Armando Sarti · F. Luca Lorini
Editors

Echocardiography for Intensivists

Forewords by A. Raffaele De Gaudio and Alfredo Zuppiroli

Springer

Echocardiography for Intensivists

Armando Sarti · F. Luca Lorini
Editors

Echocardiography for Intensivists

Forewords by A. Raffaele De Gaudio and Alfredo Zuppiroli

Springer

Editors
Armando Sarti
Department of Anesthesia and Intensive Care
Santa Maria Nuova Hospital
Florence
Italy

F. Luca Lorini
Department of Anesthesia and Intensive Care
Ospedali Riuniti di Bergamo
Bergamo
Italy

ISBN 978-88-470-2582-0 ISBN 978-88-470-2583-7 (eBook)
DOI 10.1007/978-88-470-2583-7
Springer Milan Heidelberg New York Dordrecht London

Library of Congress Control Number: 2012944384

Original Italian edition printed by Springer-Verlag Italia, 2009

Printed on acid-free paper

Springer is part of Springer Science+Business Media (www.springer.com)

Foreword by A. Raffaele De Gaudio

Since its beginning in the early 1950s by Edler and Hertz, echocardiography has developed from simple amplitude and brightness modes, through motion mode, to the present day real-time 2D and 3D imaging modalities. Its role has extended beyond cardiology into the operating rooms as a perioperative monitor and into critical care and emergency medicine. Far from being competitive or conflicting, the use of this technique by intensivists and cardiologists is complementary. In critically ill patients, echocardiography provides useful and reliable information, in a noninvasive and timely manner. This technique has become a valuable tool for diagnosing and treating a myriad of conditions commonly encountered in these patients. The hemodynamic assessment within few minutes appears to be the best approach in shock states. In addition, the evolution of technologies produced a quality of imaging that allows us to obtain clear hemodynamic data in mechanical ventilated patients. Clinical studies showed a significant role in various acute clinical situations, such us acute respiratory failure and severe chest trauma. Moreover, the use of ultrasonography for detection of pleural effusion, thoracocentesis, and central line placement is now an inevitable choice. It has long been known that ultrasonography leads to relevant changes in therapy. However, despite its easy use, the diffusion of ultrasonography among critical care physicians has been limited and the technique is not yet available in most intensive care units. A European survey demonstrated that only 20 % of intensivists have been certified. All physicians in charge of critically ill patients should be trained in ultrasonography, and in particular in echocardiography. There is an urgent need to reach this objective organizing training programs and editing new books regarding this specific topic.

Following all these reasons, it is a great pleasure to introduce this textbook that summarizes the state of the art and the standard of care for the use of echocardiography and ultrasonography in the perioperative and intensive care setting. This book is intended to highlight established principles, evolving standards of care and new opportunities to provide excellence in patient care. The editor Dr. Armando Sarti, with the contribution mainly of Italian leaders, produced a work that is a practical, handy reference for students, residents, and specialists.

This new accomplishment follows the first and already appreciated Italian edition. With this English version we now have an Italian contribution to provide a teaching program for colleagues who need a certification on ultrasonography.

A. Raffaele De Gaudio M.D.
Professor of Anesthesiology and Intensive Care
School of Medicine, University of Florence

Foreword by Alfredo Zuppiroli

The promises of the title are fully maintained, as the book is a perfect demonstration of the meaning of the term "for". This is not a sterile, academic list of topics; on the contrary, every page is deeply rooted in the daily clinical practice; every item is addressed starting from an enormous personal experience; every message shows the huge theoretical and practical background of the authors. This is not a book "of" Echocardiography, but is really a book "for" clinical bedside decision making.

As any other diagnostic tool, echocardiography has a great potential only if correct queries are made. Otherwise, inappropriate answers may be found. Every patient, particularly the critical ones, deserve that findings are interpreted in order to guide management in a safe and effective way. Therefore the book can or, better, must be read—and re-read a lot of times!—not only by intensivists, but by anyone who may face with unstable patients. I am dreaming of a health care organization where "political" decisions are made not from the physicians' or nurses' point of view, but are set on patients' needs. Critically ill patients are not only hospitalized in ICUs; critical phases of a disease can occur everywhere and at every time, even in low care settings. As a consequence, also due to the availability of miniaturized systems, the authors are providing virtually every doctor with a powerful tool for improving their diagnostic capabilities.

Today, half a century after its invention and years of use limited to cardiologists and cardiological settings, echocardiography is now mature enough to have widespread use when and where it is necessary. I am clearly reminded of my first experiences, in the 1980s, in heart surgery of ICU patients. How hard were my efforts to convince anesthesiologists to use beta-blockers, stop inotropes, and give fluids when echocardiography allowed us to recognize hypovolemia as the cause of a low output condition!

Diagnosis, that is "knowledge by means of" any tool, is not a platonic idea; it is a goal that must be pursued with humility and strictness. The authors are pointing toward the right way, providing us with a sharp, enduring light.

Florence, September 2012

Alfredo Zuppiroli
Department of Cardiology
Santa Maria Nuova Hospital, Florence

Contents

Contributors

Luciano Agati Department of Cardiology II, Policlinico Umberto I Hospital, Sapienza University of Rome, Rome, Italy

Marco Ancona Department of Cardiology, San Raffaele Hospital, Milan, Italy

Roberto Arzilla Department of Anesthesia and Intensive Care, Cardiac Surgery ICU, Policlinico Umberto I Hospital, Sapienza University of Rome, Rome, Italy

Carla Avallato Cardiovascular Anesthesia, Santa Croce & Carle Hospital, Cuneo, Italy

Piercarlo Ballo Cardiology Unit, Santa Maria Annunziata Hospital, Florence, Italy

Massimo Barattini Department of Anesthesia and Intensive Care, Santa Maria Nuova Hospital, Florence, Italy

Irene Betti Cardiology Unit, Santa Maria Annunziata Hospital, Florence, Italy

Maurizio Caruso Department of Anesthesia and Intensive Care, Cardiac Surgery ICU, Policlinico Umberto I Hospital, Sapienza University of Rome, Rome, Italy

Sergio Cattaneo Department of Anesthesia and Intensive Care, Ospedali Riuniti di Bergamo, Bergamo, Italy

Simone Cencetti UO Emergency Medicine, Santa Maria Nuova Hospital, Florence, Italy

Stefania Cerutti Department of Anesthesia and Intensive Care, Ospedali Riuniti di Bergamo, Bergamo, Italy

Simone Cipani Department of Anesthesia and Intensive Care, Santa Maria Nuova Hospital, Florence, Italy

Roger L. Click Division of Cardiology, Mayo Clinic, Rochester, MN, USA

Dionisio F. Colella Department of Anesthesia and Intensive Care, Tor Vergata University, Rome, Italy

Rachele Contri Department of Cardiology, San Raffaele Hospital, Milan, Italy

Daniele Cultrera Intensive Care Unit, Santa Maria Nuova Hospital, Florence, Italy

Giovanni Didedda Department of Anesthesia and Intensive Care, Ospedali Riuniti di Bergamo, Bergamo, Italy

Carla Farnesi Department of Anesthesia and Intensive Care, Santa Maria Nuova Hospital, Florence, Italy

Moreno Favarato Department of Anesthesia and Intensive Care, Ospedali Riuniti di Bergamo, Bergamo, Italy

Francesco Ferri Department of Anesthesia and Intensive Care, Ospedali Riuniti di Bergamo, Bergamo, Italy

Alessandro Forti Department of Anesthesia and Intensive Care, Regional Teaching Hospital, Treviso, Italy

Antonio Franco Department of Anesthesia and Intensive Care, Santa Maria Nuova Hospital, Florence, Italy

Roberto Fumagalli Cardiac Anesthesia and Intensive Care Unit, Department of Perioperative Medicine and Intensive Care, San Gerardo Hospital, University of Milano-Bicocca, Monza, Italy

Lucia Galbiati Cardiac Anesthesia and Intensive Care Unit, Department of Perioperative Medicine and Intensive Care, San Gerardo Hospital, University of Milano-Bicocca, Monza, Italy

Claudio Di Giovanni Department of Anesthesia and Intensive Care, Cardiac Surgery ICU, Policlinico Umberto I Hospital, Sapienza University of Rome, Rome, Italy

Lorenzo Grazioli Department of Anesthesia and Intensive Care, Ospedali Riuniti di Bergamo, Bergamo, Italy

Costanza Innocenti Department of Anesthesiology and Intensive Care, Careggi University Hospital, Florence, Italy

Alfonso Lagi Department of Emergency, Santa Maria Nuova Hospital, Florence, Italy

Mariavittoria Lagrotta Department of Anesthesia and Intensive Care, Ospedali Riuniti di Bergamo, Bergamo, Italy

Alessandro Locatelli Cardiovascular Anesthesia, Santa Croce and Carle Hospital, Cuneo, Italy

F. Luca Lorini Department of Anesthesia and Intensive Care, Ospedali Riuniti di Bergamo, Bergamo, Italy

Federica Manescalchi Department of Hemodialysis, Santa Maria Nuova Hospital, Florence, Italy

Lorenzo F. Mantovani Department of Anesthesia and Intensive Care, Ospedali Riuniti di Bergamo, Bergamo, Italy

Silvia Marchiani Department of Anesthesia and Intensive Care, Civil Hospital, Guastalla, Italy

Simona Marcora Unit of Pediatric Cardiology and Congenital Cardiopathy, Ospedali Riuniti di Bergamo, Bergamo, Italy

Federica Marini Department of Anesthesia and Intensive Care, Santa Maria Nuova Hospital, Florence, Italy

Andrea Masi Department of Radiology, Santa Maria Nuova Hospital, Florence, Italy

Massimo Milli Department of Cardiology, Santa Maria Nuova Hospital, Florence, Italy

Cristian O. Mirabile Department of Anesthesia and Intensive Care, Ospedali Riuniti di Bergamo, Bergamo, Italy

Cecilia Nencini Department of Anesthesia and Intensive Care, Cardiac Surgery ICU, S. Camillo Hospital, Rome, Italy

Ilaria Nicoletti Cardiovascular Anaesthesia, Santa Croce and Carle Hospital, Cuneo, Italy

Filippo Nori Bufalini Department of Radiology, Santa Maria Nuova Hospital, Florence, Italy

Michele Oppizzi Department of Cardiology, San Raffaele Hospital, Milan, Italy

Vanni Orzalesi Department of Anesthesia and Intensive Care, Civil Hospital, Guastalla, Italy

Massimo Pacilli Department of Anesthesia and Intensive Care, Cardiac Surgery ICU, Policlinico Umberto I Hospital, Sapienza University of Rome, Rome, Italy

Francesca Pacini Department of Anesthesia and Intensive Care, Cardiac Surgery ICU, Policlinico Umberto I Hospital, Sapienza University of Rome, Rome, Italy

Elena Pagani Department of Anesthesia and Intensive Care, Ospedali Riuniti di Bergamo, Bergamo, Italy

Cecilia Pelagatti Anesthesia and Intensive Care Oncologic Department, Careggi University Hospital, Florence, Italy

Mauro Pepi Monzino Cardiological Hospital, IRCCS, Milan, Italy

Laura Pera Department of Anesthesia and Intensive Care, Santa Maria Nuova Hospital, Florence, Italy

Paola Pieraccioni Department of Anesthesia and Intensive Care, Santa Maria Nuova Hospital, Florence, Italy

Claudio Poli Department of Anesthesia and Intensive Care, Santa Maria Nuova Hospital, Florence, Italy

Francesca Pompei Department of Anesthesia and Intensive Care, Cardiac Surgery ICU, Policlinico Umberto I Hospital, Sapienza University of Rome, Rome, Italy

Paolo Prati Policlinico Tor Vergata, Rome, Italy

Alessandra Rizza Intensive Care Cardiac Surgery, Ospedali Riuniti di Bergamo, Bergamo, Italy

Bruno Rossetto Department of Anesthesia and Intensive Care, Ospedali Riuniti di Bergamo, Bergamo, Italy

Marialuigia Dello Russo Department of Anesthesia and Intensive Care, Ospedali Riuniti di Bergamo, Bergamo, Italy

Valeria Salandin Department of Anesthesia and Intensive Care, Regional Teaching Hospital, Treviso, Italy

Fabio Sangalli Cardiac Anesthesia and Intensive Care Unit, Department of Perioperative Medicine and Intensive Care, San Gerardo Hospital, University of Milano-Bicocca, Monza, Italy

Vincenzo De Santis Department of Anesthesia and Intensive Care, Cardiac Surgery ICU, Policlinico Umberto I Hospital, Sapienza University of Rome, Rome, Italy

Armando Sarti Department of Anesthesia and Intensive Care, Santa Maria Nuova Hospital, Florence, Italy

Gino Soldati Emergency Medicine, Valle del Serchio General Hospital, Lucca, Italy

Carlo Sorbara Department of Anesthesia and Intensive Care, Regional Teaching Hospital, Treviso, Italy

Demetrio Tallarico Department of Cardiology I, Policlinico Umberto I Hospital, Sapienza University of Rome, Rome, Italy

Gloria Tamborini Monzino Cardiological Hospital, IRCCS, Milan, Italy

Luigi Tritapepe Department of Anesthesia and Intensive Care, Cardiac Surgery ICU Policlinico Umberto I Hospital, Sapienza University of Rome, Rome, Italy

Germana Tuccinardi Department of Anesthesiology and Intensive Care, Careggi University Hospital, Florence, Italy

Angelo Vavassori Department of Anesthesia and Intensive Care, Ospedali Riuniti di Bergamo, Bergamo, Italy

Domenico Vitale Department of Anesthesia and Intensive Care, Cardiac Surgery ICU, Policlinico Umberto I Hospital, Sapienza University of Rome, Rome, Italy

Paolo Voci Department of Cardiology, Tor Vergata University, Rome, Italy

Abbreviations

A2C	Apical two chambers
A3C	Apical three chambers
A4C	Apical four chambers
A5C	Apical five chambers
AAS	Acute aortic syndrome
ACA	Anterior cerebral artery
ACHD	Adult congenital heart defects
ACP	Acute cor pulmonale
ACS	Acute coronary syndromes
AcT	Pulmonary acceleration time
AD	Aortic dissection
AF	Atrial fibrillation
AHRQ	Agency for Healthcare Research and Quality
ALI	Acute lung injury
ALS	Advanced life support
AMI	Acute myocardial infarction
AML	Anterior mitral leaflet
APACHE	Acute physiology and chronic health evaluation
AQ	Acoustic quantification
AR	Aortic regurgitation
ARDS	Acute respiratory distress syndrome
ARF	Acute renal failure
ARV	Arrhythmogenic right ventricular dysplasia
ARVC	Arrhythmogenic right ventricular cardiomyopathy
AS	Aortic stenosis
ASD	Atrial septal defect
AT	Acceleration time
AV	Aortic valve
AVO	Aortic valve opening
AVC	Aortic valve closure
BA	Basilar artery
BCI	Blunt cardiac injury
BNP	Brain natriuretic peptide
BSA	Body surface area
BV	Basilic vein
CDC	Center for Disease Control and Prevention
CFD	Color flow Doppler
CFM	Color flow mapping

CPR	Cardiopulmonary resuscitation
CRF	Chronic renal failure
CRT	Cardiac resynchronization therapy
CSA	Cross sectional area
CSF	Cerebrospinal fluid
CUS	Compression ultrasonography
CVADs	Central vascular access devices
CVC	Central venous catheter
CV	Cephalic vein
CW	Continous wave
dB	Decibel
DCM	Dilated cardiomiopathy
DD	Diastolic dysfunction
DFR	Doppler flow ratio
DT	Deceleration time
DVI	Doppler velocity index
DVT	Deep venous thrombosis
Ea	Tissue doppler of the mitral annulus shows a prominent early diastolic velocity
ECD	Eco-color Doppler
EDA	End diastolic area
EDRVA	End diastolic right ventricle area
EDV	End diastolic volume
EF	Ejection fraction
EP	Embolia polmonare
ESA	End systolic area
ESC	European society of cardiology
ESRVA	End systolic right ventricle area
EV	Eustachian valve
FAC	Fractional area changing
FAST	Focused assessment with sonography in trauma
FATE	Focus assessed transthoracic echocardiography
FEEL	Focus echo evaluation in life support
FS	Fractional shortening
G	Gradient
GRF	Glomerular filtration rate
HCM	Hypertrofic cardiomyopathy
HOCM	Hypertrofic obstructive cardiomyopathy
IAS	Interatrial septum
ICA	Internal carotid artery
ICU	Intensive care unit
IE	Infective endocarditis
IHD	Ischemic heart disease
IMH	Intramural hematoma
IRAD	International Registry of Aortic Dissection
IVA	Isovolumic acceleration
IVC	Inferior vena cava
IVCT	Isovolumic contraction time
IVRT	Isovolumic relaxation time

IVS	Interventricular septum
IVV	Isovolumic velocity
LA	Left atrium
LAA	Left atrial appendage
LAD	Left anterior descending artery
LAP	Left atrial pressure
LGC	Lateral gain compensation
LV	Left ventricle
LVEDA	Left ventricle end diastolic area
LVEDP	Left ventricular end-diastolic pressure
LVEDD	Left ventricular internal diameter in diastole
LVEDV	Left ventricle end diastolic volume
LVEF	Left ventricular ejection fraction
LVESA	Left ventricle end systolic area
LVESD	Left ventricular internal diameter in systole
LVESV	Left ventricle end systolic volume
LVF	Left ventricle failure
LVID	Left ventricle internal diameter
LVNC	Left ventricular noncompaction
LVOT	Left ventricle outflow tract
LVOTO	Left ventricle outflow tract obstruction
LVSP	Left ventricle systolic pressure
MCA	Mean cerebral artery
ME	Midesophageal
ME LAX	Midesophageal long axis
MI	Myocardial infarction
MPAP	Mean pulmonary artery pressure
MPI	Myocardial performance index
MR	Mitral regurgitation
MS	Mitral stenosis
MV	Mitral valve
MVA	Mitral valve area
MVL	Mitral valve leale
MVP	Mitral valve prolapse
NICE	National Institute for Clinical Excellence
PA	Pulmonary artery
PADP	Pulmonary artery diastolic pressure
PAE	Paradoxical air embolism
PAOP	Pulmonary artery occlusion pressure
PAP	Pulmonary artery pressure
PAPs	Pulmonary artery systolic pressure
PAU	Penetrating atherosclerotic ulcer
PCA	Posterior cerebral artery
PCI	Primary coronary intervention
PCM	Pulse Contour Methods
PCWP	Pulmonary capillary wedge pressure
PDA	Patent ductus arteriosus
PE	Pulmonary embolism
PEA	Pulseless electric activity

PEEP	Pulmonary end espiratory pressure
PFO	Patent forame ovale
PHT	Pressure half time
PICC	Peripherically Inserted Central Catheter
PISA	Proximal isovelocity surface area
PLR	Passive leg raising
PML	Posterior mitral leaflet
PP	Plateau pressure
PR	Pulmonary regurgitation
PRF	Pulse repetition frequency
PSLAX	Parasternal long axis
PSSAX	Parasternal short axis
PV	Pulmonary valve
PVR	Pulmonary vascular resistance
PW	Pulsed wave
PWT	Posterior wall thickness
RA	Right atrium
RAP	Right atrial pressure
RCA	Right coronary artery
RCM	Restrictive cardiomyopathy
RMVD	Reumatic mitral valve disease
RV	Right ventricle
RVD	Right ventricular diameter
RVEDA	Right ventricle end diastolic area
RVEF	Right ventricle ejection fraction
RVESA	Right ventricle end systolic area
RVFAC	Right ventricle fractional area change
RVH	Right ventricle hypertrophy
RVOT	Right ventricle outflow tract
RVSP	Right ventricle systolic pressure
RWMA	Regional wall motion abnormalities
SAM	Systolic anterior motion
SBP	Systolic blood pressure
SC	Subcostal
SC4C	Four chambers subcostal view
SDI	Systolic dyssinchrony index
SPL	Spatial pulse length
SR	Strain rate
SS	Suprasternal
SV	Stroke volume
SVC	Superior vena cava
SWT	Septal wall thickness
TAI	Traumatic aortic injury
TAPSE	Tricuspid anular plane systolic excursion
TCD	Transcranial Doppler
TDI	Tissue Doppler imaging
TEE	Transesophageal ecocardiography
TG	Transgastric
TGC	Time gain compensation

TG mid SAX	Transgastric mid short axis
TR	Tricuspid regurgitation
TTE	Transthoracic ecocardiography
TV	Tricuspid valve
TVR	Tricuspid valve regurgitation
UE	Upper esophageal
ULC	Ultrasound lung comet
US	Ultrasound
VA	Veretebral arteries
VSD	Ventricular septal defect
VTI	Velocity time intergral
WMSI	Wall motion scoring index

Part I

Ultrasound and Use of the Echo Machine

Essential Physics of Ultrasound and Use of the Ultrasound Machine

1

Dionisio F. Colella, Paolo Prati, and Armando Sarti

1.1 Ultrasound

Sound is a mechanical wave made up of compressions and rarefactions of molecules in a medium (solid, liquid, or gas) (Fig. 1.1).

Sounds is characterized by some parameters:

- *Frequency* is the number of cycle per unit time (1 s), measured in hertz (Hz). The higher the frequency, the better the resolution, but the lower the penetration (Fig. 1.2).
- *Period* is the duration of a cycle (the inverse of frequency).
- *Wavelength* is the distance that sound travels in one cycle. The wavelength depends on the size of the piezoelectric crystals in the transducer and the medium through which the sound wave travels (Table 1.1).
- *Amplitude* is the amount of change in the oscillating variable. Amplitude decreases as the wave travels (attenuation), leading to echoes from deeper structures being weaker than those from superficial structures. It is measured in decibels:

$$\text{Decibel (dB)} = 20 \log_{10} A^2/A_r^2,$$

where A is the sound amplitude of interest and A_r is a standard reference sound level.

- *Intensity* is the measure of the energy in a sound beam. It is related to potential tissue damage. For example, ultrasound used for lithotripsy has high intensity to fragment renal stones. It is measured in watts per square meter.
- *Power* is the amount of energy transferred. It is expressed in watts.

  The power or the intensity levels are not represented on the ultrasound machine, but there are two other variables that indirectly change those two parameters: mechanical index and thermal index. The first one represents the risk of cavitation. The second one is related to the increase of temperature of the tissues (Table 1.1, Fig. 1.2).
- *Propagation velocity* is the velocity determined by the medium that the sound passes through. It is related to the tissue's resistance to compression. Velocity is the product of frequency and wavelength. The propagation velocity through a medium is increased by increasing stiffness of the medium and is reduced by increasing density of the medium (Table 1.2).

  Velocity is the product of wavelength and frequency:

$$v = \lambda \times f.$$

D. F. Colella (✉)
Department of Anesthesia and Intensive Care,
Tor Vergata University, Rome, Italy
e-mail: dionisio.colella@libero.it

A. Sarti and F. L. Lorini (eds.), *Echocardiography for Intensivists*,
DOI: 10.1007/978-88-470-2583-7_1,

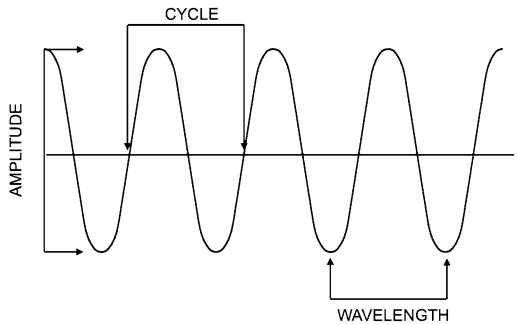

Fig. 1.1 A sound wave

Table 1.1 Relationship between frequency and wavelength

Frequency (MHz)	Wavelength (mm)
1.25	1.2
2.5	0.60
5.0	0.30
7.5	0.20
10.0	0.15

1.2 Interaction of Ultrasound with Tissues

1.2.1 Attenuation

When the ultrasound beam passes through uniform tissues, its energy is attenuated by dispersion and absorption.

Absorption is the conversion of ultrasound energy into heat. The attenuation coefficient relates the amount of attenuation to the frequency of the ultrasound beam and the distance that beam travels.

Dispersion occurs because of reflection, refraction, and scattering. The attenuation of the sound wave is increased at higher frequencies, so in order to have better penetration of deeper tissues, a lower frequency is used.

Attenuation involves less energy returning to the transducer, resulting in a poor image.

As the sound traveling through a tissue reaches another tissue with different acoustic properties, the sound energy can be reflected or change its direction, depending on the acoustic impedance of the second interface.

Acoustic impedance is the ability of a tissue to transmit sound and depends on:

- The density of the medium.
- The propagation velocity of ultrasound through the medium:

$$Z = \rho \times v,$$

where Z is the acoustic impedance, ρ is the density of the material, and v is the speed of ultrasound.

If different mediums have a large difference in acoustic impedance, there is an acoustic impedance mismatch. The greater the acoustic mismatch, the greater the percentage of ultrasound reflected and the lower the percentage transmitted.

1.2.2 Reflection

When a sound wave reaches a smooth surface, it is reflected with an angle that is opposite the incident angle. *The more the angle is near 90°, the lower the amount of energy that is lost.*

There are two types of *reflection*:

1. *Specular* reflection
2. *Scattering* reflection

If the sound wave reaches a small and irregularly shaped surface (such as red blood cells), the ultrasound energy is scattered in all directions.

Reflection can be measured by the reflection coefficient:

$$R = (Z_2 - Z_1)^2/(Z_2 + Z_1)^2,$$

where R is the reflection coefficient and Z is the acoustic impedance.

When the second medium encountered is a strong reflector, some phenomena can occur:

- Acoustic shadowing (Fig. 1.3)
- Reverberation (Fig. 1.4)
- A side lobe (Fig. 1.5)

1.2.3 Refraction

When a sound beam reaches the interface between two mediums, some of it is not reflected

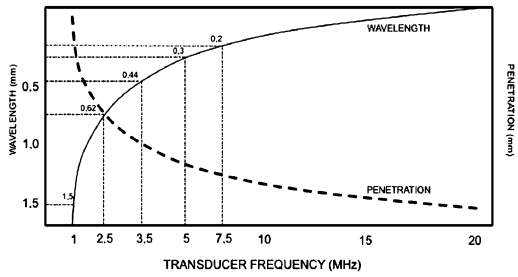

Fig. 1.2 Relationship between transducer frequency, penetration, and wavelength. As the transducer frequency increases, resolution increases and penetration decreases

Table 1.2 Ultrasound velocities in different mediums

Material	Velocity (m/s)
Air	330
Water	1,497
Fat	1,440
Blood	1,570
Soft tissue	1,540

but passes through the interface and its direction is altered. This is called refraction. The amount of refraction is proportional to the difference in the velocity of sound in the two tissues and to the angle of incidence:

$$n_1/n_2 = \sin\theta_1/\sin\theta_2,$$

where n is the refraction coefficient and θ is the angle of incidence.

It is possible to see some refraction artifact (Figs. 1.6, 1.7).

1.3 Ultrasound Wave Formation

Ultrasound waves are generated by *piezoelectric crystals*. An electrical current applied to a crystal causes vibration and consequent expansion and contraction. These changes are transmitted into the body as ultrasound waves. Modern transducers are both transmitters and receivers.

There is a strict relationship between time, distance, and velocity of ultrasound propagation. Knowing the time required for sound to travel from the transducer to an object, the time needed for the returning echo from that object to the transducer, and the propagation velocity in that medium allows one to calculate the distance the ultrasound waves have crossed. This is the basis of ultrasonic imaging.

Electrical energy is not applied to the transducer in a continuous way: ultrasound waves are produced at regular intervals with a pulsed repetition period, leading to a defined *pulse repetition frequency* (PRF; in kilohertz). The wavelength of the ultrasound generated is inversely related to the thickness of the piezoelectric elements.

The piezoelectric elements cannot emit a second pulse until the first has returned to the transducer: the ability to recognize different objects is related to the frequency of emission of the ultrasound wave pulse.

The ultrasound beam emitted from the transducer has a particular shape: it begins with a narrow beam (near field) and then the ultrasound beam diverges in the far field. The length of the near field (or Fresnel zone) is related to the diameter of the transducer (D) and the wavelength:

$$L_n = D^2/4\lambda.$$

Even the angle of divergence, forming the far field (or Fraunhofer zone), is related to the diameter of the transducer (D) and the wavelength:

$$\sin\theta = 1.22\lambda/D.$$

The resolution is improved in the near field because of the narrower diameter of the ultrasound beam. It is easy to understand that a high-diameter transducer with high frequency (short wavelength) can produce the best ultrasound beam.

There is another way to reduce the diameter of the ultrasound beam and thus improve the resolution: focusing the beam. This produces a reduction of the beam size at a particular point, ameliorating the image.

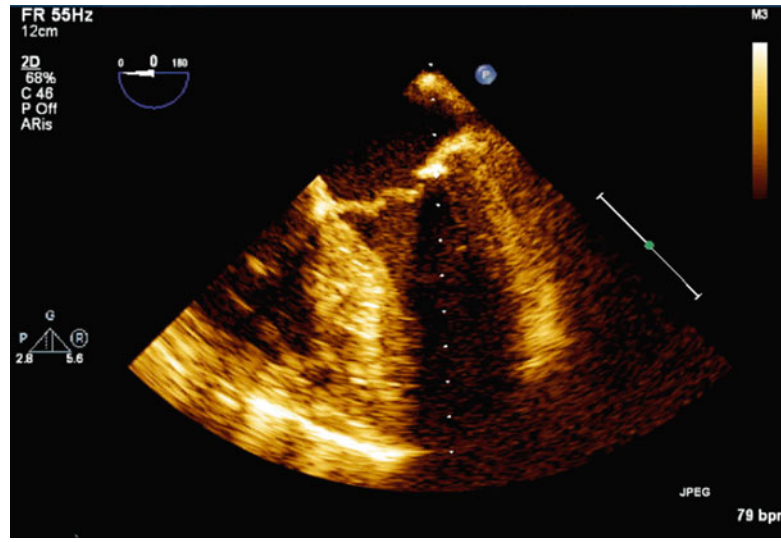

Fig. 1.3 The left ventricular wall is hidden behind a calcified posterior mitral leaflet

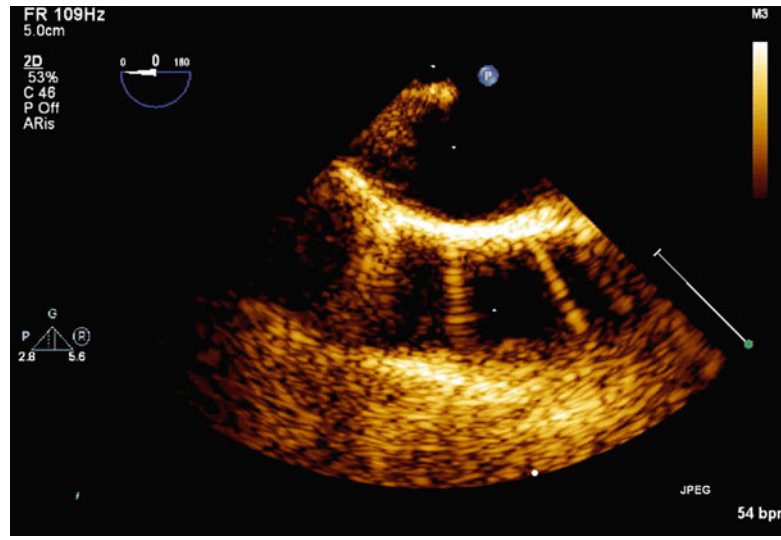

Fig. 1.4 Comet tail. Mirror image: double-barred aorta

1.3.1 Resolution

This is the ability to recognize two objects. Spatial resolution is the ability to differentiate two separate objects that are close together. Temporal resolution is the ability to place structures at a particular time.

1.3.2 Axial Resolution

This is the ability to recognize two different objects at different depths from the transducer along the axis of the ultrasound beam (Figs. 1.8, 1.9):

$$\text{Axial resolution} = \frac{\text{spatial pulse length (SPL)}}{2},$$

where SPL = $\lambda \times$ no. of cycles.

It is improved by higher-frequency (shorter-wavelength) transducers but at the expense of penetration. Higher frequencies are therefore used to image structures close to the transducer.

1.3.3 Lateral Resolution

This is the ability to distinguish objects that are side by side. It is dependent on the beam width because

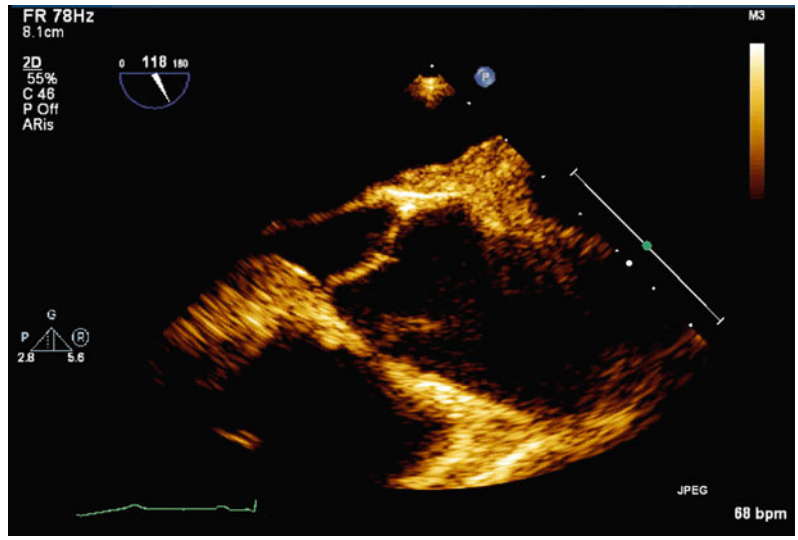

Fig. 1.5 Side lobe artifacts can create a false aortic flap

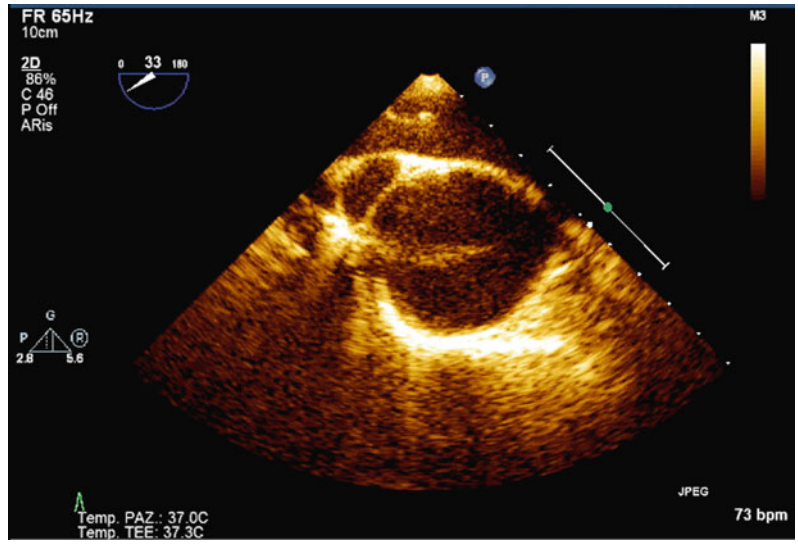

Fig. 1.6 Grading lobe. The pulmonary catheter seems to be in the aorta

two objects side by side cannot be distinguished if they are separated by less than the beam width. It is improved by use of higher-frequency transducer (which increases the beam width) and an optimized focal zone (Figs. 1.10, 1.11).

1.3.4 Temporal Resolution

This is dependent on the frame rate. It is improved by:

- Minimizing depth—the maximum distance from the transducer as this affects the PRF
- Narrowing the sector to the area of interest—narrowing the sector angle
- Minimizing the line density (but at the expense of lateral resolution)

1.4 Doppler Echocardiography

Doppler echocardiography is a method for detecting the direction and velocity of moving blood within the heart.

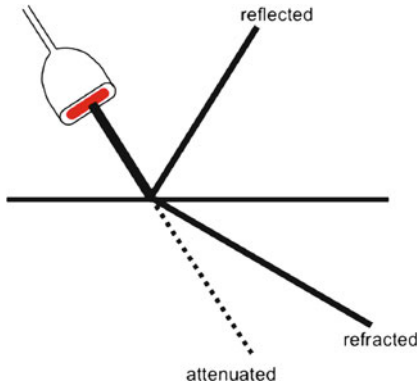

Fig. 1.7 Reflection, refraction, and attenuation

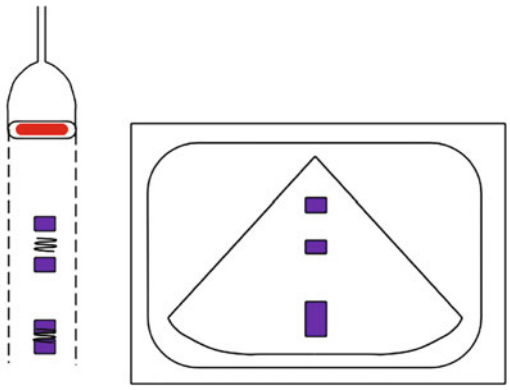

Fig. 1.8 Axial resolution. The spatial pulse length is short enough to be placed within two different structures, so they are resolved

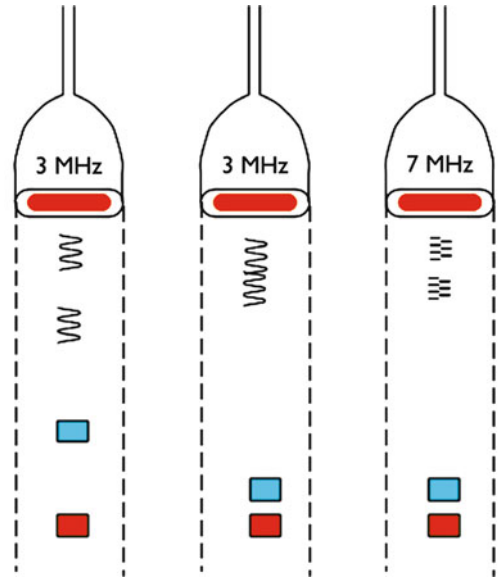

Fig. 1.9 Axial resolution and transducer frequency. Closer objects cannot be resolved by a low transducer frequency. Increasing the transducer frequency (shortening the spatial pulse length and duration) is required to resolve the objects

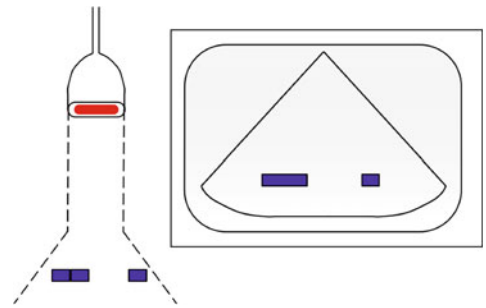

Fig. 1.10 Lateral resolution. Wider beams cannot resolve near objects

The *Doppler effect* (or *Doppler shift*) is the change in frequency of a wave for an observer moving relative to the source of the wave (Fig. 1.12).

When the source of the sound wave is moving toward the observer, each successive wave is emitted from a position closer to the observer than the previous wave and it takes less time than the previous wave to reach the observer. Then the time between the arrival of successive waves is reduced, resulting in a higher frequency. If the source of waves is moving away from the observer, the opposite effect can be seen, with increased time between the arrival

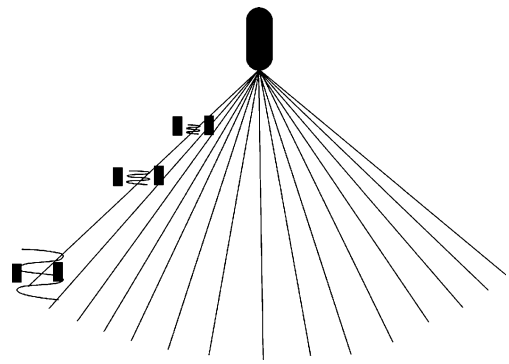

Fig. 1.11 Lateral resolution. At low depth, lateral resolution is worsened

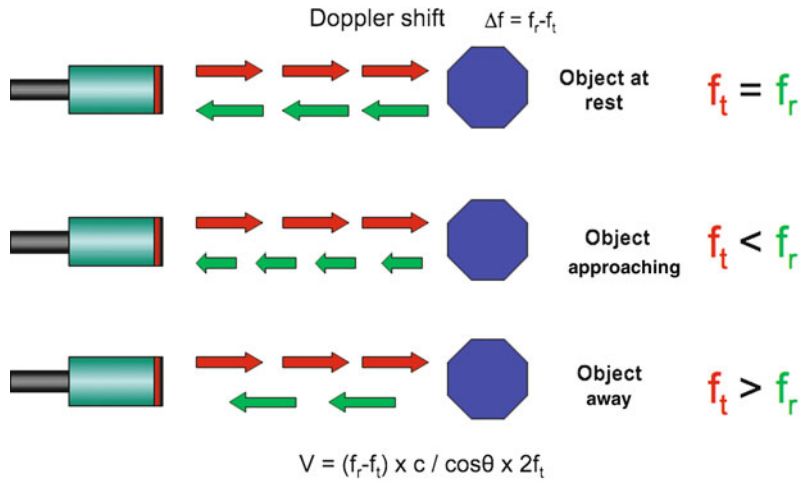

Fig. 1.12 Doppler shift

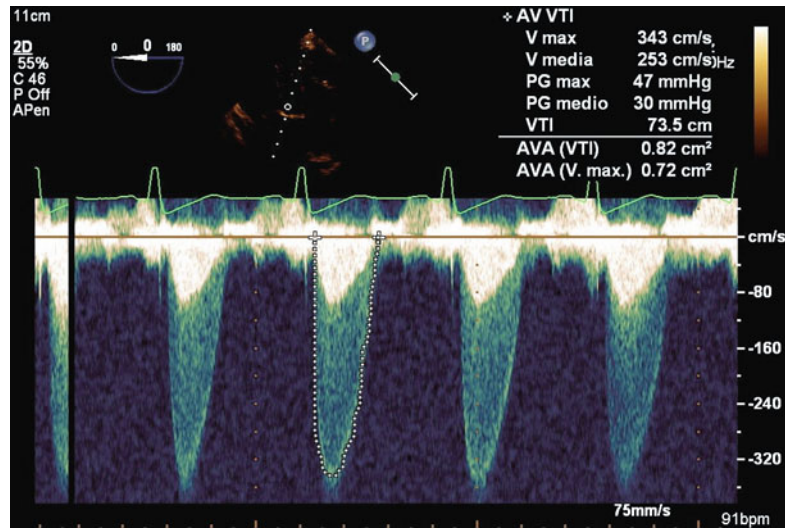

Fig. 1.13 Continuous wave Doppler imaging

of successive waves, giving them a lower frequency.

The amount of that change in frequency is the Doppler shift. Blood flow velocity (V) is related to the Doppler shift by the speed of sound in blood (C) and the intercept angle (θ) between the ultrasound beam and the direction of blood flow:

$$\text{Doppler shift} = 2 \times F(\text{transmitted}) \times [(V \times \cos\theta)]/C$$

A factor of 2 is used because the sound wave has a "round-trip" transit time to and from the transducer. If the ultrasound beam is not parallel to blood flow, an angle of incidence greater than 30° can underestimate the Doppler shift.

There are two kinds of Doppler application: pulsed wave Doppler and continuous wave Doppler.

In the *continuous wave Doppler* technique, the transducer continuously transmits and receives ultrasound waves (Fig. 1.13).

The continuous wave Doppler technique measures all velocities along the ultrasound beam. It cannot discriminate the time interval

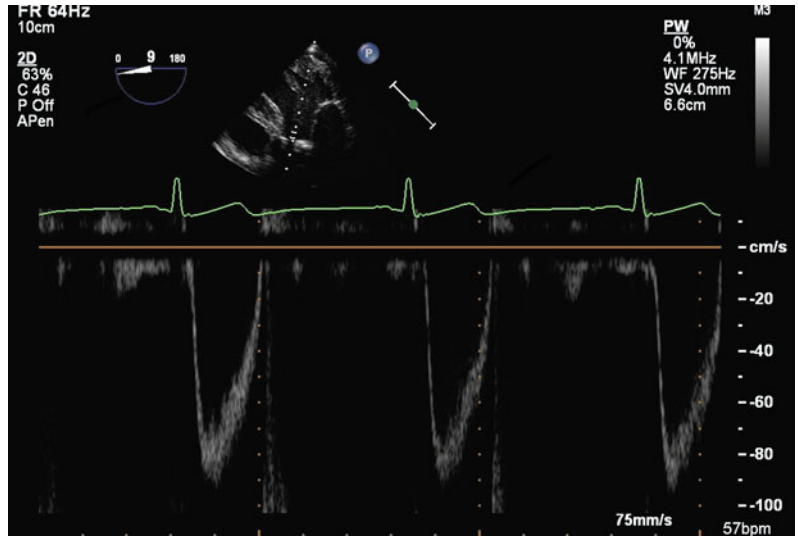

Fig. 1.14 Pulsed wave Doppler echocardiography

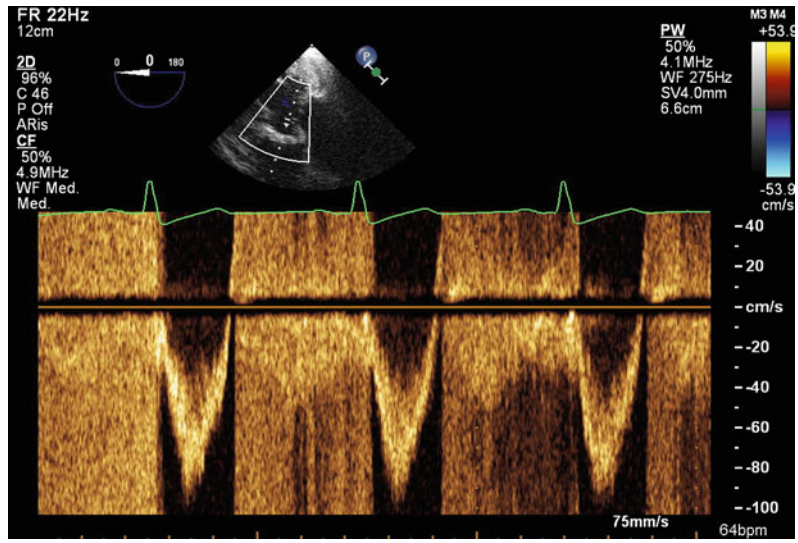

Fig. 1.15 Aliasing

from the emission and the reflection, giving no information about the depth of the received signal. The continuous wave Doppler technique is able to detect very high velocities, and it can be useful to evaluate the high velocity flow through a stenotic aortic valve.

In the *pulsed wave Doppler* technique, the transducer alternately transmits and receives the ultrasound wave and its returning echo (Fig. 1.14). The transducer must wait for the returning echo before sending out another ultrasound wave. The pulsed wave Doppler technique samples velocities at a specific point (sample volume) of the ultrasound beam.

The number of pulses transmitted from a Doppler transducer each second is called the pulse repetition frequency (PRF). The sampling rate determinates the acquisition of information. If the Doppler shift frequency is higher than the PRF, the Doppler signal is displayed on the other side of the baseline. This is the alias artifact.

Aliasing occurs when the measured velocity is greater than half of the PRF (Figs. 1.15, 1.16). This velocity is called the *Nyquist limit*.

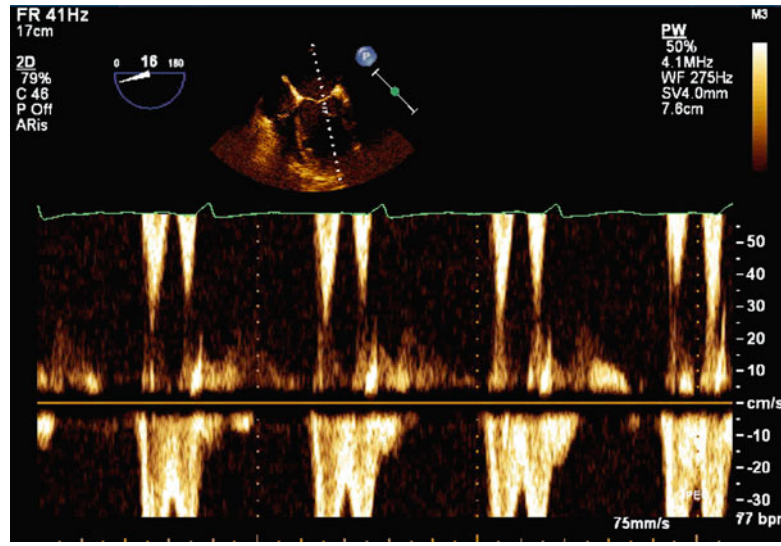

Fig. 1.16 Aliasing

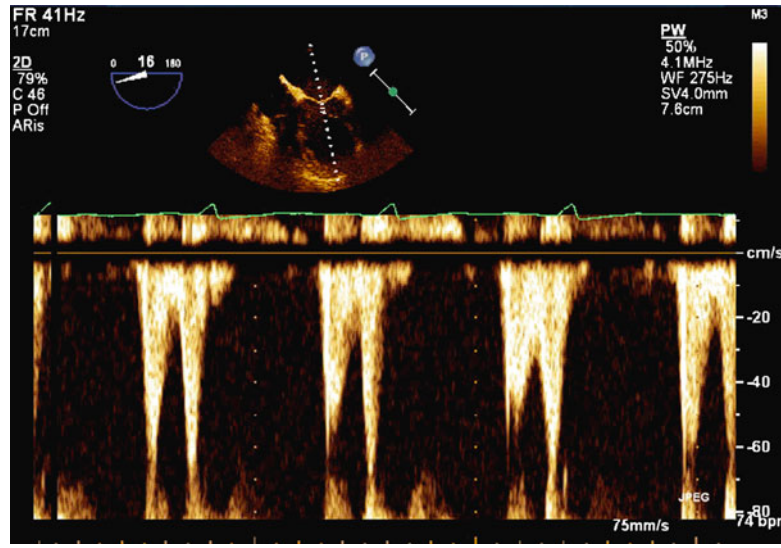

Fig. 1.17 Aliasing resolved by setting the right baseline

There are some ways to improve the velocity performance of the pulsed wave Doppler technique:

1. Decrease the distance between the transducer and the sample volume. Reducing the distance the ultrasound beam has to travel will increase the frequency of emission of the pulsed wave (PRF).
2. Choose a low frequency of emission.
3. Set the baseline to display a greater range of velocities (Fig. 1.17).

In *tissue Doppler* imaging (Fig. 1.18) a low-pass filter is used to measure only the velocity of myocardial tissues. Tissue Doppler imaging uses a small pulsed wave sample volume showing low velocity–high amplitude signals.

Color Doppler imaging combines a 2D image with a Doppler method to visualize the velocity of blood flow within an image plane. The Doppler shift of thousands of sample volumes displays the directions of the blood cells: blue for away from and red for toward the transducer (Fig. 1.19).

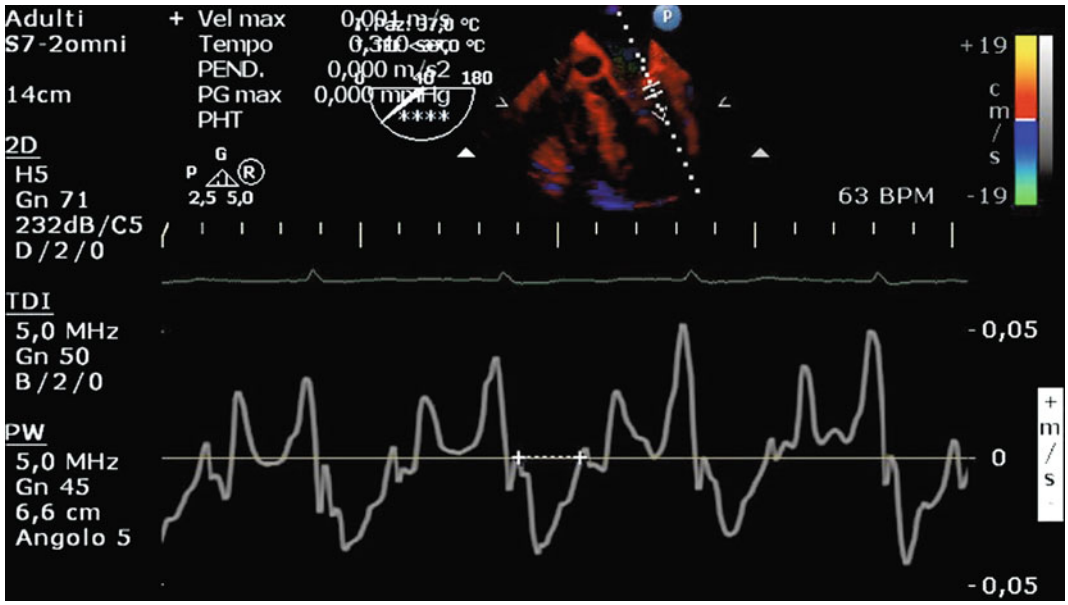

Fig. 1.18 Tissue Doppler imaging

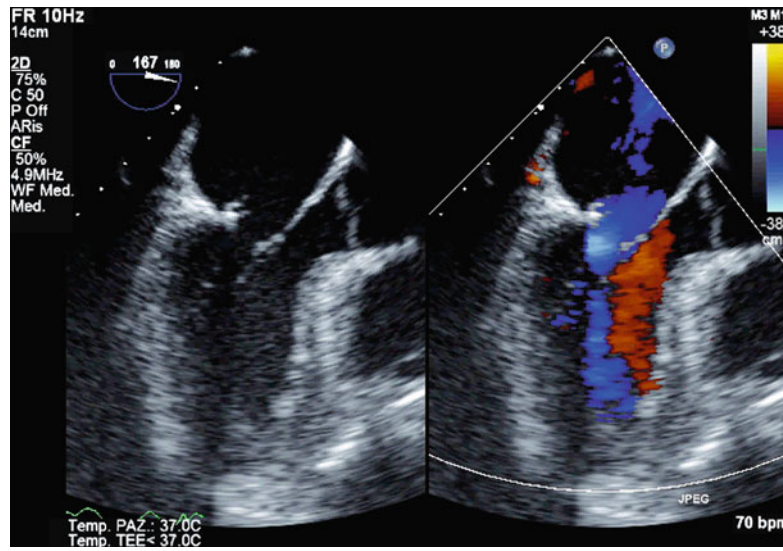

Fig. 1.19 Color Doppler imaging. *Blue* away from and *red* toward the transducer

High flow velocities are displayed in yellow (toward the transducer) and cyan (away from the transducer); green is used to visualize areas of turbulence. As with the pulsed wave Doppler technique, the color flow Doppler technique suffers from the Nyquist limit and aliasing can occur (Fig. 1.20).

Color M-mode Doppler imaging combines the spatiotemporal graphic representation of M-mode and color codification. It shows at the same time a one-dimensional view of anatomic structures and color flow visualization. It is useful to assess transmitral flow (Fig. 1.21).

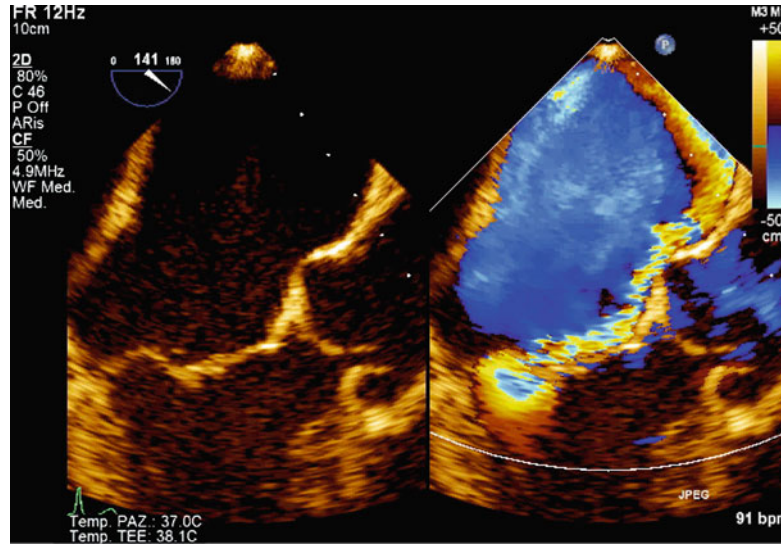

Fig. 1.20 Color Doppler aliasing

1.5 Use of the Ultrasound Machine: Optimizing the Picture

The image quality depends on the operator's skill, and also on the adjustment of the ultrasound machine according to the features of the particular patient to be examined. The positioning of the patient and the probe is discussed in Chap. 2, together with all transthoracic views. First, it is essential to study well the instruction manual of the device at one's disposal to use it optimally.

1.5.1 Environment

The brightness of the environment where the examination is done should be reduced. The examination is performed in the ICU at the bedside, so it is preferable to have beds that can be easily arranged with Trendelenburg positioning, anti-Trendelenburg positioning, head and trunk lifting, and side tilting.

1.5.2 Ultrasonograph Setting

1.5.2.1 Electrocardiogram

Despite often being omitted to save time, it is important to always connect the electrocardiogram (ECG) line of the ultrasound device to the patient electrodes. The ECG trace, recorded at the base of the display with a "marker" of time coinciding with the moving image, allows establishment of the phases of the cardiac cycle based on electrical activity of the heart, apart from monitoring the ECG. The mechanical systole usually begins immediately after the R wave and ends at about half of the T wave. The end of diastole coincides with the R-wave peak of the ECG (Fig. 1.22).

1.5.2.2 Probes

The probes used for adult echocardiography emit ultrasound with a frequency of about 3 MHz, whereas the probes used in pediatric echocardiography emit higher frequencies, from 5 to 7.5 MHz. These emissions represent the best compromise for use according to different types of patients, given that the higher the frequency, the better the image definition, but the lower the penetration of ultrasound into the tissues. Modern equipment can produce sharper images through "tissue harmonic imaging": in a nutshell, the harmonics produced by the interaction of the ultrasound beam with the tissues are enhanced and the fundamental harmonic frequencies are suppressed, resulting in better far-field quality. The image quality is better, but the very echo-reflective structures, such as pericardium and valves, can thus appear thicker

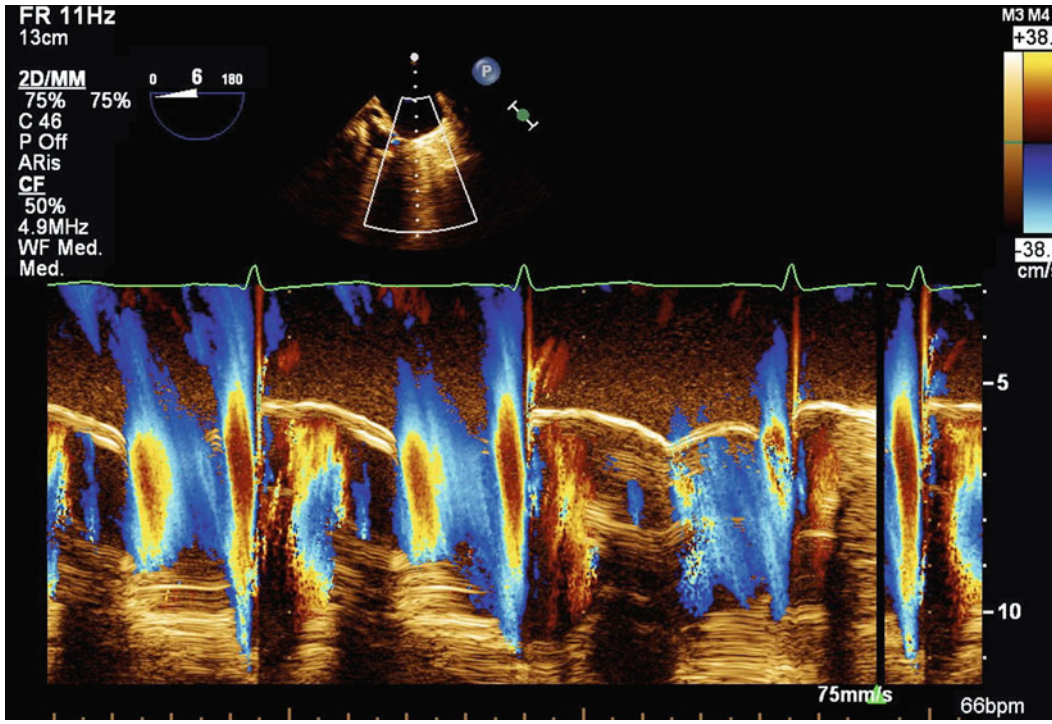

Fig. 1.21 Color M-mode imaging

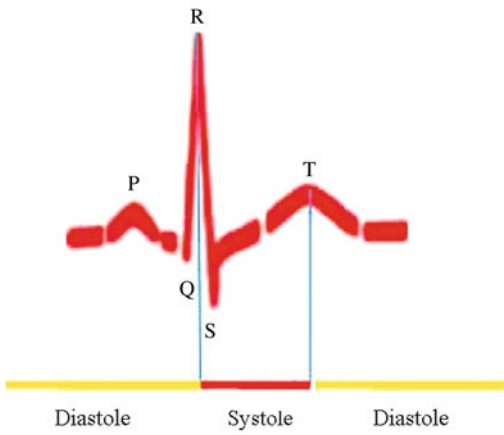

Fig. 1.22 ECG systolic and diastolic phases

than they really are. The probes have a touch and often light marker defining the scanning plane and laterality. Figure 1.23 shows the various probes used for the study of the heart with transthoracic approaches, the vessels, and the thoracic and abdominal organs.

1.5.2.3 Sector Depth

The depth can be adjusted by the operator. The machine starts with a default standard depth so that the whole heart is displayed, but the depth of the field can be varied in order to position the structures of interest in the middle of the image. If the outer edges of the heart in the default image exceed the limits of the display, the heart as a whole or some part of it is certainly enlarged.

1.5.2.4 Width of the Scanning Beam

The maximum amplitude ensures that the most lateral structures are seen, but a reduction of the amplitude may sometimes be preferable to produce greater definition of the central structures; this is because a shorter time is needed to scan a narrower angle.

1.5.2.5 Gain

The construction of the image as grayscale or monochrome images depends on the intensity of the return signal, which depends on the distance traveled and on the reflective properties of the tissues

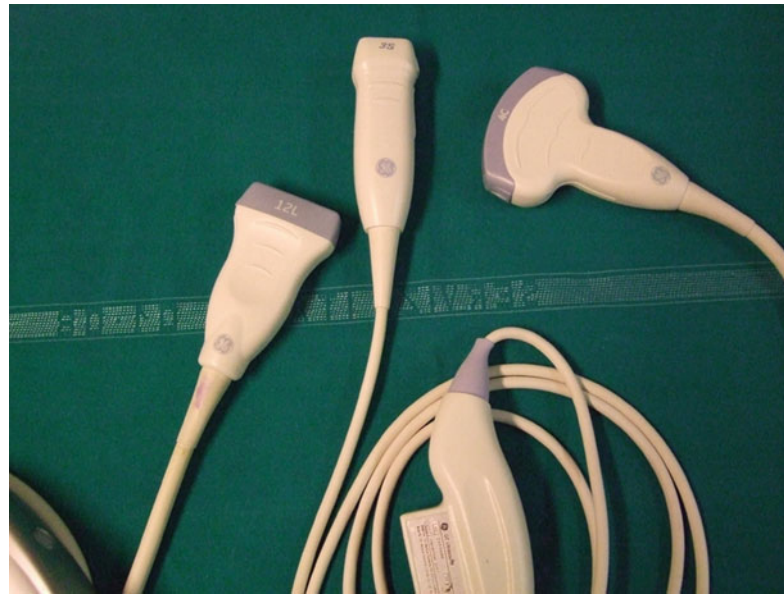

Fig. 1.23 Ultrasound probes. From *left* to *right*: vascular and soft tissue linear probe, cardiac phased-array probe, abdominal convex probe

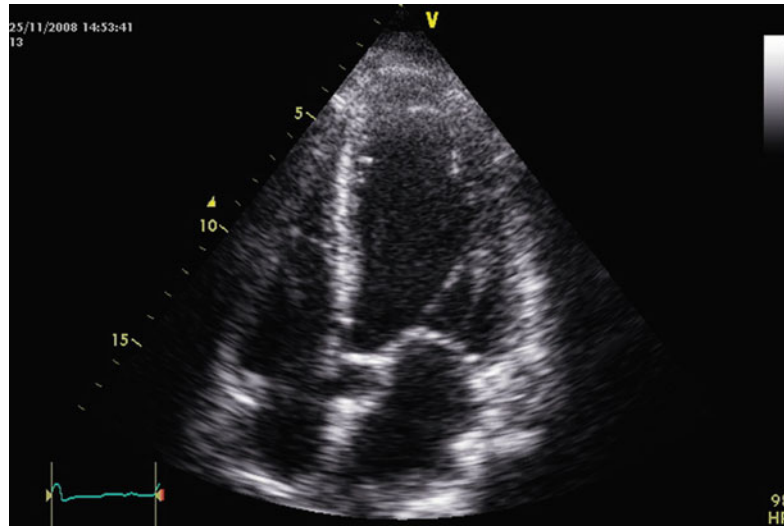

Fig. 1.24 Echo cardiographic image (apical five-chamber view) with good contrast adjustment

encountered (see earlier). Therefore, the gain can be adjusted for different depths in order to compensate for the reduction of the return signal. This adjustment (time gain compensation), which is automatic in modern equipment, usually occurs through a system of levers that correspond to vertical depths of the field. Observing the display as the default, the operator improves the image manually by moving the levers that correspond to different levels of depth. In some devices there is also a system of horizontal adjustment for adjusting the image in the lateral fields (lateral gain compensation). However, these adjustments must be done with care since excess gain produces brighter images, leading to poor definition between close structures and even artifacts. In contrast, too dark images are produced with not enough gain, hiding some low-echo-reflective structures. Even though it depends somewhat on operator preference, a well-adjusted image (Fig. 1.24) is one that has:

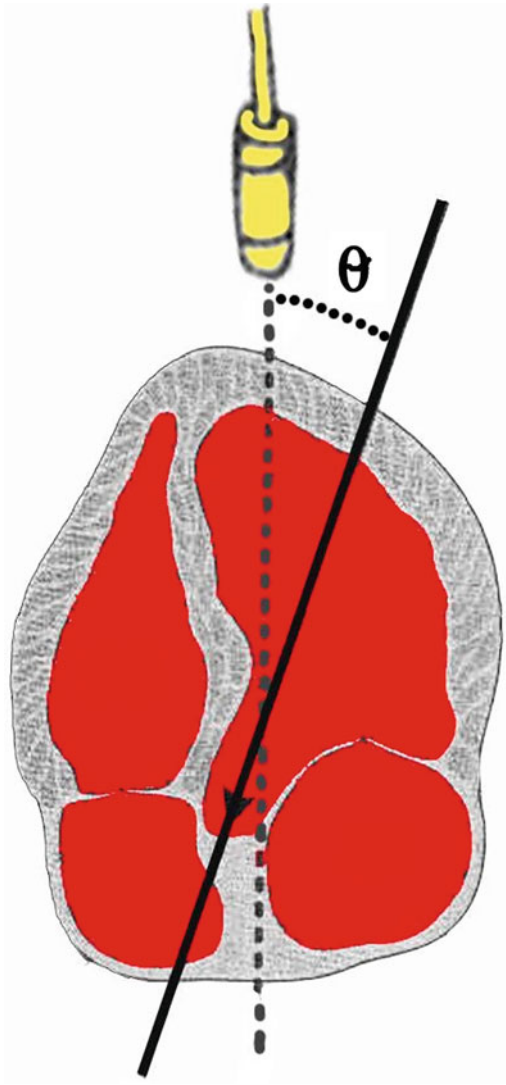

Fig. 1.25 Apical five-chamber view. Note the angle between the ultrasound beam (*dotted line*) and the blood flow through the left ventricular outflow tract (*continuous line*)

- Fairly uniform intensity of solid structures
- A slight speckling in the dark cavities full of blood

1.5.2.6 Focus

The focus of the image is usually by default in the central part of the display, but one can move the focus to higher or lower levels for further research on particular structures.

1.5.2.7 Regulating Continuous Wave Doppler and Pulsed Wave Doppler Imaging

As already mentioned, continuous wave Doppler imaging is used for the measurement of high flow rate in line with the cursor all along the stream to be examined. Pulsed wave Doppler imaging is not suitable for high-speed flows, but reproduces the flow in a specific area to be examined. The operator can adjust the gain of the Doppler signal. The optimal image is one that shows well the shape of the wave flow (changes in speed over time). By convention, the blood flow movement toward the transducer is represented above the baseline. In contrast, the movement away from the transducer is represented below the baseline. The scale of reproduction of the Doppler signal (y-axis) can be adjusted to avoid cutting high-speed-flow waves. The speed, usually 50 mm/s (x-axis), can be adjusted to better fit the times for special measures. The alignment of the ultrasound beam with the flow remains paramount for both continuous wave and pulsed wave interrogation. An angle of more than 30° between the blood flow and the Doppler cursor is not considered acceptable for reliable Doppler measurements (Fig. 1.25). A previous look with color flow mapping helps to get the proper alignment. In the evaluation of valvular regurgitation flows, the cursor is placed through the narrowest part of the jet, as previously assessed by color flow mapping.

1.5.2.8 Regulating Color Doppler Imaging (Color Flow Mapping)

The assessment area is located by the operator usually using a "trackball" to reach the structures of interest. The default width, height, and gain signal of the color area can be increased or decreased by the operator. After an initial comprehensive assessment to study the various

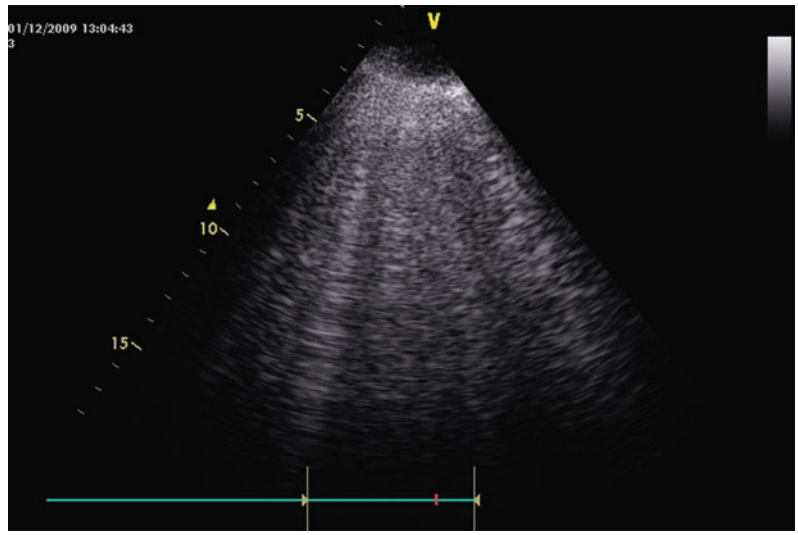

Fig. 1.26 Lung ultrasound: comet tails

streams, the field can be narrowed to obtain better definition of the single flow to be studied. Blanking out the 2D imaging sector either side of the color sector produces a better image of the flow. The gain of the color signal can also be increased in order to define small jets, even if the excess of gain alters the image by creating artifacts. A good rule is a gain that produces a minimum of speckling in areas outside the colored stream. Some assessment techniques of valvular regurgitation such as proximal isovelocity surface area are based on the phenomenon of aliasing and it is therefore necessary to adjust the base map of the color reproduction, represented in the display at the top right as a rectangle in two-tone red and blue scale graduation.

1.6 Artifacts

The shadow is an artifact produced as ultrasound reaches an object with high acoustic impedance. Attenuation of the acoustic beam occurs, and ultrasound will not be able to penetrate beyond the object any further. This linear hypoechoic or anechoic area covers deeper structures that cannot be visualized. Thus below the very echo-reflective object, such as a prosthetic valve or calcium deposit, little or nothing can be seen. This shadowing can be useful for the differential diagnosis between high-attenuation objects. In contrast, as ultrasound passes through an area of very low attenuation, it produces an acoustic enhancement and structures located beneath this area appear hyperechoic. Under other conditions ultrasound can produce solid hyperechoic rebound lines which start from the echo-reflective structure and run until the end at the bottom of the image. In the chest ultrasound assessment, these reverberation artifacts, called comet tails (B lines), originate from the pleura, producing vertical hyperechoic stripes, which are used to diagnose and quantify lung water (Fig. 1.26). An area of very high acoustic impedance may also produce an acoustic mirror, which deflects the ultrasound beam to the side. The false mirror image will be deeper than the correct anatomical reflector. Reflecting structures affected by lateral beams can also produce arcs, which appear as horizontal lines on the display. When in doubt if a structure visible in the image is an artifact, it is always useful to search for this structure using different planes since it is not likely that an artifact will be created in the same way by the ultrasound beam in different views.

Further Reading

Feigenbaum H, Armstrong WF, Ryan T (2005) Feigenbaum's echocardiography. Lippincott Williams & Wilkins, Philadelphia

Oh JK, Steward JB, Tajik AJ (2007) The echo manual, 3rd edn. Lippincott Williams & Wilkins, Philadelphia

Perrino AC (2008) A practical approach to transesophageal echocardiography, 2nd edn. Lippincott Williams & Wilkins, Philadelphia

Quiñones MA et al (2002) Recommendations for quantification of Doppler echocardiography: a report from the Doppler Quantification Task Force of the Nomenclature and Standards Committee of the American Society of Echocardiography. J Am Soc Echocardiogr 15:167–184

Savage RM (2004) Comprehensive textbook of intraoperative transesophageal echocardiography. Lippincott Williams & Wilkins, Philadelphia

Part II

Standard Echocardiographic Examination

Ultrasound Morphology of the Heart: Transthoracic Examination

2

Armando Sarti, Simone Cipani, and Costanza Innocenti

2.1 Ultrasound Morphology of the Heart: Standard Transthoracic Examination

2.1.1 Echocardiographic Anatomy

The heart is located within the chest between the lungs and in front of the esophagus. From the base toward the apex the heart is positioned:

- From top to bottom
- From back to front
- From right to left

Recalling the different structures on ultrasound images appears very complicated for the beginner operator if the various projections of the different structures are not kept in mind, according to the position of the heart within the chest under the section plane of the ultrasound scan. It should be noted that the echo image shows a thin slice of the structures crossed by the ultrasound beam. The structures first encountered by ultrasound, near the probe, are displayed at the top corner of the image and deeper structures are displayed proportionally lower on the screen, according to the progressive distance from the probe.

2.1.2 Patient Positioning

In the intensive care unit (ICU) it is not always possible to position the patient as desired. However, even small shifts can dramatically improve image acquisition. The patient should be kept with the trunk raised to 45° as is normally done in the ICU. The position on the left side or midway between the supine and the left lateral approach generally allows the heart to draw near to the chest wall, thus gaining the best acoustic windows. The patient's left arm must be raised and brought toward the head, so as to widen the left-sided intercostal spaces (Fig. 2.1) since the rib absorbs ultrasound. Aside from the ribs, aerated lung tissue is the major obstacle to the penetration of ultrasound. Therefore, patients with chronic pulmonary disease and emphysema are usually more difficult to study with transthoracic windows. Sometimes, for these patients the only approach that produces clear images is the subcostal approach. If the patient does not have acoustic windows on the chest wall and if the subcostal area is not accessible, often because of the presence of surgical wound dressings, it is essential to use transesophageal echocardiography. Nevertheless, the skilful operator, with a little patience, is almost always able to get acceptable and usable tansthoracic echocardiographic images for most patients even in the emergency and intensive care settings.

A. Sarti (✉)
Department of Anesthesia and Intensive Care,
Santa Maria Nuova Hospital, Florence, Italy
e-mail: armando.sarti@asf.toscana.it

A. Sarti and F. L. Lorini (eds.), *Echocardiography for Intensivists*,
DOI: 10.1007/978-88-470-2583-7_2, © Springer-Verlag Italia 2012

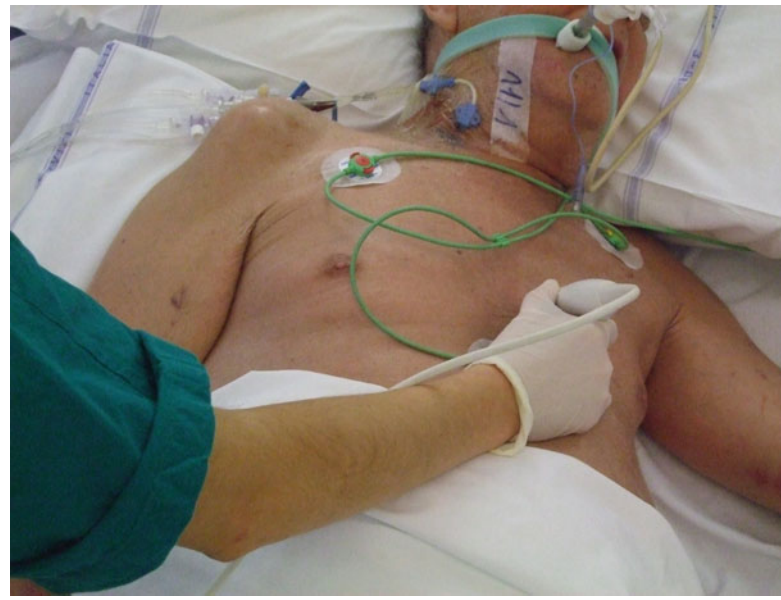

Fig. 2.1 Position of the operator and the patient for echocardiography in the intensive care unit. (From Sarti 2009 with permission)

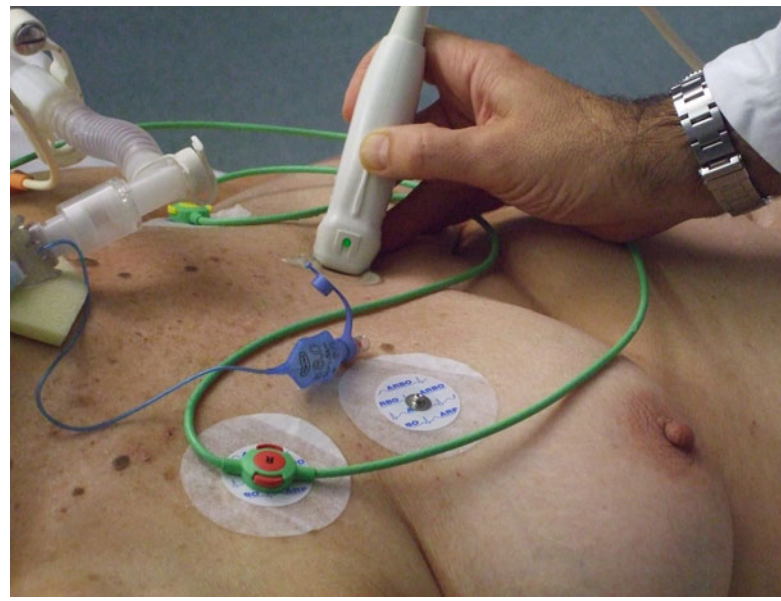

Fig. 2.2 Position of the probe for the parasternal long-axis view. Note the probe marker. (From Sarti 2009 with permission)

2.1.3 Positioning of the Probe (Acoustic Windows)

The probe, with a stream of acoustic gel at the end, is held not too tightly between the thumb and first two fingers of the gloved right hand, while maintaining contact with the chest wall with the other fingers, without causing pain or discomfort from excessive pressure, in two main locations:

1. *Left parasternal* at the second to fourth intercostal spaces (Fig. 2.2).
2. *Around the area of the apical beat,* at the fifth or sixth intecostal space along the anterior axillary line or more laterally (Fig. 2.3).

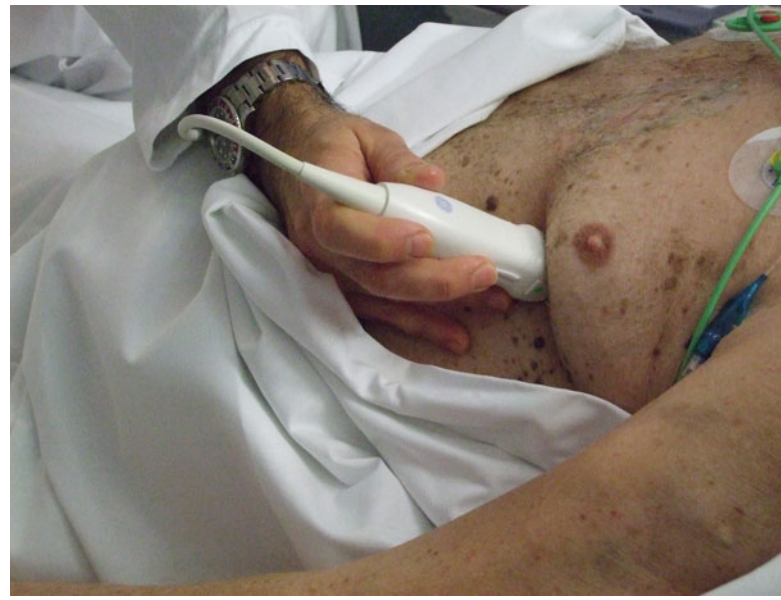

Fig. 2.3 Position of the probe for the apical four-chamber view. Note the probe marker. (From Sarti 2009 with permission)

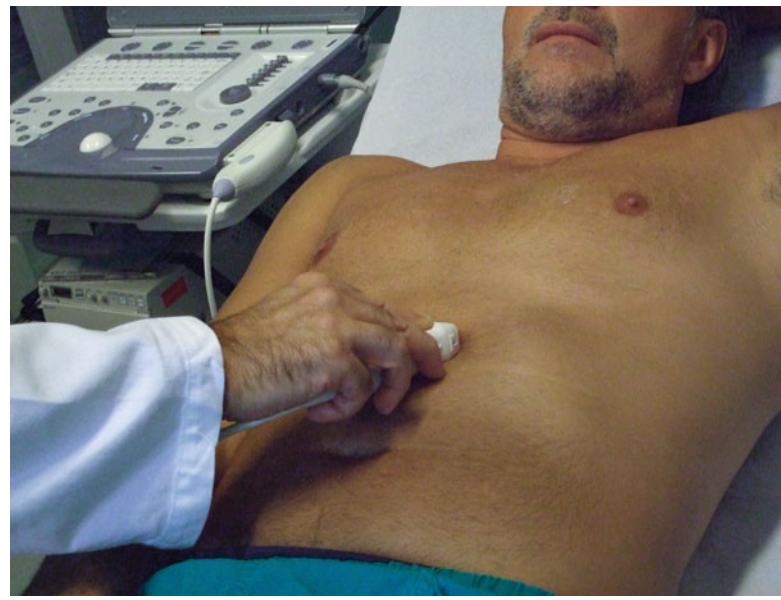

Fig. 2.4 Position of the probe for the subcostal views. (From Sarti 2009 with permission)

Another possible transthoracic location is parasternal right, which is used either in pediatrics or to assess the aortic valve (see Chap. 22).

The other basic positions of the probe, outside the chest wall, are:

- *Subcostal* central level, just below the xiphoid process (Fig. 2.4)
- *Suprasternal* level, at the jugular notch (Fig. 2.5)

2.1.4 Positioning of the Operator and the Ultrasound Machine

Most operators stay at the right side of the patient and keep the probe in the right hand. Others prefer to set themselves at the patient's left, holding the probe with the left hand, thus avoiding much contact with the patient's body. In any case, the

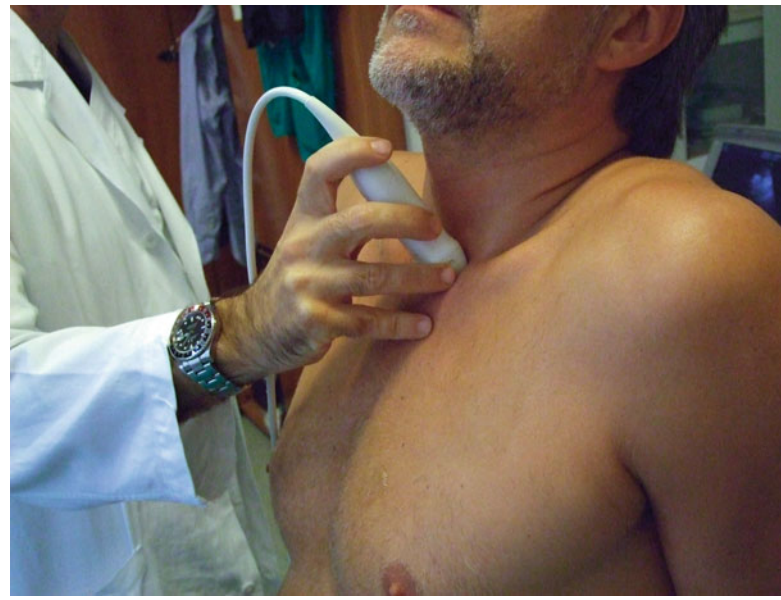

Fig. 2.5 Position of the probe for the suprasternal views. (From Sarti 2009 with permission)

position must be convenient, stable, and relaxed. Sitting is comfortable, but it is sometimes necessary to stand, lean, or even sit on the edge of the patient's bed; in this case a disposable gown should be worn. The ultrasound machine is usually placed to the right side of the patient's head, so that only small movements of the operator's head are needed to shift from the patient to the display and vice versa. In this arrangement the left hand is used to operate the controls. It is always useful to keep in mind the ultrasound section plane within the chest before looking at the images. The movement of the probe, as positioning, pointing, angling, or rotation (see Table 2.1), should be regulated while always considering what happens to the section plane inside the thorax.

2.1.5 Parasternal Long-Axis View

This is a longitudinal section of the heart (Fig. 2.6). The probe is in the left parasternal position and the marker is placed toward the right shoulder (Fig. 2.2). Initially, instead of insisting on a single point, different intercostal spaces should be tried, sliding from the second to the fourth, sometimes down to the fifth, to find the best acoustic window. The proper image is a section that shows part of the right ventricle, the septum, in a more or less horizontal position which continues toward the aortic upper wall. Below it the aortic valve and the left atrium are on the right side of the display. The left ventricle is found in the center (Figs. 2.6, 2.7). If more than one intercostal space allows one to obtain valid images, it is often preferable to use higher spaces. The parasternal long-axis view is usually the first image sought at the beginning of the examination since it highlights many structures and provides a first general idea of the heart. Positioning the cursor on the basis of the 2D image, one can obtain M-mode echograms, which are useful for measuring the size of the cardiac chambers and the thickness and the kinetics of the anterior septum (anterior descending artery) and the posterior wall (circumflex and right coronary arteries to the apex). The diameter of the left ventricular outflow tract is also measured during the systole just before the fully opened aortic cusps. The functional anatomy of aortic and mitral valves can be studied, including forward flow and any possible regurgitation, with color Doppler imaging (color flow mapping, CFM). Continuous wave and pulsed wave transvalvular flow measurements are not possible since the blood flows more or less perpendicular to the ultrasound beam. Except for

Table 2.1 Standard views, landmarks, rotation, and angling of the probe (structures and measures)

View	Probe position	Probe marker	Probe rotation	Probe angulation	Structures	Measurements
PSLAX	Parasternal 2nd to 4th intercostal space	Right shoulder	–	Variable	Left ventricle (except apex), LV septal and posterior walls, mitral and aortic valves, mitral subvalvular structures, LA, ascending aorta, RV outflow tract	LV and RV size and thickness, LV and RV kinetics, LV outflow tract and ascending aorta sizes, CFM of mitral and aortic flows
PSLAX modified for right ventricle (tricuspid plane)	Parasternal 2nd to 4th intercostal space	Right shoulder	Slightly clockwise	Inferomedial tilting from PSLAX	RV inflow, RA, tricuspid valve	CFM, PW and CW Doppler imaging of transtricuspid flow
PSLAX modified for right ventricle (pulmonary valve)	Parasternal 2nd to 4th intercostal space	Right shoulder	Slightly clockwise	Upward tilting from PSLAX-modified RV tricuspid plane	RV outflow, pulmonary valve	CFM, PW and CW imaging of transpulmonary flow, pulmonary VTI
PSSAX papillary muscle plane	Parasternal 2nd to 4th intercostal space	Left shoulder	90° clockwise from PSLAX	–	LV and RV sizes, LV walls, papillary muscles	LV and RV kinetics, FS, FAC
PSSAX mitral plane	Parasternal 2nd to 4th intercostal space	Left shoulder	90° clockwise from PSLAX	Upward tilting from PSSAX papillary muscles	Mitral valve, let ventricle, and LV sizes	Mitral valve (P1, P2, P3 and A1, A2, A3), mitral area, LV and RV kinetics
PSSAX aortic plane	Parasternal 2nd to 4th intercostal space	Left shoulder	90° clockwise from PSLAX	Upward tilting from PSSAX mitral plane	Aortic, tricuspid, and pulmonary valves, RV outflow, pulmonary trunk	Aortic valve (all cusps), aortic valve area, CFM and PW transpulmonary Doppler imaging

(continued)

Table 2.1 (continued)

View	Probe position	Probe marker	Probe rotation	Probe angulation	Structures	Measurements
A4C	Apical 4th to 6th intercostal space along the left mid-clavicular or anterior axillary line (apical beat)	Left leg	–	–	Global vision of the heart, left ventricle, right ventricle, LA, RA, LV septal and lateral walls, RV free wall, mitral and tricuspid valves	LV and RV kinetics, EF, TAPSE, CFM, PW and CW transvalvular mitral and tricuspid flows, pulmonary pressure assessment
A5C	Apical 4th to 6th intercostal space along the left mid-clavicular or anterior axillary line	Left leg	Variable	Upward tilting	Global vision of the heart plus aortic outflow valve and ascending aorta	CFM, CW and PW Doppler imaging of LV outflow, VTI
A2C	Apical 4th to 6th intercostal space along the left mid-clavicular or anterior axillary line	Right shoulder	90° counterclockwise from A4C	–	LV, LA, LV inferior and anterior walls, mitral valve	LV kinetics, EF, CFM, CW and PW Doppler imaging of transmitral flow
A3C	Apical 4th to 6th intercostal space along the left mid-clavicular or anterior axillary line	Right hand	45° counterclockwise from A2C	–	Left ventricle, LA, mitral valve, LV anteroseptal and posterior walls	LV kinetics, CFM, CW and PW Doppler imaging of transaortic flow, VTI
SC4C	Subcostal	Left shoulder	Variable	Variable	Global vision of the heart, left ventricle, right ventricle, LA, RA, LV septal and posterolateral walls, interatrial septum, liver, and intrahepatic veins	LV and RV kinetics, possible interatrial shunt
Subcostal abdominal aorta	Subcostal	Left shoulder	Variable	Downward from SC4C	Abdominal aorta	Aortic diameter
Subcostal RV and LV outflows	Subcostal	Left shoulder	Variable	Upward from SC4C	LV and RV outflow	CFM, CW and PW imaging of LV and RV outflows (if in line)

(continued)

Table 2.1 (continued)

View	Probe position	Probe marker	Probe rotation	Probe angulation	Structures	Measurements
Subcostal IVC	Subcostal, shifted a little to the left from SC4C	Left shoulder or head	Variable	Leftward tilting	IVC, RA	IVC diameter and respiratory variations
Subcostal short axis	Subcostal	Left shoulder	Variable	90° counterclockwise from SC4C	LV and RV short axis, LV and RV kinetics	–
Subcostal apical short axis	Subcostal	Left shoulder	Variable	Right tilting	LV apex	–
Subcostal basal short axis	Subcostal	Left shoulder	Variable	Left tilting	Basal LV and RV short axis	–
Suprasternal	Jugular notch	Left shoulder	Variable	Variable	Ascending aorta and aortic arch	Aortic diameter

PSLAX parasternal long axis, *RV* right ventricular, *PSSAX* parasternal short axis, *A4C* apical four chamber, *A5C* apical five chamber, *A2C* apical two chamber, *A3C* apical five chamber, *SC4C* subcostal four chamber, *IVC* inferior vena cava, *LV* left ventricular, *LA* left atrium, *RA* right atrium, *CFM* color flow mapping, *PW* pulsed wave, *CW* continuous wave, *VTI* velocity–time integral, *FS* fractional shortening, *FAC* fractional area change, *EF* ejection fraction, *TAPSE* tricuspid annular plane systolic excursion

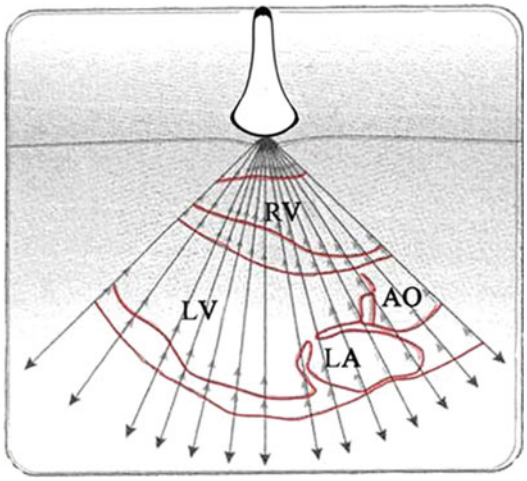

Fig. 2.6 Section plane and ultrasound beam for the parasternal long-axis view. *AO* aorta, *LA* left atrium, *LV* left ventricle, *RV* right ventricle, (From Sarti 2009 with permission)

the outflow part of the right ventricle, the right side of the heart is not generally visible. However, a broader view of the right atrium, the tricuspid valve, and the inflow tract of the right ventricle can be obtained by angling the probe down under the sternum and a fraction more medial, with a slight clockwise or, more rarely, counterclockwise rotation (Fig. 2.8), whereas an upward (cranial) angling and slight clockwise rotation from the basic parasternal long-axis view may show the right ventricular outflow tract with the pulmonary valve and the pulmonary trunk (Fig. 2.9).

2.1.6 Parasternal Short-Axis View

The probe remains in the same position as shown to obtain the parasternal long-axis view, but is rotated 90° clockwise with the marker now pointing to the left shoulder in order to obtain a cross section of the heart (Fig. 2.10). The image shows the left ventricle as a ring, more or less thick according to the thickness of the walls, with a section of the right ventricle that presents itself as a cap attached to the left ventricle by the septum, on the upper left of the display (Fig. 2.11). We must aim to produce a well-shaped circular section, avoiding oblong or oval images of the left ventricle. The assessment of the left ventricular kinetics is best performed in a plane that highlights the sections of the papillary muscles inside the ventricular cavity (Fig. 2.12). This section examines all the walls of the left ventricle, which thickens and moves toward the center in systole, with visibility of the myocardial tissue perfused by all three major coronary trunks. The upper part of the ring, starting at the eight o'clock to ten o'clock position to the two o'clock position, is attributable to the anterior descending artery. The tissue on the right side of the ventricular ring, from the two o'clock position to the six o'clock to seven o'clock position, coincides with the circumflex artery perfusion, and the bottom of the ring, shifted slightly to the left of the image, from the six o'clock to seven o'clock position to the eight o'clock to ten o'clock position, represents the myocardium perfused by the right coronary artery.

Downward (caudally) angling of the probe shows the base of the papillary muscles and then the apex of the left ventricle. An upward angulation (cranial) of the probe moves instead the section plane to cross the mitral valve, which is cut through the opening and closing motion (Fig. 2.11). A further upward angulation (Fig. 2.13) shows a central section of the aortic outflow with the valve (the aortic box, shaped as a "Mercedes star") and its three moving cusps. On the left, the tricuspid valve and the right outflow can be seen, with the pulmonary valve and the pulmonary trunk at the top of the image, above the aortic valve.

Sweeping with the probe, from an upward left side angle progressively down toward the right side shows the various sections in succession with the structures from the base toward the apex of the heart.

2.1.7 Right Parasternal View

The probe is placed on the right side of the sternum, at the third intercostal space or one intercostal space above or below. This view is used to get a better image of the aortic valve and to measure transaortic blood flow in line with the ultrasound beam. To bring the aorta forward near the anterior thoracic wall, the patient is rolled on to the right side. The 2D image shows the aortic valve and the ascending aorta. CFM can be used as a guide to place the cursor along the transaortic flow for continuous

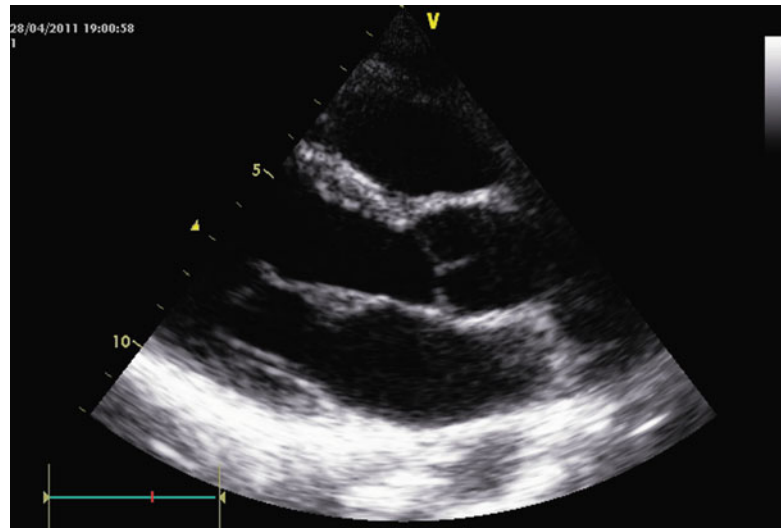

Fig. 2.7 Parasternal long-axis view

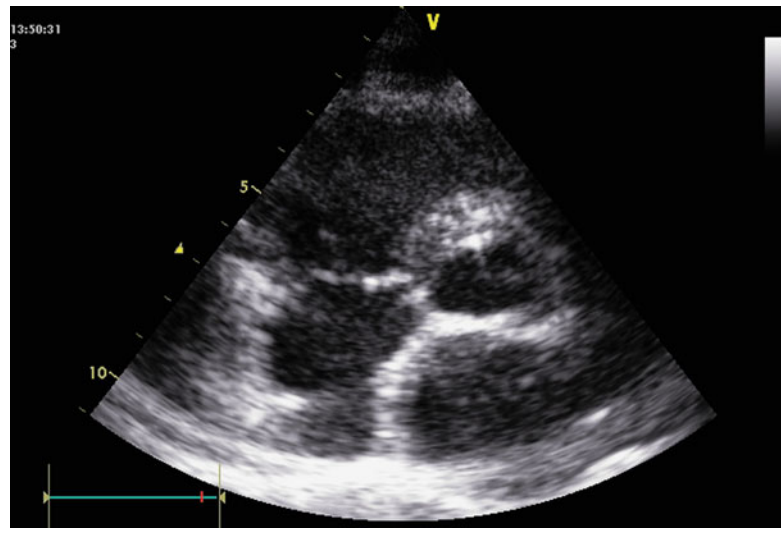

Fig. 2.8 Parasternal long-axis view modified for the right ventricular inflow tract

wave Doppler interrogation. In pediatric practice, a high right parasternal view with the marker pointing at the left leg enables examination of the right atrium, superior vena cava, and left atrium. The right pulmonary artery and upper right pulmonary vein may also be visible.

2.1.8 Apical Four-Chamber View

The probe is placed in the area of the apical cardiac beat with the marker pointing toward the left hand (raised to the head) of the patient (Fig. 2.14). The probe is slid up and down and to the side in the search for an image that dissects the heart into its four chambers with the interventricular septum in the middle, the apex at the top, the left ventricle, with its normal rugby-ball shape, on the right side, and the right ventricle, with its triangular shape, on the left of the display (Fig. 2.15). This image shows the left ventricular septal and lateral walls. Toward the bottom of the image the atrial septum can be seen, with the two atrioventricular valves

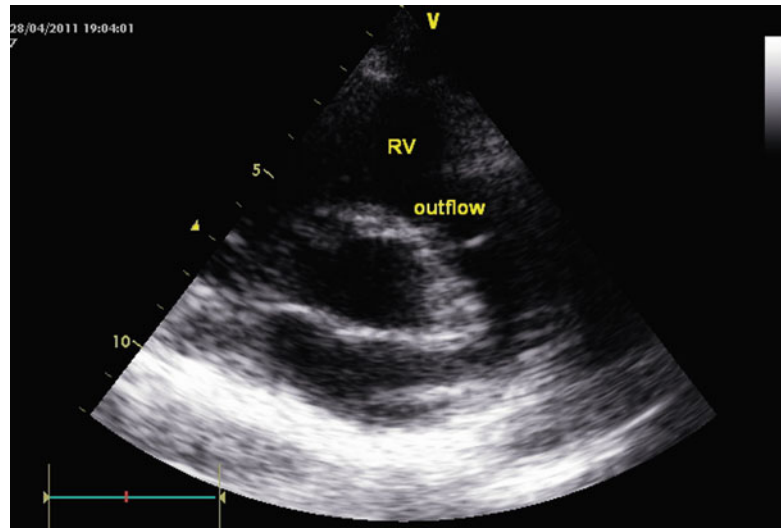

Fig. 2.9 Parasternal long-axis view modified for the right ventricular outflow tract and the right pulmonary artery. *RV* right ventricle

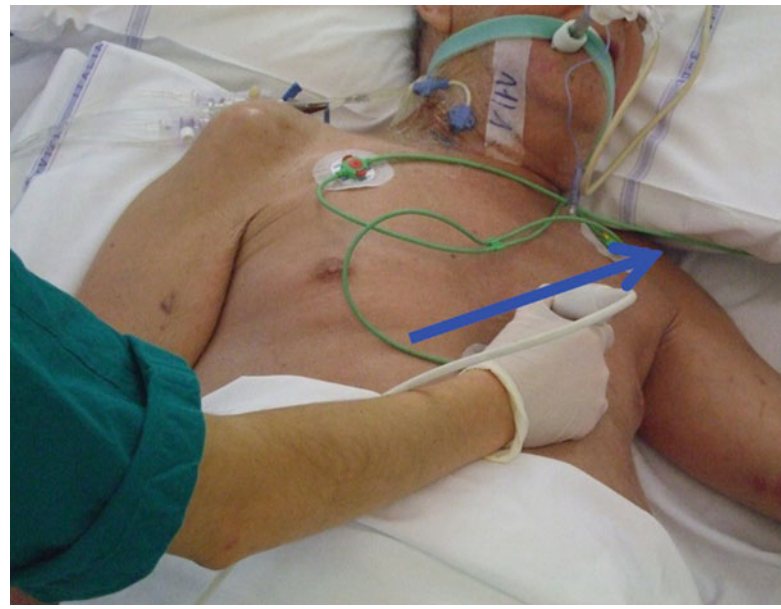

Fig. 2.10 Probe position for the parasternal short-axis view and the section line of the marker. (Modified from Sarti 2009 with permission)

horizontal, the mitral valve on the right and the tricuspid valve on the left. The atrial chambers, the left chamber on the right and right chamber on the left, take up the bottom of the image. The bottom right of the image often reveals one or two pulmonary veins draining into the left atrium.

Small movements and small changes of angles are made to try and obtain the maximum possible length of the left ventricle and evidence of both endocardial and epicardial edges of the apex. The apex thickens in systole, but does not move toward the base of the heart. If the image shows that the apex actually moves

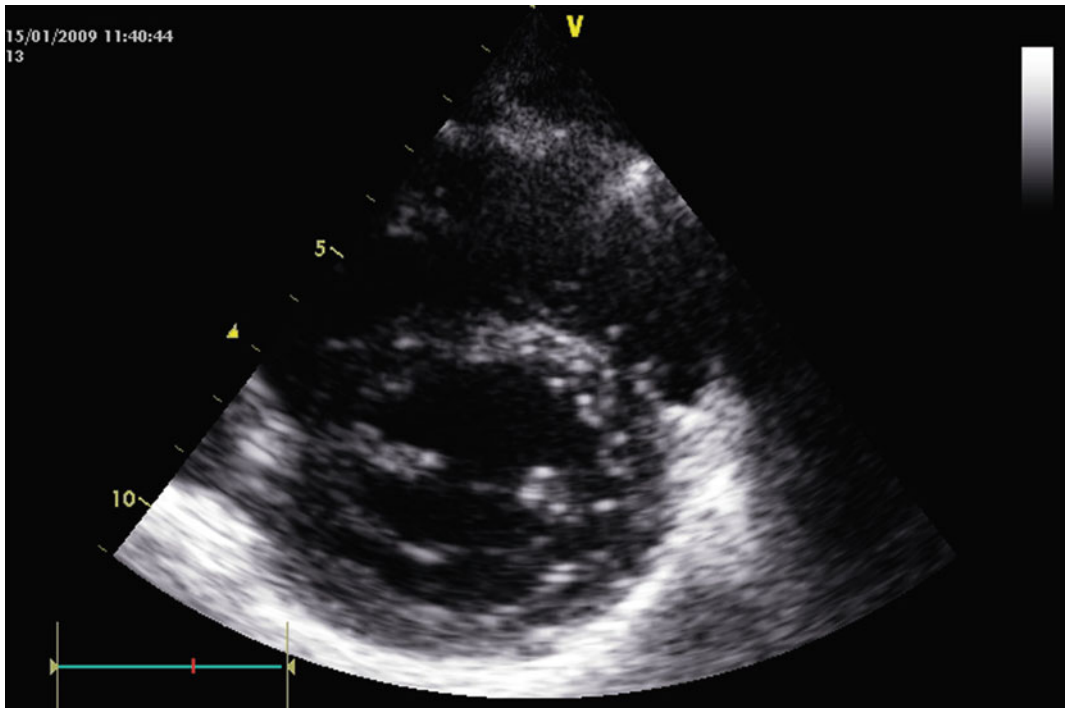

Fig. 2.11 Parasternal short-axis view at the level of the mitral valve (diastole)

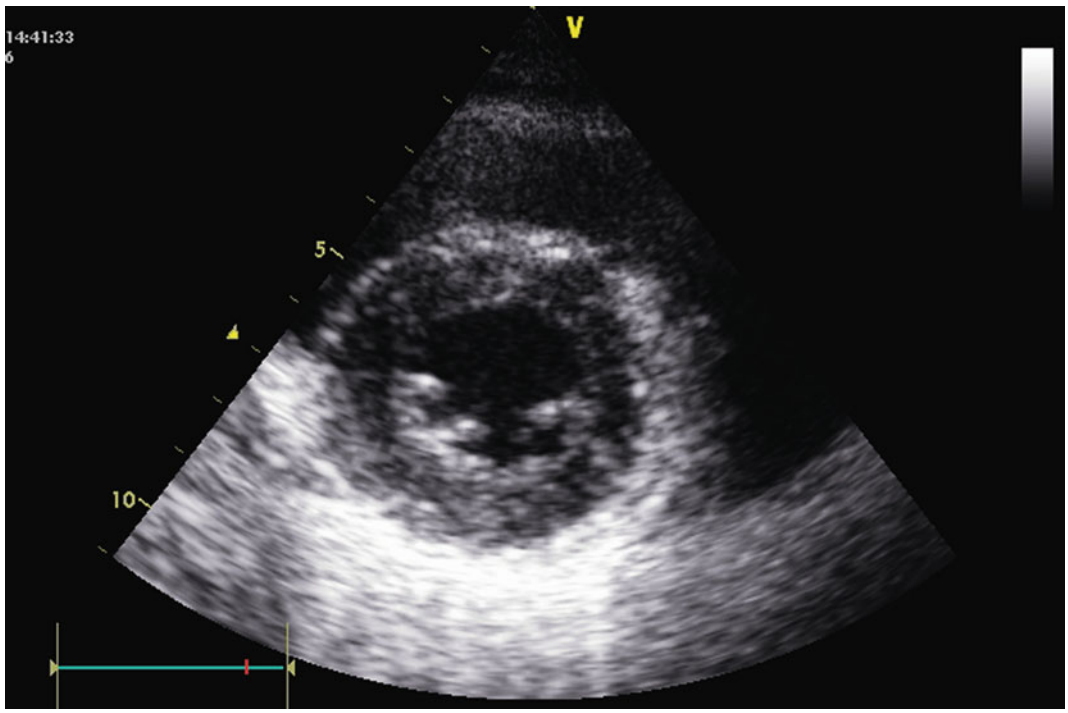

Fig. 2.12 Parasternal short-axis view at the level of the papillary muscles

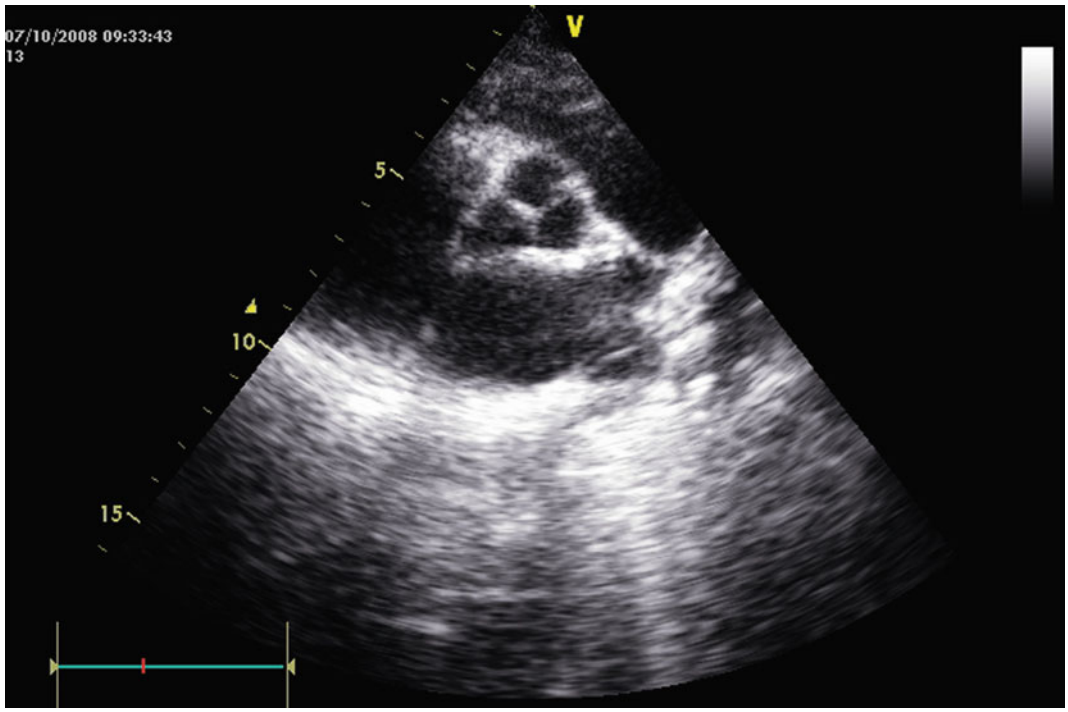

Fig. 2.13 Parasternal short-axis view at the level of the aortic valve ("Mercedes sign" in diastole) and right ventricle

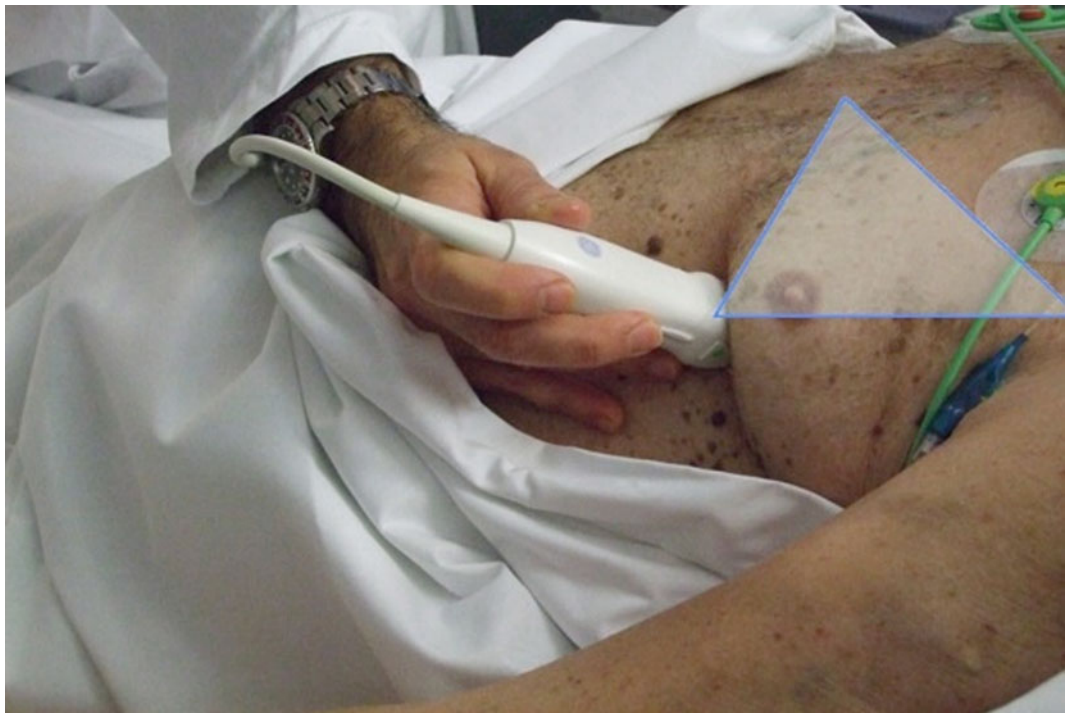

Fig. 2.14 Probe position for the apical four-chamber view and the section plane. (Modified from Sarti 2009 with permission)

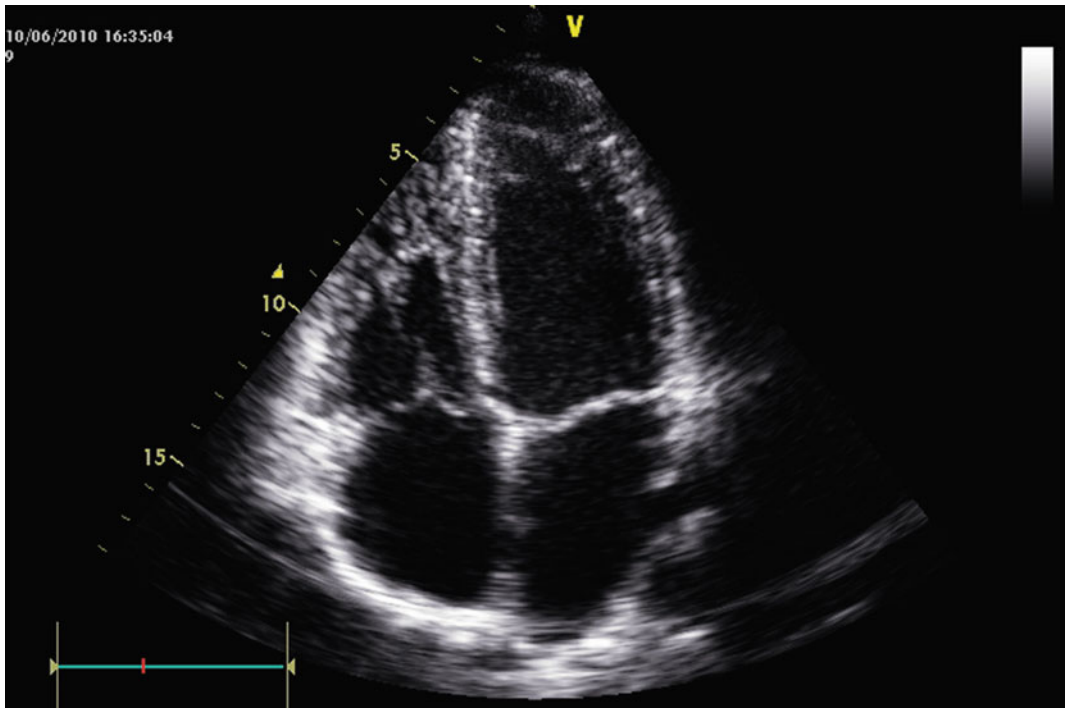

Fig. 2.15 Apical four-chamber view

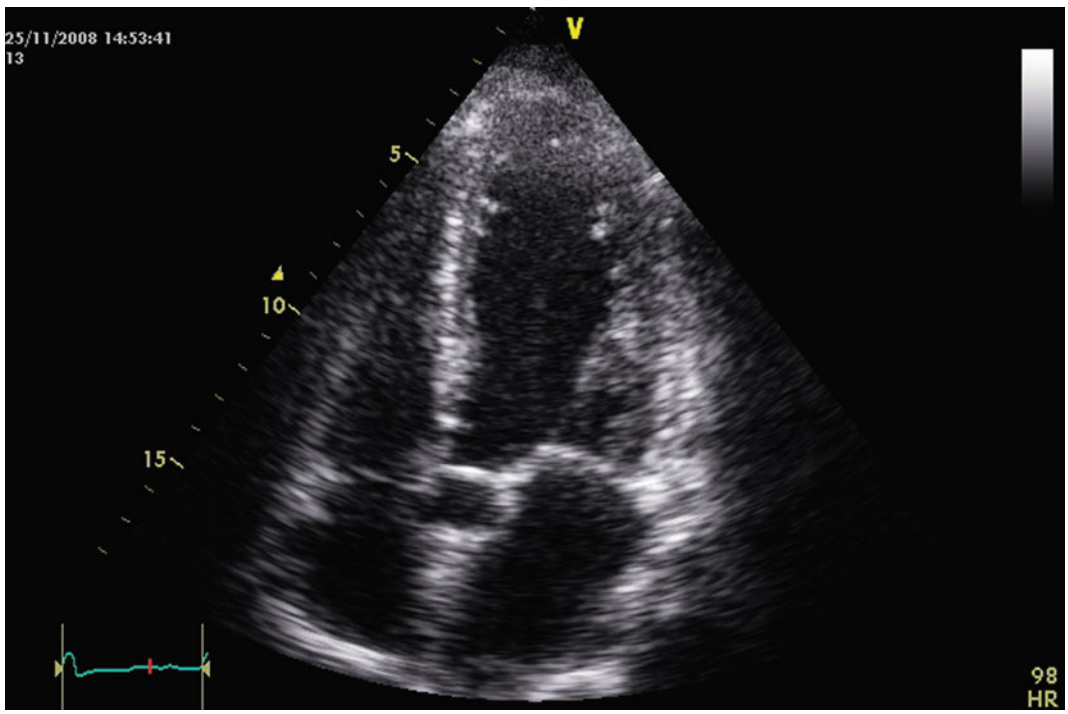

Fig. 2.16 Apical five-chamber view. (From Sarti 2009 with permission)

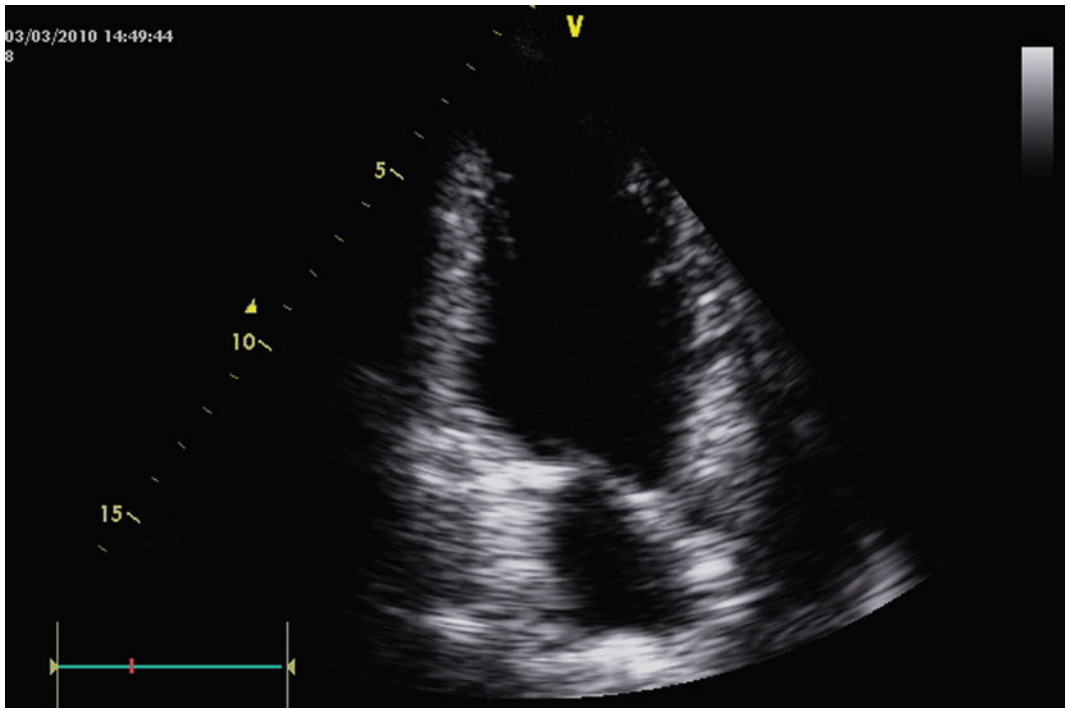

Fig. 2.17 Apical two-chamber view

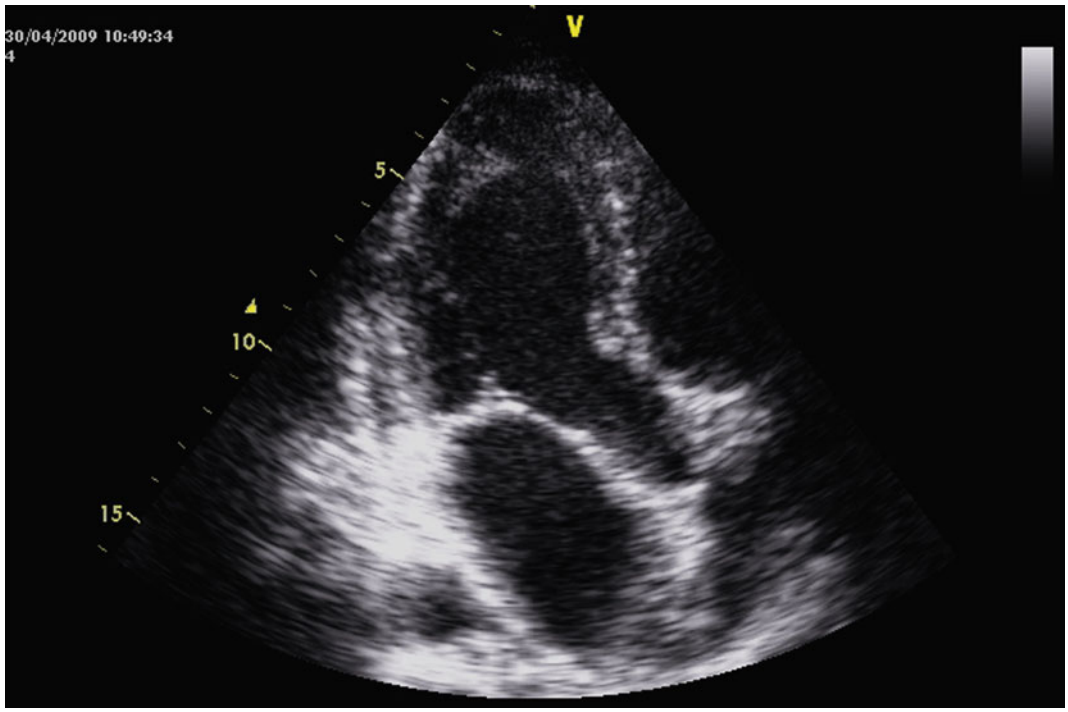

Fig. 2.18 Apical three-chamber view

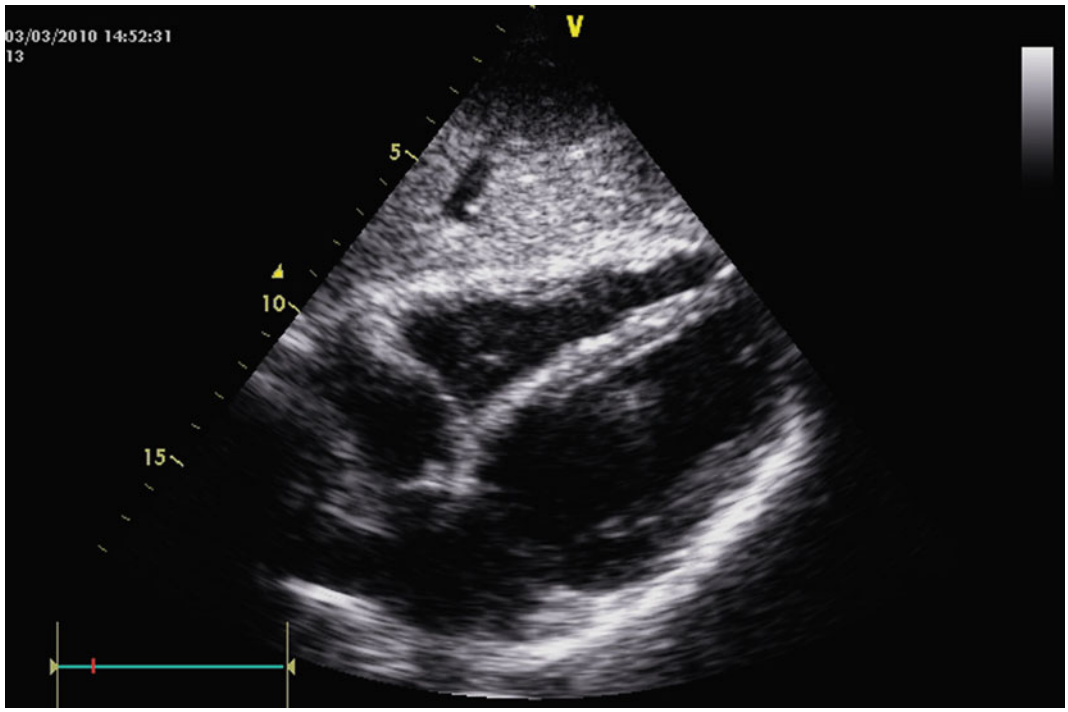

Fig. 2.19 Subcostal four-chamber view

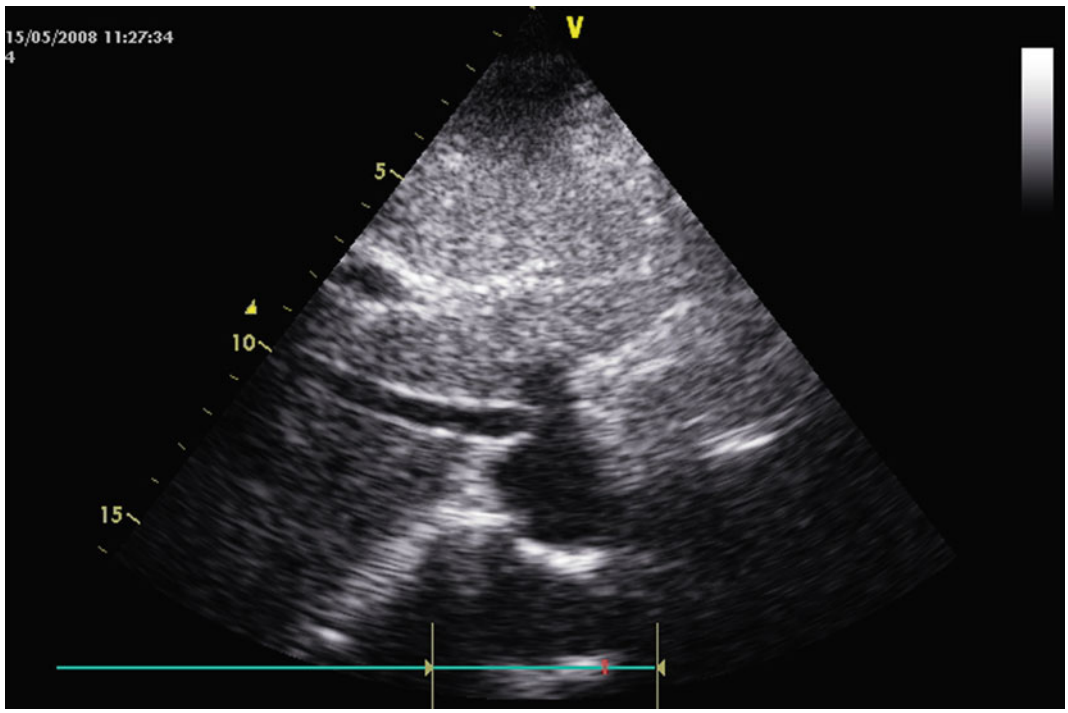

Fig. 2.20 Subcostal view modified for the inferior vena cava

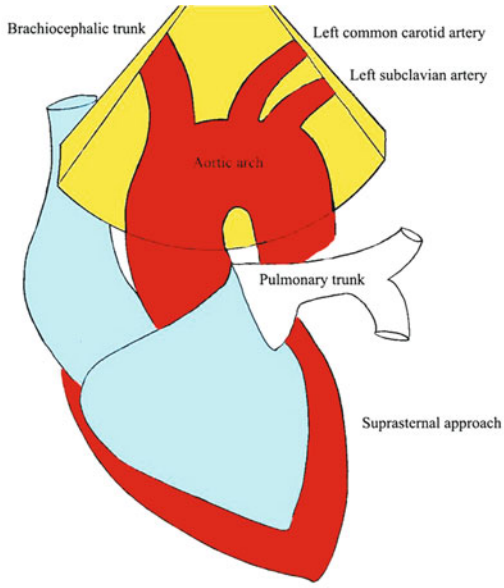

Fig. 2.21 Suprasternal view. (From Sarti 2009 with permission)

toward the atrioventricular valves, the section plane is not correct.

This view is used for various measurements, including ejection fraction, septal kinetics (right coronary artery for a short distance baseline and anterior descending artery up to the apex) and lateral wall kinetics (circumflex artery) of the left ventricle, kinetics and measurements of the right ventricle, and the morphological and Doppler study of the valves and transvalvular flows.

2.1.8.1 Apical Five-Chamber View

From the position for the apical four-chamber view, the probe is angled up slightly and sometimes rotated a little to highlight the left ventricular outflow tract (fifth chamber) with the aortic valve. This apical five-chamber view (Fig. 2.16) is used to evaluate the aortic outflow chamber and the flow toward the aorta or an aortic regurgitation because of good alignment of the ultrasound beam and thus reliable Doppler measurements.

2.1.8.2 Apical Two-Chamber View

From the position for the apical four-chamber view, the probe is rotated about 90° counterclockwise, resulting in a section plane perpendicular to the four-chamber view. Sections of the right side of the heart disappear and only the left side of the heart is now visible. The left atrium is at the bottom of the image and the left ventricle is at the top, with the mitral valve in between the two (Fig. 2.17).

The inferior wall of the left ventricle (right coronary artery from the base to the top of the apex) is on the left side of the image, and the anterior wall is on the right side (anterior descending artery).

For the biplane method, the left ventricular measurement of the ejection fraction, already done in the apical four-chamber view, is repeated in the apical two-chamber view. The mitral valve is examined in the apical two-chamber view with another plane and at a different level in relation to the apical four-chamber view.

2.1.8.3 Apical Three-Chamber View

Further rotation of the probe, approximately 45° counterclockwise from the position for the apical two-chamber view, still shows the left ventricle and left atrium (Fig. 2.18). Furthermore, on the right of the display, the left ventricular outflow tract can be seen (third chamber). This section is similar to the parasternal long-axis view but is oriented with the apex at the top and the base of the heart at the bottom. However, in contrast to the apical three-chamber view, the parasternal long-axis view does not normally show the apex. The anteroseptal wall of the left ventricle is on the right, and the posterior wall is on the left.

2.1.9 Subcostal View

This fundamental projection must never be omitted, particularly in emergency and intensive care practice. In patients on mechanical ventilation or with emphysema and in cases where the patient cannot be moved to the side, the subcostal approach may be the only approach which allows assessable images to be obtained. The patient lies in the supine position with the trunk raised to 45°, the knees bent, and the hips flexed slightly to relax the abdominal wall. The probe, held flat with the thumb and forefinger of the right hand, is placed under the xiphoid process (Fig. 2.4), with the marker toward the left

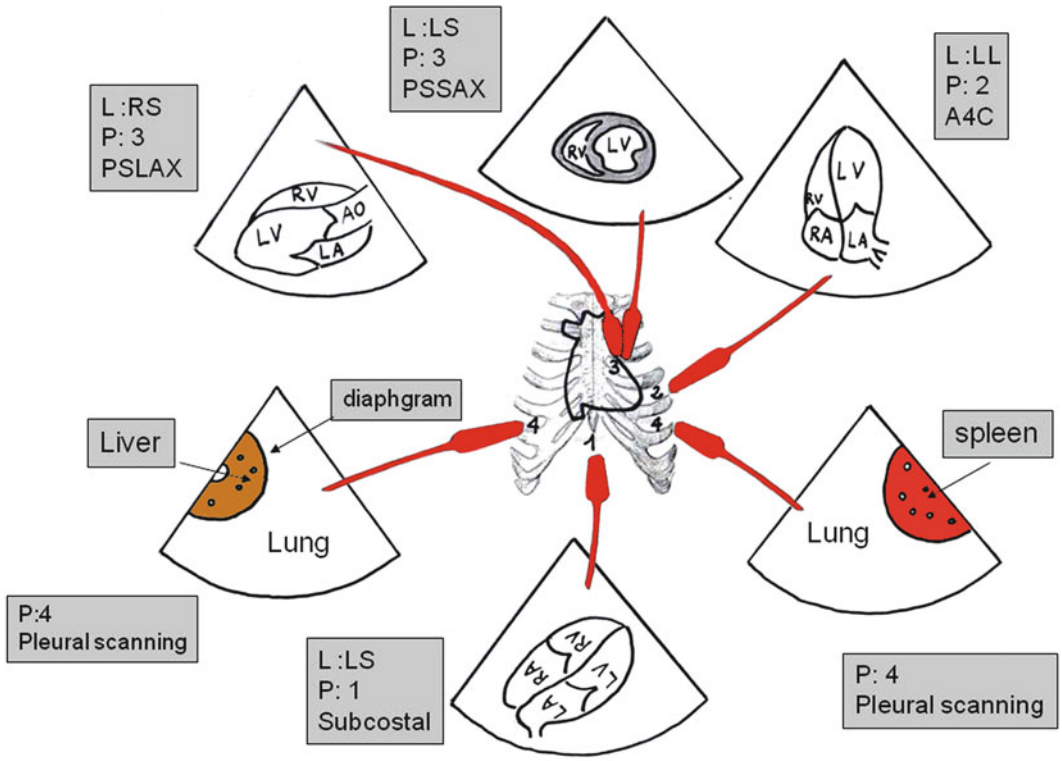

Fig. 2.22 Outline of the probe positions and main views. *L* probe landmark, *P* probe position, *RS* right shoulder, *LS* left shoulder, *LL* left leg, *PSLAX* parasternal long axis, *PSSAX* parasternal short axis, A4C apical four chamber

shoulder and a variable angle, moving slightly left or right of the midline, in the search for a subcostal four-chamber view (Fig. 2.19). The liver, with its characteristic echo structure, is the essential reference. The right side of the heart is placed at the top of the image, and the left side is placed at the bottom. The observable walls of the left ventricle are the septal and posterolateral walls. The interatrial septum is seen here in its full length with good definition of the thin foramen ovale. Any possible shunt through the open foramen ovale can be studied with this approach with CFM and pulsed wave imaging. A right-to-left shunt can also be demonstrated with the microbubble contrast produced by the quick injection of agitated saline into a vein and flowing from the right atrium to the left atrium.

A greater upward angulation of the probe shows the outflow of the left ventricle and the structures of the right side of the heart with the inflow and outflow of the right ventricle and valves. In contrast, angling the probe downward toward the abdomen may show the abdominal aorta. A shift of the probe to the left, toward the right side of the patient, brings out the inferior cava vein and hepatic veins, which enter horizontally into the right atrium (Fig. 2.20). The size of the inferior cava vein and the respiratory changes of its caliber provide information on the venous filling and blood volume of the patient. In this view, the intrahepatic veins run vertically down to reach the inferior vena cava in line with the ultrasound beam. Thus, pulsed wave Doppler echocardiography can be used to show venous intrahepatic blood flow.

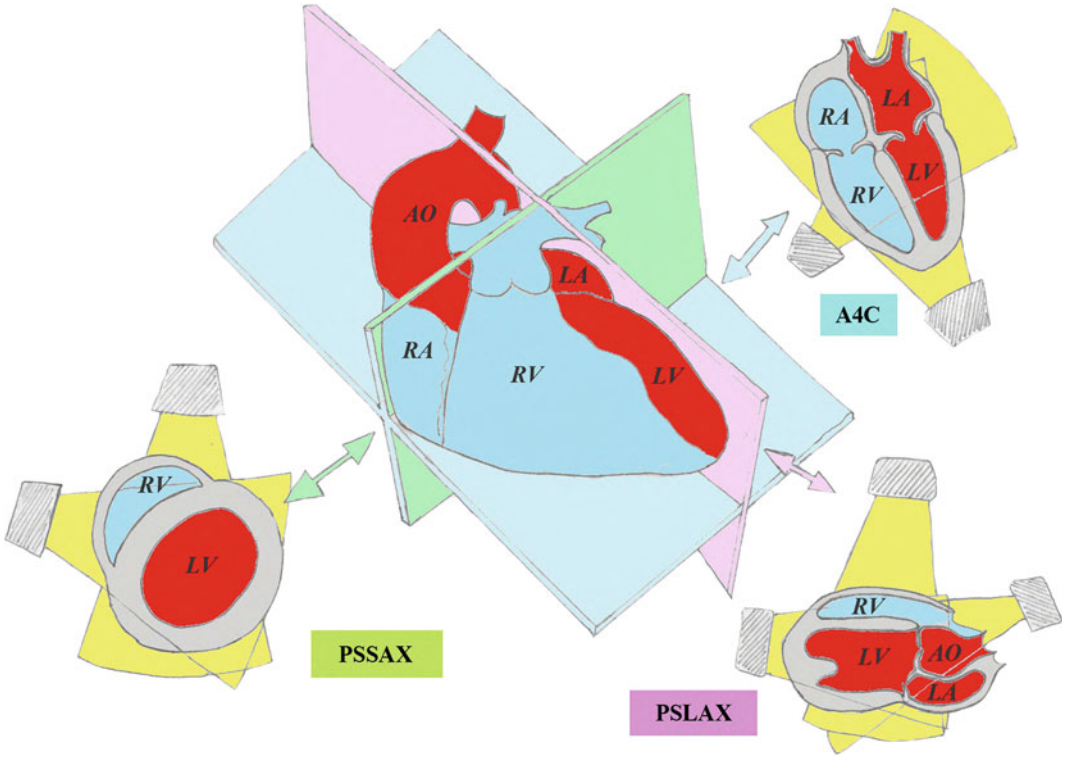

Fig. 2.23 Outline of the echocardiographic section planes and views. *A4C* apical four chamber, *AO* aorta, *LA* left atrium, *LV* left ventricle, *PSLAX* parasternal long axis, *PSSAX* parasternal short axis, *RA* right atrium, *RV* right ventricle. (Modified from [1] with permission)

A rotation of 90° counterclockwise starting from the baseline subcostal four-chamber view produces subcostal cross sections of the heart, similar to those obtained with the parasternal short-axis view. An inclination to the right gives sections toward the apex of the heart, whereas an inclination to the left explores sections of the base.

2.1.10 Suprasternal View

To obtain suprasternal images the patient is raised to at least 45°, with the head extended on the neck. In certain circumstances this approach is not easily done in the ICU or is clearly contraindicated (neck trauma). The probe is placed on the supraclavicular area just above the sternal manubrium, directed toward the chest with the marker pointing at the left shoulder (Fig. 2.5). A little movement or angulation is used to find part of the aortic arch and descending aorta (Fig. 2.21). Manipulating the probe to the right can show the ascending aorta. CFM is then used to define the aorta and its branches. A slight rotation of the probe may show the left atrium and pulmonary veins. The right branch of the pulmonary artery often appears below the aortic arch. This view is not always used. It may allow evaluation of the aorta in thoracic trauma or suspicion of dissection, but transesophageal echocardiography is far more effective for this purpose.

2.1.11 Overview

Figure 2.22 shows a summary diagram of the various probe positions with corresponding images. Fig. 2.23 outlines the main transthoracic views according to the section planes. Table 2.1 describes the movement of the probe, as position, pointing, angling, and

rotation, the structures to be seen, and the main measurements to be done.

The first echo examination of an ICU patient should include most of these views in regular sequence. Even if not all views are obtainable, a routine sequence must be tried all the same to avoid missing important unexpected information. All the structures should be identified to discriminate between normal and any deviation from normal using each usable echo modality, including M-mode echocardiography, Doppler echocardiography, and tissue Doppler imaging. Afterward, at the end of the first examination or during another assessment, the examiner focuses on particular views for specific purposes or monitoring.

Reference

1. Sarti A (2009) Ecocardiografia per l'intensivista. Springer, Milan

Further Reading

Feigenbaum H, Armstrong WF, Ryan T (2005) Feigenbaum's echocardiography. Lippincott Williams & Wilkins, Philadelphia

Oh JK, Steward JB, Tajik AJ (2007) The Echo manual, 3rd edn. Lippincott Williams & Wilkins, Philadelphia

3 Transthoracic Echocardiography in the ICU: The Patient Who Is Difficult To Study

Piercarlo Ballo

3.1 Introduction

Prompt and accurate diagnostic assessment of patients is crucial in the ICU. Transthoracic echocardiography (TTE) is of major clinical value in this setting, owing to its widespread availability and rapid diagnostic capability. However, it is well known that critically ill patients are often relatively difficulty to study by echocardiography because of unsatisfactory acoustic windows. Both factors related to the patient's condition (e.g., supine decubitus, chest wall interference) and instrumentation (e.g., artifacts due to mechanical ventilation) contribute to this technical difficulty. Early studies reported a failure rate of more than 30 % for the transthoracic approach in the ICU setting, with higher values among patients with significant body weight gain after admission, those supported by relatively high positive end-expiratory pressure, and those with chest tubes.

Thanks to dramatic technical improvements in recent years, including harmonics, contrast, and digital technologies, the failure rate has been considerably reduced. In 2004, an evaluation of 100 consecutive requests by critical care physicians for urgent echocardiograms to identify the cause of shock in ICU patients found that TTE was feasible in 99 % of cases. More recently, studies have confirmed that adequate imaging in the ICU can be obtained in the large majority of patients, even using portable echocardiographs, provided that care is taken to optimize technical settings on the echocardiograph and to minimize disturbing factors. However, when TTE does not provide adequate diagnostic information, the use of transesophageal echocardiography (TEE) is indicated. TEE can provide adequate and conclusive images in the large majority of patients, and in some conditions is currently recommended as the first-line approach (Table 3.1). However, efforts to optimize images and to achieve adequate TTE examinations should always be made to avoid inappropriate requests for TEE. These efforts should be considered mandatory particularly for patients for whom immediate availability of echocardiographic information is of major clinical importance.

On the basis of these considerations, the practical approach to the patient who is difficult to study should include the following steps: (1) minimizing patient-related disturbing factors; (2) optimizing machine settings; (3) approaching the patient using multiple and alternative views; and (4) utilizing echocardiographic indexes that are less dependent on image quality.

3.2 Minimizing Patient-Related Disturbing Factors

Patients in the ICU typically lie in the supine position. This position moves the heart behind the sternum and away from the chest anterior wall,

P. Ballo (✉)
Cardiology Unit, Santa Maria Annunziata Hospital, Florence, Italy
e-mail: pcballo@tin.it

A. Sarti and F. L. Lorini (eds.), *Echocardiography for Intensivists*,
DOI: 10.1007/978-88-470-2583-7_3,

Table 3.1 Appropriate indications for transesophageal echocardiography (*TEE*)

TEE as initial or supplemental test—general uses	
– Use of TEE when there is a high likelihood of a nondiagnostic TTE examination because of patient characteristics or inadequate visualization of relevant structures	A(8)
– Routine use of TEE when a diagnostic TTE examination is reasonably anticipated to resolve all diagnostic and management concerns	I(1)
– Reevaluation of prior TEE findings for interval change (e.g., resolution of thrombus after anticoagulation, resolution of vegetation after antibiotic therapy) when a change in therapy is anticipated	A(8)
– Surveillance of prior TEE findings for interval change (e.g., resolution of thrombus after anticoagulation, resolution of vegetation after antibiotic therapy) when no change in therapy is anticipated	I(2)
– Guidance during percutaneous noncoronary cardiac interventions including but not limited to closure device placement, radiofrequency ablation, and percutaneous valve procedures	A(9)
– Suspected acute aortic disease including but not limited to dissection/transection	A(9)
– Routine assessment of pulmonary veins in an asymptomatic patient status after pulmonary vein isolation	I(3)
TEE as initial or supplemental test—valvular disease	
– Evaluation of valvular structure and function to assess suitability for, and assist in planning of, an intervention	A(9)
– To diagnose infective endocarditis with a low pretest probability (e.g., transient fever, known alternative source of infection, or negative blood cultures/atypical pathogen for endocarditis)	I(3)
– To diagnose infective endocarditis with a moderate or high pretest probability (e.g., staphylococcal bacteremia, fungemia, prosthetic heart valve, or intracardiac device)	A(9)
TEE as initial or supplemental test—embolic event	
– Evaluation for a cardiovascular source of embolus with no identified noncardiac source	A(7)
– Evaluation for a cardiovascular source of embolus with a previously identified noncardiac source	U(5)
– Evaluation for a cardiovascular source of embolus with a known cardiac source in which a TEE examination would not change the management	I(1)
TEE as an initial test—atrial fibrillation/flutter	
– Evaluation to facilitate clinical decision making with regard to anticoagulation, cardioversion, and/or radiofrequency ablation	A(9)
– Evaluation when a decision has been made to anticoagulate the patient and not to perform cardioversion	I(2)

thus increasing the distance from the probe and favoring tissue artifacts. Most beds in the ICU can be adjusted to obtain a partial left lateral inclination. This inclination leads to relative leftward and anterior shifting of the heart, reduces the number of artifacts related to the sternum interposition, and decreases the distance from the probe, often yielding an improvement in echocardiographic image quality. Mechanical ventilation systems and chest tubes often lead to considerable numbers of image artifacts. When clinically possible in relation to the safety of the patient, transient interruption or reduction of mechanical respiratory assistance (e.g., by decreasing the positive end-expiratory pressure) eliminates or reduces the number of these artifacts, improving image quality. In some cases, image artifacts can also be produced by electrical interference with monitors or other electrical devices that are placed near the patient. Again, when clinically possible, turning off these devices in a safe manner (e.g., by using the monitor of the echocardiograph during the examination after turning off an external monitor that produces artifacts) may further improve image quality.

3.3 Optimizing Machine Settings

Sonographers working in clinics with ICUs should be trained in optimizing machine settings, in order to be able to obtain the best possible

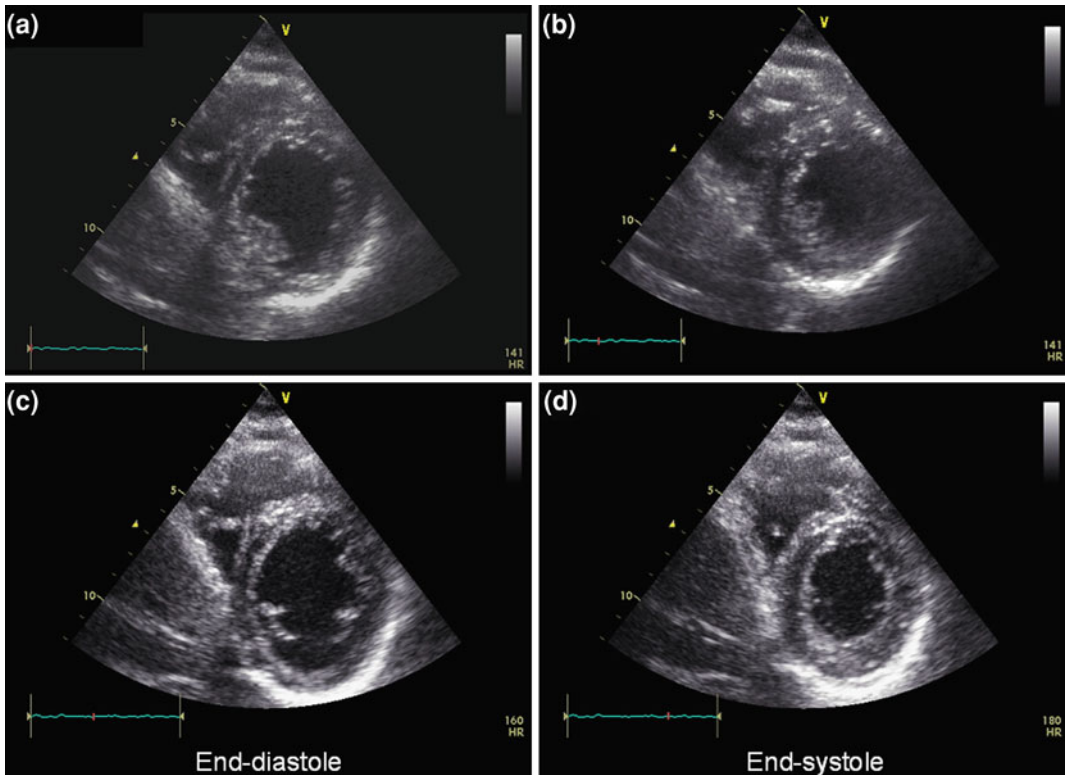

Fig. 3.1 Example of image optimization in a parasternal short-axis view at the mid-ventricular level. Before optimization (**a**, **b**), detection of endocardial borders was problematic in the end-systolic frame. A subsequent acquisition after optimization of the settings (**c**, **d**) resulted in improvement in overall image quality and adequate detection of endocardial borders at end-systole. Optimization was achieved by choosing a different two-dimensional map and adjusting the gain, compression, and rejection controls

echocardiographic images of the patient's heart. A number of parameters can be changed and modulated to achieve this. The *probe frequency* should be chosen by remembering the inverse relation between resolution and penetration. High frequencies correspond to small beam amplitudes, which allow higher axial and lateral resolution, but their penetration capability is reduced and they are less suitable for deeper structures. Conversely, low frequencies correspond to high beam amplitudes, which yield worse resolution, but have higher penetration capability, which allows adequate exploration of deeper structures. Most echocardiographs have preset controls allowing rapid selection of a configuration that enhances a particular characteristic, e.g., penetration or resolution. The correct *focus distance* should also be chosen. Adjusting the focus of the beam leads to narrowing of the ultrasound beam at the desired depth, allowing optimization of spatial resolution and improving visualization of the focused structures.

When an adequate probe frequency and focus are used, care should be taken to optimize signal processing. This can be done by adjusting a number of controls, including the pulse repetition frequency, frame rate, system gain, time gain compensation, lateral gain compensation, compression, smoothing, and postprocessing settings (which act on the image display). Among these, the *pulse repetition frequency* corresponds to the triggering frequency and determines the number of scan lines per unit time. Increasing this number enhances motion display. An increase in pulse repetition frequency can also be obtained by narrowing the

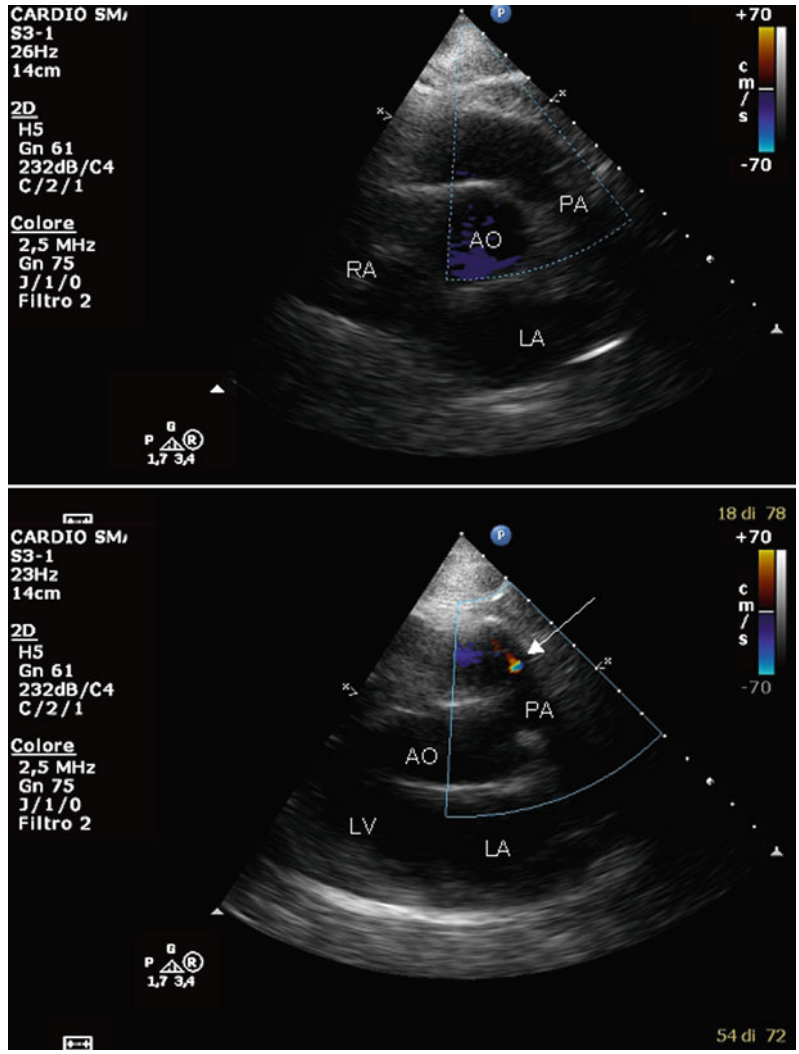

Fig. 3.2 Example of an alternative view for imaging the pulmonary valve. With the standard short-axis view at the level of the great vessels (*top*), no pulmonary regurgitation was recorded. Using an alternative view obtained starting from the parasternal long axis of the left ventricle and inclining the probe to move the ultrasonic beam toward the patient's left side, a pulmonary regurgitant flow appeared (*arrow*). This view explores the pulmonary valve and the pulmonary artery on a tomographic plane that is approximately perpendicular to that used in the classic short-axis view, so it can be used to detect eccentric regurgitant flow not seen in the standard view. Accurate detection of pulmonary regurgitation may be of clinical importance for the estimation of pulmonary artery mean and diastolic pressure. *AO* aorta, *LA* left atrium, *LV* left ventricle, *PA* pulmonary artery, *RA* right atrium

sector depth. The *frame rate* corresponds to the scanning frequency of the whole sector. Increasing the frame rate leads to better temporal resolution. The frame rate is inversely related to both sector depth and sector width. Thus, a reduction in sector depth or sector width increases the frame rate and temporal resolution.

In clinical practice, in the patient who is difficult to study, after identification of the most appropriate probe frequency, the focus should be positioned at the level of the structure to be explored to increase the spatial resolution, and both sector depth and sector width should be reduced to increase temporal resolution. Gain

controls, compression, smoothing, and postprocessing settings should then be manually adjusted to further improve image quality. Figure 3.1 shows an example of echocardiographic images before and after accurate optimization of settings. Some high-level echocardiographs have a command that activates automatic detection of the best overall control configuration to optimize image quality. However, the choice of the most suitable setting still remains dependent on the experience and the preferences of the sonographer.

3.4 Approaching the Patient Using Multiple and Alternative Views

After elimination of patient-related disturbing factors and optimization of machine settings, the third step is to approach the patient using both standard and alternative views. The use of off-axis views may facilitate visualization of heart structures not easily visualized with conventional windows. Most of these views are commonly used even in standard examinations, so the term "off-axis" may also be inappropriate for most of them. For example, a long axis of the right ventricle can be well visualized starting from a parasternal long axis of the left ventricle and inclining the probe so that the direction of the ultrasonic beam moves toward the patient's right side. This view may be of particular utility when right-sided chambers cannot be adequately visualized with apical views. A typical application of this view is related to the estimation of pulmonary artery systolic pressure from the peak velocity of the tricuspid regurgitant flow when imaging or correct alignment of the tricuspid regurgitation is not adequate with the apical four-chamber view. Starting from the parasternal long axis of the left ventricle and inclining the probe to move the ultrasonic beam toward the patient's left side allows visualization of the right ventricular (RV) outflow tract, the pulmonary valve, and the pulmonary artery on a tomographic plane that is approximately perpendicular to that seen by the standard short-axis view at the level of the great vessels. This alternative view may be useful to explore both pulmonary outflow and regurgitation when imaging is not adequate with the standard view, and can allow measurements of indexes related to pulmonary artery pressure and pulmonary bed resistance (Fig. 3.2). An alternative two-chamber visualization of the RV inflow tract can also be obtained with the apical approach, starting from the standard two-chamber view for the left ventricle and again inclining the probe so that the direction of the ultrasonic beam moves toward the patient's right side. The subxiphoid approach is of particular utility in the ICU, as it often allows good visualization of the heart in patients with poor parasternal and apical windows (e.g., related to chronic obstructive pulmonary disease or increased chest anteroposterior dimension), even when mechanical respiratory support is ongoing, and without the need to change the dorsal decubitus position of the patient. Several alternative views may also be used to image other structures that are often difficult to explore using the standard approach, e.g., the right parasternal view for the distal ascending tract of the aorta and modified parasternal short-axis and apical views for its proximal and distal intrathoracic descending tract. Overall, a large number of alternative and off-axis views exist. However, the choice of using one or more of them is strictly dependent on the experience and the preference of the sonographer, and is dictated by each individual examination.

3.5 Utilizing Echocardiographic Indexes That Are Less Dependent on Image Quality

An additional step in the approach to patients who are technically difficult to explore includes the use

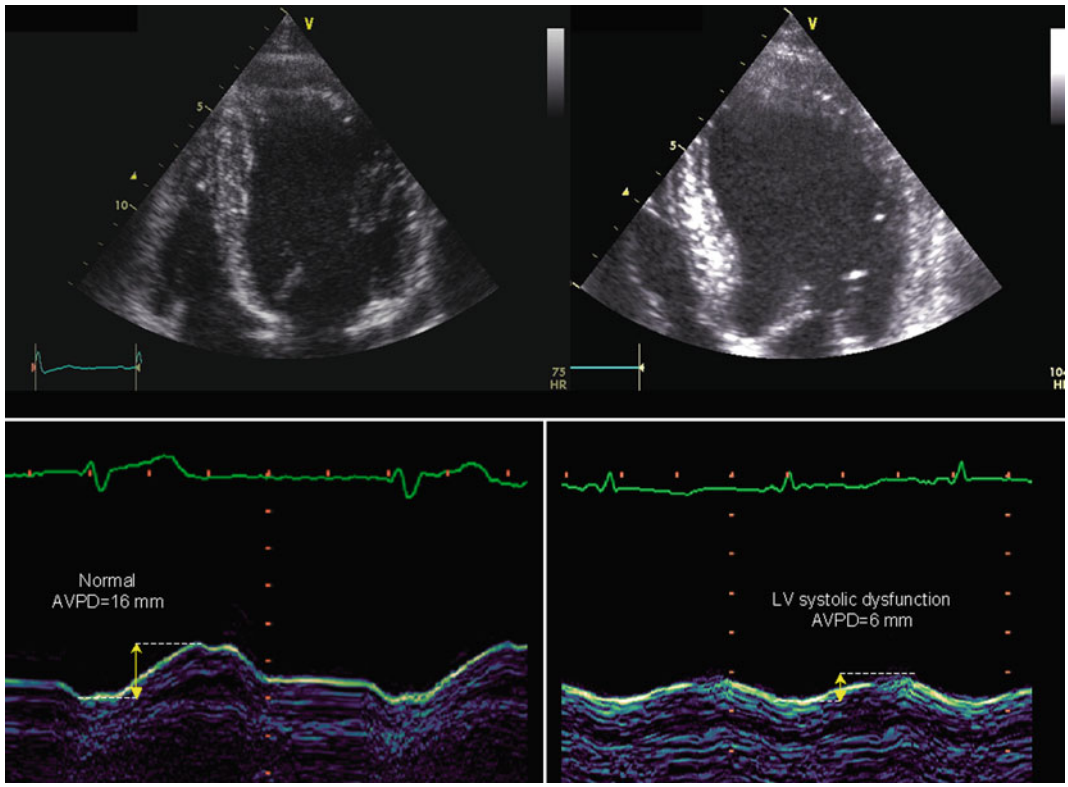

Fig. 3.3 Utility of left atrioventricular plane displacement (*AVPD*) in two patients with suboptimal quality of the four-chamber view (*top*), in whom accurate detection of the subendocardial border for the determination of left ventricular (*LV*) ejection fraction was difficult. Displacement of the annulus was normal in the first subject (*left*), but was reduced in the second subject (*right*), indicating considerable LV systolic dysfunction

of indexes that are relatively less sensitive to the quality of acoustic windows. A typical example of this is represented by the use of indexes of longitudinal function for the assessment of left ventricular (LV) and RV function.

3.5.1 LV Systolic Function

Accurate evaluation of LV systolic function is a key aspect for the treatment of patients in the ICU. LV ejection fraction as an overall index of LV systolic function is often quantitatively assessed using two-dimensional approaches aimed at measuring LV volumes (e.g., the modified Simpson rule). A rough evaluation of global LV function can also be qualitatively obtained by visual inspection alone. However, both methods rely on adequate visualization of the LV endocardial border, which is often not obtainable in critically ill patients despite appropriate harmonic imaging and efforts to optimize images. Assessment of LV segmental wall motion is dependent on detection of the endocardial border as well, and therefore suffers from similar limitations. Contrast techniques can dramatically improve visualization of the endocardial border, but they are not routinely used in critical practice. In these cases, measurement of left atrioventricular plane displacement by standard M-mode echocardiography or peak mitral annulus systolic velocity by tissue Doppler imaging (s') (Figs. 3.3, 3.4), usually

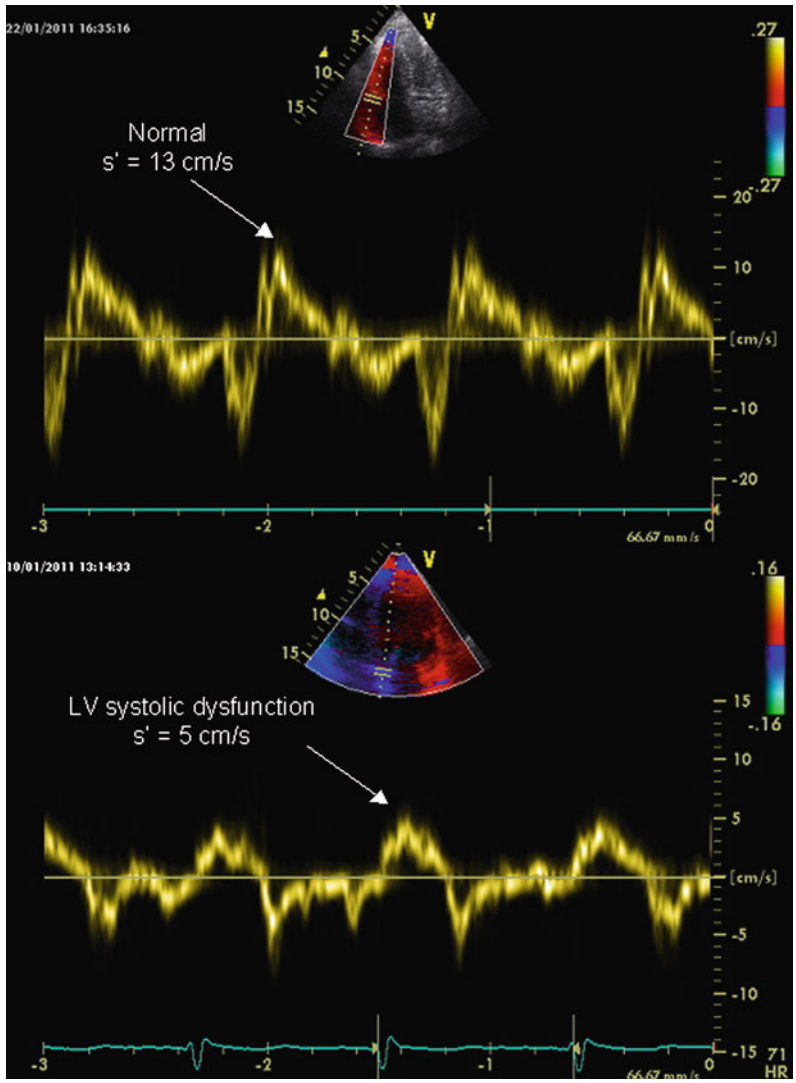

Fig. 3.4 Examples of pulsed tissue Doppler imaging of mitral annulus systolic velocity in a normal subject (*top*) and in a patient with LV systolic dysfunction (*bottom*)

calculated by averaging values measured in at least two sites of the annulus (e.g., septal and lateral from the apical four-chamber view), provides accurate indexes of LV longitudinal systolic function that are less dependent on image quality and that can often be well measured even in patients with suboptimal acoustic windows. Moreover, compared with measurement of ejection fraction, measurement of atrioventricular plane displacement and s' is more reproducible, less time consuming, and relatively less sensitive to the loading conditions.

3.5.2 LV Diastolic Function

Adequate information about LV diastolic performance can be obtained in most patients even in the case of suboptimal windows. Recording of the LV inflow pattern by pulsed Doppler

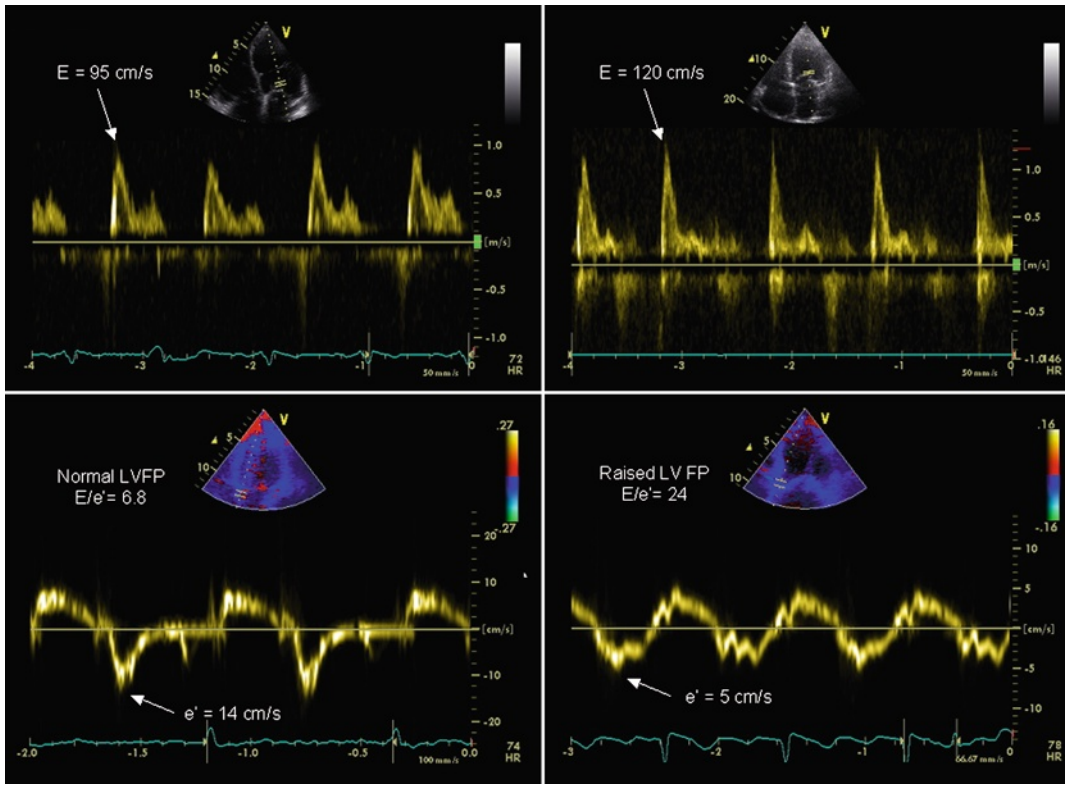

Fig. 3.5 Assessment of LV diastolic function using standard pulsed Doppler imaging of transmitral flow and tissue Doppler imaging of diastolic mitral annulus motion. *Left* recorded in a normal subject, *right* recorded in a subject with advanced left ventricular dysfunction. *LVFP* LV filling pressure

imaging after placing the sample volume at the level of the mitral tip in the apical four-chamber view is feasible in the large majority of critically ill patients. LV inflow imaging provides valuable information regarding LV diastolic dysfunction by identification of the diastolic pattern (normal, impaired relaxation, pseudonormal, and restrictive). However, it should be stressed that the simple use of LV inflow as an index of LV diastolic function is strongly limited by its strict load dependence. More reliable information regarding LV relaxation properties can be obtained by considering the peak early diastolic velocity of the mitral annulus obtain by tissue Doppler imaging (e'). As for the systolic annulus velocity, diastolic velocities are usually calculated by averaging values measured in at least two sites of the annulus (e.g., septal and lateral with the apical four-chamber view). The average e' is a relatively load-independent measure of LV relaxation. The ratio between early diastolic peak velocity of LV inflow (E) measured by standard pulsed Doppler imaging and e' provides a reliable noninvasive estimate of LV filling pressures (Fig. 3.5). Determination of e' and the E/e' ratio allows rapid and accurate assessment of LV diastolic function in the ICU, with relatively high feasibility even in the case of suboptimal windows.

3.5.3 RV Systolic Function

The same considerations made for the assessment of LV systolic function can be applied to the evaluation of RV systolic function. Assessment of RV ejection fraction by two-

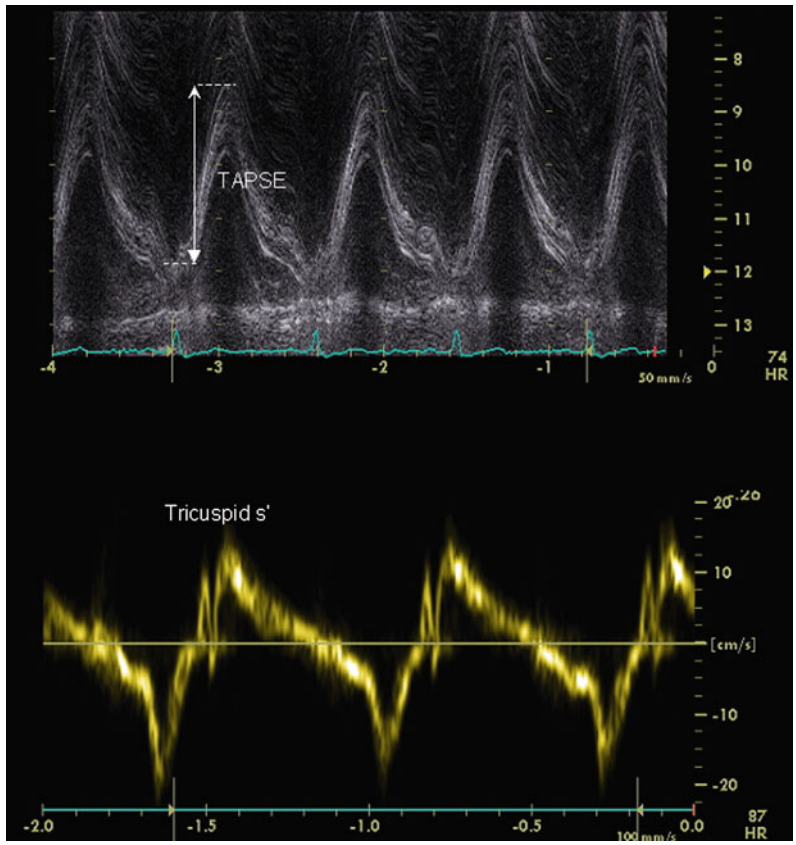

Fig. 3.6 Tricuspid annulus plane systolic excursion (*TAPSE*) (*top*) and pulsed tissue Doppler pattern of tricuspid annulus motion (*bottom*) in a normal subject

dimensional echocardiography is even more difficult than assessment of LV ejection fraction and relies on geometrical assumptions that are less valid owing to the irregular crescent/triangular shape of the right ventricle. As the use of three-dimensional echocardiography for the assessment of RV ejection fraction is still not applicable to daily practice and is affected by image quality similarly to two-dimensional methods, in practice most sonographers use indexes of RV longitudinal systolic function. M-mode tricuspid annulus systolic excursion and tissue Doppler peak systolic velocity of the tricuspid annulus are commonly used to quantify RV systolic performance and can often be measured even in patients with poor acoustic windows (Fig. 3.6). Both indexes show a good relationship with RV ejection fraction. Their advantages resemble those already explained for LV longitudinal indexes.

3.5.4 Other Applications

The opportunity of using indexes that are less dependent on image quality should be constantly taken into account for all aspects of echocardiographic examination when images are of suboptimal quality. Accordingly, in addition to the assessment of ventricular function, this concept can be applied to a number of echocardiographic evaluations (e.g., determination of pulmonary artery pressures, calculation of

cardiac output, estimation of valve regurgitation or stenosis severity, and analysis of prosthetic valve hemodynamics).

Further Reading

Cook CH, Praba AC, Beery PR et al (2002) Transthoracic echocardiography is not cost effective in critically ill surgical patients. J Trauma 52:280–284

Culp BC, Mock JD, Ball TR, Chiles CD, Culp WC Jr (2011) The pocket echocardiograph: a pilot study of its validation and feasibility in intubated patients. Echocardiography 28:371–377

Douglas PS, Garcia MJ, Haines DE, Lai WW, Manning WJ, Patel AR, Picard MH, Polk DM, Ragosta M, Ward RP, Weiner RB (2011) ACCF/ASE/AHA/ASNC/HFSA/HRS/SCAI/SCCM/SCCT/SCMR 2011 appropriate use criteria for echocardiography. A report of the American College of Cardiology Foundation Appropriate Use Criteria Task Force, American Society of Echocardiography, American Heart Association, American Society of Nuclear Cardiology, Heart Failure Society of America, Heart Rhythm Society, Society for Cardiovascular Angiography and Interventions, Society of Critical Care Medicine, Society of Cardiovascular Computed Tomography, and Society for Cardiovascular Magnetic Resonance endorsed by the American College of Chest Physicians. J Am Coll Cardiol 57:1126–1166

Hwang JJ, Shyu KG, Chen JJ et al (1993) Usefulness of transesophageal echocardiography in the treatment of critically ill patients. Chest 104:861–866

Joseph MX, Disney PJS, Da Costa R et al (2004) Transthoracic echocardiography to identify or exclude cardiac cause of shock. Chest 126:1592–1597

Ultrasound Morphology of the Heart: Transesophageal Examination

4

F. Luca Lorini, Carlo Sorbara, and Sergio Cattaneo

4.1 Introduction

A transesophageal echocardiography (TEE) examination is effective to assist in the hemodynamic treatment of patients during cardiovascular anesthesia and to make a diagnoses in the operating room during cardiac operations and in the intensive care unit. More and more anesthesiologists are involved in this practice and they provide a remarkable contribution to scientific and practical progress of perioperative echocardiography. Executing TEE requires time, but there are a lot of advantages for hemodynamic monitoring and diagnosis, which explains the increasing interest in TEE for many years.

The heart is a very complex three-dimensional structure with a lot of anatomic components bound together; therefore, perfect knowledge of the anatomy is very important to understand two-dimensional echo images of the heart. The operator's experience is very important; we think that TEE should be used in all cardiac surgery patients without contraindications, especially at the beginning of the learning curve. The simplified TEE examination usually requires 5–10 min. During the examination, the TEE operator or an anesthesiologist or a nurse can check the stability of the patient.

Sometimes images are very bad because of anatomic conditions (cardiac cavity dilatation) or air in stomach (it is possible to improve the image after suction). Instrument settings and adjustments are important for optimizing image quality and the diagnostic capabilities of TEE. Many TEE probes can obtain an image with more than one transducer frequency. Increasing the imaging frequency improves resolution but decreases penetration. Structures closer to the probe, such as the aortic valve (AV), are imaged best at a higher frequency, whereas structures farther away from the probe, such as the apical regions of the left ventricle (LV), are imaged best at a lower frequency. The depth is adjusted so that the structure being examined is centered in the display, and the focus is moved to the area of interest. Overall image gain and dynamic range (compression) are adjusted so that the blood in the chambers appears nearly black and is distinct from the gray scales representing tissue. Time compensation gain adjustments are set to create uniform brightness and contrast throughout the imaging field. The color flow Doppler (CFD) gain is set to a threshold that just eliminates any background noise within the color sector. Decreasing the size and depth of the color sector increases the aliasing velocity and frame rate. Decreasing the width of the two-dimensional imaging sector also increases the frame rate.

F. L. Lorini (✉)
Department of Anesthesia and Intensive Care,
Ospedali Riuniti di Bergamo, Bergamo, Italy
e-mail: llorini@ospedaliriuniti.bergamo.it

A. Sarti and F.L. Lorini (eds.), *Echocardiography for Intensivists*,
DOI: 10.1007/978-88-470-2583-7_4, © Springer-Verlag Italia 2012

4.2 Patient Safety

Rarely TEE can cause serious and even fatal complications; effort should be made to detect preexisting esophageal or gastric problems before performing TEE. Contraindications to TEE include esophageal stricture, diverticulum, tumor, and recent esophageal or gastric surgery. The TEE transducer should be inspected for defects and cracks in the waterproof covering before insertion. The mouth should be examined for preexisting injuries and loose teeth. The TEE probe may be inserted into an anesthetized, tracheally intubated patient with or without the use of a laryngoscope by displacing the mandible anteriorly and inserting the probe gently in the midline. Flexing the neck will help in some cases. If insertion of the probe is not easy, a laryngoscope can be used to expose the glottis and permit direct passage of the probe posteriorly into the esophagus. Once the transducer is in the esophagus, it should never be forced through a resistance. The tip of the transducer should be allowed to return to the neutral position before the probe is advanced or withdrawn, and excessive force should never be applied when the transducer is moved in the esophagus or when the tip is flexed with the control wheels. Cleaning and decontamination of the probe should be performed after each use.

4.3 The Simplified TEE Examination

The comprehensive, intraoperative TEE examination, recommended in the guidelines written by the American Society of Echocardiography and the Society of Cardiovascular Anesthesiologists in 1999 consists of a series of 20 cross-sectional views of the heart and great vessels. The views are designated by the transducer location (i.e., the echo window), a description of the imaging plane (e.g., short axis, long axis), and the main anatomic structure in the image.

One should not start to study immediately a pathological element (surgical indication); one should use a standard protocol to practice the TEE examination. One should get only one cardiac structure (valve or cavity) in focus, and analyze it and its relationship to other structures. It is very important to move the scan plane and build up a three-dimensional structure from the two-dimensional image. Everyone has to develop a personal approach to the intraoperative TEE examination; we suggest a simplified intraoperative TEE examination that reduces the number of views from the 20 standard views, and is able to analyze all the main heart structures. The main advantage of this systematic approach is the minimization of the manipulation of the TEE probe to perform a complete examination of major cardiac structures.

The cardiac examination is performed at three locations. The first location is the mid esophagus at the AV level, the second is a few centimeters distal in the mid esophagus at the level of the mitral valve, and the final location is in the stomach at the level of the LV. After completion of the cardiac examination, the aorta is evaluated throughout its thoracic course.

4.3.1 Mid-Esophageal AV Level

4.3.1.1 Mid-Esophageal AV Short-Axis View

After the probe has been inserted, it is advanced until the leaflets of the AV are seen. The imaging plane is then rotated to approximately 45° to obtain the mid-esophageal AV short-axis view. The primary structure visualized is the AV in the short axis. The size of the AV in comparison with the atrial chambers in addition to the mobility of the aortic leaflets and any leaflet calcification is carefully noted (Fig. 4.1).

The primary diagnostic goals of this view are to define the general morphology of the AV (e.g., bicuspid vs. tricuspid) and to determine if aortic stenosis is present. The intra-atrial septum can be observed for openings consistent with an atrial septal defect or patent foramen ovale.

Depth: mid-esophageal (30-40 cm from the dental rhyme) advancing or retreating until the aortic valve

Angle: 30° - 60°

Flex: none

Laterality: none

Goals: aortic valve, left atrium, right atrium, right ventricle, pulmonary valve, right ventricular outflow tract

Legend: LA: left atrium
RA: right atrium
RV: right ventricle
PV: pulmonary valve
nc: non-coronary aortic cusp
rc: right coronary aortic cusp
lc: left coronary aortic cusp

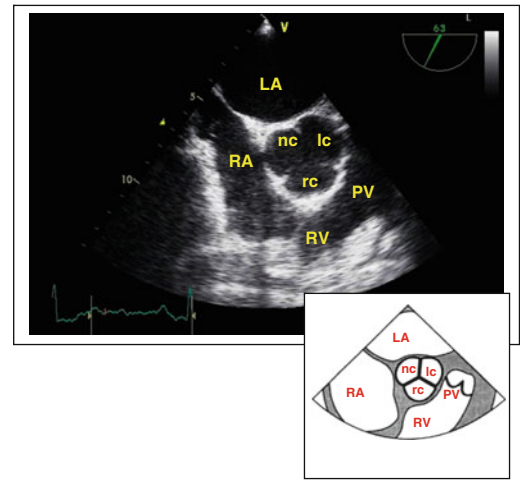

Fig. 4.1 Mid-esophageal aortic valve short-axis view

Depth: mid-esophageal (30 - 40 cm from the dental rhyme) advancing or retreating until the aortic valve

Angle: 120° - 160°

Flex: none

Laterality: none

Rotation: right-left to bring the aortic valve in the center

Goals: aortic valve, left atrium, left ventricular outflow tract

Legend: LA: left atrium
LV: left ventricle
AV: aortic valve

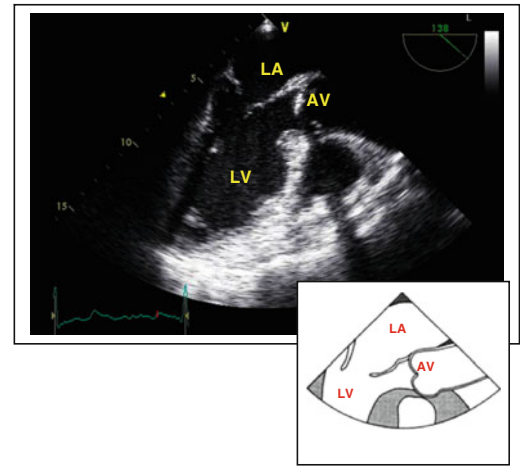

Fig. 4.2 Mid-esophageal aortic valve long-axis view

4.3.1.2 Mid-Esophageal AV Long-Axis View

The mid-esophageal AV long-axis view is obtained by further rotating the imaging angle to approximately 110–130°. A slight turn of the probe toward the patient's right may be necessary to optimize this image. The view is complete when the left ventricular outflow tract, AV, and proximal ascending aorta are displayed together. Additional structures to observe are the outflow tract itself, the sinus of Valsalva, and the sinotubular junction (Fig. 4.2).

The primary diagnostic goal of this view is to evaluate AV function. The proximal ascending aorta should be inspected for calcification, enlargement, and protruding atheroma. An important limitation of this view is that the aortic cannulation site in the distal ascending aorta cannot be visualized. After completion of a two-dimensional examination, AV function is evaluated further with CFD imaging.

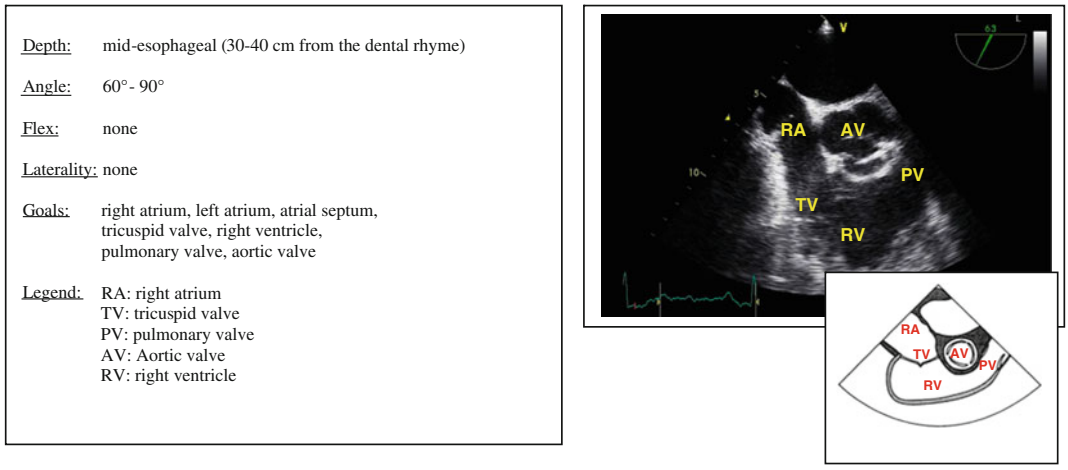

Fig. 4.3 Mid-esophageal right ventricular inflow–outflow view

4.3.1.3 Mid-Esophageal Right Ventricular Inflow–Outflow View

The next view obtained at the level of the AV is the mid-esophageal right ventricular inflow–outflow view. One starts at the mid-esophageal AV short axis and, without moving the probe, changes the rotation of the imaging angle to approximately 60–90°. The desired imaging plane will visualize the tricuspid valve, the right ventricular outflow tract, and the proximal pulmonary artery (Fig. 4.3).

The primary diagnostic goals of this view are to gauge the right ventricular chamber and pulmonary artery size and to evaluate the pulmonary valve. This view is often superior to the mid-esophageal four-chamber view for Doppler interrogation of the tricuspid valve.

4.3.1.4 Mid-Esophageal Bicaval View

The mid-esophageal bicaval view is then obtained by turning the probe further to the patient's right. This image is often best with 5–15° less rotation than in the mid-esophageal AV long-axis view. The key structures in this view are the left atrium, right atrium, superior vena cava, intra-atrial septum, and right atrial appendage (Fig. 4.4).

The primary diagnostic goals of this view are to examine for atrial chamber enlargements and the presence of a patent foramen ovale or an atrial septal defect, and to detect intra-atrial air. If the integrity of the intraatrial septum is questioned, CFD imaging or bubble contrast imaging should be performed.

4.3.2 Mid-Esophageal Mitral Valve Level

4.3.2.1 Mid-Esophageal Four-Chamber View

After completion of the mid-esophageal bicaval view, the imaging angle is returned to 0° and the TEE probe is advanced to the mitral valve level. In the transverse plane, the mid-esophageal four-chamber view is obtained. This view allows visualization of all the chambers of the heart. The image rotation is approximately 0–10° with some posterior flexion of the probe. The key structures to observe are the left atrium, the LV, the right atrium, the right ventricle, the mitral and tricuspid valves, and the septal and lateral walls of the myocardium. If a portion of the left ventricular outflow tract and AV is displayed (called the five-chamber view), retroflexion of the probe and slight advancement or rotation of

Depth: mid-esophageal (30-40 cm from the dental rhyme)

Angle: 80° - 110°

Flex: none

Laterality: none

Rotation: the right to place the right atrium in the center

Goals: right atrium, left atrium, atrial septum, inferior vena cava and superior vena cava

Legend:
LA: left atrium
RA: right atrium
IVC: inferior vena cava
SVC: superior vena cava

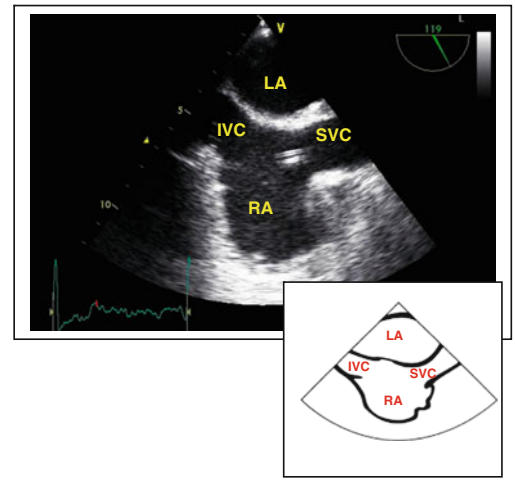

Fig. 4.4 Mid-esophageal bicaval view

Depth: mid-esophageal (30-40 cm from the dental rhyme)

Angle: 0° - 20°

Deflection: none

Laterality: none

Goals: right atrium, right ventricle, left atrium, left ventricle, mitral valve, tricuspid valve

Legend: RA: right atrium
RV: right ventricle
LA: left atrium
LV: left ventricle

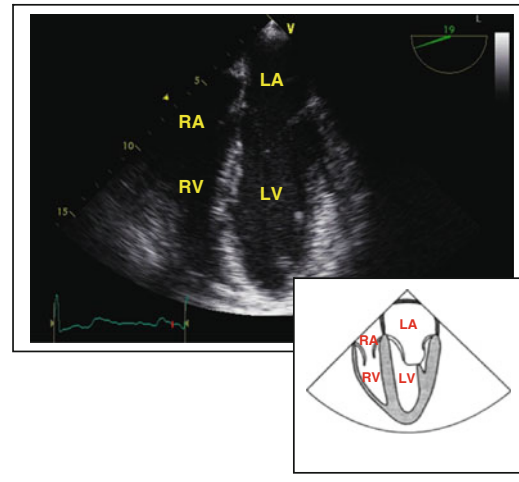

Fig. 4.5 Mid-esophageal four-chamber view

the imaging plane to 5–10° should produce the mid-esophageal four-chamber view (Fig. 4.5).

The mid-esophageal four-chamber view is one of the most diagnostically valuable views in TEE. The diagnostic goals of this view include evaluation of chamber size and function, valvular function (both mitral and tricuspid), biventricular interdependence, and regional motion of the septal and lateral walls of the LV. An additional important use of this view is to look for intraventricular air following cardiopulmonary bypass. After two-dimensional interrogation of this view, CFD imaging should be applied to the mitral and tricuspid valves to detect valvular insufficiency and stenosis.

4.3.2.2 Mid-Esophageal Two-Chamber View

From the mid-esophageal four-chamber view, the imaging angle is rotated to approximately 60° to 90° to obtain the mid-esophageal two-chamber view. This view is characterized by the

Depth: mid-esophageal (30-40 cm from the dental rhyme)

Angle: 80° - 100°

Deflection: none

Laterality: none

Goals: left atrium, mitral valve, left ventricle

Legend: LA: left atrium
LV: left ventricle

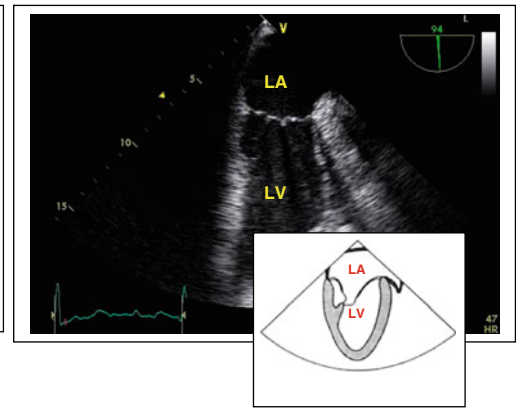

Fig. 4.6 Mid-esophageal two-chamber view

Depth: transgastric

Angle: 0 °

Flex: anteflex

Laterality: none

Goals: left atrium, left ventricle

Legend: LV: left ventricle
pmPM: posteromedial papillary muscle
alPM: anterolateral papillary muscle

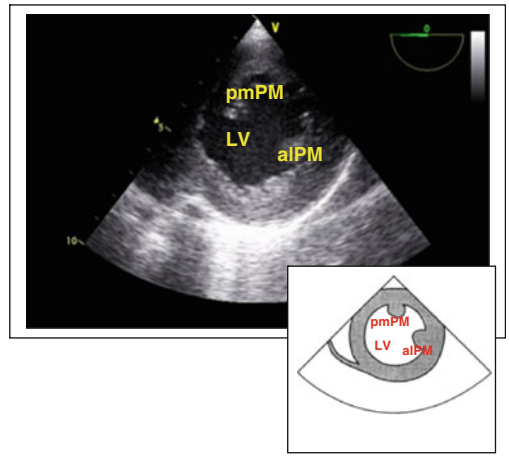

Fig. 4.7 Transgastric mid-papillary short-axis view

presence of the left atrial appendage and the absence of right-sided heart structures, and it allows visualization of the anterior and inferior walls of the LV. Occasionally, turning the probe shaft to the right will improve chamber alignment and visualization of the true left ventricular apex. Ventricular thrombus or hypokinesis at the apex is often best appreciated in this view (Fig. 4.6).

The primary goals of this view are to evaluate left ventricular function (especially the apex) and anterior and inferior regional wall motion. It can also be used to look for thrombus of the left ventricular apex and left atrial appendage.

4.3.3 Transgastric Level: Transgastric Mid-Papillary Short-Axis View

After completion of the interrogation of the heart at the aortic and mitral valve levels, the imaging plane is returned to 0° and the probe is advanced into the stomach to obtain the transgastric views. The first is the transgastric mid short-axis view. The probe is then anteflexed and withdrawn until

Fig. 4.8 Descending aortic short-axis view

contact is made with the wall of the stomach. The key structures to visualize are the left ventricular walls and cavity in addition to the posteromedial and anterolateral papillary muscles. A true short-axis cross section of the LV is confirmed when the two papillary muscles are approximately of equal size. Fine-tuning this image may be difficult (Fig. 4.7).

The primary diagnostic goals of this view are assessment of left ventricular systolic function, left ventricular volume, and regional wall motion.

4.3.4 Aortic Examination

4.3.4.1 Descending Aortic Short-Axis View

After completion of the preliminary evaluation of the heart, the aorta is examined. From the transgastric two-chamber view, the imaging angle is rotated to 0° and the probe shaft is turned to the patient's left and slightly withdrawn until a transverse view of the descending aorta is obtained (the descending aortic short-axis view). Key factors in imaging the aorta are its small size and its proximity to the TEE probe head in the esophagus. Consequently, the following maneuvers are necessary to optimize aortic imaging. First, the image depth in reduced to enlarge the displayed aortic image. Then, the frequency of the transducer can be increased to enhance resolution. The aorta is then visualized along its course as the probe is slowly withdrawn. When the aorta begins to appear elongated, the level of the aortic arch has been reached (Fig. 4.8).

4.3.4.2 Upper Esophageal Aortic Arch Short-Axis View

From the level of the aortic arch, the imaging angle is turned to 90° to obtain the upper esophageal aortic arch short-axis view. Small left and right turns of the probe shaft will allow the arch to be interrogated for calcification, enlargement, and foreign bodies. The origins of the great vessels may be at approximately three o'clock in the short axis of the aortic arch. The origin of the left subclavian artery is visualized in this view.

4.3.4.3 Descending Aortic Long-Axis View

From the upper esophageal aortic arch short-axis view with the imaging plane maintained at 90°, the probe is advanced to obtain the longitudinal view of the descending aorta (the descending aortic long-axis view). Again, as the probe is advanced, small left and right turns of the probe permit better interrogation of the aortic walls.

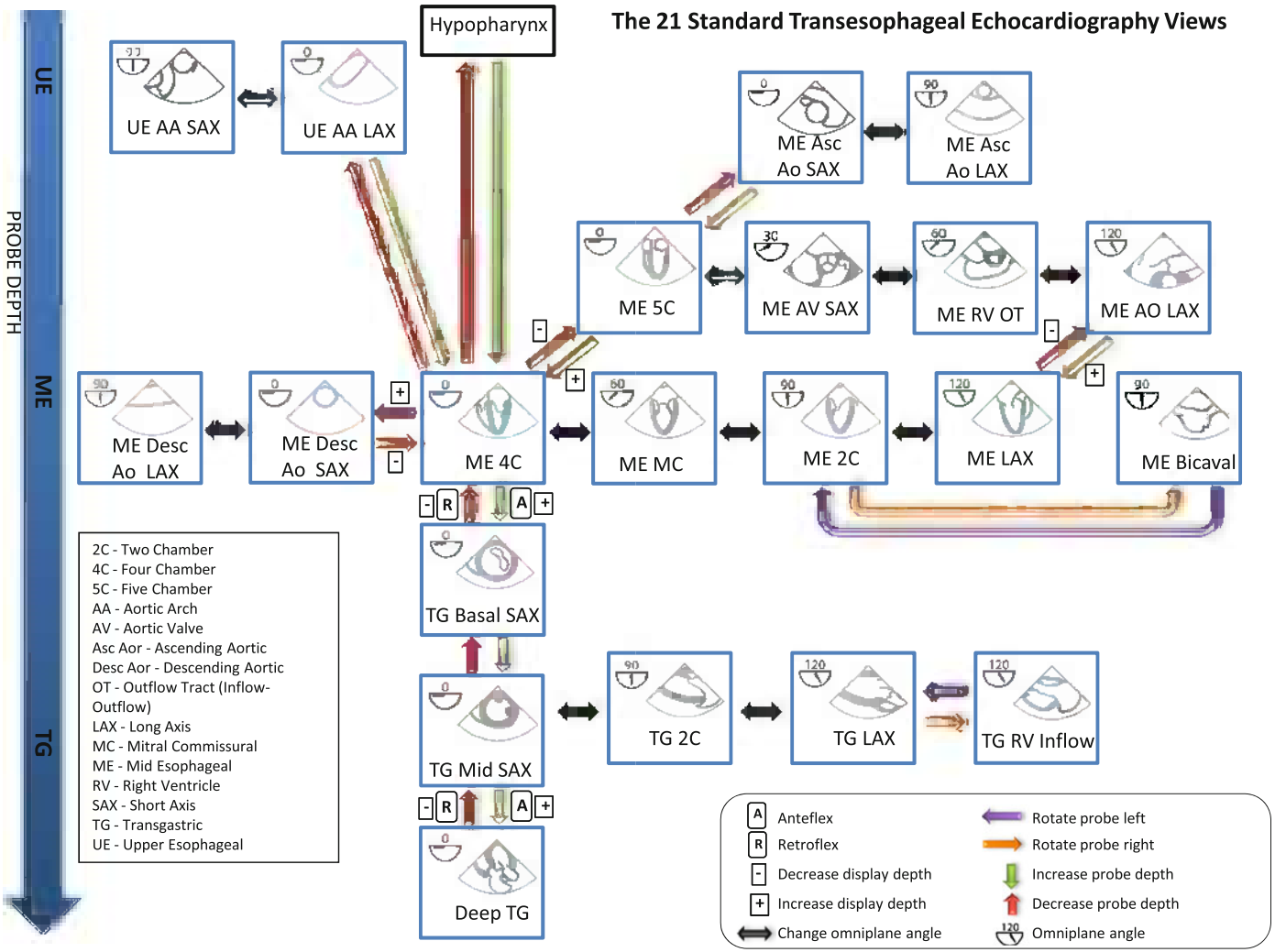

Fig. 4.9 The 21 standard transesophageal echocardiography views

4.4 Summary

To help understand the relationships between the various echocardiographic sections, Fig. 4.9 summarizes all standard views and movements of the transesophageal probe to move from one view to another.

Further Reading

Miller JP, Lambert SA, Shapiro WA et al (2001) The adequacy of basic intraoperative transesophageal echocardiography performed by experienced anesthesiologists. Anesth Analg 92:1103–1110

Shanewise JS, Cheung AT, Aronson S et al (1999) ASE/SCA guidelines for performing a comprehensive intraoperative multiplane transesophageal echocardiographic examination: recommendations of the American Society of Echocardiography Council for Intraoperative Echocardiography and the Society of Cardiovascular Anesthesiologists Task Force for Certification in Perioperative Transesophageal Echocardiography. Anesth Analg 89:870–884

Stevenson JG (1999) Adherence to physician training guidelines for pediatric transesophageal echocardiography affects the outcome of patients undergoing repair of congenital cardiac defects. J Am Soc Echocardiogr 12:165–172

Thys DM, Abel M, Bollen BA et al. (1996) Practice guidelines for perioperative transesophageal echocardiography. A report by the American Society of Anesthesiologists and the Society of Cardiovascular Anesthesiologists Task Force on Transesophageal Echocardiography. Anesthesiology 84:986–1006

Ungerleider RM, Kisslo JA, Greeley WJ et al (1995) Intraoperative echocardiography during congenital heart operations: experience from 1,000 cases. Ann Thorac Surg 60:S539–S542

Three-Dimensional Echocardiography

5

Mauro Pepi and Gloria Tamborini

5.1 Introduction

Progress in three-dimensional (3D) echocardiography was rather slow in the 1980s and 1990s mainly for technical reasons. Recently, along with the rapid evolution of probe and computer technologies, 3D echocardiography has grown into a well-developed technique able to display images of the heart that contain important new tissue and morphologic information. This new technique is now simple, rapid, and allows additional clinical information to be obtained in different fields, including evaluation of valve diseases and intracardiac masses, assessment of the volumes and function of the two ventricles, and monitoring of cardiac surgery and new interventional procedures. This chapter details the current status of 3D technology and in particular recent advances in live 3D methods (either 3D transthoracic echocardiography—TTE—or 3D transesophageal echocardiography—TEE) with their clinical applications in the main heart diseases.

M. Pepi (✉)
Monzino Cardiological Hospital, IRCCS,
Milan, Italy
e-mail: mauro.pepi@ccfm.it

5.2 Methods and New Technologies

Several methods including random and sequential scanning, free-hand techniques by both TTE and TEE have been proposed in the past and all of them required off-line reconstruction. Real-time volumetric imaging developed in the early 1990s by the group of Von Ram of Duke University was based on novel matrix phased array transducer technology. However, the first-generation instrument had several practical limitations despite its very promising clinical applications. In the early 2000s, second-generation real-time live 3D echocardiography (and nowadays the new probe and software technologies) allowed a true routine application of the method in different fields: it is simple, rapid, and may be easily integrated and associated with the standard two-dimensional (2D) examination. These new transducers (with 3,000–4,000 ultrasound elements) have multidirectional beam steering and signal processing which occurs automatically in the scanning probe itself. This technology generates true pyramidal volumes of data and creates online rendered images; since the pyramidal data sets are still limited in terms of volumes (generally 60° × 30°), it is alternatively possible to obtain a larger-volume data set of up to 100° × 100° (the so-called full-volume data set), acquiring up to seven (generally four or seven) subvolumes over consecutive cardiac cycles. Moreover, new software allows one to utilize zoom methods, to acquire 3D images also

A. Sarti and F. L. Lorini (eds.), *Echocardiography for Intensivists*,
DOI: 10.1007/978-88-470-2583-7_5, © Springer-Verlag Italia 2012

in the presence of arrhythmias, and to improve spatial and temporal resolution. The images acquired may be immediately sliced in several planes and rotated in order to visualize cardiac structures from any plane and multiple perspectives. As concerns the "old technologies," 3D sequential transesophageal acquisition (multiplane TEE with ECG and respiratory gating or new techniques with very fast acquisition without gating) is still utilized and very useful in several clinical settings. However, a new generation of TEE probes with a novel matrix array technique was recently (2008) introduced, allowing 3D presentation of cardiac structures in real time. This new tool may potentially provide fast and complete 3D information about cardiac structures, improving spatial orientation and overcoming limitations of off-line 3D technologies (acquisition and reconstruction times). Therefore, we refer to real-time 3D TTE, 3D TEE with sequential acquisition, and real-time 3D TEE. Finally, we also refer to the very new introduction of single-beat acquisition which allows a complete full volume to be acquired in a single beat.

5.3 Image Display and Analysis

After the acquisition of volumetric images in real time, the 3D the method has the problem of how to visualize the moving structures contained within the volume on a flat 2D monitor. Volume rendering is a process whereby the area of the cardiac structures is reconstructed by the computer so that the volumetric data set can be sectioned electronically in any plane. Once part of the data set has been cropped, one can see inside the heart. By this method, the size, shape, and motion of cardiac structures may be examined from any desired perspective. Moreover, the image may be manipulated, rotated, and as an example the mitral valve (MV) and the tricuspid valve may be viewed from above (simulating atriotomy, the so-called surgical view) or from below. Thanks to advances in shading techniques, an impression of perspective and depth is created. Other methods of analysis focus on the evaluation and display of cardiac chambers such as the left ventricle. Wire frame rendering or surface rendering results in the surfaces of the analyzed object facing the observer being displayed as a solid structure. These images may be obtained from manually or electronically derived contours from the data set. This method allows assessment of the chamber in terms of volume, shape, and function.

5.4 Different Clinical Applications

The main clinical applications of 3D TTE and TEE are as follows:

- Quantification of left ventricular (LV) volumes and function (and shape)
- Quantification of LV mass
- Assessment of regional wall motion of the left ventricle (rest and stress)
- Assessment of LV dyssynchrony
- Quantification of right ventricular (RV) volumes and function
- Evaluation of valve diseases
- Evaluation of congenital heart diseases
- Evaluation of cardiac masses
- Guidance of intracardiac interventions
- Monitoring of cardiac surgery

5.5 Quantification of Left Ventricular Volumes and Function (and Shape)

The biggest advancement of 3D echocardiography is the lack of dependence on geometric modeling, resulting in more accurate chamber quantification. Several studies have directly compared the accuracy of 3D versus 2D measurements of LV volumes and have demonstrated the superiority of the 3D method (less underestimation, superior reproducibility and intra- and interobserver variability). It is now possible with different software in the ultrasound units or off-line to detect endocardial surfaces from the 3D data sets and rapidly obtain the volumes and the ejection fraction. Despite this advantage, the method still slightly underestimates the LV volume in comparison with

MRI, which is considered the gold standard. There may be several reasons for this underestimation, including the resolution of 3D echocardiography, trabeculations of the left ventricle, and the different measurement methods used with the two techniques.

5.6 Quantification of Left Ventricular Mass

LV mass measurements rely on identification of not only endocardial boundaries, but also epicardial boundaries. They are therefore challenging. Nevertheless, several studies based on 3D echocardiography showed good accuracy of the method in normal and pathologic hearts. In this regard, contrast-enhanced 3D echocardiography may further improve both LV volume and LV mass measurements.

5.7 Assessment of Regional Wall Motion of the Left Ventricle (Rest and Stress)

Several studies have assessed the role of 3D echocardiography for the evaluation of regional LV function. With both the full-volume acquisition and the new single-beat acquisition, 3D echocardiography allows direct displacement of endocardial surfaces, therefore leading to an objective dynamic quantification of global and regional function. Despite the temporal and spatial resolution limitation and the dependence on optimal quality of images, this method (through the utilization of specific software in the ultrasound units or off-line) may overcome the subjective interpretation of regional analysis performed in standard examinations. Real-time 3D-derived regional motion was validated against a cardiac MRI reference. Three-dimensional regional motion may be potentially very useful in different fields: more objective quantification of the number of segments involved in regional dysfunction, stress echocardiography studies, and guidance of cardiac resynchronization therapy (CRT). In an echo–stress study, the main advantage is the unique possibility of visualizing all LV segments during one breath hold. Most stress echocardiography studies demonstrated an accuracy similar to that of standard 2D techniques, but significant advantages in terms of acquisition time and evaluation of all segments during each step of the stress (Fig. 5.1).

5.8 Left Ventricular Dyssynchrony

CRT is a very important and expanding technique in patients with symptomatic heart failure, poor LV function, and QRS duration greater than 120 ms. Several methods, including Doppler echocardiography, tissue Doppler imaging, 2D echocardiography, strain echocardiography, and speckle tracking echocardiography, have been proposed to select patients undergoing CRT, but a single parameter able to predict the response of CRT has not been demonstrated. This may be related to different reasons involving not only the echocardiographic technique but also the position of the catheters and myocardial scars and segmental function. As a consequence, 30 % of patients undergoing CRT fail to respond in terms of LV and clinical improvement. In this regard, real-time 3D echocardiography is an emerging tool to provide new indicators of myocardial dyssynchrony in selecting and monitoring patients with heart failure undergoing biventricular pacing. Several methods have been proposed. Kapetanakis et al. studied a large cohort of normal subjects and patients with real-time 3D TTE and proposed a new systolic dyssynchrony index (SDI) derived from the standard deviation of the time to the minimum regional volume for all 16 segments of the left ventricle. Normal subjects had a well-synchronized segmental function (SDI 3.5 %). In contrast, some patients had an SDI which increased with worsening of LV dysfunction (severe dysfunction SDI 14.7 %). At long-term follow-up, patients responding positively to CRT showed a marked reduction of SDI, which was associated with an increase in ejection fraction and a decrease of LV volumes. Soliman et al. also confirmed these data. An SDI > 10 % predicted CRT response with good sensitivity and

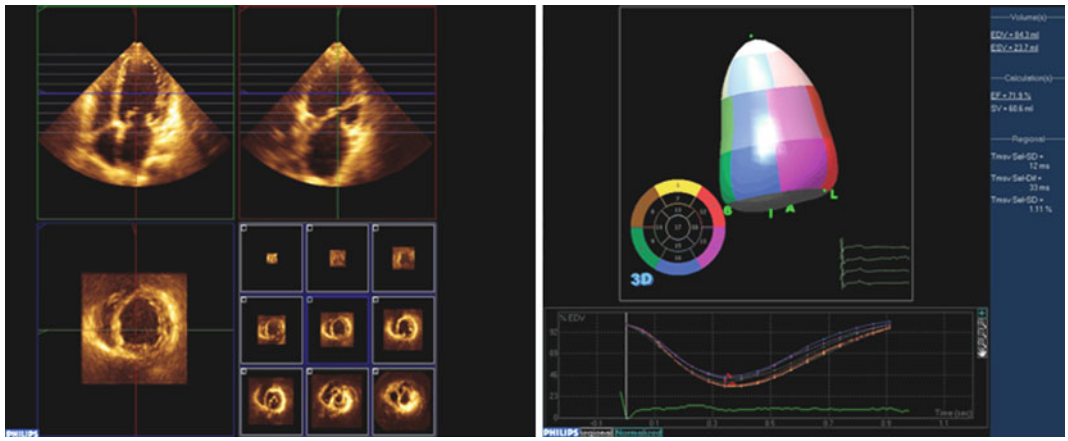

Fig. 5.1 *Left*: Three-dimensional (3D) data set as well as the short-axis view of the left ventricle at different cut planes of the chamber facilitating wall motion analysis. *Right*: A color-coded segment analysis and derived curves of the left ventricular wall motion analysis

specificity. Marsan et al. demonstrated that an SDI cutoff value of 6.4 % has high sensitivity and specificity (88 and 85 %, respectively, at long-term follow-up) and good reproducibility.

5.9 Quantification of Right Ventricular Volumes and Function

Owing to the peculiar RV morphology and function, 2D echocardiography has several limitations in the evaluation of the right ventricle which can be readily overcome by 3D echocardiography with gated wide-angle acquisition, which enables a complete assessment of geometry, volumes, and ejection fraction by displaying the surfaces of the entire right ventricle, including the inflow tract, apex, and outflow tract.

Several methods and software packages have been used to evaluate the right ventricle. Three-dimensional data are acquired in a full-volume set from the apical four-chamber view adapted to improve the visualization of the entire right ventricle.The 3D echocardiography data set is typically stored digitally and then processed off-line. On-cart dedicated RV analysis software packages will soon be available, further facilitating the use of these measurements in clinical practice. Current RV analysis software packages display 2D cut planes of the RV sagittal, four-chamber, and coronal views obtained from the full-volume 3D echocardiography data set. Most of the currently used methods of analysis automatically display these three views, which are then checked for consistency by toggling back and forth. The anatomy and disease of the tricuspid valve and the right ventricle are best visualized using volume-rendered images. The right atrium and right ventricle can be visualized using multiple cut planes. A variety of options for off-line 3D reconstruction of the right ventricle exist. After acquisition and automatic display of the RV end-diastolic and end-systolic frames, the operator traces a contour of the endocardial border in the axial plane. This traced contour generates disks of fixed height (generally 10 mm) but of differing lengths and widths as visualized in the other RV orthogonal views. The volume of the RV cavity is computed by adding the known areas of the axial traces obtained 10 mm apart, i.e., disk summation. The number of disks required to cover the entire right ventricle from the base to the apex ranges from seven to eight slices depending on RV size. Currently available software packages calculate RV volumes from end-diastolic and end-systolic endocardial border tracings of sagittal (to outline the tricuspid valve in the best possible view), four-chamber (to outline the apex), and coronal

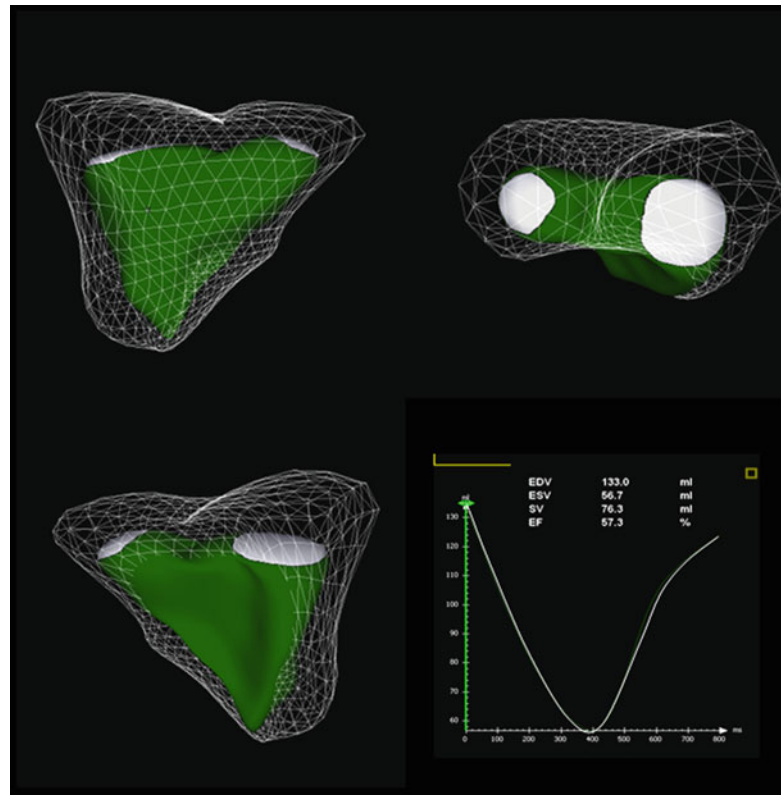

Fig. 5.2 Right ventricular (RV) end-diastolic and end-systolic surface volumes are depicted in different orientations showing the inflow, outflow, and apex segments of the right ventricle. The quantitative analysis of the curve with RV end-diastolic volume (*EDV*), end-systolic volume (*ESV*), stroke volume (*SV*), and ejection fraction (*EF*) is shown at the *bottom right*

(to outline the RV outflow tract) cross-sectional planes derived from 3D echocardiography. The operator frequently needs to manually adjust the traced contours in each frame prior to cast reconstruction and quantitative analysis. Trabeculations are generally included in the endocardial rim, but the apical component of the moderator band is excluded from the cavity. The RV volumes are calculated by summing the areas for each slice through the complete data set. Each volume data set is imported into the application and manipulated by rotating, angulating, and slicing in any of the three displayed orthogonal planes. This software analysis, which uses a semiautomated border detection algorithm with manual correction options, was validated using in vitro models as well as in vivo using cardiac MRI as the gold standard. The different software packages create a surface-rendering cast of the right ventricle. The end-diastolic and end-systolic volumes as well as the RV ejection fraction are measured and automatically displayed. Curves of global and regional RV function may be generated and analyzed (Fig. 5.2).

Data on RV volumes and function are of diagnostic and prognostic importance in a variety of cardiac diseases, including valve disease, congenital heart disease, pulmonary hypertension, and heart failure. Three-dimensional echocardiography allows the evaluation of volumes and function in normal subjects and patients, allowing identification of patients with different severity of RV dilatation and dysfunction. Several clinical studies have shown a good correlation between MRI and 3D echocardiography volumes and ejection fraction of the right ventricle in selected populations, with most studies showing a slight underestimation of volumes compared with the reference technique. Differences in RV volumes have been demonstrated between men (129 ± 25 ml) and women (102 ± 33 ml); however, adjustment to lean body mass (but not to body surface area or height) eliminated this difference.

The use of 3D TTE has been validated in patients with ostium secundum atrial septal defect, tetralogy of Fallot repair, Ebstein's anomaly, and RV cardiomyopathy. The feasibility and utility of 3D TTE for the guidance of RV endomyocardial biopsies in children has been demonstrated.

Assessment of RV function is of great interest in cardiovascular surgery because right-sided heart failure is one of the most frequent causes of morbidity and mortality after valvular surgery and surgery to correct congenital abnormalities, coronary artery bypass, and heart transplant. This highlights the importance of an accurate preoperative assessment of the right ventricle to improve risk stratification and an early and precise postoperative follow-up to optimize treatment. In this regard, 2D echocardiography and Doppler parameters (tricuspid annular plane systolic excursion, tissue Doppler imaging of the annulus) have several limitations particularly in the postoperative follow-up period. The evaluation of RV volumes and ejection fraction using 3D echocardiography overcomes many of the limitations of 2D echocardiographic methods. Very recently, reference values of RV volumes and ejection fraction have been published. Finally, preliminary data on 3D TEE acquisition and reconstruction of the right ventricle have been published.

5.10 Evaluation of Valve Diseases

Both qualitative and quantitative evaluation of valvular heart disease can be improved by 3D echocardiography. Any-plane and paraplane analysis of a stenotic valve allows accurate planimetry of the smallest orifice area. Zamorano et al. demonstrated that 3D TTE is a feasible, accurate, and highly reproducible technique for assessing MV area in patients with rheumatic mitral stenosis. In a consecutive series of 80 patients, MV area was assessed by conventional Doppler echocardiographic methods and by 3D TTE and the results were compared with those obtained invasively. Compared with the Doppler echocardiographic methods, 3D TTE had the best agreement with the invasively determined MV area and the intra- and interobserver variability of the method was very good. Zamorano et al. also studied 29 patients undergoing percutaneous balloon mitral valvuloplasty. The best agreement with the invasively determined MV area was obtained with 3D TTE, particularly in the immediate postprocedural period; thus the method may be proposed as an ideal one throughout this procedure and makes invasive evaluation unnecessary in this setting.

In addition to these very important quantitative data, 3D TTE may be integrated with 2D evaluation in the assessment of the qualitative morphology of the MV. Commissures, leaflets, the annulus calcifications, and subvalvular structures may be visualized from different and unique planes, facilitating the understanding of this complex apparatus. Each of the atrioventricular valves may be depicted both from the atrium and from ventricle with access to "en face" views or from any other angle. Vegetations, commissural diseases, subvalvular diseases (tip of the leaflets/cordae/papillary muscles), and clefts may be accurately diagnosed. MV prolapse is visualized as a bulging or protrusion on the atrial site and in this regard 3D echocardiography is the ideal method to demonstrate the disease. Several studies by 3D TEE and 3D TTE have demonstrated the importance of 3D methods in this field. Recent data showed that 3D echocardiography (either TTE or TEE) is superior in comparison with the corresponding 2D techniques in the description of MV disease. In particular, since real-time 3D TTE has an accuracy similar to that of 2D TEE, this new technique (which is also simple and rapid) may be integrated in the standard 2D examination and should be regarded as an important examination to aid in the decision regarding MV repair. MV prolapse is the most frequent cause of mitral regurgitation in industrialized countries. Since the 1970s, MV repair has become preferential to replacement and is now possible in the overwhelming majority of patients with MV prolapse. Recent studies and guidelines have underlined the importance of early surgical intervention to preserve long-term LV function in severe mitral regurgitation. In this regard, a noninvasive preoperative assessment of MV anatomy is essential

to define the feasibility and complexity of repair, to differentiate cases with simple or complex lesions, and to plan the ideal surgical strategy. For all these reasons, 3D TTE and 3D TEE should be regarded as an important examination to aid the decision regarding MV repair, particularly in patients with complex diseases and in the light of these new early surgical strategies. Recently, a large series of patients with MV prolapse evaluated with different echocardiographic methods was published by our group. One-hundred and twelve consecutive patients with severe mitral regurgitation due to degenerative MV prolapse underwent complete 2D and 3D TTE the day before surgery, and complete 2D and 3D TEE in the operating room. Echocardiographic data obtained by the different techniques (including scallops, commissures, chordal rupture identification) were compared with data from MV surgical inspection. Three-dimensional techniques were feasible in a relatively short time (3D TTE, 7 ± 4 min; 3D TEE, 8 ± 3 min), with good (3D TTE, 55 %; 3D TEE, 35 %) and optimal (3D TTE, 21 %; 3D TEE, 45 %) imaging quality in most cases. Three-dimensional TEE allowed more accurate identification (95.6 % accuracy) of all MV lesions in comparison with other techniques. Three-dimensional TTE and 2D TEE had similar accuracies (90 and 87 %, respectively), whereas the accuracy of 2D TTE (77 %) was significantly lower. Thus, these data showed that 3D TTE and 3D TEE are feasible, are not time-consuming, and are useful methods in identifying the location of MV prolapse in patients undergoing MV repair. They were superior in the description of disease in comparison with the corresponding 2D techniques and should be regarded as an important adjunct to standard 2D examinations to aid decisions regarding MV repair. Live 3D TEE technologies (miniaturization technology of the matrix array transducer) now allow one to obtain similar results in real time with obvious advances in clinical applications mainly in the operating room, giving data immediately to anesthesiologists and surgeons in the preoperative and postoperative periods. Salcedo et al. published a "state of the art" article on systematic characterization of the MV by real-time 3D TEE in which it was confirmed that several studies showed that this new technique not only provides spectacular (and immediate) images of the MV but also adds clinical value particularly in cases with complex MV prolapse. In this regard, a recent article by Tamborini et al. demonstrated that this is also true with real-time 3D TTE in patients undergoing MV repair. The overall accuracy for identification of MV scallop was 95 % (vs. surgical inspection) and the method may predict the complexity of surgical procedures. Figure 5.3 shows two cases of mitral stenosis and prolapse examined by 3D TEE.

The aortic valve may be easily evaluated by 3D TTE or 3D TEE. The morphology of the valve my be defined with high accuracy, demonstrating normality of the cusps, congenital abnormalities (bicuspid aortic valve), or acquired diseases (Fig. 5.4). Few data have been obtained on the accuracy of 3D echocardiography in the assessment of the severity of aortic valve stenosis. Very recently, Goland et al. evaluated the reproducibility and accuracy of real-time 3D TTE in 33 patients with aortic stenosis. The aortic valve area estimated by 3D TTE was compared with that estimated by 2D TTE planimetry and 2D TEE planimetry and in 15 cases with that obtained by invasive measurements. Statistical analysis showed good agreement and small absolute differences in aortic valve area between the planimetric methods. The interobserver variability was better for the 3D technique. Therefore, the authors suggested that this very rapid and novel method provides an accurate and reliable quantitative assessment of aortic stenosis.

Three-dimensional echocardiography offers a direct view to evaluate the leaflet surface of the tricuspid valve, a unique method to visualize the three leaflets simultaneously. Potentially, this offers the opportunity to study every tricuspid valve disease from different perspectives, such as from the right ventricle, from the right atrium, or from oblique planes. Leaflet coaptation and separation may therefore be visualized easily. Even though consecutive series of patients with tricuspid valve disease have not been published and no data demonstrate additional clinical value of the method, several case reports showed the

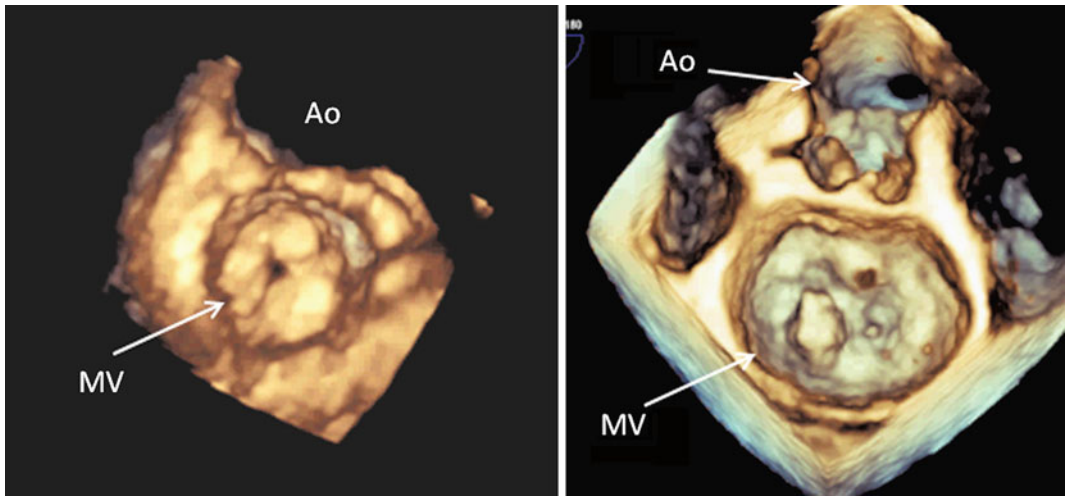

Fig. 5.3 Surgical views of a severe mitral stenosis (*left*) and of a P2 prolapse (*right*) evaluated by real-time 3D transesophageal echocardiography (TEE). *Ao* aortic valve, *MV* mitral valve

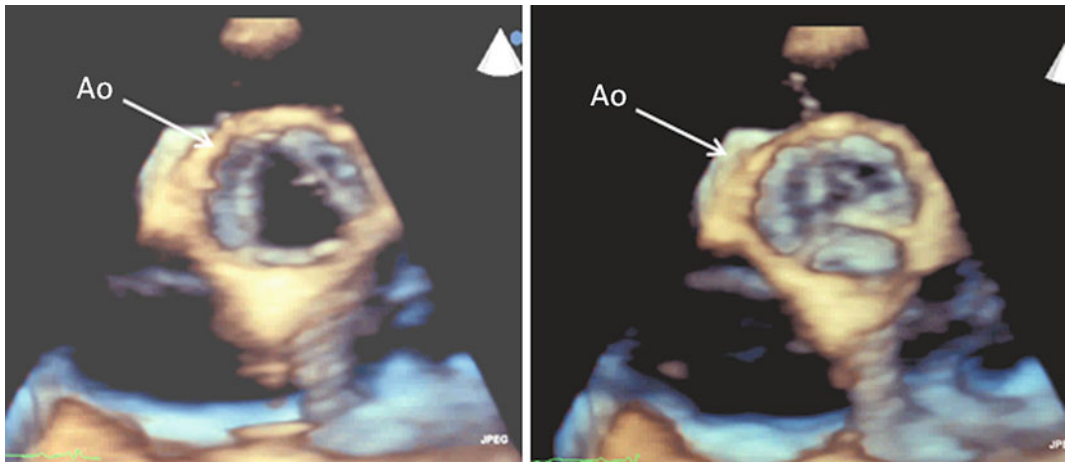

Fig. 5.4 Real-time 3D transthoracic echocardiography (TTE) of the aortic valve (*Ao*) in a systolic frame (*left*) and a diastolic frame (*right*) showing normal anatomy of the cusps

importance of this technique in Ebstein's anomaly, tricuspid stenosis, and other tricuspid valve diseases. This potential applicability in different tricuspid valve diseases may be further complemented by the measurement of RV volumes and function (ejection fraction) by off-line 3D TTE analysis. In fact, in all tricuspid valve diseases a crucial point is represented by RV function, and calculation of RV volumes is not feasible by conventional 2D echocardiography. Full-volume analysis by 3D TTE allows the acquisition of a complete data set of the RV in few seconds that allows off-line calculation of RV volume as well as recognition of tricuspid valve diseases.

5.11 Congenital Heart Diseases

The main current clinical applications of real-time TTE and 3D TEE include atrial and ventricular septal defects, several complex congenital diseases, and bicuspid aortic valve. In

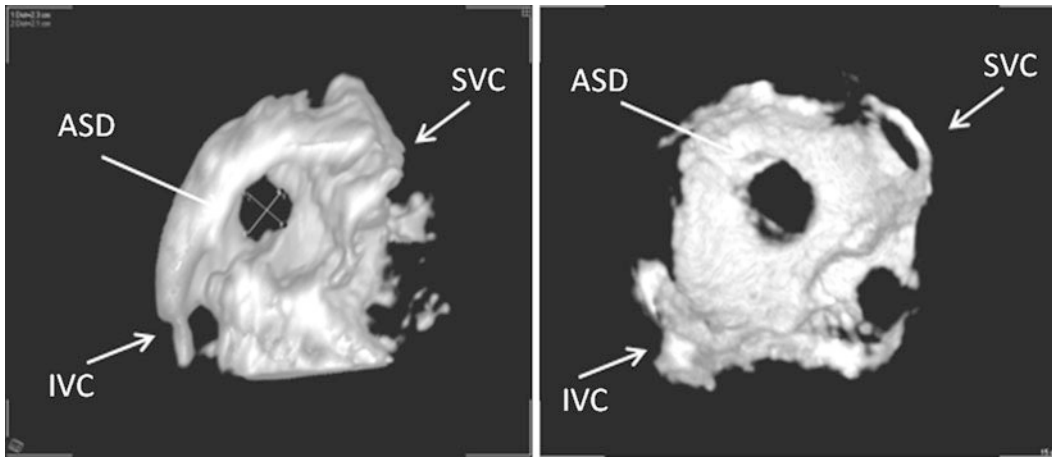

Fig. 5.5 Two cases of ostium secundum atrial septal defects evaluated by real-time 3D TTE (*left*) and real-time 3D TEE(*right*). *ASD* atrial septal defect, *IVC* inferior vena cava, *SVC* superior vena cava

children and young adults, 3D TTE (owing to their excellent acoustic window) represents an ideal technique to visualize the complex anatomy of these diseases. The position, morphology, and relation to other cardiac structures are better defined. In atrial or ventricular septal defects, the location, size, type, and rims are easily imaged by 3D TTE and 3D TEE in most cases, thus impacting the indication for percutaneous or surgical procedures (Fig. 5.5). Moreover, these methods allow an in vivo 3D assessment of devices, providing new insights into positioning and interferences with the adjacent structures.

5.12 Cardiac Masses

Three-dimensional TTE and 3D TEE are also emerging techniques for the evaluation (particularly in the preoperative assessment) of cardiac masses, including vegetations, thrombi, and tumors. The morphology, size, and location of masses may be defined accurately, and the 3D approach facilitates understanding of the relationships with the adjacent anatomical structures (Fig. 5.6). Identification of the attachment points of vegetations and tumors may improve clinical and procedural decisions. Initial experience with real-time 3D TEE in the operating room also supports the its use in this field.

5.13 Monitoring of Percutaneous Procedures

The new generation of real-time 3D TEE proves and in pediatric patients also of 3D TTE probes provides a unique new imaging technique to monitor invasive percutaneous or surgical procedures. The pathomorphology of cardiac structures may be evaluated as may be the positions of catheters and devices during procedures. Therefore, new surgical procedures, atrial septal or patent foramen ovale percutaneous closures, aortic valve implantation (Fig. 5.7), percutaneous MV repair or commisurotomy, and electrophysiological procedures may be monitored by real-time 3D echocardiography, increasing the safety, accuracy, and efficacy of these interventions. Even though in these fields there is only initial experience, several studies have demonstrated that these new imaging techniques will become an important clinical tool. Perk et al. used real-time 3D TEE to guide 72 catheter-based cardiac interventions, and described the additional clinical value of the technique. Kronzon et al. showed the importance of the 3D diagnostic approach and guidance of the procedure in cases with mitral annuloplasty and prosthetic valve dehiscence. Moreover, initial experiences suggest that in percutaneous mitral clip procedures, 3D

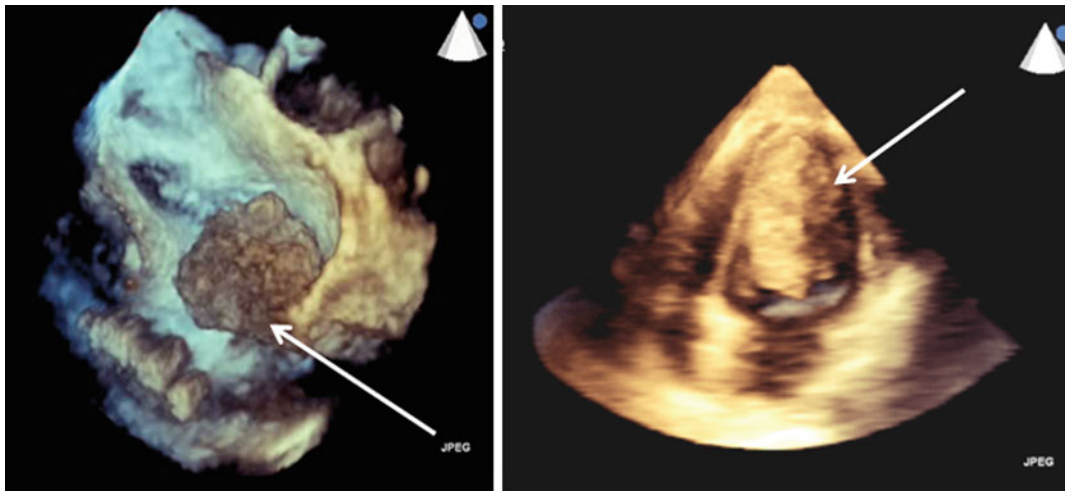

Fig. 5.6 *Left*: Left atrial myxoma visualized by real-time 3D TEE. The *arrow* shows an atypical pedunculus of the tumor attached to the posterior left atrial wall and very close to the pulmonary vein. *Right*: Real-time 3D TTE of a very large metastasis of a epidermoid carcinoma inside the left ventricle

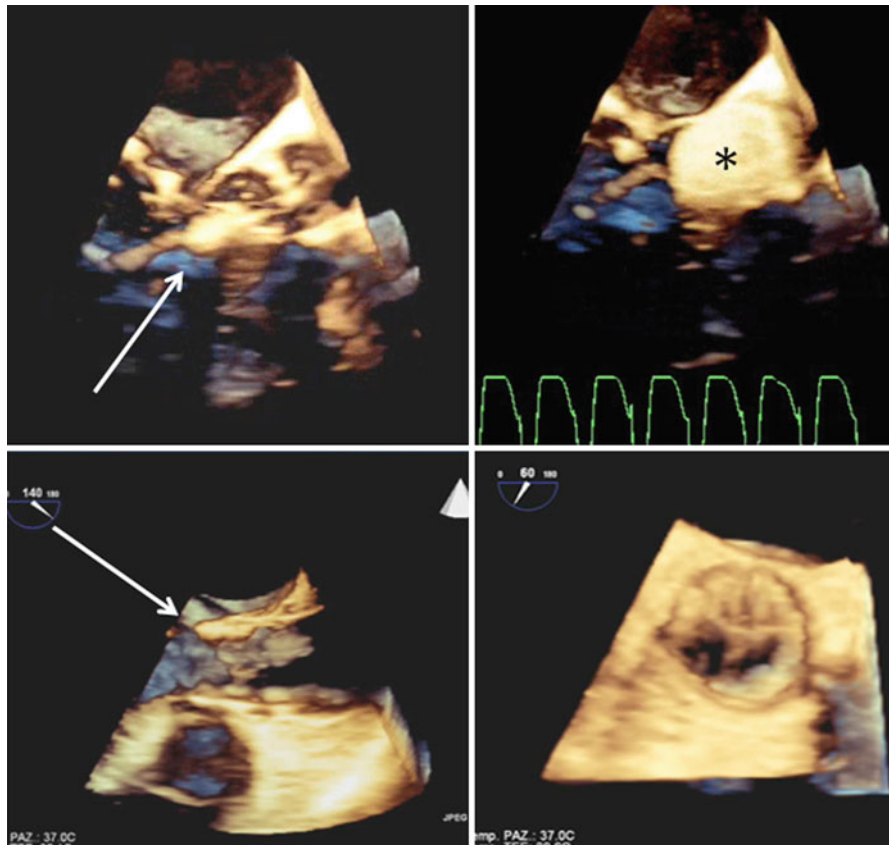

Fig. 5.7 The four main steps of a percutaneous aortic valve implantation (Edwards Sapien). The *top-left image* shows the positioning of the catheter through the valve and the *upper-right image* shows the corresponding complete opening of the balloon (*asterisk*). In the *lower images* the prosthesis has been implanted and is visualized in the long (*left*) and short (*right*) 3D views

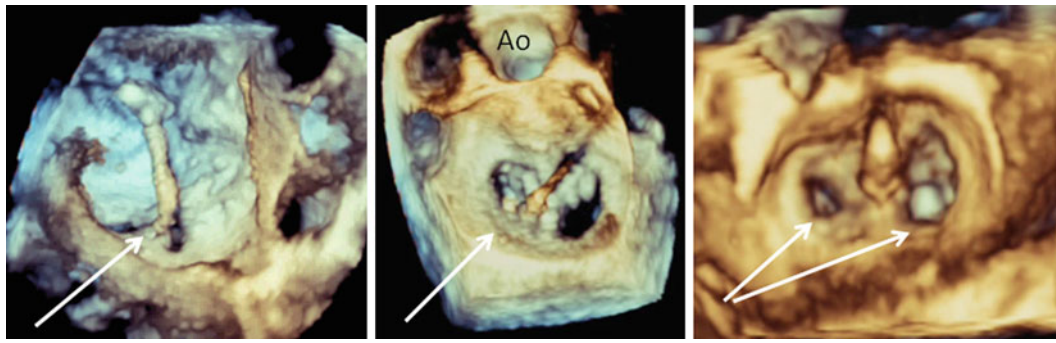

Fig. 5.8 Mitral clip implantation. In the *left image* the *arrow* shows the passage of the device from the right to the left atrium approaching the mitral valve. In the *middle image* the device is grasping the P2-A2 scallops of the mitral leaflets. In the *right image* the *arrows* show the double orifices created by the device, which is clearly seen in the center of the valve

TEE appears to be superior in comparison with sole 2D TEE monitoring (Fig. 5.8).

5.14 Monitoring of Cardiac Surgery

Multiplane 2D TEE introduced in the early 1990s has significantly improved TEE during cardiac surgery. Real-time 3D TEE has the potential to become a routine application also in this field, particularly in valve surgery, surgery to correct congenital abnormalities, and complex surgical procedures. Our first experience in 120 examinations clearly shows the feasibility, excellent imaging quality, and additional clinical value of these techniques mainly in valve surgery (either repair or replacement) not only in the preoperative period, but also in evaluating postoperative complications, as well as in cardiac mass resection.

5.15 Future Perspectives

Advances in both microindustrial design and computer technology will further reduce the size of transducers, improve temporal and spatial resolution, and permit single-beat acquisition with simple quantitative analysis. Finally, a change in display to 3D images of the heart may improve the virtual dynamic reality of the method, facilitating communication, training, and interventional procedures.

Further Reading

Tamborini G, Muratori M, Maltagliati A et al (2010) Preoperative transthoracic real time three-dimensional echocardiography in patients undergoing mitral valve repair: accuracy in cases with simple vs complex prolapse lesions. Eur J Echocard 11: 778–785.

Goland S, Trento A, Iida K, Czer LS, De Robertis M, Naqvi TZ, Tolstrup K, Akima T, Luo H, Siegel RJ (2007) Assessment of aortic stenosis by three-dimensional echocardiography: an accurate and novel approach. Heart. 93(7):801–807. Epub May 8 2007 [Epub ahead of print].

Gripari P, Tamborini G, Barbier P, Maltagliati A, Galli C, Muratori M, Salvi L, Sisillo E, Alamanni F, Pepi M (2010) Real-time three-dimensional transoesophageal echocardiography: a new intraoperative feasible and useful technology in cardiac surgery. Int J Cardiovasc Imaging 26:651–660

Kapetanakis S, Kearney MT, Siva A, Gall N, Cooklin M, Monaghan MJ (2005) Real-time three-dimensional echocardiography: a novel technique to quantify global left ventricular mechanical dyssynchrony. Circulation. 112(7):992–1000

Kronzon I, Sugeng L, Perk G, Hirsh D, Weinert L, Garcia Fernandez MA, Lang RM (2009) Real-time 3-dimensional transesophageal echocardiography in the evaluation of post-operative mitral annuloplasty ring and prosthetic valve dehiscence. J Am Coll Cardiol. 53(17):1543–1547.

Marsan NA, Bleeker GB, Ypenburg C, Van Bommel RJ, Ghio S, Van de Veire NR, Delgado V, Holman ER, van der Wall EE, Schalij MJ, Bax JJ (2008) Real-time three-dimensional echocardiography as a novel approach to assess left ventricular and left atrium reverse remodeling and to predict response to cardiac resynchronization therapy. Heart Rhythm. 5(9): 1257–1264.

Mor-Avi V, Sugeng L, Lang R (2009) Real time 3-dimensional echocardiography. An integral component of the routine echocardiographic examination in adult patients? Circulation 119:314–329

Pepi M, Tamborini G, Maltagliati A et al (2006) Head-to-head comparison of two- and three-dimensional transthoracic and transesophageal echocardiography in the localization of mitral valve prolapse. J Am Coll Cardiol 48(12):2524–2530

Perk G, Lang R, Garcia-Fernandez M et al (2009) Use of real-time three-dimensional echocardiography in intracardiac catheter based interventions. J Am Soc Echocardiogr 22:865–882

Salcedo E, Quaife R, Seres T et al (2009) A frame work for systematic characterization of the mitral valve by real-time three-dimensional transesophageal echocardiography. J Am Soc Echocardiogr 22:1087–1099

Soliman OI, Geleijnse ML, Theuns DA, van Dalen BM, Vletter WB, Jordaens LJ, Metawei AK, Al-Amin AM, ten Cate FJ (2009) Usefulness of left ventricular systolic dyssynchrony by real-time three-dimensional echocardiography to predict long-term response to cardiac resynchronization therapy. Am J Cardiol. 103(11):1586–1591. Epub Apr 8 2009. [Epub ahead-ing of print]

Zamorano J, Cordeiro P, Sugeng L, Perez de Isla L, Weinert L, Macaya C, Rodríguez E, Lang RM (2004) Real-time three-dimensional echocardiography for rheumatic mitral valve stenosis evaluation: an accurate and novel approach. J Am Coll Cardiol. 43(11):2091–2096

Part III

Essential Functional Echo-Anatomy

The Left Ventricle

6

Armando Sarti, Claudio Poli, and Silvia Marchiani

6.1 Introduction

The study of left ventricular (LV) function is crucial in the emergency department and the ICU. The left ventricle comprises an inflow and an outflow tract, the papillary muscles, and the mitral subvalvular apparatus. The two papillary muscles stick to the free wall. The transthoracic views that allow the assessment of the left ventricle are the parasternal long-axis view, the parasternal short-axis view, the apical four-chamber view, the apical two-chamber view, the apical five-chamber view (outflow tract), the apical three-chamber view (outflow tract and mitral view), and the subcostal view. The main transesophageal views are the mid-esophageal four-chamber view, the mid-esophageal two-chamber view, the mid-esophageal long-axis view, and all transgastric and deep transgastric views. The myocardial echo density is usually a bit lower than that of the valves. The myocardial tissue echo structure should be uniform. Apparent marked heterogeneity of the tissue is observed in some cardiomyopathies, such as amyloidosis and hypertrophic cardiomyopathy. The wall thickness is generally uniform, although in elderly patients, particularly if they are hypertensive, it is common to find asymmetric hypertrophy at the basal portion of the septum, proximal to the outflow tract. Ventricular interdependence must be always kept in mind. Thus, the abnormalities of LV shape and function always imply an effect on the morphology and function of the right ventricle, and vice versa.

6.2 Standard Measures

Standard measurements of the left ventricle are derived in parasternal long-axis or parasternal short-axis (transthoracic echocardiography, TTE) or transgastric (transesophageal echocardiography, TEE) M-mode from the edges of the structures. If in M-mode it is impossible to achieve alignment with the largest part of the left ventricle crossing the septum and the posterior wall in a perpendicular way, one can take measurements directly in two dimensions, although this way they may be less precise and often underestimated. The thickness of the septum, the cavity diameter at the widest point just below the mitral valve, and the posterior wall thickness are measured preferably in a M-mode track which includes a number of cycles, both when the heart is completely filled in diastole (ECG R wave) (Fig. 6.1) and at the maximum emptying in systole (normally half of the ECG T wave). The normal septum movement is toward the LV posterior wall. An asynchrony of the septal wall movement is observed in left bundle

A. Sarti (✉)
Department of Anesthesia and Intensive Care,
Santa Maria Nuova Hospital, Florence, Italy
e-mail: armando.sarti@asf.toscana.it

A. Sarti and F. L. Lorini (eds.), *Echocardiography for Intensivists*,
DOI: 10.1007/978-88-470-2583-7_6, © Springer-Verlag Italia 2012

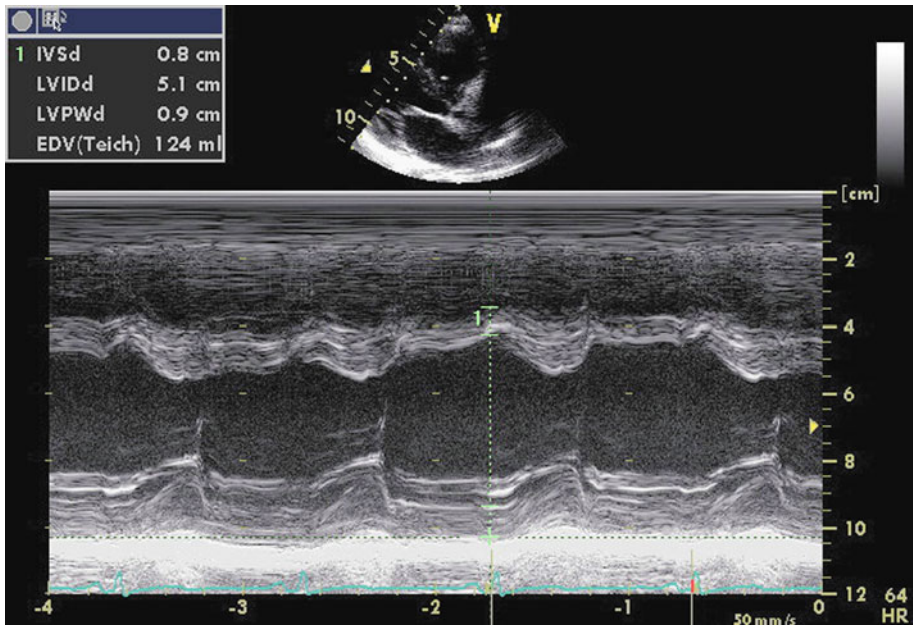

Fig. 6.1 Parasternal long-axis (transthoracic echocardiography, TTE) M-mode image just below the mitral valve: end–diastolic measurements

branch block. An abnormal movement, toward the right ventricular free wall in systole, is observed when there is a right ventricular systolic pressure overload, or diastolic volume overload, (septal dyskinesia, "right working septum"). Normal values differ with gender and size of the subject and are shown in tables of normal values. Common values in telediastole are a LV cavity diameter of 4.2–5.9 cm in men and 3.9–5.3 cm in women and a septal and posterior wall thickness of 0.6–1.0-cm in men (males) and 0.6–0.9 cm in women.

In M-mode, the normal distance between the septum and the maximum diastolic excursion of the mitral valve (mitral *E* wave corresponding to the rapid ventricular filling) must not exceed 1 cm. A wider gap shows a ventricular dilatation with LV dysfunction (Fig. 6.2).

6.3 Global Systolic Function

The left ventricle is a pump that continuously changes its complex performance according to many factors. Starting from any given level of contractility (dP/dt), the left ventricle empties in a variable fraction, from diastole to systole [aortic ejection fraction (EF), systolic volume, stroke volume], depending on the degree of the cavity filling, which depends on both preload and afterload. LV preload is related to pulmonary venous return, left atrial pressure, LV wall active relaxation and distensibility. LV afterload is related to the arterial elastic aortic distensibility (impedance), the transmural pressure, and the systemic vascular resistance. Ventricular filling is related to stroke volume by the Frank–Starling law, which accounts for an increase in stroke volume depending on increased filling of the cavity up to a plateau, which depends on the state of contraction. Beyond this plateau, further increase in filling pressure does not change the systolic ejection, but overloads the pulmonary circulation. A healthy heart has significant reserve for increasing ejection according to Starling's law, whereas as LV function worsens, this reserve progressively reduces to zero. In this case, in response to a volume load there is not an increase in stroke volume, but only an increased pulmonary pressure, which increases the amount of lung water. Generally, a left

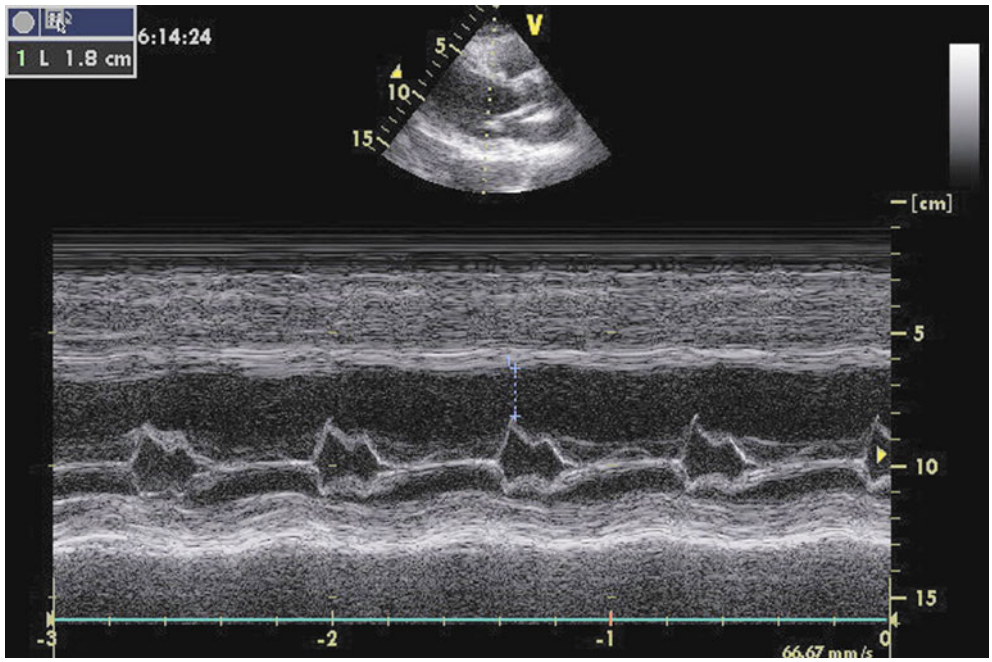

Fig. 6.2 Parasternal long axis (TTE) M-mode image at the level of mitral valve: increased distance between the septum and the maximum diastolic excursion of the mitral valve. (From Sarti with permission)

ventricle that loses the normal "truncated rugby ball" shape and becomes more spherical does not exhibit a good systolic function. All ICU treatments interfere with the preload, contractility, and afterload variables. For example, lifting of the patient's legs (passive leg raising), or a rapid intravenous fluid bolus, produces an increase in preload (greater vena cava size and lowering respiratory variations). The consequent filling of cavities produces or does not produce, depending on Starling's law, a significant increase in stroke volume, the so-called fluid responsiveness. Only repeated assessments of changes in stroke volume in response to a preload charge (administration of fluids or passive raising of the patient's legs) allow the reconstruction of the Frank–Starling curve of the patient's heart, according to the current cardiovascular condition (infusion of cathecolamines, mechanical ventilation). Indeed, hemodynamic drugs act at all levels, such as contraction, the venous tone, and the arterial vascular resistance. Mechanical positive pressure ventilation generally worsens the right ventricular function (increasing pulmonary vascular resistance), whereas it improves the LV function because of an effect on the transmural myocardial pressure. The LV systolic function, intended as the contractility state, is not easily measurable in clinical practice. The contour of a mitral regurgitation jet, if any, both as the peak level and as the speed/time curve contour profile, is related to dP/dT, which is the "true" contractility. The EF or other less precise but conceptually similar measures such as diastolic–systolic changes in diameter (fractional shortening, FS) or in area (fractional area change, FAC) are not specific measures of contractility, since they are greatly affected by both LV preload and LV afterload. Nevertheless, EF, FS, and FAC are still considered standard measures of systolic function. EF correlates well with mortality, and it is widely used as a measure of global systolic function in a stable condition, but may be misleading for a critically ill unstable patient mainly because of sudden changes of both preload and afterload.

LV wall kinetic motion and thickening are used for studying the regional systolic function (regional wall motions abnormality) (see later).

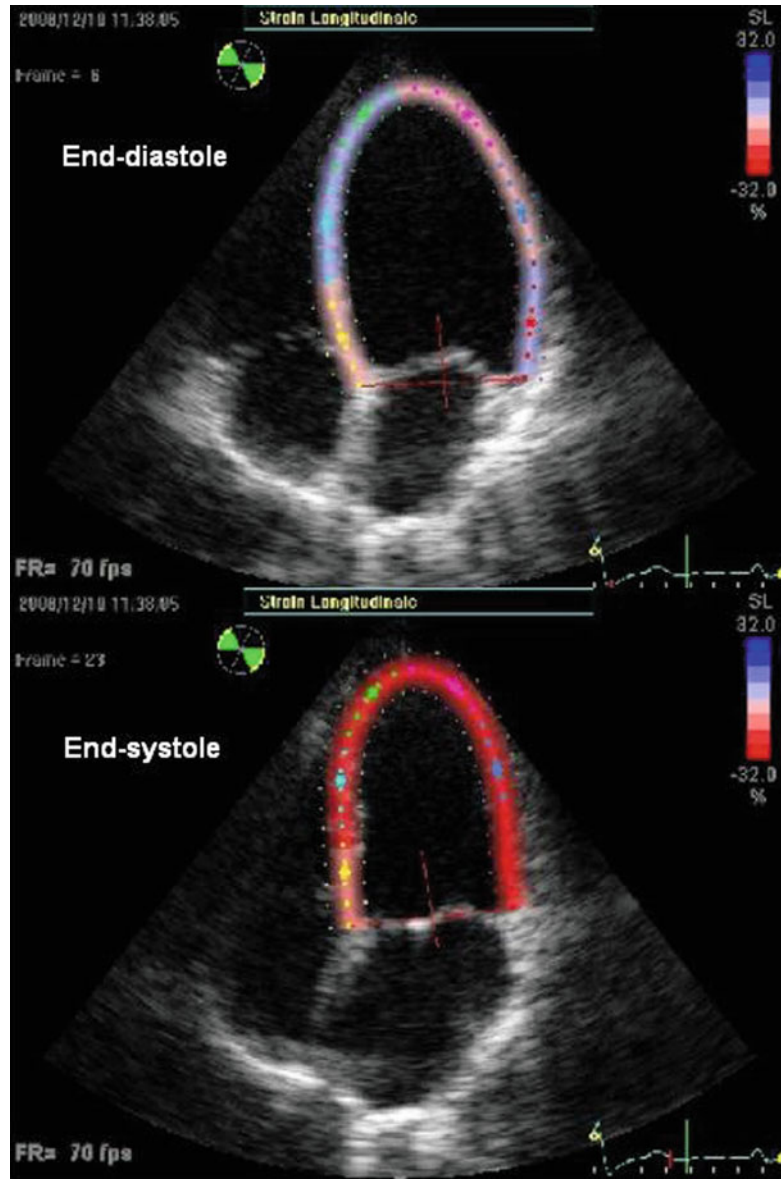

Fig. 6.3 Apical four-chamber view (TTE). Left ventricular (LV) longitudinal speckle tracking

6.3.1 Left Ventricular Rotation

The human heart rotates around its longitudinal axis during the cardiac cycle. The apex rotates clockwise during early isovolumetric contraction and counterclockwise during the LV ejection period, whereas at the same time the LV base rotates in the opposite direction. In the diastolic phase, there is untwisting, the LV recoil. Systolic LV torsion helps systolic ejection and also stores energy by twisting and shearing myofibers. Quantification of LV rotation is a sensitive tool to detect early systolic and diastolic function impairment. Nowadays it is possible to study LV rotation by using speckle tracking imaging (three-dimensional TTE), but a high-quality image is necessary and the interoperator variability is still

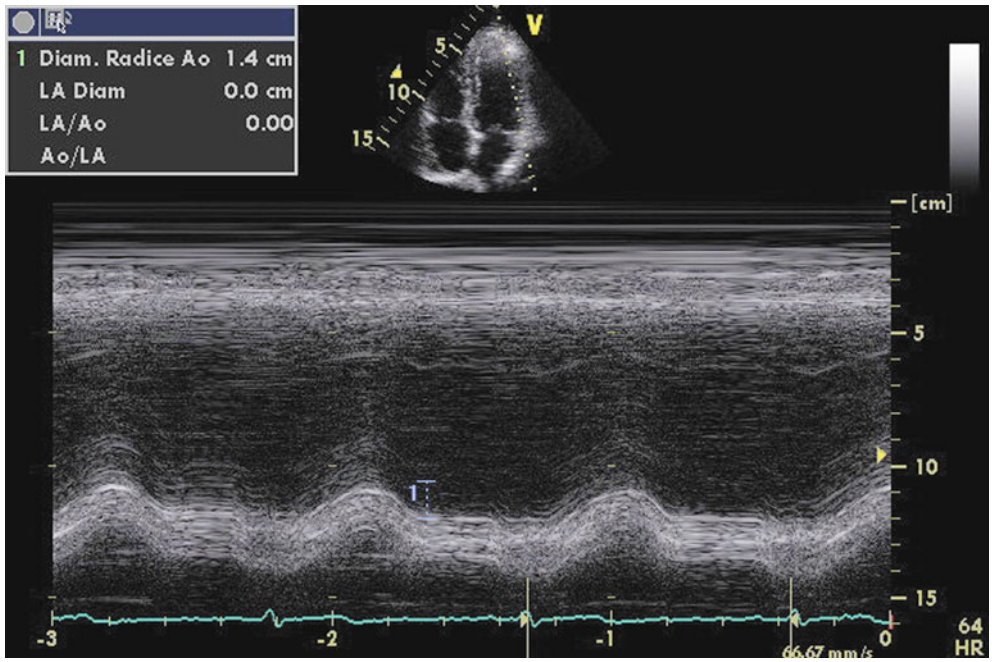

Fig. 6.4 Apical four-chamber (TTE) M-mode image. Lateral mitral ring kinetics (longitudinal shortening). (From Sarti with permission)

high (Fig. 6.3). Recently, a computed TEE system has been developed for quantifying automatically LV rotation.

6.3.2 Longitudinal Shortening

An immediate estimation of the systolic function is obtained in M-mode by observing the systolic shift of the lateral mitral ring toward the apex in the apical four-chamber view (TTE) or the mid-esophageal four-chamber view (TEE). The highest and the lowest point of the M-mode sinusoid wave are measured, having put the cursor along the mitral ring (Fig. 6.4). A value greater than 13 mm is normal, and a value below 13 mm represents beginning of a systolic dysfunction.

6.3.3 Fractional Shortening

This is the simplest parameter for quantifying the global systolic function . In the M-mode parasternal long-axis or parasternal short-axis view (TTE) or the transgastric basal short-axis view (TEE), it is difference between the LV diastolic and systolic internal diameters divided by the LV diastolic internal diameter: (LVIDd − LVIDs/LVIDd) × 100 (Fig. 6.1).

Normal values for FS range from 25 to 45 %. Normally this parameter is well correlated with the EF. The major limitation is that the systolic function of an ellipsoid, such as the left ventricle, is estimated by the change of a single diameter. Any modification of shape or alteration in the regional kinetics is not considered. So, for the FS to be an expression of the global function, it is necessary for the LV kinetics to be homogeneous along the whole ventricle.

6.3.4 Fractional Area Change

Instead of the diameters, it is possible to evaluate the area changes, end-systolic and end-diastolic, in a cross section of the heart, in the parasternal short-axis view at the mid-papillary level (TTE) (Fig. 6.5) or in the transgastric mid short-axis view (TEE). This measure is also expressed as a

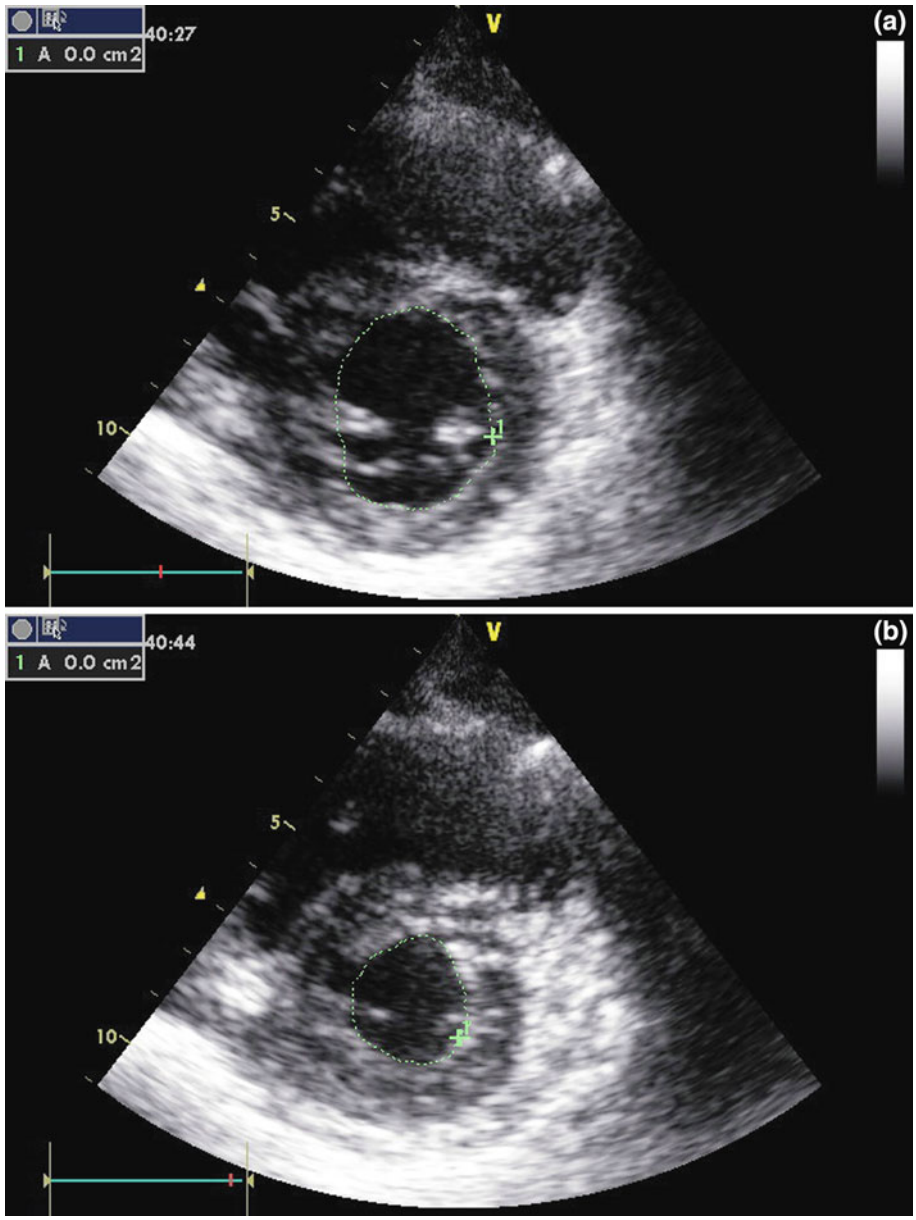

Fig. 6.5 Parasternal short-axis view (TTE). **a** LV end-diastolic area. **b** LV end-systolic area. (From Sarti with permission)

fraction: (LVEDA − LVESA/LVEDA) × 100, where LVEDA is LV end-diastolic area and LVESA is LV end-systolic area. The normal end-diastolic area indexed for body surface area is equal to or greater than 5.5 cm^2/m^2. The normal FAC value is or exceeds 45 %. Again, regional variations in shape or kinetics of the left ventricle are not recognized by this measure, which represents a single section plane of the left ventricle, at the mid-papillary level. Nevertheless, FAC and LVEDA (often in the literature end-diastolic area), although reliable only in the presence of a uniform

contraction, are easy to obtain and appear in many ultrasound-guided algorithms for classification and treatment of the patient's hemodynamics.

6.3.5 Ejection Fraction

Ejection fraction (EF) is the gold standard to measure global systolic function In fact, as already mentioned, EF is not a specific measure of contractility. Rather, it reflects the interaction between preload, contractility, and afterload. It is the amount of blood (stroke volume) pumped out the left ventricle in each cardiac cycle, reported as a percentage of the end-diastolic volume: EF = (LVEDV − LVESV/LVEDV) × 100, where LVEDV is LV end-diastolic volume and LVESV is LV end-systolic volume. The normal value is greater than 50 %. From 50 to 40 % there is a slight decrease, whereas from 40 to 30 % there is a significant reduction of the pump function. Below 30 % a severe reduction in global systolic function is diagnosed. A good emptying of the left ventricle (high EF) in a hypotensive patient, if there is no concomitant hypovolemia, evokes the suspicion that either ventricular outflow is in part ejected into a low-pressure chamber, as in mitral insufficiency, or that the ventricle empties well for a significant reduction in afterload, such as in vasoparalysis, as often happens in sepsis syndromes. In the latter case, the infusion of norepinephrine to restore vascular resistance and maintain blood pressure better shows the real state of contraction, which may be a decreased EF, unmasked by the normalized afterload. If there is severe mitral insufficiency, EF is considered normal if it exceeds 60 %. The other measures of ejection based on variations of diameters and areas should be reassessed if there is significant mitral regurgitation.

It is better consider that since EF is related to diastolic volume, even a very low EF such as 25 % in a patient with dilated cardiomyopathy may reflect an adequate or only slightly reduced stroke volume, because it is 25 % of a greatly increased end-diastolic volume, and thus a normal or near-normal cardiac output at rest. In these cases an effort, however slight, or an acute disease, unmasks the inability of the left ventricle to increase its performance, that is, stroke volume and cardiac output, in response to increased oxygen demand. Then all the symptoms and signs of acute cardiac failure become manifest.

The method now recommended for the measurement of EF is the modified Simpson method that estimates systolic and diastolic volumes in two different planes perpendicular to each other, in practice in the apical apical four-chamber and apical two-chamber projections (TTE) or the mid-esophageal four-chamber and mid-esophageal two-chamber projections (TEE). The ultrasound machine automatically calculates the values for the media. The inner edges of the LV endocardium, including the papillary muscles, are outlined using the "trackball" tracer both in diastole and in systole. It is necessary, therefore, that the endocardium be visible along the entire cavity and for the entire cycle. The maximum length from the apical endocardium to the mitral annulus is also measured. The calculation, which results in a volume (area for length), is automatically computed by splitting the cavity into small cylinders (Fig. 6.6). It is important to search for the maximum length of the left ventricle, the true long axis, avoiding cutting the LV ellipsoid with an oblique section (in this case excessive mobility and altered shape of the apex are showed on the display). Also, cardiac cycles originating from extrasystoles should be avoided. For better accuracy, especially if the aortic ejection is particularly variable (i.e., changes in systolic blood pressure monitored invasively or changes in the maximum amplitude of the plethysmographic wave measured by a pulse oximeter), the measurement must be repeated for three cycles in sinus rhythm and for at least five cycles if there is atrial fibrillation. Note that for a skilled echocardiographer, according to data confirmed in the literature, the simple inspection of some cardiac cycles in motion ("eyeball measurement") provides a reliable estimate of EF, which correlates well with more accurate measurements.

6.3.6 Tissue Doppler Imaging

The speed wave produced by the movement of myocardial tissue at the lateral or septal mitral ring in the apical four-chamber view (TTE) or

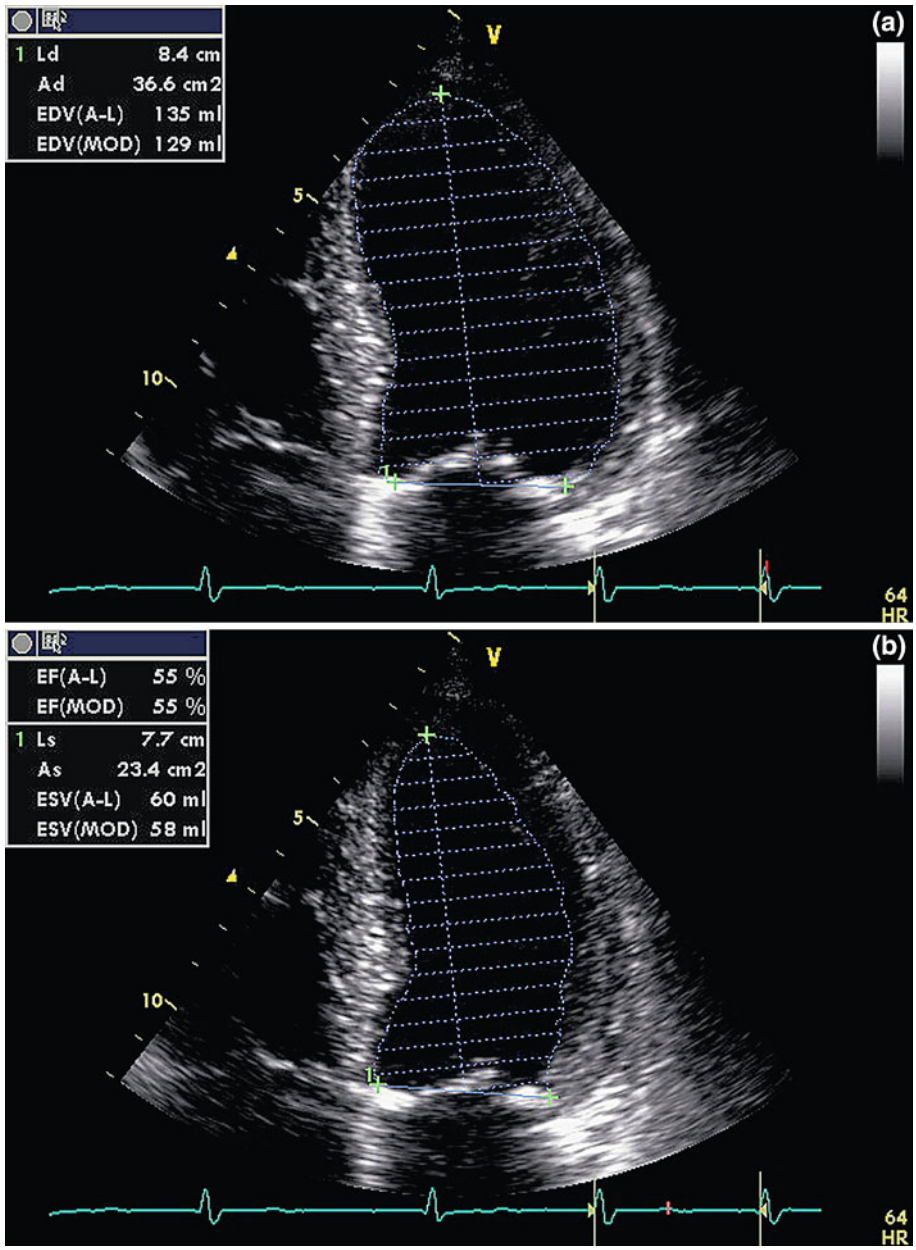

Fig. 6.6 Apical four-chamber view (TTE). **a** LV end-diastolic volume. **b** LV end-systolic volume. See the text

the mid-esophageal four-chamber view (TEE) is related to EF. Tissue Doppler imaging (TDI) thus allows an immediate assessment of global LV systolic function. The normal systolic velocity (S wave; Fig. 6.7) is 8–10 cm/s at the lateral ring side. Below 8 cm/s there is a systolic depression, reflecting the corresponding reduction of the EF. The function is reduced gradually between 8 and 3 cm/s. A severe alteration, corresponding to EF < 30 %, is below 3 cm/s.

6.3.7 Ventricular Wall Kinetics

The following walls of the left ventricle are examined with TTE:

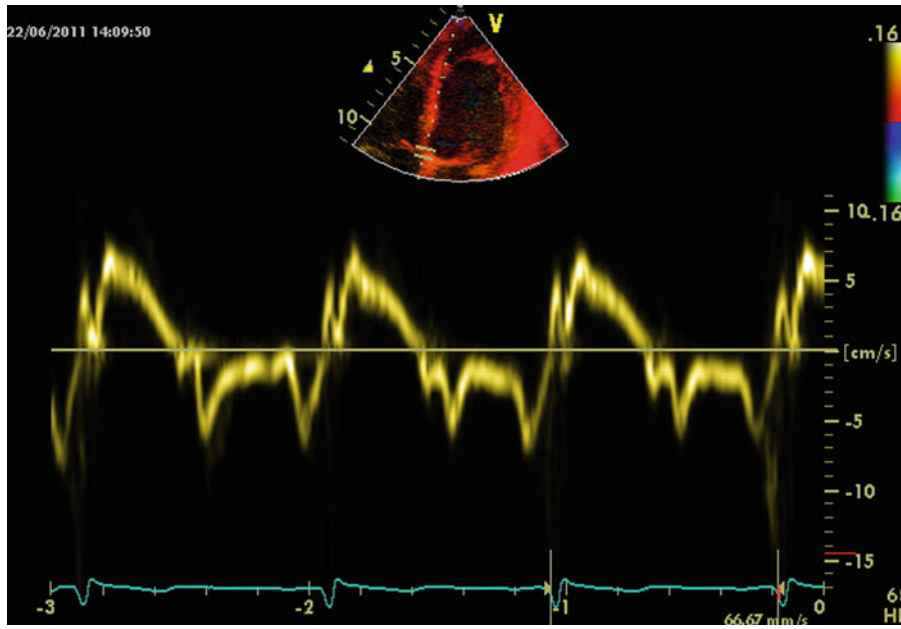

Fig. 6.7 Apical four-chamber view (TTE). LV tissue Doppler imaging at the septal level

- The anteroseptal and posterior walls: parasternal long-axis and apical three-chamber views
- All the walls at mid-papillary level: parasternal short-axis view
- The septal and lateral walls: apical four-chamber view
- The inferior wall on the left of the display and the anterior wall on the right: apical two-chamber view
- The septal and posterior–lateral walls: subcostal view

The following LV walls are examined using TEE:

- The septal and lateral walls: mid-esophageal four-chamber view
- The inferior (on the left on the display) and anterior (on the right on the display) walls: mid-esophageal two-chamber view
- The posterior (on the left on the display) and anteroseptal (on the right on the display) walls: mid-esophageal long-axis view
- All the walls at the mid-papillary level: transgastric mid short-axis view
- All the walls at the basal level: transgastric basal short-axis view

Although there are variations, it can be stated that:

- The anterior wall, most of the septum, and the apex are typically perfused by the left descending artery.
- The lateral wall and the posterior wall are perfused by the circumflex artery.
- The inferior wall is perfused by the right coronary artery (Fig. 6.8).

For the assessment of the wall motion, each wall in the four-chamber view and in the two-chamber view is divided into three segments: basal, medial, and apical, which are characterized by a number. We can examine these segments also in the parasternal short-axis (TTE) or transgastric (TEE) view (the only one that shows all the sections of myocardium perfused by the three main coronary trunks) at the basal (six segments), medial (six segments), and apical (four segments) levels. This 16-segment model has recently been integrated with the 17th segment, the apical cap, without myocardial endocardial borders (Fig. 6.9), which is useful for comparison with other cardiac imaging techniques (magnetic resonance imaging, scintigraphy, CT).

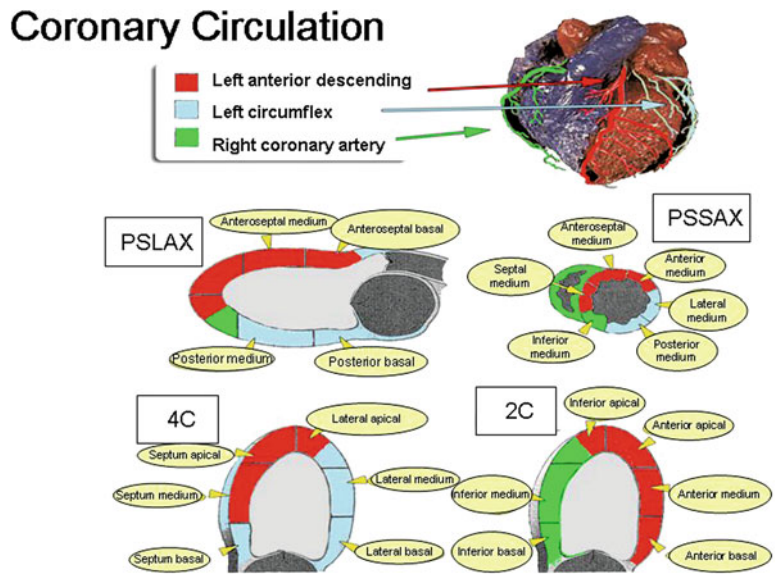

Fig. 6.8 Summary of the ventricular walls and relative coronary perfusion in various TTE views. *2C* two chamber, *4C* four chamber, *PSLAX* parasternal long axis, *PSSAX* parasternal short axis. (Modified from Sarti with permission)

The wall contractility is evaluated by two simultaneous assessments:

1. Systolic thickening, which must typically be greater than 30 %
2. The convergent movement of the wall toward the LV lumen

The former is prevalent in the assessment of the kinetics because the latter is also affected by tractions exerted by adjacent tissues. The study of regional kinetics may not be easy for the beginner. The index finger placed on the "display" in the center of the LV cavity, in the parasternal short-axis view (TTE) or the transgastric view (TEE), can help in the evaluation of centripetal motion and thickening. The individual segments are qualitatively evaluated for:

1. Normal contraction
2. Hypokinesia (reduction)
3. Akinesia (absence)
4. Dyskinesia (paradoxical centrifugal motion in systole)
5. Aneurysm (a visible deformation both in systole and in diastole, which causes an excessive thinning of the wall)

Changes 2–5 are defined as regional wall motion abnormalities. From the findings of the individual segments, it is then possible to indicate the affected coronary artery (Fig. 6.8). By assigning a score of contractility to each segment, one can calculate the wall motion scoring index. It is the sum of the scores divided by the number of segments studied (Table 6.1). The normal value is therefore 1.

6.4 Diastolic Function

6.4.1 Introduction and Background

The heart is a variable-volume pump inserted into a system of elastic tubes with one-way valves, filled with blood. So the pump function is not only related to the systolic squeeze, but it also depends on the degree of relaxation of the heart chambers, which creates the reserve volume required for an effective ejection. Echocardiography is the only clinical method that allows easy assessment of LV diastolic filling. Diastolic function, which has only recently been thoroughly and regularly evaluated, may be considered "the dark side of the moon" of the cardiac function. Diastolic dysfunction, although not

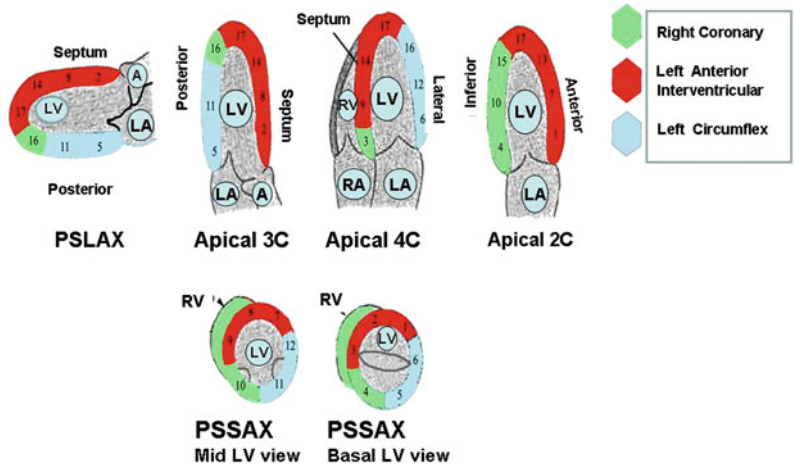

Fig. 6.9 Classification of LV myocardial segments and coronary perfusion in different TTE views. *A* ascending aorta, *2C* two chamber, *3C* three chamber, *4C* four chamber, *LA* left atrium, *LV* left ventricle, *PSLAX* parasternal long axis, *PSSAX* parasternal short axis. (Modified from Sarti with permission)

Table 6.1 Wall motion scoring index

Score	Definition
1	Normal. Thickening of more than 30 % and movement toward the inner cavity
2	Hypokinesia. Reduction of movement and thickening of less than 30 %
3	Akinesia. Absence of thickening (a remnant movement can be transmitted)
4	Dyskinesia. Paradoxical movement outward in systole
5	Aneurysm. Permanent dilation deformation in both diastole and systole with a thin and hyper-echo-reflective wall

The score is the sum of individual segment scores divided by the number of segments examined. A normal left ventricle has a wall motion scoring index of 1.

present at rest, often appears during myocardial stress due to myocardial ischemia or during weaning from mechanical ventilation. Many pathological conditions which are often seen in the emergency department and ICU and are characterized by impending pulmonary edema and low cardiac output with normal EF are well explained by diastolic dysfunction. As the left ventricle relaxes slowly and compliance decreases, cardiac filling is reduced and the pressure load in the left atrium increases. The overloaded left atrium tends to enlarge. Pulmonary capillary pressure is also increased, thus facilitating interstitial edema and ultimately alveoli flooding. The increase in lung water can be easily studied by ultrasonography of the lung (comet tails; see Chaps. 34 and 45). Most of the coronary flow of the left ventricle occurs during the diastolic phase. Therefore, a deficit of coronary perfusion (e.g., when associated with a reduction in diastolic time, such as during tachycardia, or in hypotension) is accompanied by an impaired relaxation, thus reducing cardiac output and increasing pulmonary capillary pressure. Concentric LV hypertrophy and myocardial fibrosis reduce compliance and therefore the distensibility of the cavity. These mechanisms are the most common precipitating cause of perioperative ischemia, even without significant coronary obstruction, along with the increase in oxygen consumption due to tachycardia, possible high blood pressure due to pain, or reduced coronary perfusion pressure due to hypotension. In fact, perioperative myocardial infarctions do not

always show a thrombotic coronary obstruction. Often, they are characterized by more or less extended subendocardial necrosis. The onset of high-frequency atrial fibrillation may suddenly worsen an ischemic borderline condition. So in these patients the arrhythmia should be treated promptly, often combining antiarrhythmic drugs with electric shock.

In general, diastolic dysfunction is suspected in:

- Elderly patients
- Diabetic patients
- Patients with metabolic syndrome
- Hypertensive patients
- The presence of ventricular hypertrophy
- The presence of aortic stenosis
- Restrictive heart disease

6.4.2 Phases of Diastole

Diastole is divided into four stages:

1. Isovolumetric relaxation. This is an active, energy-requiring phenomenon and therefore needs good perfusion. It begins with the closure of the aortic valve and continues until the opening of the mitral valve.
2. Rapid ventricular filling. The active muscle relaxation continues and the left ventricle is filled according to its own compliance. It starts as the ventricular pressure drops below the left atrial pressure, thus, the mitral valve opens and most of the ventricular filling occurs (diastolic *E* wave of the transmitral pulsed wave Doppler flow). Ageing can reduce the *E* wave peak.
3. Mesodiastolic phase. the flow is very slow following the minimum pressure gradient between the left atrium and the left ventricle.
4. Atrial contraction, *A* wave of the transmitral pulsed wave Doppler flow; normally 20–30 % of the total filling volume. It may increase in importance as the left ventricle becomes stiffer. This atrial filling contribution is obviously lost if there is atrial fibrillation.

6.4.3 Pulsed Wave Doppler Assessment of Transmitral Flow

The transmitral diastolic flow is examined with pulsed wave Doppler echocardiography in the apical four-chamber or two-chamber view (TTE) or the mid-esophageal four-chamber or two-chamber view (TEE) 2–3 mm beyond the level of the valve's opening. To obtain a reliable assessment, it is necessary to have good alignment of the ultrasound beam with the flow. Diastolic transmitral flow presents in succession the protodiastolic rapid filling (*E* wave), the mesodiastolic pause, and the telediastolic filling, "atrial systole" (*A* wave) (Fig. 6.10).

The parameters of interest are:

- The *E* peak velocity (72 ± 14 cm/s under the age of 50 years and 62 ± 14 cm/s above the age of 50 years).
- The *E* wave deceleration time, from the apex of the *E* wave to the isoelectric line; normal below 200 ms (below 180 ± 20 ms from 20 to 50 years and below 210 ± 36 ms above 50 years).
- The *A* peak velocity (40 ± 10 cm/s below the age of 50 years and 59 ± 14 cm/s above the age of 50 years).
- The *E*/*A* ratio. Normally, $E > A$), but *E* is usually equal to *A*, or slightly less, in older people (1.9 ± 0.6 below 50 years and 1.1 ± 0.3 above 50 years).

A stiff left ventricle leads to increased end-diastolic pressure and increased left atrial pressure. Thus, the volume of the atrium augments. Diastolic function is characterized by four stages with changes in the parameters shown above (Fig. 6.11). For heart frequencies greater than 100 beats per minute, transmitral Doppler waves are generally less recognizable. Of course, this classification does not apply if there is atrial fibrillation because of the disappearance of the *A* wave. In the course of atrial fibrillation it is possible to evaluate LV diastolic function by the *E* wave (Fig. 6.12) and the deceleration time, together with TDI (see below).

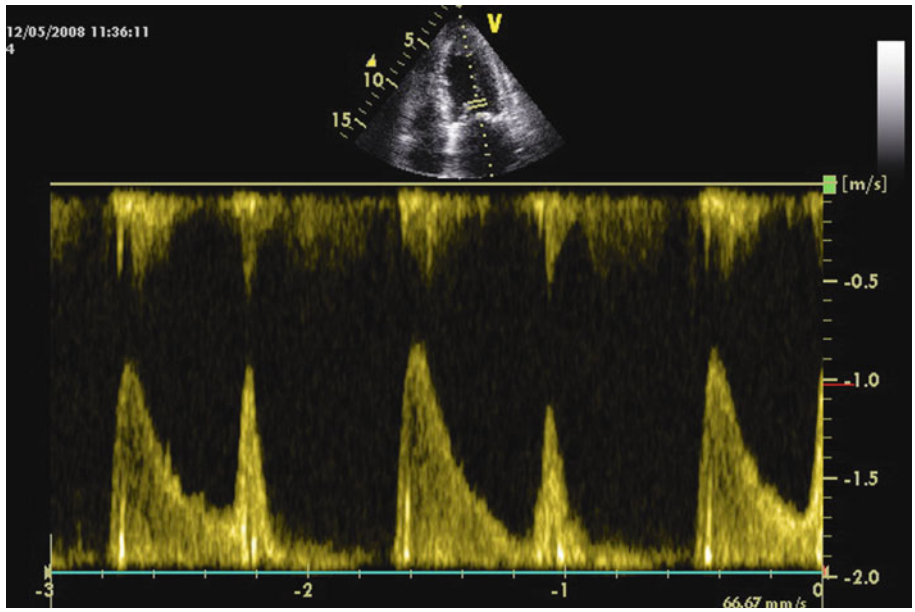

Fig. 6.10 Apical four-chamber view (TTE). Pulsed wave Doppler image of diastolic transmitral flow (normal pattern). (From Sarti with permission)

Fig. 6.11 Classification of diastolic function. See the text for details. *DT* deceleration time. (Modified from Sarti with permission)

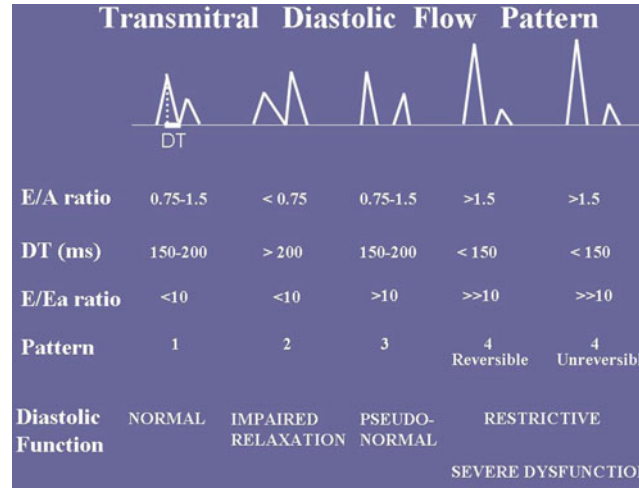

Pattern 1 is the normal one (Fig. 6.10). In altered relaxation (pattern 2), the *E* wave loses speed and the *E*/*A* ratio is reversed (Fig. 6.13). However, as the left atrial pressure progressively increases, the *E* wave rises again and the *E*/*A* ratio becomes greater than 1 again (pseudonormal, pattern 3). With advanced diastolic dysfunction, the *E*/*A* ratio becomes greater than 2 (restrictive pattern, pattern 4) (Fig. 6.14). It should be considered that as far as the *E*/*A* ratio is concerned, normal and pseudonormal functions are not distinguishable, but a heart with pseudonormal diastolic dysfunction also has other pathological changes as seen on ultrasongraphic examination such as LV hypertrophy and atrial dilatation. Moreover, any doubt can be clarified by TDI evaluation that examines directly the speed of movement of the myocardium (see below).

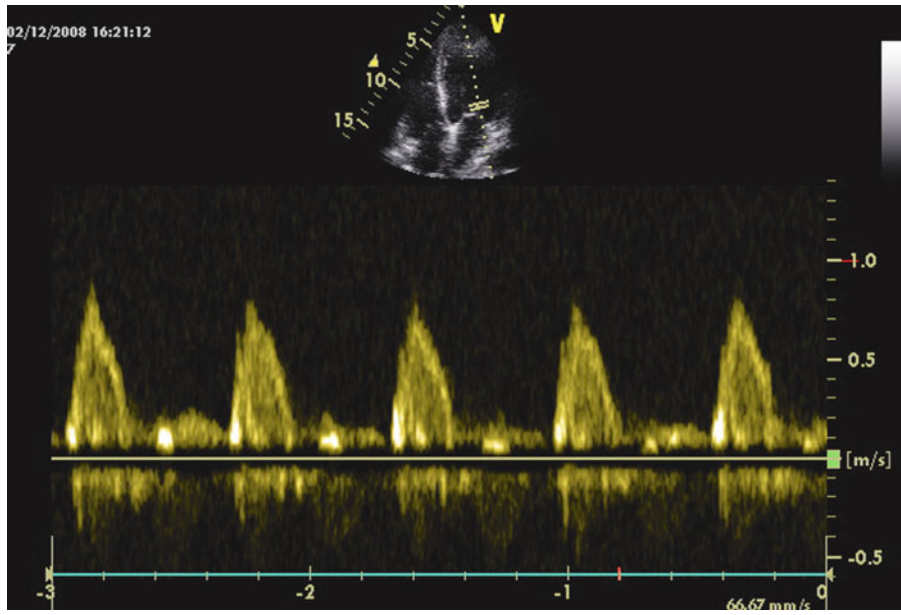

Fig. 6.12 Apical four-chamber view (TTE). Pulsed wave Doppler image of mitral flow in atrial fibrillation (absence of *A* wave). (From Sarti with permission)

The release phase of the Valsalva maneuver allows one to distinguish a reversible phase of the restrictive dysfunction from the final irreversible stage. As the restrictive pattern is still reversible, an increasing *A* wave (due to increased venous return) is observed together with an *E*/*A* ratio equal to or even greater than 1. Instead, in the irreversible phase, no significant change in the *A* wave peak is observed in the release phase of the Valsalva maneuver. In the ICU, with a mechanically ventilated patient, a sort of Valsalva maneuver may be done by stretching slowly the lungs by manual ventilation using a bag valve mask. A sudden release of the positive pressure produces the release phase of this modified Valsalva maneuver.

6.4.4 Tissue Doppler Imaging

TDI is a very sensitive technique for evaluating LV diastolic function because it directly evaluates the speed of movement of the myocardial tissue (Fig. 6.7). At the level of the lateral mitral annulus in the apical four-chamber view (TTE) or the mid-esophageal four-chamber view (TEE), a tissue Doppler wave of relaxation directed toward the base of the heart because of the LV diastolic filling expansion is recorded in diastole. This wave is called E', Ea, or Em in the literature. E' is temporally correlated with the transmitral flow Doppler *E* wave. A further tissue stretch is then recorded as an A' (or Aa or Am) wave, which is related to further LV expansion due to atrial systole and is concomitant with the Doppler *A* wave of telediastolic transmitral flow. Of course, the A' wave, like the *A* wave, disappears if there is atrial fibrillation. The parameters of interest are:

1. The speed of early relaxation, E'. Normally this is 10 cm/s or greater. A value less than 10 cm/s (or less than 8 cm/s at the septal level of the mitral annulus) defines a diastolic dysfunction.
2. The E/E' ratio (or *E*/Ea, or *E*/Em), which is the ratio between the peak velocity of early flow (pulsed wave Doppler echocardiography) and the speed of tissue relaxation movement (TDI). It is rather intuitive that the ratio between the peak flow, which depends on the transmitral pressure gradient, and the speed of

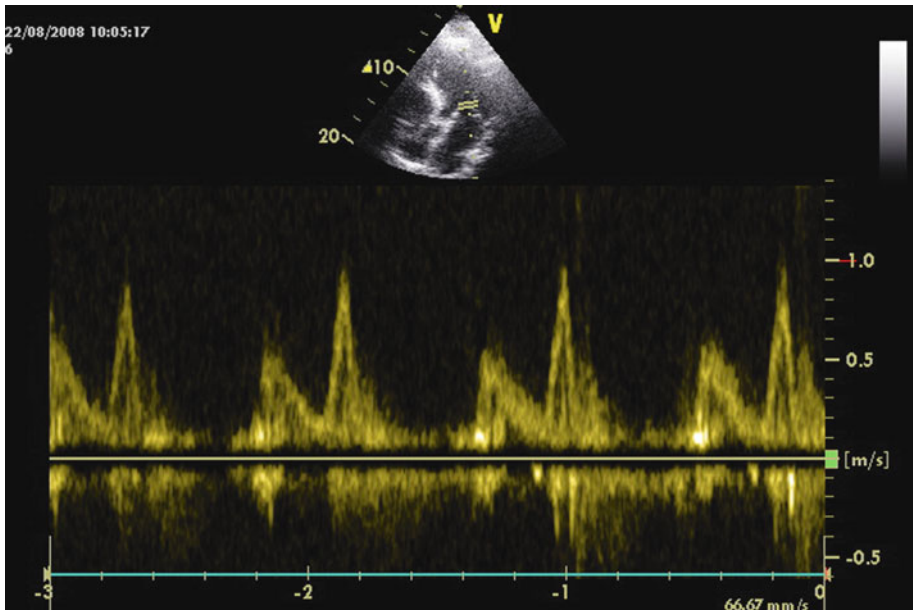

Fig. 6.13 Pulsed wave Doppler image of transmitral diastolic flow: inversion of the *E*/*A* wave. Apical four-chamber view (TTE). Pattern 2. Impaired relaxation. (From Sarti with permission)

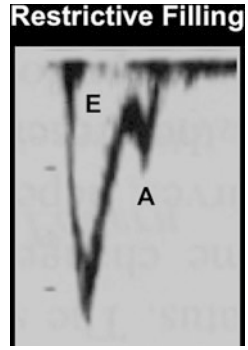

Fig. 6.14 Severe diastolic dysfunction. Trasesophageal echocardiography image of a restrictive pattern

the myocardial relaxation can represent LV filling pressure. This ratio is considered normal under 10 and abnormal (impaired diastolic relaxation) over 10. In particular, a value greater than 15 is associated with a marked increase in left atrial pressure and pulmonary capillary wedge pressure, and also with a significant increase of atrial B-type natriuretic peptide (see Chap. 25).

6.5 Myocardial Performance Index

By placing the pulsed wave Doppler sample volume between the two streams of the mitral valve (diastolic) and aortic valve (systolic) flows in the apical five-chamber view (TTE) or the deep transgastric long-axis view (TEE), one can study these two flows and the isovolumetric diastolic and systolic phases in succession:

- The isovolumetric relaxation time at the beginning of diastole.
- The isovolumetric contraction time at the beginning of systole.
- The aortic ejection time between the two (Fig. 6.15).

The myocardial performance index (MPI) is defined as $(a - b)/b$, where a corresponds to the time between closing of the mitral valve and its reopening in the next cycle (end of A wave and beginning of the subsequent E wave in transmitral flow Doppler measurements) and

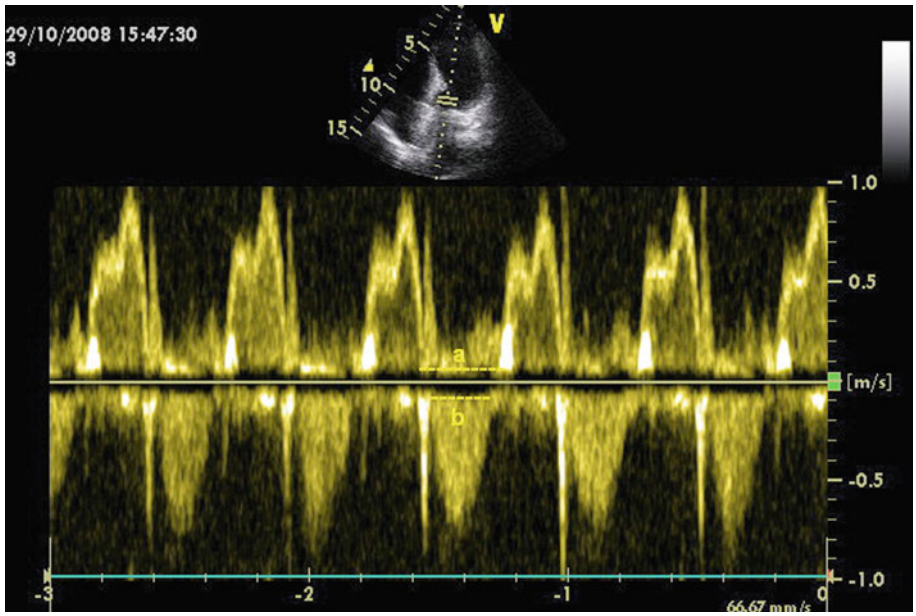

Fig. 6.15 Pulsed wave Doppler sample volume positioned between the inflow and outflow of the left ventricle **a**: is the time between the opening and closing of the mitral valve, **b**: is the aortic ejection time. Apical five-chamber view (TTE) (see the text). (From Sarti with permission)

b corresponds to the aortic ejection time, as evidenced by the Doppler flow (velocity–time integral) at the LV outflow tract (Fig. 6.15). The normal value is between 0.30 and 0.38. This index is altered both by systolic dysfunction (+d*P*/d*t*, time of isovolumetric contraction) and by diastolic dysfunction (−d*P*/d*t*, isovolumetric relaxation time) and it is therefore a general index of LV performance.

Further Reading

Bloechlinger S, Grander W, Bryner J et al (2010) Left ventricular rotation: a neglected aspect of the cardiac cycle. Intensive Care Med 37:156–163

Bouhemad B, Nicolas-Robin A, Arbelot C et al (2008) Isolated and reversible impairment of ventricular relaxation in patients with septic shock. Crit Care Med 36:766–774

Brian DH (2007) Left ventricular diastolic function. Crit Care Med 35(Suppl):S340–S347

Combes A, Arnoult F, Trouillet JL (2004) Tissue Doppler imaging estimation of pulmonary artery occlusion pressure in ICU patients. Intensive Care Med 30:75–81

Lang RM, Bierig M, Devereux RB, Flachskampf FA et al (2005) Recommendations for chamber quantification: a report from the American Society of Echocardiography's Guidelines and Standards Committee and the Chamber Quantification Writing Group, developed in conjunction with the European Association of Echocardiography, a branch of the European Society of Cardiology. J Am Soc Echocardiogr 18:1440–1463

Matyal R, Skubas NJ, Shernan SK et al (2011) Perioperative assessment of diastolic dysfunction. Anesth Analg 113:449–472

Poelaert J, Osipowska E, Verborgh C (2008) Diastolic dysfunction and cardiac failure in the intensive care unit. In: Vincent JL (ed) 2008 yearbook of intensive and emergency medicine. Springer, Berlin, pp 76–87

Sarti A (2009) Ecocardiografia per l'intensivista. Springer, Milan

Slama M, Maizel J (2006) Echocardiographic measurement of ventricular function. Curr Opin Crit Care 12:241–248

Sturgess DJ, Marwick TH, Joyce CJ et al (2007) Tissue Doppler in critical illness: a retrospective cohort study. Crit Care 11:R97

The Right Ventricle and Pulmonary Artery

7

Luigi Tritapepe, Vincenzo De Santis, and Massimo Pacilli

7.1 The Right Ventricle: Anatomy

The right ventricle is positioned anterior to the left ventricle directly behind the sternum. It has a complex geometry, appearing triangular at the frontal view, and semilunar when viewed in a transverse section of the heart, with the septum being the most important determinant of shape. Under normal loading conditions, the septum moves toward the right ventricle in both systole and diastole. This complex geometry cannot be simply represented with geometric models, which presents important limitations for the estimation of right ventricular (RV) volume and function based on two-dimensional (2D) tomographic views. The ventricles extend from the atrioventricular junction leftward to the apex and cephalad to the ventriculoarterial junction. For the right ventricle, the annuli of the leaflets of the tricuspid and pulmonary valves delimit the chamber at the respective junctions with the atrium and the arterial trunk. The RV chamber is commonly viewed as having two sections, the sinus (inflow) and the conus or infundibulum (outflow). The right ventricle contracts in a "peristaltic" pattern that proceeds from the sinus, where fibers are mostly oriented obliquely with an average major radius of curvature of nearly 4 cm, to the infundibulum, whose fibers are circumconal with a small radius of curvature of 0.8 cm. Because of the complex shape of the right ventricle, triangular from the frontal aspect and crescentic from the apex, it is necessary to image the right ventricle from several projections, each characterized by specific anatomic landmarks. The thickness of the RV free wall is in the range of only 3–5 mm, and the RV mass is approximately one fourth of that of the left ventricle. Still, owing to the lower impedance and greater distensibility of the pulmonary artery bed, the right ventricle can pump blood at the same rate and volume as the left ventricle. The ability of both ventricles to maintain a normal cardiac output, ensuring sufficient organ perfusion, depends on three key factors: the contractile status of myocardial tissue, the preload, which represents the initial stretching of cardiac myocytes prior to contraction, and the afterload, defined as the load against which the heart must contract to eject blood. In addition, RV performance is directly influenced by left ventricular (LV) functional status owing to ventricular interaction. The interventricular septum, the pericardium, and common muscle fibers all play an important role in facilitating the transfer of force from the left ventricle to the right ventricle during the cardiac cycle. Around one third of the pressure generated in the right ventricle is determined by LV contraction. The right ventricle is affected much by the increase in pulmonary artery pressure, which can the acute dilation of the right ventricle resulting in

L. Tritapepe (✉)
Department of Anesthesia and Intensive Care, Cardiac Surgery ICU, Policlinico Umberto I Hospital, Sapienza University of Rome, Rome, Italy
e-mail: luigi.tritapepe@uniroma1.it

A. Sarti and F. L. Lorini (eds.), *Echocardiography for Intensivists*,
DOI: 10.1007/978-88-470-2583-7_7, © Springer-Verlag Italia 2012

tricuspid regurgitation. The increase in RV pressure and dilation of the right ventricle may cause the interventricular septum to shift itself to the left, with decreased compliance of the left ventricle and increased LV end-diastolic pressure. In other words, the right ventricle also tolerates a large increase in volume, but immediately suffers from any increase in afterload.

7.2 The Pulmonary Artery: Anatomy

The pulmonary artery is a large artery originating from the superior surface of the right ventricle and carrying deoxygenated blood from the heart to the lungs. The pulmonary artery is the exception to the rule that arteries carry oxygenated blood from the heart to other parts of the body. The pulmonary trunk (pulmonary artery or main pulmonary artery) is approximately 5 cm in length and 3 cm in diameter. It branches into two pulmonary arteries (left and right), which deliver deoxygenated blood to the corresponding lung. The right pulmonary artery commences below the arch of the aorta, and runs to the right and slightly downward to reach the hilum of the right lung. In its course, it passes behind the ascending aorta and the superior vena cava, and in front of the esophagus and the stem of the right bronchus. Near the lung it gives off a large branch which accompanies the eparterial bronchus. The left pulmonary artery runs to the left and backward, across the front of the descending aorta and the left bronchus, to the hilum of the left lung.

7.3 The Right Ventricle: Echocardiography

The right ventricle has been less studied than the left ventricle in terms of physiopathology and echocardiography. However, this ventricle is more involved in respiratory diseases in the ICU, both acute and chronic. Its functionality may determine the load response and blood volume in unstable patients, and whenever the hypotensive patient does not respond to a fluid challenge, involvement of the right ventricle is suspected. Owing to its widespread availability, echocardiography is used as the first-line imaging modality for assessment of RV size and function. The quantitative assessment of RV size and function is often difficult, because of the complex anatomy. With transthoracic echocardiography (TTE) we may explore with sufficient precision the dimension and function of the right ventricle. A qualitative evaluation of the right ventricle can be obtained by assessing the shape of the right ventricle, which can be visualized in the parasternal short-axis view, the parasternal long-axis view and its modification, and the apical four-chamber view. The location of the right ventricle behind the sternum restricts somewhat the transthoracic parasternal windows that can be accessed by the ultrasound beam. Thick trabeculations in the chamber may occasionally be confused with a thrombus or a tumor or may be misdiagnosed as hypertrophic cardiomyopathy. Because of the triangular shape of the right ventricle, its apex is normally not well evaluated in the apical for-chamber view, so when the apex is well visible or exceeds the LV apex, this means there is enlargement or hypertrophy of the right ventricle. Then this is an important point in the echocardiographic evaluation of the RV dilation and function: immediately, we can exclude an involvement of the right ventricle in determination of contingent disease. However, we need other measures to confirm the diagnosis of RV dilation. In the apical four-chamber view, we can measure the transverse and the longitudinal diameter of the right ventricle to assess the size of the right ventricle. Two transverse diameters are measured in the apical four-chamber view: the annulus or basal diameter, which is about 3.5 cm in diastole and 2.9 cm in systole; and the mid diameter, at the mid-ventricular level, which is about 3.0 cm in diastole and 2.4 cm in systole. Finally, we measure the length of the right ventricle from the annulus to the apex, which is about 7.1 cm in diastole and 5.5 cm in systole. Still in the apical four-chamber view, it is important to measure the RV end-diastolic area (RVEDA), which, generally, is about two thirds

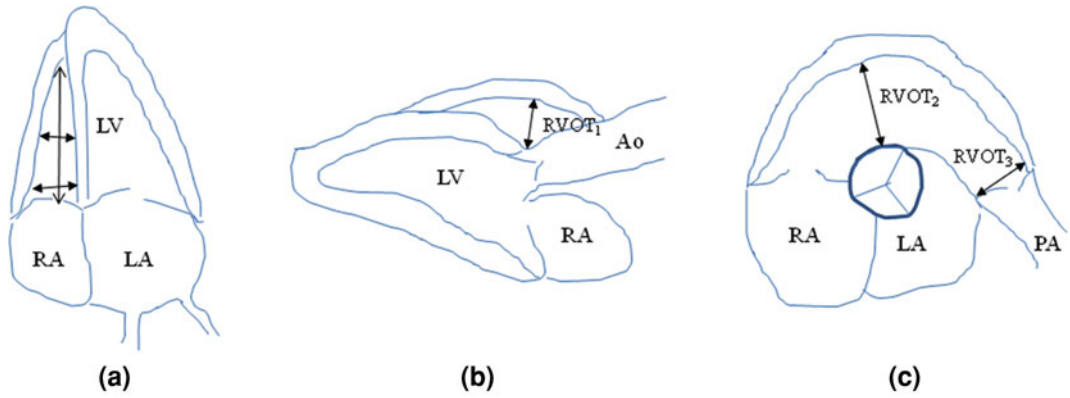

Fig. 7.1 The echocardiographic views used for evaluating the diameters of the ventricle. **a** apical four-chamber view, **b** parasternal long-axis view, and **c** parasternal short-axis view at the base of the heart. *Ao* aorta, *LA* left atrium, *LV* left ventricle, *PA* pulmonary artery, *RV* right ventricle

of the LV end-diastolic area (LVEDA), and is about 20 cm^2. The relationship between the RVEDA and the LVEDA is very important to make the diagnosis of primary or secondary involvement of the right ventricle. An RVEDA/LVEDA ratio less than 0.6 is considered normal, whereas an RVEDA/LVEDA ratio between 0.6 and 1.0 is typical of RV dilation, which becomes a huge dilation for a ratio greater than 1.0.

The wall thickness of the right ventricle, as measured in the apical four-chamber view or better in the subcostal four-chamber view, is usually less than 0.5 cm. Any increase of the thickness above 0.5 cm shows hypertrophy of the right ventricle. In the parasternal long-axis view, it is also possible to measure the RV diameter at the outflow tract by 2D echocardiography and in M-mode ($RVOT_1$). $RVOT_1$ is measured at the maximal diastolic expansion of the right ventricle. Two other diameters, $RVOT_2$ and $RVOT_3$, are measured at the outflow tract of the right ventricle in the parasternal short-axis view at the basal level of the heart. $RVOT_2$ is the widest part of outflow tract and $RVOT_3$ is measured at the pulmonary annulus plane. These diameters are more important for the trend modifications due to loading and contractile conditions than as isolated values. Then, without difficult calculations, but almost at a glance, we can get an idea of the function of the right ventricle at that time (Figs. 7.1, 7.2).

In the parasternal short-axis view, at the mid-papillary level, we can observe the short axis of the left ventricle and the right ventricle but especially the shape of the interventricular septum. The movement of the interventricular septum is very important for the diagnosis of overload of the right ventricle or overpressure inside the right ventricle. In fact, the flattening of the septum can represent an increase in volume or in pressure of the right ventricle, and the left ventricle takes the form of the letter D. In this condition the left ventricle is unloaded (hypodiastolic) and the right ventricle is overloaded. In the case of increased afterload of the right ventricle, the septum moves toward the left ventricle in systole and diastole, whereas in the case of overload, the movement toward the left ventricle is visible only during diastole. These circumstances should be immediately diagnosed particularly in patients ventilated with high levels of positive end-expiratory pressure in mechanical ventilation, because, while presenting all forms of dynamic change of the hemodynamic indices explored, such patients do not respond to the fluidic load during the hemodynamic instability period. The eccentricity index is an index for grading the level of RV hypertension (i.e., in the case of pulmonary embolism or excessive positive end-expiratory pressure in the acute respiratory distress syndrome patient), and is measured in the parasternal short-axis view at the mid-ventricular level. This index is the ratio

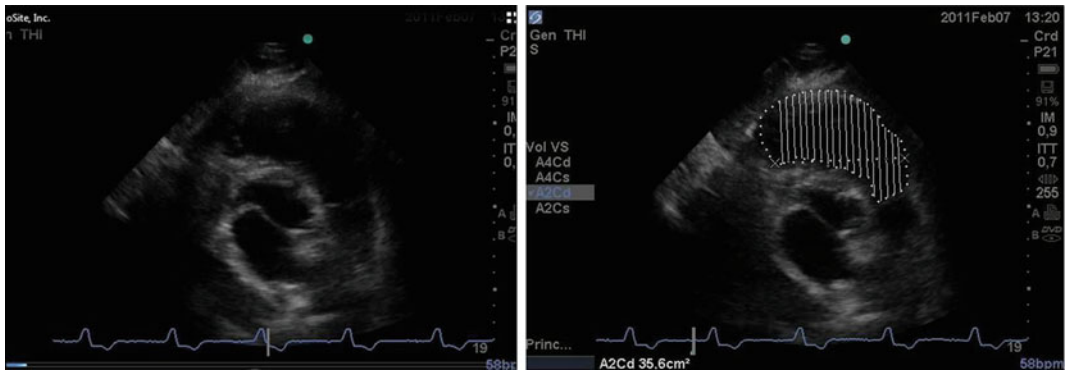

Fig. 7.2 Transthoracic echocardiography (TTE), parasternal short-axis view of the right ventricle and its volume measurement

between the anteroposterior diameter of the left ventricle and the lateroseptal diameter of the same ventricle, measured in diastole. Normally the eccentricity index is 1; every elevation of this value (above 1) means an increase of the RV overload if it is measured at the end of diastole, whereas it shows an increase of pressure if it is measured at the end of systole and diastole.

With transesophageal echocardiography, however, the right-side structures are farthest from the esophagus, and the definition of the right ventricle is sufficiently good. The tomographic views in which we can recognize the shape, function, and volume of the right ventricle are the same but specular of TTE. The best evaluation of the right ventricle is obtained in the mid-esophageal four-chamber view, the mid-esophageal RV inflow–outflow view, the transgastric short-axis view, and the transgastric RV inflow view. The classic mid-esophageal four-chamber view puts the right ventricle on the left side of the screen, but the apex is far from the transducer. An optimal tomography is represented by the mid-esophageal RV inflow–outflow view, where the right ventricle is positioned on the left and at the bottom of the screen and we can obtain good alignment for Doppler investigation of tricuspid valve. In the transgastric short-axis view, we can observe, especially in ventilated patients, in which there are not good windows for exploration, the ratio between both ventricles, which is so important to manage fluid loading and diagnose RV failure in the case of hypocontractility and enlargement of the right ventricle. At this level, rotating the multiplane angle to about 100° and turning the probe slightly to the right, we obtain the transgastric RV inflow view, in which projection we can study well the subvalvular structures of the tricuspid valve and we can evaluate the movement and thickness of the inferior portion of the RV free wall.

7.4 The Pulmonary Artery: Echocardiography

The pulmonary artery is studied with TTE in the parasternal short-axis view at the base of the heart and in the modified parasternal long-axis view. In the subcostal short-axis view it is possible to obtain useful images to study the right ventricle and the pulmonary artery. The pulmonary artery and/or its right branch are visible as a little circle below the aortic arch in suprasternal tomography. Transesophageal echocardiography allows us to completely evaluate the pulmonary artery and its right branch. The left branch is not visible because of the presence of the left main bronchus, which, with its air content, prevents the passage of the ultrasound beam. The mid-esophageal RV inflow–outflow view is a good tomographic view to evaluate the diameter of the pulmonary artery, the flow through the pulmonary valve, and the tricuspid regurgitation, which, sampled with continuous wave Doppler imaging, allows us to measure the systolic pulmonary pressure when the right atrial pressure

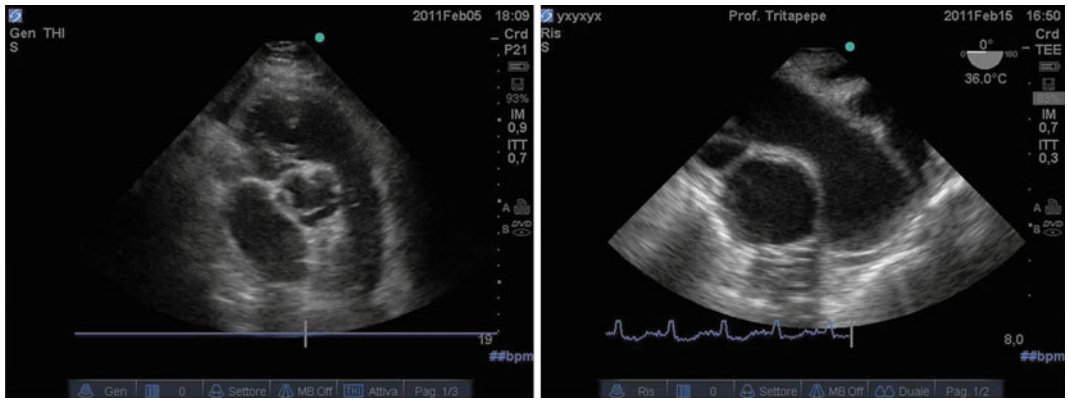

Fig. 7.3 TTE and transesophageal echocardiography of the trunk of the pulmonary artery

is known [pulmonary artery pressure = 4 × (peak velocity of tricuspid regurgitation)^2 + central venous pressure] (Fig. 7.3).

Two other views are fundamental to study the pulmonary artery: the mid-esophageal ascending aortic short-axis view and the upper esophageal aortic arch short-axis view. The first one shows the trunk of the pulmonary artery and the right branch of pulmonary artery. This tomographic view is important because the trunk of the pulmonary artery is parallel to the pulsed wave Doppler beam and the pulmonary velocity–time integral can be measured, which essential to determine the right cardiac output and to show the cyclic variation of velocity–time integral with different intrathoracic pressure levels (Fig. 7.4).

Furthermore, we can follow the positioning of a Swan-Ganz catheter, and detect formation of thrombosis around the pulmonary catheter. In the case of pulmonary embolism, we can observe the thrombi throughout the pulmonary artery bed.

7.5 Assessment of Right Ventricular Systolic Function

Unlike the left ventricle, the assessment of systolic function of the right ventricle with the biplane method to quantify RV function is complicated by its particular shape and geometry. Nevertheless, some surrogate methods are used and now accepted because of MRI validation. The RV outflow tract shortening fraction is obtained in the parasternal short-axis view at the base of heart, where we can measure (in M-mode) the RV outflow tract diameter in systole and diastole. The difference between the two diameters divided by the diastolic diameter gives the RV outflow tract shortening fraction. RV fractional area change describes the percentage change in RV area between diastole and systole. It is measured in the apical four-chamber view and is calculated by measuring the RVEDA and the RV end-systolic area and diving the difference between these areas by the RVEDA. It is very well related to the ejection fraction calculated from MRI and is used to stratify patients after myocardial infarction, pulmonary hypertension, or cardiac surgery. Some errors are possible because of the endocardial border determination of the right ventricle is complicated by the presence of widely represented trabeculae. For this reason, the RV ejection fraction is not normally measured (Table 7.1).

7.6 Tricuspid Annular Plane Systolic Excursion

A quantitative method to evaluation of RV systolic function that is well accepted and confirmed by the literature is the tricuspid annular plane systolic excursion (TAPSE). In other words, because the right ventricle contracts in a "peristaltic" pattern that proceeds from the sinus to the infundibulum, it is sufficient to measure the

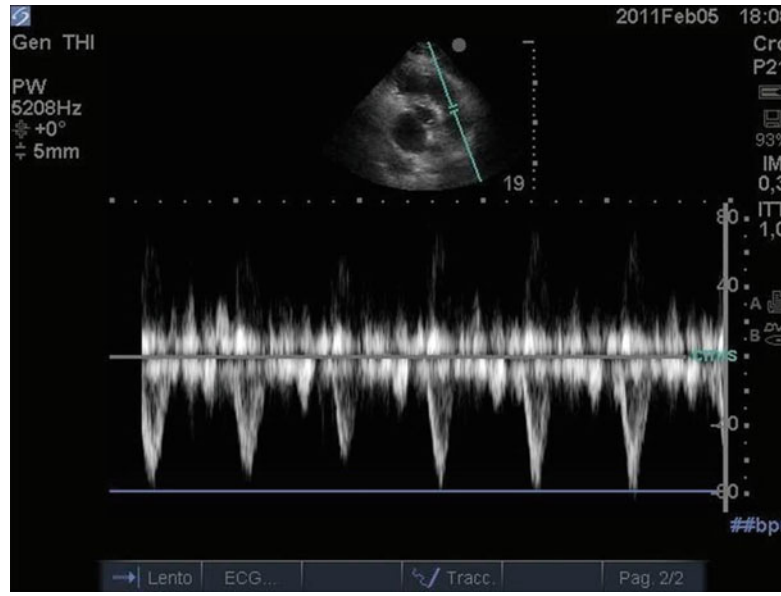

Fig. 7.4 Pulsed wave Doppler imaging of the pulmonary artery and variation of the velocity–time integral with the respiratory cycle

Table 7.1 Normal values for parameters of right ventricular systolic function

Parameter	Normal value
RVOT-SF (%) = (EDRVOTD − ESRVOTD)/EDRVOTD × 100	61 ± 13[a]
RVFAC (%) = RVEDA − RVESA/RVEDA × 100	56 ± 13[b]

EDRVOTD right ventricular outflow tract diameter in diastole, *ESRVOTD* right ventricular outflow tract diameter in systole, *RVEDA* right ventricular end-diastolic area, *RVESA* right ventricular end-systolic area, *RVFAC* right ventricular fractional area change, *RVOT-SF* right ventricular outflow tract shortening fraction

[a] Lindqvist et al.

[b] Lopez-Candales et al.

extent of dislodgement of the lateral portion of the tricuspid annulus toward the apex to quantify RV efficiency. The TAPSE is measured in M-mode utilizing the apical four-chamber view. The cursor is positioned on the image of the lateral tricuspid annulus and the distance between the above and below point formed by the excursion of the tricuspid annular plane is measured. Normally, the TAPSE is more than 2 cm. A value below 2 cm shows a reduction of RV systolic function. When TAPSE is very low (less than 1.3 cm), the right ventricle is in a very bad condition and has a serious systolic dysfunction. Samad et al. assessed TAPSE in patients after a first acute myocardial infarction, and showed that TAPSE of 15 mm or less was associated with increased mortality (45 % at 2 years) compared with patients having TAPSE greater than 20 mm (4 %). Special care must be taken when interpreting this parameter in longitudinal studies of patients undergoing procedures that affect the overall heart motion (i.e., cardiac surgery).

7.7 Tissue Doppler Imaging and Tei Index

Tissue Doppler imaging (TDI) allows quantitative assessment of RV systolic and diastolic function by means of measurement of myocardial velocities. Tissue velocities can be measured using pulsed wave tissue Doppler imaging at different levels of the RV free wall, but because of the difficulties to explore the apical segment of the right ventricle and because of physiological

considerations, we use TDI on the basal segment of the RV free wall. The peak systolic velocities registered at this level fit with RV systolic function and represent a good prognostic index of survival in patients with RV myocardial infarction. A peak systolic velocity greater than 11 cm/s is considered normal, but patients with myocardial infarction velocities greater than 8 cm/s have a significantly better event-free survival at 1 year than patients with systolic annular velocities below 8 cm/s. The Doppler index of myocardial performance (Tei index or myocardial performance index) is yet another parameter that can be used for evaluation of RV performance. It is expressed by the formula (isovolumic contraction time + isovolumic relaxation time)/RV ejection time. It is established that it is actually unaffected by heart rate, loading conditions, or the presence and the severity of tricuspid regurgitation. To calculate the Tei index, one needs to measure the inflow and the outflow of the right ventricle with pulsed wave Doppler imaging. The velocities, sampled in conjunction with ECG registration, emphasize the isovolumic contraction time and relaxation time, and so Tei index can be calculated with the formula previously mentioned.

7.8 Right Ventricular Diastolic Function

RV filling is different from LV filling for two reasons: the time, which is shorter for the right ventricle, and the velocity, which is slower than for the left ventricle. In fact, the tricuspid valve area is greater than the mitral orifice and a large quantity of blood passes through the valve slowly. Nevertheless, it is possible, as for the left ventricle, to study the transtricuspid flow with pulsed wave Doppler imaging in the parasternal short-axis view at the base of heart or in the apical four-chamber view, two views that present good alignment of Doppler beam. The *E* and *A* velocities can be collected and the *E*/*A* ratio represents the grading of RV diastolic dysfunction. Diastolic dysfunction is characterized by a decrease in the *E*/*A* ratio, but a detailed definition of the values to describe the different pattern of disease is lacking. The transtricuspid flow is affected by the loading condition, heart rate, aging, and respiration. The study of RV diastolic function is completed by TDI at the level of the tricuspid lateral annular plane and measurement of the inferior vena cava (IVC). The E1 and A1 waves measure RV diastolic function with minor influence of the loading condition. The diameter and the collapsibility of the inferior vena cava can help to identify the function of the right ventricle, especially the diastolic function. Finally, the hepatic vein change on the Doppler flow pattern can identify a RV diastolic dysfunction when the ratio of the total hepatic reverse flow integral to the total forward flow integral increases.

Further Reading

Bleeker GB, Steendijk P, Holman ER et al (2006) Assessing right ventricular function: the role of echocardiography and complementary technologies. Heart 92(1):i19–i26

Ho SY, Nihoyannopoulos P (2006) Anatomy, echocardiography, and normal right ventricular dimensions. Heart 92(1):i2–i13

Jurcut R, Giusca S, La Gerche A et al (2010) The echocardiographic assessment of the right ventricle: what to do in 2010? Eur J Echocardiogr 11:81–96

Lindqvist P, Henein M, Kazzam E (2003) Right ventricular outflow-tract fractional shortening: an applicable measure of right ventricular systolic function. Eur J Echocardiogr 4:29–35

Lopez-Candales A, Rajagopalan N, Saxena N, Gulyasy B, Edelman K, Bazaz R (2006) Right ventricular systolic function is not the sole determinant of tricuspid annular motion. Am J Cardiol 98:973–977

Mathew JP, Ayoub CM (2005) Clinical manual and review of transesophageal echocardiography. McGraw-Hill, Columbus

Samad BA, Alam M, Jensen-Urstad K (2002) Prognostic impact of right ventricular involvement as assessed by tricuspid annular motion in patients with acute myocardial infarction. Am J Cardiol 90:778–781

Sheehan F, Redington A (2008) The right ventricle: anatomy, physiology and clinical imaging. Heart 94:1510–1515

Vieillard-Baron A (2009) Assessment of right ventricular function. Curr Opin Crit Care 15:254–260

Left and Right Atria

8

Luigi Tritapepe, Francesca Pompei,
and Claudio Di Giovanni

8.1 Anatomy

Compared with the right atrium, the left atrium is characterized by lower volume and greater wall thickness. However, owing to its transverse axis, it forms a large part of the base of the heart and extends to the right, covering, in part, that side of the atrium. Considering the heart in situ, there are the following walls: anterior–superior wall, corresponding to the rib and sternum face that has a relationship with the ascending aorta and the pulmonary trunk; the posterior–superior wall, which, with the interposition of the pericardium, has a relationship with the esophagus. Four pulmonary veins, two on each side, open into the posterior–superior wall of the atrium. The four orifices of the pulmonary veins have no valves; the posteroinferior wall is very large and flat, and corresponds to the diaphragmatic face; the anteroinferior wall is where the mitral valve is positioned; the medial wall (or septum) corresponds to the atrial septum. The medial wall has a slight depression that corresponds to the fossa ovalis of the right atrium. In front, this depression is limited by a semilunar fold, which is the residue of the foramen ovalis valve, the lateral wall through which one accesses the left atrial (LA) appendage (LAA). The cavity of the atrium has smooth walls; trabeculae carneae are found only near the LAA anastomosed to the network. The left atrioventricular orifice is positioned low and anteriorly and leads into the ventricular cavity; it has a valve apparatus, consisting of two cusps called the bicuspid or mitral valve.

The right atrium is on the right and forward of the left atrium. It has, roughly, a cube shape and consists of six walls. Considering the heart in situ: the anterior–superior wall corresponds to the rib–sternum face; the posterior–superior wall corresponds to the base of the heart and has the openings of the cavae veins, superior and inferior; the posterior–inferior wall corresponds to the diaphragmatic face where the coronary sinus ends; the anterior–inferior wall corresponds to the orifice of the tricuspid valve; the medial wall is formed by the interatrial septum; and the lateral wall communicates with the right atrial appendage.

The inner surface of the right atrium, with the other chambers of the heart, is covered with endocardium and has a smooth posterior portion, the sinus of caval veins, and an anterolateral corrugate surface caused by the presence of fleshy pads that are regularly arranged, the pectinate muscles. The boundary between these two portions is marked by a ridge, the crista terminalis.

In the posterior–superior surface of the right atrium, to the limits with the anterosuperior and posteroinferior faces, are the outlets of the upper

L. Tritapepe (✉)
Department of Anesthesia and Intensive Care, Cardiac Surgery ICU, Policlinico Umberto I Hospital, Sapienza University of Rome, Rome, Italy
e-mail: luigi.tritapepe@uniroma1.it

A. Sarti and F. L. Lorini (eds.), *Echocardiography for Intensivists*,
DOI: 10.1007/978-88-470-2583-7_8, © Springer-Verlag Italia 2012

and lower caval veins. The contour of the anterolateral orifice of the superior vena cava is defined by the crista terminalis, and the flow around the mouth of the inferior vena cava (IVC) passes through a rudimentary valve, the Eustachian valve, which goes from the contour of the orifice to the edge of the fossa ovalis. To the left and in front of the orifice of the IVC, near the atrioventricular orifice, is the mouth of the coronary sinus, which carries most of the effluent blood from the walls of the heart, the coronary sinus ends with the Thebesius valve, which has the task of preventing the reflux of blood into the coronary sinus during atrial systole.

The medial wall (or septum) is smooth and has an elongated depression in the vertical direction, the fossa ovalis. This depression is bordered in front and above by a crescent-shaped pad, the flap of the fossa ovalis representing the free end of the septum secundum. The lateral wall has the atrial appendage, an appendix cavity whose walls show numerous anastomosed muscles that continue to network with those covering much of the atrial wall.

Forward and further down at the anteroinferior wall lies the atrioventricular orifice, which leads into the ventricular cavity. It has a valve apparatus which consists of three leaflets or cusps, hence the name of the tricuspid valve.

8.2 Echocardiography

The atria can go into dilation when stenosis or insufficiency of valvular apparatus occurs. The atrial kick contributes to a stroke volume of around 20 % and its contribution increases when there is diastolic dysfunction owing to the elevation of atrial pressure. When atrial fibrillation occurs, the atrial contribution to cardiac output is lost and in this case a worsening degree of diastolic dysfunction may cause a low-output syndrome. An increased atrial volume is an independent predictor of adverse cardiovascular events, including stroke and congestive heart failure. Accordingly, accurate measurement of the atrial size has become increasingly relevant to clinical practice. Most clinical studies have used echocardiographic measurements, because echocardiography is the most accepted and best validated modality for atrial volume quantification. The area–length method has often been chosen for atrial volume quantification, because it is simple, relatively quick, and can be done using standard acquisitions. Echocardiographic apical two- and four-chamber views are used with the subject in the left lateral decubitus position to demonstrate the left ventricular apex and mitral valve.

8.3 Left Atrium

The left atrium has three important roles: it contributes 20–30 % of cardiac output, it is an anatomical reservoir during ventricular systole, and is a passive conduit for the flow during the early phase of diastole. All these functions can be explored with the echocardiography. With transthoracic echocardiography (TTE), the left atrium is seen in many standard projections, such as the apical four-chamber, apical two-chamber, apical three-chamber, parasternal short-axis, parasternal long-axis, and subcostal projections (Fig. 8.1). The mean longitudinal diameter of the left atrium is about 4.1 cm and the mean transverse diameter is about 3.8 cm. The diameter is measured at the end of the systole, when the atrium is very full. An optimal view is represented by the parasternal long-axis view, where, with the help of M-mode, it is very easy to measure the LA diameter. The LA area is less than 20 cm^2 and can be easily obtained with the apical four-chamber and apical two-chamber projections. The LA volume and diameters are increased in many pathological conditions, but mitral valve disease and left ventricular function are the major determinants for the enlargement and the loss of LA function. With the apical four-chamber view, we observe the ends of the pulmonary veins as the pass into the left atrium and we can measure their flow through pulsed wave Doppler imaging, which useful to study the degree of diastolic dysfunction, mitral valve regurgitation and LA pressure. With transesophageal echocardiography (TEE) we may see the left atrium in most of the recommended two-dimensional tomographic views. Not only the left

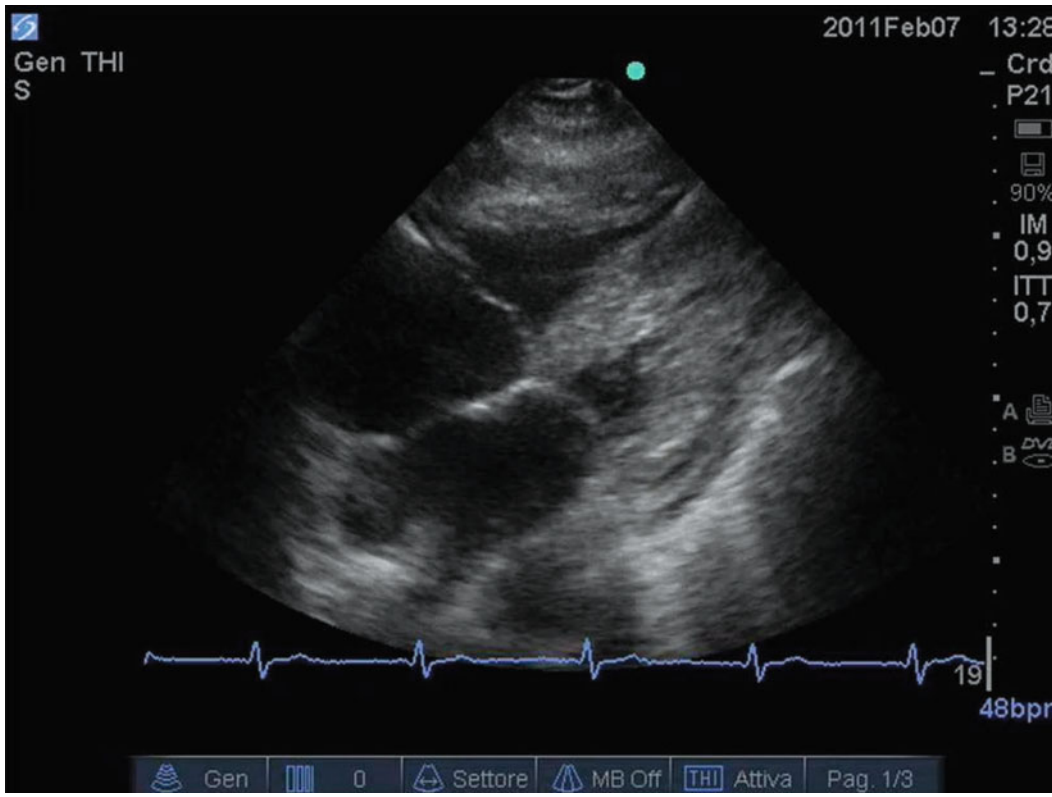

Fig. 8.1 Transthoracic echocardiography of the right and left atria at the end of systole

atrium, but especially the LAA can be visualized with TEE. The mid-esophageal four-chamber, mid-esophageal two-chamber, mid-esophageal long-axis, transgastric two-chamber, mid-esophageal mitral commissural, mid-esophageal aortic valve short-axis, mid-esophageal aortic valve long-axis, deep transgastric long-axis, mid-esophageal bicaval, and mid-esophageal right ventricular inflow–outflow views are all tomographic views that allow us to explore the dimensions and function of the left atrium and the relationship between the left atrium and the left ventricle. The mid-esophageal four-chamber view and the mid-esophageal two-chamber view are the projections used to measure the left atrium and the apical four-chamber view with TTE that allows us to visualize more accurately the superior margin of the left atrium. The LAA is an important structure that is well visualized with the mid-esophageal two-chamber between 60° and 90° or with the transgastric two-chamber view around 90°. The LAA is a triangular structure divided from the left superior pulmonary vein by a ridge called the Coumadin ridge, which is often confused with a thrombotic formation or a mass. With the use of tissue Doppler imaging, we can differentiate the ridge from a thrombus. Pulsed wave Doppler imaging is utilized to measure the different flow rates in the pulmonary vein and in the LAA. When the patient suffers of atrial fibrillation we can explore with TEE the LAA where clots can form. The presence of slow flow (smoke effect) in the left atrium or thrombi inside the LAA can be always detected before the use of DC shock to reverse atrial fibrillation. If there is mitral rigurgitation, it is possible to determine LA pressure by sampling the regurgitant jet with continuous wave Doppler imaging. In particular, LA pressure = systolic arterial blood pressure − [4 × (peak mitral regurgitant velocity)^2].

Especially in the ICU, patients with hemodynamic instability can have different degrees of mitral insufficiency. It is very important to measure the atrial diameter because this may help to differentiate between the acute and subacute or chronic forms of mitral insufficiency. It is crucial to assess the cause of the hemodynamic instability and consider other abnormalities that lead to hypotension. Some abnormalities in the zone near the left atrium, such as aortic dissection, aortic aneurysm, pericardial hematoma after cardiac surgery or after percutaneous cardiac intervention, and lung or mediastinal tumors, can cause LA compression, directly or through compression of pulmonary veins. Chronic LA compression can lead to symptoms mimicking congestive heart failure. Unlike LA compression, congestive heart failure is associated with an enlarged left atrium. Acute LA compression causes immediate hypotension and low-output syndrome. Analysis with TEE can be used to obtain more information about the compromising structure or can be used when TTE has limitations.

8.4 Right Atrium

With TTE, the right atrium is seen in the apical four-chamber, parasternal short-axis, and subcostal projections (Fig. 8.1). Moving the probe slightly to the right of the patient, in the subcostal position, one can see flow from the IVC into the right atrium. This is a very important view used to assess the preload of the patient and the response to volume load. The lateral diameter of the right atrium is evaluated in the apical four-chamber view and is usually less than 4.5 cm. It is not possible with TTE to estimate precisely the volume in orthogonal projections as it is when studying the left atrium.

With TEE, the right atrium is seen in the mid-esophageal four-chamber, mid-esophageal aortic valve short-axis, mid-esophageal bicaval, mid-esophageal right ventricular inflow–outflow, and transgastric right ventricular inflow views. The right atrium can be evaluated in the mid-esophageal four-chamber view, but the mid-esophageal bicaval view is the best projection to estimate the volume of the right atrium and the ends of the superior (on the right side of the display screen) and inferior (on the left side) venae cavae. This bicaval view allows us to measure the bicaval diameters in M-mode and see the bicaval diameter modification during the respiratory cycle, which is important to define fluid responsiveness of hemodynamically unstable patients. Also, the mid-esophageal bicaval view is the crucial projection to monitor the positioning of venous cannulae in extracorporeal membrane oxygenation or extracorporeal life support procedures. Patients with atrial or ventricular catheters (Swan–Ganz or pacemaker cables) can have thrombotic masses near or on the indwelling devices that are well evaluated in the mid-esophageal bicaval view. In this projection, the atrial septum is also well visualized and may reveal pathological loss of continuity (atrial septal defects) or paraphysiological loss as a patent foramen ovale (PFO). Especially in acute lung injury/acute respiratory distress syndrome patients ventilated with positive end-expiratory pressure, the inversion of the pressure gradient between the right and left atria at the level of PFO causes shunt with hypoxia and allows passage of air bubbles or fibrin aggregates through the PFO, with consequent paradoxical embolization. The arrangement of the septum, moved down to the right or straight or even prominent at the upper left, shows the current pressure in the right atrium and can be a sign of right ventricular failure, along with an enlarged right atrium itself.

8.5 Interatrial Septum

The interatrial septum is always a structure worth exploring, especially in the patient in the ICU. The different pressure regimes, related to high levels of intrathoracic pressure in mechanically ventilated patients, can determine the patency of the foramen ovale or reverse shunt in atrial septal defects. The subcostal four-chamber projection is easily visible with TTE, and by aligning the probe perpendicular to the septum, we can use pulsed wave Doppler

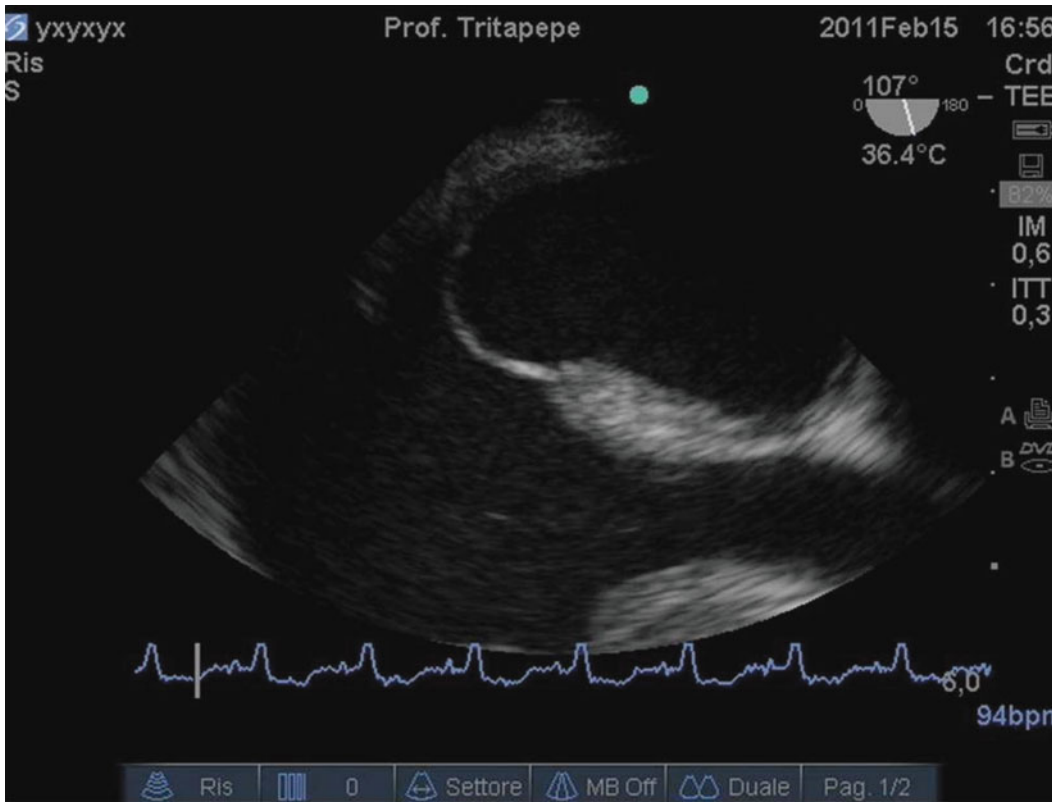

Fig. 8.2 Transesophageal echocardiography of the right atrium in the bicaval view, with the septum at the level of the fossa ovalis

imaging to study any interatrial flow. In the apical four-chamber view, we visualize the septal wall to the roof of the atria and the portion near the valve plane losing the continuity of the echoes of the septum (the phenomenon of dropout) near the fossa ovalis. This should not be confused with an atrial septal defect. It is often difficult to distinguish between a slightly redundant septum and a true aneurysm. In both cases, the wall of separation between the left atrium and right atrium rather than remaining in a fixed position during contraction and relaxation of the heart, according to the different pressures present in the left atrium can tend to shift to the left or right. This condition may be associated with the presence of a small permeability of the wall (atrial septum), a condition that could be the cause of the transient ischemic attack. The interatrial septum is well evaluated with TEE, especially in the mid-esophageal bicaval view (Fig. 8.2), but also in the mid-esophageal aortic valve short-axis view.

Lipomatosis of the interatrial septum is a rare benign disease characterized by accumulation of fatty tissue of the atrial septum. Typically, the thickening of the lipomatous septum saves the fossa ovalis. It may be associated with supraventricular arrhythmias and may sometimes result in hemodynamic complications. For this reason, it is always considered in the differential diagnosis of cardiac masses.

8.6 Chiari Network

Another element found on echocardiography of the right atrium is the presence of the Chiari network, a remnant of the embryonic venous sinus

valve. It has no pathological significance, but, appearing as a floating weblike structure that generates echoes in motion, it can be mistaken as a thrombus or vegetation or mass. It is well evaluated in the apical four-chamber projection.

8.7 Eustachian Valve

The Eustachian valve is an endocardial fold extending from the anterior inferior margin of the inferior vena cava to the anterior part of the limbus of the fossa ovalis. The Eustachian valve is programmed to regress completely after birth. In about 30 % of adults it persists with variable size and structure. It is well evaluated with TTE in the subcostal view, in the projection to explore the inferior vena cava. It can be confused with thrombus or vegetation and could promote the migration of thrombi or embolization toward the fossa ovalis. In case of doubt, TEE examination is recommended.

Further Reading

Kenneth KE (2008) Anatomy of the left atrial appendage. Echocardiography 25:669–673

Oh JK, Steward JB, Tajik AJ (2007) The echo manual. Lippincott Williams & Wilkins, Philadelphia

Whitlock M, Garg A, Gelow J, Jacobson T, Broberg C (2010) Comparison of left and right atrial volume by echocardiography versus cardiac magnetic resonance imaging using the area-length method. Am J Cardiol 106:1345–1350

Pericardium and Pericardial Diseases

9

F. Luca Lorini, Stefania Cerutti, and Giovanni Didedda

9.1 Introduction

The normal pericardium is a thin, linear structure that echocardiographically is outlined as a bright, highly echogenic line. Within the two layers of the pericardium, the inner serosal layer and the outer fibrous pericardium, about 10–50 ml of pericardial fluid accumulates physiologically; it is generally visualized only in systole as an echo-free space surrounding the heart.

Transthoracic echocardiography is a milestone and the first-line imaging modality for diagnosing pericardial diseases such as pericardial effusion (PE) and cardiac tamponade, constrictive pericarditis, pericardial cysts and tumors, and partial and complete absence of the pericardium. The limitations of this imaging are very few, mainly represented by a poor echocardiographic window and the lack of details of the pericardium's anatomy, which need to be investigated with a further examination (CT or MRI). Although transthoracic echocardiography is almost always the ideal technique to detect and grade pericardial diseases, several factors in the period after cardiac surgery may contribute to the need for transesophageal echocardiography.

F. L. Lorini (✉)
Department of Anesthesia and Intensive Care,
Ospedali Riuniti di Bergamo,
Bergamo, Italy
e-mail: llorini@ospedaliriuniti.bergamo.it

9.2 Pericardial Effusion

The causes of PE range from inflammatory effusions (secondary to bacterial or viral infections, myocardial infarction, trauma, or neoplasm) to hemorrhagic effusions, mostly common in the period after cardiac surgery. The clinical signs and symptoms are related to the cause of the PE and to the hemodynamic significance of the effusion itself. If the PE is secondary to pericarditis, a prodrome of fever, malaise, and myalgia could precede major symptoms such as retrosternal or left precordial chest pain and shortness of breath. A pericardial friction rub could be present, although it could be transient, and the heart rate is usually rapid and regular. If the PE develops slowly, it can be remarkably asymptomatic, whereas rapidly accumulating effusions manifest themselves clinically with tamponade (see the next section). Echocardiography should be the first modality to determine the size and the hemodynamic significance of PE, as it is an even more accurate imaging technique than CT in quantitative assessment of nonloculated PE, always keeping in mind the few limitations that this examination has. The hemodynamic consequences of PE will be examined in the next section. In this section we will examine the classification and the characteristics of PE.

The size of the effusion has been graded by the European Society of Cardiology as small, moderate, large, and very large (Table 9.1). PE may be seen not only in systole (as it is common for the physiological pericardial fluid), but they

A. Sarti and F. L. Lorini (eds.), *Echocardiography for Intensivists*,
DOI: 10.1007/978-88-470-2583-7_9,

Table 9.1 Classification of pericardial effusion by the European Society of Cardiology

Classification of pericardial effusion	Dimension in diastole (mm)	Location
Small	<10	Posterior atrioventricular groove
Moderate	10–20	
Large	>20	Usually extends behind the left atrium, may determine a compression of the heart
Very large	>20	Extends behind the left atrium and determines a compression of the heart

may become visible throughout the entire cardiac cycle. As the amount of pericardial fluid increases, fluid moves from the posterobasilar left ventricle to the apex and anterior wall and then laterally and posteriorly to the left atrium (Fig. 9.1). It is important to emphasize that the mere presence of an effusion, even when large, does not indicate hemodynamic significance. Since the rapidity of pericardial fluid accumulation and the compliance of the pericardium influence the pressure elevation for any given fluid volume, effusion volume alone does not determine hemodynamic significance. Therefore, the presence of an effusion must be related to other echocardiographic parameters of cardiac filling and transvalvular flow and must be correlated with the clinical features (see the next section).

Although PE generally appears as an echo-free space encircling the heart, sometimes echogenic materials such as fibrinous strands and a shaggy exudative coating are found. These findings are important as well, because the initial echocardiographic characteristics of PE determine the pericardial complication. More precisely, echogenic PE, including an exudative frond-like coating and fibrinous strands in PE, are the major risk factors for pericardial complications such as constrictive pericarditis and PE recurrence. Diffuse echogenic PE results in the highest incidence of events, followed by PE with an exudative coating, and fibrinous strands. Echocardiography could, then, be used not only for diagnostic purposes, but also for a prognostic evaluation.

PE are a possible complication of cardiac surgery, with a reported incidence that ranges between 50 and 64 % of cases depending on the study definitions and designs. They compromise cardiac function in 0.8–7 % of cases and have a peak incidence on the tenth postoperative day. Echocardiographic monitoring of surgical patients should be, therefore, done up to 20 days to 1 month after surgical intervention, because late PE are an important cause of morbidity. Persisting PE is more frequent after coronary artery bypass graft surgery than after valve replacement surgery. In contrast, the incidence of late cardiac tamponade is higher in patients undergoing valve replacement surgery. The use of transthoracic echocardiography is important not only for the follow-up of cardiac surgical patients, but it has also been validated for the classification of postoperative PE for predicting late postoperative cardiac tamponade. Indeed, the incidence of late cardiac tamponade is significantly increased in patients with a loculated effusion larger than 15 mm or a circumferential effusion larger than 10 mm on transthoracic echocardiography on postoperative day 20.

The risk of PE has to be considered not only in the adult population, but also after congenital cardiac surgery. Serial echocardiographic monitoring up to 28 days postoperatively is indicated in selected high-risk patients such as those with symptoms of postpericardiotomy syndrome and those given warfarin. Interestingly, PE that eventually becomes moderate to large tends to occur later and occurs more commonly after Fontan-type procedures.

Although transthoracic echocardiography is almost always the ideal technique to detect and grade PE, several factors in the postoperative

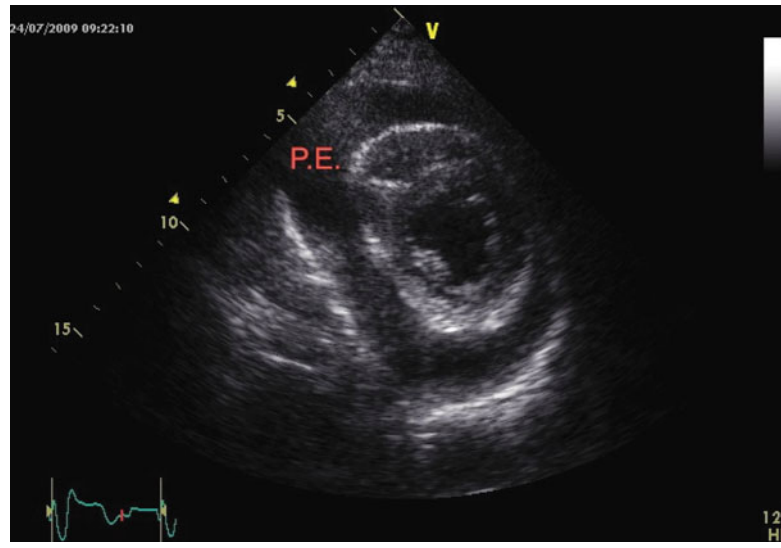

Fig. 9.1 Transesophageal echocardiography transgastric short-axis view of the left ventricle showing a circumferential large pericardial effusion (*P.E.*)

patient after cardiac surgery may contribute to the need for transesophageal echocardiography: the surgical site may preclude the use of the optimal transthoracic window, chest tubes may prevent proper positioning of the patient, and some loculated effusions or intrapericardial clots may not be amenable to transthoracic imaging.

As a final consideration, the differential diagnosis of echo-free spaces should include PE, pleural effusions, and pericardial fat. As a rule, in the different views pericardial fluid reflects at the posterior atrioventricular groove, whereas PE continues under the left atrium, posterior to the descending aorta. Pericardial fat can be identified as the hypoechoic space anterior to the epicardial fat; it is more prominent anteriorly, but may appear circumferentially, thus mimicking effusion. Pericardial fat is slightly echogenic and tends to move with the heart; in contrast, the effusion is generally echolucent and motionless.

Echocardiography is very important not only for diagnostic purposes, but also as a guide for percutaneous needle pericardiocentesis: it has an excellent profile in terms of simplicity, safety, and efficacy. Echocardiography identifies the shortest route by which the pericardium can be entered intercostally, allows clear localization of the needle, and shows the immediate benefit of the removal of the excess of pericardial fluid. Finally, the approach to the PE should be selected according to the distribution of the PE on echocardiography. If the effusion is equally large in the apical position and in front of the right ventricle from the subxiphoid view, both an apical and a subxiphoid approach can be attempted, according to the operator's preference. However, if the effusion is significantly asymmetrically distributed, it should be approached from the side where the accumulation of fluid is largest. The reported incidence of major complication ranges from 1.3 to 1.6 %.

9.3 Cardiac Tamponade

When the accumulation of pericardial fluid causes an increase in the pericardial pressure exceeding the intracardiac pressure, the positive transmural pressure gradient compresses cardiac chambers at different points in the cardiac cycle, compromising cardiac filling. Depending on the type and the severity of tamponade, a variety of physical findings may be present: chest pain radiating to the neck and jaw, orthopnea, cough, and dysphagia. The jugular venous pressure is elevated and there is commonly an exaggeration of the normal variation in the pulse pressure during the inspiratory phase of respiration greater than 10 mmHg (pulsus paradoxus) as well as an elevation in the venous jugular

pressure during inspiration (Kussmaul sign). On chest radiography, large effusions are depicted as globular cardiomegaly with sharp margins ("water bottle" silhouette). Electrocardiography may demonstrate diminished QRS and T-wave voltages, PR-segment depression, ST-T changes, bundle-branch block, and electrical alternans. Patients after cardiac surgery present a much more specific diagnostic challenge, since effusions may be localized, underlying cardiac disease is present, and positive pressure ventilation is used, all factors likely to alter the classic clinical findings.

Echocardiography is a powerful tool to quickly identify the hemodynamic significance of the PE and the cardiac tamponade. The basic elements that allow this identification are as follows:

- The low pressure of the right chambers makes them the first structures susceptible to the increased transmural pressure. Right atrial wall inversion during ventricular systole is usually an early sign of cardiac tamponade, followed by diastolic compression of the right ventricular outflow tract (evaluated by both M-mode and 2D echocardiography) (Fig. 9.2). The longer is the duration of the right atrial invagination relative to the length of the cardiac cycle, the greater is the likelihood of significant hemodynamic compromise: a duration of right atrial collapse exceeding one third of the cardiac cycle increases specificity without sacrificing sensitivity. Right chamber collapse may be delayed in the setting of pulmonary hypertension; in such cases, left atrial collapse may precede right atrial collapse.
- "Swinging heart": when a large PE accumulates, the heart will be swinging in the pericardial fluid beat-to-beat.
- Ventricular interdependence: during inspiration the interventricular septum bulges into the left ventricle owing to increased systemic venous return to the right ventricle and limited expansion of the free wall of the right ventricle.
- Respiratory variation in tricuspid and pulmonary flow detected with Doppler echocardiography. Tricuspid flow increases and mitral flow decreases during inspiration: the respiratory variations in mitral inflow of more than 35% and tricuspid inflow of more than 40% correlate well with cardiac tamponade. These respiratory variations cannot be seen in the invasively ventilated patient.
- Plethora of the inferior vena cava: there is a lack of change in vena cava caliper (less than 50% reduction in diameter) during inspiration.
- Prominence of diastolic reversals in hepatic veins by pulsed Doppler echocardiography: with expiration, systemic venous return decreases with reversal of diastolic flow in the hepatic veins.

9.4 Constrictive Pericarditis

Chronic inflammation of the pericardium results in thickening fibrosis and fusion of both layers of the pericardium. Constrictive pericarditis represents the end stage of this chronic inflammatory process leading to a limit in diastolic filling and resulting in diastolic failure, with relatively preserved global systolic function. The most common symptoms are related to either fluid overload (peripheral edema, elevated central venous pressure, hepatomegaly, pleural effusion, ascites, and anasarca) or decreased cardiac output (dyspnea, fatigue, palpitations, weakness, and exercise intolerance). An important reason to use echocardiography early in the diagnostic process is to rule out more common causes of right-sided heart failure, including left or right ventricular systolic dysfunction, severe pulmonary hypertension, or unrecognized left-sided valvular diseases. Once these diseases have been excluded, echocardiography is very useful in recognizing the pericardial thickening and the elements that characterize constrictive pericarditis. Visualization of the pericardium thickening (Fig. 9.3) could be done in a more accurate way with transoesophageal echocardiography, with a significant cutoff value of 3 mm.

The echocardiographic characteristics of constrictive pericarditis are secondary to the impaired diastolic cardiac filling and elevated ventricular filling pressures:

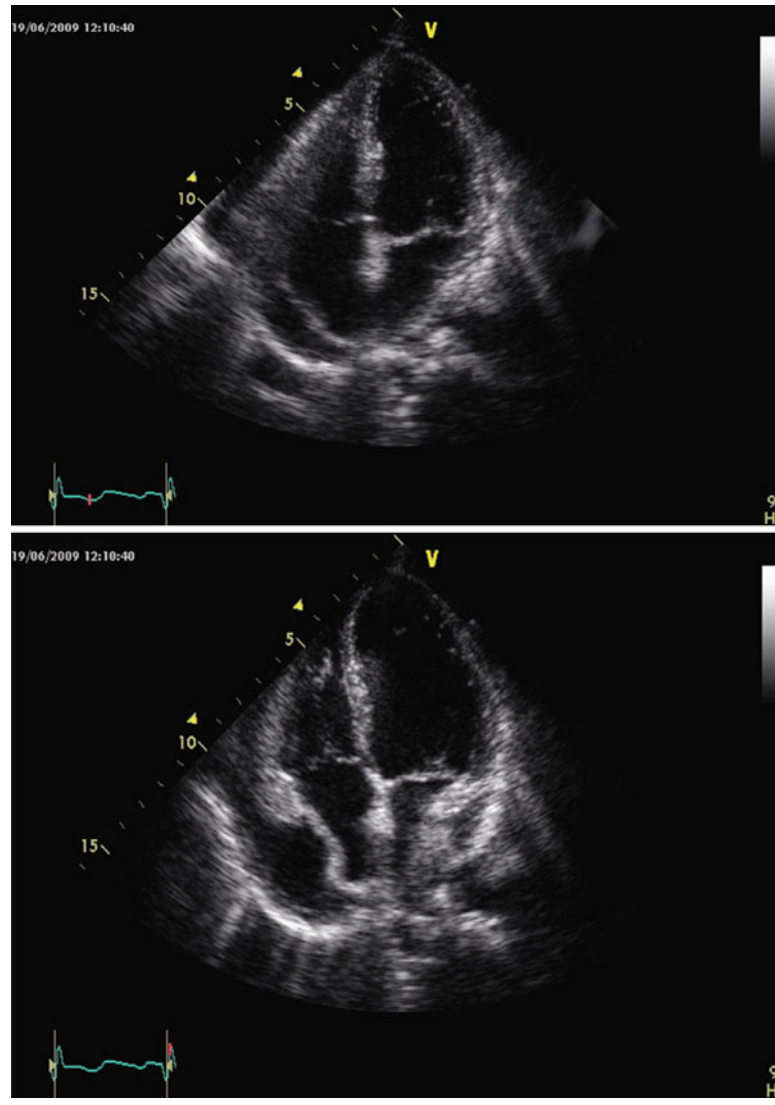

Fig. 9.2 Transthoracic echocardiography apical four-chamber view showing a large pericardial effusion with right atrial wall inversion during ventricular systole (*bottom*)

- Mitral inflow assessed by Doppler echocardiography demonstrates a rapid increase in ventricular diastolic pressure that creates the dip-and-plateau pattern with an increased early diastolic filling (E-wave) velocity with a rapid deceleration time and a small or absent A wave.
- Marked respiratory variation in left and right ventricular inflow velocities are seen with Doppler echocardiography. There is an increase in early diastolic mitral inflow of more than 25% during expiration. After complete pericardiectomy, mitral inflow patterns return to normal, and little respiratory variation is seen.
- Tissue Doppler imaging of the mitral annulus shows a prominent early diastolic velocity (Ea). A lateral or septal early diastolic mitral annular velocity of more than 8 cm/s on pulsed tissue Doppler imaging is in general the accepted cutoff value to diagnose constrictive pericarditis. Mitral annular velocities are particularly useful when pronounced respiratory variations in peak early mitral inflow velocities are not seen.
- There is increased ventricular interdependence with a classic respiratory shift in the position of the interventricular septum

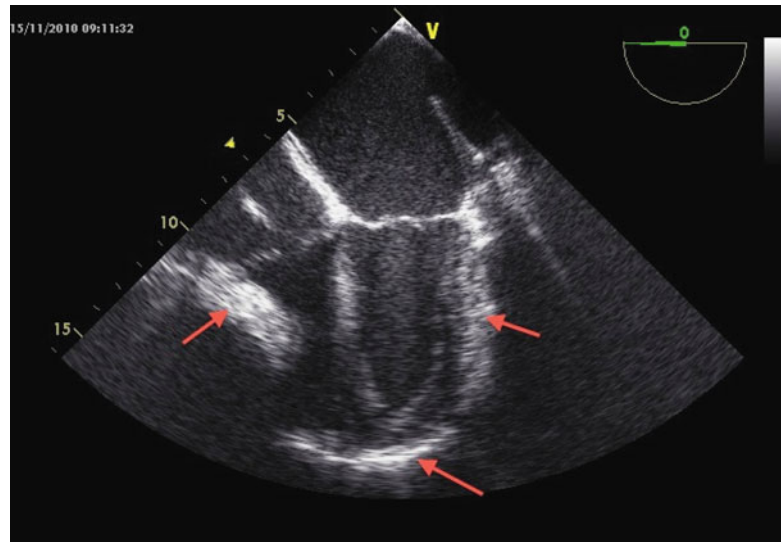

Fig. 9.3 Transesophageal echocardiography mid-esophageal four-chamber view showing pericardial thickening and calcification in constrictive pericarditis

towards the left ventricle during inspiration ("septal bounce").

- The flow propagation velocity into the left ventricle detected by color Doppler M-mode echocardiography is greater than 45 cm/s.
- Marked diastolic flow reversal that increases in expiration is evident in the hepatic veins.
- There is rapid flattening of the posterior wall of the left ventricle in early diastole with normal or exaggerated longitudinal deformation of the left ventricle.

The above criteria are important not only to diagnose constrictive pericarditis, but they also help to distinguish it from restrictive cardiomyopathy (see Chap. 13). Doppler echocardiographic techniques, in particular, have been shown to be useful in differentiating between these two diseases: a marked respiratory variation in mitral inflow and pulmonary venous flow is present in patients with constrictive pericarditis but is absent in those with restrictive cardiomyopathy. Recently, the newer echocardiographic modalities of tissue Doppler imaging and color M-mode flow propagation have been validated as ancillary tools to distinguish between these diseases, although they are equivalent and complementary to Doppler respiratory variation in distinguishing between constrictive pericarditis and restrictive cardiomyopathy. The additive role of the new methods needs to be established in difficult cases of constrictive pericarditis where respiratory variation may be absent or decreased. Of the two newer modalities, tissue Doppler imaging of the mitral annulus tends to have greater specificity and sensitivity than color M-mode flow propagation and is generally easier to use. As the velocity of propagation of early ventricular inflow from color M-mode echocardiography and the early mitral annular velocity from tissue Doppler imaging are markers of myocardial relaxation, their values are generally normal or supranormal in pure constrictive pericarditis, in which myocardial relaxation is normal or raised. By contrast, these values are decreased in restrictive cardiomyopathy, in which myocardial relaxation is impaired.

Patients with chronic obstructive pulmonary diseases or severe right ventricular dysfunction and large respiratory variations in intrathoracic pressure may also show inspiratory decreases in early mitral inflow velocities, such as in constrictive pericarditis. To distinguish these two conditions, the intensivist should consider that in chronic obstructive pulmonary disease there is a greater decrease in intrathoracic pressure in inspiration, which generates greater negative pressure changes in the thoracic cavity, and augments blood flow to the right atrium from the superior vena cava during inspiration.

9.5 Effusive-Constrictive Pericarditis

The features of cardiac tamponade and constrictive pericarditis may combine and cause effusive-constrictive pericarditis. These rare and particular cases should be diagnosed not only with the important help of echocardiography, but also taking into consideration hemodynamic variations before and after the removal of the excess pericardial fluid. The clinical diagnosis of this condition is based on the demonstration that in a patient with PE and tamponade a clinical and hemodynamic picture consistent with pericardial constriction persists after the removal of enough pericardial fluid to lower the intrapericardial pressure to the normal level.

9.6 Pericardial Masses

Primary pericardial tumors are rare; secondary tumors are far most common. Pericardial masses are often detected incidentally during routine echocardiography; although echocardiography should be considered important in the identification of these masses, CT or cardiac MRI should always be performed as they are the imaging modalities of choice when further evaluating these tumors.

9.7 Pericardial Cysts

Pericardial cysts are rare, benign congenital or inflammatory malformations; they can also be acquired after cardiothoracic surgery. They are usually found incidentally during routine X-ray or echocardiographic examinations and appear as echo-free fluid-filled loculated masses located mostly at the right costophrenic angle, and less frequently in the left costophrenic angle or in the posterior or anterior superior mediastinum. Color flow and pulsed Doppler interrogation at a low-velocity setting can be used to ensure there is no phasic flow within the structure and can be used to differentiate pericardial cysts from coronary aneurysm, left ventricular aneurysm, prominent left atrial appendage, aortic aneurysm, or solid tumors. Transesophageal echocardiography can be useful if transthoracic echocardiography is inadequate in delineating the diagnosis and can help to identify a pericardial cyst in atypical locations and distinguish it from other posteriorly located lesions.

9.8 Congenital Absence of the Pericardium

Congenital absence of the pericardium is a rare anomaly whose reported prevalence is 0.002–0.004 %. This defect can be partial or complete, mostly located on the left side of the heart and more frequently asymptomatic and detected incidentally. The foramen-type defects are the most dangerous subgroup of partial defects, because they can be fatal when they allow herniation of part of the heart. The absence of the pericardium results in an exaggerated cardiac motion, particularly of the posterior wall of the left ventricle. Traditional echocardiography shows prominence of the right-sided cardiac chambers and abnormal septal motion. If the right ventricle shifts to the left, its cavity may falsely appear enlarged. Finally, there is typically a displacement of the apical imaging window into the axilla and the atria appear compressed. An echocardiogram should be useful as well in the identification of the associated heart defects, such as atrial septal defects and bicuspid aortic valve.

Further Reading

Ashikhmina EA et al (2010) Pericardial effusion after cardiac surgery: risk factors, patient profiles, and contemporary management. Ann Thorac Surg 89:112–118

Dal-Bianco JP et al (2009) Role of echocardiography in the diagnosis of constrictive pericarditis. J Am Soc Echocardiogr 22:24–33

The Task Force on the Diagnosis and Management of Pericardial Diseases of the European Society of Cardiology (2004) Guidelines on the diagnosis and

management of pericardial diseases. Eur Heart J 25:587–610.
Wann Samuel, Passen Edward (2008) Echocardiography in pericardial disease. J Am Soc Echocardiogr 21:7–13
Yared K et al (2010) Multimodality imaging of pericardial diseases. JACC Cardiovasc Imaging 3:650–660

The Aorta

10

Luigi Tritapepe, Domenico Vitale, and Roberto Arzilla

10.1 Anatomy

The aorta is the largest artery in the body. It arises from the left ventricle, ascends for a short distance in the thorax, then forms an arch, and finally descends through the chest and through the abdomen, where ends by dividing into two arteries called the common iliac arteries. Anatomically, the aorta is traditionally divided into the ascending aorta, the aortic arch, and the descending aorta. In its initial part, divided into the ascending aorta, aortic arch and descending aorta, the aorta takes the form of an umbrella handle. The descending aorta is, in turn, subdivided into the thoracic aorta (which descends within the chest) and the abdominal aorta (which descends within the abdomen). The division into the thoracic aorta and abdominal aorta depends on the location to the diaphragm muscle. The thoracic aorta is characterized by the ascending tract, which ends at the brachiocephalic trunk, the arch to the left subclavian artery, and the descending tract to the diaphragm. The walls of the aorta consist of three layers. They are the tunica adventitia, the tunica media, and the tunica intima. The intima is a thin layer of endothelial cells arranged on a basal lamina. Normally it is not very echogenic, but that can change in pathological conditions. The media, which forms 80 % of the wall thickness, is formed of smooth muscle fibres arranged in a matrix of elastin and collagen in a spiral fashion. This layer provides the primary structural support and vascular tone of the aorta. The outermost layer is the adventitia, which provides nutrient supply by means of its lymphatics and the vasa vasorum. The aorta gives off branches that go to the heart, the head and neck, the arms, the major organs in the chest and abdomen, and the legs. It serves to supply them all with oxygenated blood. Many aortic diseases immediately damage the organs to which it supplies blood. The aorta is separated from the heart in the anterior mediastinum and turns left in front of the trachea and the left main bronchus, projecting into the posterior mediastinum, where it comes down behind the esophagus and in front of the vertebrae. The ascending aorta is about 5 cm long and has two distinct portions. The ascending aorta arises from the left ventricle and the portion distal to the valve is called the aortic root, where one can see the sinuses of Valsalva and the branching off of the two coronary arteries. The aortic root beginning at the aortic orifice and extends to the sinotubular junction, which is marked by a ledge or circumferential line that is called the supra-aortic ridge. The arch gives rise to three branches from its superior aspect, from where they course posterosuperiorly. The innominate and the left common carotid

L. Tritapepe (✉)
Department of Anesthesia and Intensive Care, Cardiac Surgery ICU, Policlinico Umberto I Hospital, Sapienza University of Rome, Rome, Italy
e-mail: luigi.tritapepe@uniroma1.it

A. Sarti and F. L. Lorini (eds.), *Echocardiography for Intensivists*,
DOI: 10.1007/978-88-470-2583-7_10, © Springer-Verlag Italia 2012

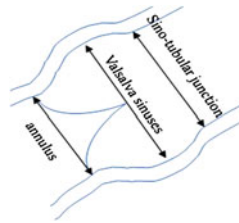

Fig. 10.1 The ascending aorta with measurement points

artery are in close proximity to the anterior aspect of the trachea. The descending aorta begins distal to the left subclavian artery at the ligamentum arteriosum, a remnant of the fetal patent ductus arteriosus. This area is called the aortic isthmus and it is important to visualize it in cases of coarctation of the aorta or patent ductus arteriosus. This region is also used as a landmark since the location of any disease in the descending aorta is described in relation to the isthmus.

The abdominal aorta is made up of suprarenal, renal, and infrarenal segments. In the adult, the aorta has a diameter of about 3 cm at the origin, 2.5 cm in the descending thoracic portion, and 1.8–2 cm in the abdomen.

10.2 Echocardiography

Echocardiography plays an important role in the diagnosis and follow-up of aortic diseases. Evaluation of the aorta must always be performed during the echocardiographic examination. Echocardiography is useful for every aortic disease that involves size, shape, and atherosclerotic degeneration of the thoracic aorta. With transesophageal echocardiography (TEE) we can easily visualize and study the aortic root and the proximal ascending aorta, and TEE can resolve the technical limitation of transthoracic echocardiography (TTE) in the examination of the thoracic aorta. TEE is the technique of choice in the diagnosis of aortic dissection, but in the emergency setting, TTE may be used as the initial screening mode. The discovery of an intimal flap in the ascending aorta, pericardial effusion/tamponade, and acute aortic valve insufficiency is possible with TTE. However, a negative TTE finding does not rule out aortic dissection and other imaging techniques must be considered. TEE is more accurate in defining the location of an entry tear, the severity of aortic regurgitation, and true lumen compression. TEE is recommended in selecting and monitoring surgical and endovascular treatment especially to detect every possible complication. CT and MRI have a greater field of view and may yield complementary information, but echocardiography is portable, rapid, accurate, and cost-effective in the diagnosis of most aortic diseases. The echocardiographic view of the aorta shows it to be circular in the perpendicular sections and tube shaped in the parallel sections relative to its largest axis. The echocardiographic image shows the wall as echo-reflecting and the aortic lumen as echo-free.

10.3 TTE of the Aorta

TTE is one of the techniques most used to measure proximal aortic segments in clinical practice. The proximal ascending aorta is visualized in the parasternal long-axis view, and also in the modified right parasternal long-axis view, and in the basal parasternal short-axis view, but for a lesser extent. The parasternal long-axis view allows us to correctly measure the aortic root diameters (Fig. 10.1). In the parasternal long-axis view, directly in two dimensions or in M-mode, we can study the aortic root and the proximal ascending aorta at the end of diastole with the aortic leaflets closed. We can measure the annulus, where the leaflets are attached, the Valsalva sinuses, in the maximal diameter, and the sino-tubular junction, at the end of the sinuses and the beginning of tubular tract. The root and the proximal aorta measure less than 3.7 cm in an adult of mean size. With the same view, we can observe the descending aorta as a circular image below the left atrium, posteriorly. In all patients with suspected aortic disease, the right parasternal long-axis view, also if it is not routinely performed, is recommended for estimating the true size of the ascending aorta. The ascending aorta is also visualized in the apical three-chamber and modified apical five-chamber views; however, in

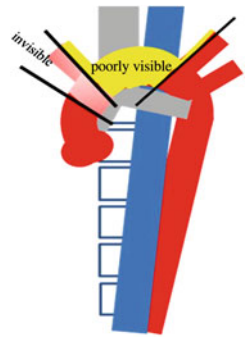

Fig. 10.2 Evaluation of the aorta by transesophageal echocardiography (TEE)

these views, the aortic walls are seen with suboptimal lateral resolution and the diagnosis could be misinterpreted or unrecognized. The subcostal views may in some cases be helpful, and allow one to visualize the suprarenal aorta. All these tomographies also allow us to study optimally the aortic valve, which is often involved in disorders of the ascending aorta (e.g., bicuspid valve, aortic regurgitation due to dilatation of the ascending aorta or aortic dissection, and other diseases). The suprasternal view is a crucial view to visualize, above the right pulmonary artery, the aortic arch and the three supra-aortic trunks (innominate, left carotid, and left subclavian arteries), and again a variable tract of the descending and the ascending aorta. However, if inconclusive information or abnormalities are present, another imaging modality (e.g., TEE) is required to either the complete information or add diagnostic information.

10.4 TEE of the Aorta

TEE has been shown to be a very sensitive diagnostic tool in the delineation and management of different aortic diseases. It is a fundamental examination to diagnose the aortic syndrome and differentiate other diseases in the case of chest pain. TEE represents a diagnostic tool for the cardiologist, intensivist, and anesthesiologist wishing to practice cardiac anesthesia. The anatomic proximity of the aorta to the esophagus allows one to have a good view of the aorta, almost entirely. The only invisible tract is the distal portion of the ascending aorta owing to the presence of air in the right main bronchus, whereas the proximal portion of the aortic arch is poorly visible because of the proximity of the trachea, which could cause a virtual blind spot in that area (Fig. 10.2).

In routine practice, evaluation of the aorta by TEE is possible through six views (Table 10.1): mid-esophageal ascending aortic short-axis view, mid-esophageal ascending aortic long-axis view, upper esophageal aortic arch view, upper esophageal aortic arch long-axis view, descending aortic short-axis view, and descending aortic long-axis view. In the mid-esophageal four-chamber view at 0°, the probe should be withdrawn 2 cm and the ascending aorta can be shown in the short axis. This produces a circular image of the aortic root between the left atrium and the right atrium. Rotating the imaging plane to 90° will produce the long-axis view showing the ascending aorta. In this projection, however, the distal ascending aorta cannot be visualized owing to the dispersion of echoes due to tracheal air. The ascending aortic long-axis view is a good view to measure the wall thickness, the aortic diameter and the turbulence of flow. To view the descending thoracic aorta, we must return to the mid-esophageal four-chamber view and then rotate the probe through 180°; we then see the aorta positioned behind the esophagus. The aorta is circular at the top of the screen and changing the depth and frequency, we may well see it in an appropriate manner. If the probe is moved down, the aorta is no longer displayed when we reach the diaphragm muscle. With slight shifts of the probe back, we obtain the short-axis view of the thoracic aorta at various levels, making sure to rotate the probe slightly to center the image of the aorta because it runs laterally and then posteriorly to the esophagus at this level. Thus, we can fully display the descending thoracic aorta, which is very useful, for example, in the positioning of an endoluminal stent. Rotating the imaging plane to 90° will bring into view the long-axis image of the descending aorta.

To view the arch, we go back to the mid-esophageal four-chamber view at 0° and pull the probe back slowly until the aortic arch is seen.

Table 10.1 Tomographic views for evaluation of the ascending aorta, aortic arch and descending thoracic aorta

TTE	TEE
PSLAX, PSSAX (Asc + Desc Ao)	ME Asc Aortic LAX, ME Asc Aortic SAX (Asc Ao)
A4C, A2C, ALAX (Desc Ao)	UE Aortic Arch, UE Aortic Arch LAX (arch + Asc Ao)
Suprasternal (Arch, Asc and Desc Ao)	Desc Aortic LAX, Desc Aortic SAX (Desc Ao)
Subcostal (Abdominal and Asc Ao)	

TTE transthoracic echocardiography, *TEE* transesophageal echocardiography, *PSLAX* parasternal long axis, *PSSAX* parasternal short axis, *Asc* ascending, *Desc* descending, *Ao* aorta, *A4C* apical four chamber, *A2C* apical two chamber, *ALAX* apical long axis, *ME* mid esophageal, *LAX* long axis, *SAX* short axis, *UE* upper esophageal

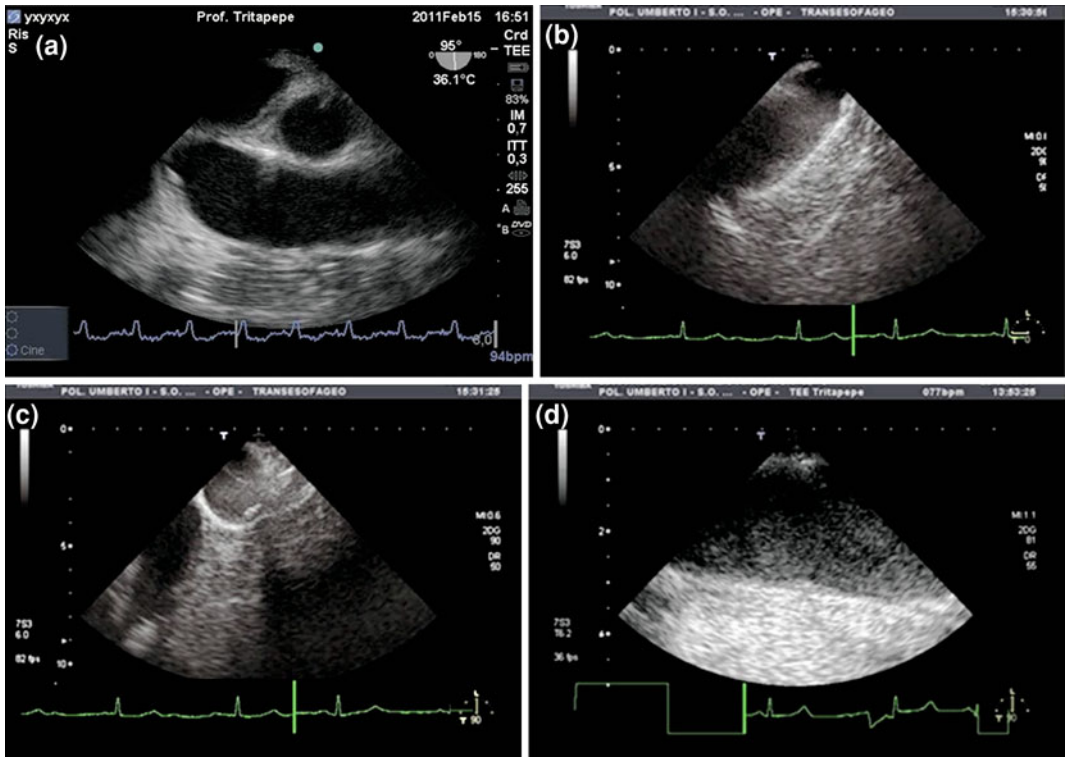

Fig. 10.3 TEE of the aorta: **a** ascending aorta, **b** arch, **c** at level of the origin of the subclavian artery, **d** descending aorta

This is displayed in the upper esophageal long-axis view about 20 cm from the mouth rhymes. The proximal part of the aortic arch is not viewable because of air in the trachea; however, we have a good view of the arch that shows the proximal portion on the left of the screen and the distal part on the right, with the posterior wall near the probe and at the top of the screen and the anterior wall farther and down. To obtain short-axis images of the aortic arch, we need to rotate the probe 90° clockwise. The left subclavian artery and the left common carotid artery can also be viewed by pulling the probe further back (Fig. 10.3).

Near the aortic arch we can see the trunk of the pulmonary artery and part of its left branch. It is impossible to see the brachiocephalic arterial trunk because of the presence of tracheal air, which prevents the penetration of the echoes. Study of the thoracic aorta should include wall

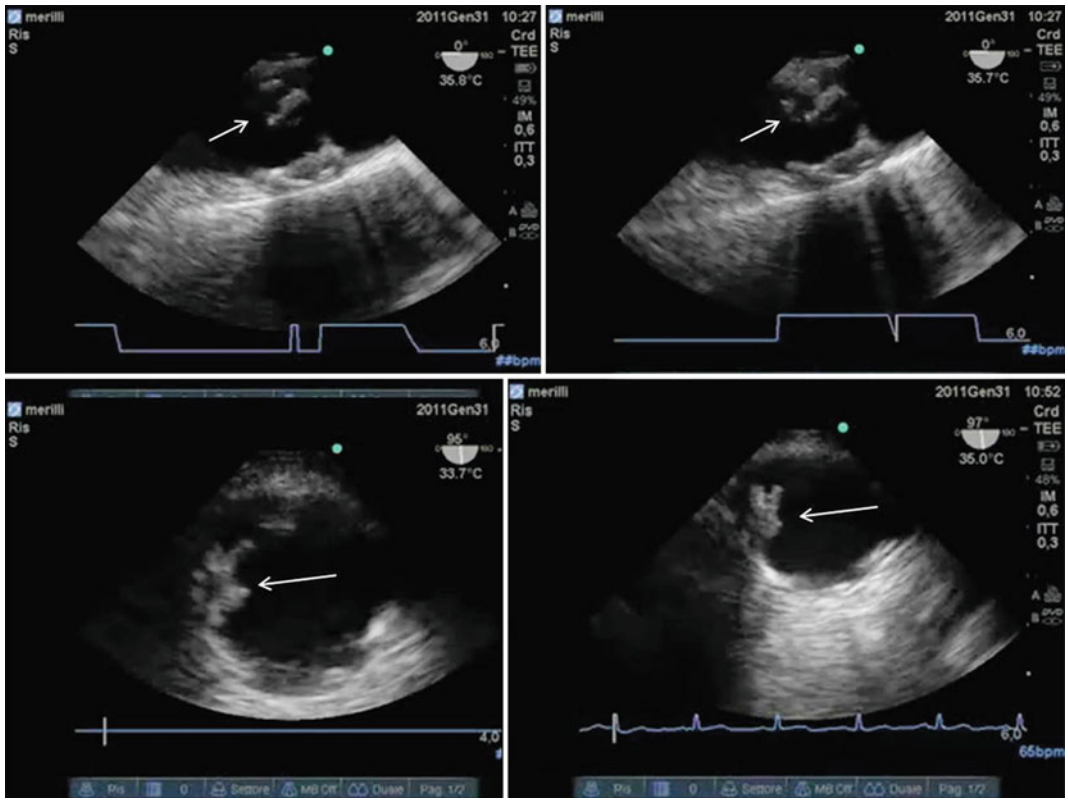

Fig. 10.4 TEE of the aorta at the level of the arch and of the origin of the subclavian artery. Note the presence of a huge mobile atheroma (*arrow*)

thickness, tissue characteristics, dimensions, and blood flow patterns by Doppler assessment.

10.5 Aortic Atheroma

Aortic atheroma appears as a thickening of the aortic wall localized or extended, either circumferential or more irregular. In recent years, the presence of protruding atheromas in the aortic arch has been recognized as a potential cause of cerebral or peripheral embolization in the elderly. The complexity of the atheroma (the presence of ulcerations on its luminal surface or of mobile components) has been considered as a potential cofactor in further enhancing the risk of stroke. Several case–control studies with either autopsy findings or TEE have identified large atheromas (i.e., more than 5 mm thick) as one of the most powerful independent risk factors for ischemic stroke in patients over 60 years of age. Aortic atheroma complexity rather than size is strongly associated with ischemic stroke in the elderly. For aortic disease, TEE provides real-time images that allow the evaluation of plaque morphology, ulceration, and mobility (Fig. 10.4, Table 10.2).

Table 10.2 One of many classifications for aortic atheroma as proposed by Katz and colleagues

Grade	Findings
I	No disease or minor intimal thickening
II	Extensive intimal thickening but without discrete measurable plaques
III	Protruding plaques less than 5 mm thick
IV	Protruding plaques more than 5 mm
V	Any mobile atheroma

TEE or epicardial echocardiography is useful in cardiac surgery to detect the presence of aortic atheroma. In fact, many surgeons still palpate the aorta for atheroma scanning before making an aortotomy or placing a vascular clamp, but this method can only detect the most severe cases of atherosclerosis, and in some instances the palpation itself can dislodge the plaques and lead to embolic sequelae. The aortic atheroma must always be detected before intra-aortic devices (intra-aortic balloon pump, cannulae, endovascular stents) are positioned.

10.6 Aortic Aneurysm

The aneurysm is considered a dilation of an aorta whose diameter is least more than 50% the diameter of the expected normal value for age, height, and sex. In an aortic aneurysm, the three layers of the vessel wall are preserved but the luminal diameter is increased. An aneurysm can be described as saccular and fusiform depending on its morphology and it can occur along the whole length of the aorta. Most aortic aneurysms (about 65 %) occur in the abdominal aorta. They are often related to systemic arterial hypertension and atherosclerosis, but, especially in the ascending aortic tract, also to Marfan syndrome and other collagenopathies, aortic bicuspid valve, and other aortic valve diseases.

The aneurysm of the descending thoracic aorta can be due to aortic atherosclerosis but it can also be consequence of previous thoracic trauma with the mechanism of incomplete wall rupture or strain at the level of the isthmus tract of the aorta. The ascending aortic aneurysm can be easily detected with TTE in the parasternal long-axis view, in which we can recognize not only the aortic diameter and the systolic expansion of the aneurysm, but also the remodeling of the aortic valve with its consequent insufficiency. The importance of echocardiography is in evaluating the growing of the aortic aneurysm, in detecting the presence of intramural thrombi, and in preventing rupture by referring the patient to the surgeon when the diameter generally exceeds more than 5 cm. TEE is more accurate to study the aortic arch and the descending thoracic aorta. This method is now usually employed in all procedures of endovascular aortic stenting and recently in monitoring and guiding percutaneous aortic valve replacement. The implantation of transluminally placed endovascular grafts or stents has become an alternative to aortic surgery especially in the treatment of a thoracoabdominal aneurysm. TEE monitoring is crucial to detect, during the whole procedure, the exact positioning of stents and to search for endoleaks to exclude aortic lesions.

10.7 Aortic Dissection

Aortic dissection is characterized by an intimal tear near an aortic plaque or by an aortic penetration from an ulcerated plaque and the extension of an intramural hematoma affecting the media and allows the hematoma to expand throughout the aortic wall. The detachment of the intima from the aortic wall is a result of the thrust due to the systolic blood pressure and cardiac contractility. This mechanism promotes the formation of two lumens in the aorta: the false lumen and the true lumen. When the dissection involves the aortic root, correct functioning of the aortic valve is of importance because aortic valve insufficiency can precipitate the hemodynamics. Also, the dissection can proceed toward the coronary ostia, causing acute myocardial ischemia or infarction that has to be accurately detected by echocardiography before these lesions are treated with antiplatelets or with percutaneous transluminal coronary angioplasty or an intra-aortic balloon pump. In the absence of a diagnosis or in the case of misinterpretation, we may have a disaster related to massive bleeding or organ malperfusion at the time of emergent surgery. TEE is the technique of choice in the diagnosis of aortic dissection, but in the emergency setting, TTE may be used as the initial screening mode. Although CT angiography and MRI images are more sensitive and specific, they cannot be used in unstable patients, which is more often the case in this clinical scenario. In the case of doubt or absence

of a clear landmark with TTE, TEE is required to differentiate a dissection from the other abnormalities that cause chest pain. Depending on the location of dissection, we distinguish a dissection as Stanford type A (type I and II of the DeBakey classification) when the lesion involves the ascending aorta and arch and as Stanford type B (DeBakey type III) when it affects the descending aorta, below the emergence of the subclavian artery. Type A aortic dissection is a true surgical emergency with a mortality rate that increases from the time of onset. A criterion that determines the extreme urgency is the presence of pericardial effusion or tamponade as well as the condition of shock. In type B aortic dissection, in the absence of malperfusion of splanchnic organs, we have to treat the patient aggressively with antihypertensive drugs associated with beta blockers, and only after stabilizing the lesion can we treat the aortic dissection with endoluminal stents. Echocardiographic diagnosis is fundamental to resolve some doubts and to help the surgeon, in case of type A, or radiologist, in case of type B, to correct the aortic dissection with success. Echocardiographic diagnosis needs to detect a mobile intraluminal flap, the presence of a false lumen, and one or more entry tears where the flow goes from a true lumen into the false lumen. Doppler and color Doppler imaging may help to identify the true lumen from the false lumen and to evidence the aortic tear. Doppler imaging does not show a normal wave typical of aortic flow in the false lumen, which may have a flat wave due to luminal thrombosis. The differences between the false lumen and the true lumen can be summarized as follows: the false lumen is bigger than the true lumen; during systole the true lumen expands whereas the false lumen is compressed; the direction of flow is antegrade in the true lumen and reduced or absent in the false lumen.

10.8 Intramural Hematoma

Intramural hematoma is a bleeding inside the layers of the aortic wall. It can resolve spontaneously or following medical therapy or can develop into an aortic aneurysm or dissection. The diagnosis of intramural hematoma can be straightforward in typical cases, but an intramural hematoma can be confused with a thrombus or a thrombosis of the false lumen in aortic dissection. TEE may facilitate the diagnosis of intramural hematoma, whereas TTE does not have accuracy on the aortic wall. On echocardiography an intramural hematoma appears as concentric or more localized thickening (more than 5 mm) of the aortic wall without measurable flow within. The International Registry of Aortic Dissection data demonstrate a 5.7 % prevalence of intramural hematoma in patients with acute aortic syndromes. Like classic aortic dissection, intramural hematoma is a highly lethal condition when it involves the ascending aorta, and surgical therapy should be considered, but this condition is less critical when it is limited to the arch or the descending aorta.

10.9 Sinus of Valsalva Aneurysm

The spaces between the luminal surface of the three bulges on the aortic root and their respective valvar leaflets are known as the aortic sinuses of Valsalva. A sinus of Valsalva aneurysm is often a congenital abnormality caused by a dilation, usually of a single sinus of Valsalva, from a separation between the aortic media and the annulus fibrosus. Other disease processes that involve the aortic root (e.g, atherosclerotic aneurysms, endocarditis, cystic medial necrosis, chest trauma) may also produce a sinus of Valsalva aneurysm, although this usually involves multiple sinuses. Rupture of the dilated sinus may lead to intracardiac shunting when a communication is established with the right atrium or directly into the right ventricle (60–90 %). Cardiac tamponade may occur if the rupture involves the pericardial space. TTE and TEE are accurate in the diagnosis of a sinus of Valsalva aneurysm both in the parasternal long-axis view and the mid-esophageal aortic valve long-axis view and in the short-axis view.

10.10 Aortic Coarctation

Coarctation of the aorta is a narrowing of the aorta between the upper and the lower body. It typically occurs in an isolated location just after the aortic arch at the level of the aortic isthmus. It can be associated with other congenital abnormalities such as a bicuspid aortic valve. The narrowing of the aortic lumen increases the blood pressure in the upper body, and reduces it in the lower part. It is a rare diagnosis in an adult patient, but it can occasionally be detected during a complete screening for idiopathic hypertension. TEE is more sensitive than TTE in visualizing the coarctation of the aorta. In addition, apart from imaging the ridge of the aortic lumen, Doppler imaging is accurate in determining the severity of aortic coarctation. In fact, the presence of a high-velocity turbulent flow and a gradient with continuous wave Doppler imaging could justify the suspicion of an aortic coarctation that will be classified as severe when the gradient exceeds 25 mmHg.

10.11 Patent Ductus Arteriosus

Patent ductus arteriosus is a heart defect that occurs soon after birth in some babies. Before birth the aorta and the pulmonary artery are connected by the ductus arteriosus. This vessel is an essential part of fetal blood circulation. Within minutes or up to a few days after birth, the ductus arteriosus is closed. In some babies, however, the ductus arteriosus remains open (patent). This opening allows mixing of oxygenated blood from the aorta to the pulmonary artery. This could cause heart failure and increase blood pressure in the lung arteries. Patent ductus arteriosus can be detected with TTE in the parasternal short-axis view, in which we can observe, with color Doppler imaging, a jet from the aorta to the pulmonary artery.

Further Reading

Evangelista A, Mukherjee D, Mehta RH et al (2005) Acute intramural hematoma of the aorta a mystery in evolution. Circulation 111:1063–1070

Evangelista A, Flachskampf FA, Erbel R et al (2010) Echocardiography in aortic diseases: EAE recommendations for clinical practice. Eur J Echocardiogr 11:645–658

Harloff A, Simon J, Brendecke S et al (2010) Complex plaques in the proximal descending aorta an underestimated embolic source of stroke. Stroke 41: 1145–1150

Ho SY (2009) Structure and anatomy of the aortic root. Eur J Echocardiogr 10:i3–i10

Kabirdas D, Scridon C, Brenes J-C et al (2010) Accuracy of transthoracic echocardiography for the measurement of the ascending aorta: comparison with transesophageal echocardiography. Clin Cardiol 33:502–507

Shiga T, Wajima Z, Apfel CC, Inoue T, Ohe Y (2006) Diagnostic accuracy of transesophageal echocardiography, helical computed tomography, and magnetic resonance imaging for suspected thoracic aortic dissection. Arch Intern Med 166:1350–1356

Vasaiwala S, Vidovich MI, Connolly J, Frazin L (2010) Transesophageal echocardiography of the descending thoracic aorta: establishing an accurate anatomic marker using the celiac artery. Echocardiography 27:1093–1097

Willoteaux S, Nedelcu C, Bouvier A et al (2011) Syndrome aortique: quelle imagerie réaliser? Presse Med 40:43–53

Inferior and Superior Venae Cavae 11

Massimo Milli

11.1 Inferior Vena Cava

11.1.1 Visualization

The inferior vena cava (IVC) in a subcostal approach appears like a horizontal tube supplied by the intrahepatic veins, in continuity with the right atrium (Fig. 11.1).

Guidelines suggest acquiring the IVC diameter:

- With the patient in the left lateral decubitus position 1 or 2 cm from the outflow in the atrium (sometimes it is possible to obtain better images with the patient in the dorsal decubitus position)
- In M-mode using the zoom function

The factors that influence the vessel diameter are the position of the patient, the age of the patient, respiratory variations (Figs. 11.2, 11.3, 11.4), and mechanical ventilation.

Normal values for IVC diameters in elderly patients may be helpful to detect the hydration status. For this reason the variation of normal values in relation to age need to be considered. In particular, we can observe an age-related decrease in the maximum IVC diameter and an increase in respirophasic variations of IVC diameter. Therefore, elderly patients with decreased maximum IVC diameter and increased respirophasic IVC collapsibility should be monitored for risk of dehydration.

11.1.2 Hypovolemia

A decrease of IVC diameter under 1.2 cm and, in particular, under 1 cm with complete inspiratory collapse is related to a hypovolemic status and low central venous pressure during spontaneous respiration. During mechanical ventilation the cutoff value of the IVC diameter for hypovolemic status increases to 1.5 cm.

11.1.3 Evaluation of Right Atrial Pressure and Prediction of Fluid Responsiveness in Patients with Spontaneous and Mechanical Breathing Support

In healthy subjects, during inspiration, we observe a physiological reduction of IVC diameter. During spontaneous ventilation, the normal IVC diameter is under 1.7 cm and normally we can observe an inspiratory collapse of 50 % or more during the respiratory cycle; these values usually correspond to a 0–5-mmHg right atrial pressure. An IVC dilatation (diameter more than 1.7 cm) with a normal inspiratory collapse (50 %) corresponds to 6–10-mmHg right atrial pressure. If we detect an IVC dilatation with an inspiratory collapse of less than 50 %, the right atrial pressure increase to

M. Milli (✉)
Department of Cardiology, Santa Maria Nuova Hospital, Florence, Italy
e-mail: massimo.milli@asf.toscana.it

A. Sarti and F. L. Lorini (eds.), *Echocardiography for Intensivists*,
DOI: 10.1007/978-88-470-2583-7_11, © Springer-Verlag Italia 2012

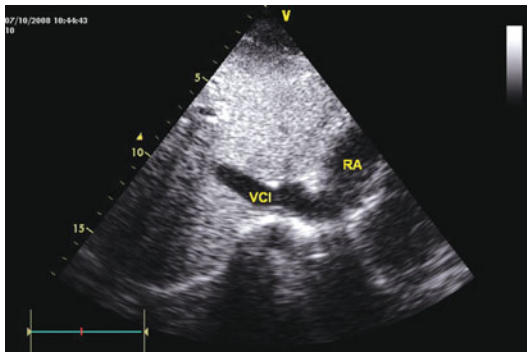

Fig. 11.1 Subcostal view: inferior vena cava. *RA* right atrium, *VCI* inferior vena cava. (From Sarti [1] with permission)

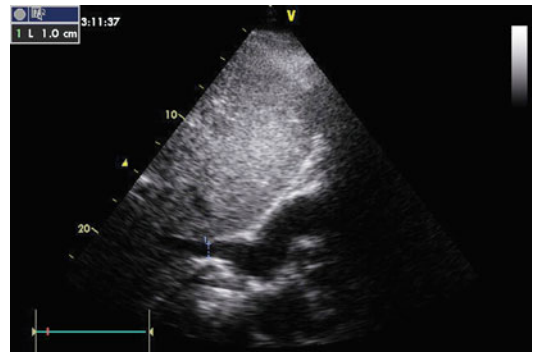

Fig. 11.3 Subcostal view: inferior vena cava diameter during inspiration (spontaneous breathing). (From Sarti [1] with permission)

Fig. 11.2 Subcostal view (M-mode): inferior vena cava. Respirophasic variations of inferior vena cava diameter. (From Sarti [1] with permission)

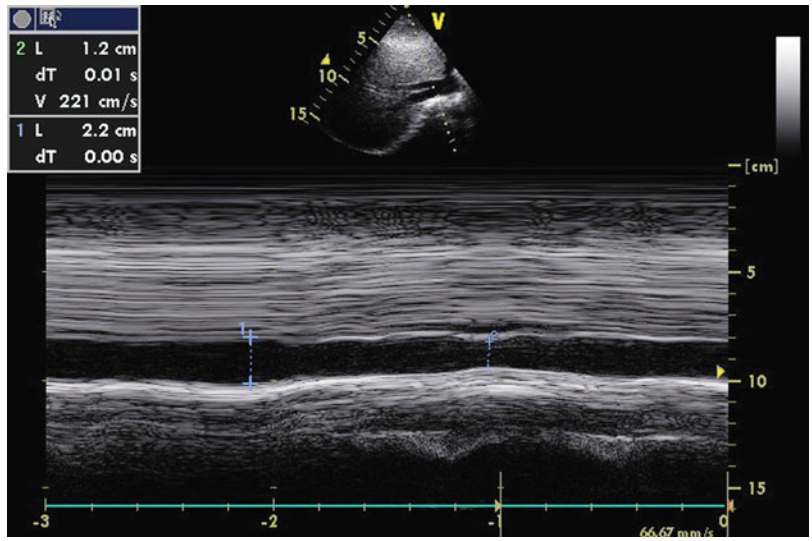

10–15 mmHg. Finally, an IVC dilatation without any inspiratory collapse point to a right atrial pressure of more than 15 mmHg (Table 11.1).

During mechanical insufflation, the pressure inside the thorax increases more than the pressure outside; therefore, the pressure gradient to venous return is reduced and the systemic venous return decreases during mechanical insufflation. As a consequence, mechanical insufflation increases the volume of extrathoracic venous blood, and then the endoluminal diameter of the distensible IVC. For these reasons, in patients with mechanical ventilation with positive pressure, the dilatation of the IVC should be used carefully to estimate the right atrial pressure. In any case, if the IVC diameter is less than 1.2 cm during mechanical ventilation, this measure is highly specific for right atrial pressure below 10 mmHg.

A specific distensibility index of the IVC is available to evaluate fluid responsiveness in septic mechanically ventilated patients. The IVC diameter at end-expiration (D_{min}) and at end-inspiration (D_{max}) is measured by echocardiography using a subcostal approach. The distensibility index of the IVC, calculated as $(D_{max} - D_{min})/D_{min}$, can be used in the treatment of ventilated intensive care patients. In circulatory failure during severe sepsis,

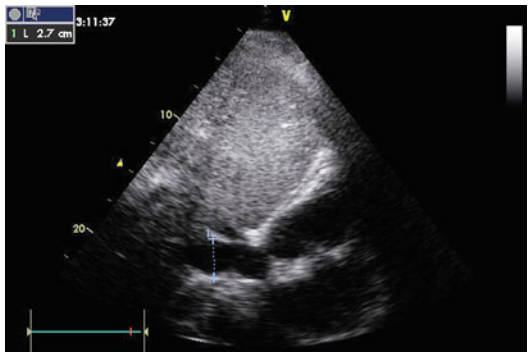

Fig. 11.4 Subcostal view: inferior vena cava diameter during expiration (spontaneous breathing). (From Sarti [1] with permission)

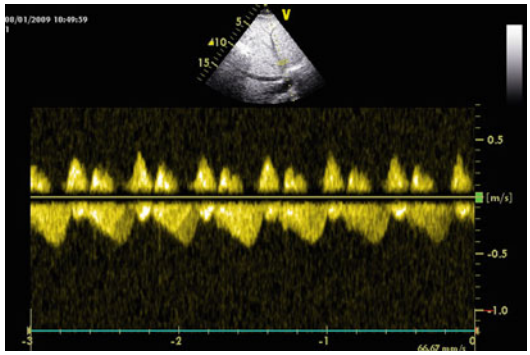

Fig. 11.5 Subcostal view: pulsed wave Doppler imaging of an intrahepatic vein. (From Sarti [1] with permission)

a distensibility index above 18 % suggests volume expansion.

11.1.4 Intrahepatic Veins

The dimensions of the intrahepatic veins are related to the central venous pressure. Very branched "star" images of intrahepatic venous vessels are consistent with caval hypertension. With the transthoracic echocardiographic approach, we cannot perform a correct Doppler evaluation of IVC flow because of alignment problems. With good alignment, it is possible to correctly evaluate the systolic and diastolic flow components, with the pulsed Doppler beam positioned into an intrahepatic vein lumen, about 1 cm before the outflow in the IVC (Fig. 11.5).

Table 11.1 Inferior vena cava: evaluation of right atrial pressure and central venous pressure

Diameter (cm)	Inspiratory collapse	Right atrial pressure (mmHg)
<1.5	>50 %	0–5
>1.5	>50 %	6–10
>1.7	<50 %	10–15
>1.7	No collapse	>15

From Sarti [1] with permission

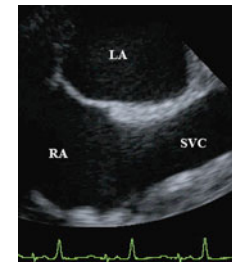

Fig. 11.6 Transesophageal echocardiography mid-esophageal bicaval 90° view. *LA* left atrium, *RA* right atrium, *SVC* superior vena cava

11.2 Superior Vena Cava

11.2.1 Visualization

The superior vena cava (SVC) is a large vein located in the upper chest, which collects blood from the head and arms and delivers it to the right atrium of the heart. The SVC can be visualized with transesophageal echocardiography, in the transverse plane (0°) in the proximal esophagus, down to the outflow in the right atrium. In the vertical plane (90°), the longitudinal axis can be studied (Fig. 11.6). In an intensive care setting, the evaluation of the SVC can be used to detect the presence of compression of the vein (SVC syndrome), which is frequently related to cancer, and less often to thrombotic obstruction or infections.

As for the IVC, the distensibility index of the SVC is a good index to evaluate the response to volume expansion in ventilated septic patients.

Reference

1. Sarti A (2009) Ecocardiografia per l'intensivista. Springer, Milan

Further Reading

Barbier C (2004) Respiratory changes in inferior vena cava diameter are helpful in predicting fluid responsiveness in ventilated septic patients. Intensive Care Med 30:1740–1746

Feissel M (2004) the respiratory variation in inferior vena cava diameter as a guide to fluid therapy. Intensive Care Med 30:1834–1837

Jue J, Chung W, Schiller NB (1992) Does inferior vena cava size predict right atrial pressures in patients receiving mechanical ventilation? J Am Soc Echocardiogr 5:613

Lang RM, Bierig M, Devereux RB et al (2008) Recommendations for chamber quantification: a report from the American Society of Echocardiography's Guidelines and Standard Committee and the Chamber Quantification Writing Group, developed in conjunction with the European Society of Cardiology. J Am Soc Echocardiogr 18:1440–1463

Masugata H et al (2010) Age related decrease in inferior vena cava diameter measured with echocardiography. Tohoku J Exp Med 222:141–147

Vieillard-Baron A et al (2004) Superior vena caval collapsibility as a gauge of volume status in ventilated septic patients. Intensive Care Med 30:1734–1739

Wallace DJ, Allison M, Stone MB (2010) Inferior vena cava percentage collapse during respiration is affected by the sampling location: an ultrasound study in healthy volunteers. Acad Emerg Med 17(1):96–99

Ischemia and Myocardial Infarction

12

F. Luca Lorini, Marialuigia Dello Russo, and Elena Pagani

12.1 Introduction

The echocardiogram is a standard tool in the treatment of patients with acute myocardial infarction (AMI). The role of echocardiography in establishing the diagnosis, location, and extent of myocardial infarction, in diagnosing mechanical complications of infarction, and providing prognostic information that is important for risk stratification will be reviewed.

A 2003 task force of the American College of Cardiology, the American Heart Association, and the American Society of Echocardiography gave a class I recommendation for the use of echocardiography in the diagnosis of suspected acute ischemia or infarction not evident by standard means, but did not recommend echocardiography when the diagnosis was already apparent.

The task force recommended against the routine use of echocardiography for diagnosis of chest pain in patients with electrocardiographic changes diagnostic of myocardial ischemia or infarction.

12.2 Diagnosis of AMI

The diagnosis of AMI is typically based upon the

- History and symptoms
- Electrocardiogram
- Cardiac enzymes, particularly serum troponins and myocardial-bound creatine kinase.

Although not routinely performed for diagnosis, echocardiography is an accurate, noninvasive test that is able to detect evidence of myocardial ischemia or necrosis.

Severe ischemia produces regional wall motion abnormalities (RWMAs) that can be visualized echocardiographically. The RWMAs reflect a localized decrease in the amplitude and rate of myocardial excursion, as well as a blunted degree of myocardial thickening.

Since ischemic RWMAs develop prior to symptoms, chest pain in the absence of RWMAs should not be due to active myocardial ischemia. However, the converse is not true; the presence of RWMAs does not establish the diagnosis of ischemia. There are a number of other causes of RWMAs, including a prior infarction, focal myocarditis, prior surgery, left bundle branch block, ventricular preexcitation via an accessory pathway, and cardiomyopathy.

12.3 Role of Echocardiography in Ischemic Heart Disease

The use of echocardiography in ischemic heart disease is based upon the rapid change in wall motion of a segment after an interruption or critical decrease in its blood supply. This phenomenon occurs within a few seconds of the onset of coronary occlusion (12 ± 5 and 19 ± 8 s in two series of patients evaluated during transient coronary occlusion induced by

F. L. Lorini (✉)
Department of Anesthesia and Intensive Care,
Ospedali Riuniti di Bergamo,
Bergamo, Italy
e-mail: llorini@ospedaliriuniti.bergamo.it

A. Sarti and F. L. Lorini (eds.), *Echocardiography for Intensivists*,
DOI: 10.1007/978-88-470-2583-7_12,

angioplasty), just after the onset of diastolic abnormalities and many seconds before electrocardiographic changes and angina.

Experimental as well as clinical studies have shown that wall motion abnormalities have a high sensitivity for predicting myocardial infarction. Other studies, performed in the emergency department on patients evaluated for myocardial ischemia, have reported similar results. An important aspect is that necrosis is not necessary to cause wall motion abnormalities; therefore, echocardiography can also be used to identify patients with ischemia without infarction.

Importantly, the sensitivity is significantly higher than that for electrocardiography and is comparable to that for myocardial perfusion imaging.

Transthoracic echocardiography (TTE) is often underutilized in this setting. TTE has the advantages of being readily accessible, portable, noninvasive, and fast; it may detect significant findings that are misdiagnosed or not detected on initial clinical evaluation. In one study of 124 patients, it identified a patient with a significant abnormality with a sensitivity, specificity, positive predictive value, negative predictive value, and overall accuracy of 84, 88, 89, 83, and 86 %, respectively.

Although TTE has been most commonly used for evaluation of regional wall changes, transesophageal echocardiography (TEE) is an alternative, more invasive technique that may be of particular importance during surgery or in the patient with inadequate transthoracic echocardiographic images. As an example, the continuous high-quality imaging of the left ventricle afforded by TEE during surgical procedures makes it ideally suited for the early detection of ischemia. These intraoperative changes in wall motion are more predictive of postoperative ischemia or infarction than ECG changes or hemodynamic abnormalities as documented with Swan-Ganz catheter measurements, such as an increase in pulmonary capillary wedge pressure (PCWP). In a study of 98 patients studied before and after the induction of anesthesia prior to coronary artery bypass graft surgery, ischemia as defined by TEE was associated with a small elevation in PCWP (3.5 mmHg); however, a rise in PCWP itself had a low sensitivity and predictive value for myocardial ischemia.

Echocardiography is a valuable, noninvasive diagnostic tool that can provide information about systolic function and valvular abnormalities and can provide alternative explanations for the causes of chest pain, such as aortic dissection, aortic stenosis, cardiac tamponade, pericarditis, and hypertrophic cardiomyopathy.

12.4 Evaluation of Regional Wall Motion

The abnormalities in wall motion associated with ischemia are characterized by

- Diminished or absent inward endocardial motion
- Impaired systolic myocardial thickening (in the normal condition it is greater than 30 %)

TEE is highly sensitive for the detection of acute ischemia and is therefore used extensively for real-time monitoring of regional wall motion as well as global left ventricular (LV) function.

Basic routine echocardiography views allow imaging of the anterior, inferior, posterior, and lateral walls from different locations in the heart (from the base of the heart in the plane of the mitral valve to the apex).

Echocardiographic signs of ischemia/infarction are as follows:

- Wall motion abnormalities (hypokinetic, akinetic)
- Reduced ejection fraction
- Mechanical complications of infarction (ischemic mitral regurgitation, ventricular septal defect, myocardial rupture)

The location of the wall motion abnormality correlates well with the involved coronary artery (Fig. 12.1):

1. Inferior wall motion abnormality is a sign of infarction involving the posterior descending artery of the right coronary artery or the distal left circumflex artery—seen best on the short-axis view and the parasternal long-axis view.
2. Septal, apical, and anterior wall motion abnormality is a sign of infarction involving the left anterior descending artery—seen best

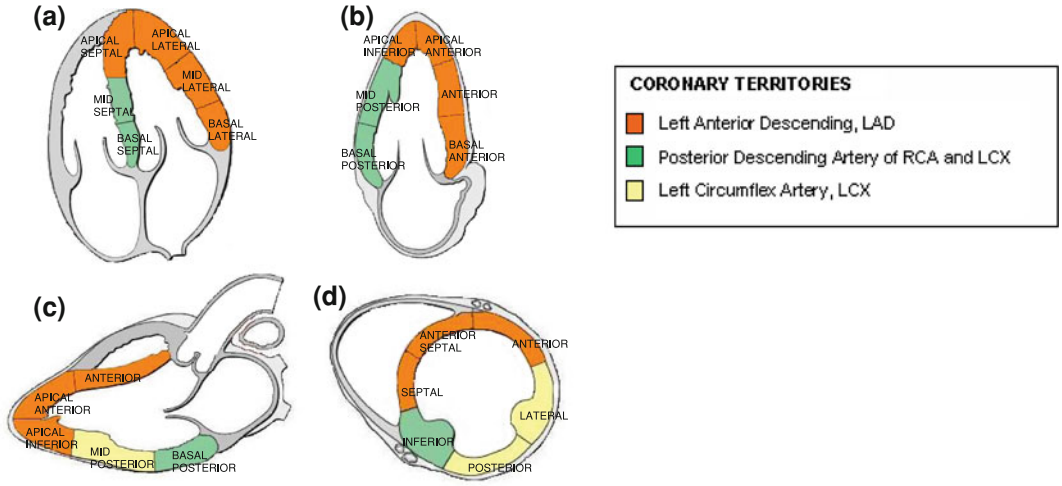

Fig. 12.1 Exemplary scheme of main the transthoracic echocardiography (TTE) views and coronary distribution: **a** apical four-chamber view, **b** apical two-chamber view, **c** parasternal long-axis view, **d** short-axis view

on the short-axis view and the four-chamber view.

3. Lateral and posterior wall motion abnormality is a sign of infarction involving the circumflex artery—seen best on the short-axis view.

12.4.1 Transthoracic Echocardiography

The main TTE views used for evaluation of AMI and RWMA are as follows:

1. Four-chamber view: septum and lateral wall (Fig. 12.2a)
2. Two-chamber view: inferior (left of display) and anterior (right of display) walls (Fig. 12.2b)
3. Parasternal short-axis view: all walls at the papillary level (Fig. 12.2c)
4. Parasternal long-axis view: septum and posterior wall (Fig. 12.2d)

12.4.2 Transesophageal Echocardiography

The TEE views most widely used for evaluation of AMI and RWMA (Fig. 12.3) are as follows:

1. Mid-esophageal four-chamber view
2. Mid-esophageal two-chamber view
3. Mid-esophageal long-axis view
4. Transgastric mid short-axis view

The standard transesophageal LV short-axis view (horizontal plane) is obtained by the transgastric view at the level of the papillary muscle tips. At this level, the myocardium is supplied by all three major coronary vessels and can be divided into four or six segments for standardization purposes: anterior, anterolateral, inferolateral, inferior, inferoseptal, and anteroseptal (Fig. 12.3).

12.5 Echocardiography and Complications of AMI

Papillary muscle rupture is an infrequent but often fatal mechanical complication of AMI (Fig. 12.4). Despite its rarity, it is an important cause of severe mitral regurgitation usually proceeding to heart failure and, if not corrected, to cardiogenic shock and eventually death. Echocardiography is one of the noninvasive imaging assessment techniques that can identify mechanical complications such as acute mitral regurgitation in the setting of AMI, and it allows precise location of the papillary muscle rupture and leaflet involvement, and evaluation of the modality and entity of mitral regurgitation and

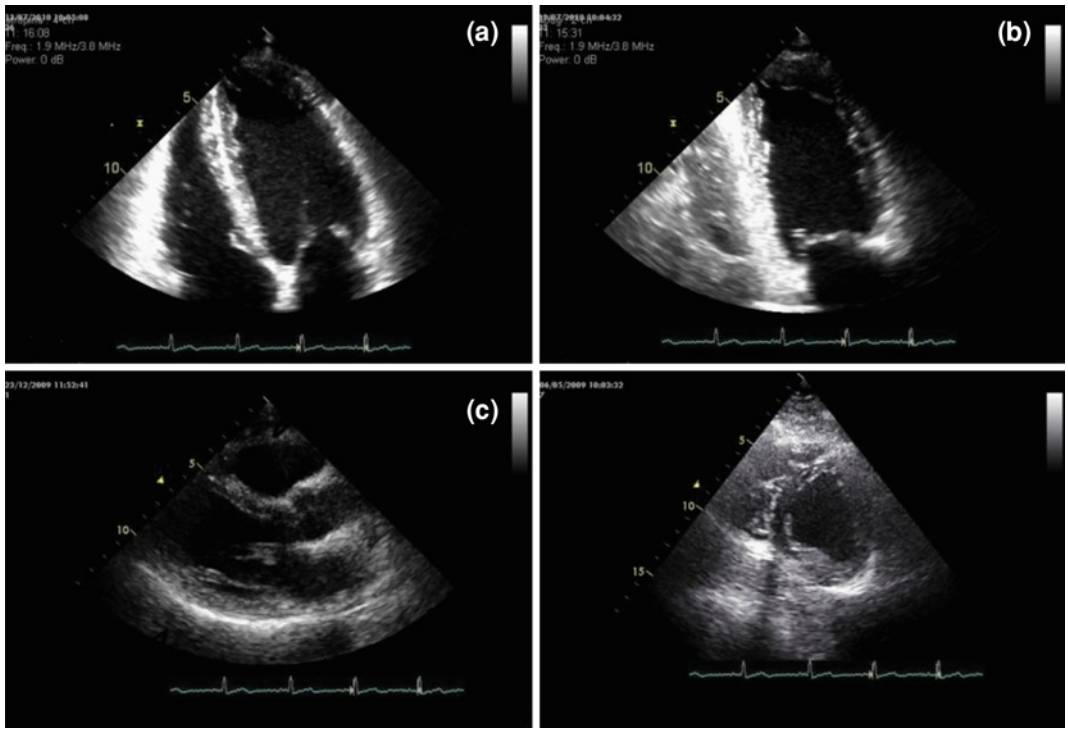

Fig. 12.2 Main TTE views used for evaluation of acute myocardial infarction (AMI): **a** four-chamber view, **b** two-chamber view, **c** parasternal short-axis view, **d** parasternal long-axis view

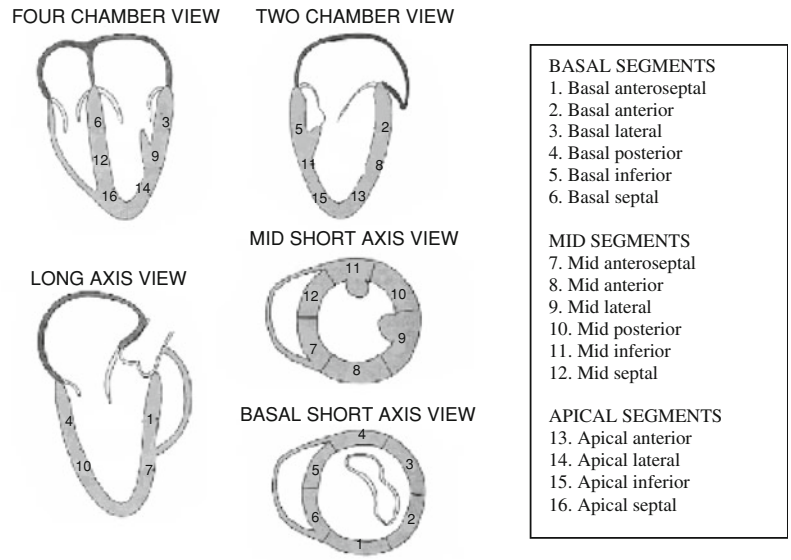

Fig. 12.3 Transesophageal echocardiography (TEE) views most widely used for evaluation of AMI and regional wall motion abnormality and selective study of 16 segments of the left ventricle

hemodynamic complications. TTE has an important role in diagnosing mechanical acute complications during AMI and in the decision making for patients with sudden onset of hemodynamic compromise. Echocardiography is the imaging technique of choice for detecting

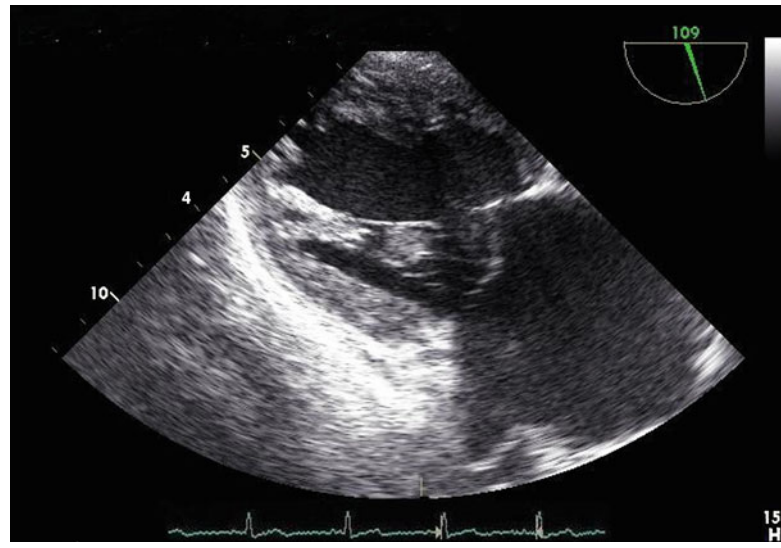

Fig. 12.4 TEE transgastric long-axis view of the left ventricle. The *arrow* shows papillary muscle rupture, an acute complication of AMI

complications of acute infarction, including myocardial free wall rupture, acute ventricular septal defect, and mitral regurgitation secondary to papillary muscle rupture or ischemia. TTE is able to identify a papillary muscle rupture with a diagnostic sensitivity of 65–85 %, but TEE is more sensitive. TTE is particularly useful in showing complications of ruptured papillary muscle such as the "flail" of mitral flaps and the papillary stump interested by the prolapsing rupture in the left atrium.

12.6 Assessment of Myocardial Ischemia and Viability Using Tissue Doppler and Deformation Imaging

The accurate evaluation of LV regional systolic function remains an important goal in clinical echocardiography. As explained before, conventional evaluation of LV regional function using two-dimensional echocardiography is based on the subjective assessment of endocardial excursion and myocardial thickening. However, it is mostly related to the negative effect of poor image quality, which makes interpretation difficult and observer variability high.

Recent advances in ultrasound technology have enabled us to acquire regional myocardial velocities, strain, and strain rate using the tissue Doppler imaging (TDI) technique. They potentially offer new and unique ultrasonic parameters to describe the regional deformation properties of myocardial tissue, which could reveal new information about myocardial structure and function.

Conventional assessment of contractile function is based on the measurement of the transmural thickening and does not provide information regarding the transmural distribution of contractile performance. TDI and strain rate imaging have been introduced as quantitative methods for assessing myocardial function and have been shown to overcome the limitations of current ultrasound methods for assessing the complex changes in regional myocardial function that occur in differing ischemic substrates. TDI analyzes in real time endocardial and epicardial velocities, and measures the myocardial velocity gradient, which is an index of myocardial deformation. Strain/strain rate imaging has been shown to be a sensitive technique for quantifying regional myocardial deformation compared with other cardiac imaging modalities. Strain and strain rate are measures of changes in shape and therefore represent deformations.

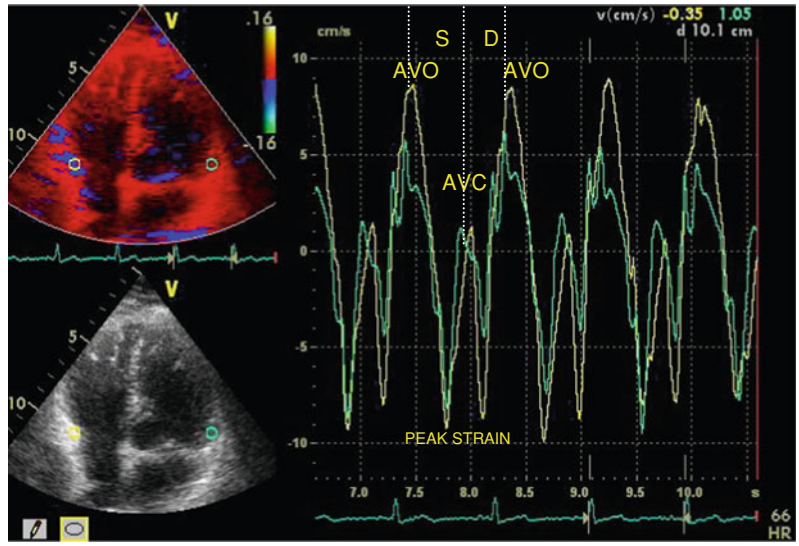

Fig. 12.5 Strain and strain rate imaging by tissue Doppler imaging. The strain rate at the basal septal wall of the left ventricle (*green*) and the right ventricle (*yellow*) is shown. Note the negative strain rate in systole (*S*) and the positive strain rates during diastole (*D*). In this example, the peak systolic strain is about 10 %, which occurs during left ventricular ejection defined as the interval between aortic valve opening (*AVO*) and aortic valve closure (*AVC*)

Strain, represented by the symbol ε, is a dimensionless index that refers to the amount of tissue deformation normalized to its original shape. It can be written mathematically as

$$\varepsilon = (L - L_0)/L_0,$$

where L is the length of the myocardium after deformation and L_0 is its original length. By convention, strain is defined as positive when the distance between the points of measurement is increasing (i.e., lengthening), whereas shortening is represented by negative strain. When strain is acquired at the LV apex, normal LV myocardium has a negative strain in systole and a positive strain in diastole in the longitudinal direction. Strain and strain rate imaging have also been applied recently in the assessment of left atrial function. When strain is acquired at the LV apex, the left atrium has a positive strain in ventricular systole and a negative strain during ventricular diastole.

Strain rate is the first derivative of strain, or the speed at which deformation (i.e., strain) occurs. Strain rate can also be considered as the velocity gradient between two points in the myocardium. When strain rate is acquired at the LV apex, normal ventricular myocardium has a negative strain rate in systole and a positive strain rate during diastole (Fig. 12.5). The left atrium has a positive strain rate in ventricular systole and a negative strain rate during ventricular diastole. Peak strain, peak systolic strain, and strain rate are the more commonly used parameters. Peak strain is the maximum strain which may occur during LV ejection (defined as the interval between aortic valve opening and closure). TDI is a Doppler technique that allows quantification of myocardial tissue velocities.

Strain and strain rate imaging have been shown to be able to differentiate between transmural and nontransmural infarcts. Patients with transmural infarction were shown to have significantly lower circumferential and longitudinal strain and strain rate compared with those with subendocardial infarct, with no significant differences in radial strain.

In myocardial infarction, transmural extension of scar distribution in the infarct zone is proportionally related to the reduction in systolic function measured by the radial transmural

velocity gradient or by strain rate imaging. Measurement of both systolic and postsystolic deformation both at rest and during a graded dobutamine infusion may help to distinguish between transmural and nontransmural infarcts.

Although TDI measurement of regional function by peak systolic ejection velocity is easy to perform, reproducible, and validated, and regional function is typically reduced during ischemia, many experimental studies have demonstrated its limited ability to differentiate between different grades of ischemic dysfunction and to distinguish ischemic from postischemic dysfunction. This important limitation of TDI is related to the fact that velocities in one myocardial segment are determined by function in other segments as well, which is due to tethering between segments and cardiac translational motion.

In conclusion, strain imaging has the ability to evaluate regional myocardial function. Strain rate has not replaced conventional grayscale imaging in the assessment of regional LV function, and the implementation of these new indices in routine clinical practice will need additional clinical and large-scale studies.

Further Reading

Chen X, Nakatani S (2011) Transmural myocardial strain gradient: a new and robust quantitative index of left ventricular wall motion based on myocardial strain imaging. Echocardiography 28(2):181–187

Cheitlin MD, Armstrong WF, Aurigemma GP et al (2006) ACC/AHA/ASE 2003 guideline update for the clinical application ofechocardiography: summary article. A report of the American College of Cardiology/AmericanHeart Association Task Force on Practice Guidelines (ACC/AHA/ASE committee to update the1997 guidelines for the clinical application of echocardiography). J Am Soc Echocardiogr 16(10):1091–1110

Greaves SC (2010) Role of echocardiography in acute coronary syndromes. Heart 88(4):419–425

Leung DY, Arnold CT (2010) Emerging clinical role of strain imaging in echocardiography. Heart Lung Circ 19:161–174

Muttreja MR, Mohler ER 3rd (1999) Clinical use of ischemic markers and echocardiography in the emergency department. Echocardiography 16(2):187–192

The Cardiomyopathies

13

F Luca Lorini, Alessandra Rizza, and Francesco Ferri

13.1 Introduction

Cardiomyopathies comprise a heterogeneous group of disease of the myocardium. Historically in the WHO/International Society and Federation of Cardiology classification of 1996, cardiomyopathies were defined as primary disorders of unknown cause. Heart muscle diseases of known cause or associated with systemic disorders were classified as secondary. However, this distinction between primary and secondary heart muscle disease has become redundant, as the cause of previously idiopathic disorders has been discovered.

Recently the American Heart Association proposed that cardiomyopathies are "myocardial diseases associated with mechanical and/or electrical dysfunction that usually—but not invariably—exhibit inappropriate ventricular hypertrophy or dilatation and are due to a variety of causes that are frequently genetic." The American Heart Association panel also suggested that ion channelopathies and disorders of conduction should be considered cardiomyopathies as well because channel mutations alter biophysical properties and protein structure, thereby creating structurally abnormal ion channel interfaces and architecture.

A. Rizza (✉)
Intensive Care Cardiac Surgery, Ospedali Riuniti di Bergamo, Bergamo, Italy
e-mail: alessandra.rizza@virgilio.it

The European Society of Cardiology (ESC) has assumed that the clinically most useful method for diagnosing and managing the cardiomyopathies is a classification in which heart muscle diseases are grouped according to ventricular morphology and function. The ESC has defined cardiomyopathies as "myocardial disorders in which the heart muscle is structurally and functionally abnormal, in the absence of coronary artery disease, hypertension, valvular disease and congenital heart disease sufficient to cause the observed myocardial abnormality." The ESC classification consists of the following categories:

- Hypertrophic cardiomyopathy (HCM)
- Dilated cardiomyopathy (DCM)
- Restrictive cardiomyopathy (RCM)
- Arrhythmogenic right ventricular (RV) cardiomyopathy (ARVC)
- Unclassified, e.g., left ventricular (LV) noncompaction

The cause of each cardiomyopathy is taken into account by replacing the traditional division of primary and secondary by a new division into *familial* (or genetic) and *nonfamilial* (nongenetic). The nonfamilial category is subdivided into idiopathic cause and acquired cardiomyopathies in which LV dysfunction is a complication of another disorder (e.g., myocarditis, drugs, pregnancy, endocrine disorders, tachycardiomyopathy).

There is no ideal classification; however, from an echocardiographic point of view, the classification based on structure and function is the most useful. This chapter will describe

A. Sarti and F. L. Lorini (eds.), *Echocardiography for Intensivists*,
DOI: 10.1007/978-88-470-2583-7_13,

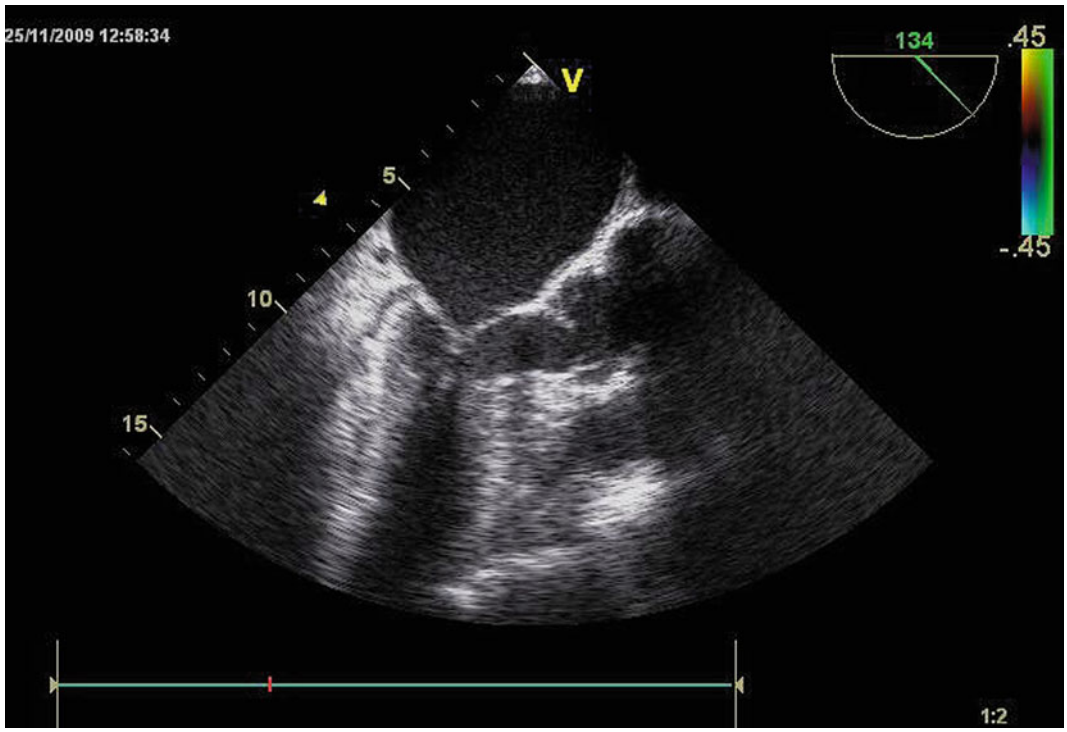

Fig. 13.1 Asymmetrical hypertrophy in hypertrophic cardiomyopathy

HCM, DCM, RCM, ARVC, and LV non-compaction according to the ESC classification.

13.2 Hypertrophic Cardiomyopathy

HCM is clinically defined in the presence of LV hypertrophy and in the absence of hypertension and valve disease. LV hypertrophy occurs in one in 500 of the general population and this incidence includes all kinds of hypertrophy. HCM is a familial disease with an autosomal pattern of inheritance, caused by mutations in genes encoding for sarcomeric proteins, usually resulting in an asymmetrical pattern of LV hypertrophy.

The echocardiographic diagnostic criteria in HCM include:

1. *Asymmetrical septal hypertrophy*. LV thickness, evaluated at the septum and free wall level, is considered abnormal when it is greater than 15 mm (Fig. 13.1) and is defined as asymmetrical when there is a septal to free wall thickness ratio between 1.3 and 1.5. A value greater than 30 mm is a risk factor for sudden cardiac death.
   The distribution of hypertrophy may be anterior septal, anterior and posterior septal, posterior basal wall, or apical (e.g., in Japanese people).
2. *Systolic anterior motion (SAM) of the mitral valve*. SAM is characterized by an abrupt anterior movement of the mitral valve in systole (Fig. 13.2), reaching its peak before maximum movement of the posterior wall (this characteristic allows one to differentiate true SAM from "pseudo SAM," which is produced by an exaggerated anterior motion of the mitral valve and reaches its peak after the full contraction of the posterior wall). A Venturi effect is thought to be responsible for dragging the anterior mitral leaflet into the LV outflow tract (LVOT). The severity of SAM is correlated with the severity of LVOT obstruction.
3. *Pressure gradient across the LVOT*. This gradient may be variable, because obstruction is dynamic. A value of 30 mmHg or greater has physiological consequences, and is associated

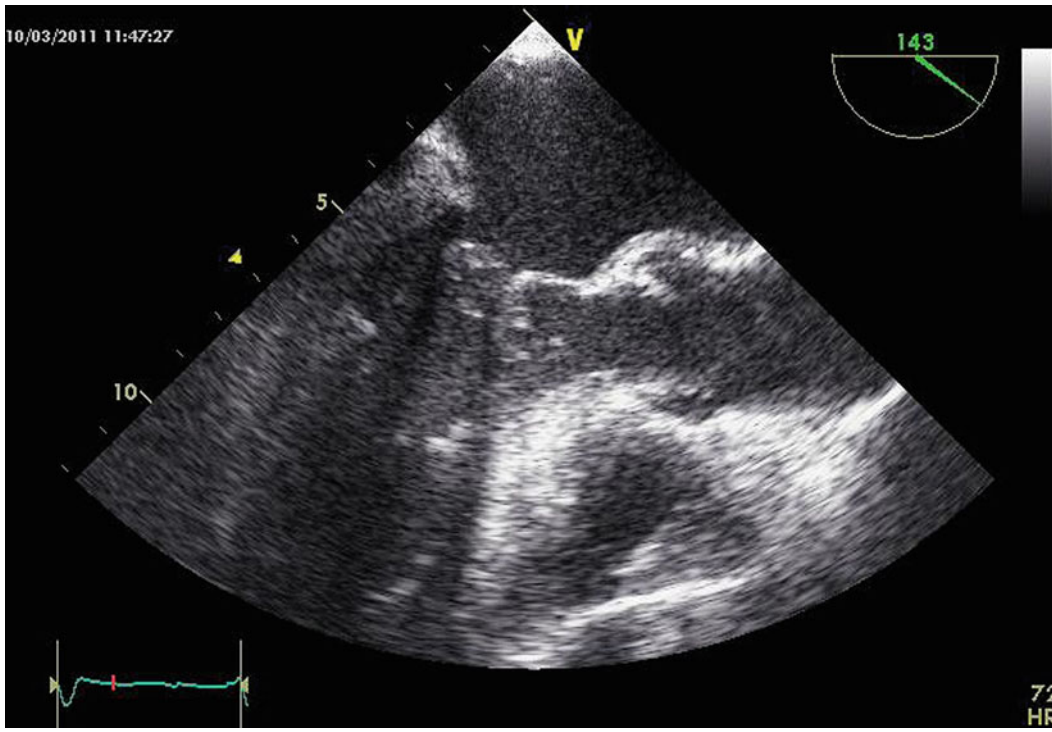

Fig. 13.2 Systolic anterior motion in hypertrophic cardiomyopathy

with progression to New York Heart Association class III–IV and death from heart failure or stroke, especially in patients aged over 40 years.

4. *Dynamic mitral regurgitation*. Mitral regurgitation is a consequence of SAM which induces abnormal mitral leaflet coaptation. The evaluation of the presence and degree of mitral regurgitation is performed by color Doppler echocardiography. The regurgitant jet is usually posteriorly directed, and an anterior or central jet may occur in the presence of an intrinsic mitral valve disease due to annular, papillary, or leaflet disease (Fig. 13.3).
5. *Small LV cavity*. Mid-cavity obstruction may occur owing to muscular apposition in a small LV cavity, with excessive hypertrophy of the mid-ventricle and papillary muscles.
6. *Diastolic dysfunction*. Almost all patients with HCM have some degree of LV diastolic dysfunction. The mechanisms linked to diastolic dysfunction are complex and include altered contraction and relaxation of sarcomeric protein, altered sensitivity to calcium, disarray of and increased amount of extracellular matrix, increased wall thickness, and ischemia.

Diastolic dysfunction is assessed by analysis of both transmitral spectral Doppler flow velocity (E) and mitral annular velocity (E').

Transmitral blood flow is represented by an early E wave and a late A wave on pulsed wave Doppler echocardiography, isovolumic relaxation is slowed, the rate of rapid filling is diminished, the atrial contribution to filling is increased, as well is LV stiffness. Unfortunately in HCM, the E wave varies with preload and does not correlate well with LV hypertrophy.

Tissue Doppler imaging (TDI) provides more accurate evaluation of diastolic dysfunction. Early diastolic mitral annular velocities are significantly reduced, and the ratio of transmitral velocity E/E' is higher and appears to correlate with New York Heart Association functional class. The ratio of early transmitral (E) to tissue Doppler early diastolic (e') velocities of the lateral mitral annulus accurately quantifies LV pressures, in particular before atrial contraction; $E/e' > 10$ showed the best sensitivity

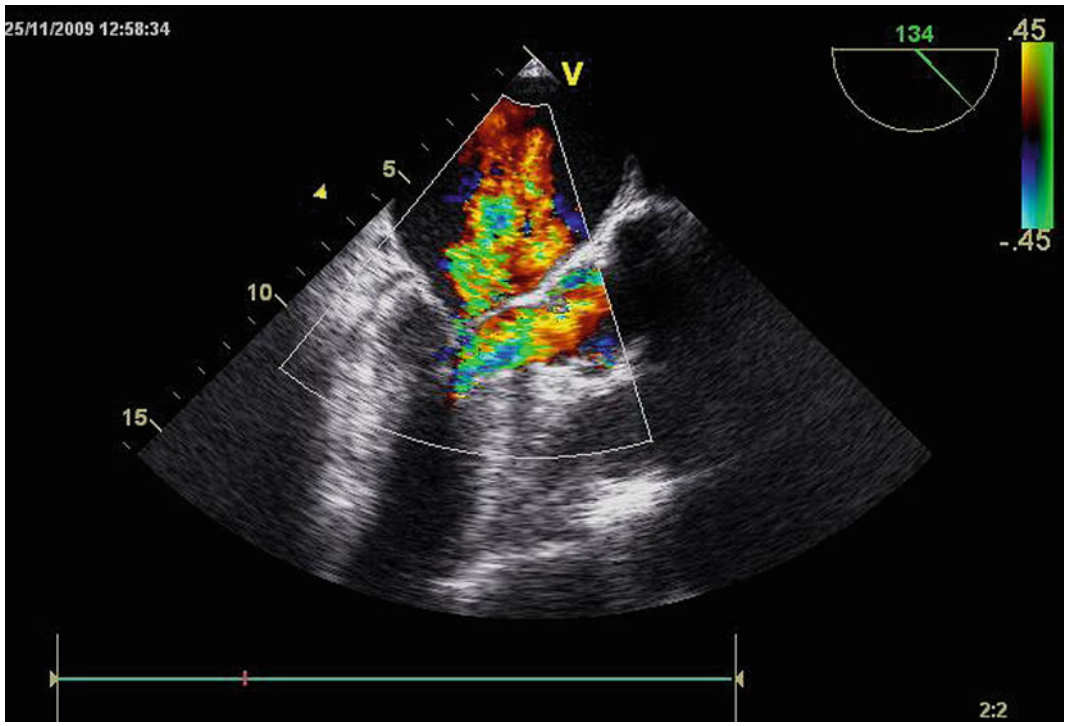

Fig. 13.3 Mitral regurgitation and systolic anterior motion in hypertrophic cardiomyopathy

and specificity for identifying LV pre-A pressure greater than 15 mmHg. However, that ratio shows only a modest correlation when related to mean left atrial pressure, although this parameter identifies patients with low exercise capacity.

TDI has been investigated in the preclinical diagnosis of HCM, but additional data are needed to determine TDI velocity values that provide the highest diagnostic accuracy.

Differential diagnosis of HCM includes:

- LV hypertrophy due to hypertension: LV hypertrophy in HCM is asymmetrical, whereas that of LV hypertrophy caused by hypertension has a concentric appearance.
- LV hypertrophy in athletes: the criteria that may be utilized to support the diagnosis of pathological HCM are LVOT obstruction, impaired diastolic function, enlarged left atrium, family history, left bundle branch block, and ST-segment depression.

The management of HCM, in addition to β-blockers, includes surgical septal miectomy (if the LVOT gradient is greater than 50 mmHg) or percutaneous alcohol septal ablation. The abnormal insertion of papillary muscle may contribute to mitral regurgitation, requiring a more extended septal myectomy or mitral valve replacement. Intraoperative echocardiography is used to check:

- Residual gradient across the LVOT
- Iatrogenic ventricular septal defect
- SAM of the mitral valve
- Residual mitral regurgitation

Echocardiography can provide important information for the appropriate diagnosis of HCM; however, it cannot distinguish conditions based on myocyte hypertrophy from those in which LV mass and wall thickness are increased by interstitial infiltration or intracellular accumulation of metabolic substrates. Cardiac

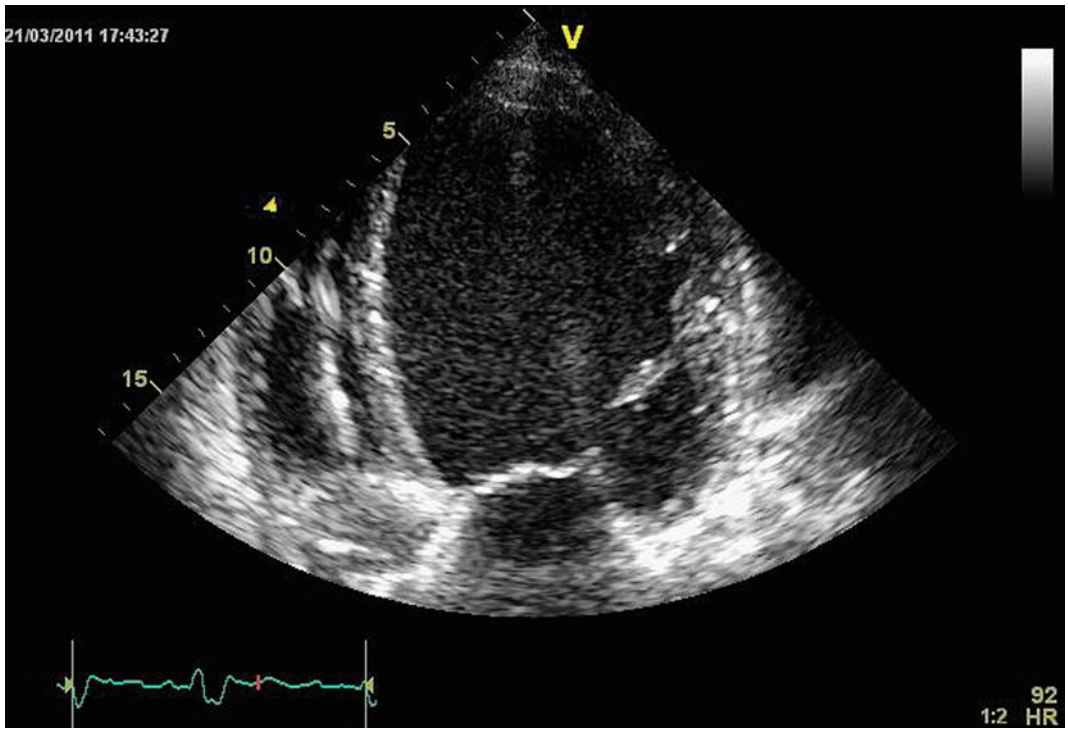

Fig. 13.4 Dilated left ventricle in dilatative cardiomyopathy

magnetic resonance imaging may help in the diagnosis, even if the final diagnosis in some specific conditions can only be obtained by myocardial biopsy.

13.3 Dilated Cardiomyopathy

DCM is a primary myocardial disease characterized by differing degrees of LV dysfunction and dilatation in the absence of chronic increased afterload (e.g., aortic stenosis or hypertension) or volume overload (e.g., mitral regurgitation).

Although there are many different causes of DCM, in most cases it is idiopathic. DCM may be a final consequence of a variety of pathways, such as hypertension, ischemia, severe valvular disease, myocarditis, endocrine or congenital heart disorders, toxins, chemotherapy, and LV noncompaction. In the absence of these etiological factors, DCM may occurs as a result of gene mutations.

Echocardiography not only facilitates evaluation of strict diagnostic criteria, but also provides us with a comprehensive assessment of cardiac anatomy, pathophysiological changes, and hemodynamics.

The following are echocardiographic features of DCM:

- Ventricular dilation. The left ventricle is considered dilated if its end-diastolic volume is more than 117% of the predicted value, corrected for age and body surface area (Fig. 13.4).
- Severe ventricular dysfunction. Typically LV fractional shortening is less than 20% and LV ejection fraction is less than 35%.
- Functional mitral regurgitation with a central jet.
- Dilatation of the mitral annulus associated with an increase of the annulus dimensions.
- Tethering of both mitral leaflets by displaced papillary muscles. The degree of tethering is reflected in the angle between each leaflet and the annular plane, the height between the

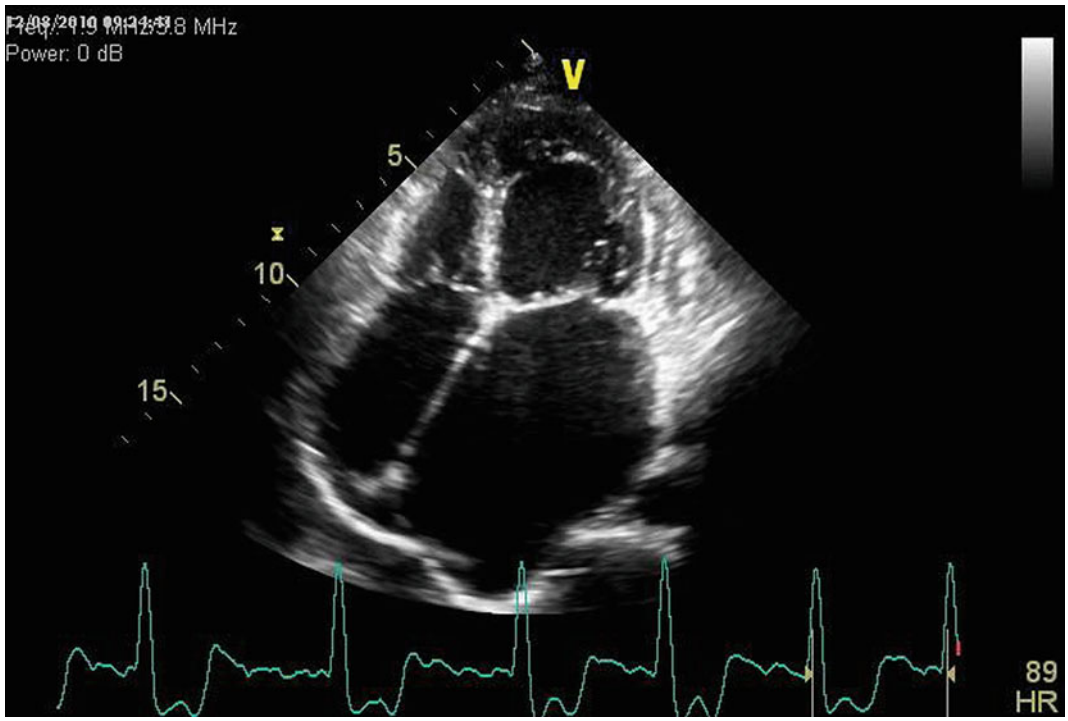

Fig. 13.5 Restrictive cardiomyopathy

annular plane and leaflet point of coaptation, and the tenting area bordered by the annular plane and the two leaflets.

- Functional tricuspid regurgitation.

The differential diagnosis includes ischemic heart disease and primary mitral valve disease: in both conditions there is a low ejection fraction, but in DCM there is a dilated mitral annulus, abnormal papillary muscle angle, leaflet tethering, and absence of severe leaflet disease, e.g., rheumatic disease, flail, or prolapse.

13.4 Restrictive Cardiomyopathy

RCM is characterized by increased stiffness of the myocardium, normal or reduced ventricular diastolic volumes, normal or mildly increased wall thickness, and preserved systolic function. Unlike the other cardiomyopathies, which are classified according to morphological criteria, RCM is a functional classification. The classic echocardiographic features include:

- A small (not dilated neither hypertrophied) left ventricle
- Marked dilatation of both atria (Fig. 13.5)
- Normal systolic function in the absence of a pericardial disease
- Mild to moderate mitral and tricuspid valve regurgitation
- Increased pulmonary pressures
- Pulmonary venous flow showing a blunted S wave and pronounced diastolic and atrial waves (with sinus rhythm)
- A restrictive filling pattern, as transmitral velocity is characterized by a rapid but ill-sustained ventricular filling on pulsed wave Doppler echocardiography (E wave), little or no late ventricular filling (A wave), an *E*/*A* ratio greater than 2 and the deceleration time of the E wave shortened to less than 150 ms

However, as in the case of HCM, transmitral velocity in the early stage of RCM is reduced; when compliance of the heart decreases the left atrial pressure increases, leading to pseudonormalization of the diastolic pattern and then to a restrictive pattern. The early mitral tissue Doppler velocity may be a more reliable guide to LV filling pressure as the E/E' ratio increases with the severity of the disease. In RCM—unlike in constrictive pericarditis—E' is blunted and this reduction is consistent with the finding that RCM is a disease of the myocardium.

Systemic amyloidosis is a disorder of protein metabolism in which abnormal extracellular protein material is deposited in organs and tissue. Primary amyloidosis involves the heart in 90% of cases, and cardiac amyloidosis is the commonest cause of RCM: interstitial infiltration of the atria and ventricles leads to a firm and rubbery consistency of the myocardium. Secondary amyloidosis only rarely affects the heart.

The echocardiographic features of cardiac amyloidosis include thickened RV and LV walls, granular or "sparkling" appearance of the myocardium, normal-sized or small LV, enlarged atria, depressed LV systolic and diastolic function, mild mitral regurgitation, restrictive pattern of E/A, high E/e' ratio suggestive of elevated filling pressures, and pericardial effusion in advanced disease.

Tissue Doppler echocardiography can contribute to the earlier diagnosis of amyloid infiltration of the heart. Peak systolic and early diastolic mitral annular velocities, as well as myocardial velocity gradients (strain rate) in systole and early diastole, are equally reduced in patients with or without a restrictive pattern of transmitral Doppler velocities.

13.5 Arrhythmogenic Right Ventricular Cardiomyopathy

ARVC is a syndrome characterized by myocardial disease, predominantly involving the right ventricle and associated with ventricular tachycardia arising from this chamber, syncope, and sudden death. At autopsy there is an unusual distribution of fatty and fibrotic tissue within the right ventricle, preferentially affecting the apex, the inflow tract, and the outflow tract. ARVC is a genetic cardiac disease involving genes encoding for specialized intercellular adhesion junctions known as desmosomes and thus is mechanistically distinct from either HCM or DCM.

The original descriptions of ARVC focused on the fatty replacement in the right ventricle. Replacement infers that the muscle develops normally and subsequently undergoes dysplastic degeneration with replacement of muscle by fibrous scarring and fatty tissue. There is important histologic evidence of fibrofatty involvement of the left ventricle in 30–75% of ARVC cases.

The intrinsic difficulties in making a diagnosis of ARVC are evident from the existence of the task force criteria (1994).

ECG may be useful, but only in the appropriate clinical context. Major criteria include ε waves or localized prolongation of the QRS duration (greater than 110 ms) in right precordial leads. Minor criteria include inverted T waves in right precordial leads in individuals older than 12 years in the absence of right bundle branch block.

Early diagnosis by echocardiography is difficult, because of the irregular shape and trabeculation of the normal right ventricle. However, some echocardiographic features suggestive of ARVC have been showed and include (Fig. 13.6):

- RV and RV outflow tract dilatation (diameter 30 mm)
- Trabecular derangement
- Global RV dysfunction with fractional shortening less than 32%
- RV regional wall motion abnormality, especially of the apex and anterior wall
- Focal RV aneurysms.

Echocardiographic assessment in ARVC requires considerable expertise given the complex geometry of the right ventricle, the lack of standard reference views, and the load dependence of RV function.

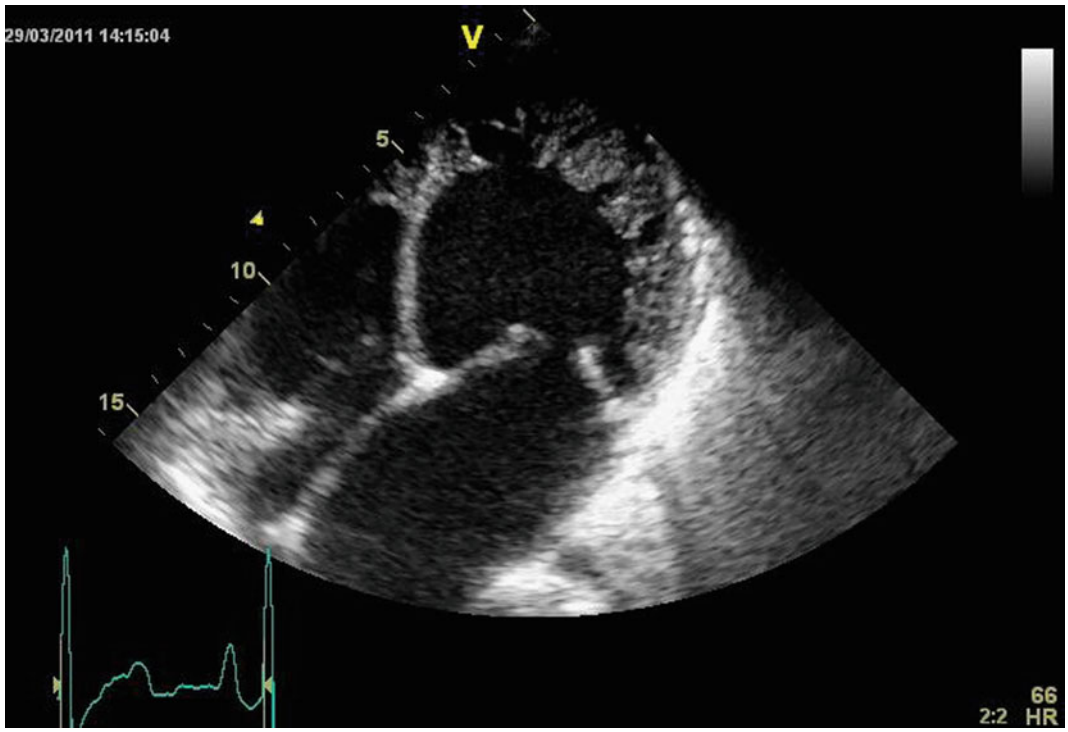

Fig. 13.6 Left ventricular noncompaction

13.6 Left Ventricular Noncompaction

LV noncompaction is a sarcomeric cardiomyopathy. Sporadic or familial adult forms are genetically distinct from X-linked infantile cases, and they are transmitted by an autosomal dominant trait. The reported prevalence is 0.014–0.05%. The major clinical manifestations in patients with reduced LV function include heart failure, arrhythmias (atrial fibrillation, ventricular tachyarrhythmias, sudden cardiac death, and Wolff–Parkinson–White syndrome in pediatric patients) and systemic embolic events. The diagnosis is often delayed (3.5–5.7 years). Echocardiography is considered the reference standard for the diagnosis, and the features includes:

- Absence of coexisting cardiac abnormalities by definition
- Typical two-layered structure of the myocardium with a thin, compacted epicardial band and a much thicker, noncompacted endocardial layer consisting of trabecular meshwork with deep endocardial spaces (with a ratio of the noncompacted layer to the compacted layer greater than 2)
- Multiple ventricular trabeculations, prominent in the middle and apical segments (Fig. 13.6)
- Predominant segmental location of the abnormality (noncompacted myocardium greater than 80%) found in the apical and mid-ventricular regions of both inferior and lateral walls
- Color Doppler evidence of deeply perfused intertrabecular recesses (not communicating with the coronary circulation, unlike for myocardial sinusoids)

Further Reading

Elliott P, Andersson R, Arbustini E (2008) Classification of the cardiomyopathies: a position statement from the ESC working group on myocardial and pericardial disease. Eur Heart J 29:270–276

Kaski JP, Elliott P (2007) The classification concept of the ESC working group on myocardial and pericardial diseases for dilated cardiomyopathy. Herz 32:446–451

Losi A, Nistri S, Galderisi M (2010) Echocardiography in patients with hypetrophic cardiomyopathy: usefulness of old and new techniques in the diagnosis and pathophysiological assessment. Cardiovasc Ultrasound 8(7):1–19

Maron BJ, Towbin JA (2006) Contemporary definitions and classifications of the cardiomyopathies: an AHA scientific statement from the Council on Clinical Cardiology, Heart Failure and Transplantation Committee. Circulation 113:1807–1816

Malla R, Sharma R et al (2009) J Nepal Med Assoc 48(174):180–184

McKenna WJ, Thiene G, Nava A (1994) Diagnosis of arrhythmogenic right ventricular aysplasia cardiomyopathy. Br Heart J 71:215–218

Nihoyannopoulos P, Dawson D (2009) Restrictive cardiomyopathies. Eur J Echocardiogr 10:23–33

Patrick T, Calum A et al (2010) Arrhythmogenic right ventricular cardiomyopathy. Heart Failure Clin 6:161–177

Thomas DE, Wheeler R, Zaheer R et al (2009) The role of echocardiography in guiding management in dilated cardiomyopathy Eur J Echocardiogr 10: iii15–iii21

Cor Pulmonale and Pulmonary Hypertension

14

Lorenzo Grazioli, F. Luca Lorini, and Angelo Vavassori

14.1 Introduction

Cor pulmonale is a condition in which there is a right ventricular enlargement secondary to a lung disorder that produces pulmonary arterial hypertension. Right ventricular (RV) failure may follow this type of condition. Cor pulmonale may be acute or chronic.

A lung disorder can cause pulmonary hypertension by several mechanisms:

- Loss of capillary bed
- Vasoconstriction (hypoxia, hypercapnia)
- Hypertrophy of arterioles in the pulmonary vessel tree

In this condition, echocardiography is a useful method for evaluation of RV function and pulmonary hypertension.

In the first phase there is only pulmonary hypertension, but with the progression of the disorder, right-sided heart failure can occur with worsening of Po_2 and Pco_2 and peripheral edema. However, it has been demonstrated that in the subclinical period, COPD patients can develop the initial signs of RV failure before pulmonary hypertension.

Pulmonary hypertension complicating chronic respiratory disease, particularly COPD, is generally defined by a mean pulmonary artery pressure (PAP) greater than 20 mmHg, which is slightly different from the definition of idiopathic pulmonary arterial hypertension (mean PAP $>$ 25 mmHg).

Echocardiography is an important tool to identify and classify pulmonary hypertension and its degree.

14.2 Common Right Ventricular Measurements

Estimation of RV function is not so well codified as that of LV function because of the complex shape of the right ventricle—triangular when viewed from the front and a crescent wrapping partway around the left ventricle when viewed in the transverse section; the septum in the normal condition is an arch into the right ventricle both in systole and in diastole.

The right ventricle is divided into three parts: inflow tract (starting with the tricuspid valve), apex, and infundibulum (ending with the pulmonary valve). RV diameter (RVD) is the first measurement we perform. It is necessary to use a four-chamber view and to measure, in diastole, in the middle of the RV cavity the distance between the free wall and the septum. The diameter of the right ventricle measured in the middle of the cavity is normally 2.7–3.3 cm.

In patients with COPD, we can observe enlargement of the right ventricle. We can observe this by measuring the transverse mid-cavity diameter in the four-chamber view. This parameter is also useful for determination of right-sided heart failure, in which there is a

L. Grazioli (✉)
Department of Anesthesia and Intensive Care, Ospedali Riuniti di Bergamo, Bergamo, Italy
e-mail: lgrazioli@ospedaliriuniti.bergamo.it

A. Sarti and F. L. Lorini (eds.), *Echocardiography for Intensivists*,
DOI: 10.1007/978-88-470-2583-7_14, © Springer-Verlag Italia 2012

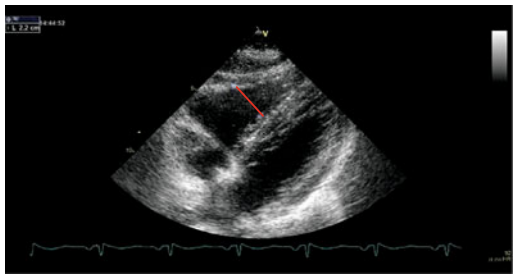

Fig. 14.1 Right ventricular diameter

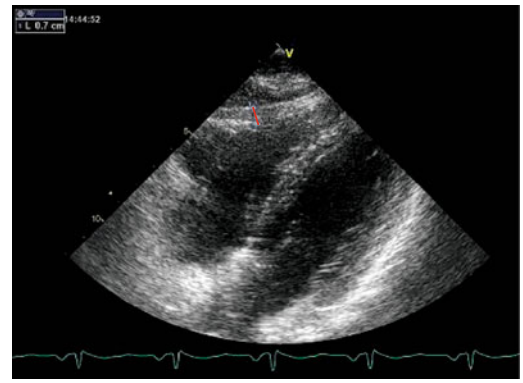

Fig. 14.2 Right ventricular wall thickness

further increase in diameter respect who have only pulmonary hypertension (Fig. 14.1).

The normal wall thickness (measured in diastole) is less than 5 mm; a greater thickness indicates RV hypertrophy and may suggest pressure overload.

Guidelines suggest acquiring the wall thickness using the subcostal four-chamber view and excluding epicardial fat (Fig. 14.2).

RV fractional area change is the percentage variation between the RV end-diastolic area and the RV end-systolic area. This parameter is well correlated with MRI-derived RV ejection fraction. In this case the cutoff for RV myocardial dysfunction is 35%. The limitation of this method is the difficulty recognizing of endocardial border delineation.

Tricuspid annular plane systolic excursion (TAPSE) is a parameter which indicates the systolic displacement of the tricuspid annular plane; it is the expression of the RV longitudinal function. To obtain TAPSE, we need to use M-mode on the lateral tricuspid annulus in the four-chamber view. A value greater than 15 mm is correlated with normal systolic function, and a value below 8 mm is correlated with significant RV dysfunction; there is also a relation between TAPSE and RV ejection fraction (Table 14.1).

Table 14.1 Relation between tricuspid annular plane systolic excursion (*TAPSE*) and right ventricular ejection fraction (*EF*)

TAPSE (mm)	EF (%)
5	20
10	30
15	40
20	50

In COPD patients, TAPSE represents an independent risk factor for mortality, with a cutoff of 14 mm, and doubling of the TAPSE value is correlated with a reduction of mortality of 26% (Fig. 14.3).

Important in the definition of pulmonary hypertension is the estimation of systolic pulmonary artery pressure (PAPs) through the tricuspid regurgitation with a simplified Bernoulli equation: PAP $= 4V^2 +$ right arterial pressure, where V (m/s) is the peak velocity of the regurgitant jet (Fig. 14.4). We need to use a four-chamber view and continuous Doppler echocardiography of tricuspid regurgitation.

The European guidelines for the diagnosis and treatment of pulmonary hypertension consider the echocardiographic diagnosis of pulmonary hypertension "likely" when the tricuspid regurgitation velocity is greater than 3.4 m/s (or systolic PAP is greater than 50 mm Hg) and "possible" when the tricuspid regurgitation velocity is between 2.9 and 3.4 m/s (or systolic PAP is between 37 and 50 mmHg), with or without additional echocardiographic signs suggestive of pulmonary hypertension, or when the tricuspid regurgitation velocity is less than 2.8 m/s (or systolic PAP is less than 36 mm Hg) with additional variables suggestive of pulmonary hypertension such as RV hypertrophy or dilation.

Because the estimation of the pressure is angle-dependent, to minimize the risk of error the measurement has to be acquired in multiple views to be sure of using the maximum velocity.

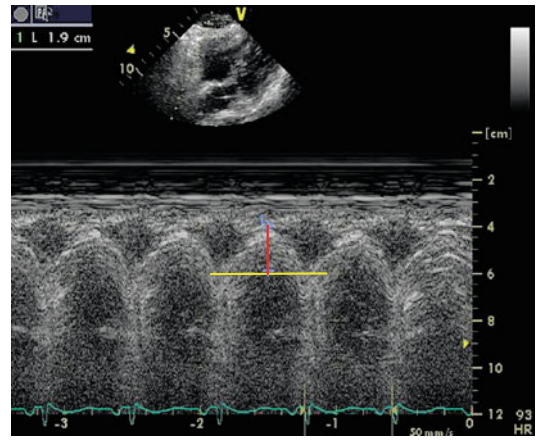

Fig. 14.3 Calculation of tricuspid annular plane systolic excursion (in *red*)

Diastolic pulmonary pressure can be estimated by the Bernoulli equation applied to the velocity of the end-diastolic pulmonary regurgitant jet as follows: [pulmonary artery diastolic pressure = 4 × (end-diastolic pulmonary regurgitant velocity)^2 + right atrial pressure].

There are a lot methods which can be used to estimate mean PAP by sampling the pulmonary valve regurgitation or by use of empirical formulas. A simple method which correlates well with catheter measurements has been described recently. The mean systolic gradient (between the right atrium and the right ventricle) is calculated by tracing the transcuspid regurgitation velocity–time integral. Mean PAP = right atrial pressure + mean systolic gradient.

14.3 Advanced Right Ventricular Measurements

The function of the right ventricle can be investigated by use of novel technique such as tissue Doppler imaging (TDI), strain, and strain rate. With this type of imaging, the focus is on the myocardium and not on blood.

14.3.1 Tissue Doppler Imaging

TDI reveals the velocity of the myocardium in a region of interest; in our case, the right ventricle. The use of TDI allows us to study the right ventricle in a way that is less preload dependent compared with the conventional methods.

The conventional approach is the four-chamber view.

There are two types of TDI: pulsed-based and color-based.

Pulsed-based TDI is simpler to use, but has poor spatial resolution owing to the movement of the heart. We can record the maximum instantaneous velocity.

Color-based TDI has better spatial resolution and enables us to analyze the waves offline and also to acquire measurements simultaneously.

It has poorer temporal resolution than pulsed-based TDI, but increasing the frame rate (more than 120–150 frames per second) makes the acquisition acceptable. Other limitations are the insonation angle and translational myocardial motion.

The values we sample with color-based TDI are mean values and on average the values are 25% lower than those obtained by pulsed-based TDI.

With TDI, we can see five distinct waveforms:

1. Isovolumic contraction time velocity: early systole; above or below the baseline.
2. Systolic peak (S′): during RV mechanical systole, pulmonary valve opening; always above the baseline.
3. Isovolumic relaxation time velocity: early diastole (end of T wave); it can be above or below the baseline.
4. Early diastolic wave (E′): during RV relaxation; it is usually under the baseline.
5. Late diastolic wave (A′): represents atrial contraction (just after the P wave on ECG); always under zero (Fig. 14.5).

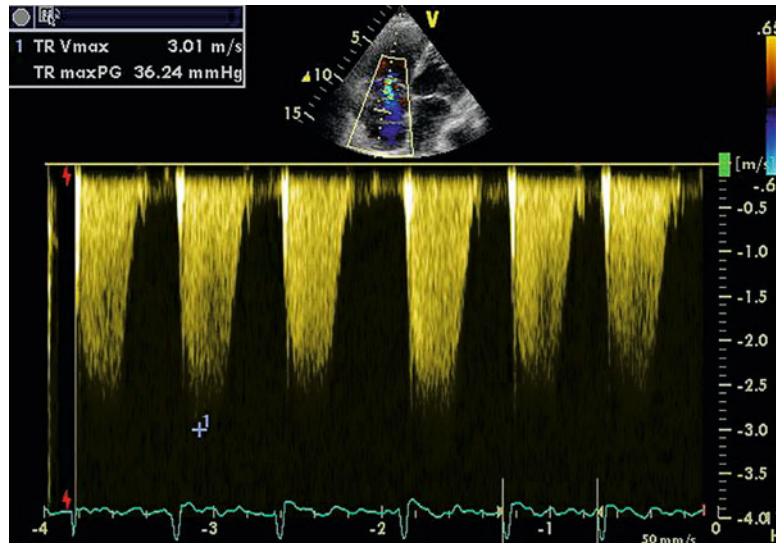

Fig. 14.4 Image for calculation of pulmonary artery pressure with the tricuspid gradient and atrial pressure

These parameters are considered at the tricuspid annulus; TDI of the free wall is not considered in normal clinical practice because of the high variability of the signal.

The septum should not be considered alone for the study of the right ventricle because it is not only linked to RV function.

A simple and reproducible measurement is that of the systolic peak; the cutoff used is 10 cm/s. Below this limit there is suggestion of RV failure.

We consider the systolic peak at the annular free wall and measure it with pulsed TDI. Lower velocities are found for the mid and apical zones of the right ventricle, and the velocity can be lower with increasing age.

Color-based TDI measurements have lower velocities, but more studies are required before they can be used as a guideline.

In particular, in a study on COPD patients, the cutoff for RV failure was 9.2 cm/s, with a sensitivity of 80% and a specificity of 62%. There was also good correlation with conventional parameters such as RV diameter and systolic PAP.

The disadvantage is that it is load-dependent.

Another parameter is the isovolumic acceleration (IVA), which is obtained by dividing the isovolumic velocity or the isovolumic contraction time velocity by the acceleration time (from the baseline to the peak of the isovolumic velocity).

IVA has to be sampled on the tricuspid annulus. In COPD patients, IVA is impaired and is correlated with the forced expiratory volume in 1 s and with the severity of the disease.

The cutoff is quite variable in the literature, the value depending on the control population, COPD without right-side heart failure, and COPD with right-sided heart failure.

However, with pulsed TDI a value under 1.9 m/s^2 reveals a COPD patient with right-sided heart failure with 82% sensitivity and 77% specificity; in the literature there is not an univocal range for the lower limit of this parameter because of its variability with age. We can consider only the range for a homogeneous population as a reference.

The color-based TDI IVA reference value is 20% lower than the pulse-based TDI value.

IVA is not affected by the loading condition and reflects RV contractility but is dependent on age and is influenced by heart rate (Fig. 14.6).

14.3.2 Strain and Strain Rate

Strain is defined as the change of distance between two points divided by the initial length: $(L–L_0)/L_0$. It is expressed as a percentage; conventionally, shortening or thinning has a negative value, and lengthening or thickening has a positive value.

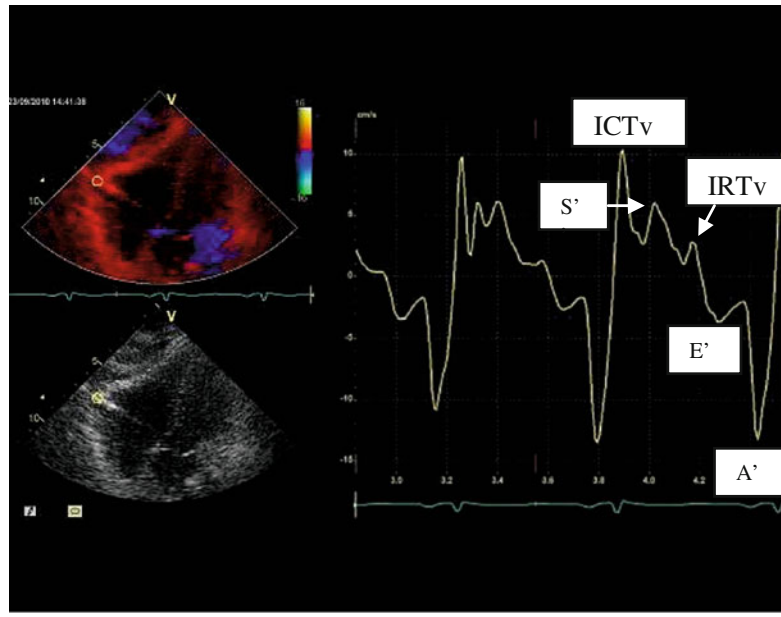

Fig. 14.5 Tissue Doppler imaging (TDI) waves. *A′* late diastolic wave, *E′* early diastolic wave, *ICTv* isovolumic contraction time velocity, *IRTv* isovolumic relaxation time velocity, *S′* systolic peak

Strain rate is the first derivative of strain and represents the change of velocity between two points divided by the distance between them. The unit of measure is reciprocal seconds. These parameters are derived from TDI. Acquisition of the images usually has to be performed in the four-chamber view at high frame rate (more than 150 frames per second).

Strain is influenced by the presence of pulmonary hypertension. Systolic strain is closely related to stroke volume and contractility.

Strain can be sampled on the tricuspid annulus, on the free wall, or on the apex. Strain and strain rate have higher values for the apical segment.

Strain and strain rate are angle-dependent and the angle should be under 30 ° from the beam direction. To compensate for this type of bias, there is a novel technique—2D speckle tracking—that is relatively angle independent and also is less influenced by the frame rate and the quality of the image.

The peak systolic strain (at the end of the T wave on ECG) is maximum in a normal subject, decreases in pulmonary hypertension patients, and decreases further if the right ventricle is decompensated.

The systolic wave correlates well with the regional ejection fraction.

Dysfunction of the right side of the heart starts early in the COPD patient and strain and strain rate can detect it.

The normal strain value for the basal fraction of the right ventricle is about −27% and for the free wall it is −29% (±9.9%) with regional strain.

COPD and pulmonary hypertension decrease the wave (more positive) of peak systolic wall strain in particular on the free wall (Fig. 14.7).

Also strain rate correlates well with the contractility of the right ventricle. It has the advantage of not being load-dependent like strain.

In particular, systolic wall strain rate (reference from -1.5 ± 0.41 to -2.23 ± 0.91) worsens in COPD patients and worsens further in cor pulmonale patients (Fig. 14.8).

14.3.3 Myocardial Performance Index or Tei Index

The myocardial performance index (MPI) is a useful method to assess the systolic and diastolic function of the right ventricle. To calculate the

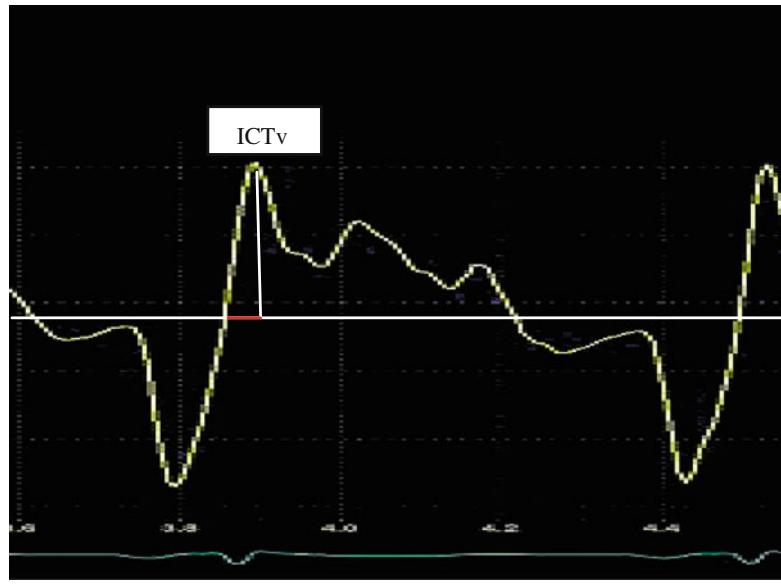

Fig. 14.6 Calculation of isovolumic acceleration (by color TDI waves). *Red* acceleration time, *white* baseline

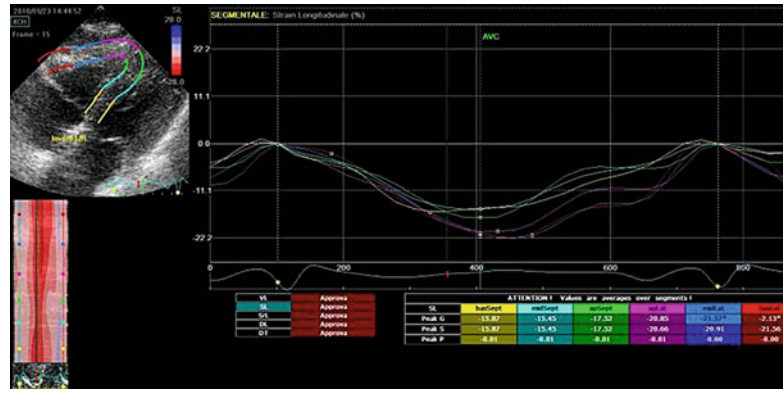

Fig. 14.7 Peak systolic strain (obtained by analysis of 2D strain)

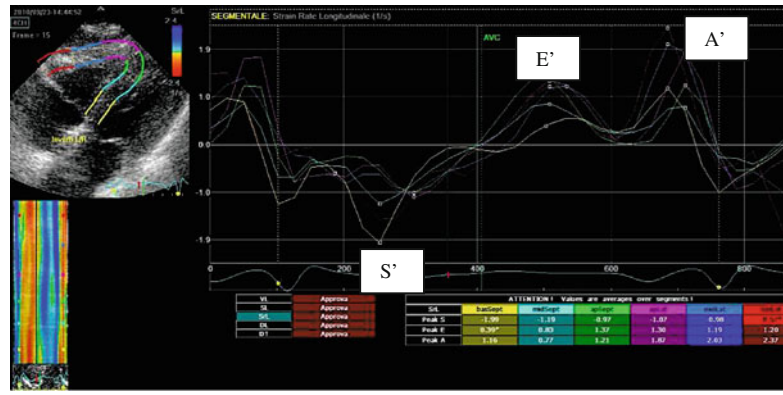

Fig. 14.8 Strain rate imaging E', A', and S' (peak systolic strain rate) obtained by analysis of 2D strain

MPI we can sample time intervals using pulsed Doppler echocardiography or TDI: MPI = (isovolumic relaxation time + isovolumic contraction time)/ejection time.

With pulsed Doppler echocardiography, the ejection time is measured from the onset to the cessation of the flow for the RV outflow tract. The sum of the isovolumic relaxation time and

the isovolumic contraction time is the time between the E wave and the A wave of the next beat, seen on Tricuspid Valve Doppler, minus the ejection time. The parasternal long-axis view is recommended for visualization of the both pulmonary valve and the tricuspid valve.

More user-friendly is the calculation of the MPI from TDI because we do not need to acquire the image of the two valves.

The upper reference of the MPI calculated with pulsed wave Doppler echocardiography is 0.40 and with TDI it is 0.55. Patients with pulmonary hypertension and decompensation of the right side of the heart have values above these limits.

The disadvantage of this method is that it is load-dependent and is not useful in arrhythmia such as atrial fibrillation and when right atrial pressure is high.

The use of this tool is, however, recommended as a complement of other methods for evaluation of the right ventricle.

Further Reading

Horton KD, Meece RW, Hill JC (2009) J Am Soc Echocardiogr 22:776–792

Lòpez-Candales A, Rajagopalan N, Dohi K, Gulyasy B, Edelman K, Bazaz R (2007) Echocardiography 24:615–622

Milan A, Magnino C, Veglio F (2010) J Am Soc Echocardiogr 23:225–239

Turhan S, Dinçer I, Ozdol C, Rahimov U, Kiliçkap M, Altin T, Tulunay C, Akgun G, Erol C (2007) Echocardiography 24:126–133

Vitarelli, Conde Y, Cimino E, Stellato S, D'Orazio S, D'Angeli I, Nguyen BL, Padella V, Caranci F, Petroianni A, D'Antoni L, Terzano C (2006) Eur Respir J 27:268–275

Mitral Valve

15

Ilaria Nicoletti, Carla Avallato, and Alessandro Locatelli

15.1 Introduction

The mitral valve (MV) apparatus includes the mitral annulus, two leaflets, approximately 1 mm thick, chordae tendineae, and papillary muscles.

The anterior mitral leaflet (AML) and the posterior mitral leaflet (PML) cover approximately one third and two thirds, respectively, of the circumference of the annulus (Fig. 15.1). The AML is longer than the PML; the distance from the base to the free edge of the AML is about 1.5–2.5 cm, whereas the distance from the base to the free edge of the PML is about 1 cm.

The PML is divided into three segments or scallops: P_1, P_2, and P_3 (Fig. 15.2). P_1 is the lateral scallop and it is close to the anterolateral commissure and atrial appendage. P_2 is the central scallop and generally the largest. P_3 is the medial scallop; it is close to the posteromedial commissure and the tricuspid valve.

The AML has a semicircular shape and its fibrous core is continuous with the noncoronary cusp of the aortic valve. In the AML, although it is not anatomically divided into scallops, three regions (A_1, A_2, and A_3) have also been identified for the sake of classification, and in accordance with the PML.

In systole the two leaflets of the MV overlap in an area known as the coaptation zone (Fig. 15.3). It is about 7–10 mm long.

The chordae tendineae arise from the papillary muscles or directly from the ventricular walls and are inserted on the leaflets; according to their insertion site, the chordae tendineae are classified into three types of chordae:

1. *Primary or marginal chordae*: they are attached to the tip of the leaflets. The rupture of these chordae causes insufficiency. These chordae, being inserted at the level of the commissures, are called commissural chordae.
2. *Secondary chordae*: they are inserted on the ventricular surface of the leaflets and relieve the leaflets of tension. The "strut chordae" belong to this type; these robust chordae maintain the shape and function of the left ventricle.
3. *Tertiary chordae*: they are attached on the base of PML and arise from the ventricular wall.

There are two papillary muscles, anterolateral and posteromedial; they arise from the distal third of the left ventricle wall and attach to the anterolateral and posteromedial sites. They exert a dynamic force on the valve leaflets which counterbalances the pressure rise in the ventricle during systole. The anterolateral papillary muscle has a dual blood supply, from the circumflex artery and from the diagonal branches of the left anterior descending artery. The posteromedial papillary muscle is usually supplied by the right coronary artery and it is, therefore, more susceptible to risk of ischemic damage.

I. Nicoletti (✉)
Cardiovascular Anesthesia, Santa Croce & Carle Hospital, Cuneo, Italy
e-mail: nicoletti.i@ospedale.cuneo.it

A. Sarti and F. L. Lorini (eds.), *Echocardiography for Intensivists*,
DOI: 10.1007/978-88-470-2583-7_15,

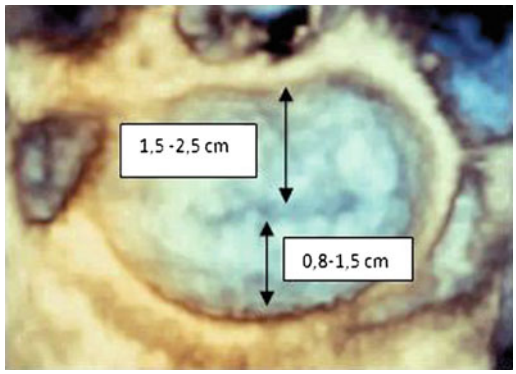

Fig. 15.1 Anterior mitral leaflet and posterior mitral leaflet

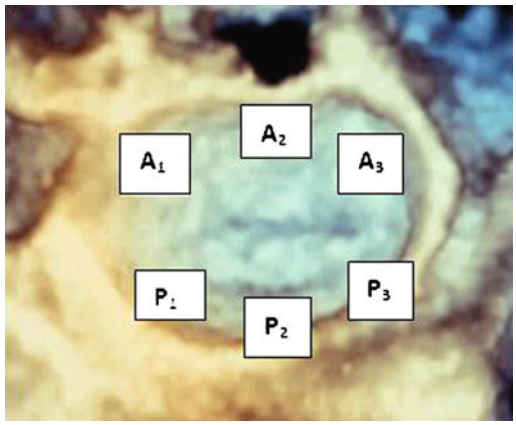

Fig. 15.2 Scallops of anterior and posterior mitral leaflets

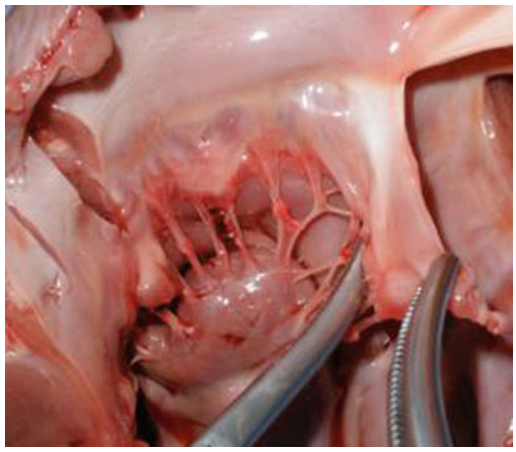

Fig. 15.3 Coaptation zone

A perfect interplay among all of these structures, namely, the mitral leaflets, the subvalvular apparatus, the annulus, and the left ventricle, is critical for normal functioning of the MV.

15.2 Mitral Valve and Transthoracic Echocardiography and Transesophageal Echocardiography

The views used for studying both the anatomy and the function of the MV by transthoracic echocardiography (TTE) are as follows:

- Parasternal long-axis and short-axis views (Figs. 15.4, 15.5)
- Apical four-chamber and two-chamber views (Figs. 15.6, 15.7)

The views used in transesophageal echocardiography (TEE) are as follows:

- Mid-esophageal view (four-chamber, commissural, two-chamber, and long-axis views) (Figs. 15.8, 15.9, 15.10, 15.11)
- Transgastric basal views (short-axis and two-chamber views) (Figs. 15.12, 15.13)

15.3 Mitral Valvulopathy

Stenosis and insufficiency of the MV, which can be concomitant, are the common result of several forms of disease.

15.4 Mitral Regurgitation

Two types of mitral regurgitation (MR) are recognized: organic and functional. The first type is due to an intrinsic malformation of the valve; the second is due to a regional and/or global remodeling of the left ventricle.

Organic MR is due to intrinsic valve diseases such as degenerative diseases (Barlow's disease, fibroelastic degeneration, Marfan's syndrome, Ehlers–Danlos syndrome), rheumatic heart disease, endocarditis, and ischemic papillary muscle rupture.

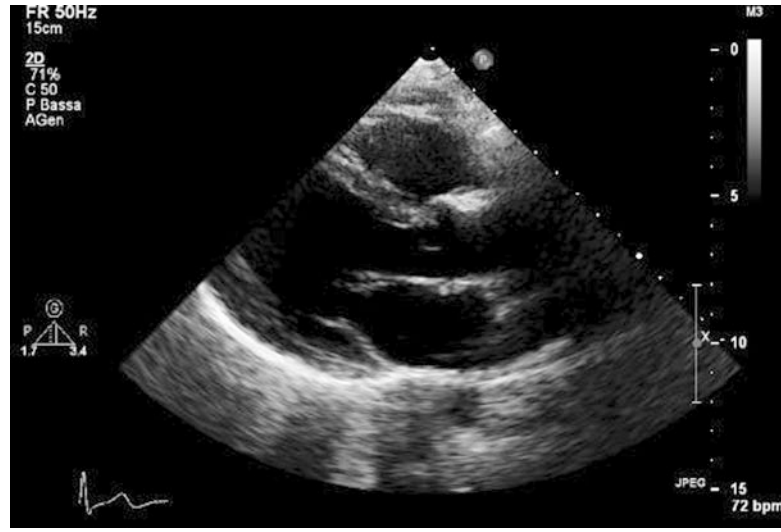

Fig. 15.4 Parasternal long-axis view

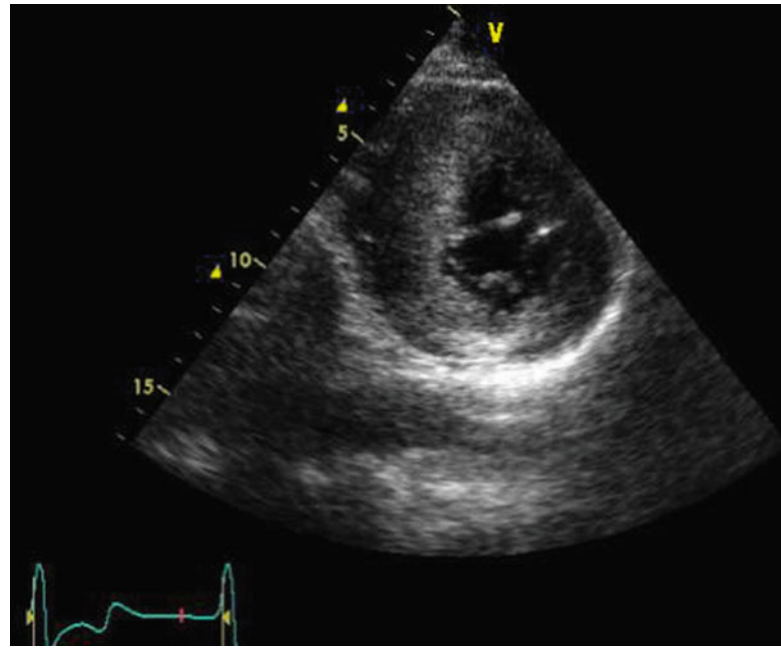

Fig. 15.5 Parasternal short-axis view

In *functional MR*, ischemic heart disease and dilated cardiomyopathy are common underlying diseases. Functional MR is due to an alteration of the geometry of the left ventricle (dilation and spherical enlargement) followed by dilation of the mitral annulus and dislocation of the papillary muscles. The MV is morphologically normal but the systolic coaptation of its leaflets is impaired, owing to both reduced contractility and loss of synchronization of the left ventricle and the papillary muscles. The mitral annulus also shows an altered systolic contraction.

15.4.1 Mechanisms of Mitral Regurgitation

Carpentier's classification is most commonly used. It identifies three types of MR on the basis of leaflet motion.

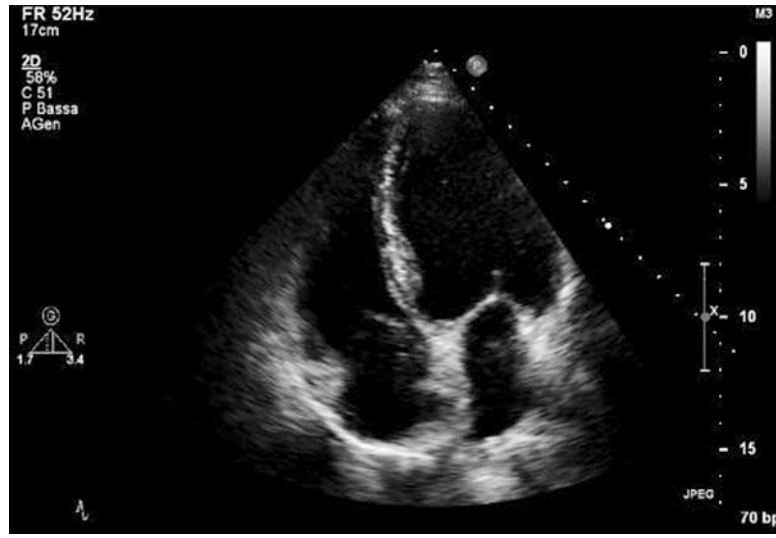

Fig. 15.6 Apical four-chamber view

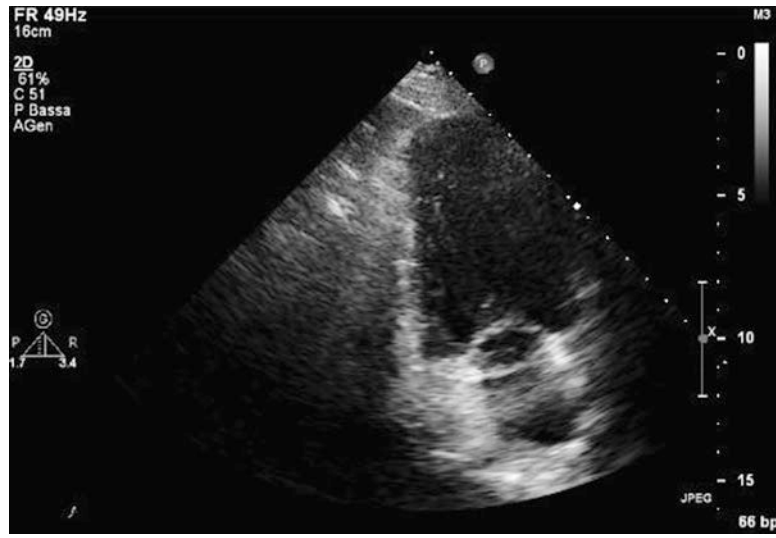

Fig. 15.7 Apical two-chamber view

1. Type I: normal leaflet motion with a coaptation defect. Degenerative or ischemic annular ectasia and leaflet perforation due to endocarditis may be present.
2. Type II: excessive leaflet motion. Cordal stretching or rupture, papillary muscle rupture, or degenerative disease may be present.
   - Billowing leaflet. There is a mitral leaflet bulge above the annulus toward the left atrium during systole, but the coaptation line is maintained below the mitral anulus.
   - Floppy valve. Myxomatous valvular degeneration is present. The leaflets are thickened (more than 5 mm in diastole) and redundant. The chordae often appear elongated.
   - Prolapse. In this case the line of coaptation is above the mitral annulus, about 2 mm or more, but the leaflet tip is directed toward the left ventricle. It can be assessed in the mid-esophageal long-axis view at the end of systole (Figs. 15.14, 15.15).
   - Flail. The free edge of the leaflet is upturned in the left atrium and its tip is directed toward the left atrium. Chordal rupture, due to degenerative, infective, or ischemic causes, is usually the cause; the PML, especially P_2,

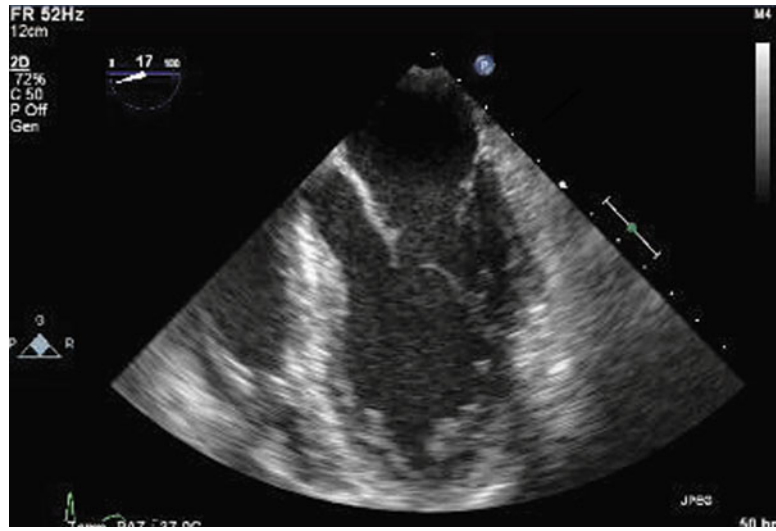

Fig. 15.8 Mid-esophageal four-chamber view

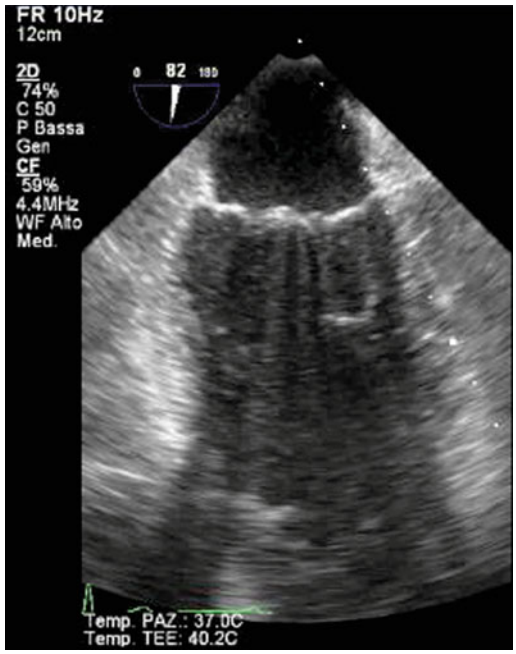

Fig. 15.9 Mid-esophageal commissural view

is more often involved. The regurgitant jet is usually eccentric, moving away the side of the lesion (Fig. 15.16).

3. Type III: restricted leaflet motion. It may be associated with rheumatic heart disease, dilated cardiomyopathy, and ischemic cardiomyopathy. This type is further subdivided into types IIIa and IIIb.
   - Type IIIa. Leaflet movement is restricted because of organic causes (mostly rheumatic disease), both in systole and in diastole.
   - Type IIIb. Leaflet movement is restricted because of functional causes (mostly ischemic heart disease). Systolic tethering of the leaflets, papillary muscle displacement, or left ventricular dilation are present; leaflet motion is normal during diastole.

15.4.2 Echocardiographic Assessment of Mitral Regurgitation

Normally a standard approach is employed, using the same views as used in the morphological examination of the MV. Quantification requires a Doppler technique with qualitative (spectral Doppler echocardiography), semi-quantitative (color Doppler echocardiography), and quantitative (regurgitation volume, regurgitation area, regurgitation fraction) assessments.

15.4.2.1 Qualitative Assessment

The presence and severity of a mitral insufficiency can be assessed by using some of the qualitative parameters obtained from Doppler curves for the regurgitant flow, pulmonary venous flow, and transmitral flow.

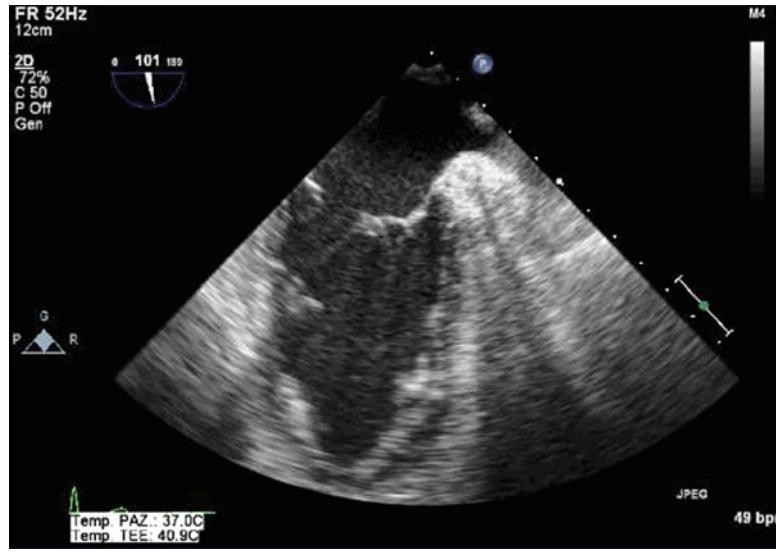

Fig. 15.10 Mid-esophageal two-chamber view

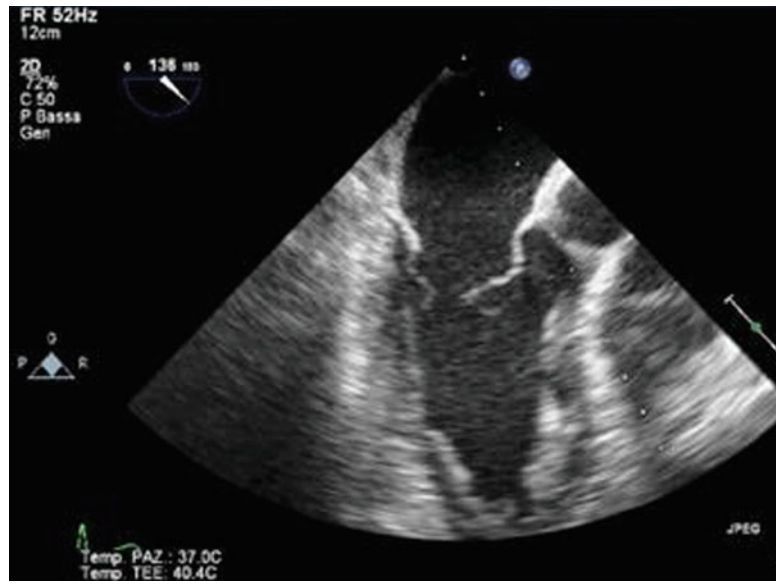

Fig. 15.11 Mid-esophageal long-axis view

Applying continuous wave Doppler analysis to the regurgitant jet, one obtains a flow profile whose intensity is correlated with the extent of the regurgitation: a thicker and more evident curve is associated with a severer regurgitation.

Under normal conditions pulmonary venous flow shows three waves. Two are positive, namely, S and D (peaks of systolic and diastolic velocity, normally $S > D$), and one is negative, *a*, due to atrial contraction. MR causes an increase in left atrial pressure and a decrease in the peak of systolic velocity; in severe MR the S wave is reduced and may even be inverted.

Under normal conditions transmitral flow shows two waves: E and A (peaks of velocity produced by rapid diastolic filling and atrial contraction); in the absence of mitral stenosis, an E-wave velocity greater than 1.4 m/s indicate significant MR, whereas a dominant A wave excludes significant MR.

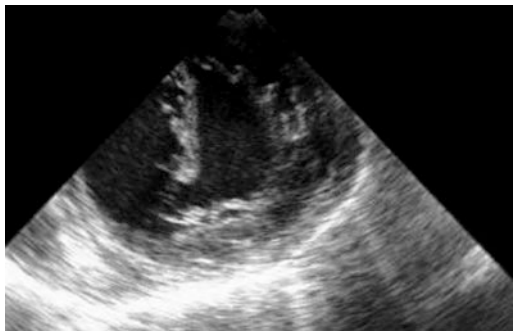

Fig. 15.12 Transgastric basal short-axis view

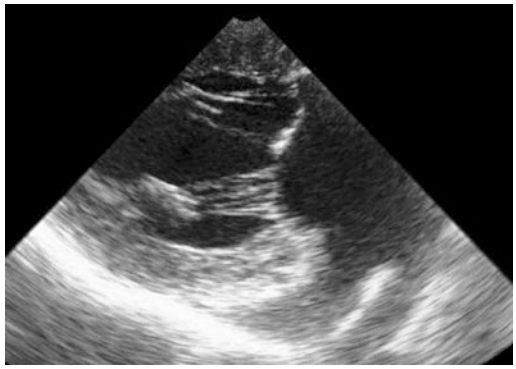

Fig. 15.13 Transgastric basal two-chamber view

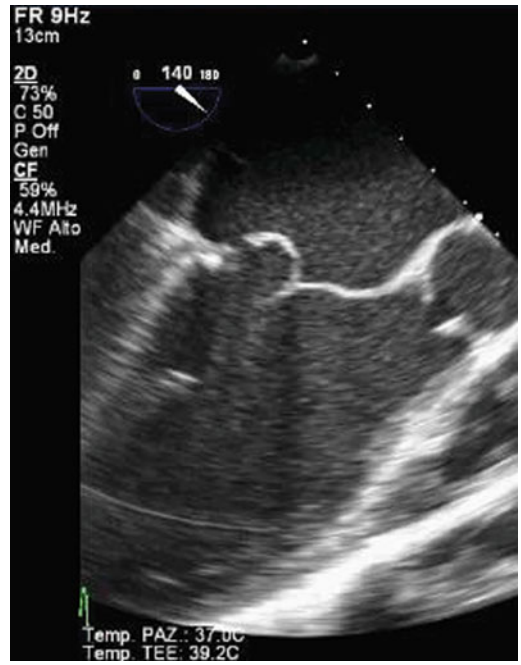

Fig. 15.14 Prolapse

15.4.2.2 Semiquantitative Assessment

Visualization of a regurgitant jet in the left atrium starting from the MV shows the presence of valvular insufficiency. Using color Doppler echocardiography, one examines the regurgitant jet to assess both its area and its relationship with left atrial area.

The regurgitant jet area is the spatial representation of the velocity of the blood which regurgitates into the left atrium. This area of turbulence is influenced by the pressure gradient between the left ventricle and the left atrium. If the pressure in the former is lowered (e.g., by hypovolemia or reduced left ventricular contraction), a parallel reduction is observed in the regurgitant jet. Fine control of color gain is essential in the assessment of the regurgitant jet area: in fact, higher or lower gains translate into the representation of a larger or smaller turbulence area. The color gain scale should be adjusted to eliminate all color in the areas without flow or with low flow, and a color-coded velocity around 50–60 cm/s should be used. The timing of regurgitation is also an important element in the assessment of the regurgitant jet: color M-mode echocardiography, owing to its high temporal resolution, visualizes how much of the systole is involved in regurgitation: large areas of turbulence may appear to be limited to early systole or end-systole, and therefore may be less significant.

The perimeter of the regurgitant jet is traced with the cursor and the area is measured:

A perimeter less than 4 cm^2 signifies mild MR

A perimeter greater than 8 cm^2 signifies severe MR

Both the regurgitant jet area and the area of the left atrium are traced with the cursor and the ratio is calculated:

A ratio less than 20 % signifies mild MR

A ratio of 25–30 % signifies moderate MR

A ratio of 30–40 % signifies moderate to severe MR

A ratio greater than 40 % signifies severe MR

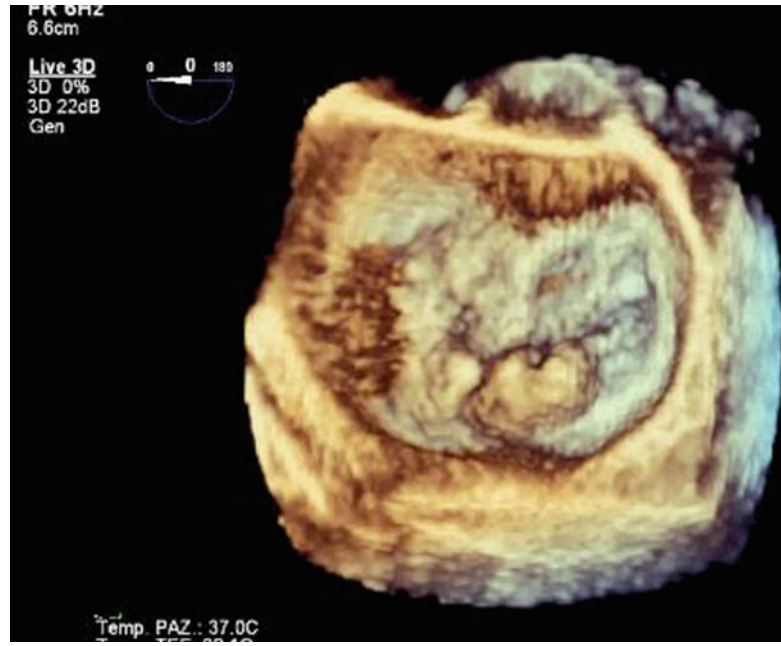

Fig. 15.15 Prolapse

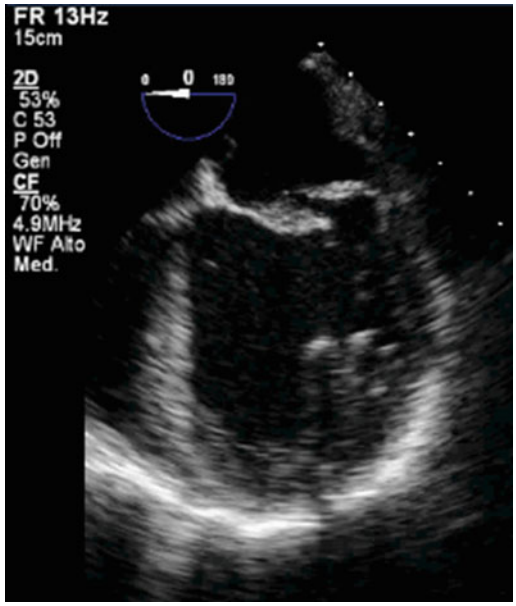

Fig. 15.16 Flail

15.4.2.3 Quantitative Assessment

The most common methods used for quantifying the severity of regurgitation are the *vena contracta method* and the *proximal isovelocity surface area (PISA) method*, both of which require color Doppler echocardiography.

The vena contracta (Fig. 15.17) is the narrowest portion of the regurgitant jet and is positioned just above the regurgitant orifice between the convergence area and the postorifice turbulence area. It is independent of hemodynamic variations and applies to jets whose origin may be either central or not central. Views should be used which are perpendicular to the commissural line, such as the mid-esophageal long-axis view for TEE and the parasternal long-axis view for TTE. Both zooming and reduction of the examining angle of the color Doppler imaging can be helpful, by improving temporal resolution. In the case of multiple jets, the individual vena contracta values should not be added up. A vena contracta width of less than 3 mm signifies mild MR and a width greater than 7 mm signifies severe MR.

The PISA method, or flow convergence method, is based on the principal of flow conservation and of the continuity equation. When a flow approaches a circular orifice, it converges and accelerates, forming concentric hemispheres whose surfaces have the same velocity (isovelocity). The velocity

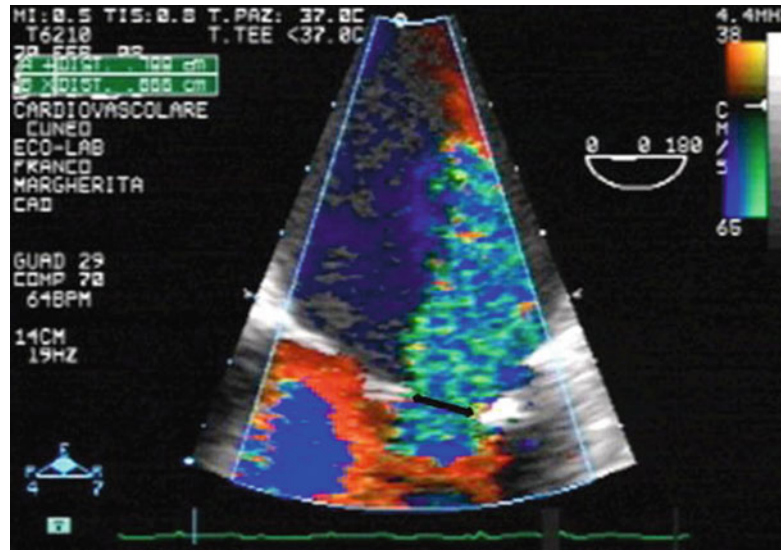

Fig. 15.17 Vena contracta

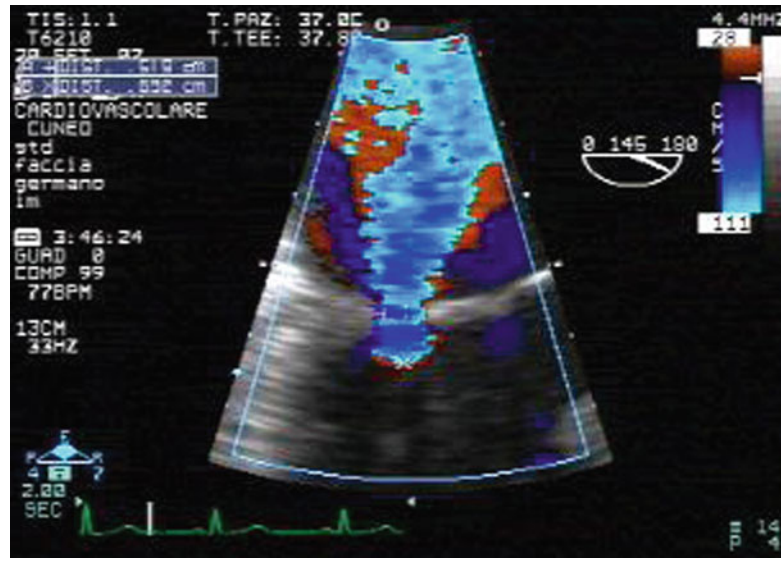

Fig. 15.18 Proximal isovelocity surface area or flow convergence method

of flow at the level of these hemispheres is equal to that of the flow through the regurgitant orifice. Regulating the aliasing velocity (Nyquist limits, i.e., the velocity beyond which the color is inverted; in the case of TEE the color of the regurgitant jet from red to blue), one obtains a well-defined external hemisphere. This allows calculation of the flow through the regurgitant orifice as the product of the area of the hemisphere and the velocity of aliasing, $Q = 2\pi r^2 \times V_{\text{aliasing}}$, where r is the distance between the surface of the first hemisphere and the regurgitant orifice (Fig. 15.18).

Owing to the principle of conversion of mass, the quantity of flow through the surface of the hemisphere coincides with that of the regurgitant orifice; therefore, dividing the flow by the maximum velocity of the MR (measured with continuous wave Doppler interrogation of the regurgitant jet), one obtains the effective regurgitant orifice area (EROA). This, multiplied by the time–velocity integral (TVI) obtained with continuous wave Doppler interrogation of the regurgitant jet, gives the regurgitant volume (RV):

$$Q = 2\pi r^2 \times V_{\text{aliasing}},$$

$$\text{EROA} = Q/\text{Vmax},$$

$$\text{RV (ml)} = \text{EROA}\left(\text{cm}^2\right) \times \text{TVI (cm)}.$$

If V_{aliasing} is 40 cm/s and V_{max} of the MR is 500 cm/s, then EROA $= 6.28 \times r^2 \times 40/500 = r^2/2$.

PISA assessment is improved by reducing the depth of the image and reducing the Nyquist limit to 20–40 cm/s. The radius is measured in mesosystole using the first velocity of aliasing. The presence of a flow convergence with a Nyquist limit of 50/60 cm/s immediately suggests a significant MR. For a velocity aliasing of 40 cm/s, a PISA radius greater than 1cm indicates severe MR.

The values of the parameters for quantifying the severity of MR are different in organic and functional MR.

In organic MR:

- Mild MR is characterized by EROA $<$ 20 mm^2 and RV $<$ 30 ml.
- Mild to moderate MR is characterized by EROA = 20–29 mm^2 and RV = 30–44 ml.
- Moderate to severe MR is characterized by EROA = 30–39 mm^2 and RV = 45–59 ml.
- Severe MR is characterized by EROA $>$ 40mm^2 and RV $>$ 60 ml

In functional MR, severe MR is characterized by EROA $>$ 20 mm^2 and RV $>$ 30 ml.

Quantitative assessment of the RV and the regurgitant area can be performed also with pulse waved and continuous wave Doppler echocardiography. The RV is given as the difference between the quantities of blood which enter and exit the left ventricle. The flow through the regurgitant valve, in this case the MV, and the flow through the left ventricular outflow tract (LVOT) are used to calculate the RV. The diameter of the MV is measured in early diastole, in the mid-esophageal four and two chamber view; the diameter of the LVOT is measured in the mid-esophageal long-axis view just beneath the aortic valvular plane. The flow through the MV is recorded at the level of the mitral annulus and the flow through the LVOT is measured beneath the aortic valvular plane. In the case of aortic insufficiency, the flow through the pulmonary valve is used.

$$\text{RV} = \text{SV}_{\text{regurgitant valve}} - \text{SV}_{\text{competent valve}},$$

$$\text{SV}_{\text{MV}} = \text{area}_{\text{MV}} \times \text{TVI}_{\text{MV}},$$

$$\text{SV}_{\text{LVOT}} = \text{area}_{\text{LVOT}} \times \text{TVI}_{\text{LVOT}},$$

$$\text{Area} = \pi r^2 = (d/2)^2 = 0.785 \times d^2,$$

where SV is stroke volume.

To obtain the TVI, PW Doppler echocardiography is used:

$$\text{EROA} = \text{RV}/\text{TVI}_{\text{MV}},$$

$$\text{FR} = (\text{RV}/\text{SV}_{\text{MV}}) \times 100.$$

The Doppler Volumetric method is a time-consuming approach and is, therefore, discouraged as a first-line method to quantify valvular regurgitation severity. The ratio between the mitral TVI and the aortic TVI gives a quick idea of the MR severity. The transmitral flow is sampled at the level of the mitral anulus, and the aortic flow is sampled at the level of the aortic annulus.

A $\text{TVI}_{\text{MV}}/\text{TVI}_{\text{AoV}}$ ratio greater than 1.4 indicates severe MR; $\text{TVI}_{\text{MR}}/\text{TVI}_{\text{AoV}} < 1$ indicates mild MR.

15.4.3 Physiopathology of Mitral Regurgitation

15.4.3.1 Functional Mitral Regurgitation

Common causes are ischemic and dilated cardiopathies.

In this type of insufficiency the valve and subvalvular apparatus are unaffected and impaired leaflet coaptation is a result of reduced function and distorted geometry of the left ventricle. The imbalance between the tethering forces (as result of left ventricular distorted geometry) and the closure forces (due to the left

ventricular impaired contraction), associated with asynchronous papillary contraction and dilation of the mitral annulus, result in functional MR. Remodeling of the left ventricle is responsible for the transition from an ellipsoidal to a spherical geometry, resulting in a displacement of the papillary muscles, mitral annulus, and subvalvular apparatus. The papillary muscles undergo apical and posterior displacement with tethering of leaflets and apical displacement of the coaptation area of the leaflets; the leaflet apposition is usually normal, i.e., the tips of the leaflets are at the same level in systole. These abnormalities cause MR; the presence and degree of MR seem to be more closely related to the extent of geometric remodeling and dysfunction than to the severity of systolic impairment of the left ventricle. Global ventricular remodeling is more evident in anterior myocardial infarction than in the inferior myocardial infarction. However, the incidence of MR is greater in inferior myocardial infarction owing to the anatomical and functional involvement of the basal segment of the posteroinferior wall adjacent to the papillary muscles. Posterior papillary muscles undergo apical and posterior repositioning with tethering of both mitral leaflets, and so their coaptation point is not at the center of the ventricular cavity but is positioned posteriorly. The AML, tethered by the secondary chords, is reshaped in a "hockey stick" figure and, during valve closure, slides toward the PML, generating a posteriorly oriented, eccentric MR. In anterior and inferior myocardial infarction and in dilated cardiomyopathy, a posterior and apical displacement of the papillary muscles occurs, with symmetrical tenting on both leaflets. The coaptation zone is shifted toward the apex and posteriorly. Since the leaflets are similarly tethered, apposition is normal and the regurgitation jet is central. Global left ventricular remodeling can be assessed by measuring left ventricular volumes and by calculation of the spherical index, which is the relationship between the short axis and the long axis in mid esophageal four-chamber views at end-systole. The following parameters are measured:

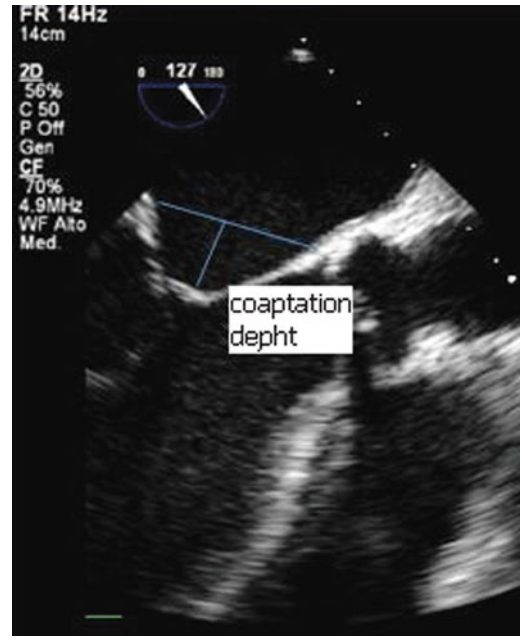

Fig. 15.19 Coaptation depth

- Coaptation depth. This is the distance between the line of coaptation of the leaflets and the mitral annulus plane. This is an index of the dislocation of the papillary muscles and of left ventricular remodeling. In pathological conditions it is equal to or more than 10 mm (Fig. 15.19).
- Tenting area. This is measured in mesosystole as the space between the valve leaflets and the line which connects the two furthest points from the annulus. A tenting area of more than 4 cm^2 indicates moderate MR (Fig. 15.20).

These parameters were obtained in mid-esophageal long-axis views at mid-systole.

15.4.3.2 Degenerative Mitral Regurgitation

Common causes are rheumatic valve disease and myxoid degeneration. The myxoid degeneration involves both the leaflets and the chordae. The leaflets are redundant and thickened (more than 5 mm), especially in their more distal part, showing a clubbed shape. Flail and prolapse are the most frequent scenarios. Careful assessment of annular calcifications should be performed, as they may complicate surgical repair efforts.

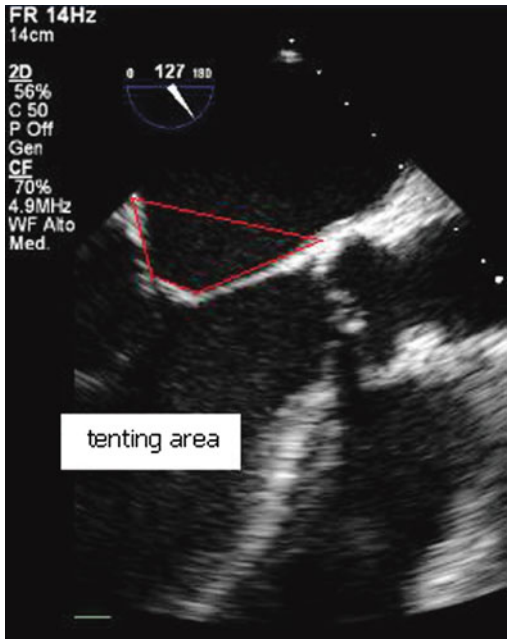

Fig. 15.20 Tenting area

15.5 Transesophageal Echocardiography and Mitral Valve Surgery

TEE can be of help during two separate stages of surgical MV repair. The first stage is prior to cardiopulmonary bypass (CPB), when it is necessary to assess the regurgitation, its mechanism, and the possibility of valve repair. Evaluation of the regurgitation site and mechanism allows the surgeon to plan the surgical strategy. The appraisal of MR severity is less reliable than that performed preoperatively since both the preload and the afterload conditions can be changed by anesthesia. The second stage is after complete weaning from CPB, when the result of MV repair is evaluated by the assessment of residual regurgitant jets, and possible complications such as valve stenosis, systolic anterior motion (SAM), coronary injury, left ventricular rupture, and aortic valve damage can be detected. In the case of valve replacement, TEE is used as well to assess the functioning of the prosthesis and possible perivalvular leaks. The most common complications are:

- Stenosis. The presence of a peak E-wave velocity greater than 2 m/s in transmitral flow should point to stenosis, which can be confirmed by a mean gradient of more than 6 mmHg and a maximum gradient of more than 16 mmHg.
- SAM (Fig. 15.21). This is most often observed after repair of a myxomatous valve. Redundant leaflets, reduced mitral–aortic angle, a small left ventricle, anterior displacement of the point of coaptation, and a small annulus are all baseline features associated with this complication. Pre-CPB TEE (mid-esophageal five-chamber and long-axis views) showing an AML/PML ratio below 1 and a distance between the coaptation point and septum less than 2.5 cm can identify subjects who are at increased risk of SAM. On the echocardiogram it can be apparent as a dynamic obstruction of the LVOT and the presence of a regurgitant jet directed posteriorly. Volume loading and—possibly—vasoconstrictors and beta-blockers can be of help in these cases but, if conservative measures fail, surgical revision of the MV repair is required for the resolution of the SAM.
- Coronary artery injury. The circumflex artery runs along the atrioventricular groove at the level of the posterior mitral annulus. If, during mitral ring placement, the sutures are placed too deeply into the MV annulus, coronary disruption can occur with impairment of coronary flow. TEE shows new ischemic wall motion abnormalities in the lateral or inferolateral wall.
- Left ventricular rupture. This can occur at the level of the atrioventricular groove or the free wall of the left ventricle between the insertion of the papillary muscles and the atrioventricular groove. This is a much-feared and devastating complication. Female gender, advanced age, and calcification of the annulus are predisposing factors. TEE shows persistent bubbling of air into the left ventricular cavity. Surgical placement of a ventricular patch is the only therapy.
- Aortic valve leaflet injury. Sutures which are placed too deep at the level of the anterior

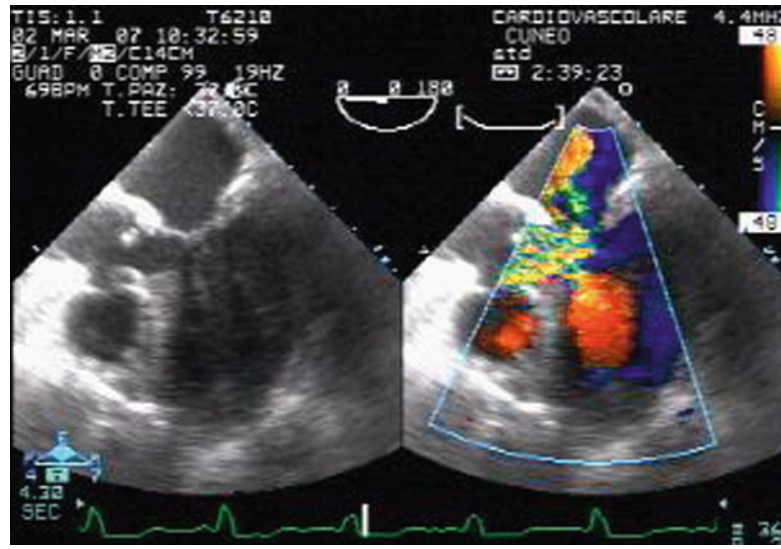

Fig. 15.21 Systolic anterior motion

mitral annulus can damage the aortic leaflets (mainly the left coronary or the noncoronary cusp) causing lesions or inappropriate pulling; the result is massive aortic regurgitation requiring surgical correction.

15.6 Mitral Stenosis

The valve area is between 4 and 6 cm^2. In the case of stenosis, the valvular orifice is reduced; the leaflets appear thickened owing to fibrosis and calcium deposits, and the commissures are usually fused. The subvalvular apparatus appears retracted and the chordae are fused together. Rheumatic disease is the most common cause; rare nonrheumatic forms can be congenital (as in congenital stenosis, parachute MV), or acquired as in calcified degeneration of the annulus and tumors of the annulus or leaflets.

Careful morphological examination by TEE is crucial; on the basis of ultrasonography findings, a decision can be made for a more or less conservative treatment. Next, quantification of stenosis severity is performed via valve area planimetry, the pressure gradient, and calculating the valve area.

Morphological analysis includes the assessment of:

- Thickening of the leaflets, which are typically more marked at the free edge in rheumatic disease
- Thickening, shortening, and degree of fusion of the chordae
- Altered leaflet movement: in particular, the AML tends to fold in, looking like a "hockey stick"
- Commissural fusion

Continuous wave Doppler echocardiography (in mid-esophageal four-chamber or long-axis views) measures the mitral flow velocity and, through the Bernoulli equation, transforms it into mean and maximum gradient values. The gradient can be overestimated in the case of concomitant severe MR. A similar situation arises in the presence of increased cardiac output and restrictive diastolic patterns.

Calculation of the valve area can performed by planimetry, the pressure half time (PHT), the continuity equation, or the PISA method.

In planimetry using the transgastric basal short-axis view, the valve area is measured in diastole. Difficulties can be found in the correct alignment of the scan to the valve, and an oblique view will result in overestimation of the valve area.

PHT is the time for the early diastolic pressure gradient to fall from the maximum value to half that value. This time increases proportionally to

the degree of mitral stenosis. The volume sample is positioned through the mitral orifice, parallel to the flow; sampling can be facilitated using color Doppler echocardiography. The PHT is calculated directly by the machine once the maximum and minimum velocities have been identified. From the PHT, the valve area can be derived: valve area = 220/PHT. The PHT is influenced by various factors which can lead to overestimation of the valve area. Reduced left ventricular compliance or severe aortic regurgitation rapidly increases the ventricular pressure, which causes PHT shortening and in consequence valve area overestimation. Also a rapid increase in cardiac output, following the use of inotropes and/or volume loading, can cause PHT shortening.

The continuity equation is based on the principle of conservation of mass. In the absence of regurgitation and shunts, the volume of flow through the MV is the same as the cardiac output. The flow through the MV is obtained from $\text{area}_{MV} \times \text{TVI}_{MV}$. Cardiac output is mainly calculated at the LVOT or, in the case of aortic regurgitation, at the pulmonary valve. The flow through the LVOT is given by the product $\text{area}_{LVOT} \times \text{TVI}_{LVOT}$:

$$\text{Area}_{MV} \times \text{TVI}_{MV} = \text{area}_{LVOT} \times \text{TVI}_{LVOT},$$

$$\text{Area}_{MV} = \text{area}_{LVOT} \times (\text{TVI}_{LVOT}/\text{TVI}_{MV}),$$

$$\text{Area}_{LVOT} = \pi \times r^2.$$

The continuity equation is independent of the transvalvular pressure gradients, left ventricular compliance, and hemodynamic modifications. The absence of regurgitation in the valves being examined is important in order to application of the continuity equation to be valid. Indeed, in the presence of regurgitation, the forward flows are not equal.

In the PISA method, the continuity equation and color Doppler interrogation are used together to assess the flow through the stenotic MV and the same principles are used as those discussed above for insufficiency. However, in this case acceleration of blood with the formation of concentric hemispheres occurs in the atrium rather than the ventricle. Because of the principle of flow conservation, the calculated flow through these hemispheres is the same as that through a stenotic valve. Flow is calculated as the product of the area of the hemisphere and the velocity of aliasing $\left(Q = 2\pi \times r^2 \times V_{al}\right)$. The most external hemisphere is selected because it is the easiest to identify and its velocity is distinguished by corresponding to the set velocity of aliasing. The radius r in the first hemisphere is measured from the border of the same hemisphere to the extremity of the leaflets. Using the continuity equation, $A_{MV} \times V_{\text{max MV}} = \text{area}_{PISA} \times V_{al}$, for which

$$A_{MV} = \text{area}_{PISA} \times V_{al}/V_{\text{max MV}}.$$

Further Reading

Baumgartner H (2009) Echocardiographic assessment of valve stenosis: EAE/ASE recommendations for clinical practice. J Am Soc Echocardiogr 22(1):1–23

Gary PF et al (1998) Accurate localization of mitral regurgitant defects using multiplane transesophageal echocardiography. Ann Thorac Surg 65:1025–1031

Grayburn PA (2008) How to measure severity of mitral regurgitation. Heart 94:376–383

Lambert AS (2007) Proximal isovelocity surface area should be routinely measured in evaluating mitral regurgitation: a core review. Anesth Analg 105:940–943

Levine RA et al (2005) Ischemic mitral regurgitation on the threshold of a solution: from paradoxes to unifying concepts. Circulation 112:745–758

Naqui TZ (2007) Perioperative clinical decision making in surgery for mitral valve repair. Minerva Cardioangiol 55:213–227

Roberts WC (1983) Morphologic features of the normal and abnormal mitral valve. Am J Cardiol 51:1005–1028

Shanewise J et al (1999) ASE/SCA guidelines for performing a comprehensive intraoperative multiplane transesophageal examination: recommendation of the America Society of Echocardiography and the Society of Cardiovascular Anesthesiologist task force for certification in perioperative transesophageal echocardiography. J Am Soc Echocardiogr 12:884–900

Yiu SF et al (2000) Determinants of the degree of functional mitral regurgitation in patients with systolic left ventricular dysfunction. A clinical study. Circulation 102:1400–1406

Zoghbi WA et al (2003) Recommendations for evaluation of the severity of native valvular regurgitation with two-dimensional and Doppler echocardiography. J Am Soc Echocardiogr 16:777–802

The Aortic Valve

16

Irene Betti

16.1 Morphology (2-D and M-Mode Echocardiography)

The whole left ventricular outflow tract (LVOT) comprises:

1. The subvalvular LVOT: the portion of the left ventricle extending from the free edges of the mitral leaflets to the aortic annulus.
2. The aortic valve (AV)
3. The aortic root (between the AV annulus and the sinotubular junction) and the proximal ascending aorta

The AV is composed of three leaflets; behind each leaflet is the respective sinus of Valsalva. Each sinus and leaflet is named according to the adjacent coronary artery.

A detailed 2-D examination of the AV is an important first step: the AV is seen in the following views: parasternal long-axis view, parasternal short-axis view, apical five-chamber view, and subcostal view.

In the parasternal short-axis view (Fig. 16.1) the AV is viewable in circular section as a star-shaped orifice:

- The right leaflet is on the top (adjacent to the right ventricular outflow tract).
- The noncoronary leaflet is at the bottom left.
- The left leaflet is at the bottom right.

In the parasternal long-axis view the subvalvular LVOT, the aortic annulus, the leaflets (the right leaflet at the top in the image and the noncoronary leaflet at the bottom), the aortic root, the sinotubular junction, and the proximal ascending aorta are viewable. The annular diameter is normally less than 2.5 cm.

Usually the leaflets are thin (thickness less than 2 mm) and mobile and the normal mesosystolic cusp separation is 2 cm or greater. With M-mode it is possible to evaluate the morphology and the systolic opening (aortic box).

A decreased cusp separation with a morphologically normal AV is viewable in hypovolemia and in other conditions with low systolic ejection.

16.2 Doppler Imaging

Transvalvular flow is assessed with color flow Doppler imaging and with continuous wave (CW) Doppler imaging in the apical five-chamber view, and with alignment with the ultrasound beam.

Transvalvular velocity and pressure gradients can be estimated from a CW Doppler envelope directed through the AV. The flow peak velocity across AV is normally less than 2 m/s.

I. Betti (✉)
Cardiology Unit, Santa Maria Annunziata Hospital, Florence, Italy
e-mail: irenebetti@yahoo.it

A. Sarti and F. L. Lorini (eds.), *Echocardiography for Intensivists*,
DOI: 10.1007/978-88-470-2583-7_16, © Springer-Verlag Italia 2012

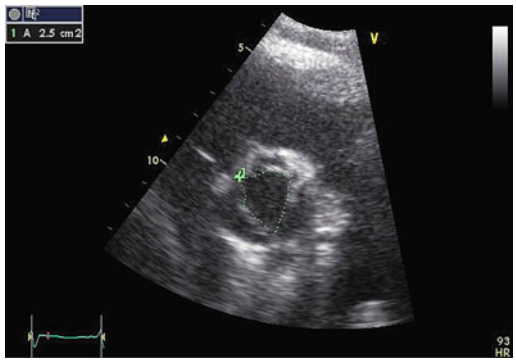

Fig. 16.1 Parasternal short-axis view of the aortic valve (AV) in circular section during systole

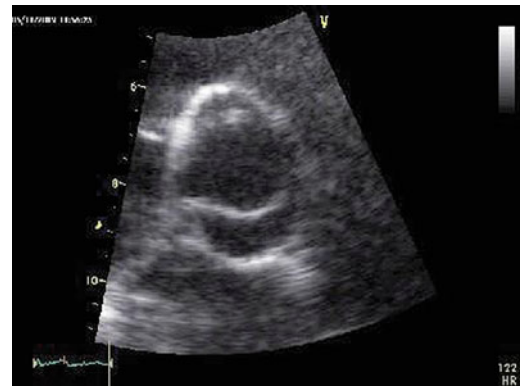

Fig. 16.2 Parasternal short-axis view of a bicuspid AV in systole: there are two cusps (differently dimensioned) rather than the normal three cusps, resulting in an elliptical rather than a star-shaped orifice

16.3 Aortic Sclerosis

Typical of the elderly, aortic sclerosis is characterized by thickened and sometimes calcified leaflets but without a significant restriction of their motion. Therefore, aortic sclerosis is not associated with a flow obstruction, and the peak velocity across the AV is less than 2 m/s.

16.4 Bicuspid Aortic Valve

A bicuspid AV is one of the most common congenital cardiac anomalies. A first echocardiographic criterion for making a diagnosis utilizing 2-D echocardiography in the parasternal short-axis view is two cusps (frequently differently dimensioned) opening in systole rather than the normal three cusps, resulting in an elliptical rather than a star-shaped orifice (Fig. 16.2). It can occasionally be difficult to make this diagnosis in diastole because a fused commissure (raphe) may resemble a third leaflet, so the diagnosis of a bicuspid AV can reliably be made only in systole.

A second criterion for diagnosis utilizes M-mode echocardiography: in the parasternal long-axis view, this technique identifies eccentric closure of the AV within the aorta.

In the adult, a bicuspid AV is frequently not identifiable because of heavy calcification of leaflets (a severely calcified bicuspid AV may be indistinguishable from a trileaflet valve). If this valve anomaly is detected, it is necessary to rule out other associated abnormalities, including subaortic obstruction, coarctation of the aorta, and dilatation of the aortic root and/or of the ascending aorta. Rarely, an AV may be congenitally unicuspid or quadricuspid.

16.5 Aortic Stenosis

Aortic stenosis may be caused by calcific degeneration of a normal valve (the most common form), rheumatic disease, or congenital valve abnormality (frequently bicuspid AV). In the adult the leaflets are commonly heavily calcified, so the cause is difficult to determine.

Calcific aortic stenosis generally occurs in patients over 70 years of age. It is characterized by fibrocalcific changes in the body and along the free edges of the cusps, resulting in a significant increase in echogenicity and thickness and restriction of leaflet motion during systole. Nevertheless, although the absence of valvular calcification makes significant stenosis unlikely, the presence of calcification does not necessarily imply relevant aortic stenosis.

In M-mode echocardiography of the aortic box in the parasternal long-axis view, a maximal cusp separation of less than 6 mm is suggestive of severe stenosis; on the other hand, a maximal

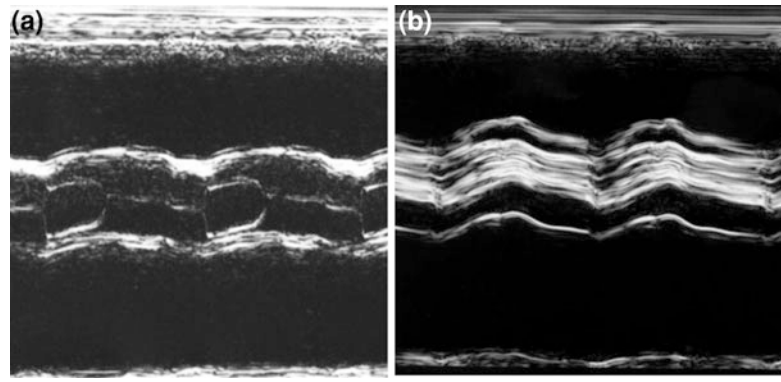

Fig. 16.3 M-mode echocardiography of the aortic box in the parasternal long-axis view: **a** normal cusp separation, **b** cusp separation less than 6 mm, suggestive of severe stenosis

cusp separation of more than 12 mm indicates a no more then mild stenosis (Fig. 16.3).

Color flow Doppler imaging cannot be used to quantify the severity of aortic stenosis; nevertheless, a turbulent, high-velocity flow in the proximal aorta suggests a poststenotic flow pattern. The quantitative diagnosis of aortic stenosis can be obtained using CW Doppler imaging but it is crucial that the ultrasound beam is parallel to the aortic jet.

Using the modified Bernoulli equation, one can measure the pressure gradient across the valve (echocardiography machines directly indicate it on the basis of the transvalvular flow velocity of the CW spectrum during systole): $G = 4 \times v^2$ (where G is the pressure gradient and v is the transvalvular flow velocity). If a high-velocity jet is identified (greater than 4 m/s) in presence of a significant AV disease, a severe aortic stenosis is highly probable (Fig. 16.4); however, if the flow velocity is within normal limits or mildly increased, a critical aortic stenosis can be excluded in patients with a normal left ventricular function. Obviously, the gradient is dependent on both the valve area and the transvalvular flow: an increased transvalvular flow (such as occurs in relevant aortic regurgitation or in elevated cardiac output conditions) can determine a high gradient, and a low cardiac output can determine a small gradient in patients with a severe aortic stenosis. Then in these cases or when the peak pressure gradient is between 25 and 60 mmHg, other measures for quantitative assessment such as planimetry of the AV orifice in the parasternal short axis-view and/or a valve area estimation by the continuity equation are crucial.

For assessment of AV area by the continuity equation it is necessary to acquire the following measurements:

1. The AV velocity–time integral (VTI_{AV}), which is obtained by tracing the outline of the CW Doppler envelope directed through the AV from an apical five-chamber view
2. The area of the subvalvular LVOT obtained from the diameter of the AV annulus in the parasternal long-axis view
3. The velocity–time integral at the level of the LVOT (VTI_{LVOT}), which is obtained by placing a pulsed wave sample volume at the level of the subvalvular LVOT in the apical view

AV area = LVOT area $\times$ VTI_{LVOT}/VTI_{AV}. More simply, for the evaluation of AV area using the continuity equation, the peak velocity has been shown to be a valid substitute for the velocity–time integral. Then AV area = LVOT area $\times$ $V_{max,\ LVOT}/V_{max,\ AV}$.

Another parameter not dependent on the transvalvular flow for severity assessment of aortic stenosis is the ratio of the peak velocities across the subvalvular LVOT and the AV (Doppler velocity index).

Peak velocity of transvalvular flow greater than 4 m/s, mean transvalvular pressure gradient greater than 40 mmHg, AV area less than 1.0 cm^2, indexed AV area less than 0.6 cm^2/m^2 body surface area, and Doppler velocity index less than 0.25 are echocardiographic criteria for the diagnosis of severe aortic stenosis.

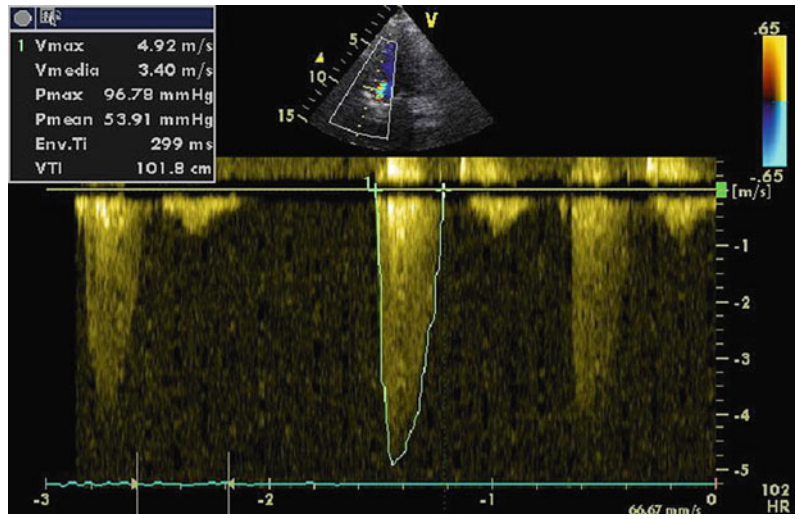

Fig. 16.4 Continuous wave Doppler envelope directed through the AV in severe aortic stenosis: a high-velocity jet is identified (peak velocity greater than 4 m/s, mean pressure gradient greater than 40 mmHg)

Finally, in severe aortic stenosis, left ventricular hypertrophy is generally detectable as a secondary sign.

16.6 Aortic Regurgitation

Aortic regurgitation is caused by abnormalities of the AV and/or the aortic root and may be acute or chronic. Commonly, acute aortic regurgitation results from aortic dissection or endocarditis. In AV endocarditis, cusps are perforated or distorted; sometimes an aortic root abscess distorts the sinotubular junction.

Chronic aortic regurgitation frequently results from calcific degeneration, rheumatic disease, or congenital abnormalities (e.g., bicuspid AV); more rarely it results from a leaflet prolapse in myxomatous disease, which commonly affects also the mitral valve. Another common cause of chronic aortic regurgitation is dilatation of the aortic root (annulus, Valsalva sinus, sinotubular junction) or of the ascending aorta with a reduced overlap between the leaflets in diastole.

By 2-D imaging, abnormalities of the AV and aorta can be detected (e.g., bicuspid AV, calcifications, vegetations, abscess); severe regurgitation is unlikely in the absence of disease on 2-D imaging. Left ventricular volume overload is a significant finding in chronic severe regurgitation.

Color flow Doppler imaging is useful for evaluation of the origin of the jet: the area of the regurgitant jet can be determined from the parasternal short-axis view and can be compared with the area of the subvalvular LVOT by tracing the two areas on the same frame in mid diastole: a ratio less than 25 % suggests mild regurgitation, whereas a ratio greater than 60 % is consistent with severe regurgitation. The parasternal long-axis view can be used for the estimation of width of the regurgitant jet: a jet width to outflow tract diameter ratio of 65 % or greater suggests severe aortic regurgitation.

Another measure for severity assessment of aortic regurgitation is the width of the vena contracta, which is the narrowest portion of the jet located just distal to the regurgitant orifice (Fig. 16.5). A vena contracta wider than 0.6 cm is associated with severe regurgitation, a width less than 0.3 cm is associated with mild regurgitation, and a width between 0.3 and 0.6 cm is associated with moderate regurgitation. Jet length can also be useful to evaluate the severity of aortic regurgitation (Fig. 16.6): a jet is likely severe if its extends past the level of the papillary muscles and mild if it extends less than 2 cm beyond the level of the AV.

Moreover, if a large proximal convergence zone is noted (proximal isovelocity surface area radius greater than 0.7 cm) severe regurgitation is usually present.

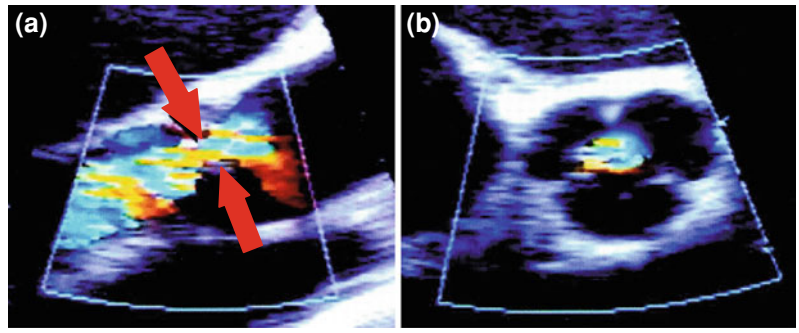

Fig. 16.5 Color flow Doppler imaging of aortic regurgitation. **a** Parasternal long-axis view, *arrows* vena contracta evaluation (the narrowest portion of the jet located just distal to the regurgitant orifice). **b** Parasternal short-axis view

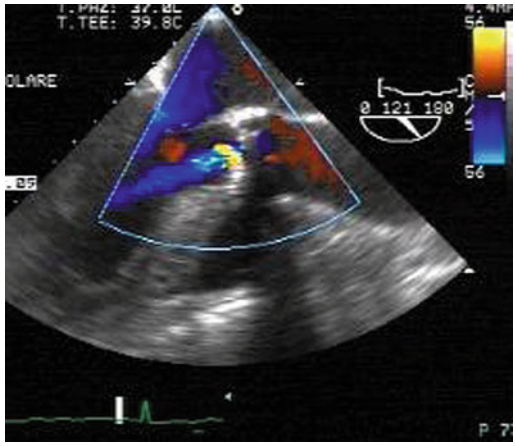

Fig. 16.6 Transesophageal echocardiography mid-esophageal long-axis view at 120°. Severe regurgitation of the aortic valve. The valve cusps appear very thickened; a high peak transvalvular flow in another view showed concomitant severe stenosis

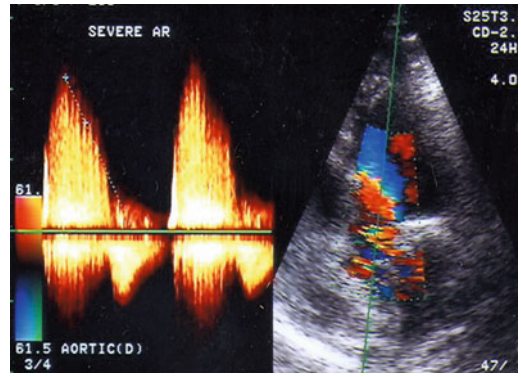

Fig. 16.7 Continuous wave Doppler imaging of aortic transvalvular flow in the apical five-chamber view. Pressure half time (*PHT*) evaluation of aortic regurgitation: a PHT of less than 200 ms is associated with severe regurgitation

The intensity of the regurgitant jet obtained by using spectral Doppler imaging in the apical five-chamber view is proportional to the blood flow across the AV in diastole (it is crucial to compare the regurgitant jet with the anterograde flow signal to eliminate the confounding effect of the difference in the Doppler gain setting).

Another very useful index of severity is the slope of the regurgitant Doppler envelope obtained by using CW Doppler imaging in the apical five-chamber view and the pressure half time (PHT), which is defined as the time required for the pressure gradient across the AV to decrease to half of its maximal value. PHT is inversely proportional to the severity of regurgitation: a PHT greater than 500 ms is associated with mild regurgitation, whereas a PHT less than 200 ms is associated with severe regurgitation (Fig. 16.7).

Increasing severity of aortic regurgitation causes a more prolonged reversal of diastolic flow in the descending aorta: holodiastolic flow reversal has a very high sensitivity for severe regurgitation.

An additional sign suggestive of severe aortic regurgitation is the presystolic closure of the mitral valve (severe aortic regurgitation causes a rapid

diastolic rise in left ventricular pressure, which can cause a premature closure of the mitral valve).

Further Reading

Feigenbaum H (1994) Echocardiography. Lea & Febiger, Malvern

Sidebotham D, Merry A, Legget M (2003) Practical perioperative transoesophageal echocardiography. Butterworth-Heinemann, Edinburgh

The Task Force on the Management of Valvular Heart Disease of the European Society of Cardiology (2007) Guidelines on the management of valvular heart disease. Eur Heart J 28:230–268

Tricuspid and Pulmonary Valves

17

Claudio Poli, Armando Sarti, and Vanni Orzalesi

17.1 Tricuspid Valve Morphology and Function

The tricuspid valve (TV), as the name implies, has three cusps, as does the pulmonary valve (PV). The TV is morphologically similar to the mitral valve, but it is placed downward, toward the apex of the heart. The subvalvular apparatus, including the papillary muscles and chordae tendinae, sticks mainly to the septum, and it is not easily visible in ultrasound images.

The TV is visible mainly in the parasternal long-axis view modified for the right sections, in the parasternal short-axis view at the "big vessels level," in the apical four-chamber view, and in subcostal projections by transthoracic echocardiography (TTE). With transesophageal echocardiography (TEE), this valve is easily seen in the mid-esophageal four-chamber view, the mid-esophageal right ventricular inflow-outflow view, the mid-esophageal aortic valve short-axis view, the transgastric right ventricular inflow view, and the deep transgastric long-axis view. The cusps should not be thicker than 4 mm. The annulus, well visible in TTE apical four-chamber and TEE mid-esophageal four-chamber views, has a diameter ranging typically between 2 and 3.8 cm. With use of color flow mapping (CFM) Doppler echocardiography it is possible to detect a slight tricuspid regurgitation in most subjects. This is normal. On the other hand, moderate or severe regurgitations are never normal.

It is possible to estimate the systolic pulmonary pressure on the basis of tricuspid regurgitation (see Chap. 14).

The respiratory changes in transtricuspid flow are very marked, up to 40 % in normal subjects, so a reliable Doppler assessment of pulmonary artery systolic pressure needs many measurements during the respiratory cycle.

By TTE it is not possible to study the Doppler flow in the inferior cava vein, which is essential to assess the right side of the heart, because of the impossibility of a proper ultrasound alignment. However, with use of pulsed wave Doppler imaging in the subcostal projection for the inferior vena cava, it is possible to evaluate the ultrasound-aligned vertical flow in a hepatic vein, about 1 cm before it merges into the inferior vena cava (see Chap. 14).

The hepatic vein's flow is a good mirror of the vena cava's flow. The normal flow pattern has:

- A dominant systolic component
- A diastolic velocity of no more than 50 % of the systolic velocity

If there is significant tricuspid regurgitation, the flow in the hepatic veins can be dramatically reduced in systole and even reversed, whereas its diastolic component becomes predominant. The normal atrioventricular flow through the TV, estimated with pulsed wave Doppler imaging

C. Poli (✉)
Department of Anesthesia and Intensive Care, Santa Maria Nuova Hospital, Florence, Italy
e-mail: claudio106@yahoo.it

A. Sarti and F. L. Lorini (eds.), *Echocardiography for Intensivists*,
DOI: 10.1007/978-88-470-2583-7_17, © Springer-Verlag Italia 2012

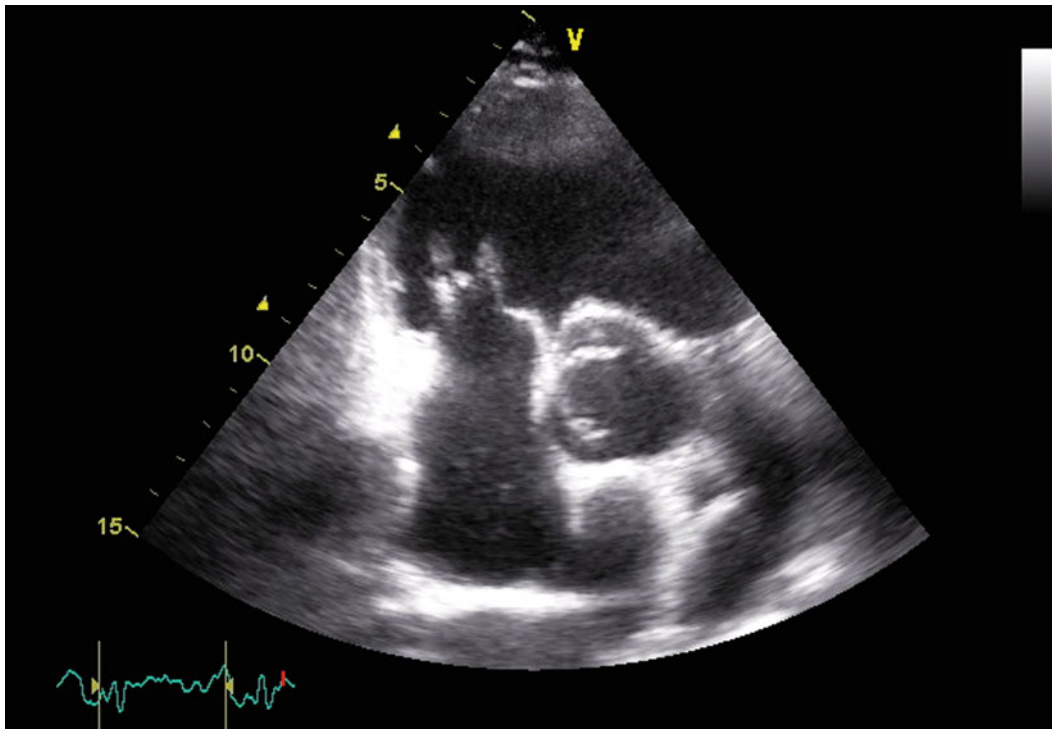

Fig. 17.1 Carcinoid syndrome. Transthoracic echocardiography (TTE) parasternal short-axis view. Thickened leaflets of the tricuspid valve causing severe regurgitation and stenosis

with the apical four-chamber view (TTE) (Fig. 17.5) or in the mid-esophageal four-chamber view (TEE), is a low-speed flow, well below 1 m/s.

17.2 Pulmonary Valve Morphology and Function

The PV is visible by TTE in the modified parasternal long-axis projection (cranial inclination), in the parasternal short-axis view, and in the subcostal short-axis view at the level of the aortic valve. With use of TEE this valve is mainly seen in the mid-esophageal right ventricular inflow-outflow, mid-esophageal aortic valve short-axis, and upper esophageal aortic arch short-axis views. The cusps' thickness normally does not exceed 2 mm. The transpulmonary flow is studied by TTE in the parasternal short-axis view with pulsed wave or continuous wave Doppler imaging. Normally, the peak does not exceed 0.9 m/s. A slight regurgitation is visible in most healthy subjects. The diastolic pulmonary artery pressure can be estimated by means of the pulmonary regurgitation jet (see Chap. 14).

17.3 Carcinoid Syndrome

A serotonin-producing carcinoid tumor causes damage to the valves of the right side of the heart. They gradually thicken and lose their normal mobility (Figs. 17.1, 17.2), causing valvular insufficiency and sometimes even stenosis. If there are no carcinoid lung metastases, left-sided heart structures are not affected.

Alterations of the TV and of the PV are also described in amphetamine-addicted patients. Amphetamine-derived drugs have also been widely used in the past to reduce the sense of hunger with the purpose of weight loss.

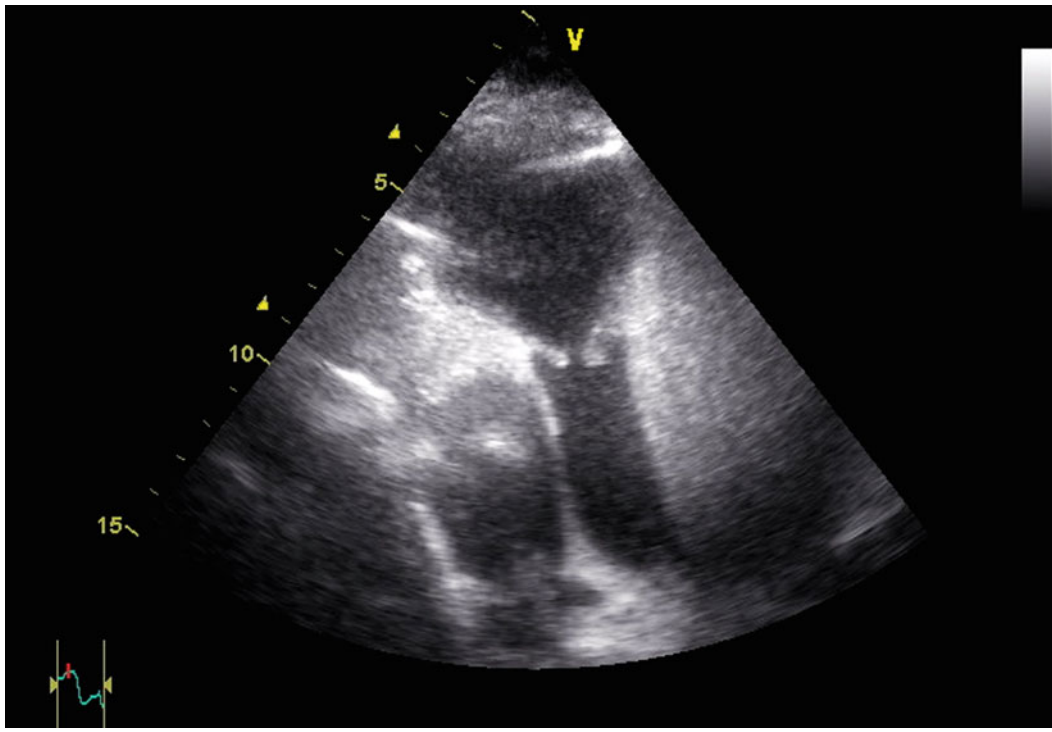

Fig. 17.2 Carcinoid syndrome. TTE modified parasternal short-axis view for right ventricular outflow and pulmonary valve. Thickened leaflets of the pulmonary valve leading to severe regurgitation and stenosis

17.4 Tricuspid Stenosis

This is a rare condition observed in relation to carcinoid syndrome (Fig. 17.1), rheumatic heart disease, or Löffler's endomyocardial fibrosis. The diagnostic principles are like those used for mitral stenosis. The valve exhibits morphological changes in relation to the underlying disease. The average gradient obtained from the continuous wave Doppler transvalvular flow is considered severely impaired if it is more than 5 mmHg. Caval congestion is observed with severe tricuspid stenosis.

17.5 Pulmonary Stenosis

This is known to be associated with Noonan's syndrome. Apart from the congenital forms, pulmonary stenosis can also be caused by carcinoid syndrome (Fig. 17.2) or rheumatic disease. Among the congenital forms, the most common, subvalvular, with a dynamic obstruction component, is most often related to Fallot's tetralogy. The right ventricle thickens in response to obstruction.

17.6 Tricuspid Regurgitation

The most common cause of tricuspid regurgitation is related to TV annulus enlargement due to right ventricular cavity dilatation (caused by reduced right ventricular contractility and pressure or volume overload). In this case, apart from the annulus expansion, the valve is morphologically normal. The other most common cause of tricuspid regurgitation is endocarditis, particularly in intravenous-drug-addicted patients, in carcinoid syndrome, and in rheumatic disease. The congenital defect of the

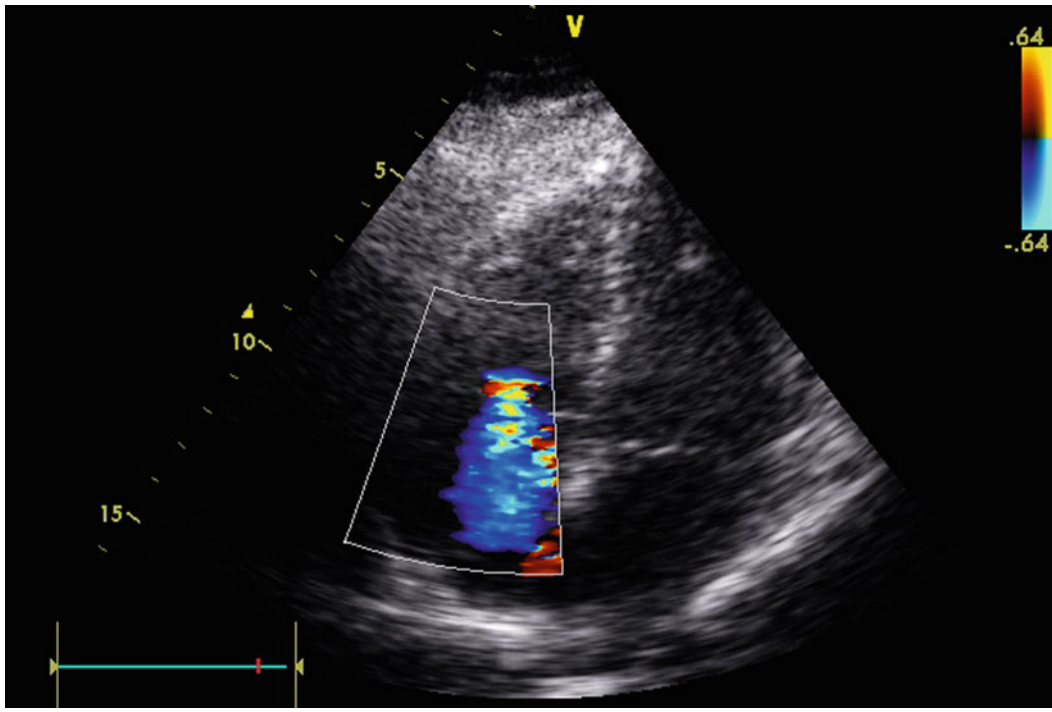

Fig. 17.3 Severe tricuspid regurgitation. TTE subcostal four-chamber view. (From Sarti [3] with permission)

perimembranous ventricular septum may be complicated by tricuspid regurgitation. Even Ebstein's anomaly, which consists of a displacement of the septal cusp toward the apex, with right ventricular "atrialization," is associated with tricuspid regurgitation. The valve leaflets appear dysplastic. Sometimes Ebstein's anomaly is diagnosed in adulthood with the onset of right-sided heart failure. The association with Wolff–Parkinson–White syndrome is not uncommon.

A CFM Doppler echocardiography study through the TV should not be omitted in each cardiac ultrasound assessment. First, the possible morphological alterations are considered. The simple visual observation of the regurgitant jet gives an idea of the insufficiency, despite the large fluctuations caused by breathing (Fig. 17.3). Moreover, the flow is also affected by the pressure generated by the right ventricle. With pulmonary hypertension the high right ventricular pressure generates a well-defined, high-speed jet (Fig. 17.4). So, tricuspid regurgitation cannot be measured by visual CFM of the jet only. The most reliable and easiest to apply method to estimate the amount of tricuspid regurgitation is to measure the diameter of the narrowest point of the jet, just beyond the valvular level (vena contracta). A diameter that exceeds 0.7 cm reveals severe regurgitation.

17.7 Pulmonary Insufficiency

Pulmonary regurgitation in adults is substantially in relation with rheumatic disease, carcinoid syndrome, or endocarditis. Also, pulmonary hypertension may dilate the annulus and cause valvular leakage. The anterograde flow and regurgitation is studied in the parasternal short-axis view (TTE), (Fig. 17.5), or in the mid-esophageal aortic valve short-axis and right ventricular inflow-outflow views (TEE) with CFM. A large jet in relation to the area of right ventricular outflow tract, with a

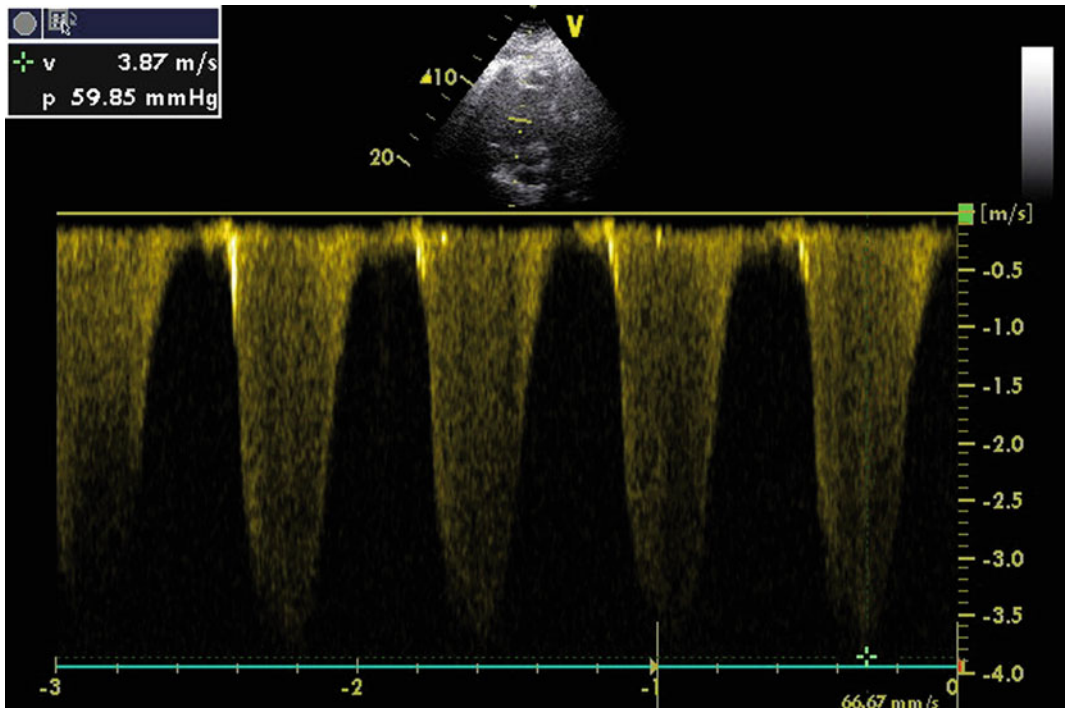

Fig. 17.4 Continuous wave Doppler imaging of a high-speed tricuspid regurgitation jet. TTE apical four-chamber view

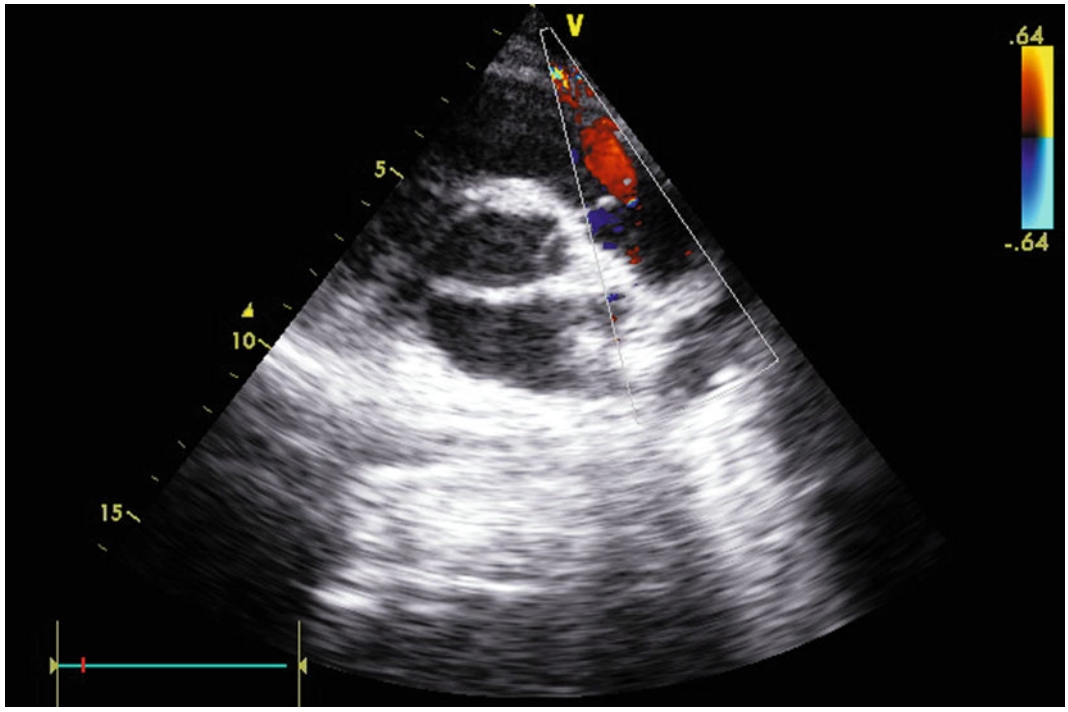

Fig. 17.5 Pulmonary insufficiency. TTE parasternal short-axis view. (From Sarti [3] with the permission)

length 20 mm or more and an area of 1.5 cm^2 or more, shows a significant regurgitation. By continuous wave Doppler imaging it is possible to study the pressure half time (time for the peak to reach the half value) of pulmonary insufficiency. A value below 100 m/s reveals significant regurgitation. An important regurgitation first causes right ventricular dilatation and later right ventricular hypertrophy.

References

1. Feigenbaum H, Armstrong WF, Ryan T (2005) Feigenbaum's echocardiography. Lippincott Williams & Wilkins, Philadelphia
2. Oh JK, Tajik AJ, Stewart JB (2007) The echo manual, 3rd edn. Lippincott Williams & Wilkins, Philadelphia
3. Sarti A (2009) Ecocardiografia per l'intensivista. Springer, Milan

Endocarditis

18

Roger L. Click

18.1 Introduction

Endocarditis is not common but can be a life-threatening inflammation of the endocardium, particularly the heart valves, native or prosthetic. Vegetative material is the hallmark of endocarditis and may be infective or noninfective. The diagnosis can be challenging because in some cases symptoms are vague and nonspecific. The diagnosis is based on positive blood cultures and clinical and echocardiographic features. Since patients with endocarditis can become critically ill and it may be fatal, the diagnosis must be made quickly and appropriate treatment must be initiated. In this chapter, the role of echocardiography in the diagnosis and management of endocarditis is reviewed.

18.2 Classification

Infective endocarditis is usually the result of a bacterial or fungal infection of the heart valves. With a transient bacteremia, e.g., from dental cleaning, bacteria can seed abnormal valves and grow, form a vegetation and damage the valve, potentially be embolic, or form an abscess.

Noninfective endocarditis, also known as nonbacterial thrombotic endocarditis or marantic endocarditis, may occur on normal valves. Often it is associated with other systemic illnesses such as cancer, a hypercoagulable state, and lupus (Libman–Sacks). The vegetations are sterile and are usually smaller than in infective endocarditis and nondestructive to the valve. The greatest risk is embolism.

18.3 Diagnostic Criteria

There are three general criteria to diagnose endocarditis: bacteremia, active endocardial disease, and predisposing heart disease. More specifically, in 1994 the Duke clinical criteria for the diagnosis of infective endocarditis established guidelines. There are major and minor criteria for the diagnosis (see Table 18.1).

To make the diagnosis with the Duke criteria, two major criteria, one major and three minor criteria, or five minor criteria must be fulfilled.

The Duke criteria define echocardiographic evidence as an oscillating intracardiac mass on a heart valve or supporting structure in the path of a regurgitant jet or prosthetic material, cardiac abscess, new dehiscence of a prosthetic valve, or new valvular regurgitation. Echocardiographic assessment of the patient for endocarditis can be divided into two general areas: recognize/differentiate and complications.

R. L. Click (✉)
Division of Cardiology, Mayo Clinic,
Rochester, MN, USA
e-mail: click.roger@mayo.edu

A. Sarti and F. L. Lorini (eds.), *Echocardiography for Intensivists*,
DOI: 10.1007/978-88-470-2583-7_18, © Springer-Verlag Italia 2012

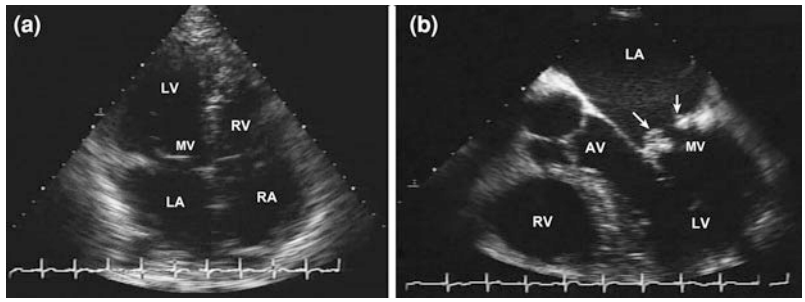

Fig. 18.1 **a** Transthoracic echocardiography four-chamber view of a patient with suspected endocarditis. The image is difficult to interpret and no obvious vegetations are seen. **b** A transesophageal echocardiography (TEE) long-axis view of the same patient shows obvious mitral valve (*MV*) vegetations (*arrows*). *AV* aortic valve, *LA* left atrium, *LV* left ventricle, *RA* right atrium, *RV* right ventricle

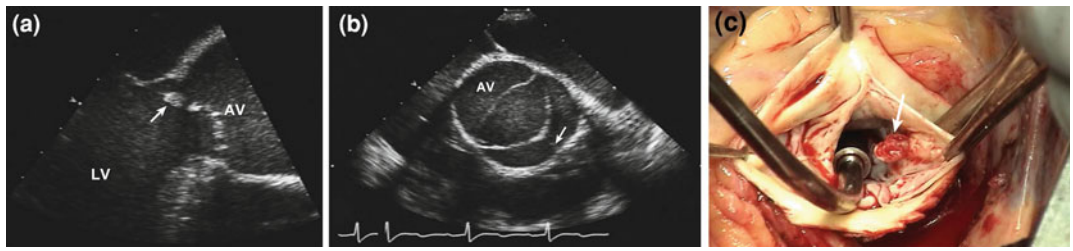

Fig. 18.2 **a** TEE long-axis view (**a**) of the aortic valve (*AV*) with a vegetation (*arrow*). **b** Short-axis view of the bicuspid AV with raphe (*arrow*). **c** An intraoperative photograph of the valve and vegetation (*arrow*). *LV* left ventricle

Table 18.1 Duke criteria for diagnosis of endocarditis

Major criteria	Minor criteria
Positive blood cultures	Predisposition
Endocardial involvement	Fever
Positive echocardiogram	Vascular phenomenon
New valvular regurgitation	Immunologic phenomenon
	Microbiological evidence[a]
	Echocardiographic evidence[a]

[a] Less than major criteria

18.3.1 Recognize/Differentiate

Recognizing the presence of endocarditis refers to identifying vegetations and abnormal valves and differentiating endocarditis from other noninfective valve lesions or abnormalities. Transthoracic echocardiography (TTE) is less than half as sensitive as transesophageal echocardiography (TEE), 44 % vercsus 94 %. The specificity is, however, better (98 % for TTE vs. 100 % for TEE). For this reason it is recommended that TEE be performed on all patients, if possible, when endocarditis is suspected. Figure 18.1 shows an example of a mitral valve observed with TTE and TEE and the presence of vegetations easily missed by TTE.

To recognize a vegetation, the echocardiographic features have to be appreciated. Most vegetations are on left-sided heart valves because of the higher pressure jet lesions from regurgitation and the more common anatomical variants of left-sided valves, i.e., bicuspid aortic valve (Fig. 18.2), mitral stenosis, and prolapse.

Right-sided heart lesions are less common but may be seen with intravenous drug use and right-sided heart indwelling catheters and pacemakers. The vegetations tend to be irregular, bulky, and may be multiple and lead to valve destruction (Figs. 18.3, 18.4). The sites of vegetations are as follows:

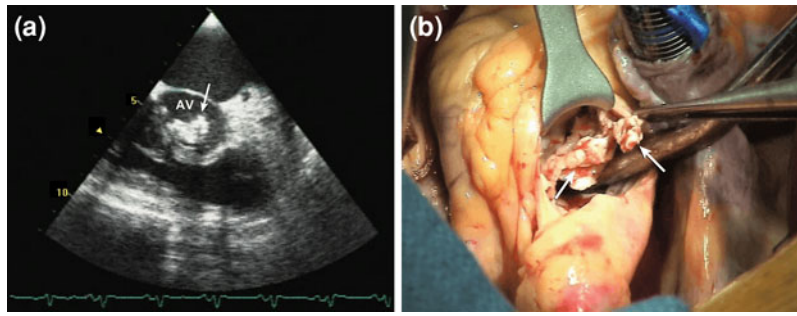

Fig. 18.3 **a** TEE short-axis view of the AV with vegetation (*arrow*). **b** An intraoperative picture of the AV vegetation and significant valve destruction

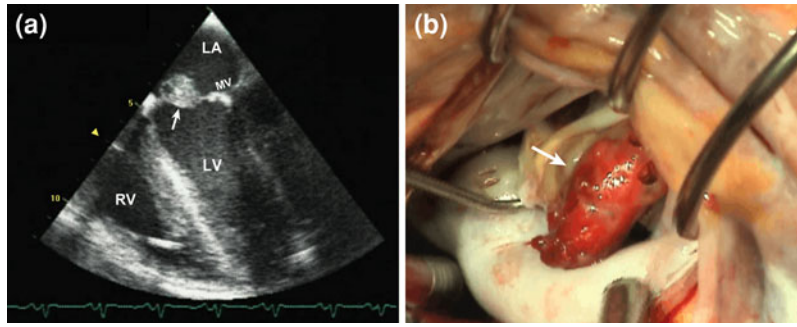

Fig. 18.4 **a** TEE four-chamber view of the MV with vegetation (*arrow*). **b** An intraoperative picture of the MV vegetation (*arrow*). *LA* left atrium, *LV* left ventricle, *RV* right ventricle

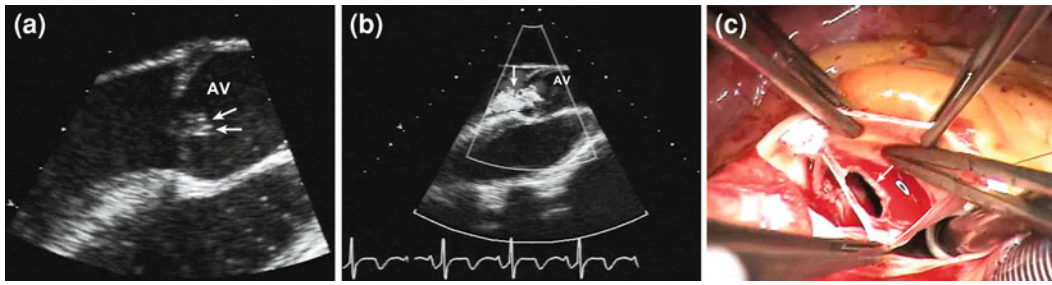

Fig. 18.5 **a** TEE of the AV in the long-axis view with vegetation (*arrows*). **b** The same AV with color flow Doppler imaging shows extensive aortic regurgitation (*arrow*). **c** Intraoperative picture of large AV leaflet perforation (*arrow*) from the endocarditis

- Atrial surfaces of atrioventricular valve
- Ventricular surface of aortic and pulmonary valves
- Prosthetic valve sewing ring
- Cusps of bioprosthetic valves
- Sites affected by turbulent flow
- Patches, pacing wires, and catheters

Once an abnormal mass on a valve has been identified, one has to differentiate it from other types of valve masses. Endocarditis vegetations occur more often on an abnormal valve. Other lesions, e.g., fibroelastomas, are more commonly seen on normal valves. They are usually discrete, singular, and do not cause valve erosion or destruction.

The strands often called degenerative strands are often seen in the older population. The main differentiators of vegetations from other valve lesions are the presence of other features

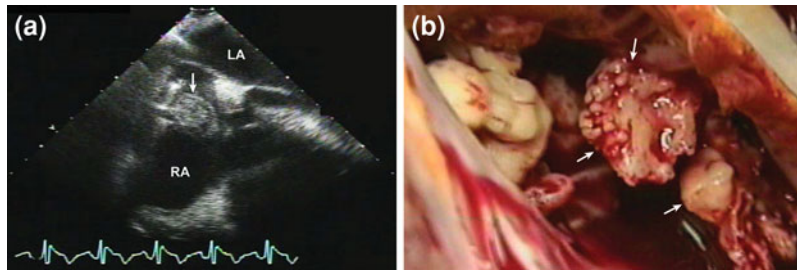

Fig. 18.6 **a** TEE of a large mass (*arrow*) in the right atrium (*RA*). **b** Intraoperative photograph of multiple right atrial masses from a fungal infection. *LA* left atrium

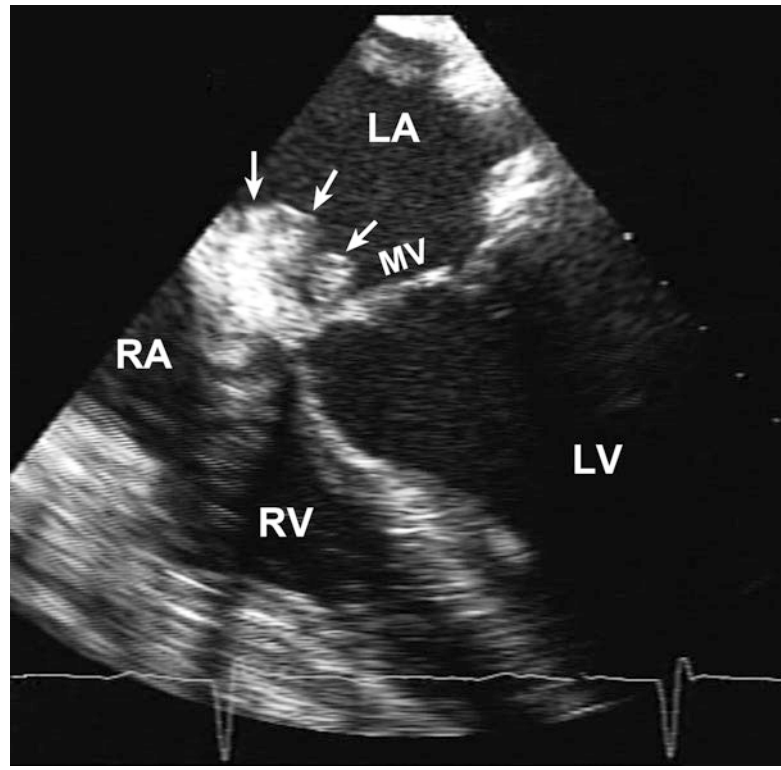

Fig. 18.7 TEE four-chamber view showing MV endocarditis with extension into the intervalvular fibrosa area (*arrows*). *LA* left atrium, *LV* left ventricle, *RA* right atrium, *RV* right ventricle

indicating endocarditis, e.g., fever, positive blood cultures, and clinical presentation. Rarely does a patient have ongoing active endocarditis and not appear ill or have other associated features. Other types of valve lesions usually do not have accompanying features, e.g., ill patient, fever, or positive blood cultures. Other causes of lesions seen on valves are as follows:

- Thrombus
- Myxomatous tissue
- Ruptured chordae/flail scallop
- Fibroelastoma (papilloma)
- Nonbacterial thrombotic endocarditis
- Valve fenestration (especially torn)
- Healed vegetation
- Torn tissue prosthesis
- Strands/excrescences

18.3.2 Complications

Patients with endocarditis can avoid many of the complications of the infection if it is diagnosed

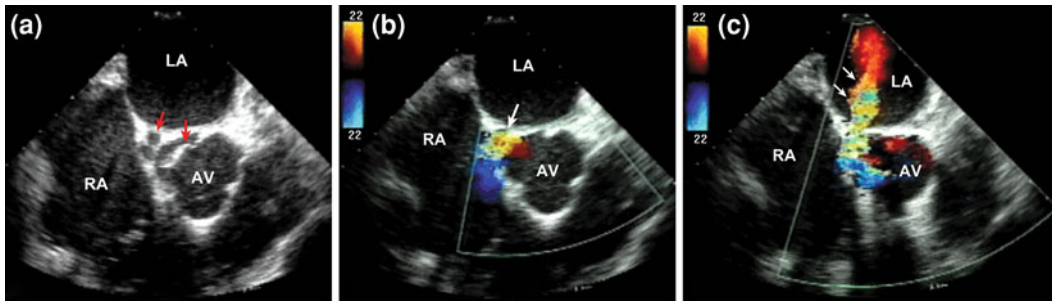

Fig. 18.8 **a** TEE of the AV with perivalvular abscess (*arrows*). **b** Same view with color flow Doppler imaging. **c** Same view several days later showing perforation (*arrows*) of the perivalvular abscess into the left atrium (*LA*) on color flow Doppler imaging. *RA* right atrium

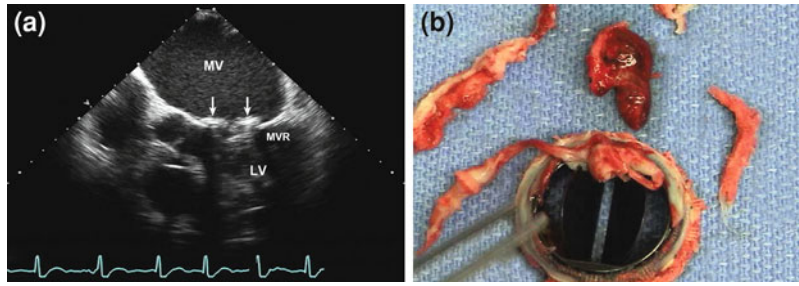

Fig. 18.9 **a** TEE four-chamber view of a mechanical MV replacement (*MVR*) with "shaggy" echos coming from the sewing ring (*arrows*). **b** Removed mitral prosthesis with vegetative material and thrombus. *LV* left ventricle

and treated promptly. However, many patients are diagnosed after weeks or months of lingering illness because of vague symptoms. These patients are at significant increased risk of developing complications: emboli, abscess formation, mycotic aneurysm, valve destruction (regurgitation), and valve stenosis (bulky masses, obstruction).

It has been shown that vegetations larger than 1.0 cm^2 pose a greater risk and are associated with more complications, including heart failure, emboli, and need for surgery. When vegetations seed an abnormal valve, they break down the valve tissue and perforation can occur, leading to significant regurgitation (Fig. 18.5).Perforations can be difficult to see echocardiographically, but eccentric color flow jets may be a clue. Surgically, they may be repairable with a small pericardial patch.

Fungal vegetations tend to be larger and bulky and can be obstructive. Fungal endocarditis is more often seen in intravenous drug users and those who are immunocompromised or receiving broad-spectrum antibiotics. Fungal endocarditis may be more difficult to diagnose as blood cultures may be negative and may also be more of a challenge to treat. Figure 18.6 shows the typical echocardiographic and intraoperative picture of a fungal infection involving the right side of the heart.

If left untreated, vegetations can extend from valves to other structures. Mitral and aortic vegetations will frequently extend into the intervalvular fibrosa (the anatomical area between the aortic root and the mitral annulus). Once a vegetation has seeded, an abscess space may form (Fig. 18.7).

Likewise, extension from the valve leaflets can occur and cause a perivalvular abscess which may stay contained or can rupture through to an adjacent chamber and cause a perivalvular fistula (Fig. 18.8).

Valvular prostheses are particularly vulnerable to infection. Echocardiographically it may be a challenge to see infection on a prosthesis. The sewing ring is the most common location and the only clue may be "haziness." Rarely there is obstruction or a stuck leaflet (Fig. 18.9).

18.4 Conclusion

Endocarditis is a serious, potentially fatal infection of cardiac valves. If it is treated early, complications may be avoided; however, the diagnosis is often delayed because of nonspecific symptoms. Complications are not uncommon and include emboli, valve destruction, and abscess formation. If there is significant valve destruction and hemodynamic instability, emboli, or abscess formation, patients are often faced with valve replacement. Echocardiography plays a key role in the diagnosis and treatment of patients with endocarditis and therefore should be one of the first tests performed if endocarditis is suspected.

Further Reading

Bayer AS, Bolger AF, Taubert KA et al (1998) Diagnosis and management of infective endocarditis and its complications. Circulation 98:2936–2948

Daniel WG, Mugge A, Martin RP et al (1991) Improvement in the diagnosis of abscesses associated with endocarditis by transesophageal echocardiography. N Engl J Med 324:795–800

Durack DT, Lukes AS, Bright DK et al (1994) New criteria for diagnosis of infective endocarditis: utilization of specific echocardiographic findings. Am J Med 96:200–209

Erbel R, Rohmann S, Drexler M et al (1988) Improved diagnostic value of echocardiography in patients with infective endocarditis by transesophageal approach: a prospective study. Eur Heart J 9:43–53

Shively BK, Gurule FT, Roldan CA et al (1991) Diagnostic value of transesophageal compared with transthoracic echocardiography in infective endocarditis. J Am Coll Cardiol 18:391–397

Prosthetic Valve Evaluation

19

Roger L. Click

19.1 Introduction

With the aging population has come an increased number of cardiac operative procedures, including valve replacement and repair and the percutaneous valve replacement approach. Echocardiography plays a significant role in the assessment of prosthetic valves. The primary goal of echocardiography is to determine if a prosthetic valve is normal or abnormal. All echocardiographic parameters, including 2D appearance, color flow Doppler features, and pressure gradients, must be obtained to determine if a valve is normal. Finally, the echocardiographer has to be familiar with what is normal for a given type of valve and location. In this chapter, the echocardiographic features of prosthetic heart valves are reviewed.

19.2 General Considerations

In many applications, 2D echocardiography, either transthoracic echocardiography (TTE) or transesophageal echocardiography (TEE), will provide most of the diagnostic information. To determine if a valve prosthesis is normal, one must rely as much or more on Doppler information in addition to the 2D appearance of the valve. In addition, the type of prosthetic valve and the Doppler characteristics of the valve in a specific location have to be appreciated. The hemodynamics of each patient has to be assessed at the time of the prosthetic assessment. Is there tachycardia, high or low cardiac output, or other factors that may effect the Doppler velocities, e.g., anemia, fever, or thyroid disease?

Each prosthesis has a normal-appearing 2D motion and color flow Doppler pattern. Also, each prosthesis has a normal Doppler velocity range depending on the prosthesis type and location. It is always helpful to have a baseline echocardiogram of a prosthesis shortly after it has been placed to compare the appearance and velocities on follow-up echocardiograms. Most patients who have had a new prosthetic valve fitted will have a dismissal echocardiogram to establish this baseline.

19.3 Normal 2D Echocardiographic Appearance

In general, TEE is superior to TTE to assess the echocardiographic appearance and motion of prosthetic leaflets. The mitral valve leaflets are easier to see for all prostheses (Fig. 19.1), whereas an aortic prosthesis leaflet motion may be more difficult to see with TEE or TTE. In many cases, an aortic prosthesis can be seen best from the transgastric view. The leaflet motion as well as the parallel Doppler angle is best seen

R. L. Click (✉)
Division of Cardiology, Mayo Clinic,
Rochester, MN, USA
e-mail: click.roger@mayo.edu

A. Sarti and F. L. Lorini (eds.), *Echocardiography for Intensivists*,
DOI: 10.1007/978-88-470-2583-7_19,

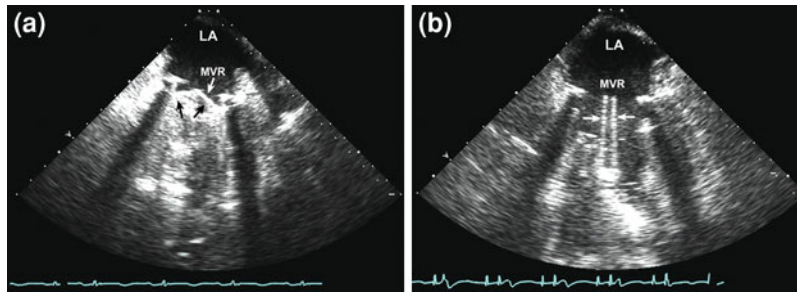

Fig. 19.1 Transesophageal echocardiography (TEE) image of a normal mitral bileaflet disc prosthesis (*MVR*). The *arrows* show a normal closed position (**a**) and open position (**b**). *LA* left atrium

from this position and velocity assessment is more accurate (Fig. 19.2).

Tissue prostheses (Hancock, Ionescu–Shiley, or homograft) usually have struts and thin leaflets which may be hard to see on TTE, but which may be easier to see with TEE (Fig. 19.3).

If normal opening and closing excursion of a mechanical prosthesis is not seen from multiple angles, then one has to suspect a stuck or obstructed prosthesis (see Fig. 19.4). This is usually confirmed with color flow Doppler and velocity measurements. If it is still not clear, fluoroscopy can determine if there is normal mechanical leaflet motion.

Likewise, tissue prostheses may have a subtle 2D appearance that shows incomplete coaptation and resulting significant regurgitation (Fig. 19.5).

19.4 Color Flow Characteristics

After one has examined a prosthesis with 2D echocardiography, either with TTE or with TEE, the next step is color flow Doppler assessment of the valve. Each type of valve has a specific color flow Doppler flow profile. Tissue prostheses usually have a small central jet, mild at most. Mechanical prostheses have closing volume jets. The more popular bileaflet tilting disc prostheses (St. Jude) have several closing volume jets (Fig. 19.6), whereas a single tilting disc prosthesis will have either a single larger central jet (Medtronic Hall) or smaller closing jets on each side (Bjork–Shiley).

Regardless of the closing volume jets, one must identify the sewing ring. All closing volume jets will be inside the ring. Perivalvular jets will be outside the sewing ring (Fig. 19.7). If the 2D appearance of a prosthesis suggests dysfunction, e.g., stuck valve or abnormal coaptation of a tissue prosthesis, then a large regurgitant jet will be seen coming through the valve leaflets and would not be confused with closing velocity jets (Fig. 19.8).

19.5 Doppler Imaging

The final check on a prosthesis to determine if it is normal is to determine the hemodynamic profile. This is done with Doppler imaging. In most cases continuous wave Doppler imaging can be used to determine the peak and mean gradients. Using the modified Bernoulli equation (pressure gradient $= 4V^2$), one can determine pressure gradients across the prosthesis. Studies have shown a good correlation between gradients measured noninvasively by Doppler echocardiography and those obtained by invasive catheter measurements. Both peak and mean gradients across a prosthesis should be determined. These values will depend on the type and location of the prosthesis. Normal ranges for all types of prostheses and locations have been established and reported from studies of the Mayo Clinic Echocardiography Laboratory (see references). Aortic mechanical prostheses, bileaflet and single tilting

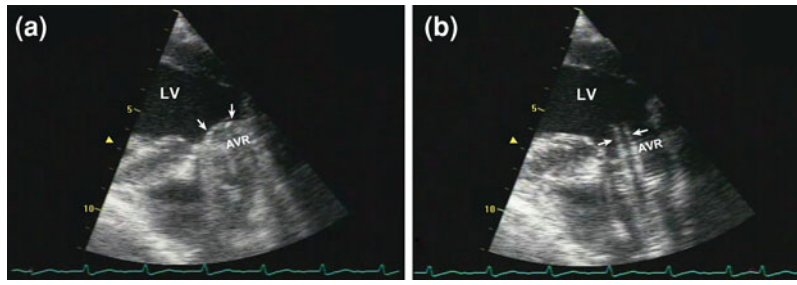

Fig. 19.2 TEE transgastric view of a normal aortic bileaflet disc prosthesis (*AVR*). The *arrows* show a normal closed position (**a**) and open position (**b**). *LV* left ventricle

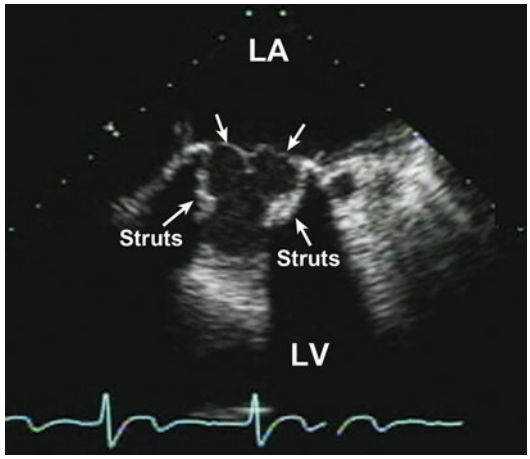

Fig. 19.3 TEE image of a normal-appearing mitral tissue prosthesis. Typical thin leaflets (*arrows*) and supporting struts (*arrows*). *LA* left atrium, *LV* left ventricle

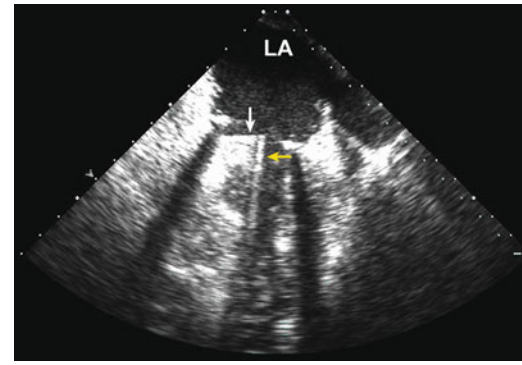

Fig. 19.4 TEE image of a bileaflet mechanical prosthesis. Only one leaflet opens (*yellow arrow*), and the other leaflet is frozen closed (*white arrow*). *LA* left atrium

disc, have mean gradients in the 13–15-mmHg range. The older ball cage prostheses in the aortic position have higher values (average mean gradient 23 mmHg). Aortic tissue valves have lower mean gradients of less than 10 mmHg for homografts, and other tissue aortic prostheses have a mean gradient around 13 mmHg.

In the mitral position, there is not a lot of difference between mechanical and tissue prostheses. Average mean gradients for all are in the 4–5-mmHg range. Normal mean gradients for tricuspid and pulmonic prostheses have also been determined (see references). These are reference guidelines for most normal prostheses. It is always helpful to have the early postoperative Doppler velocities of a prosthesis. Presumably, these will be normal for that valve in that location for a given patient. If follow-up Doppler imaging shows a significant variance from this baseline or values outside the established values, then the prosthesis may be abnormal.

If the Doppler gradients have changed or are increased, one must determine if the prosthesis is abnormal, e.g., stuck valve, pannus ingrowth, or stiffened tissue valve leaflets. Other issues that can result in abnormally high velocities across a prosthesis need to be ruled out, e.g., anemia, high cardiac output, significant regurgitation, tachycardia, or thyrotoxicosis.

It is usually the combination of 2D imaging, color flow Doppler features, and Doppler velocities that is used to assess a prosthesis and determine if it is malfunctioning, either obstructive or regurgitant.

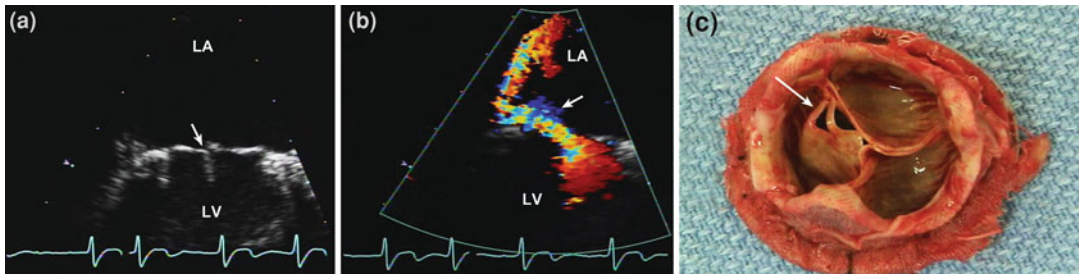

Fig. 19.5 TEE image of an abnormal mitral tissue prosthesis. **a** Incomplete coaptation of the leaflets (*arrow*). **b** An eccentric mitral regurgitant jet (*arrow*). **c** The surgical specimen and torn leaflet (*arrow*). *LA* left atrium, *LV* left ventricle

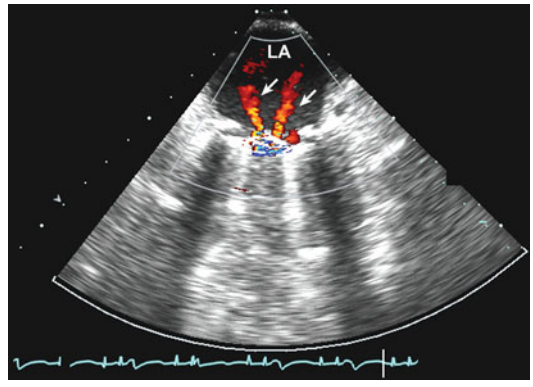

Fig. 19.6 TEE image of a mitral bileaflet mechanical prosthesis in the closed position showing normal closing volume jets (*arrows*). *LA* left atrium

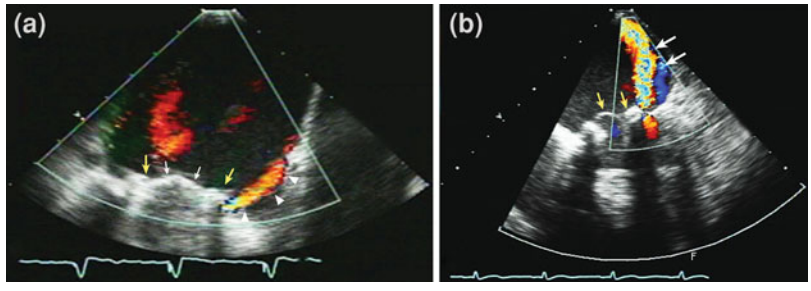

Fig. 19.7 **a** TEE image of an abnormal mitral bileaflet mechanical prosthesis. The leaflets (*small white arrows*) are shown in the closed position, and the sewing ring (*yellow arrows*) and a large perivalvular regurgitant jet (*white arrowheads*) are seen. **b** TEE image of an abnormal mitral tissue prosthesis with a large perivalvular jet (*arrows*)

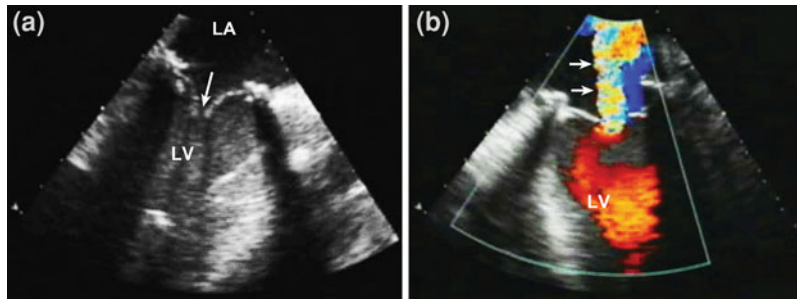

Fig. 19.8 *a* TEE image of an abnormal mitral tissue prosthesis with incomplete coaptation of leaflets (*arrow*). **b** Large valvular regurgitation (*arrows*). *LA* left atrium, *LV* left ventricle

19.6 Management

If a mechanical prosthesis seems abnormal, e.g., abnormal motion, abnormal color profile, or higher than normal velocities, echocardiography may help determine the cause. If the valve is abnormal because of thrombus, in addition to maximizing anticoagulation, lytic therapy has been successful in freeing up a prosthetic leaflet. If this is unsuccessful, the valve may have to be replaced.

If a tissue valve is stenotic or torn with significant regurgitation, then surgery may be the best option.

19.7 Summary

Two-dimensional echocardiography, color flow Doppler features, and Doppler gradients must all be employed to accurately assess a valve prosthesis and determine if it is normal or abnormal. Baseline and routine follow-up echocardiograms are helpful to determine if the features of a given prosthesis have changed. This is especially true for Doppler gradients. Finally, echocardiographers must be familiar with all types of prostheses in various locations with regard to the normal 2D appearance, color flow pattern, and Doppler gradients. Only then can they interpret the echocardiographic data accurately and determine if a prosthetic valve is normal or abnormal.

Further Reading

Burstow DJ, Nishimura RA, Bailey KR et al (1990) Continuous wave Doppler echocardiographic measurement of prosthetic valve gradients: a simultaneous Doppler-catheter correlative study. Circulation 82:1467–1475

Connolly HM, Miller FA Jr, Taylor CL et al (1993) Doppler hemodynamic profiles of 82 clinically and echocardiographically normal tricuspid valve prostheses. Circulation 88:2711–2717

Lengyel M, Miller F Jr, Taylor CL et al (1990) Doppler Hemodynamic profiles in 456 clinically and echonormal mitral valve prostheses. Circulation 82(Suppl 3):3–43

Miller F Jr, Callahan J, Taylor C et al (1989) Normal aortic valve prosthesis hemodynamics: 609 prospective Doppler examinations. Circulation 80(Suppl 2):2–169

Novaro GM, Connolly HM, Miller FA (2001) Doppler hemodynamics of 51 clinically and echocardiographically normal pulmonary valve prostheses. Mayo Clin Proc 76:155–160

Cardiac Tumors and Masses

20

Roger L. Click

20.1 Introduction

Echocardiography is the imaging modality most often used to identify intracardiac masses. An echocardiogram can be performed quickly in any situation or setting, e.g., outpatient setting, bedside, emergency room, ICU, or operating room. The results are usually available immediately for clinical decision making. Most intracardiac masses found by echocardiography are thrombi and vegetations usually in the setting of cardiomyopathy, atrial fibrillation, valvular heart disease, or endocarditis. Endocarditis and vegetations are discussed in Chap. 18. In this chapter, the focus is on cardiac thrombi and tumors.

Intracardiac thrombi generally have caused an embolus or have embolic potential, whereas cardiac tumors are much less common, but can produce a variety of symptoms and frequently require urgent surgical removal. Most cardiac masses are found incidentally in patients referred for an echocardiogram for other reasons. Less frequently, patients are referred for an echocardiogram specifically to rule out a cardiac mass, e.g., the source of embolism.

Transthoracic echocardiography (TTE) is often the first imaging modality when an intracardiac mass or tumor is discovered. The size, location, mobility, and hemodynamic effects can all be delineated by TTE. TEE can provide additional information in many cases or can be helpful to see certain structures, e.g., the left atrial appendage.

20.2 Intracardiac Thrombi

Intracardiac thrombi are usually located in the left atrium, the left atrial appendage (LAA), or the left ventricle. Left ventricular (LV) thrombi are usually found in the LV apex in patients with a dilated cardiomyopathy or coronary artery disease and an apical infarct. The thrombus can be laminated (Fig. 20.1), with generally low embolic potential, or pedunculated (Fig. 20.2), with higher risk of embolization.

Sometimes, it may be difficult to determine if "haziness" in the LV apex is a thrombus. Changing depths, gain, and frequency may help differentiate a true apical thrombus from an artifact. Injection of a contrast medium may also prove beneficial to differentiate a real thrombus from an artifact. Aggressive revascularization treatment with lytic agents or primary angioplasty has decreased the incidence of severe apical wall motion abnormalities and aneurysms and has lessened the likelihood of LV apical thrombus formation. Unlike other applications, TTE may show the LV apex better than transesophageal

R. L. Click (✉)
Division of Cardiology, Mayo Clinic,
Rochester, MN, USA
e-mail: click.roger@mayo.edu

A. Sarti and F. L. Lorini (eds.), *Echocardiography for Intensivists*,
DOI: 10.1007/978-88-470-2583-7_20,

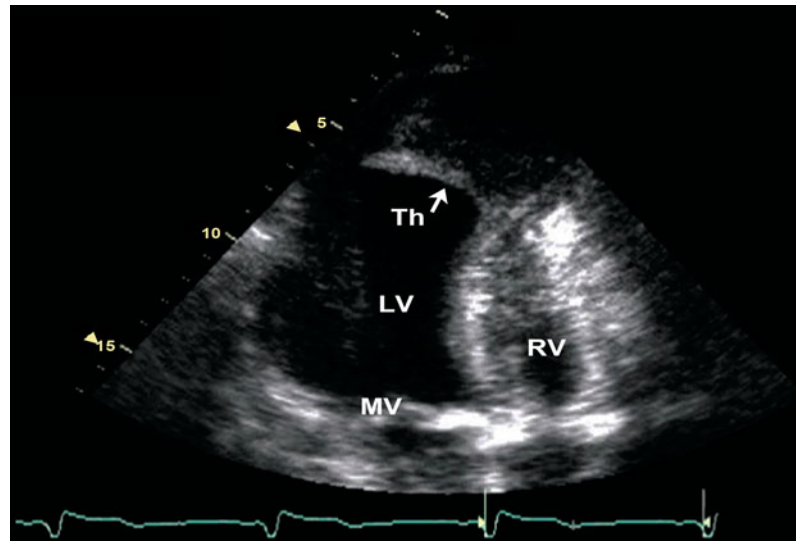

Fig. 20.1 Transthoracic echocardiography (TTE) apical four-chamber view showing an apical aneurysm and a laminated thrombus (*Th*). *LV* left ventricle, *MV* mitral valve, *RV* right ventricle

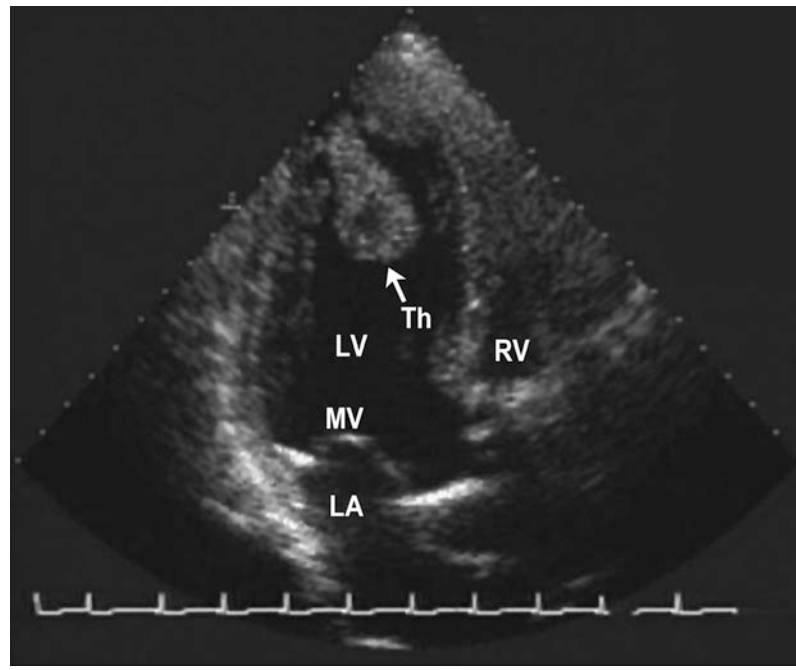

Fig. 20.2 TTE apical long-axis view showing a pedunculated thrombus (*Th*) in the left ventriclular apex. *MV* mitral valve, *LA* left atrium, *LV* left ventricle, *RV* right ventricle

echocardiography (TEE). The LV apex may be foreshortened on TEE, whereas the true LV apex is best seen by TTE to rule out an apical thrombus.

The left atrium and LAA are other common locations for thrombi in patients with atrial fibrillation, mitral stenosis, or a prosthetic mitral valve. Unlike the LV apex, the left atrium and especially the LAA are best viewed by TEE. Patients with atrial fibrillation are particularly at increased risk of the development of left atrial and LAA thrombi. In patients with atrial fibrillation who have had a suspected embolism or precardioversion, TEE is the imaging modality of choice (Fig. 20.3).

Imaging the LAA can be a challenge. Contrast medium can help determine if haziness or "smoke" in the LAA is a formed thrombus. The presence of spontaneous echo contrast and low

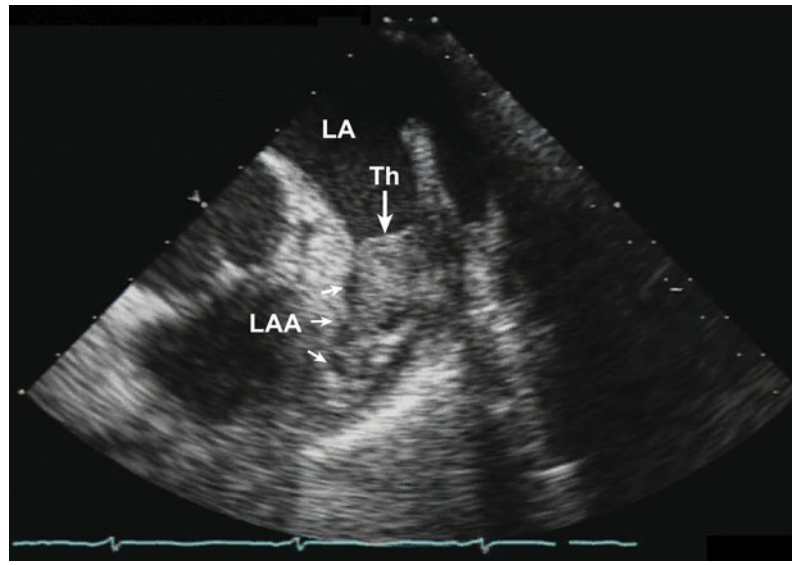

Fig. 20.3 Transesophageal echocardiography (TEE) of the left atrial appendage (*LAA*) showing LAA thrombus (*Th*). *LA* left atrium

emptying velocities of the LAA determined by TEE may also predict the risk of thrombus and embolization.

20.3 Intracardiac Tumors

Tumors of the heart can be divided into primary, either benign or malignant, or secondary from metastases or extension from surrounding tissue. Primary intracardiac tumors are uncommon, with an autopsy incidence of 0.002–0.28 %. Metastatic tumors of the heart are more common by about 20 times.

Table 20.1 shows the distribution of primary cardiac tumors, both benign and malignant, in an autopsy series.

In a surgical series [1], 75 cardiac masses were surgically removed. Most were benign. Most malignant tumors would not be managed surgically. Myxoma is the most common primary tumor of the heart, accounting for 41 % in the autopsy series (Table 20.1) and in the operative series. Of the 31 myxomas in the operative series, 24 were in the left atrium. Atrial myxomas can be silent or can cause a variety of symptoms, including fever, arthralgias, arrhythmias, hemodynamic obstruction, and most serious, embolization. Therefore, when they are discovered, most are surgically removed urgently.

Table 20.1 Cardiac tumor distribution (autopsy series)

Benign cardiac tumors ($N = 319$)	Primary malignant tumors ($N = 125$)
Myxoma 41 %	Angiosarcoma 31 %
Lipoma 14 %	Rhabdomyosarcoma 21 %
Papillary fibroelastoma 13 %	Mesothelioma 15 %
Rhabdomyoma 11 %	Fibrosarcoma 11 %
Fibroma 5 %	Other sarcomas 9 %
Hemangioma 5 %	Lymphoma 6 %
Teratoma 4 %	Miscellaneous 7 %
Mesothelioma 4 %	
Miscellaneous 3 %	

Used with permission from Freeman et al., Transesophageal Echocardiography, modified from McAllister and Fenoglio [2]

The echocardiographic appearance is typical. Usually a myxoma is pedunculated and attached to the atrial septum by a stalk. Most occur singly, but in Carney syndrome, multiple myxomas are accompanied by lentiginosis and endocrine abnormalities. Figure 20.4 shows the typical echocardiographic features of a left atrial myxoma and the corresponding surgical specimen.

Cardiac fibromas are benign, occur more commonly in children, and may cause arrhythmias, obstruction, heart failure, and chest pain. They are well-demarcated masses usually

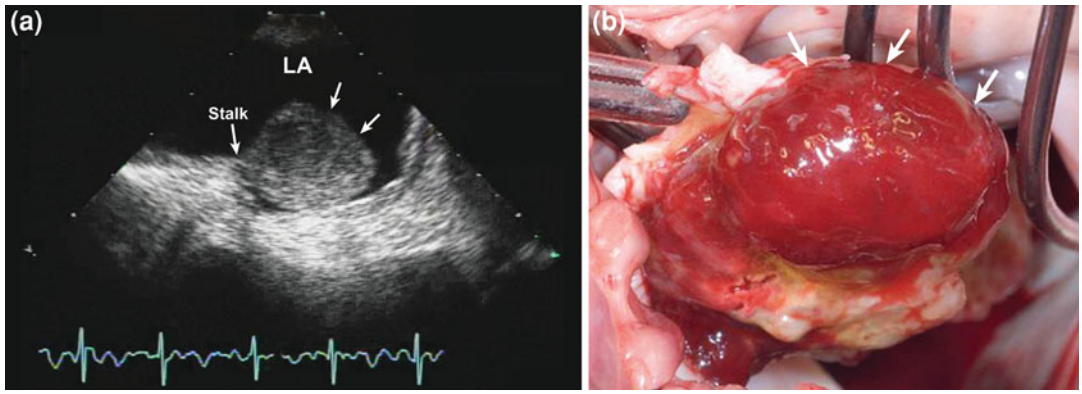

Fig. 20.4 TEE of a left atrial myxoma (**a**) and corresponding surgical specimen (**b**). The attachment stalk of the myxoma (*arrows*) is shown in **a**. In the surgical view (**b**) the myxoma is seen (*arrows*)

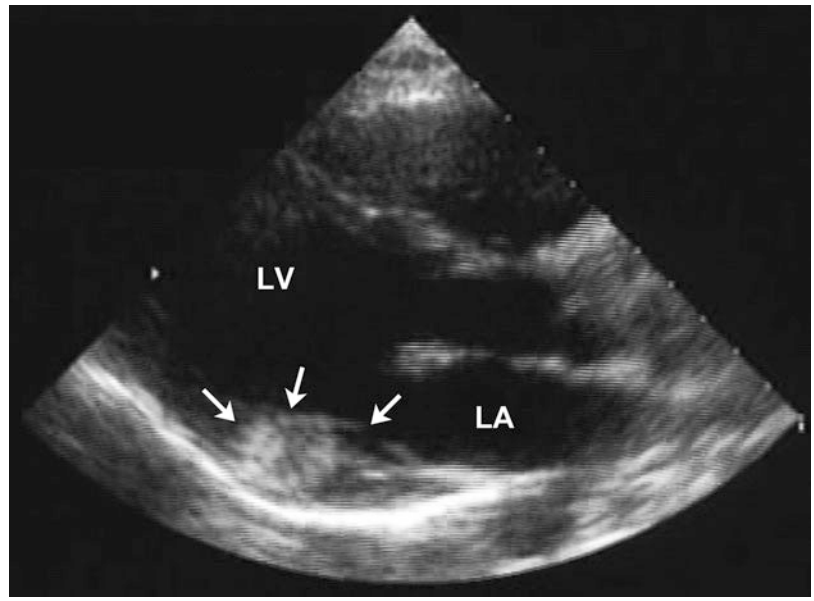

Fig. 20.5 TTE parasternal long-axis view of a fibroma (*arrows*) in the inferior lateral wall of the left ventricle (*LV*). *LA* left atrium

within the wall of the left ventricle or septum. Figure 20.5 shows the typical echocardiographic appearance of a fibroma. Embolization is rare.

Rhabdomyomas, also benign, are the most common tumor in children. They can be associated with tuberous sclerosis and may be multiple in the left and right ventricles, right ventricular outflow, or pulmonary artery (Fig. 20.6).

Fibroelastomas or papillomas are small benign tumors usually attached to the valves. They are often well demarcated and pedunculated (Fig. 20.7). They are often found incidentally, and the greatest risk is embolization and so they should be considered for surgical removal if no other embolic source is found. Fibroelastomas may at times be difficult to differentiate from other valvular masses such as vegetations, Lambl's excrescences, or other degenerative strands. Other clinical features, e.g., fever and positive blood cultures, most often point to vegetation rather than fibroelastoma.

Malignant tumors can appear anywhere in the heart. Usually they have an invasive, infiltrative, irregular appearance and may be associated with

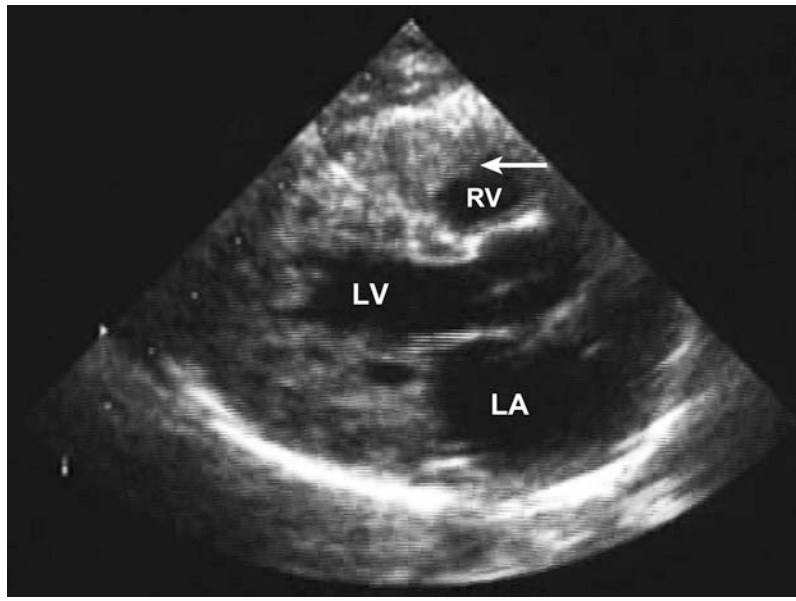

Fig. 20.6 TTE parasternal long-axis view of a rhabdomyoma (*arrow*) in the right ventricle (*RV*). *LA* left atrium, *LV* left ventricle

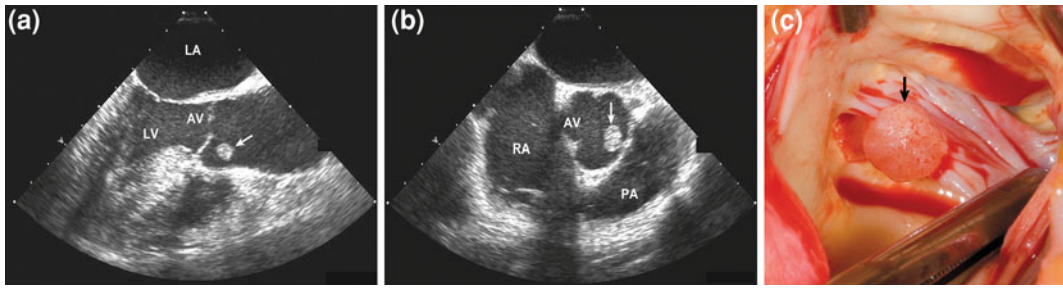

Fig. 20.7 TEE of an aortic valve (*AV*) fibroelastoma (*arrow*) shown in the long-axis view (**a**), short-axis view (**b**), and the surgical specimen (**c**). *LA* left atrium, *LV* left ventricle, *RA* right atrium, *PA* pulmonary artery

pericardial involvement or a pericardial effusion. Angiosarcomas are more common and frequently occur in the right atrium (Fig. 20.8).

Metastatic tumors of the heart can be from any primary tumor elsewhere. Most commonly they are from the lung, breast, kidney, liver, lymphoma, melanoma, and osteogenic sarcoma. Like other malignant tumors, they have an irregular invasive appearance and often there is pericardial involvement. Malignant tumors, primary or metastatic, have a poor prognosis and are often not resectable. Malignant tumors from the pelvic organs and kidney can extend up the inferior vena cava and have a "snake"-like appearance and may extend into the right atrium and appear as a mass in the right atrium. If surgical resection of the primary tumor is performed, intraoperative echocardiography needs to be done simultaneously to ensure all the tumor is removed. These extensions are usually not adherent to the inferior vena cava or right atrium, and the entire extension will slide out with the primary tumor (Fig. 20.9).

Local extension into the cardiac structures from malignant mediastinal or lung tumors can occur. These can be identified by their obvious extension from the primary tumor. They are invasive and irregular with pericardial involvement (Fig. 20.10).

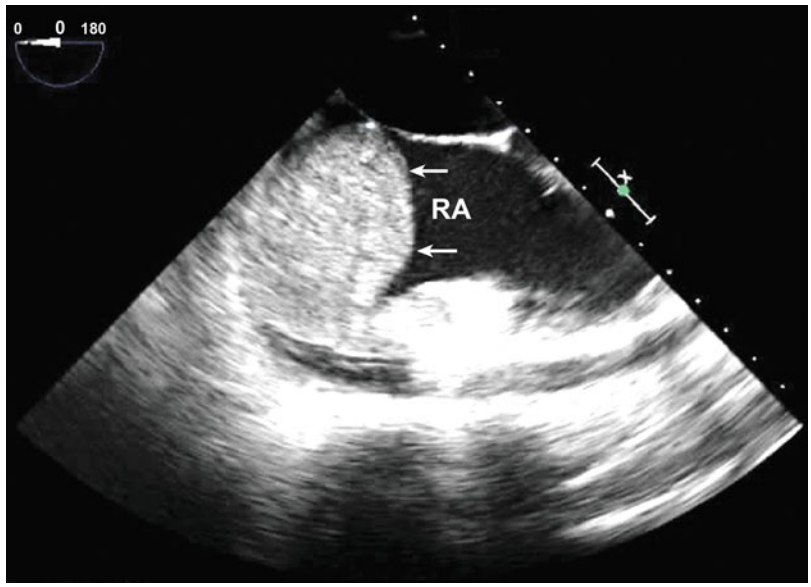

Fig. 20.8 TEE of a right atrial invasive angiosarcoma (*arrows*). *RA* right atrium

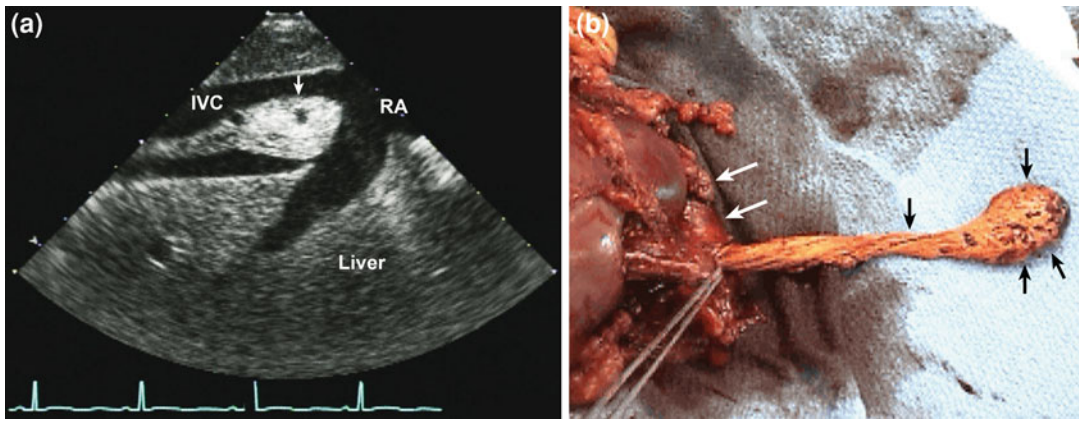

Fig. 20.9 **a** TEE of the inferior vena cava (*IVC*) and hypernephroma (*arrow*) extending up the IVC just to outside the right atrium (*RA*). **b** The hypernephroma (*white arrows*) and the stalk and extension of the tumor/thrombus (*black arrows*)

20.4 Management

LV thrombi if pedunculated are usually managed with maximizing anticoagulation, lytic therapy, or surgery (generally not recommended). A laminated LV thrombus usually does not necessitate anticoagulation. All atrial thrombi require anticoagulation. Benign intracardiac tumors such as myxomas and fibromas should usually be urgently removed surgically. The embolic risk is unpredictable. Malignant or metastatic tumors of the heart most are often not resectable and the prognosis is poor.

20.5 Summary

Intracardiac masses are not common. Usually they are first discovered echocardiographically. The echocardiographic features can help distinguish the type of mass, its location, attachment

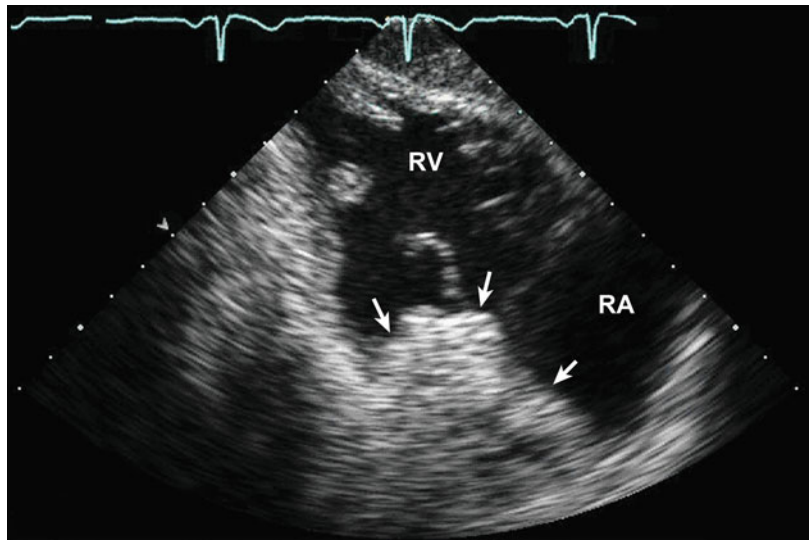

Fig. 20.10 TEE transgastric view of an invasive right atrial tumor (*arrows*) from extension secondary to an adjacent lung tumor. *RA* right atrium, *RV* right ventricle

site, demarcation, and invasiveness. Also, the clinical situation may aide in distinguishing masses, e.g., age of patient, history of myocardial infarction, atrial fibrillation, fever, embolization, or other primary tumor with metastases or extension. Once they have been discovered, echocardiography is helpful in the management and surgical resection and surveillance for any recurrence.

References

1. Dujardin KS, Click RL, Oh JK (2000) The role of intraoperative transesophageal echocardiography in patients undergoing cardiac mass removal. J Am Soc Echocardiogr 13(12):1080–1083
2. McAllister HA Jr, Fenoglio JJ Jr (1978) Tumors of the cardiovascular system. In: Atlas of tumor pathology, 2nd series. Fascicle 15. Armed Forces Institute of Pathology, Washington

Further Reading

DeVille JB, Corely D, Jin BS et al (1995) Assessment of intracardiac masses by transesophageal echocardiography. Tex Heart Inst J 22(2):134–137
Klarich KW, Enriquez-Sarano M, Gura GM et al (1997) Papillary fibroelastoma: echocardiographic characteristics for diagnosis and pathologic correlation. J Am Coll Cardiol 30(3):784–790
Wysokinski WE, Ammash NM, Soande F et al (2010) Predicting left atrial thrombi in atrial fibrillation. Am Heart J 159:665–671

Congenital Septal Abnormalities in the Adult Patient

21

F. Luca Lorini, Cristian O. Mirabile, and Moreno Favarato

21.1 Atrial Septal Defects

Atrial septal defect (ASD) is one of the most common adult congenital heart defects (ACHDs), accounting for 30 % of all cases.

21.1.1 Anatomy and Physiopathology of ASDs

ASD is a persistent communication between atria. Ostium primum ASD (OP) results from deficiency/absence of the lower part of the atrial septum, near the crux of the heart. Ostium secundum ASD (OS) is in the region of the fossa ovale. Sinus venosus ASD (SV) may be located in the superior part of the atrial septum with connection of the right pulmonary vein to the right atrium. In some patients, the septum may be aneurysmal and/or fenestrated. ASDs are singular or associated with other lesions (Table 21.1).

Shunt flow occurs in systole and diastole and can be from left to right or from right to left. Blood in each atrium can flow either through the atrioventricular (AV) valve to the ventricle or across the defect to the opposite ventricle. Ventricular compliance affects the direction of flow through the ASD in diastole. Left ventricle has less capacitance for blood than the right ventricle; therefore, blood in the left atrium is more likely to fill the more expandable right ventricle. When the right ventricle loses its compliance because of other pathological processes (i.e., right ventricular outflow tract obstruction, RVOTO), the shunt flow is from right to left. In systole, the different compliance of atria and other abnormalities (i.e., valve regurgitation) determines shunt flow and the size of the ASD determines the volume of the shunt.

21.1.2 Clinical Aspects

In an unrepaired ASD there is left-to-right shunt with right ventricular (RV) volume overload and pulmonary overcirculation. The main clinical features associated with it are pulmonary infections, fatigue, exercise intolerance, palpitations, cardiomegaly, new audible murmur in pregnancy, atrial arrhythmias, flow-related pulmonary arterial hypertension (PAH) and vascular obstructive disease, ictus cerebri in paradoxical embolism, atrial fibrillation, and indwelling venous catheters.

ASDs should be diagnosed by demonstration of shunting across the defects, RV volume overload, and associated anomalies. Patients with unexplained RV volume overload should be referred to an ACHD center.

In a repaired ASD the clinical aspects are most dependent on the original abnormality and its correction.

Many patients with ASD are asymptomatic, so they may present for primary repair in adulthood. Complications such as tachyarrhythmias and paradoxical emboli increase in frequency with age, so repair is ideally performed in childhood.

F. L. Lorini (✉)
Department of Anesthesia and Intensive Care, Ospedali Riuniti di Bergamo, Bergamo, Italy
e-mail: llorini@ospedaliriuniti.bergamo.it

A. Sarti and F. L. Lorini (eds.), *Echocardiography for Intensivists*,
DOI: 10.1007/978-88-470-2583-7_21, © Springer-Verlag Italia 2012

Table 21.1 Lesions associated with atrial septal defects

Type of atrial septal defect	Associated lesions
Ostium secundum	Pulmonary stenosis, mitral valve prolapse, partial anomalous pulmonary venous connection
Ostium primum	Mitral cleft, subaortic stenosis
Sinus venosus	Partial anomalous pulmonary venous connection
Coronary sinus	Partial anomalous pulmonary venous connection, persistent left superior vena cava

Closure after 5 years of age is associated with incomplete resolution of RV hypertrophy and survival is worse when the ASD is closed after 24 years of age.

21.1.3 Echocardiography

PAH and paradoxical movement of the atrial septum in patients with unexplained RV overload may be correlated with ASD.

21.1.3.1 Transthoracic Echocardiography

This is the primary diagnostic imaging modality for ASD. The study includes 2-D imaging of the atrial septum from parasternal, apical, and subcostal views with color demonstration of shunting. Subcostal views with deep inspiration and high right parasternal views are particularly helpful in adults. The atrial septum from the orifice of the superior vena cava to the orifice of the inferior vena cava should be visualized to detect SV defects or the extension of large OS in these regions.

21.1.3.2 Transesophageal Echocardiography

The recommended views for imaging the atrial septum are the mid-esophageal four-chamber view for OS and OP ASDs (Fig. 21.1), the mid-esophageal bicaval view for an SV defect and for detection of anomalous pulmonary veins, and the mid-esophageal short-axis view at the aortic valve level to bring the atrial septum into the center of the screen.

Transesophageal echocardiography (TEE) is necessary to detect connection of the pulmonary veins to the left atrium in patients with ASD. In addition, it is useful for optimal views of the atrial septum (better localization and sizing of the ASD, measurement of septal rims) and so for a good therapeutic approach. A large coronary sinus (CS) orifice with evidence of atrial shunting may indicate a defect in the roof of the CS, so the entire CS roof should be imaged when this is suspected. When a coronary sinoseptal defect is associated with lesions that cause right-to-left shunting, the orifice of the CS may not be enlarged, and the defect may not be recognized until after definitive surgery, at which time a left-to-right shunt may occur. With PAH, the low velocity of the shunt flow across the coronary sinoseptal defect may be difficult to distinguish from other low-velocity flow within the atria. Right atrial (RA) and RV enlargement with diastolic flattening and paradoxical motion of the interventricular septum are evidence of RV volume overload and significant left-to-right shunt. The RV systolic pressure should be estimated from the peak velocity of the tricuspid regurgitant jet if it is present. Two-dimensional imaging should assess associated lesions, and their functional significance should be determined by color Doppler and spectral Doppler imaging.

21.1.3.3 Doppler Echocardiography

It can be useful in the diagnosis of ASDs to evaluate the pressure gradient between atria. The pulsed wave Doppler transASD shows a continuous flow with end-systolic peak flow. The pulmonary to systemic flow ratio can be used to assess patients with ASDs or ventricular septal defects (VSDs) by comparing the different stroke volumes through the left ventricular (LV) outflow tract and the RV outflow tract.

21.1.3.4 Contrast Echocardiography

Contrast echocardiography with intravenous agitated saline injection is used to confirm the presence of a right-to-left atrial shunt if the findings from imaging and color Doppler echocardiography are inconclusive. Additionally, the

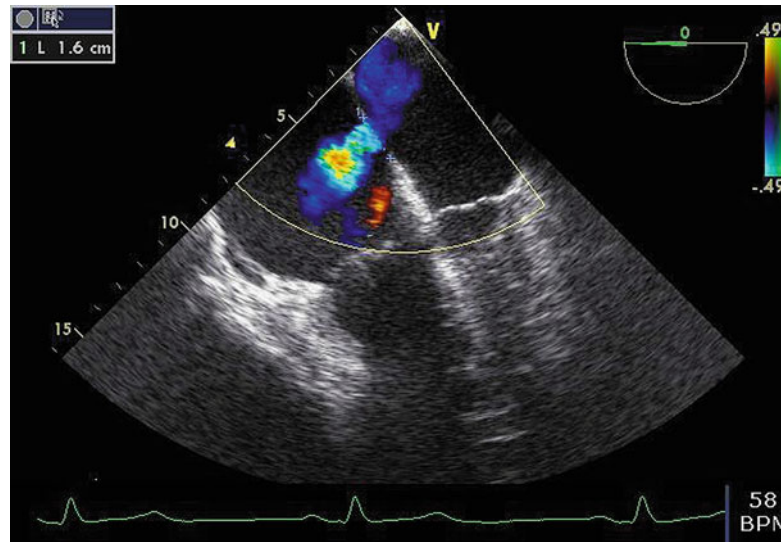

Fig. 21.1 Ostium secundum atrial septal defect: transesophageal echocardiography (TEE) image with color Doppler imaging (0°, transverse, mid-esophageal four-chamber view)

presence of negative contrast in the right atrium may be helpful in identifying a left-to-right shunt. If a left-to-right shunt or RV volume overload is recognized but unexplained, the patient should be referred to an ACHD center.

21.1.3.5 TEE for Closure of ASDs

The use of TEE has spread greatly because of its use in closure of OS ASD by the percutaneous technique. Factors that determine suitability for transcatheter closure of OS include the size of the defect and the presence of adequate tissue rims around the ASD. Accurate imaging of the anatomic features of the ASD is critical for case selection, planning, and guidance during the procedure. Conventionally, a margin of 5 mm is considered adequate. For a comprehensive evaluation during the percutaneous closure procedure, TEE is performed in three different planes: transverse (0°), longitudinal (90°), and at 45°; it plays a critical role for patient selection, guidance, and postclosure evaluation.

21.1.4 Patent Foramen Ovale

Patent foramen ovale (PFO) is found in up to 25 % of adults in the general population, it is generally discovered accidentally, and has no consequences. However, association of PFO with various clinical conditions has been reported (embolic stroke, platypnea orthodeoxia, decompression sickness in divers, and migraine). Optimal treatment has not been established and there are contradictory results from different studies.

Patients with suspected PFO should undergo a contrast study, as color Doppler echocardiography detects only 5–10 % of interatrial shunts. The most widely used technique is the injection of agitated saline solution microbubbles. This should be performed at rest and during maneuvers that increase RA pressure (i.e., Valsalva), because this can improve diagnostic sensitivity. The presence of a single microbubble in the left atrium and left ventricle in the first three beats after right cavity opacification is considered diagnostic of PFO. Microbubbles after the third beat may correspond to intrapulmonary shunt. The number of microbubbles crossing the PFO enables us to quantify shunting. Instead of counting microbubbles, some echocardiography laboratories classify severity as complete to almost complete to slight left chamber opacification. The principal limitation of transthoracic echocardiography (TTE) is its relatively poor sensitivity compared with TEE (Fig. 21.2).

TEE should be considered if the findings of the TTE study are negative or inconclusive but strong clinical suspicion of PFO remains. PFO morphology is heterogeneous and ranges from

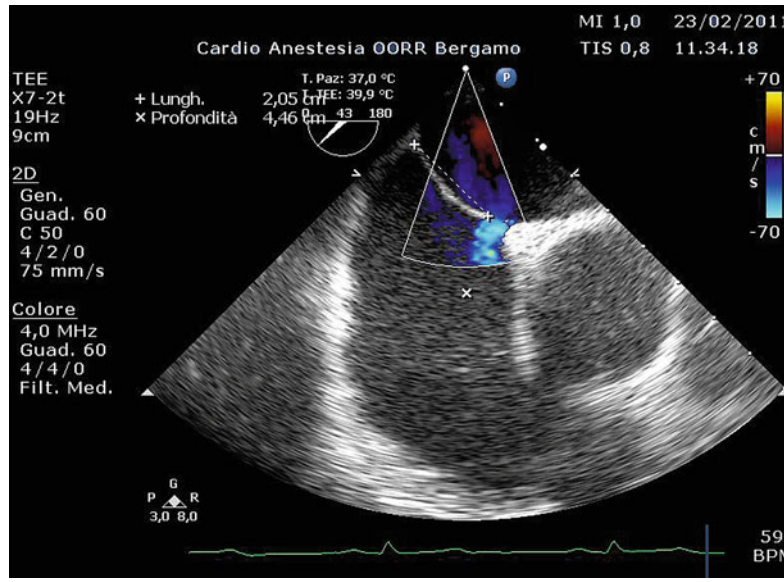

Fig. 21.2 Patent foramen ovale: TEE image before closure with color Doppler imaging across the defect (mid-esophageal view, 45°)

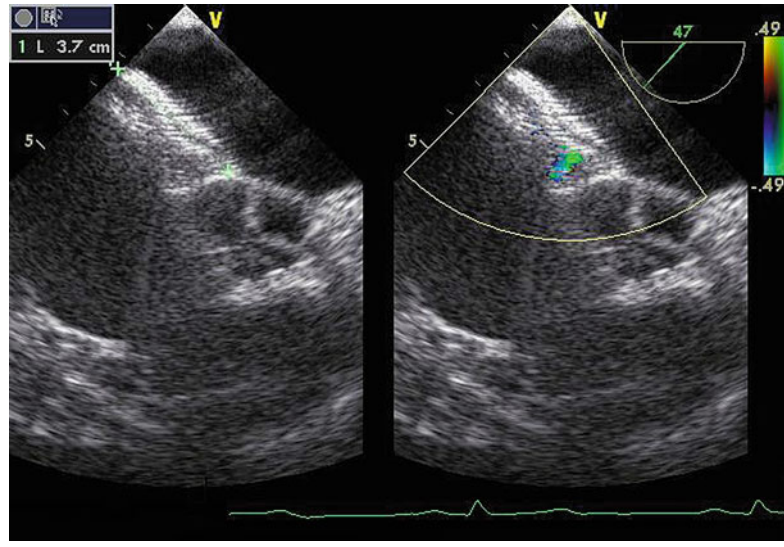

Fig. 21.3 Patent foramen ovale. TEE control after closure with an Amplatzer device

simple, large defects to long, oblique, and tunnel-like defects. TEE enables detailed assessment of the interatrial septum, which is important for successful transcatheter closure. For example, long tunnels represent a problem for devices with a fixed distance between RA and left atrial (LA) components, as there is the potential for both disks to be partially deployed within the tunnel. Long tunnels can be identified with TEE measurement of the maximum opening diameter of the communicating channel (septum primum–septum secundum distance) at the entrance to the left atrium. During intervention, TEE is useful in determining the size of the device to be implanted and provides direct visual guidance in device deployment, avoiding interference with other structures (Fig. 21.3).

21.2 Ventricular Septal Defects

VSD is the most common congenital heart defect at birth and occurs in three in every 1,000 live births. There is high incidence of spontaneous

closure of most small-to-moderate VSDs in the first decade of life, so the incidence is much lower in older infants and particularly in adults: VSDs account for approximately 10 % of all cases of ACHD. There are four anatomic types of VSDs, with multiple synonyms for each one.

21.2.1 Anatomy and Physiopathology of VSDs

Incorrect embryological development of the ventricular septum results in VSD. Type 1 VSDs (conal, subpulmonary, infundibular, supracristal, doubly committed juxta-arterial) occur in the RV outflow tract. Spontaneous closure is uncommon. Type 2 or perimembranous VSDs are the most common defects, and nearly 80 % of VSDs are of this type. The defect is in the septum membrane next to the septal tricuspid leaflet, which can become adherent to the VSD, so creating an aneurysm of the ventricular septum and limiting shunt by closure of the VSD. On the LV side of the septum, the defect is next to the aortic valve. Type 3 VSDs (inlet VSDs) occur in the lower part of the right ventricle and adjacent to the tricuspid valve. These defects typically occur in patients with Down syndrome. Type 4 or muscular VSDs can be located centrally, apically, and at the margin of the septum, near RV free wall: they result from excessive fetal muscular resorption. They are multiple in limited numbers of patients. Spontaneous closure is common in children.

VSD is most often an isolated lesion. It is a component of complex abnormalities such as conotruncal defects or is associated with left-sided obstructive lesions. A subpulmonary VSD is often associated with progressive aortic valve regurgitation caused by prolapse of the aortic cusp through the defect. Another mechanism of aortic valve regurgitation is the passage of a noncoronary cusp in restrictive VSD by the Venturi principle (difference in pressure between the two chambers).

The degree of VSD intracardiac shunting depends on defect size, location, pulmonary vascular resistance, and compliance of the left and right ventricles.

The volume and the route of the flow through the VSD is based on the size and the comparative resistance between the usual ventricular and the VSD outflow tracts. Left-to-right shunt may result from a large VSD along with a low pulmonary vascular resistance as compared with the systemic circulation, and vice versa; in a left-to-right shunt, there is low output of the left ventricle. To gain a normal cardiac output, the response is an elevation in LV volumes and so in LA pressure. The consequence is congestion of the pulmonary venous circulation. In addition to systolic flow, we must consider a diastolic flow through the VSD that depends on the differences in compliance, contractility, and volume between the two ventricles.

It has been demonstrated that in patients with a small VSD, infective endocarditis may occur on the rim of the VSD and this event is also related with the injury of the endocardium by the turbulent flow. A progressive aortic insufficiency may result from aortic cusp prolapse. If the defects are large, these patients have the typical spectrum of symptoms of congestive heart failure. Particularly the LV overload may predispose to the development of pulmonary vascular disease, which can progress to Eisenmenger syndrome. There will be cyanosis when there is a relevant right-to-left shunt from the right ventricle to the aorta through the VSD.

A physiological classification of an isolated VSD in adults is as follows: in *restrictive* VSD, RV pressure is lower than LV pressure and there is no RVOTO; in *unrestrictive* VSD, RV pressure is equal to LV pressure without RVOTO.

21.2.2 Clinical Aspects

Isolated VSDs are uncommon in adults because larger VSDs are clinically evident and repaired early; spontaneous closure is more frequent in small-to-moderate VSDs; the mortality of young patients with very large unrepaired VSDs is high.

Typical clinical presentations are as follows: a patient with a VSD corrected when he/she was a child; an asymptomatic patient but with a systolic murmur; infective endocarditis with fever and bacteremia, with pulmonary embolism

or cerebral abscess; diagnosis of an aortic regurgitation; a patient with right-to-left shunt and progressive development of PAH affected by cyanosis and exercise intolerance.

In patients with an isolated VSD, the clinical features depend on size of the defect and the status of vascular pulmonary resistance.

The clinical severity grading for isolated VSDs is as follows:

- *Small VSD*: less than or 25 % of aortic annulus diameter, small left-to-right shunt, absent LV overload, no PAH.
- *Moderate VSD*: more than 25 % to less than 75 % of aortic diameter, with small to moderate left-to-right shunts, mild to moderate LV volume overload, absent or mild PAH. The patients remain asymptomatic or have mild congestive heart failure; symptoms are usually controlled with drugs.
- *Large VSD*: greater than or 75 % of aortic diameter, moderate to large left-to-right shunt, volume overloading of the left ventricle, developing PAH; congestive heart failure is frequent in childhood and a change in shunt to right to left is possible, thus resulting in Eisenmenger syndrome.

21.2.3 Echocardiography

Patients with hemodynamically significant VSDs with evidence of volume overload and progressive aortic insufficiency due to chamber dilation are referred for closure of the defect.

21.2.3.1 Transthoracic Echocardiography

This remains the mainstay of diagnosis for VSDs. The windows used to investigate a VSD are subcostal and apical views (Fig. 21.4) and these are useful if there are good echocardiographic windows. TTE is fundamental in the preoperative phase to obtain information about the number and location of the VSDs, biventricular function, and size of left and right chambers, and for imaging of the aortic valve to detect possible prolapse/regurgitation, the presence/absence of RVOTO or LV outflow tract obstruction (LVOTO), and the presence of tricuspid valve insufficiency. By Doppler analysis, tricuspid regurgitation jet may be detected, and a Doppler study of the flow through the VSD is desirable. The description of septal configuration and movement is routine in the study.

In a patient operated on for closure of a VSD with new symptoms and signs of cardiac failure and PAH, a Doppler echocardiographic analysis of possible residual shunting and evaluation of pulmonary arterial pressure by tricuspid regurgitation and pulmonary regurgitation is mandatory; in addition, for a good evaluation it is necessary to investigate if there is aortic regurgitation, ventricular function, and the presence of LVOTO and RVOTO.

21.2.3.2 Transesophageal Echocardiography

TEE is useful but not so essential for evaluating isolated defects of the interventricular septum because visualization of the defect can usually be achieved using TTE. Nevertheless TEE is useful in the evaluation of associated valvular abnormalities. The commonest defect (perimembranous) is located near the tricuspid valve just beneath the aortic valve. This kind of VSD is better seen in the five-chamber view in the low esophageal position. In the short-axis view at the aortic valve level, the defect can be seen near the tricuspid valve. Obtaining images of the membranous septum, we may see ventricular septal aneurysms or tricuspid tissue tags. In perimembranous VSD in which there is aortic regurgitation, the aortic cusp may herniate in the defect. Perimembranous defects have been seen in subvalvular aortic stenosis.

Muscular septal defects are located centrally or near the apex in the muscular part of septum: the best views are the mid-esophageal four-chamber view (0–20°) and the transgastric mid short-axis view (0°).

The inlet type of VSDs is generally a feature of a partial AV septal defect (AVSD): they are located in the posterior or inlet septum in close proximity to the AV valves (echocardiographically, AV valves are on the same level without

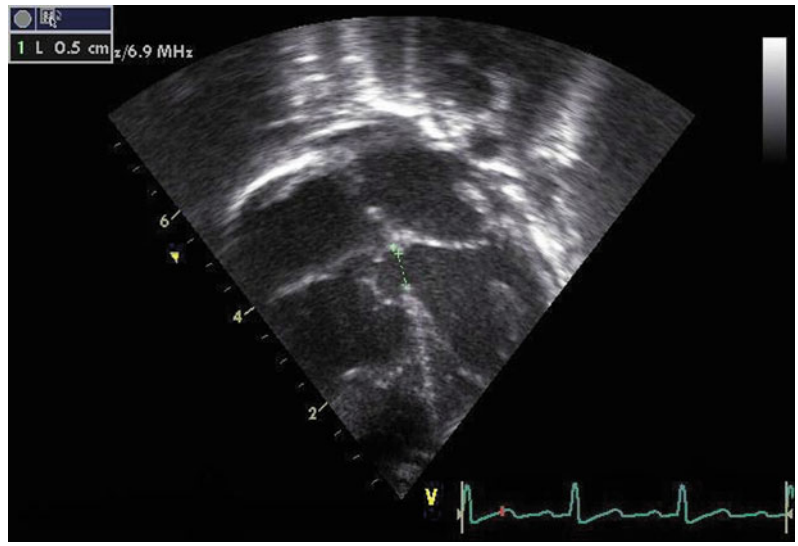

Fig. 21.4 A perimembranous ventricular septal defect: TTE, apical view, short axis

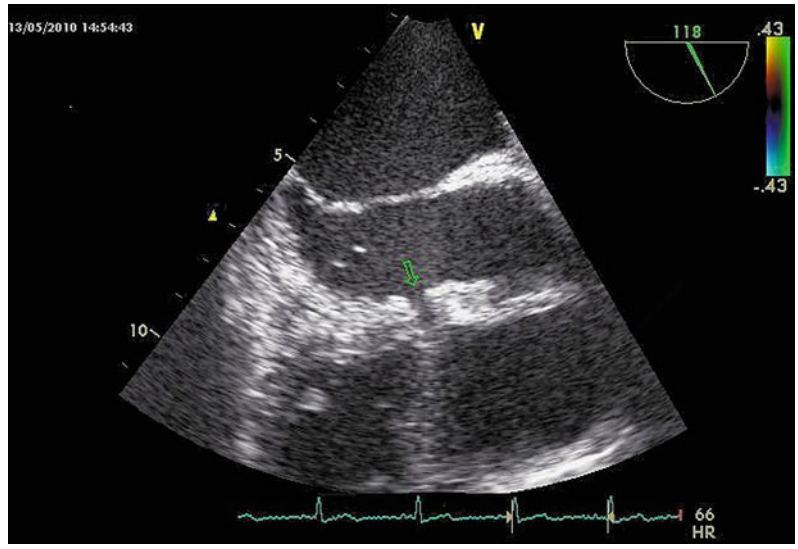

Fig. 21.5 A ventricular septal defect in the subaoartic position (*arrow*) and the left ventricular outflow tract: TEE image (mid-esophageal, aortic valve level, long axis, 120°)

offset as and are located inferior to the tricuspid valve).

Defects in the outlet septum are referred to supracristal, infundibular, doubly committed or subarterial VSDs. The longitudinal plane of the outflow tract (Fig. 21.5; mid-esophageal, long axis, 120°) provides adequate visualization of this defect and anatomic/functional characterization of aortic valve. Another useful view for VSD is gained by plane rotation from 0° to 30–45°: it is similar to an inverted parasternal short-axis view.

In conclusion, for an adequate TTE study of VSDs, the following must be included: identification of the region of the septum involved, the identification of all defects, assessment of the size of the defect and its borders, evaluation of chamber sizes and wall thickness, assessment of shunt size (pulmonary to systemic flow ratio), estimation of RV pressure and pulmonary arterial pressures, and identification of additional associated lesions. By evaluation of the peak systolic velocity through the VSD velocity, we

may acquire the RV systolic pressure (RVSP) and pulmonary artery systolic pressure (PASP):

$$\text{RVSP (or PASP)} = \text{SBP} - 4 \times \text{PVSD}^2,$$

where SBP is the systolic blood pressure and PVSD is peak velocity of the VSD jet.

21.2.3.3 Contrast Echocardiography

This is employed to detect relatively small right-to-left ventricular level shunts. This simple and effective technique is useful to identify small defects: only a few microbubbles in the left ventricle are required for diagnostic confirmation. Contrast echocardiography is particularly useful for suspected defects that cannot to be imaged by standard approaches, for small muscular defects in association with PAH, and in the intraoperative evaluation of postrepair residual defects. It is useful to use a deep Valsalva maneuver during intravenous injection to optimize visualization of microbubbles across the defect.

21.2.3.4 TEE for Closure of VSDs

Advances in operative hemodynamic device engineering have permitted safe and feasible percutaneous closure of VSDs; the basic principles of TEE guiding the process of closure of these defects are similar to those for ASDs. The ACHD patients suitable to undergo a percutaneous closure procedure are those with perimembranous and muscular VSDs.

21.3 Atrioventricular Septal Defects

21.3.1 Anatomy and Physiopathology of AVSDs

The AV canal results from incomplete development of endocardial cushions. Defects in AVSDs may be only at the atrial septum (OP) or may include an inlet VSD. AV valves are abnormal, composed of five leaflets, separated into right and left AV valves, or like a common valve.

The AV valve may be misaligned with respect to the ventricles and it is possibly associated with RV or LV hypoplasia. The posteromedial papillary muscle may be rotated abnormally to the lateral wall of the ventricle. Conotruncal abnormalities may be associated.

In partial AVSD, the ventricular septum is intact. There is an OP ASD, a cleft in the left AV valve and two separate AV valve annuli. Intermediate AVSD is a part of spectrum between complete and partial AVSD. It is characterized by OP ASD, restrictive VSD, and mitral cleft. There are due to a distinct AV valve because anterior and posterior leaflets are fused. In complete AVSD, there is an unrestrictive inlet VSD, often a primum ASD, the atrial septum is rarely intact, and the AV valve is common.

21.3.2 Clinical Aspects

Unrepaired adults may be asymptomatic or present with symptoms. The principal cause of becoming symptomatic in young patients is a significant left AV valve regurgitation. Subaortic stenosis may occur initially or may develop and progress later. Surgical correction involves closure of the ASD and VSD, division of the AV valve, and closure of a cleft in the anterior leaflet of the mitral valve. Repair is usually performed in infants because the risk of evolution in end-stage PAH is very high if the defect is closed too late.

21.3.3 Echocardiography

In a patient with a partial unrepaired AVSD, TTE is the primary imaging modality and should include demonstration of the rims of the OP (Fig. 21.6), a VSD (if present), the morphology and function of the AV valve, ventricular size, shunting, and subaortic stenosis (if present). In a patient with a complete and unrepaired AVSD, the study must include the presence and size of the septal defect, the morphology and function of the common AV valve, and ventricular size and function. When the ventricular portion of the septal defect is large, the ventricular septum may be deficient apically and inferiorly. Pulmonary arterial pressures should be evaluated by measuring tricuspid insufficiency and pulmonary regurgitation jet velocity with simultaneous systemic blood pressure measurement. Evidence of subaortic obstruction, caused by attachment of the AV valve to the crest of the interventricular

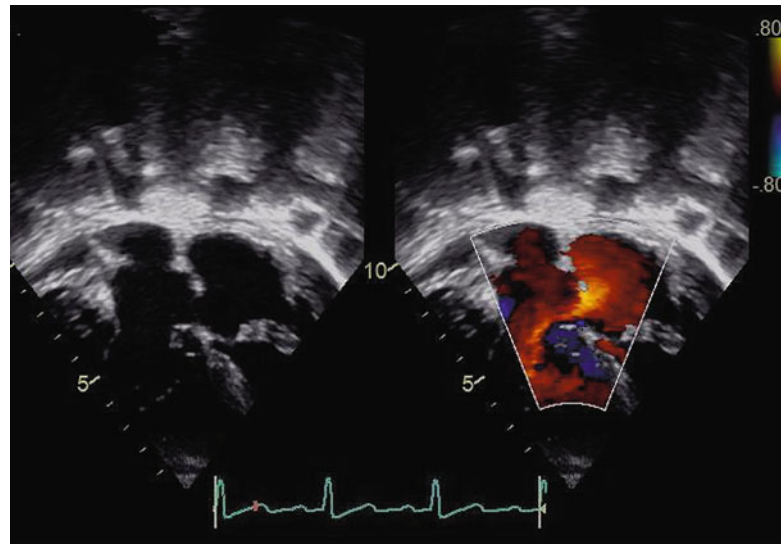

Fig. 21.6 Ostium primum atrial septal defect in partial atrioventricular septal defect: TTE, apical view, without and with color Doppler imaging

septum, should be sought by imaging and Doppler echocardiography. In the postrepair patient, residua include left AV valve dysfunction, subaortic stenosis, shunt flow in the VSD patch, and uncontrolled PAH. It may be difficult to distinguish residual LV to RA shunt from tricuspid regurgitation with RV hypertension, resulting in erroneous diagnosis of PAH.

Further Reading

Kim MS, Klein AJ, Carroll JD (2007) Transcatheter closure of intracardiac defects in adults. J Interv Cardiol 20(6):524–545

McManus B (2010) Adult congenital heart disease-challenges and opportunities for pathologists. Cardiovasc Pathol 19:281–285

Miller-Hance WC, Silverman NH (2000) Transesophageal echocardiography (TEE) in congenital heart disease with focus on the adult. Cardiol Clin 18(4):861–892

Silvesides CK, Dore A, Poirier N et al (2010) Canadian Cardiovascular Society 2009 consensus conference on the management of adults with congenital heart disease: shunt lesions. Can J Cardiol 26(3):e70–e79

Warnes CA, Williams RG, Bashore TM et al (2008) ACC/AHA 2008 guidelines for the management of adults with congenital heart disease. A report of the American College of Cardiology/American Heart Association Task Force on practice guidelines (writing committee to develop guidelines on the management of adults with congenital heart disease). Circulation 118:e714–e833

Essential Pediatric Echocardiography 22

F. Luca Lorini, Simona Marcora,
and Mariavittoria Lagrotta

22.1 Introduction

Echocardiography in intensive care settings has widespread utilization to evaluate hemodynamically unstable patients. Transthoracic echocardiography (TTE) is the easiest and least invasive way to image cardiac structures. In a pediatric echocardiographic examination, it is important to choose the correct probe: 10 MHz for neonates and 5 MHz for infants and children. Certain views are of added importance for pediatric examinations: subxiphoid or subcostal, suprasternal notch, and right parasternal views (Fig. 22.1).

However, in many critically ill patients, low-quality images are obtained because the acoustic windows are suboptimal because of the presence of chest tubes, extensive dressings, and mechanical ventilation. Transesophageal echocardiography (TEE) provides images of better quality. In addition, the TEE probe can be left in place for continuous monitoring. The world's smallest multiplane TEE probe was released recently. The micro TEE probe can be used in newborns and infants of less than 5-kg weight.

Close collaboration between the anesthetist and the pediatric cardiologist is important for acquisition and interpretation of echocardiographic examinations because of the complex anatomy of congenital heart disease (CHD) and the many surgical procedures used to palliate or repair them.

The recent introduction of functional echocardiography has improved the bedside use of echocardiography to assess myocardial and pulmonary function, the changes in cardiovascular status in response to treatment, and systemic and pulmonary blood flow. This chapter discusses its use in the more common diagnostic dilemmas confronting the intensivist.

22.2 Systolic and Diastolic Ventricular Function

Bidimensional and Doppler echocardiography are the main tools used to evaluate left ventricular (LV) function noninvasively in children with heart disease.

The evaluation of systolic function in children can be easily achieved with the fractional shortening, which is calculated by subtracting the LV internal diameter in systole from the LV internal diameter in diastole, and multiplying by 100. The normal value is more than 25 %. This method has some limitations in this setting as it is not valid in the case of hypokinesia/akinesia (e.g., paradoxical septum in pulmonary hypertension or atrial septal defect, postbypass septum), is dependent on loading conditions, and is inadequate in the case of abnormal LV geometry (e.g., univentricular heart). Ejection fraction calculated by two-dimensional echocardiography can be a valid alternative in the case of regional hypokinesia but

F. L. Lorini (✉)
Department of Anesthesia and Intensive Care,
Ospedali Riuniti di Bergamo, Bergamo, Italy
e-mail: llorini@ospedaliriuniti.bergamo.it

A. Sarti and F. L. Lorini (eds.), *Echocardiography for Intensivists*,
DOI: 10.1007/978-88-470-2583-7_22, © Springer-Verlag Italia 2012

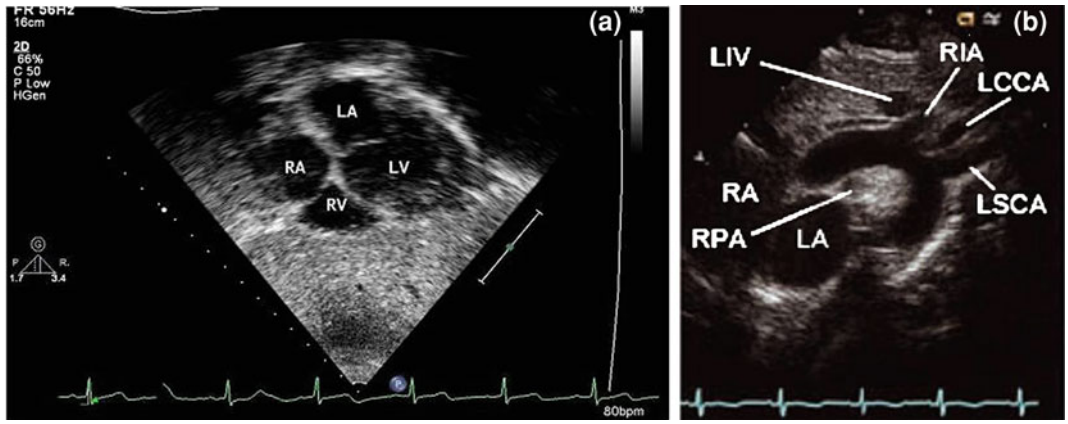

Fig. 22.1 Echocardiographic views in pediatric echocardiography. The subcostal view (**a**) was obtained by applying the transducer in the subcostal space and tilting the transducer from anterior to posterior. All cardiac chambers can be seen, particularly the interatrial septum. The suprasternal view (**b**) was obtained by placing the transducer in the suprasternal notch with the plane of the sound oriented between the right nipple and the left shoulder. This view is good to evaluate the arch and the ductus (rotating the probe perpendicularly). *LA* left atrium, *LCCA* left common carotid artery, *LIV* left innominate vein, *LSCA* left subclavian artery, *LV* left ventricle, *RA* right atrium, *RIV* right innominate vein, *RPA* right pulmonary artery, RV right ventricle

it is dependent on loading conditions and ventricular geometry. Three-dimensional echocardiography has been introduced recently, and new high-frequency matrix transducers allow a better and more reliable evaluation of ventricular function and volumes.

The methods employed for the evaluation of diastolic function include the following:(1) Pulsed Doppler evaluation of transmitral inflow, with evaluation of the peak E and A wave velocities and the *E*/*A* ratio; (2) pulmonary vein Doppler imaging with evaluation of the peak S and D wave velocities; (3) tissue Doppler evaluation of the mitral valve annulus with measurement of the myocardial peak E and A wave velocities, as well as the isovolumic relaxation time; (4) evaluation by M-mode color Doppler imaging of LV inflow and measurement of the velocity of flow propagation. Normal reference values for children are available in the literature but it would be preferable if every echocardiography laboratory were to give the normal range according to its population.

The increased availability of several newer techniques such as tissue Doppler imaging (TDI), strain, and strain rate to assess ventricular function has stimulated interest in their use in CHD. Several characteristics of tissue velocity and deformation imaging make them attractive for assessment of ventricular function in CHD. These methods are independent of ventricular geometry and therefore may be useful for the evaluation of ventricles with variable morphology, in particular right ventricular (RV) function and hearts with a functionally single ventricle. Furthermore, these methods allow quantification of myocardial motion and deformation in different directions (longitudinal, radial, circumferential), whereas conventional techniques allow only the assessment of radial function. This is very important for the evaluation of the right ventricle, the most important ventricle in most of CHD, where the fibers are arranged in a predominantly longitudinal orientation. Finally, these techniques quantify regional myocardial function in addition to global ventricular function.

To perform a good evaluation of ventricular function with tissue doppler and strain techniques it is of fundamental importance to obtain good images and curves. Moreover, it is important to use the same protocols to obtain reproducible data. Nowadays, no pediatric guidelines exist regarding the acquisition of tissue Doppler and strain measurements. Normal values for the pediatric range of TDI and strain parameters

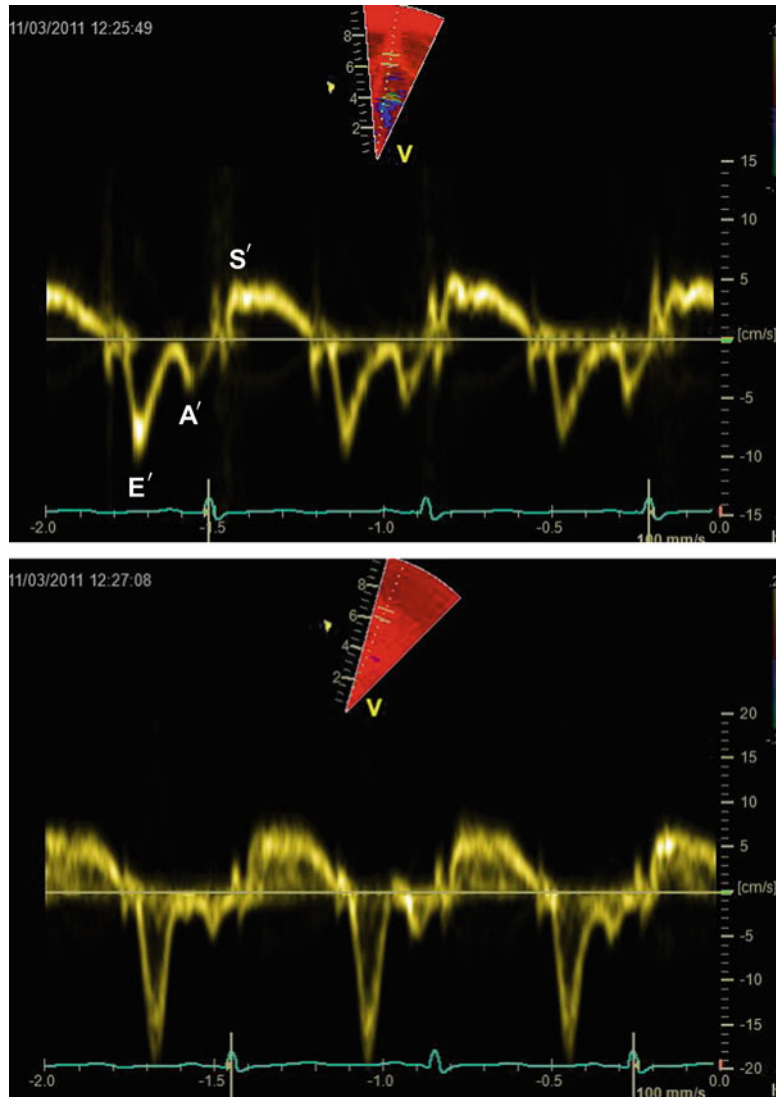

Fig. 22.2 Four-chamber view. Pulsed tissue Doppler imaging of the left ventricle at the level of the septum and the lateral wall. Case of a child with left ventricular dysfunction after myocarditis. Note the reduction of the S′ wave

(Fig. 22.2) are beginning to appear in the literature, but we think it is important to collect them before and after the operation so that each patient is his or her own control.

Our protocol, produced with pediatric cardiologists, is described below.

The TDI-derived velocity is obtained by pulsed Doppler imaging (angle-dependent) or color TDI (less angle dependent). Strain is obtained by speckle tracking.

22.2.1 Pulsed TDI

During image acquisition it is important:

1. To have a good and stable QRS pattern on the EGG
2. To optimize the temporal resolution by selecting as narrow an image sector as possible (a frame rate greater than 150 is recommended)
3. To select the appropriate velocity scale (around 15–20 cm/s)
4. To put the ventricle wall to be interrogated in the center of the imaging sector (tilting function)
5. To select the velocity–time integral (VTI) function and align the pulsed Doppler probe perpendicular to the structure to be studied

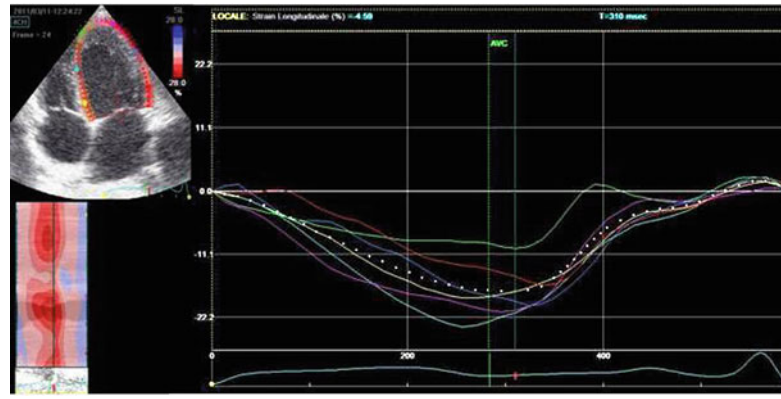

Fig. 22.3 Longitudinal strain. Strain measurement is obtained using a two-dimensional four-chamber view with speckle tracking

Sedation of the baby to keep it still and allow good images to be obtained. An ECG trace is always needed. Postprocessing analysis is not possible.

22.2.1.1 Color TDI

During image acquisition it is important:

1. To have a good and stable QRS pattern on the ECG (sedation)
2. To optimally visualize the myocardial wall with a clear delineation of myocardial tissue and extracardiac structures
3. To optimize the FPR to more than 180 by narrowing the imaging sector until it is slightly wider than the wall investigated
4. To adjust the velocity scale to avoid aliasing
5. To record three complete cycles at the same heart rate when activating the VTI function Postprocessing is possible.

22.2.1.2 Speckle Tracking Strain

During image acquisition it is important:

1. To have a good and stable ECG (sedation).
2. To optimize a standard two-dimensional image view (two-, three-, four-chamber views for longitudinal strain; parasternal short-axis view for radial strain) in order to obtain a clear delineation of the myocardial walls.
3. To obtain an FPR between 50 and 80. This is achieved by narrowing the imaging sector to include little other than the wall segment interrogated.
4. To store images in cineloop format for offline analysis (at least two cycles) (Fig. 22.3).

22.3 Hemodynamic Management

In cardiac diseases such as univentricular heart, a surgical shunt or a stent in ductus arteriosus puts the systemic and pulmonary circulation in parallel (Fig. 22.4c) . In this situation, maldistribution of cardiac output between the systemic and pulmonary circulation can be one of the major causes of hemodynamic instability in the ICU. Sudden shifts in the resistance ratio between the two vascular beds can have deleterious effects on the distribution of flow: for example, a decrease in pulmonary vascular resistance, an increase in pulmonary overcirculation, or both may result in pulmonary overcirculation and systemic hypoperfusion. A Doppler index has been introduced to measure the pulmonary flow ratio. The Doppler flow ratio (Fig. 22.4) is the mean VTI of retrograde flow divided by the VTI of the antegrade flow calculated with pulsed Doppler imaging distal to the shunt in the descending aorta using a sagittal suprasternal notch. A Doppler flow ratio of 1 predicts a Qp/Qs ratio of 1.

22.4 Unexplained Hypoxemia

Children admitted in ICU may have a level of hypoxemia disproportionate to the degree of disease. TEE or TTE can help to diagnose an intracardiac shunt through a patent foramen ovale or an atrial septal defect. Using normal saline solution usually agitated with two syringes and TTE with

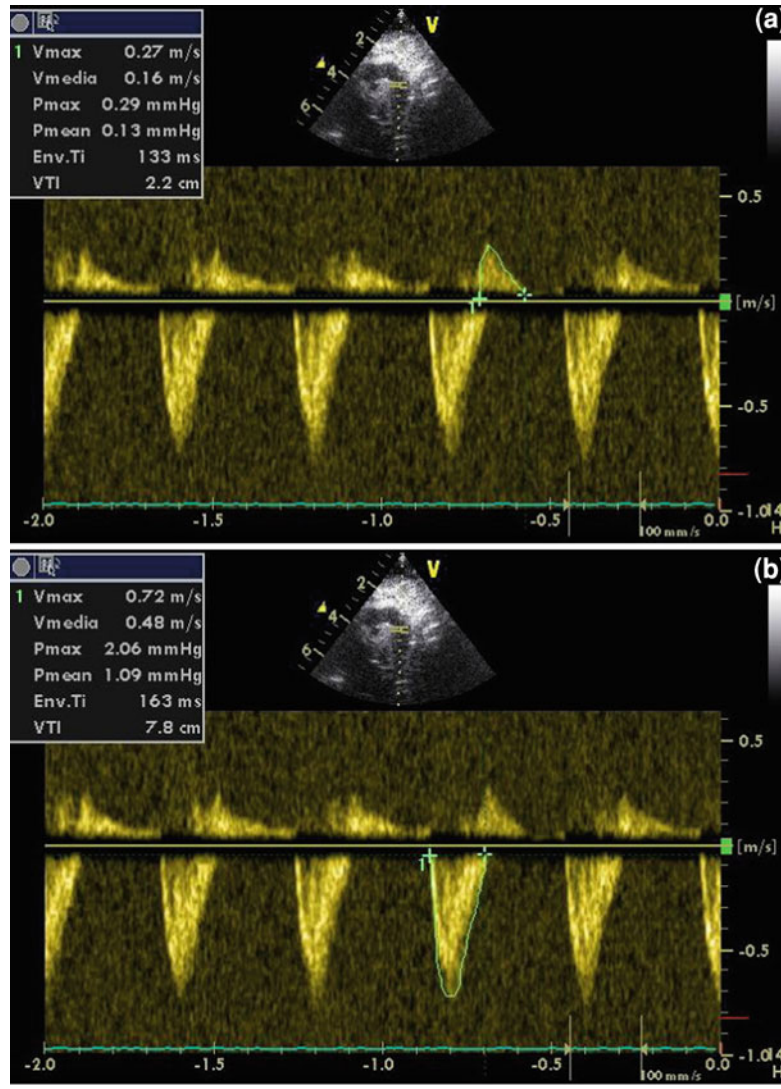

Fig. 22.4 **a** Velocity–time integral (VTI) of retrograde flow. **b** VTI of anterograde flow. A low Doppler flow ratio with almost absent retrograde flow in the aortic arch suggests a partial closure of the shunt (**c**) in a patient with Ebstein anomaly with pulmonary atresia

an apical four-chamber view with color flow Doppler imaging or TEE with mid-esophageal bicaval and four-chamber views with color flow Doppler imaging, one can demonstrate right-to-left intracardiac shunt. If there is right-to-left shunting, left atrial contrast is observed in three to five cardiac cycles and the density does not match that of the right atrium. When intrapulmonary shunting occurs, the intensity of contrast in right side diminishes, whereas in left side it increases and the contrast passes the left atrium via the pulmonary veins. Another source of high oxygen demand is patent ductus arteriosus with pulmonary hypertension and right-to-left ductal shunting.

22.5 Pulmonary Hypertension

Systolic pulmonary artery pressure can be estimated from the tricuspid regurgitation velocity, and pulmonary artery diastolic pressure can be estimated from the end-diastolic pulmonary regurgitation velocity. Mean pulmonary artery pressure can be estimated from the pulmonary artery acceleration time or can be derived from the systolic and diastolic pressures. RV systolic pressure (RVSP) can be evaluated from the peak tricuspid regurgitation jet velocity, using the simplified Bernoulli equation and combining this

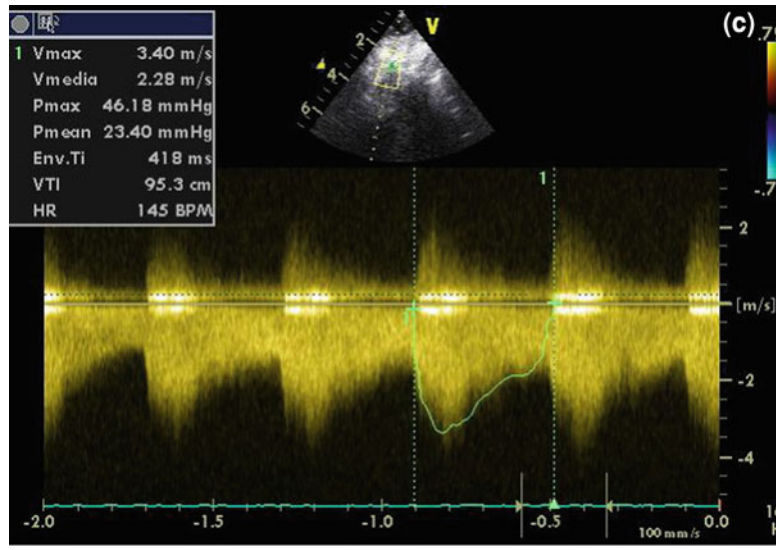

Fig. 22.4 c. Continued

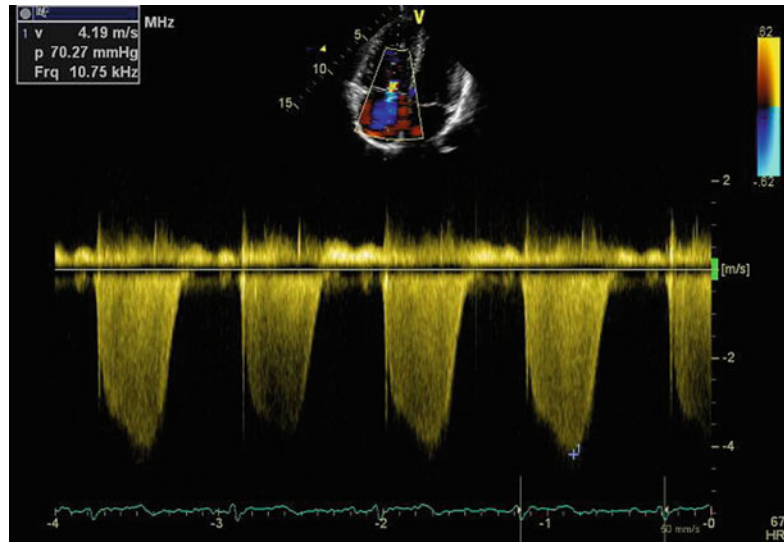

Fig. 22.5 Transtricuspid continuous wave Doppler imaging for indirect estimation of right ventricular (RV) pressure, which in the absence of a stenotic pulmonary valve is equal to systolic pulmonary artery pressure

value with an estimation of right atrial (RA) pressure: RVSP $= 4V^2 +$ RA pressure, where V is the peak velocity of the tricuspid valve regurgitant jet in meters per second, and RA pressure is estimated from the inferior vena cava diameter and respiratory variation if there is not a direct measure of RA pressure. In the absence of a gradient at the level of the pulmonary valve or the RV outflow tract, systolic pulmonary artery pressure is equal to RVSP. In the case of RVSP elevation, obstruction at the level of the RV outflow tract or pulmonary valve should be excluded, especially in patients with CHD or who have undergone pulmonary valve surgery. Sometimes, the simplified Bernoulli equation may underestimate the RV–RA gradient. Some cardiologists who care for patients with CHD will consider systolic pulmonary artery pressure greater than two thirds of the systolic blood pressure as a sign of severe pulmonary hypertension (Figs. 22.5, 22.6, 22.7).

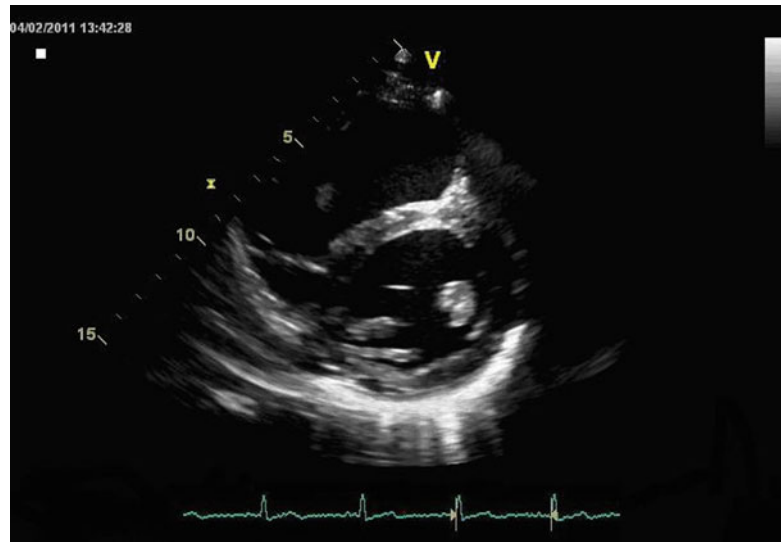

Fig. 22.6 Stopped frame in the parasternal RV short-axis view at the papillary muscle (PM) level from a patient with isolated RV pressure overload due to primary pulmonary hypertension. There is a leftward ventricular septal (VS) shift and reversal of septal curvature with relative sparing of left ventricular deformation at end-diastole

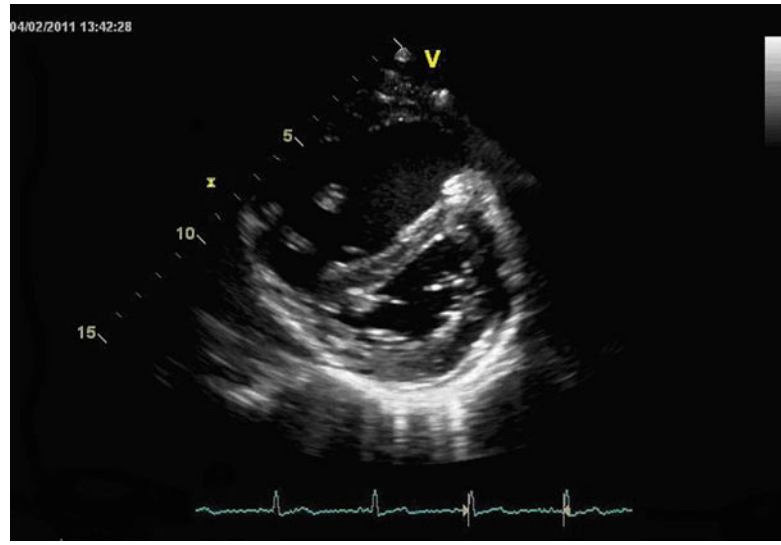

Fig. 22.7 Stopped frame in the parasternal RV short-axis view at the papillary muscle level from a patient with isolated RV pressure overload due to primary pulmonary hypertension. There is a leftward ventricular septal shift and reversal of septal curvature with most marked deformation of the left ventricle at end-systole (flattening)

22.6 Intracardiac Vegetations

Suspected infective endocarditis is rather common in children with a central line or an endotracheal tube. With TTE it is possible to obtain accurate imaging of the valves, but TEE is the procedure of choice to identify complications such as abscess, perforation, and mycotic aneurysm. For right-sided vegetations, TEE does not offer a substantial benefit compared with TTE. Multiplane TEE has a sensibility of more than 90 % in detecting left-sided vegetations. The image is of echo-dense, pedunculated, or adherent vegetations with different degrees of movement. The size of the vegetations, the

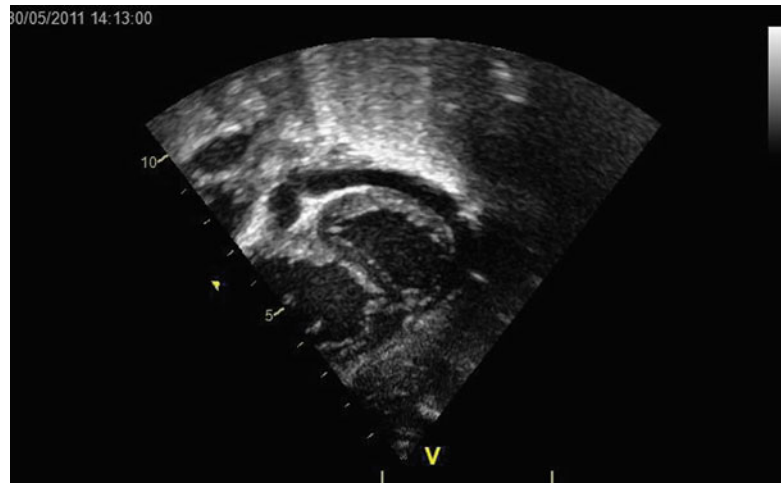

Fig. 22.8 The subcostal view is a good view for evaluating pericardial effusion

mobility, the position, and the number of valves involved are related to complications such as systemic embolization, heart failure, poor response to treatment, and resurgery in patients with a prosthetic valve. The pitfalls during echocardiographic examination are myxomatous changes, suture material, and thrombus.

22.7 Cardiac Tamponade and Pericardial Effusion

The quantity of pericardial fluid cannot be determined with echocardiography, but many echocardiographers are used to quantifying the pericardial fluid with terms such as "trivial," "moderate," and "severe." Even though such words do not reveal the actual quantity of fluid, they are useful for serial evaluations. The position of the fluid can be anterior, posterior, or circumferential. However, the most sensitive two-dimensional sign of cardiac tamponade is RV collapse during diastole. The left atrium and left ventricle can collapse too, especially if LV pressures are low. M-mode includes persistence of effusion throughout the cardiac cycle, a characteristic "swinging motion" of the heart. The images can be obtained with TTE with parasternal short-axis, subcostal coronal and apical four- to five-chamber views. In addition, hemopericardium and cardiac tamponade can be easily diagnosed with TEE. Two-dimensional echocardiographic identification of pericardial effusion usually reveals an echo-free space (Figs. 22.8, 22.9). The diagnosis of pericardial tamponade includes the identification of changes with breathing in atrial and ventricular Doppler inflow profiles. As usual, during spontaneous breathing, intrathoracic pressures are transmitted equally to the pericardial space and intracardiac chambers. The transmission of intrathoracic pressure is prevented by noncompliant pericardium in patients with pericardial effusion. Consequently, LA and LV filling pressure gradients are decreased during spontaneous inspiration, resulting in diminished pulmonary vein forward diastolic velocities, delayed mitral valve opening, prolonged isovolumic relaxation time, and decreased mitral E-wave velocity. So relative increases in LA and LV filling pressure gradients during spontaneous expiration are responsible for increases in Doppler LA and LV inflow velocities. The ventricular interdependence is responsible for reciprocal changes in right-sided intracardiac flows that result in increased tricuspid E-wave velocities during spontaneous inspiration. In addition, hepatic venous forward flow decreases during expiration.

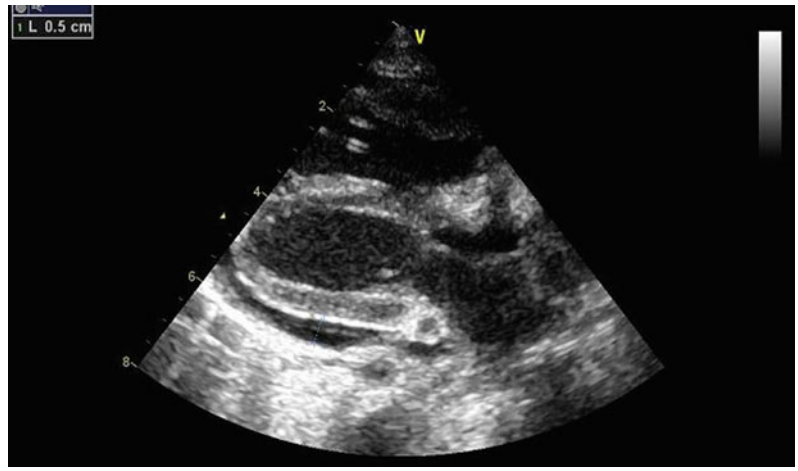

Fig. 22.9 Long axis. It is possible to detect the apex in the evaluation of pericardial effusion

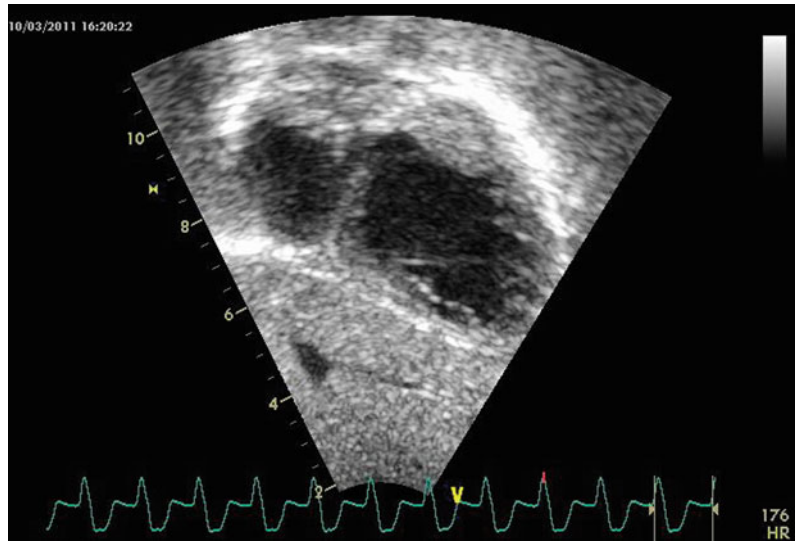

Fig. 22.10 Subxyphoid view. Thrombus at the level of the apex after double-inlet ventricle closure with a patch in a double-outlet right ventricle

22.8 Residual Postoperative Lesion

Residual heart lesions in patients who have undergone cardiac surgery or lesions not previously identified can result in difficult clinical management in the ICU. Echocardiography provides useful information for the intensivist about residual intracardiac shunts, persistent mitral insufficiency following mitral valve repair, the patch being dehisced, and sutures coming loose. The images from TTE can be limited by postoperative dressings, so TEE can be useful in the ICU.

22.9 Intracardiac Thrombus

Echocardiography is useful in determining the source of emboli in patients with atrial arrhythmias, prosthetic valves, central lines, and severe

cardiac dysfunction. Findings include atrial and ventricular thrombi (Fig. 22.10), vegetations, tumors, and atrial septal aneurysm. Spontaneous echo contrast ("smoke") in the atrium indicates a low flow that may lead to thrombus formation. TEE can provide increased sensitivity in the detection of intracavitary thrombi, especially those in the left atrium and left atrial appendage.

22.10 Pleural Effusion, Pneumothorax, and Diaphragmatic Paralysis

Chest ultrasonography represents a promising technique for the detection and follow-up of pleural effusion, lung embolism, pneumonia, pneumothorax, and atelectasis in the adult. Recently, its use has been increased in children too, because of higher sensitivity to ionizing radiation during chest X-ray. Ideally, an emission frequency of 5–7 MHz is desirable for optimizing visualization of the lung. The probe should be small with a convex tip so it can be easily placed in intercostal spaces. Generally, a convex probe of 3–5 MHz, as available with multipurpose ultrasound machines, allows good visualization of the lung. The probe is placed perpendicular, oblique, or parallel to the ribs in the anterior, lateral, and posterior thorax. For the examination of the posterior thorax, the child is put in the lateral decubitus position and in the sitting position. With use of anterior and posterior axillary lines as anatomical landmarks, each chest wall can be divided into six lung regions: upper and lower parts of the anterior, posterior, and lateral chest wall. Chest ultrasonography also provides information on the need for additional procedures, such as thoracentesis, and it may also guide the procedure. Another peculiarity of ultrasonography is its ability to provide some information about the type of effusion, an unorganized anechogenic effusion, or an organized effusion. Whereas chest X-ray gives a more panoramic view in a shorter time, ultrasonography takes longer to explore the entire surface of the two hemithoraces (anterior, posterior, lateral). In the case of peripheral consolidation not extending to the subpleura, ultrasonography is unable to image the area owing to interposition of the ventilated lung. The only regions inaccessible to ultrasonography are the posterior apical regions that are covered by the scapulae. In normal chest ultrasonography, the ribs, on longitudinal scans, appear as curvilinear structures with posterior acoustic shadowing. The pleura appears as a regular echogenic line, pleural line, that moves with respiration. Pleural motion has been described as a "lung-sliding sign." Beyond the pleura–lung interface, the lung is filled with air and does not allow additional views of the normal lung. However, the large change in acoustic impedance at the pleura–lung interface results in horizontal artifacts that are seen as a series of echogenic parallel lines equidistant from one another below the pleural line. Such artifacts are known as A lines. Vertically oriented comet-tail artifacts arising from the pleural line, known as B lines according to Lichtenstein's classification, are absent in the normal lung. They arise from the pleural line, move with lung sliding, reach the border of the screen, and delete the A line. The presence of these artifacts is due to fluid-rich interlobular septae, which are surrounded by air and are considered pathological findings. The evidence of air inside the bronchograms that moves with respiration is defined as a "dynamic air bronchogram." It is a sign of patency of the bronchus and excludes the diagnosis of atelectasis. Pleural effusion can be easily identified and appears as an anechogenic area in the pleural space. The presence of lung sliding excludes the diagnosis of pneumothorax. Further, the presence of a comet tail excludes the diagnosis of pneumothorax. The presence of air within the pleural spaces prevents full expansion of the lung and generates parallel horizontal reverberation artifacts that are diagnostic of pneumothorax. When the question of diaphragmatic paresis or paralysis arises, fluoroscopy can be performed. Because this procedure involves transport, TTE can be performed at the bedside. TTE can evaluate movement of each hemidiaphragm.

Further Reading

Jensen MB, Sloth E, Larsen KM, Schmidt B (2004) Transthoracic echocardiography for cardiopulmonary monitoring in intensive care. Eur J Anaesthesiol 21:700–707

Karski JM (2006) Transesophageal echocardiography in the intensive care unit. Semin Cardiothorac Vasc Anaesth 10:162–166

Kluckow M, Seri I, Evans N (2007) Functional echocardiography: an emerging clinical tool for the neonatologist. J Pediatr 150:125–130

Lai WW, Geva T, Shirali GS, Rychik J (2006) Guidelines and standards for performance of a pediatric echocardiogram: a report from the Task Force of the Pediatric Council of the American Society of Echocardiography. J Am Soc Echocardiogr 19:1413–1430

Lichtenstein DA, Lascols N, Prin S, Mezière G (2003) The "lung pulse": an early ultrasound sign of complete atelectasis. Intensive Care Med 29:2187–2192

Rudski LG, Lai WW, Afilalo J, Hua L, Handschumacher MD, Chandrasekaran K, Solomon SD, Louie EK, Schiller NB (2010) Guidelines for the echocardiographic assessment of right heart in adults: a report from the American Society of Echocardiography endorsed by the European Association of Echocardiography, a registered branch of the European Society of Cardiology, and the Canadian Society of Echocardiography. J Am Soc Echocardiogr 23:685–713

Part IV

Echocardiography in the ICU and OR: Basic and Advanced Applications

23 Echocardiographic History, Echocardiographic Monitoring, and Goal-Directed, Focus-Oriented, and Comprehensive Examination

Armando Sarti, Simone Cipani, and Massimo Barattini

23.1 What Kind of Examination?

Echocardiography is applied in the emergency and ICU setting according to specific needs as follows.

1. First, ultrasonographic examination of the patient. This assessment by transthoracic echocardiography (TTE) or transesophageal echocardiography (TEE) is performed systematically, according to a logical and reproducible sequence which includes all major cardiovascular structures and measurements from all echocardiographic views. Chronic findings, such as hypertrophy or left-sided heart dilatation, must be distinguished from acute changes in order to reconstruct the morphofunctional history of the patient's heart.
2. Further examination to reassess the patient. This is more targeted to obtain more specific information and is done in order to follow the evolution of the clinical picture and the response to drugs and general treatment over time, including mechanical positive pressure ventilation.
3. Focus-oriented or goal-directed clinical interrogation and assessment. This occurs any time during the clinical course of hospitalization in order to resolve a specific question or problem. A focus-oriented or goal-directed examination is not a basic assessment, but is an examination specifically designed to support the making of quick decisions in relation to the diagnosis and treatment following a logical algorithm or predefined flowchart. This Chapter and Chaps. 24–41 deal with many focus-oriented and goal-directed assessments.
4. Rapid emergency examination. For very unstable patients the ultrasonographic assessment will only concentrate on the essential information that can be obtained in a few minutes or even seconds. Examples are the focused assessment with sonography in trauma (FAST) examination (see Chap. 46), designed to help in the diagnosis of and the treatment plan for the traumatized patient, and the focused emergency echocardiography in life support (FEEL) examination (see Chap. 42), used to obtain a rapid diagnosis and an immediate intervention, such as the administration of epinephrine, a pericardium drainage, or a fluid bolus during advanced life support.

23.2 Operator's Skill

An inexperienced operator will be limited in terms of what he/she is able to obtain and interpret and will need to seek help with any questions or doubts. As the intensivist's skills improve progressively, he/she will be able to enhance his/her ability to use diagnostic ultrasonography in assessing and treating critically ill or injured patients.

A. Sarti (✉)
Department of Anesthesia and Intensive Care, Santa Maria Nuova Hospital, Florence, Italy
e-mail: armando.sarti@asf.toscana.it

A. Sarti and F. L. Lorini (eds.), *Echocardiography for Intensivists*,
DOI: 10.1007/978-88-470-2583-7_23,

Cholley et al. [2] have set out a pyramid for the progressive acquisition of echocardiographic expertise by intensivists. At the base there are the less experienced workers, ideally all ICU physicians, who are required to recognize:

- Large pericardial effusion.
- The diameter of the inferior vena cava and its changes throughout the respiratory cycle.
- Right ventricular (RV) dilatation.
- An evident left ventricular (LV) dysfunction.
- Basic ultrasonographic appearance of the pleura and lung.

At the center of the pyramid we find operators with more advanced training who are able to:

- Detect severe valvular dysfunction.
- Measure RV (tricuspid annular plane systolic excursion, TAPSE) and LV (fractional shortening, fractional area change, ejection fraction, pulsed wave Doppler measurement of transmitral flow) systolic and diastolic function.
- Measure the systolic pulmonary pressure.
- Assess "fluid responsiveness".
- Perform thoracic echography.

At the top of the pyramid we have the skilled operators, of which there is often just one or only a few in each ICU, who have a substantial "background" in cardiology and who are able to use and integrate all the techniques, including Doppler echocardiography and tissue Doppler imaging (TDI), and who can perform the full range of echocardiographic diagnoses and hemodynamic assessments.

In my opinion, junior intensivists should be trained and certified in performing at least basic heart and lung ultrasonography. The standard of training courses and accreditation is highly variable around the world. Acceptable competency requires both cognitive and technical knowledge of ultrasound instrumentation, image acquisition, and cardiopulmonary anatomy, physiology, and pathology. Enough evidence from the literature shows that reading a book in advance, a TTE/TEE course involving both theoretical and practical training, and ongoing mentoring and supervision after the course can provide a high standard of practice. Many scientific societies define procedural competency on the basis of a minimum number of supervised echocardiographic examinations performed by the intensivist. However, regular reaccreditation and continuous comparison with adequate standards are still required to maintain competency. A recent international round table of the European Society of Intensive Care Medicine, endorsed by many other societies [6], states that there was a 100 % agreement among the participants that basic critical care echocardiography and general critical care ultrasonography should be mandatory in the curriculum of ICU physicians.

23.3 First Comprehensive Examination of the Patient

A systematic assessment implies the need for substantial experience and mastery of most of the echocardiographic techniques, including B-mode, M-mode, continuous wave Doppler, pulsed wave Doppler, color flow mapping (CFM), and TDI. During the training phase, the intensivist would be better off requesting the intervention of the cardiologist, or another skilful intensivist, so as to perform the first systematic assessment in conjunction with an experienced colleague.

First, it is advisable to review all previous echocardiographic examinations, if available. The comparison is useful to determine the starting point of the patient before the episode that led him/her to the emergency department or ICU. Currently observed findings are often very different from those produced previously, even recently. In fact, the ICU ultrasound assessment is performed on patients in a critical or unstable condition due to acute changes in arterial pressure, hypovolemia or hypervolemia, hypoxemia, hypercapnia, mechanical ventilation, and high levels of circulating catecholamines. This "stress echocardiography" examination may thus show latent disorders which are not visible at rest.

Echocardiography always starts from the patient and must keep the patient at the center of clinical reasoning. Before the echocardiography machine is switched on, the patient's medical history, the physical examination, and all the

results of laboratory and radiographic findings should be reviewed.

Each operator may follow his or her own particular sequence of image acquisition, so as not to overlook some data. With experience, as soon as the operator places the probe on the chest, a general idea of the patient's heart will be readily obtained. Nevertheless, it is better to proceed in a systematic way and then come back to specific views and focus on specific changes in the light of the findings already detected.

A possible TTE sequence used by the author, with the elements not to be overlooked, is as follows.

- Parasternal long-axis view: examination of the whole heart, pericardium, measurements of LV outflow tract diameter, left atrium, aortic valve, mitral valve, mitral subvalvular apparatus, CFM Doppler assessment of transvalvular flows and possible regurgitation, RV outflow tract dimension and kinetics, septum, and LV posterior wall motion
- Modified parasternal long-axis view for the right side of the heart: inflow and outflow of the right ventricle, tricuspid and pulmonary valves and flows, and possible pericardial effusion
- Parasternal short-axis view: basal sections, aortic box and mitral valve, RV inflow and outflow Doppler and CFM interrogation, segmental wall thickness and kinetics at submitral level, papillary and apical segmental wall thickness and motility, LV diastolic and systolic areas
- Apical four-chamber view: general morphology of the heart, the atria and ventricles, RV systolic function (TAPSE), segmental wall motion of left ventricle, atrioventricular valves with ongoing flows and possible regurgitation (continuous wave, pulsed wave, and CFM Doppler echocardiography), systolic pulmonary artery pressure, LV ejection fraction, LV diastolic function (transmitral flow peak ratio, morphology, and *E*/*A*), LV and RV TDI, *E*/Ea ratio, and possible pericardial effusion
- Apical two-chamber view: left atrium and left ventricle, mitral valve, LV ejection fraction, and segmental wall kinetics
- Apical five-chamber view: LV outflow tract with pulsed wave and CFM Doppler interrogation, aortic valve, and transaortic flow (peak velocity and velocity–time integral)
- Apical three-chamber view: LV outflow tract, mitral and aortic valves, transaortic flow, and segmental wall kinetics
- Subcostal four-chamber view: general morphology of the heart, size and thickness, atrial septum, right ventricle, any pleural or pericardial effusion
- Subcostal short-axis view: valves, RV and LV kinetics
- Subcostal view modified for the vena cava: diameter and respiratory variations of the inferior vena cava, shape and size of the intrahepatic veins, and intrahepatic venous pulsed wave Doppler interrogation
- Suprasternal view (if feasible and not contraindicated): aortic arch, pulmonary artery, and descending aorta
- Lung ultrasonography: search for possible pleural effusion, pneumothorax, pulmonary atelectasis or consolidation, and lung water (comet tails)

23.4 Echocardiographic History: General Ultrasonographic Morphofunctional Study of the Heart

It should always be considered that, in ICU echocardiography, acute changes are often superimposed on chronic alterations and remodeling. Since new-onset modification overlaps with preexisting alteration, the intensivist ultrasonography operator is faced with and must interpret a myriad of different and complex findings. This is more and more frequent today, with ICU patients who are often characterized by advanced age and various associated comorbidities. All the echocardiographic information must be integrated within the clinical context of the patient, putting together the physical examination, including the cardiac auscultation and the anamnesis, with all other available data. Ultrasonography of the lung further contributes to outlining the whole diagnostic picture.

Some echocardiographic findings are frequently encountered in ICU practice:

1. Diffuse hypokinesia of the left ventricle without cardiac remodeling (i.e., without hypertrophy or dilatation) suggests an acute dysfunction due to sepsis, myocarditis, or postischemic or postanoxic disturbance (stunned myocardium). Drug toxicity or other toxic substances should also be suspected. If remodeling with dilatation is associated with diffuse hypokinesia, it is natural to suspect a dilated cardiomyopathy, either postischemic or a primitive myocardial alteration.
2. Hypokinesia or akinesia of one or more LV walls is typical of acute myocardial ischemia, but may also reflect chronic alterations. Even if there are individual variations, most of the septum (except for the basal part of it, which is supplied by the right coronary artery) and the LV anterior wall are supplied by the left anterior descending artery. The LV inferior wall and the RV free wall reflect the perfusion of the right coronary artery, whereas the LV lateral and posterior walls (except for a small portion near the apex supplied by the right coronary artery) are supplied by the circumflex artery. An old myocardial infarction scar appears as a hypokinetic–akinetic wall, which is also thinned and echo-hyperreflective.
3. Diffuse hyperkinesia of the left ventricle is a common finding in the ICU (Fig. 23.1). It is visible as a marked reduction, or even a collapse, of the ventricular cavity in systole (kissing ventricle). If hypovolemia is the cause, LV end-systolic obliteration is associated with:
   - Reduction of LV end-diastolic volume or area.
   - Reduced diameter of the inferior vena cava and superior vena cava with marked respiratory variations.

   Otherwise, if the LV end-diastolic area or volume is normal or increased, LV hyperkinesia may be linked to the ventricular emptying made easier because of decreased systemic vascular resistance, as occurs with:
   - Sepsis.
   - Anaphylaxis.
   - Vasodilators.
   - Epidural or spinal anesthesia.
   - Vasovagal syndrome.
   - Hyperthyroidism.
   - Cirrhosis.
   - Advanced pregnancy.

   An easier unloading of the left ventricle (and thus a higher ejection fraction) may also be due to the systolic ejection which in part flows in a low-pressure chamber, as occurs with:
   - Mitral regurgitation.
   - Left-to-right shunt through the ventricular septum.

   To confirm the systemic vasodilatation as the cause of the hypotension associated with the left kissing ventricle, one may consider an easy algorithm (Fig. 23.2).
4. The LV dilatation suggests an adaptation that has been shaped in months or years. It can be achieved while maintaining the elliptical shape or with an increase of lateral ventricular diameter leading to a spheroidal ventricle, almost always associated with annulus dilatation and mitral regurgitation. The patient's clinical history helps to distinguish a postischemic cause from a myocardial primitive disorder, or valve diseases. The study of aortic and mitral valves is thus mandatory.
5. The dilatation of the left atrium is frequently found in critically ill patients, especially in the elderly. It always implies diagnostic and prognostic significance. If significant mitral valve disease can be ruled out, LV systolic and/or diastolic dysfunction should be always suspected. Right atrial dilatation is generally observed with RV dysfunction and tricuspid regurgitation. The interatrial septum tends to arch with convexity directed toward the lower-pressure chamber.
6. Acute mitral or aortic regurgitation is not accompanied by ventricular dilatation. Although CFM Doppler interrogation may show only a modest regurgitant jet, there is a significant increase in ventricular and atrial pressures. This must be kept in mind when face with an unstable or critically ill patient with a mild valvular regurgitation and symptoms and

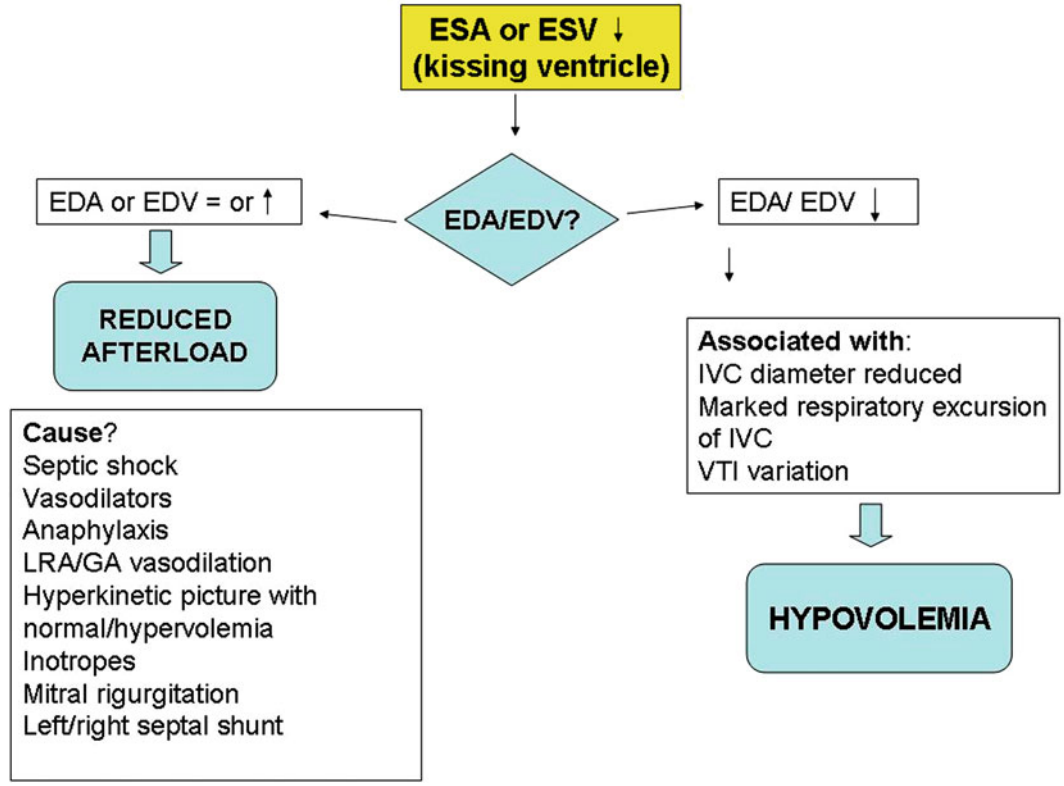

Fig. 23.1 Ultrasound-guided algorithm for the assessment of left ventricular hyperkinesia. Differential diagnosis between hypovolemia and afterload reduction. *EDA* end-diastolic area, *EDV* end-diastolic volume, *ESA* end-systolic area, *ESV* end-systolic volume, *IVC* inferior vena cava, *GA* general anesthesia, *RA* regional analgesia, *VTI* velocity–time integral. (Modified from Sarti [7] with permission)

signs of pulmonary edema and low cardiac output. The overall echocardiographic assessment is very helpful in clarifying the differential diagnostic interpretation of acute valvular insufficiency (e.g., ischemia, myocardial infarction, or endocarditis vegetations).

7. LV hypertrophy always suggests chronic remodeling. The morphology and function of all cardiac valves must never be omitted from the examination. Eccentric hypertrophy occurs with severe aortic regurgitation. Concentric hypertrophy of the septum, particularly prominent in the basal portion, is typical of hypertensive subjects, especially if they have not been adequately managed. A very thick septum or marked general LV hypertrophy is observed in hypertrophic cardiomyopathy. Aortic stenosis is another frequent cause of concentric LV hypertrophy, particularly in the elderly. LV hypertrophy is often accompanied by diastolic dysfunction. Basal septal hypertrophy increases the risk of dynamic outflow obstruction, which is not a steady phenomenon, can be transient, and is greatly facilitated by hypovolemia, reduced LV afterload, and hypercontractility. The recognition of this disorder always has a significant therapeutic impact.
8. RV dilatation without hypertrophy is related to acute volume overload or increased impedance of the right ventricle. In the emergency and ICU setting, this is often caused by pulmonary embolism or acute lung injury/acute respiratory distress syndrome associated with positive pressure mechanical ventilation. With severe RV dysfunction, the interventricular septum progressively flattens before moving toward the left ventricle, producing the "D" image of the left ventricle in the TTE

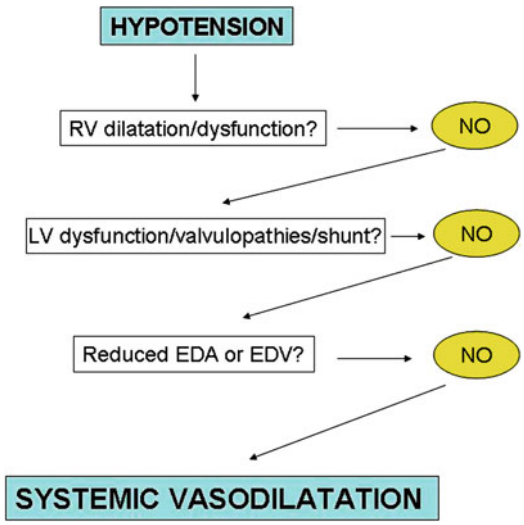

Fig. 23.2 Scheme of confirmation of vasodilatation as the cause of hypotension. *EDA* end-diastolic area, *EDV* end-diastolic volume, *LV* left ventricular, *RV* right ventricular. (Modified from Sarti [7] with permission)

parasternal short-axis view, or the TEE transgastric 0° view. Septal dyskinesia is also observed in acute cor pulmonale. Hypokinesia of the basal part of the right ventricle, with concomitant maintenance of the kinetics of the apical part, may be seen in pulmonary embolism (McConnell sign).

9. RV free wall hypertrophy, with or without dilatation, is a chronic remodeling induced by chronic obstructive pulmonary disease, chronic pulmonary embolization, or other causes of pulmonary hypertension. With significant right-sided heart hypertrophy and dilatation, the right ventricle takes up the apex of the heart.
10. RV hypokinesia without remodeling may occur in the course of
    - Sepsis.
    - Pulmonary embolization.
    - Acute respiratory distress syndrome.
    - Mechanical ventilation.
    - RV myocardial infarction, usually combined with the involvement of the inferior wall of the left ventricle.

The right ventricle may dilate more or less in relation to central venous filling, the contractility condition, and pulmonary artery pressure. Primary RV myocardial failure must be distinguished from secondary involvement, which is associated with pulmonary hypertension.

23.5 Echocardiographic Monitoring: Serial Examinations

In the acute phase of hemodynamic instability, the echocardiographic assessment is regularly repeated to check the clinical evolution and the response to management according to specific therapeutic goals, such as central venous hemoglobin saturation greater than 75 %, decreasing lactate levels, and adequate diuresis. In practice, the ultrasonographic assessment is often repeated:

- To determine the "fluid responsiveness" and follow the effect of a fluid bolus or of the passive leg raising maneuver.
- After starting the infusion of vasopressors, vasodilators, or inotropes and after any significant change in their dosage.
- To check the effect of mechanical ventilation, after any significant change on plateau pressure, mean airway pressure, or positive end-expiratory pressure.
- To study a difficult weaning from positive pressure ventilation.

So the ultrasonographic examination becomes primarily designed to follow the spontaneous evolution of the clinical condition of the patient, and the results of the management plan supervising some physiological variables, such as:

- Ejection fraction, considered together with LV end-diastolic volume.
- Stroke volume, or more often LV velocity–time integral.
- Systolic and diastolic diameters, areas, or volumes of the cardiac chambers.
- Size and respiratory variations of the inferior vena cava (TTE) or superior vena cava (TEE).
- LV filling pressures, including the evaluation of the *E*/Ea ratio.
- RV area, septal dyskinesia, pulmonary artery systolic pressure, and TAPSE.
- Pleural or pericardial effusion size before and after drainage.
- Lung comets (B lines) and pulmonary consolidation after a diuretic or another drug

therapy, the start of mechanical ventilation, or any change of the ventilator setting.

Echocardiography, supplemented by chest ultrasonography often provides all the necessary information to achieve hemodynamic stabilization of the patient. Nevertheless, a nonechocardiographic method for continuously monitoring cardiac output is normally associated with cardiovascular ultrasonography in order to monitor the patient at the bedside.

References

1. Noble VE, Nelson B, Sutingo AN (2007) Emergency and critical care ultrasound. Cambridge Medicine, Cambridge
2. Cholley BP, Vieillard-Baron A, Mebazaa A (2005) Echocardiography in the ICU: time for widespread use! Intensive Care Med 32:9–10
3. Jensen MB (2004) Transthoracic echocardiography for cardiopulmonary monitoring in intensive care. Eur J Anaesthesiol 21:700–707
4. Breitkreutz R, Walcher F, Seeger F (2007) Focused echocardiographic evaluation in resuscitation management: concept of an advanced life support-conformed algorithm. Crit Care Med 35:S150–S161
5. Tayal VS, Kline JA (2005) Emergency echocardiography to detect pericardial effusion in patients in PEA and near-PEA states. Resuscitation 59:315–319
6. Expert Round Table on Ultrasound in ICU (2011) International expert statement on training standards for critical care ultrasonography. Intensive Care Med 37:1077–1083
7. Sarti A (2009) Ecocardiografia per l'intensivista. Springer, Milan

Intraoperative Echocardiography in Cardiac Surgery

24

Carlo Sorbara, Alessandro Forti, and F. Luca Lorini

24.1 Introduction

Intraoperative decision-making and patient outcome can be improved by the correct performance of transesophageal echocardiography (TEE) and correct interpretation of the findings. Since its first use in the operating room (over 20 years ago), TEE has been used as an important diagnostic tool during cardiac surgery, and it has a significant impact on surgical care and anesthesia management. In 1999, the American Society of Echocardiography/Society of Cardiothoracic Anesthesiologists (ASA/SCA) Task Force published guidelines for performing a comprehensive intraoperative TEE examination. The guidelines describe 20 views of the heart and great vessels that include all four chambers and valves of the heart as well as the thoracic aorta and the pulmonary artery. However, additional views are often required to assess a particular abnormality detected during a surgical procedure.

24.2 Indications for Intraoperative TEE

There are three categories of indications for intraoperative TEE described by the ASA/SCA practice guidelines:

1. Hemodynamic instability and valve repair surgery (supported by the strongest evidence in the literature and expert opinion.
2. Patient at risk of myocardial ischemia during surgery and operations to remove cardiac tumors (supported by less evidence in the literature and expert consensus)
3. Monitoring for emboli during orthopedic procedures and intraoperative assessment of graft patency (supported by little evidence in the literature and expert opinion)

The echo-tailored management of hemodynamic instability is reviewed in Chaps. 28 and 30.

24.3 Warning To Avoid Complications

It is necessary before the TEE examination to review the medical history of the patient regarding the presence of dysphagia, hematemesis, or esophageal disease. In cases where they are present, an evaluation by an internist such as a gastroenterologist may be helpful to assess the risk of the TEE procedure.

An important maneuver is insertion of the probe. Excessive force should never be used to insert the probe in the esophagus. The easiest

F. L. Lorini (✉)
Department of Anesthesia and Intensive Care, Ospedali Riuniti di Bergamo, Bergamo, Italy
e-mail: llorini@ospedaliriuniti.bergamo.it

A. Sarti and F. L. Lorini (eds.), *Echocardiography for Intensivists*,
DOI: 10.1007/978-88-470-2583-7_24,

Table 24.1 Contraindications for transesophageal echocardiography

Absolute	Relative
Recent esophageal or gastric surgery	History of mediastinal radiation
Symptomatic esophageal stricture	Symptomatic hiatal hernia
Esophageal diverticulum	Coagulopathy
Esophageal tumor or abscess	Unexplained upper gastrointestinal tract bleeding
	Esophageal varices
	Cervical spine disease

way to perform this procedure is by grabbing the mandible with the left hand and inserting the probe with the right hand. The probe has to be inserted with constant gentle pressure in addition to a slight turning back and forth and from left to right to find the esophageal opening. It is very important to know when the TEE examination is contraindicated (Table 24.1).

24.4 Valve Repair Surgery

24.4.1 Mitral Valve Repair

Mitral valve reconstruction is clearly favored over prosthetic replacement for the surgical treatment of mitral regurgitation. Mitral valve repair is associated with improved operative and late mortality and with minimization of potential complications associated with mitral prostheses, such as thromboembolism, infective endocarditis, and bleeding secondary to anticoagulant therapy. Vital to the effectiveness of mitral valve repair is the intraoperative assessment of mitral competence after reconstructive procedures. Accordingly, several techniques of intraoperative echocardiography have been described. With the escalating surgical trend toward mitral valve repair for mitral regurgitation, this procedure has become the primary indication for intraoperative TEE in adult patients. This technique readily offers high-resolution real-time delineation of the functional pathoanatomy of the mitral valve leaflets, annulus, and support apparatus, aiding the surgeon in planning approaches to mitral valve repair.

In contemporary practice, degenerative mitral valve disease is clearly the most common cause of mitral regurgitation requiring operative repair. Mitral leaflet redundancy, prolapse, ruptured chordae, and flail leaflet segments caused by myxomatous degeneration of the mitral valve are readily demonstrable on TEE. The location and degree of mitral leaflet malcoaptation can be visualized on tomographic four-chamber and two-chamber scanning of the entirety of the valve with transverse and longitudinal TEE, respectively. Determination of the extent of mitral annular dilatation and calcification is possible with these imaging planes. It is also important, especially in patients with ischemic heart disease, to examine the myocardial support of the mitral apparatus. The best approach is from the transgastric window. Transverse TEE short-axis imaging delineates global and regional left ventricular (LV) function. Localized myocardial dysfunction may range from segmental hypokinesis to regional thinning with infarct expansion and may have a significant effect on the technique or even the feasibility of mitral valve repair in patients with ischemic mitral regurgitation. Examination of the mitral support apparatus has also been greatly supplemented by transgastric longitudinal imaging.

24.4.2 Aortic Valve Repair

Intraoperative TEE for the evaluation of repair procedures is likely to become of use much more for aortic regurgitation than for aortic stenosis. Intraoperative two-dimensional examination is useful for the delineation of the mechanism of aortic regurgitation, such as cusp prolapse or incomplete coaptation due to enlargement of the aortic root and annulus. Semiquantitation of associated regurgitation should be performed by composite biplanar long-axis and short-axis color Doppler imaging. With central regurgitant jets, the ratio of the subvalvular jet to outflow

tract dimensions (on long-axis imaging) and the ratio of the subvalvular jet to outflow tract areas (on short-axis imaging) correlate well with angiographic gradation of aortic regurgitation. The trajectory of the aortic regurgitant jet also aids in the clarification of the mechanism and insufficiency; defects in central coaptation cause central jets, and asymmetrical cusp malcoaptation produces eccentric jets usually directed away from the most affected cusp. Longitudinal short-axis color Doppler imaging of the aortic valve can usually pinpoint the exact site and size of the regurgitant orifice, further guiding surgical repair efforts. Significant residual aortic regurgitation shown by intraoperative color Doppler evaluation after initial aortic valve repair was noted in 7 % of patients studied by Cosgrove et al. [2], prompting immediate successful revision of the repair in all patients in this series.

24.5 Monitoring of Myocardial Ischemia

Monitoring of myocardial ischemia and segmental LV regional wall motion abnormalities (RMWA) is reviewed in detail in Chaps. 12 and 27. Ideally, complete evaluation of regional LV performance requires that multiple views of the left ventricle be obtained, e.g., at the base, midcavity, and apex. A qualitative impression of LV contraction is obtained by evaluating LV wall thickening and endocardial motion. Qualitative schemes describe regional wall motion as normal, hypokinetic, akinetic, or dyskinetic. Regional wall motion is normal if there is obvious systolic wall thickening and inward endocardial motion. "Hypokinesia" refers to abnormal systolic wall thickening or inward endocardial motion and may be graded as mild, moderate, or severe. "Akinesia" refers to the absence of systolic wall thickening or inward endocardial motion. "Dyskinesia" refers to paradoxical motion in which a portion of the wall moves in the opposite direction to the rest of the left ventricle and may even become thinner rather than thicker during systole. This is a pattern typical of transmural myocardial infarction and LV aneurysm. A scoring system based on regional systolic function can be readily applied to this scheme (see Chap. 12).

24.5.1 Limitation of TEE To Diagnose Myocardial Ischemia

Errors in the interpretation of RWMA are often due to images of poor quality or to operator inexperience. Poor quality may be caused by inappropriate settings on the ultrasound machine or dropout in the lateral segments of the sector arc. Occasionally, a true short-axis view of the left ventricle cannot be obtained. Oblique views may produce a false impression of RWMA. Misinterpretation of regional wall motion may be related to translational or rotational changes in cardiac position throughout the cardiac or respiratory cycle that can be amplified after pericardiotomy. Omission of short-axis views at the base and apex of the left ventricle may overlook RWMA present only in these cross sections. Temporal heterogeneity of LV contraction due to abnormal LV activation (bundle-branch block or paced rhythm) may lead to a false interpretation of regional systolic function, because even though all the ventricular wall segments may contract normally, they do so at slightly different times, so the impression given is regional dysfunction within segments with delayed electrical activation. There is also increasing uncertainty about the specificity of transient RWMA as a marker of myocardial ischemia. Intermittent myocardial ischemia can produce areas of postischemic ("stunned") myocardium. Although all methods have some limitations, TEE has provided a unique opportunity for further elucidation of the complex interactions of the heart in response to anesthesia and surgery.

24.6 Mass Lesions

Cardiac tumors and masses are reviewed in Chap. 20. Intraoperative TEE provides valuable

information to the surgeon both before and after tumor resection. As also used during surgery for intracardiac myxoma, TEE can precisely localize tumor attachment, define the tumor's effect on and potential invasion of surrounding anatomic structures, and identify multifocal tumors within the heart. After tumor resection, TEE is useful to confirm complete removal, to detect residual valvular regurgitation caused by trauma from either the tumor or surgical excision, and to exclude a possible intracardiac communication precipitated by surgical resection.

Intraoperative TEE has also been used to delineate the nature and extent of secondary neoplastic invasion of the heart, particularly in patients with renal cell carcinoma. It has been demonstrated that TEE provides highly accurate definition of intracaval neoplastic preoperative extension of renal cell carcinoma into the right side of the heart; the images were superior to characterization by preoperative computed tomography, magnetic resonance imaging, or inferior venacavography. After tumor resection, absence of tumor embolization, residual tumor, and inferior vena caval obstruction has been reliably confirmed by TEE in such cases. We also use intraoperative TEE to evaluate intracaval extension of other genitourinary neoplasms.

24.7 Monitoring for Intraoperative Embolism

24.7.1 Cardiac Surgery

Intracardiac air is routinely encountered in patients after cardiac operations, such as valvular or congenital heart surgery, in which the chambers of the heart are opened to air. At the end of the cardiac surgical procedure, maneuvers are undertaken to ensure that intracardiac air has been eliminated. These procedures include placement of the patient in the Trendelenburg position, transient carotid artery compression, and prolonged venting of the left ventricle. TEE is an exquisitely sensitive monitor of intracardiac air and should be used to detect intracardiac air before cardiopulmonary bypass is discontinued. Significant amounts of air necessitate prolonged venting maneuvers to avoid potential arterial air embolism.

24.7.2 Orthopedic Surgery

During surgery for total hip arthroplasty, significant hemodynamic deterioration occasionally develops during reaming of the femoral shaft or at the time of insertion of methylmethacrylate cement. Preliminary studies have suggested that embolization of air, fat, or cement occurs at these times or later with manipulation of the joint. Because cemented total hip arthroplasty is associated with a significantly greater degree of embolism than the noncemented operation, the increases in intramedullary pressure that occur with cementing may be the cause of embolism. Several studies suggest that TEE may have a role in monitoring selected patients undergoing major orthopedic operations. TEE is also useful for the detection of other causes of hypotension, such as venous thromboembolism and hypovolemia.

24.7.3 Liver Surgery

Occasionally, isolated right ventricular failure can account for some of the hemodynamic instability seen during liver transplant. More often, venous, pulmonary, and paradoxical embolization of air and thrombi contribute to right ventricular failure. Air embolism during liver transplant occurs particularly at the time of vein-to-vein bypass, and TEE is the ideal tool for recognizing this. The risk of disrupting esophageal varices in patients with portal hypertension is minimal, but does exist. Hence, the potential benefit of TEE monitoring for air embolism in patients undergoing liver surgery must be weighed against the risks of variceal bleeding.

24.7.4 Neurosurgery

TEE has several intraoperative applications in neuroanesthesia and neurosurgery. Specifically, TEE can be used as a monitor of venous air

embolism (VAE) and paradoxical air embolism (PAE).

VAE is a well-recognized complication of neurosurgical procedures in patients who are in the sitting position. The most important factors that limit morbidity and mortality from VAE are early diagnosis and prompt treatment. Presently, the most sensitive monitor for intraoperative detection of VAE is two-dimensional TEE.

PAE is a rare complication in patients undergoing neurosurgical procedures, but when it occurs, the results can be devastating. It has been postulated that a patent foramen ovale (PFO) predisposes patients to development of PAE during episodes of VAE. Venous air entering the pulmonary circulation results in an increase in pulmonary artery pressure secondary to obstruction of pulmonary arterial blood flow and, possibly, reflex vasoconstriction. The resultant pulmonary hypertension may cause increases in right atrial and ventricular pressures relative to left-sided pressures. Thus, a right-to-left atrial pressure gradient may occur that predisposes to development of PAE if a PFO exists. TEE may be used preoperatively to identify patients with a PFO and thus alert the clinician to the potential increased risk of PAE (see Chaps. 21 and 35). Intraoperative TEE with provocative maneuvers may be used after induction of anesthesia to detect a PFO. When a PFO is identified before the surgical procedure begins, one may choose to perform the operation with the patient in a position associated with a lower incidence of VAE than the sitting position. Performing the operation with the patient in this alternative position with lower risk of VAE might, theoretically, lower the risk of PAE.

Further Reading

Carpentier A et al (1980) Recostructive surgery of mitral valve incompetence: ten year appraisal. J Thorac Cardiovasc Surg 79:2338–2348

Cosgrove DM et al (1991) Valvuloplasty for aortic insufficiency. J Thorac Cardiovasc Surg 102:571–577

Lang RM, Bierig M, Devereux RB et al (2005) Recommendations for chamber quantification: a report from the American Society of Echocardiography's Guidelines and Standards Committee and the Chamber Quantification Writing Group, in conjunction with the European Association of Echocardiography. J Am Soc Echocardiogr 18:1440–1463

Zoghbi WA, Enriquez-Sarano M, Foster E et al (2003) Recommendations for evaluation of the severity of native valvular regurgitation with two-dimensional and Doppler echocardiography. J Am Soc Echocardiogr 16:777–802

General Hemodynamic Assessment

25

Carla Avallato, Ilaria Nicoletti,
and Alessandro Locatelli

25.1 Introduction

The assessment of hemodynamic parameters is the foundation for the correct diagnosis and treatment of patients hospitalized in intensive care. Both transthoracic echocardiography (TTE) and transesophageal echocardiography (TEE) have proven to be versatile tools in providing a large amount of information on cardiac function, in real time and directly at the bedside, also thanks to the application of Doppler technology. Assessment of the hemodynamic parameters is based on an estimate of pressures and volumes, and we shall see how echocardiography can provide the data in a minimally invasive manner. However, the limitations of this technique should also be highlighted, which are often operator-dependent and related to the quality of the images obtained. This can compromise both the accurate assessment of the parameters and the correct application of the physical principles of Doppler echocardiography, such as the proper alignment of the Doppler beam with the estimated direction of blood flow and the precise location of the sample (or sample point).

25.2 Pressure Assessment

The intravascular pressure cannot be measured directly, but, with Doppler echocardiography, it is possible to obtain the necessary data to apply the Bernoulli equation. The Bernoulli equation shows the difference in pressure generated by the passage of blood flow through a narrowed orifice as, for example, a heart valve. The estimate of the pressures inside the heart chambers assumes the presence of a jet of valvular regurgitation in the cavity ahead. In its clinical application, the equation can be simplified as follows (Fig. 25.1):

$$P_1 - P_2 = 1/2\,\rho\,(V_{2^2} - V_{1^2}),$$

where ρ is blood density (1.06×10^3 kg/m^3), V_2 is the velocity at the distal point of the narrowed orifice, at V_1 is the velocity at the proximal point of the narrowed orifice.

Because V_1 is much lower than V_2, it can be disregarded in the final simplified formula, which is

$$\Delta P = 4 \times V_{2^2}$$

Modern ultrasound machines automatically provide the value of the pressure gradient, which is obtained by measuring with continuous wave Doppler echocardiography the peak velocity of the regurgitant flow. Continuous wave Doppler echocardiography is necessary to deal with high speeds (Fig. 25.2).

C. Avallato (✉)
Cardiovascular Anesthesia, Santa Croce and Carle Hospital, Cuneo, Italy
e-mail: avallato.c@ospedale.cuneo.it

A. Sarti and F. L. Lorini (eds.), *Echocardiography for Intensivists*,
DOI: 10.1007/978-88-470-2583-7_25,

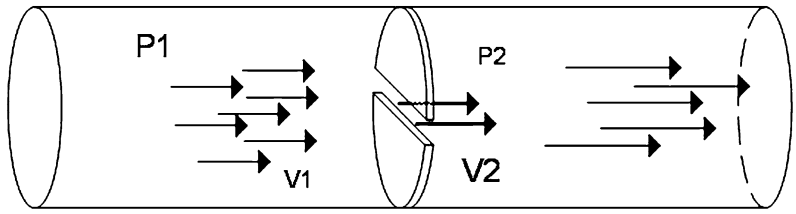

Fig. 25.1 The pressure gradient created by flow passing through a restricted orifice is correlated with the difference of the square of velocity. This is simplified in the Bernoulli equation

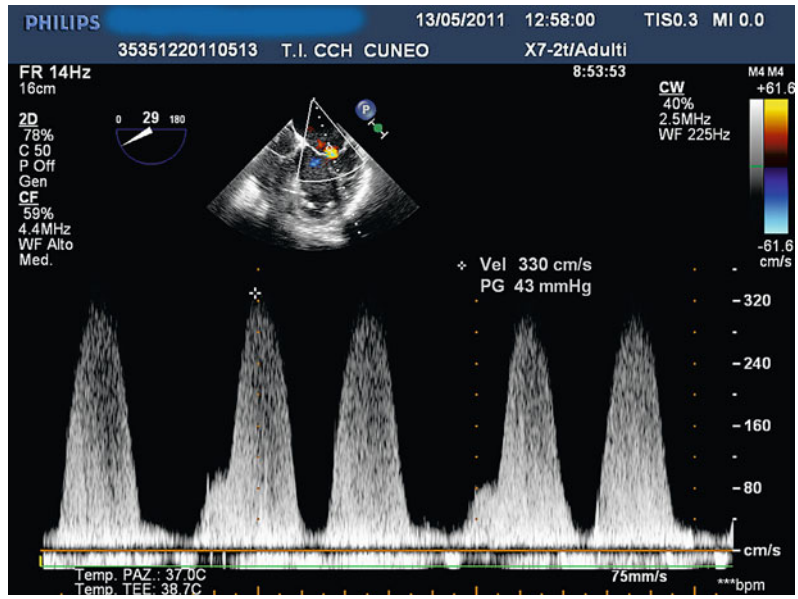

Fig. 25.2 Peak velocity assessment of the mitral regurgitant flow using continuous wave Doppler echocardiography

Considered this, using the heart valve regurgitation flow and the pressure of the heart chambers that determines it, we can calculate the left atrial pressure (LAP), the end-diastolic pressure of the left ventricle (LVEDP), and the systolic pulmonary artery pressure (sPAP).

LAP is calculated using the mitral regurgitation. The driving pressure is the aortic systolic blood pressure (sBP), which, in the absence of stenosis of the aortic valve, is considered equal to the left ventricular pressure. The resulting equation is

$$\mathrm{LAP} = \mathrm{sBP} - 4\mathrm{V}_{\mathrm{MR}^2},$$

where $\mathrm{V}_{\mathrm{MR}^2}$ is the peak velocity of the mitral regurgitant jet.

Several factors may make the value obtained less reliable, such as the load conditions and compliance of the left ventricle, the use of inotropic drugs, and mitral insufficiency characterized by multiple regurgitation jets.

The determination of LVEDP uses the regurgitation jet of the aortic valve. The LVEDP is calculated by measuring the difference between the driving pressure (systemic diastolic blood pressure, dBP) and the end-diastolic gradient of aortic regurgitation. The resulting equation is

$$\mathrm{LVEDP} = \mathrm{dBP} - 4\mathrm{V}_{\mathrm{AR-EDV}^2}$$

where $\mathrm{V}_{\mathrm{AR-EDV}^2}$ is the end-diastolic velocity of the regurgitation jet of the aortic valve.

Left ventricular filling pressure (pulmonary capillary wedge pressure) is calculated by the *E*/*E*′ ratio (or *E*/Ea ratio), which is the ratio between the peak velocity of early transmitral flow (pulsed wave Doppler echocardiography)

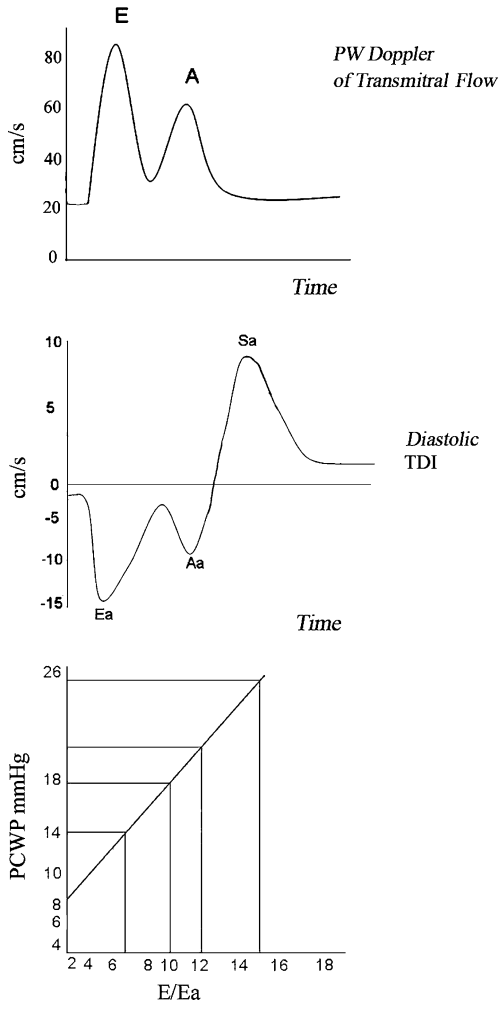

Fig. 25.3 *Top* to *bottom*: Transthoracic echocardiography (TTE) apical four chamber pulsed wave (*PW*) Doppler measurement of transmitral flow, TTE apical four chamber lateral mitral ring tissue Doppler imaging (*TDI*), and the relationship between *E*/Ea (*E*/*E*′) and pulmonary capillary wedge pressure (*PCWP*)

and the speed of early tissue relaxation velocity (tissue Doppler imaging). It is rather intuitive that the ratio between the peak flow, which depends on the transmitral pressure gradient, and the speed of the myocardial relaxation can represent left ventricular filling pressure. This ratio is considered normal under 8–10 and abnormal (increased filling pressure) over 10. In particular, a value over 15 is associated with a marked increase in left ventricular filling pressure and pulmonary capillary wedge pressure (Fig. 25.3) especially if left ventricular systolic function is preserved, and also with a significant increase of the level of atrial natriuretic peptide (Fig. 25.3).

The sPAP is equal to the systolic right ventricular pressure in absence of stenosis of the right ventricular outflow tract or of the pulmonary valve. It is determined by measuring the peak velocity of the tricuspid valve regurgitation jet, obtained with continuous wave Doppler echocardiography. The equation is

$$\text{sPAP} = 4V_{TR}{}^2 + \text{RAP},$$

where RAP is the pressure in the right atrium. This pressure is 8–10 mmHg but, if the patient shows signs of congestive heart failure or jugular venous distension, it can be estimated by ultrasound measurement of the inferior vena cava and its variations during the respiratory cycle. A dilated vena cava (diameter greater than 2 cm) and its variations inferior to 50% during inspiration is significant for RAP > 15 mmHg.

Mean pulmonary artery pressure can be estimated by pulsed wave Doppler echocardiography by measuring the acceleration time of the velocity–time integral (VTI) of the pulmonary artery flow, using the TTE parsternal short-axis view (Fig. 25.4) or the TEE ascending aortic short-axis view. The shorter the time to reach the peak velocity, the higher the mean pressure in the pulmonary artery:

$$\text{Mean PAP} = 79 - 0.45 \times \text{AT},$$

where PAP is pulmonary artery pressure and AT is acceleration time.

A sharp rise of pulmonary peak velocity by simple visual inspection can immediately suggest a high pulmonary pressure as the ascending velocity slope is very sharp (Fig. 25.5).

25.3 Cardiac Output

Echocardiography allows us to obtain a qualitative and quantitative estimation of ventricular volumes and therefore to measure cardiac output. This is accomplished either through the use

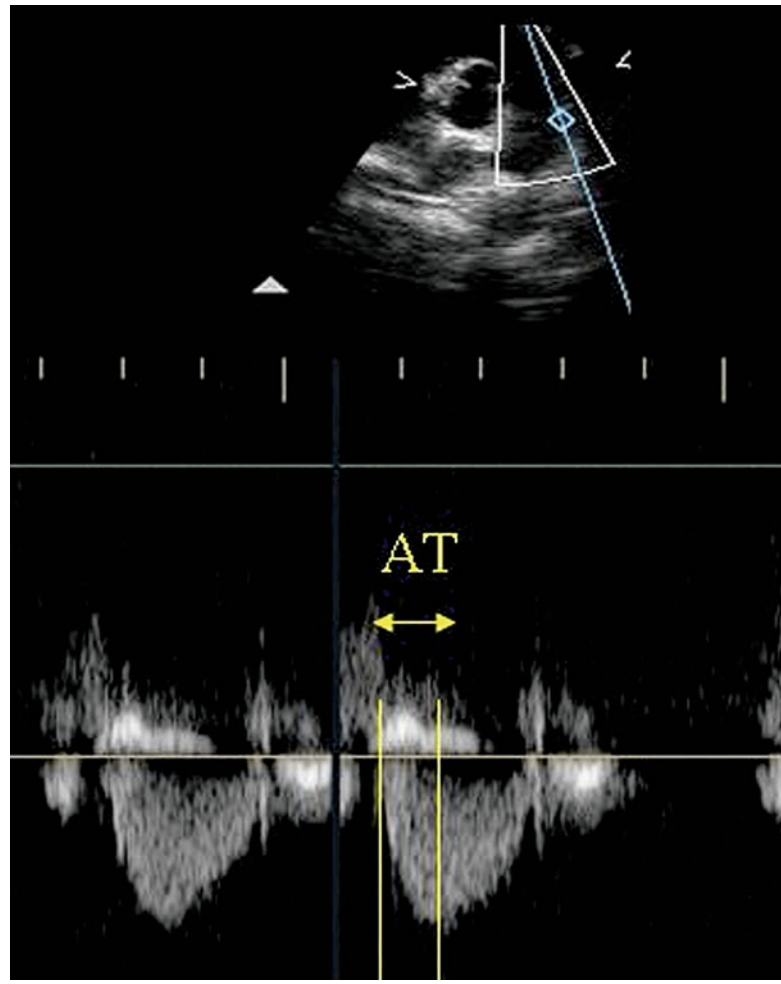

Fig. 25.4 TTE parasternal short-axis view, pulmonary artery velocity–time integral (VTI). *AT* acceleration time

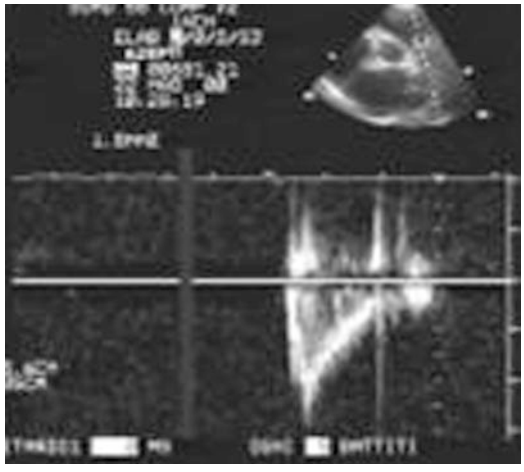

Fig. 25.5 TTE parasternal short-axis view, pulmonary artery VTI: short acceleration time in pulmonary hypertension

of Doppler technology or through volumetric measurements and derived applications (e.g., acoustic quantification and real-time three-dimensional echocardiography).

The application of Doppler echocardiography in this context uses the flow equation: the flow or volume is the product of the cross-sectional area (CSA) through which the blood sample moves and the distance that this blood volume covers in a given time. In echocardiography, this distance, corresponding to the column of blood moving through the CSA in a heartbeat, can be calculated using the velocity–time integral of the Doppler wave (pulsed wave Doppler echocardiography or continuous wave Doppler echocardiography) found in the specific CSA. All echocardiographic

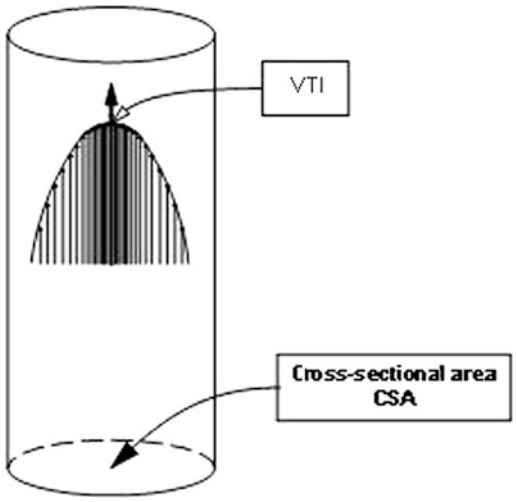

Fig. 25.6 Flow equation: the flow is the product of the cross-sectional area (*CSA*) and the distance that the blood volume covers in a given time, assessed by the VTI

devices provide automatic calculation of the VTI by tracing the outline of the corresponding Doppler signal (Fig. 25.6).

This is illustrated by the following equation:

$$\text{Volume}\ \left(\text{cm}^3\right) = \text{CSA}\ \left(\text{cm}^2\right) \times \text{VTI}\ (\text{cm}).$$

In this way, the stroke volume (SV) is calculated, i.e., the volume of blood ejected with each heartbeat. With echocardiography, the SV is obtained with several methods, properly correlating the measure of CSA with the point of detection of the Doppler signal:

For the left ventricular outflow tract, the pulsed Doppler spectrum is used (pulse wave Doppler echocardiography). The sample is placed 5 mm below the plane of the aortic valve. The ultrasound Doppler beam must be as parallel as possible to the direction of the blood flow so that the angle of incidence between the two directions does not exceed 20° (in this way the possible error produced will be less than 6%). With TEE the best alignment is achieved with transgastric projections (transgastric long-axis view at 90–120° or deep transgastric view), whereas with TTE the apical five-chamber view is used. The CSA is calculated using the diameter of the left ventricular outflow tract measured with M-mode at the aortic annulus during systole (Figs. 25.7, 25.8).

The CSA of the aortic valve can be obtained by tracing its plane during systole or, more accurately, considering the valve like an equilateral triangle and using the same mathematical formula based on the length of one side. The aortic valve is the narrowest point through which the flow passes: a reduction of the diameter results in an increase in blood velocity. For this reason it is necessary to use continuous wave Doppler echocardiography.

With use of the mitral valve for SV calculation, the VTI profile is obtained more easily. The transmitral flow is obtained during diastole in the four-chamber long-axis view with pulsed wave Doppler echocardiography. The sample is placed in the middle of the mitral valve in the annulus plane. It is more difficult to obtain the correct value of the valve area because the mitral annulus is elliptical, not circular. With the same projection the diameter from the rise of the anterior leaflet to the posterior leaflet of the valve is measured during diastole. The mitral valve has a funnel shape. For this reason, planimetry is inaccurate to compute the CSA with TEE. Instead, planimetry has been validated with TTE: it is performed in the parasternal short-axis view, moving carefully from the apex to the base of the heart.

Another way to estimate the SV is to use the systolic and diastolic volumes of the left ventricle. The SV is calculated by

$$\text{SV} = \text{LVEDV} - \text{LVESV},$$

where LVEDV is the left ventricular end-diastolic volume and LVESV is the left ventricular end-systolic volume.

Different methods are used, but the most used ones are:

- The area–length method. The projection used is the four-chamber long-axis view, for both TTE and TEE. This method is based on the assumption that the left ventricle has a geometric elliptical shape. To obtain the volume

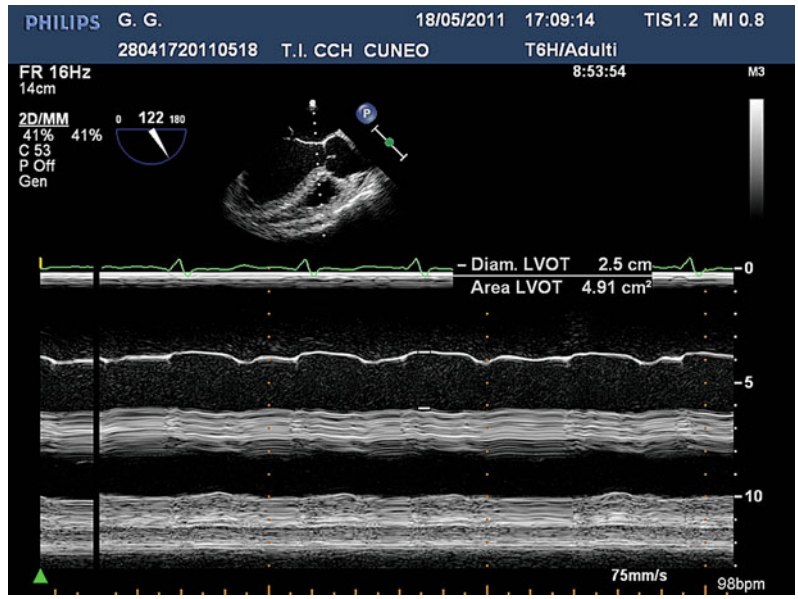

Fig. 25.7 CSA assessment using M-mode. The diameter of the left ventricular outflow tract (*LVOT*) is measured at the aortic annulus during systole

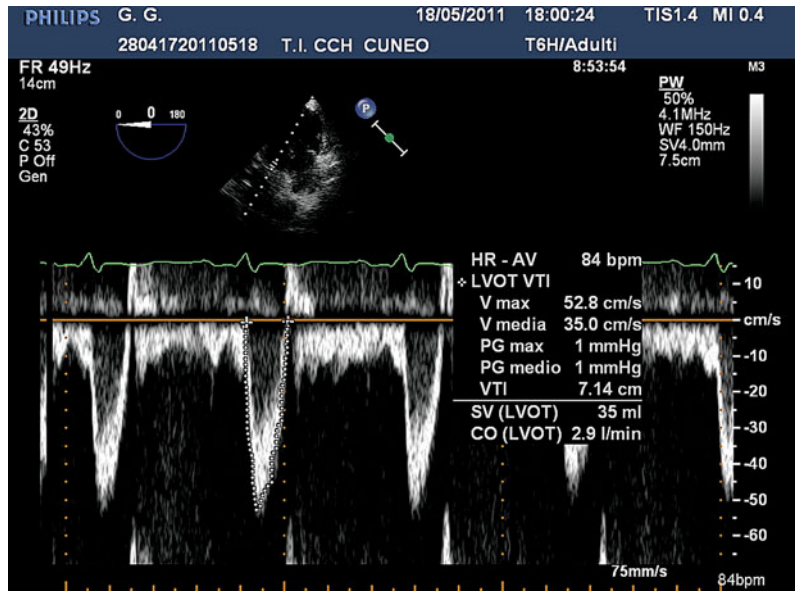

Fig. 25.8 VTI assessment using the PW Doppler spectrum. The sample is placed 5 mm below the plane of the aortic valve (*AV*)

it is necessary to trace the areas and the largest longitudinal diameter of the left ventricle at the end of systole and the end of diastole. In order to not underestimate the volume, it is also important to obtain the view of the true apex.

– Simpson's rule. This method is often used in echocardiography software. The ventricle is divided into multiple slices of known thickness, each considered as a cylinder. The total volume of the ventricle is obtained automatically by adding all the volume of individual slices. It is necessary to set the machine up correctly to get the best resolution and visualization of the endocardium, the inner edge of which is traced. Again, the measurements are made at the end of systole and the end of diastole. By convention, the papillary muscles are included in the cavity of the ventricle. If the patient has a sinus rhythm, it is sufficient

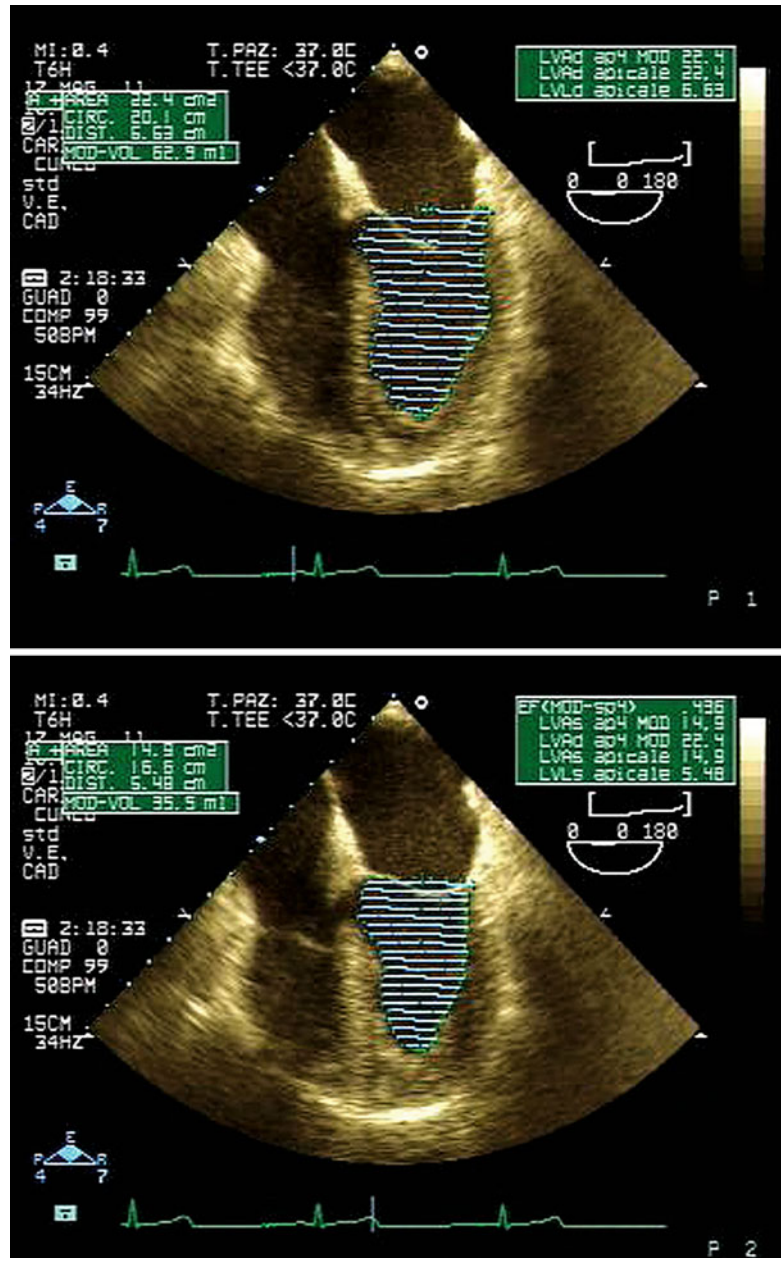

Fig. 25.9 and Fig. 25.10 Application of the echocardiography software for the measurement of ejection fraction by Simpson's rule. Left ventricular long-axis views measuring end-diastolic and end-systolic volumes

to perform measurements on three different heart beats; if the patient has atrial fibrillation, the measurement needs to be repeated for seven to nine beats (Figs. 25.9, 25.10).

The limitation of these volumetric methods is related to the echocardiographic image resolution and the ventricular geometry itself. The resolution of 2D echocardiography ranges between 0.3 and 1.5 mm, depending on the frequency and the number of cycles employed. Therefore, variations of a few millimeters are sufficient to provide significant changes in SV. Also, variations in regional contractility may lead to errors in determining the absolute value of SV and therefore of cardiac output.

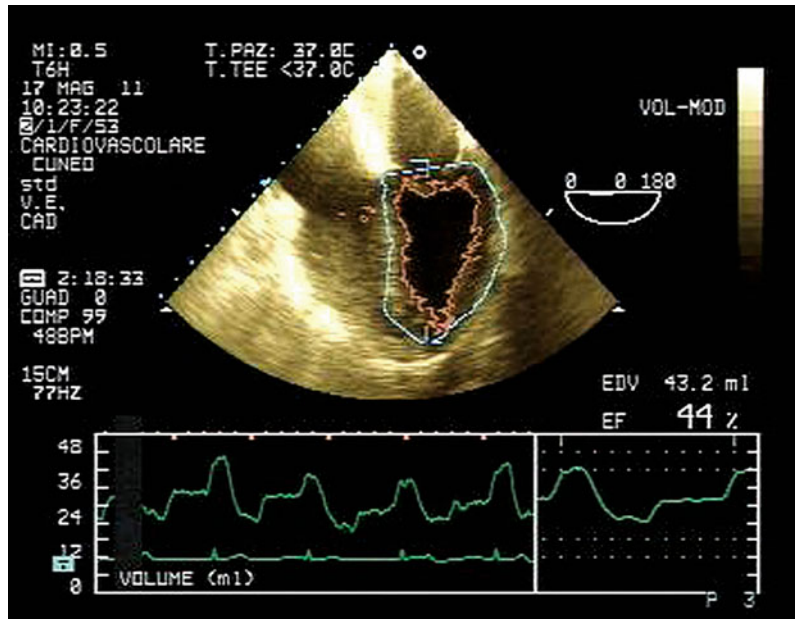

Fig. 25.11 Acoustic quantification. The software is used to select the region of interest, which is the inner cavity of the left ventricle. The resultant waveform is associated with the value of the ejection fraction (*EF*)

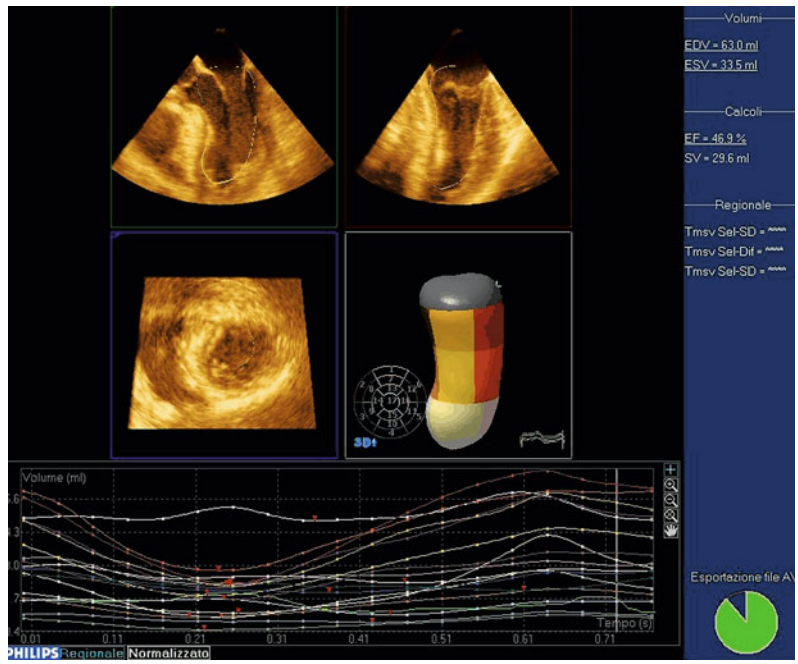

Fig. 25.12 Left ventricular volume and left ventricular EF calculation from a 3D dataset

25.4 New Approaches

25.4.1 Acoustic Quantification

Acoustic quantification represents an ultrasound imaging system which provides detection and tracking of endocardial blood boundaries based on quantitative assessment of acoustic properties of tissue in real time. It is a noninvasive method for online quantification of left ventricular end-diastolic volume, end-systolic volume, and ejection fraction. The acoustic technique has the ability to identify, view, and automatically

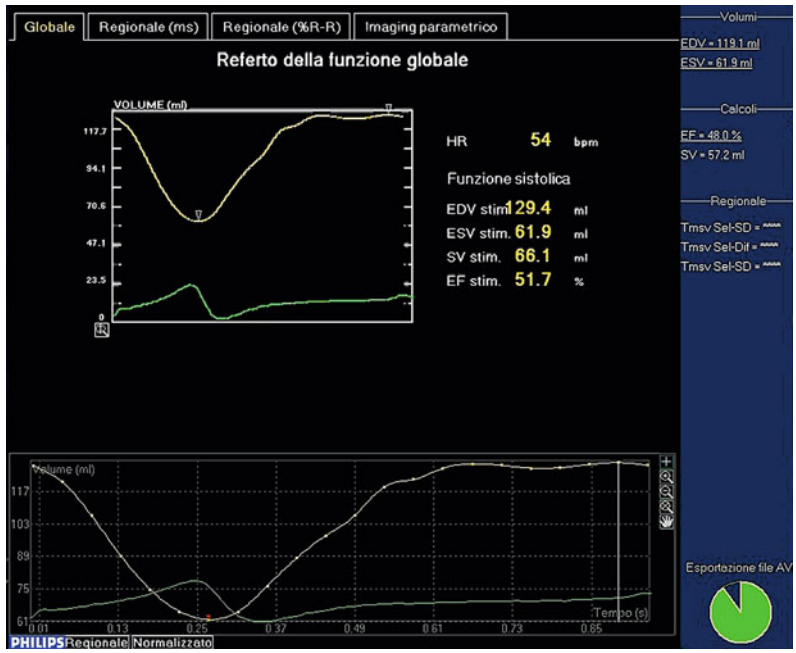

Fig. 25.13 Quantitative panel analysis provided by 3D echocardiography

highlight the endocardium–blood interface. The software allows one to select the area of interest, which is the inner cavity of the left ventricle. The ECG trace is needed to correlate the area variations with the cardiac cycle. The resultant waveform is associated with the value of the ejection fraction, the end-diastolic and end-systolic volumes, and then SV (Fig. 25.11).

25.4.2 Real-Time 3D Echocardiography

The spatial limit of 2D echocardiography has been partly surpassed by technological evolution of ultrasound physics and computerized image processing that has allowed the development of 3D echocardiography.

Real-time 3D echocardiography can currently use three different picture modes: live 3D (a 50° × 30° pyramidal volume), 3D zoom (a truncated pyramid that can be changed in size and in the sections, by the operator), and full-volume 3D (a pyramid volume built from the sum of four to seven images acquired on the ECG trace). This last mode allows one, by aligning the images, to reconstruct the whole left ventricle. Several mathematical algorithms process the image (in which one has to introduce different points of reference oneself and, if necessary, correct the autotracing of the endocardium), providing time–volume curves and calculating the end-diastolic volume, end-systolic volume, and ejection fraction. Several studies have demonstrated a high correlation between the volumes calculated by real-time 3D echocardiography and volumes obtained by magnetic resonance imaging (Figs. 25.12, 25.13).

Further Reading

Brown JM (2002) Use of echocardiography for hemodynamic monitoring. Crit Care Med 30:1361–1364

Hüttemann E (2006) Transoesophageal echocardiography in critical care. Minerva Anestesiol 72:891–913

Poelaert JI, Schüpfer G (2005) Hemodynamic monitoring utilizing transesophageal echocardiography: the relationships among pressure, flow and function. Chest 127:379–390

Szokol JW, Murphy GS (2004) Transesophageal echocardiographic monitoring of hemodynamic. Int Anesthesiol Clin 42:59–81

Vignon P (2005) Hemodynamic assessment of critically ill patients using echocardiography Doppler. Curr Opin Crit Care 11:227–234

Contrast Echocardiography in the ICU and OR

26

Paolo Voci, Luigi Tritapepe, Demetrio Tallarico, and Luciano Agati

26.1 Ultrasound Contrast Agents

Ultrasound contrast agents can be divided into first-generation and second-generation agents. First-generation hand-agitated saline solutions contain large and unstable air microbubbles which cannot pass through the pulmonary microcirculation and are used only for the opacification of the right side of the heart. These agents have been used for about 40 years to rule out a shunt at the level of the fossa ovalis. Second-generation agents are made of smaller, more standardized and stable microbubbles containing a low-diffusable gas. They can easily cross the pulmonary circulation and provide left ventricular (LV) cavity and LV myocardial opacification. These agents are used for better delineation of the endocardial contour and for myocardial perfusion studies.

26.2 Intracardiac Shunts

Critically ill patients with unexplained embolic stroke or refractory hypoxemia may have an intracardiac (atrial septal defect or patency of the fossa ovalis, PFO) or an intrapulmonary (pulmonary arteriovenous fistula) shunt. Another rare cause, but from iatrogenic stroke, is anomalous drainage of a persistent left superior vena cava to the left atrium. PFO affects 25–30% of the general population and is usually a virtual, valve-shaped communication between the atria allowing only small and transient passage of blood from the right to the left atrium after a Valsalva maneuver or cough, which temporarily increase right atrial pressure. However, when the pressure in the right atrium permanently exceeds that of the left atrium (as in pulmonary hypertension, right ventricular failure, and severe tricuspid valve regurgitation) the foramen ovale can be widely and constantly opened, producing a hemodynamically significant right-to-left shunt and hypoxemia. Color Doppler imaging may detect intra-atrial shunts, but contrast echocardiography significantly helps in the diagnosis. Agitated saline solution is good enough for this application. About 0.5 mL of air is mixed with 10 mL of saline solution and 1 mL of the patient's blood, and is pushed back and forth between two syringes connected by a three-way stopcock to produce cavitation bubbles. The solution is then forcefully injected into a peripheral vein, with the syringe maintained perpendicular to the injection site, to prevent injection of large bubbles. Normally, most of the bubbles are trapped in the pulmonary microcirculation, and only a small number of them may occasionally reach the left atrium and ventricle, with a delay of three to seven beats due to the transpulmonary passage. In PFO, however, the bubbles may cross the atrial septum immediately

L. Tritapepe (✉)
Department of Anesthesia and Intensive Care, Cardiac Surgery ICU, Policlinico Umberto I Hospital, Sapienza University of Rome, Rome, Italy
e-mail: luigi.tritapepe@uniroma1.it

A. Sarti and F. L. Lorini (eds.), *Echocardiography for Intensivists*,
DOI: 10.1007/978-88-470-2583-7_26,

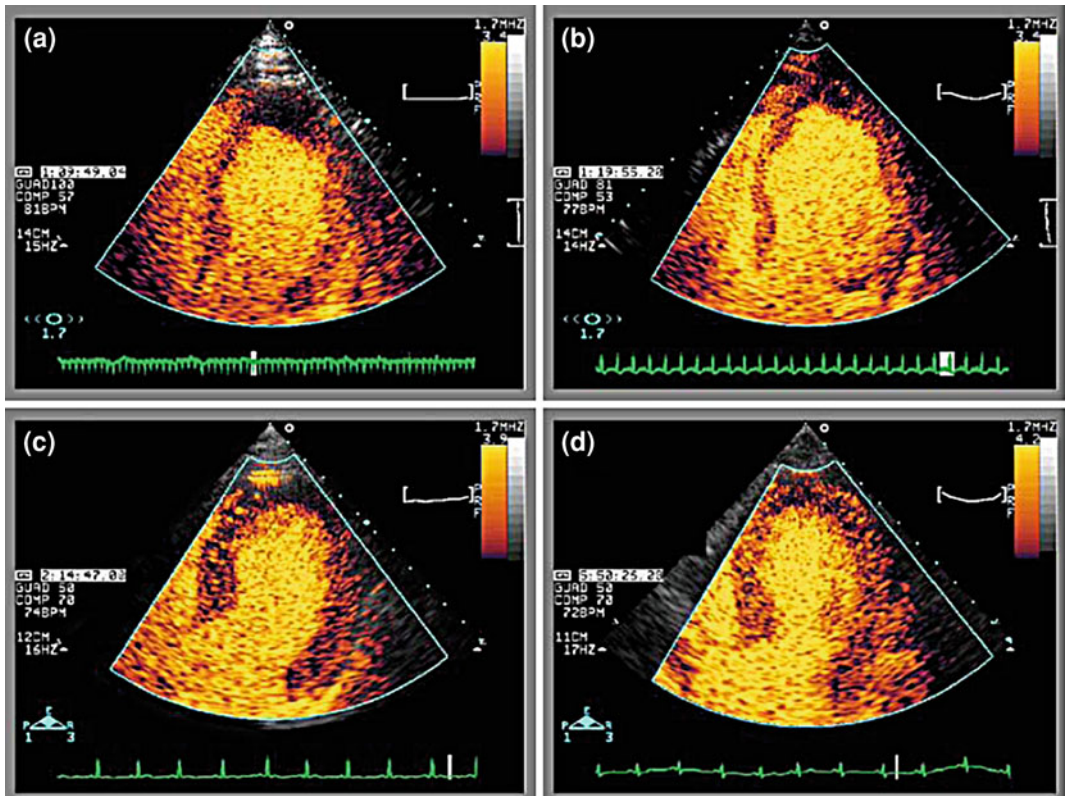

Fig. 26.1 Contrast-enhanced apical four-chamber view in patients with acute myocardial infarction treated with primary coronary intervention (**a**, **b**) or with early primary coronary intervention after lysis (**c**, **d**)

after right-sided opacification, most often during a Valsalva maneuver.

26.3 Improvement of Image Quality

In critically ill patients with poor acoustic windows, endocardial visualization may be inadequate, making the assessment of wall motion, cavity volumes, and ejection fraction difficult. In these patients, second-generation contrast agents producing LV cavity opacification from a venous injection can dramatically improve delineation of the LV cavity, detection of wall motion abnormalities, and correct measurement of ejection fraction (Fig. 26.1). Therefore, contrast echocardiography may be a noninvasive alternative to transesophageal echocardiography for determination of regional and global LV function at rest and during pharmacological stimulation. By the use of second-generation contrast agents, up to 75% of nondiagnostic echocardiograms in the intensive care unit may be diagnostic. Contrast agents also improve detection of endoventricular thrombosis (Fig. 26.2), noncompaction of the left ventricle, and heart rupture, and may definitely improve the Doppler signal to detect tricuspid regurgitation, pulmonary artery pressure, aortic transvalvular flow, and pulmonary venous flow.

26.4 Coronary Flow

Transthoracic imaging of coronary flow is a new imaging modality that can be improved by contrast ultrasonography. The left anterior descending (LAD) coronary artery can be studied at the middle-distal tract in almost all patients. Resting flow measurements may show focal velocity acceleration, suggesting the presence of a coronary stenosis,

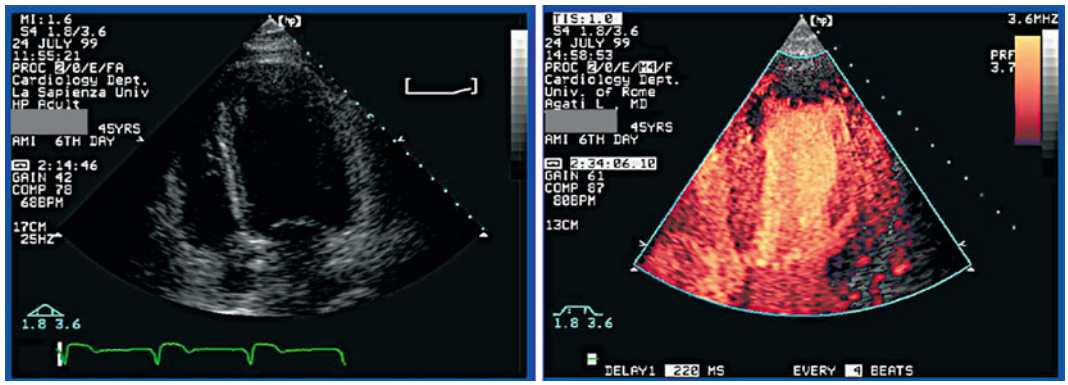

Fig. 26.2 Four-chamber view: the apical thrombus is well visualized only in the contrast-enhanced image (*right*)

even though coronary tortuosity may produce the same effect. Coronary flow reserve (CFR; the ratio between hyperemic and baseline flow velocities) is a useful surrogate of coronary output measurement during maximal microcirculatory vasodilation induced by adenosine, ATP, or dipyridamole, reflecting the functional impact of a coronary stenosis CFR > 2.5 indicates the absence of a flow-limiting coronary stenosis, whereas CFR < 2 suggests the presence of a flow-limiting coronary stenosis. CFR ≤ 1 occurs in coronary subocclusion, when the vasodilator reserve is completely exhausted or coronary steal occurs. In the gray zone ranging from 2 to 2.5, the correlation with angiography is less strong, but usually an intermediate stenosis is found. About 25–30% of patients treated with primary coronary intervention for acute myocardial infarction have a no-reflow or low-reflow phenomenon, despite successful coronary recanalization. These patients may exhibit no significant contractile reserve or functional recovery at follow-up. CFR early after the procedure allows prediction of functional recovery after primary coronary intervention as it is directly proportional to the level of viable myocardium. Perforating branches of the LAD coronary artery can also be visualized as a useful sign of tissue reperfusion and viability after acute anterior myocardial infarction. Graft patency to the LAD coronary artery can be easily imaged, particularly at the suture level, because the mammary artery is not affected by wall motion artifacts, and graft function can be accordingly assessed by vasodilator stress focusing on the LAD coronary artery, not on the graft itself, to prevent the bias introduced by flow competition.

26.5 Myocardial Perfusion

Second-generation contrast agents reach the coronary microcirculation after venous injection, and enhance the grayscale level of the LV myocardium (myocardial contrast echocardiography). This technique allows measurement of the extent of the myocardial area at risk subtended by an occluded coronary artery and the detection of the no-reflow phenomenon after reperfusion in acute myocardial infarction, and may ultimately predict irreversible LV dysfunction at follow-up.

26.6 Safety and Research Applications

Gas embolism is a potential side effect of galenic contrast agents, but has never been a major problem in large series of patients. Nevertheless, caution is recommended in the case of right-to-left shunt at the level of the fossa ovalis. Levovist, a hyperosmolar galactose-containing agent, is contraindicated in patients with galactosemia and must be used with caution in patients with severe heart failure. Optison is made of an albumin shell, and must not be administered to patients with known or suspected hypersensitivity to blood, hemoderivates,

or albumin. SonoVue contains sulfur hexafluoride, and is contraindicated in patients with known hypersensitivity to the agent, right-to-left shunt, pulmonary hypertension (more than 90 mmHg), uncontrolled systemic hypertension, adult respiratory distress syndrome, assisted mechanical ventilation, unstable neuropathies, and acute coronary syndromes. No studies have evaluated the safety of intracoronary injection of commercial contrast agents as their rheological behavior has not been studied in the absence of filtering by the pulmonary microcirculation. Therefore, these agents should not be used for intracoronary injection. The interaction between the ultrasound beam and microbubbles produces energy with potential effects on tissue, namely, inertial cavitation and acoustic current production. Inertial cavitation refers to formation, growth, and collapse of the gas cavities within a fluid as a result of exposure to ultrasound. A high energy level is produced in a very small volume of gas, resulting in a very high but focal temperature increase in the collapsing zone, free-radical generation, and emission of electromagnetic radiation (sonoluminescence). This phenomenon may cause extrasystole, which is frequently seen with sonicated albumin microbubbles and the appearance of contrast agent in the right atrium. Potential membrane damage has been reported in red blood cells in vitro and in animal cells in vivo. An increase in membrane permeability was demonstrated by electron microscopy in cell membranes surrounding oscillating microbubbles, an effect which could be used for local drug delivery using microbubbles as carriers of drugs and genetic material.

26.7 Intraoperative Ultrasonography

Contrast-enhanced cardioplegia has been shown both experimentally and clinically to detect nonuniform cardioplegia distribution in patients with coronary occlusion and poor collateral circulation, in whom a retrograde administration through the coronary sinus may restore uniform protection and reduce postoperative events. In surgical repair of aortic dissection, contrast agents allow immediate visualization of retrograde aortic perfusion, and may prevent severe postoperative neurologic complications in the case of inadvertent false lumen cannulation/perfusion.

Further Reading

Agati L, Funaro S, Madonna MP, Sardella G, Garramone B, Galiuto L (2007) Does coronary angioplasty after timely thrombolysis improve microvascular perfusion and left ventricular function after acute myocardial infarction? Am Heart J 154:15127

Agati L, Tonti G, Galiuto L, Di Bello V, Funaro S, Madonna MP, Garramone B, Magri F (2005) Quantification methods in contrast echocardiography. Eur J Echocardiogr 6(Suppl 2):S14–S20

Feinstein SB, Voci P, Segil LJ, Harper PV (1991) Contrast echocardiography. In: Marcus ML, Skorton DJ, Wolf GL (eds) Cardiac imaging. A companion to Braunwald's heart disease. Saunders, Philadelphia, pp 557–574

Galiuto L, Garramone B, Scarà A, Rebuzzi AG, Crea F, La Torre G, Funaro S, Madonna MP, Fedele F, Agati L (2008) The extent of microvascular damage during myocardial contrast echocardiography is superior to other known indexes of post-infarct reperfusion in predicting left ventricular remodeling. J Am Coll Cardiol 51:552–559

Pizzuto F, Voci P, Mariano E, Puddu PE, Aprile A, Romeo F (2005) Evaluation of flow in the left anterior descending coronary artery but not in the left internal mammary artery graft predicts significant stenosis of the arterial conduit. J Am Coll Cardiol 45:424–432

Voci P (2000) The bubbles and the science of life. J Am Coll Cardiol 36:625–627

Voci P, Testa G, Tritapepe L (1996) Demonstration of false lumen perfusion during repair of type A aortic dissection. Anesthesiology 85:926–928

Voci P, Pizzuto F, Romeo F (2004) Coronary flow: a new asset for the echo lab? Eur Heart J 25:1867–1879

Echo-Guided Therapy for Myocardial Ischemia

27

Michele Oppizzi, Marco Ancona, and Rachele Contri

27.1 Introduction

Definitive studies on the ideal treatment strategy for the management of intraoperative myocardial ischemia and infarction are lacking. Therefore, we suggest a personal approach, tailored on the basis of hemodynamic and echocardiographic data, that can be summarized in the following scenarios (Fig. 27.1).

27.2 Left Ventricular Ischemia/Infarction

In patients with an *increased mean arterial pressure/heart rate ratio*, transesophageal echocardiograpy (TEE) usually shows a normal end-diastolic area (EDA; transgastric short-axis view), a fractional area change (FAC) of more than 40% (transgastric short-axis view), and no or mild mitral regurgitation (mid-esophageal four-chamber view). In such cases myocardial ischemia can be the manifestation of inappropriate anesthetic management. Therefore, the first step is deepening anesthesia and analgesia.

If this maneuver is not successful and *both the mean arterial pressure and the heart rate* remain high, heart rate control takes priority. An intravenous beta blocker with a short half-life such as esmolol is the first choice in most patients with ST segment depression or elevation, whereas diltiazem is preferred whenever coronary spasm is suspected (previous history of rest angina and normal coronary angiography findings). The effects of both drugs on ventricular function in the context of ongoing ischemia must be monitored with TEE (transgastric short-axis view) in order to avoid hypotension and heart failure.

If only *the mean arterial pressure is increased but heart rate is normal or below the normal rate*, beta or calcium blockers must be used with caution because of the risks of bradycardia and low-output syndrome. Nitrate infusion is usually well tolerated and is the treatment of choice. Before nitrate infusion is started, right ventricular (RV) dysfunction, in terms of an enlarged, hypokinetic right ventricle with reduced tricuspid annular plane systolic excursion (TAPSE) and systolic component of the electrocardiogram (Sa) (mid-esophageal four-chamber view, transgastric short-axis view to visualize the right ventricle), or low left ventricular (LV) preload (small EDA, transgastric short-axis view) must be ruled out to avoid the risk of severe hypotension. In some patients, the effects of a large myocardial ischemia combined with an increase in afterload due to hypertension carry the risk of acute LV dysfunction by a stunning mechanism which may be detected by TEE (transgastric short-axis or mid-esophageal views). In such cases it is better to start nitrate infusion with a rapid titration in order to reduce arterial pressure and to administer a bolus

M. Oppizzi (✉)
Department of Cardiology, San Raffaele Hospital, Milan, Italy
e-mail: oppizzi.michele@hsr.it

A. Sarti and F. L. Lorini (eds.), *Echocardiography for Intensivists*,
DOI: 10.1007/978-88-470-2583-7_27, © Springer-Verlag Italia 2012

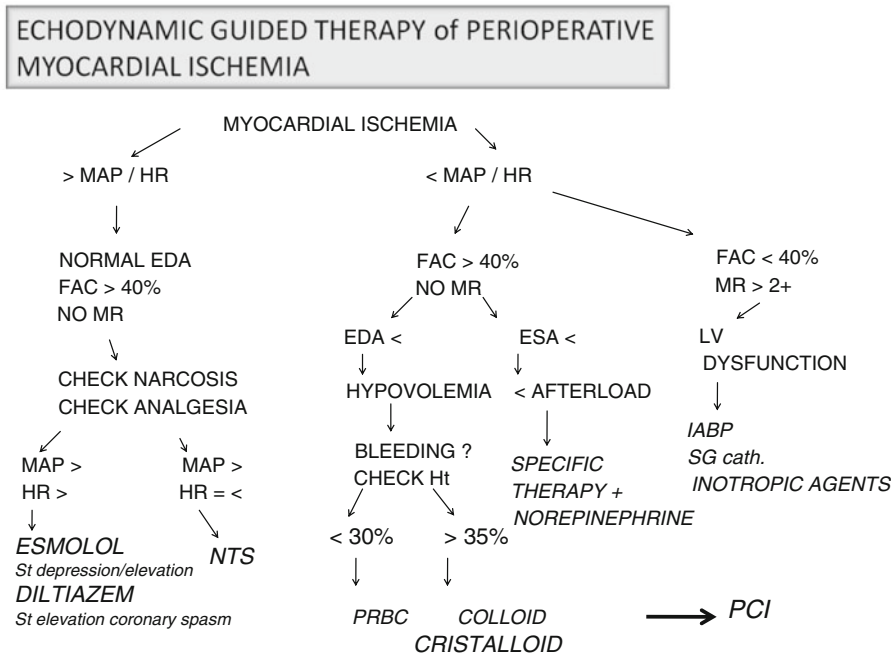

Fig. 27.1 Echo–dynamic-guided therapy for perioperative myocardial ischemia. *MAP* mean arterial pressure, *HR* heart rate, *EDA* end-diastolic area, *FAC* fractional area changes, *MR* mitral regurgitation, *NTS* nitrates, *ESA* end-systolic area, *PRBC* packed red blood cells, *IABP* intra-aortic balloon pump, *SG cath.* Swan–Ganz catheter, *PCI* percutaneous coronary inteventions, *cath.* catheter, *Ht* hematocrit,*St* segment of the electrocardiogram

of furosemide to prevent the development of pulmonary edema.

Among patients with a *decreased mean arterial pressure/heart rate* ratio, TEE identifies two groups: the first characterized by a normal LV systolic function (FAC > 40% in the absence of mitral regurgitation) and the other characterized by LV systolic dysfunction (FAC < 40%) and/or significant functional mitral regurgitation.

Many of the patients belonging to the first group have a *reduction in LV EDA*. Hypovolemia associated with acute anemia from surgical bleeding is the cause of hypotension and subsequent subendocardial ischemia in most cases. RV dysfunction must be excluded and other echocardiographic signs supportive of hypovolemia, such as a collapsed inferior vena cava (bicaval view), respiratory variations in stroke volume (transgastric long-axis view), and a good response to the leg-raising maneuver, must be confirmed before starting fluid therapy. Rapid volume infusion, based on hematocrit values, is recommended as the first step, and LV filling and function (transgastric view) are monitored through echocardiography.

In a few patients from the first group *LV end-systolic area (ESA) is also decreased* to such an extent that during systole the LV cavity may become virtual. In these patients a severe afterload reduction is the main mechanism of hypotension. All the possible causes should be evaluated and treated: spinal anesthesia, improper use of anesthetic or vasodilating agents, drug interactions with a preexisting antihypertensive therapy, especially with ACE-I, and an acute allergic reaction. Concomitantly, norepinephrine infusion at low or medium dose is recommended to correct hypotension.

Patients with a *low mean arterial pressure/heart rate ratio with LV dysfunction* and/or functional mitral regurgitation are at higher risk of in-hospital mortality for two reasons: (1) the underlying heart condition—if the arterial pressure is low, then the ischemic area is large or

akinetic areas from a previous acute myocardial infarction are present; (2) the therapeutic options are limited: beta blockers, calcium antagonists and nitrates are contraindicated or may be used at low doses. Patients with severe LV dysfunction have a higher incidence of myocardial ischemia compared with patients with a normal function since they have a lower coronary perfusion pressure (lower arterial pressure, higher LV end-diastolic pressure) and higher myocardial oxygen consumption (more enlarged left ventricle; la Place law). Most patients with LV dysfunction are receiving chronic therapy with beta blockers and ACE-I because of their beneficial effect on long-term survival; nonetheless, it has been well demonstrated that ACE and angiotensin I inhibitors potentiate the hypotensive effect of anesthetic agents and that beta blockers prevent the compensatory adrenergic responses. Finally, patients with LV dysfunction are more prone to the hemodynamic consequences of myocardial ischemia.

The mechanisms of hypotension responsible for myocardial ischemia in patients with LV dysfunction are several: an overzealous induction, an interaction between anesthetic drugs and ACE or angiotensin I inhibitors, an LV distension during aortic cross-clamping, and excessive volume expansion.

The demonstration of severe LV dysfunction associated with myocardial ischemia by TEE has important implications for the diagnostic and therapeutic decision-making, i.e., choice of medications, and devices, and for monitoring. Early coronary angiography followed by percutaneous myocardial revascularization is mandatory. Until coronary flow is restored, in-hospital mortality is high and drugs are poorly efficacious. If available, concomitant percutaneous intra-aortic balloon pump (IABP) insertion through the femoral artery is the treatment of choice because of its beneficial effects on myocardial oxygen balance, but its use may worsen aortic valve regurgitation and may be dangerous in patients with aortic aneurysm or peripheral vascular disease. Before IABP insertion, severe aortic regurgitation (mid-esophageal long-axis view of the aorta) and diffuse aortic type 5 atheromas complicated by mobile thrombus (descending aorta views) should be ruled out by TEE. During IABP insertion, echocardiography (proximal tract of descending thoracic aorta) assesses the correct positioning of the balloon distal to the left subclavian artery and excludes an uncommon but life-threatening complication, i.e., aortic dissection. When the IABP is started, complete balloon inflation and deflation can be seen in the same view (short and long axis). In those patients with a moderate aortic regurgitation, a worsening of the insufficiency (mid-esophageal long-axis view) and its effects on LV dimensions and function (mid-esophageal four-chamber or transgastric short-axis view) can and should be identified. An improvement in coronary blood flow in the left anterior descending (LAD) artery caused by the IABP can be confirmed by a skilled echocardiographer (in the mid-esophageal short-axis view at 30°, a few millimeters above the aortic valve, or in the mid-esophageal view at 150°). A few minutes after initiation of the IABP, its benefits on regional wall motion and LV function can be seen.

Inotropic agents, which are considered dangerous in patients with acute myocardial ischemia because of their adverse effects on myocardial oxygen balance, can be used safely provided that an associated LV severe systolic dysfunction is demonstrated by TEE (mid-esophageal four-chamber or transgastric short-axis views). The choice of the specific inotropic agent is based mainly on hemodynamic parameters, but echocardiography may be of additional help. Patients with severe mitral regurgitation (mid-esophageal views for the mitral valve) benefit from vasodilators with no risk of further reduction in systemic arterial pressure because of the improvements in cardiac output and systolic pressure consequent to the reduction of mitral regurgitation; ischemic mitral insufficiency is significantly improved by an IABP in most patients. Levosimendan and phosphodiesterase 3 inhibitors are theoretically recommended in patients with an associated diastolic dysfunction because of their lusitropic properties, but they have to be used with caution in patients with severe LV hypertrophy, especially if the LV cavity is reduced (transgastric short-

axis view), in order to avoid the risks of preload mismatch, hypotension, and worsening of myocardial ischemia, which are amplified by the long half-life of these drugs. Both drugs are contraindicated if LV outflow tract obstruction (by aortic stenosis or hypertrophic cardiomyopathy) is present. Aortic stenosis is well visualized in the upper esophageal short-axis view for the aortic valve, whereas LV outflow tract obstruction is well visualized in the in mid-esophageal four-chamber view or long-axis view at 120° of the aorta. The gradient can be measured with continuous wave Doppler echocardiography in the long-axis view at 120° or in the deep transgastric view.

In the evaluation of LV function, echocardiography is helpful in distinguishing scarred areas, caused by a previous transmural myocardial infarction and which have no possibility of recovery, from ischemic viable myocardium. Scar areas appear bright and their wall thickness is less than 5 mm. These echocardiographic characteristics of scarred areas correlate well with the presence of myocardial fibrosis on magnetic resonance imaging. The extension of myocardial scarred areas is useful to anticipate a poor response to inotropic agents.

The effects of revascularization on regional wall motion and of inotropic agents on LV function can be monitored by echocardiography in the mid-esophageal and transgastric views. In most patients, regional wall motion abnormalities and LV dysfunction persist for hours to days even after effective myocardial revascularization, owing to a reversible stunning phenomenon. Therefore, a lack of early improvement must not be interpreted as an ominous sign.

Insertion of a Swan–Ganz (SG) catheter may be considered in these patients in order to guide the administration of inotropic agents and fluids. The tip of the SG catheter is well visualized by ultrasonography, so TEE may be useful to guide positioning of the SG catheter from the right atrium (mid-esophageal bicaval view), through the tricuspid valve, the right ventricle, and the pulmonary valve (mid-esophageal inflow-outflow view of the right ventricle) to the right pulmonary artery (upper esophageal short-axis view of the aorta).

27.3 RV Involvement

An enlarged and hypokinetic right ventricle (mid-esophageal four-chamber, transgastric short- and long-axis views of the right ventricle) with specific markers of dysfunction (i.e., reduced TAPSE, Sa, RV FAC) complicated by functional tricuspid valve regurgitation with normal or only mildly elevated pulmonary arterial pressure (mid-esophageal LV inflow and outflow views) associated with LV inferior wall akinesia is diagnostic of RV ischemia. It is imperative that myocardial revascularization of the right coronary artery be performed as soon as possible, even more so in patients with the complication of cardiogenic shock. The recognition of RV stunning is important because, in addition to specific therapy for the underlying cause (i.e., myocardial revascularization), the appropriate treatment strategy is quite different from that for LV dysfunction. A careful balance between optimized preload and decreased afterload is essential. Drugs (mainly nitrates, diuretics, and opioids) and maneuvers that reduce RV preload and some subsets of mechanical ventilation must be avoided. RV preload is maintained by fluid loading. Initially, a volume challenge of 500–1,000 ml should be administered, provided that the pulmonary arterial pressure (mid-esophageal LV inflow and outflow views) is normal or only mildly increased, the left ventricle is not severely dysfunctional (transgastric short-axis view), and mitral regurgitation is no more than moderate (mid-esophageal four-chamber, commissural, and long-axis views). Subsequently, fluid infusion velocity should be reduced and no further volume challenge should be administered if no hemodynamic benefit has been achieved. Whether traditional predictors of fluid responsiveness (e.g., stroke volume variations, passive leg raising) are applicable to isolated RV dysfunction is not known and needs further study; respiratory variations in vena cava diameter are useless because of the high right atrial pressure. Passive leg raising may be a better predictor of fluid responsiveness in patients with

spontaneous respiration. Careful hemodynamic and echocardiographic monitoring is nonetheless required during fluid expansion. If fluid administration is too vigorous and preload increases excessively, the interventricular septum shifts leftward (transgastric short-axis view) and LV stroke volume (deep transgastric view) decreases; diuretics may be indicated in this case.

Mechanical ventilation, especially if a high tidal volume and a positive end-expiratory pressure are used, increases intrathoracic pressures and RV afterload and decreases RV preload. Therefore, the lowest tidal volume, plateau pressure, and positive end-expiratory pressure necessary to provide adequate ventilation and oxygenation should be used, avoiding at the same time the development of a degree of permissive hypercapnia capable of determining pulmonary vasoconstriction and a subsequent increase in RV afterload. Adequate oxygenation is of utmost importance in order to avoid afterload increases due to hypoxic pulmonary vasoconstriction. Patency of the fossa ovalis, especially if a septal aneurysm coexists, may be associated with a right-to-left shunt and with a subsequent worsening of hypoxia and therefore should be visualized by TEE (bicaval view). The effects of ventilation on RV shape and function are monitored by echocardiography: a leftward shift of the atrial or ventricular septum (mid-esophageal four-chamber view) and a worsening of tricuspid valve regurgitation (RV inflow–outflow view) indicates an excessive increase in afterload.

The choice of the most appropriate inotropic agent is mainly based on hemodynamic parameters. Dobutamine remains the preferred drug in patients with no significant hypotension; norepinephrine is usually beneficial in hypotensive and tachycardic patients who do not respond to dobutamine. Levosimendan has a more specific pulmonary vasodilatory effect but its use is limited by hypotension and arrhythmias; therefore, further studies are needed before its use can be recommended. The effect of inotropic drugs on RV function are immediately visible as an improvement in regional wall motion (mid-esophageal four-chamber, inflow–outflow, and transgastric short-axis views) and a reduction of tricuspid valve regurgitation and can be quantified (mid-esophageal four-chamber view) by means of TAPSE, tissue Doppler imaging, and RV FAC.

Since the right ventricle poorly tolerates afterload increases, pulmonary vasodilators may be used. The combination of inhaled NO and dobutamine is supported by the best current evidence; sildenafil may be of particular benefit when combined with dobutamine or inodilators.

In evaluating the benefits of treatment on RV function, attention must be paid to the ambiguous behavior of the pulmonary pressure. A decrease in systolic pulmonary arterial pressure may be due to a beneficial effect of pulmonary vasodilators on vascular resistances (improvement of RV function), but it may also reflect a worsening of RV failure.

27.4 How To Do It

The best views for identifying myocardial ischemia and for therapeutic monitoring are the transgastric short-axis views. These cross-section views have the advantages of showing the LV territories supplied by all three coronary arteries simultaneously and at the same time of monitoring ventricular filling (EDA), afterload (ESA), and the effects of ischemia on LV (FACs) and RV function.

The transgastric views are acquired by advancing the probe into the stomach and anteflexing the tip to obtain the short axis, in which the left ventricle has a circular shape and the right ventricle a crescent-like shape. The image depth is adjusted to include the entire left ventricle, usually at 12 cm. The probe is advanced or withdrawn in order to reach the appropriate level: basal (at the mitral valve height), mid (at the height of the papillary muscles), and apical (apex).

Myocardial ischemia appears as a reduction in regional wall motion and systolic thickening. Regional systolic thickening is best appreciated by M-mode echocardiography, which has a better temporal and spatial resolution. In short-

axis views, only inferior and anterior walls are perpendicular to the M-mode ultrasonic beam; long-axis views are needed to align the beam with the septum and lateral wall. Some limitations of echocardiography in the detection of ischemia should be recognized. Interpretation of regional wall motion may be difficult because of the rotation and translation movements of the heart, asynchrony due to left bundle branch block or pacing, and the tethering of a contiguous zone of myocardial fibrosis.

An abnormal motion of the anterior wall (transgastric short-axis view) indicates an obstruction of the LAD artery. The outcome for patients with an inferior ST-segment elevation myocardial infarction depends in large part on the occluded artery: the right coronary (80%) or left circumflex (20%) artery. In-hospital survival is lower in patients with right coronary occlusion because of its associated complications, i.e., RV involvement and conduction disturbances. When the inferior and the posterior wall (posterolateral branch) and the ventricular septum are involved, the culprit lesion involves the right coronary artery. Motion abnormalities in the lateral and possibly the posterior walls (posterolateral branch) suggest involvement of the left circumflex artery.

Counterclockwise rotation of the biplane probe shows the right ventricle (transgastric short-axis view), where kinesis of the RV lateral and anterior wall can be inspected.

Akinesia of the segments associated with LV proximal inferior wall motion abnormalities is diagnostic of RV infarction. Akinesia involving the basal segments is indicative of a proximal coronary obstruction and carries a high risk of severe LV (anterior wall) or RV (inferior wall) dysfunction.

In most patients, TEE can be used to visualize the left main coronary artery (visible in the upper esophageal short-axis view, 1 cm above the aortic valve and with the probe rotated about 15–30°), the proximal tract of the LAD artery, the left circumflex artery (mid-esophageal view at 130–160° at the level of the left atrioventricular sulcus) and the ostium odf the right coronary artery (mid-esophageal long-axis view at 120° of the ascending aorta). Coronary blood flow can be measured by color Doppler imaging. The occurrence of the aliasing phenomenon is a marker of flow turbulence due to a significant coronary stenosis. Diastolic velocity can be quantified by pulsed Doppler imaging. The normal values of the peak diastolic velocity are 1.4 m/s in the left main truncus, 0.9 m/s in the LAD artery, and 1.1 m/s in the common carotid artery. In patients with a coronary stenosis, the transstenotic blood velocity is significantly increased. The aliasing phenomenon and abnormal coronary Doppler flow patterns of velocities associated with regional wall motion abnormalities are indicative of severe and proximal coronary artery disease. Break of color mapping, absence of a Doppler spectrum, and retrograde diastolic blood flow are echocardiographic criteria for coronary artery occlusion.

The effects of myocardial ischemia on global LV systolic function can be quantified by calculation of the FAC (EDA − ESA/EDA) in the transgastric short-axis view at the mid-papillary level or by the ejection fraction (end-diastolic volume − end-systolic volume/end-diastolic volume) in the mid-esophageal four-chamber view. This view is useful to complete the study of wall motion abnormalities, to evaluate the degree of mitral valve and tricuspid valve regurgitation, to study the diastolic function, and to measure the left atrial pressure. By rotating of the probe from the mid-esophageal four-chamber view to the long-axis view at 120°, one can visualize all walls of the left ventricle and can quantify the extent of ischemia. Color Doppler imaging applied to the long-axis view is necessary to exclude an aortic valve regurgitation that would contraindicate IABP use. Mitral valve regurgitation is quantified by color Doppler imaging in the four-chamber, commissural, and long-axis views.

After completion of the estimation of the mitral valve regurgitation, pulsed wave Doppler imaging and tissue Doppler imaging of mitral valve annulus are performed to evaluate the severity of associated diastolic dysfunction and to measure the left atrial pressure.

In patients with an acute inferior myocardial infarction, RV function is quantified (mid-esophageal four-chamber view) by M-mode echocardiography (TAPSE), tissue Doppler imaging evaluation of tricuspid annulus (Sa), and 2D FACs. Withdrawal of the probe to the inflow–outflow view and subsequent application of color Doppler imaging allows the visualization of tricuspid valve regurgitation; systolic pulmonary arterial pressure can be measured through continuous wave Doppler imaging (adding the right atrial pressure).

Finally, a study of the descending thoracic aorta is performed to detect complicated atheromas that are dangerous for IABP placement.

Hypovolemia and Fluid Responsiveness 28

Armando Sarti, Simone Cipani, and Massimo Barattini

28.1 Introduction

The veins contain around 70% of the body's entire blood volume. They contain a large volume even when their transmural pressure is near zero (venous capacitance). This reserve unstressed volume does not produce ongoing flow to the heart. According to Guyton's description of cardiocirculatory function, only the stressed volume within the venous system generates the venous return, which is determined by the difference between the mean systemic filling pressure (the intravascular pressure at cardiac arrest) and right atrial pressure against the resistance to venous flow (Fig. 28.1). The mean systemic filling pressure may increase because of augmented blood volume or the transfer of venous blood from the unstressed to the stressed volume, due to venoconstriction through adrenergic stimulation. In contrast, a reduced mean systemic filling pressure, whether absolute (hypovolemia) or relative (transfer of blood from the stressed to the unstressed volume due to increased venous compliance), always causes a reduced venous return.

As blood volume decreases, a critical balance may be suddenly disturbed through an increase of intrathoracic pressure. Indeed, in clinical practice a compensated hypovolemia is promptly unmasked by severe hypotension just after the institution of positive pressure mechanical ventilation with or without positive end-expiratory pressure.

28.2 Is the Blood Volume Adequate?

Inadequate cardiovascular filling is very common in emergency department and ICU patients. Obvious causes of hypovolemia include external or internal bleeding and loss of circulating body fluid due to insufficient oral or parenteral intake, excessive diuresis, diarrhea, or the redistribution of fluid between the intravascular and extravascular compartments. Inappropriate or excessive diuretic therapy is common in both medical and surgical wards for treating oliguria and fluid retention. The traumatic or surgical insult produces hemorrhages and capillary leakage of fluid and albumin from the vascular space. The clinical picture of severe sepsis and septic shock includes either absolute hypovolemia, due to third space losses, or relative hypovolemia, caused by peripheral redistribution of blood volume. Whether hypovolemia is absolute or relative, the heart is not properly filled and cardiac output decreases. Initially, arterial pressure

A. Sarti (✉)
Department of Anesthesia and Intensive Care, Santa Maria Nuova Hospital, Florence, Italy
e-mail: armando.sarti@asf.toscana.it

A. Sarti and F.L. Lorini (eds.), *Echocardiography for Intensivists*,
DOI: 10.1007/978-88-470-2583-7_28,

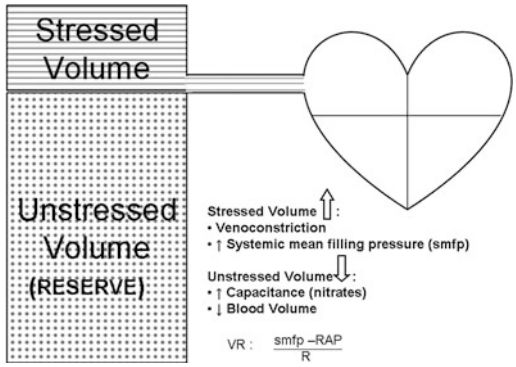

Fig. 28.1 Stress volume and unstressed volume. Only the stress volume generates the venous return (*VR*). See the text for details. *Smfp* mean systemic filling pressure, *RAP* right atrial pressure. *R* resistance to flow

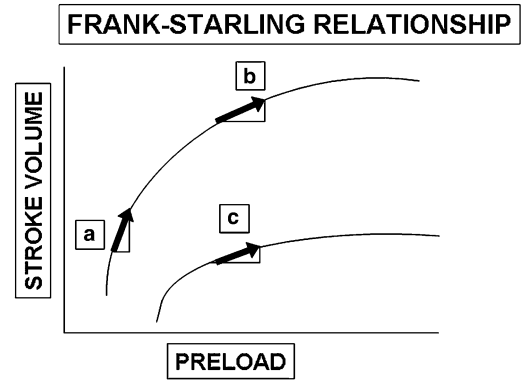

Fig. 28.2 Frank–Starling relationship. Two curves reflecting different heart performance conditions. **a** Fluid responsive (a small increase in preload induces a significant increase of stroke volume). **b**, **c** Fluid unresponsive (a big increase of preload does not induce a significant increase of stroke volume)

may not decrease if systemic vascular resistance increases sufficiently.

Systematic large volume expansion in the first few hours of circulatory failure due to severe sepsis and septic shock decreases mortality. Also, uncorrected hypovolemia leads to improper infusion of vasopressors such as norepinephrine, with subsequent organ hypoperfusion and aggravating tissue ischemia.

28.3 Should I Provide a Fluid Bolus?

On the admission of the patient to the emergency department or ICU, the clinical signs of manifest hypovolemia, such as tachycardia, hypotension, oliguria, altered mental status, and mottled or pale skin with augmented capillary refill time, may immediately suggest a positive response to a bolus of fluid infusion. In this case there is initially no need for more sophisticated information. However, for hospitalized patients who experience hemodynamic instability, a favorable response to fluid resuscitation should not be always expected. Indeed, excessive volume expansion may cause interstitial edema in many organs, including the lungs, and is clearly associated with increased morbidity and mortality.

Traditionally, fluid responsiveness has been assessed by graded volume loading, but this may easily lead to fluid overload. Indeed, in septic patients, positive cumulative fluid balance has been shown to be an independent risk factor for death. The end point of fluid resuscitation may often be unclear and hence arbitrary. Occasionally, the futility (or worse, the harmfulness) of ineffective volume expansion is realized only after multiple, ineffective fluid boluses have been given.

Therefore, it is not surprising that rapid volume expansion as a first-line therapy is a crucial decision and has a vital key role in the cardiovascular resuscitation of seriously ill patients. Hypotension and signs of tissue hypoperfusion, such as central venous desaturation, increased levels of lactates, augmentation of the venous–arterial carbon dioxide gradient, and oliguria elicit a possible role for volume expansion. It has been reported that only around 50% of critically ill patients will respond to a volume bolus with significant increase in stroke volume and cardiac output (fluid responsiveness). The response depends on where the heart of the patient with hemodynamic instability and hypoperfusion is located on the Frank–Starling curve (Fig. 28.2). On the steep portion of the curve the heart will respond to a fluid bolus with an increase of end-diastolic volume, stroke volume, and cardiac output (preload reserve). In contrast, on the flat part of the curve the heart does not respond with a significantly increased

stroke volume (Fig. 28.2), but responds only with fluid overload and rising filling pressure (preload unresponsiveness). Also, for the single patient the Frank–Starling relationship between preload and stroke volume is not stable, but changes with its position with different ventricular contractility, which can be extremely variable and not easily measured in clinical practice. At a determined preload, many other factors may influence the Frank–Starling curve, such as aortic impedance and the complex effects of mechanical positive pressure ventilation.

Thus, whether to provide a fluid bolus is a critical decision of the utmost importance, particularly in the current practice of intensive care characterized by ageing patients with preexistent chronic cardiovascular dysfunction. These patients have a greater chance of being fluid-unresponsive. So the only way to avoid useless or even harmful fluid load is simply to challenge the Frank–Starling relationship to establish the possible positive response to a fluid bolus before giving it, that is, predicting fluid responsiveness. Echocardiography, with all the vital information on cardiovascular functional anatomy it provides, has become the best tool to assess volume status, predict fluid responsiveness, and guide fluid therapy in the emergency and ICU setting.

28.4 Hypovolemia

Central venous pressure (CVP) and pulmonary artery occlusion pressure (PAOP) are both generally decreased during manifest hypovolemia, even if previous right ventricular (RV) or left ventricular (LV) dysfunction or valve disease may well alter these measures. A low CVP, such as below 3–4 cmH_2O, may suggest emptiness of the central veins, but no information can be obtained above this pressure. Doppler interrogations of the regurgitation jets of the atrioventricular valves can be used to estimate CVP and PAOP without central venous or pulmonary artery catheters, but their effectiveness as a guide to fluid therapy is limited. Thus, cardiac filling pressures are poor predictors of preload and neither CVP nor PAOP can be used to predict fluid responsiveness in patients who breathe spontaneously or in patients on positive pressure ventilation. End-diastolic dimensions are considered better indicators of cardiac preload than filling pressure, but nonetheless they cannot accurately predict fluid responsiveness because the chamber dimensions may be reduced or dilated as a result of many previous or concomitant alterations. It must always be remembered that an assessment of preload is not an assessment of fluid responsiveness, particularly in critically ill patients.

If previous biventricular function is preserved, the echocardiographic appearance of a full-blown picture of hypovolemia is consistent with a small hyperkinetic fast-beating heart. Both end-diastolic and end-systolic dimensions of all cardiac chambers are decreased, with LV cavity end-systolic obliteration. In spontaneously breathing patients, a small inferior vena cava (IVC; transthoracic echocardiograpy, TTE) or superior vena cava (SVC; transesophageal echocardiography, TEE) is visualized with complete inspiratory collapse. In mechanically ventilated patients, small dimensions of the venae cavae with evident respiratory changes are seen at end expiration. All echocardiographic views can show this hypovolemic small-chamber-low-flow imaging:

- No distance is seen during diastole between the septum and the anterior leaflet of the mitral valve in the parasternal long-axis view (TTE) because of the reduced ventricular diameter, as well as the reduced width of the aortic cusps opening in systole with a slowing of aortic closure in diastole.
- In the parasternal short-axis view (TTE) or the transgastric short-axis view (TEE), the section of the left ventricle at the level of the papillary muscles shows reduced LV end-diastolic area (below 5.5 cm^2/m^2) and end-systolic area with a complete, or almost complete, systolic obliteration of the cavity (kissing ventricle). (Fig. 28.3).
- Reduction of all end-diastolic and end-systolic volumes in the apical four-chamber view (TTE) (Fig. 28.4) and mid-esophageal four-

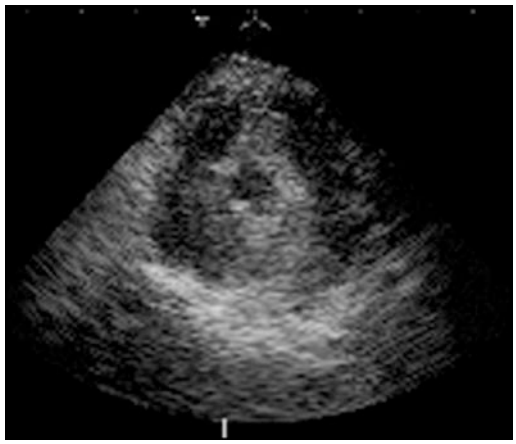

Fig. 28.3 Parasternal short-axis view, papillary muscle level, transthoracic echocardiography (TTE). Obliteration of the left ventricular (RV) cavity in systole (kissing ventricle)

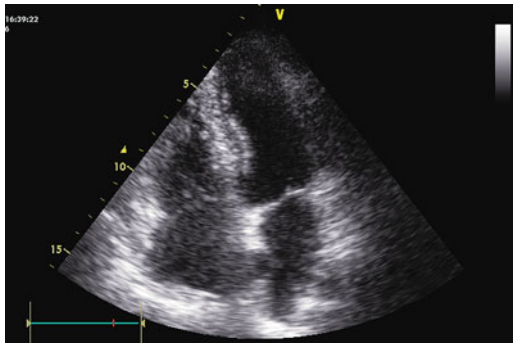

Fig. 28.4 Apical four-chamber view TTE. Reduced volumes of all the cardiac chambers in hypovolemia

chamber view at 0° (TEE) with reduced transmitral flow (E wave).

- Reduced velocity–time integral (VTI) in the RV outflow tract and pulmonary trunk (parasternal short-axis view, TTE, and mid-esophageal ascending aorta view, TEE) and in the LV outflow tract (LVOT) (apical five-chamber or three-chamber view, TTE, and deep transgastric view, TEE) owing to reduced stroke volume.
- Small IVC (subcostal TTE, transgastric 60° off-axis TEE) less than 12 mm in spontaneously breathing patients and less than 15 mm in patients with mechanical ventilation and small SVC (mid-esophageal bicaval view, TEE) together with large respiratory changes.

28.5 Passive Leg Raising

Emergency rescuers have raised the lower limbs for years in order to increase heart filling and blood arterial pressure. Passive leg raising (PLR) has been proposed as a preload-modifying maneuver without any potentially harmful fluid infusion. ICU patients are normally kept in a semirecumbent position with the trunk lifted to 45° and the legs in the horizontal plane. Lifting the legs to around 45°, while at the same time lowering the trunk to the horizontal plane, induces a gravitational transfer of blood from the lower part of the body and the abdomen to the thoracic central circulatory compartment (Fig. 28.5). LV filling, stroke volume, and then cardiac output will increase if the right ventricle and then the left ventricle are fluid-responsive. This autotransfusion, estimated to be between 300 and 500 ml, is immediately and fully reversed when the trunk is lifted and the legs are laid down. This technique of predicting fluid responsiveness can also be used in spontaneously breathing patients and in the presence of arrhythmias. This is particularly important, since dynamic indices based on oscillation of preload (see below) are not reliable in patients who breathe spontaneously or with atrial fibrillation. An increase of stroke volume greater than 15% after PLR can predict a positive response to a fluid bolus with good sensitivity and specificity. Since the response to PLR is transient, the possible change of stroke volume (or only VTI since the LVOT cross-sectional area does not change acutely) must been assessed using TTE or TEE just after the maneuver and continuing for at least 1 min. Sometimes the PLR maneuver may stress or cause pain to the patient, especially after surgery or trauma.

28.6 Heart–Lung Interactions

28.6.1 Pulse Pressure, Stroke Volume, and VTI Variation

In spontaneously breathing patients the systolic arterial pressure falls slightly during inspiration. This is due to increased venous return and

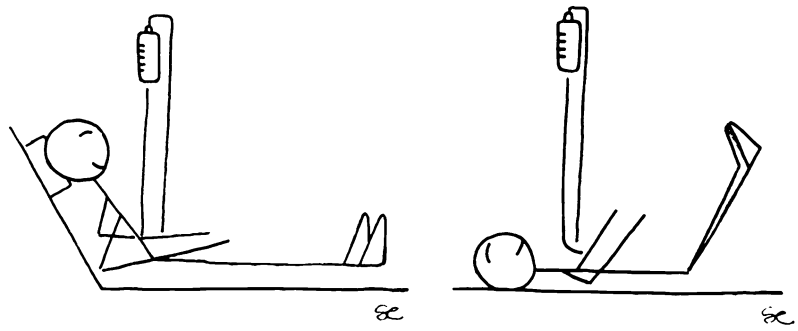

Fig. 28.5 Passive leg raising maneuver. *Left* The normal position of the ICU patient. *Right* Legs lifted to around 45° and trunk lowered to the horizontal plane. The blood is transferred from the lower part of the body and the abdomen to the thoracic central circulatory compartment (autotransfusion)

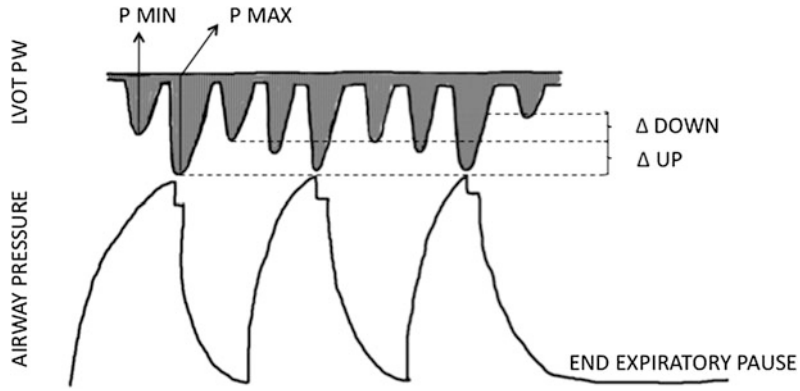

Fig. 28.6 Pulsed wave Doppler velocity–time integral (VTI) at the LV outflow tract recorded continuously during mechanical ventilation. Changes in VTI (below the baseline because the flow runs away from the probe) directly reflect changes in LV stroke volume. Note Δdown and Δup. Δdown reflects fluid responsiveness. $P = \mathrm{VTI}_{\mathrm{peak}}$. See the text for details and limitations

ventricular interdependence. A greater fall (more than 10 mmHg) is observed in many clinical conditions, such as hypovolemia, cardiac tamponade, acute severe asthma, massive pleural effusion, anaphylactic shock, and pulmonary embolization (pulsus paradoxus). Mechanical ventilation with or without positive end-expiratory pressure decreases venous return owing to an increase in intrathoracic pressure if the chest is not opened. During mechanical ventilation, cyclic changes are observed in pulse pressure (reversed pulsus paradoxus). Small changes in arterial pulse pressure during positive pressure ventilation are also frequently caused by ventricular interdependence. In this case, because of diminished LV afterload and enhanced LV pulmonary venous flow (squeezing of blood out of the lungs), the LV systolic ejection transiently increases during the ventilator-derived inspiration relative to the level observed during the expiratory pause (Δup). This Δup effect has been described in congestive heart failure, and it might actually suggest the need for volume reduction rather than expansion.

At the end of positive pressure inspiration, the LV stroke volume (and pulsed wave Doppler VTI at the LVOT, which directly reflects the stroke volume) decreases as a result of depressed RV preload and ejection due to increased intrathoracic pressure, which propagates to the left ventricle after a few heartbeats (Δdown) (Fig. 28.6). Disappearance or clear blunting of Δdown during mechanical ventilation is a marker of preload insensitivity (Fig. 28.7). Preload

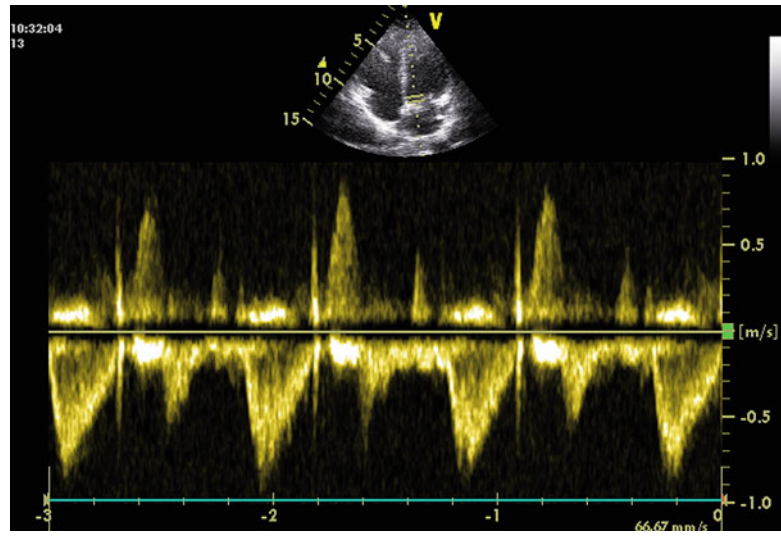

Fig. 28.7 Apical five-chamber view, TTE. Pulsed wave Doppler VTI at the LV outflow tract recorded during a mechanical breath. No fluctuation of the VTI (preload insensitivity)

sensitivity and fluid responsiveness is thus associated with and is proportional to Δdown, which is linked to the heart operating in the steep portion of the Frank–Starling relationship. This has been demonstrated in both ventilated surgical and septic patients. The entire fluctuation (Δdown plus Δup) (Fig. 28.8) of stroke volume or pulse pressure (ΔPP, maximal–minimal systolic pressure) induced by mechanical breathing (inspiration and expiration) has been similarly validated.

28.6.2 Vena Cava Variation

The cyclic effects of positive pressure ventilation are also evident in the geometry of the venae cavae with increased diameter during inspiration and decreased diameter in the expiratory phase (Fig. 28.9). Ventilator-derived positive intrathoracic pressure will dilate more an incompletely-filled IVC because of the transmission of increased pleural pressure and increased transmural pressure, since intrabdominal pressure only increases partially. It is intuitive that the transmural pressure change of the venae cave will more readily translate into cross-sectional size variations during mechanical ventilation when imposed on a partially empty vessel (hypovolemia). Studies have demonstrated that the amplitude of phasic changes in the diameter of the venae cavae is highly predictive of an increase of cardiac output after a fluid bolus has been given. The SVC is not influenced by intra-abdominal pressure and it is only subjected to pleural pressure, directly reflecting the interaction between central volume and intrathoracic pressure. Thus, the wider SVC variation during mechanical ventilation correlates particularly well with fluid responsiveness and is considered even more reliable.

28.7 Screening for the Tolerance to Volume Load and Assessment of the Effect of Fluid Boluses

Low tolerance to fluid load and relative fluid unresponsiveness are expected in patients who present with signs of systemic or pulmonary venous congestion and left and right systolic or diastolic ventricular dysfunction.

An enlarged right ventricle with septal dyskinesia is consistent with right-sided heart dysfunction. The echocardiographic parameters of LV diastolic dysfunction and elevated LV filling pressure are as follows:

- Left atrium enlargement
- *E*/*A* ratio of the Doppler transmitral flow - greater than 1.5
- Deceleration time less than 150 m/s
- E/E' (or E/E_a) ratio greater than 15
- S < D wave of pulsed wave Doppler pulmonary vein flow

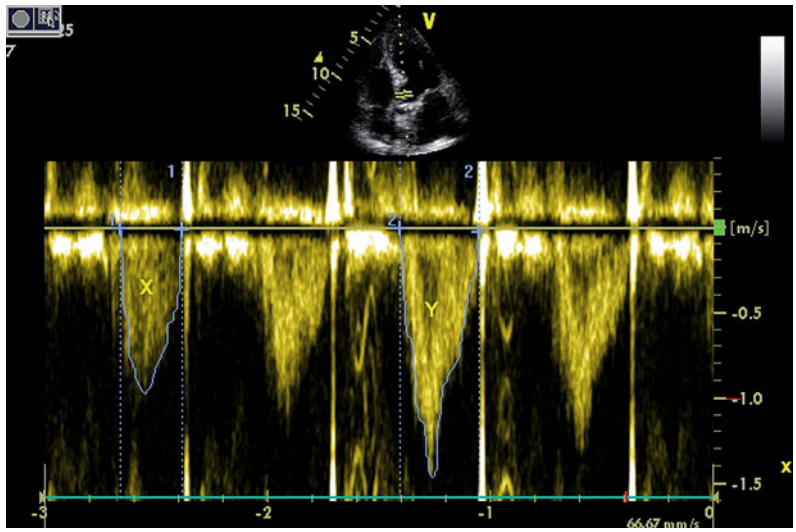

Fig. 28.8 Apical five-chamber view, TTE. Wide VTI fluctuation during a mechanical breath in a clearly fluid responsive patient. X = VTI 19.1 cm; Y = VTI 29 cm. $\Delta VTI = 100 \times (VTI_{max} - VTI_{min})/(VTI_{max} + VTI_{min}/2) = 43\%$. See the text for further details

- Reversed pulmonary vein flow time (A_r) greater than atrial systole time (A) of the mitral forward flow

These parameters of RV and LV function, as well as the filling patterns, must be assessed before fluid expansion and again during volume loading, after each bolus has been given, to detect early signs of dysfunction and increasing filling pressure.

28.8 Limitations of Fluid Responsiveness Indices Derived from Heart–Lung Interaction

1. Functional hemodynamic parameters can be used only in patients who are on fully and stable mechanical ventilation. No spontaneous respiratory effort should be observed. A tidal volume of 8 ml/kg was shown to be necessary to produce the indices of fluid responsiveness. Patients with acute lung injury or acute respiratory distress syndrome are normally ventilated with lower tidal volumes, but they also exhibit markedly decreased lung compliance. Thus, a lower tidal volume should still generate a large variation of airway and intrathoracic pressure.
2. Respiratory variations in LV stroke volume can be influenced by increasing respiratory rate, whereas SVC variations seem to be unaffected. This may suggest that right and left indices of preload variations can be dissociated.
3. In RV failure, the inspiratory increase of RV impedance is a major determinant of stroke volume variations. These patients should not be considered fluid-responsive since volume expansion may simply not reach the left ventricle, and may only increase RV filling pressure. This is seen particularly in patients on mechanical ventilation who show severe RV dysfunction.
4. Arrhythmias can certainly produce stroke volume variations unrelated to fluid responsiveness. Thus, a regular and stable sinus rhythm is an essential requirement.
5. Acute changes of aortic impedance might alter stroke volume variations. Some animal studies have shown that norepinephrine infusion might reduce the value of dynamic changes, but further study is needed to clear up this point.
6. An increase in intra-abdominal pressure might alter the cyclic variation of the IVC. Theoretically, the SVC could be less affected, but no data are available to confirm this.

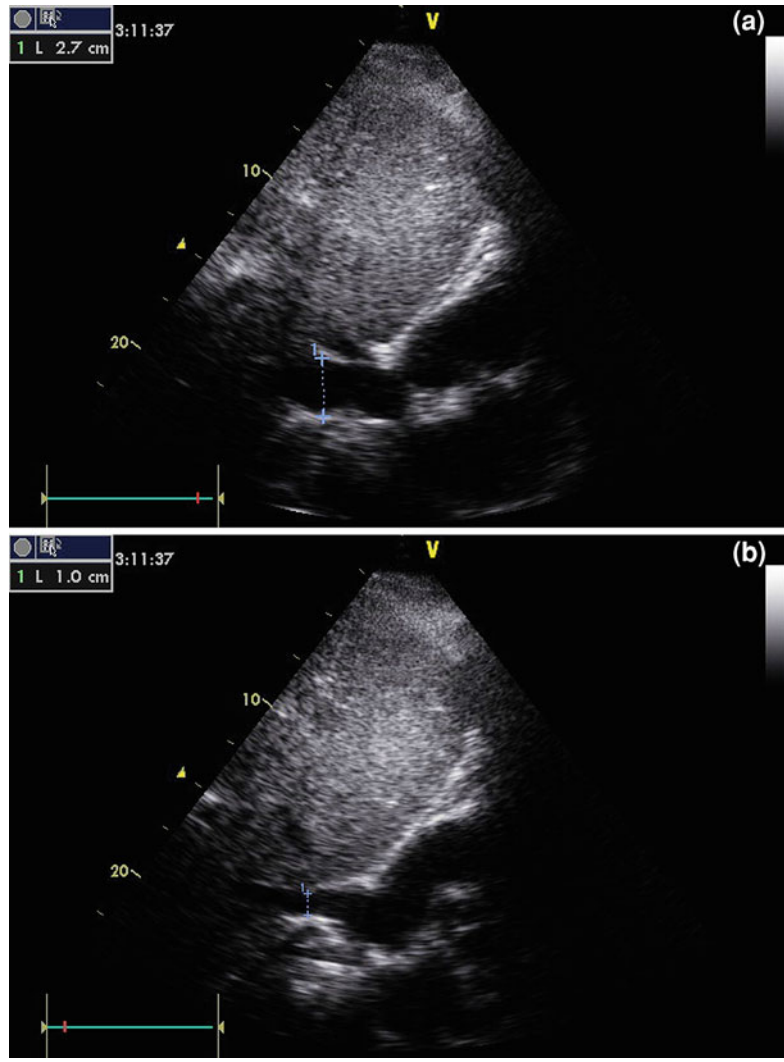

Fig. 28.9 Subcostal TTE for the inferior vena cava. Inferior vena cava diameter variation during a mechanical breath. **a** Inspiration and **b** expiration

If all these limitations cannot be ruled out, the only way to predict fluid responsiveness is by observing the effect of the PLR maneuver on stroke volume .

28.9 Indices of Fluid Responsiveness

28.9.1 Vena Cava Collapsibility

The vena cava collapsibility index (ΔVC) is the percentage variation of the cava diameter during inspiration versus expiration (IVC, subcostal TTE, and SVC, mid-esophageal bicaval TEE):

$\Delta IVC = 100 \times (IVC_{insp} - IVC_{exp})/IVC_{insp}$ (Fig. 28.9). A variation greater than 18% predicts fluid responsiveness.

$\Delta SVC = 100 \times (SVC_{insp} - SVC_{exp})/SVC_{insp}$. In this case a variation greater than 36% is used as a predictor.

28.9.2 Stroke Volume Variations

Using pulsed wave Doppler interrogation (apical five-chamber or three-chamber view, TTE, and deep transgastric view at 0°, TEE) at the level of the LVOT (aortic annulus), one can detect the VTI of LV ejection. The product of VTI and LVOT cross-sectional area equals stroke volume. This

method is normally used to measure cardiac output (stroke volume times heart rate) through echocardiography. Considering that the area of the aortic annulus does not change acutely, it is only possible to measure VTI to detect changes in stroke volume. The variation of either the VTI or the peak velocity (P) of LV ejection (the highest level of the VTI curve) can be used to predict fluid responsiveness as follows:

$\Delta VTI = 100 \times (VTI_{max} - VTI_{min})/(VTI_{max} + VTI_{min}/2)$;

$\Delta P = 100 \times (P_{max} - P_{min})/(P_{max} + P_{min}/2)$.

$\Delta VTI > 18\%$ (Fig. 28.8) and $\Delta P > 12\%$ are expressive of fluid responsiveness.

Further Reading

Charron C, Caille V, Jardin F et al (2006) Echocardiobraphic measurement of fluid responsiveness. Curr Opin Crit Care 12:249–254

De Backer D, Taccone FS, Holsten R et al (2009) Influence of respiratory rate on stroke volume variation in mechanically ventilated patients. Anesthesiology 110:1092–1097

Fehil F, Broccard AF (2009) Interactions between respiration and systemic hemodynamics. Part I: basic concepts. Intensive Care Med 35:45–54

Feihl F, Broccard AF (2009) Interactions between respiration and systemic hemodynamics. Part II: practical implications in critical care. Intensive Care Med 35:198–205

Gerstle J, Shahul S, Mahmood F (2010) Echocardiographically derived parameters of fluid responsiveness. Int Anesthesiol Clin 48(1):37–44

Pinsky MR (2007) Heart-lung interactions. Curr Opin Crit Care 13:528–531

Teboul JL, Monnet X (2008) Prediction of volume responsiveness in critically ill patients with spontaneous breathing activity. Curr Opin Crit Care 14:334–339

ARDS, ALI, Mechanical Ventilation, and Weaning

29

Federica Marini, Carla Farnesi, and Armando Sarti

29.1 Introduction

Mechanical ventilation for acute respiratory failure is a routine aspect of patient treatment in the ICU. Acute lung injury (ALI) and its more severe subset acute respiratory distress syndrome (ARDS) are the results of bilateral and diffuse alveolar damage due to an acute insult.

Lung computerized tomography (CT) is the gold standard for evaluating lung morphology and for assessing the effects of different therapies on lung reaeration. However, performing a lung CT scan generally requires transportation of the patient to the radiology department, the presence of trained physicians, and sophisticated cardiorespiratory monitoring. Moreover, radiation exposure limits its repeatability.

Ultrasonography is increasingly being used in the treatment of the critically ill patient as a noninvasive diagnostic and monitoring tool. Chest ultrasonography in patients with ALI/ARDS has been proposed to assess initial abnormalities of lung morphology, to monitor the effects of the therapy, and to optimize positive end-expiratory pressure (PEEP).

Lung ultrasonography has intrinsic patient-dependent limitations, such as obesity and the presence of subcutaneous emphysema, which makes the examination difficult. There is also an operator-dependent limitation even though the learning curve for general transthoracic lung ultrasonography is rather short for residents (less than 3 weeks).

Pulmonary processes can be visualized when they come up to the pleura, and are accessible via a sound window without subcutaneous emphysema or pneumothorax. Purely central processes cannot be visualized sonographically and therefore cannot be ruled out with this technique.

29.2 Pneumonia

The sonographic findings of pneumonia (see also Chap. 45) are as follows:

1. Liver-like in the early stage. The echo texture of the consolidated lung is similar to that of the liver.
2. Air bronchogram. Viral or fungal pneumonias are quite often more poorly ventilated and produce less marked air bronchograms.
3. Air trapping, which can be focal or diffuse. Severe airflow obstruction increases airway resistance and causes intrinsic PEEP.
4. The fluid bronchogram is characterized by anechoic/hypoechoic branched tubular structures in the course of the bronchial tree. A persistent fluid bronchogram arouses suspicion of poststenotic pneumonitis and requires bronchoscopic investigation.

F. Marini (✉)
Department of Anesthesia and Intensive Care, Santa Maria Nuova Hospital, Florence, Italy
e-mail: federica.marini@asf.toscana.it

A. Sarti and F. L. Lorini (eds.), *Echocardiography for Intensivists*,
DOI: 10.1007/978-88-470-2583-7_29,

5. Blurred, irregular, and serrated margins of a consolidated area are characteristic of pneumonia.
6. Reverberation echos in the margin of the consolidation areas.
7. Hypoechoic abscess formation. Bacterial pneumonias tend to fuse and form abscesses: round or oval and largely anechoic foci. Depending on the formation of a capsule, the margin is smooth and echodense.

29.3 Acute Respiratory Distress Syndrome

In patient with ALI/ARDS (see also Chap. 45), a given ultrasound pattern corresponds to a given degree of lung aeration. Four conditions are possible as a progression of consolidation:

1. Normal: presence of artifactual horizontal A lines beyond the pleural line.
2. Interstitial syndrome: presence of multiple vertical B lines (comet tails) with well-defined spacing corresponds to moderate decrease in lung aeration (regularly spaced B lines 7 mm apart) or to disseminated foci of pneumonia (irregularly spaced B lines).
3. Alveolar-interstitial syndrome: presence of coalescent B lines less than 3 mm apart corresponds to more severe decrease in lung aeration resulting from partial filling of the alveolar space by edema or confluent bronchopneumonia.
4. Alveolar consolidation: presence of lung consolidation characterized by an inspiratory reinforcement—dynamic bronchograms—corresponds to complete loss of lung aeration with persisting aeration of distal bronchioles. The size of the consolidation does not vary with respiratory movements.

In patients with focal loss of lung aeration, any increase in intrathoracic pressure simultaneously induces hyperinflation of normally aerated lung regions and possible recruitment of nonaerated parts of the lung.

Patients with ALI/ARDS can be classified according to the initial distribution of aeration loss:

- Focal loss of aeration: the aeration loss predominates in dependent lung regions
- Diffuse loss of lung aeration: aeration loss is equally distributed between all lung regions.

The improvement in gas exchange with the use of artificial ventilator techniques is probably related to the number of recruitable alveoli that initially were not involved in gas exchange because of edema or atelectasis. Alveoli that are involved in a consolidation process, such as pneumonia, are less amenable to recruitment.

29.4 Lung Atelectases

Lung atelectases (see also Chap. 45) are characterized by partial or complete absence of ventilation:

- Compression atelectasis is caused by voluminous pleural effusion, with floating of the lung. The parenchyma could be partial reventilated during inspiration and recruitment maneuvers and after effusion drainage. Color Doppler ultrasonography shows increased branch-like vessel visualization (Fig. 29.1).
- Obstructive atelectasis is marked by a largely homogeneous hypoechoic presentation of lung tissue in terms of hepatization. Effusion is absent or small. The image is similar to that for pneumonia, but with significantly fewer air bronchograms.

29.5 The Ultrasound Lung Reaeration Score

Lung ultrasonography is a promising tool for assessing PEEP-induced alveolar recruitment, lung reexpansion after pleural drainage, and recovery from ventilator-associated pneumonia. Lung recruitability is higher in patients with diffuse loss of aeration than in patients with focal loss of aeration.

In ALI/ARDS, lung consolidation predominates over alveolar interstitial syndrome. In the studies of Bouhemad et al. [1] the reaeration score is defined by four stages of aeration,

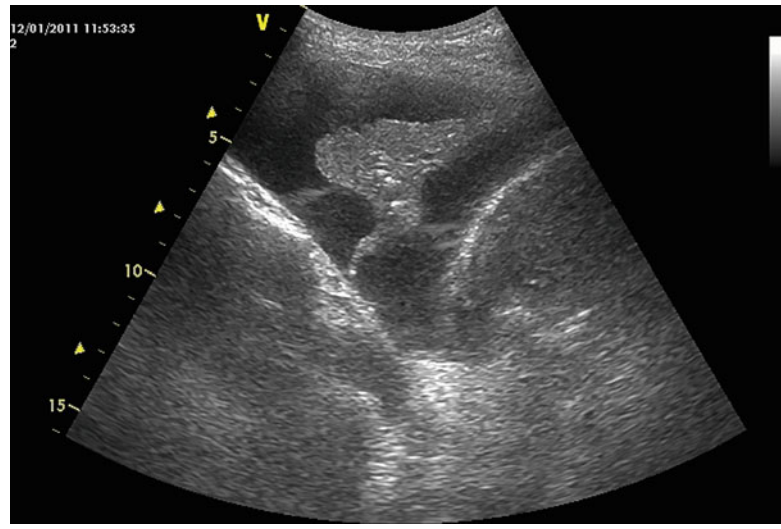

Fig. 29.1 Compression atelectasis caused by voluminous pleural effusion, with floating of the lung

Table 29.1 Ultrasound lung reaeration score

Quantification of reaeration[a]			Quantification of loss of aeration		
1 point	3 points	5 points	−5 points	−3 points	−1 point
B1→N	B2→N	C→N	N→C	N→B2	N→B1
B2→B1	C→B1			B1→C	B1→B2
C→B2					B2→C

Modified from Bouhemad et al. [1]

B1 ultrasound lung comets with well-defined and irregular spacing, moderate loss of lung aeration, *B2* abutting ultrasound lung comets, severe loss of lung aeration, *C* alveolar consolidation, *N* normal pattern

[a] First, ultrasound lung aeration was measured in each of the examined lung regions before and after any treatment; then the score was calculated as the sum of each score characterizing each region of interest.

including normal aeration, decreased lung aeration (number and type of B lines), and consolidation (Table 29.1). It is calculated from changes in the ultrasound pattern of each of the eight or 12 regions of interest after any treatment or after a defined period of therapy.

The ultrasound reaeration score could be appropriate for measuring recruitment resulting from any treatment aimed at increasing lung aeration, such as PEEP, negative fluid balance, patient positioning, or recruitment maneuvers. The score has also been used to compare lung reaeration measured by bedside chest radiography, lung CT, and lung ultrasonography in patients with ventilator-associated pneumonia treated with antibiotics.

29.6 Mechanical Ventilation and Weaning

Reducing tidal volume during mechanical ventilation decreases mortality in patients with ARDS. However, selecting the right level of PEEP is difficult. Alveolar recruitment is defined as the volume of gas penetrating into poorly aerated and nonaerated lung areas after PEEP. In ARDS, the percentage of potentially recruitable lung is extremely variable and is strongly associated with the response to PEEP (Figs. 29.2, 29.3).

To provide a bedside estimate of the percentage of potentially recruitable lung, it has been shown that at least two of the following

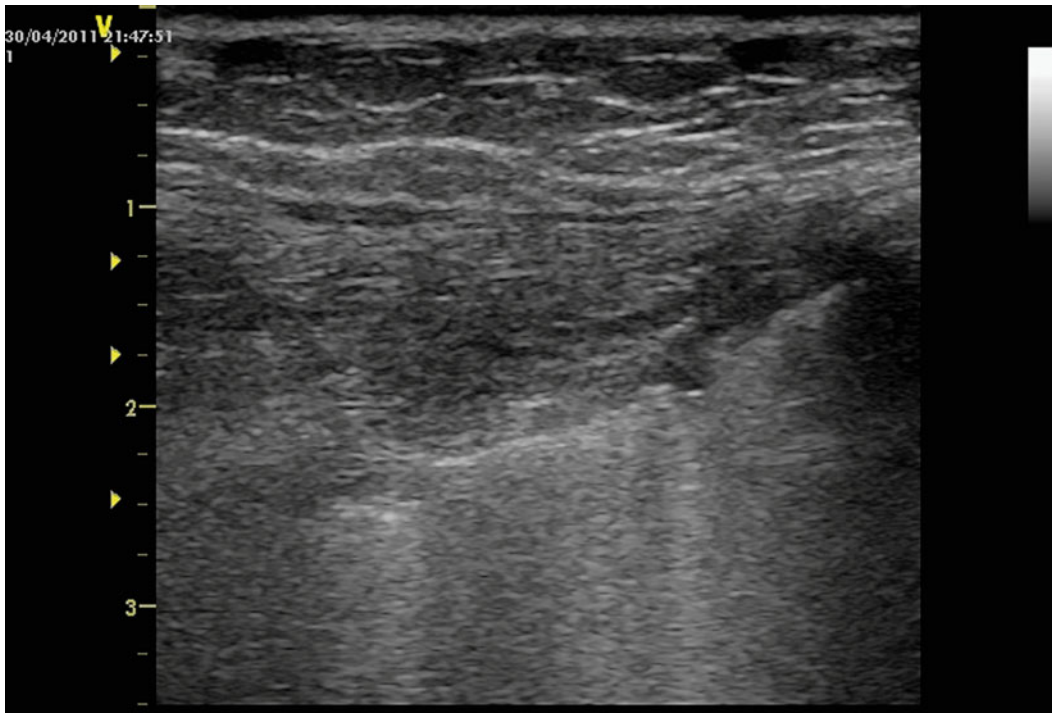

Fig. 29.2 Lung before recruitment maneuvers

three changes in respiratory variables can occur when PEEP is increased from 5 to 15 cmH_2O:

1. An increase in PaO_2/FiO_2.
2. A decrease, even slight, in $PaCO_2$.
3. An increase in respiratory-system compliance

Lung ultrasonography was also compared, by Bouhemad et al. [1] with the pressure–volume curve for assessing PEEP that induced lung recruitment in ARDS/ALI patients. A highly statistically significant correlation was found between PEEP-induced lung recruitment measured by the pressure–volume curve method and the ultrasound reaeration score. The ultrasound reaeration score was accurate in detecting a significant increase in lung aeration associated with a significant increase in arterial oxygenation. However, it was less accurate in detecting smaller changes of lung aeration.

So, ultrasonography can be used at the bedside for measuring lung recruitment, is noninvasive, and is easily repeatable. The quasi-static pressure–volume curve method requires deep sedation and muscle paralysis, disconnection of the patient from the ventilator, and specific software on the ventilator to avoid a complex and time-consuming analysis of the data.

Distribution of transthoracic lung ultrasound aeration loss (lung consolidation and B lines) is predominant in the most dependent lung regions (posterior parts of lower lobes). PEEP-induced lung reaeration is predominantly seen as the disappearance of B lines in the anterior and lateral parts of the chest wall, whereas consolidation in posterior lung regions is marginally modified by PEEP.

However, lung ultrasonography cannot detect PEEP-induced lung hyperinflation, so it should not be the sole method for PEEP titration. Ultrasonographic evidence of PEEP-induced recruitment is insufficient to consider the PEEP applied as optimum (Fig. 29.4).

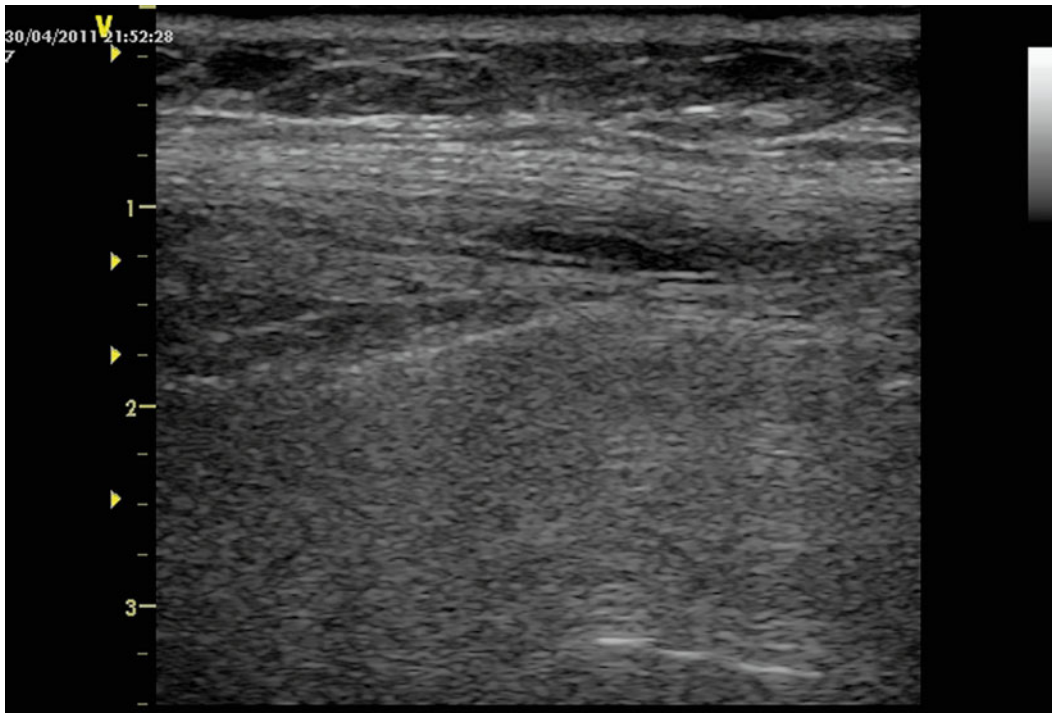

Fig. 29.3 Lung after recruitment maneuvers when positive end-expiratory pressure was increased from 5 to 15 cmH_2O

29.7 Weaning

Once the underlying process necessitating mechanical ventilation has started to resolve itself, withdrawal of ventilation support should be considered. Many parameters such as neuromuscular state, muscle strength and adequate coughing, ability to cooperate, cardiovascular stability, age, comorbidity, and prolonged mechanical ventilation must be taken into account.

Weaning from mechanical ventilatory support is a real cardiovascular stress test. Cardiac dysfunction is a leading cause of weaning failure. During weaning, the support provided by the ventilator is reduced, and the patient progressively takes over the work of breathing. Changes associated with the transition from mechanical ventilation to spontaneous ventilation overload the cardiorespiratory system, with increase in venous return (preload), left ventricular (LV) afterload, O_2 consumption, and sympathoadrenergic tone, with predictable consequences on heart rate and blood pressure. Hypoxia and high $PaCO_2$ may acutely increase pulmonary arterial pressure, leading to right ventricular (RV) impairment and failure. In patients with preexisting heart disease (coronary artery disease and LV insufficiency), these physiological changes associated with spontaneous breathing can trigger LV failure and cardiac ischemia, which in turn may lead to respiratory failure and unsuccessful weaning. The cardiovascular changes are:

- Increases in mean systemic filling pressure due to venoconstriction and associated reduction in venous compliance
- Decreased intrathoracic pressure
- Increases in LV afterload
- Increases of RV and LV end-diastolic volumes by the venous return

All these changes augment myocardial O_2 demand and the heart must be able to cope with this situation. With diminished cardiovascular reserve, myocardial ischemia may appear with an increase of LV filling pressure. In a recent study, it was demonstrated that weaning-failure patients had

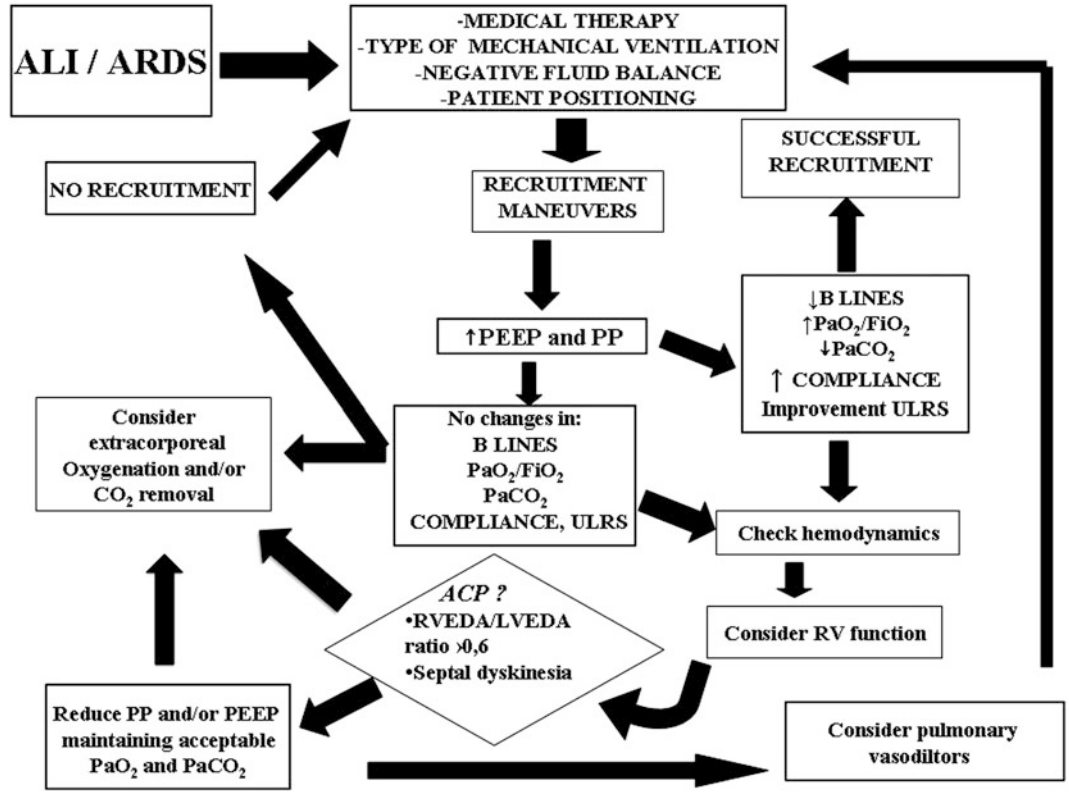

Fig. 29.4 Echo-guided treatment of acute lung injury (*ALI*)/acute respiratory distress syndrome (*ARDS*). *PP* plateau pressure, *PEEP* positive end-expiratory pressure, *ULRS* ultrasound lung reaeration score, *RVEDA* end-diastolic right ventricular area, *LVEDA* end-diastolic left ventricular area, *ACP* acute cor pulmonale, *RV* right ventricular

significantly larger left atrial and LV diameters and a significantly thicker intraventricular septum and posterior wall than weaning-success patients. These parameters are predictive of a difficult weaning. In another recent transthoracic echocardiography (TTE) study [2], patients for whom weaning failed had a low *E*/*E*′ ratio, reduced stroke volume, and shortened deceleration time. Thus, altered LV diastolic properties may well contribute to the rise of filling pressure and unsuccessful weaning from mechanical ventilation. In fact, in ventilated ICU patients, a lateral *E*/*E*′ ratio above 8.0 predicted a pulmonary artery occlusion pressure of more than 18 mmHg with good sensitivity and specificity. Similarly, other authors showed that an *E*/*A* ratio above 0.95 and an *E*/*E*′ ratio above 8.5 at the end of a spontaneous breathing trial could predict a high pulmonary artery occlusion pressure in patients difficult to wean.

To summarize:

- Echocardiography is suited to screening patients at risk of weaning failure.
- Patients who exhibit an LV ejection fraction less than 35 % must be considered at high risk of cardiac-related weaning failure, particularly when LV diastolic dysfunction (shortened deceleration time) and increased filling pressure (elevated *E*/*E*′) are associated with the systolic dysfunction.
- In patients for whom weaning ultimately failed owing to cardiogenic pulmonary edema, median *E*/*A* and *E*/*E*′ ratios increase when pressure-support ventilation is switched to a spontaneous breathing trial.
- Echocardiography before, during, and after the weaning process is very helpful to assess hemodynamics and tailor a specific therapy (diuretics, antihypertensive drugs, noninvasive

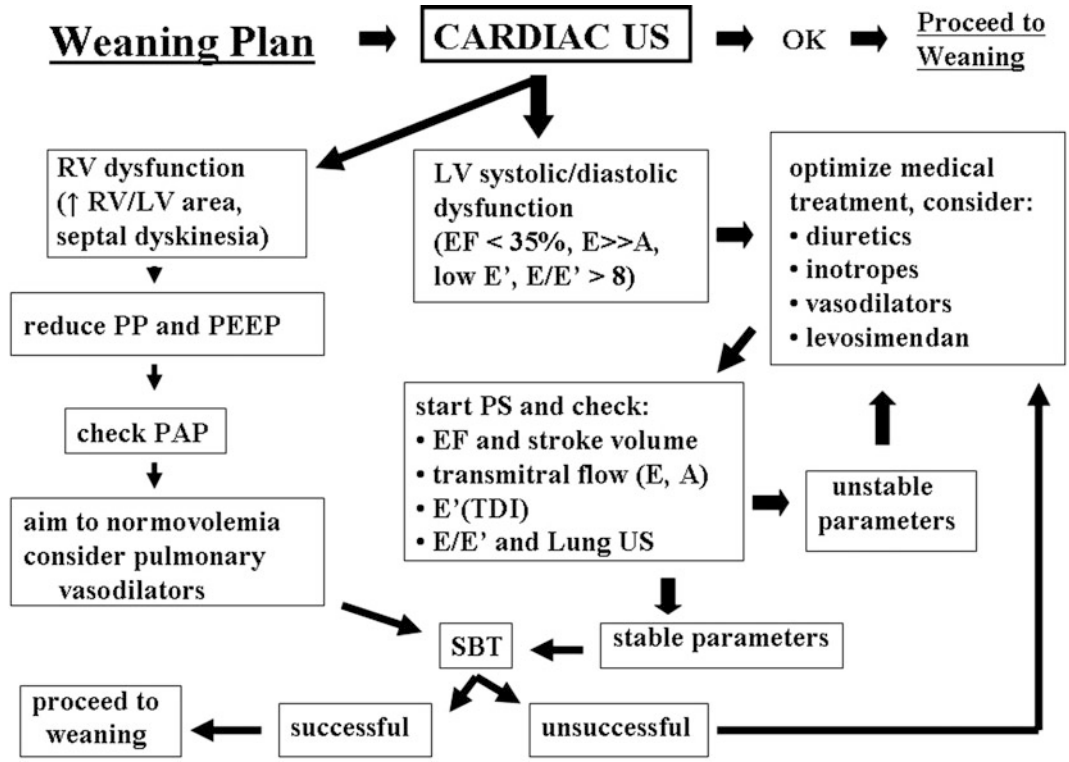

Fig. 29.5 Echo-guided weaning algorithm. *PP* plateau pressure, *PS* pressure support ventilation, *PEEP* positive end-expiratory pressure, *PAP* pulmonary arterial pressure, *SBT* spontaneous breathing trial, *US* ultrasonography, *RV* right ventricular, *LV* left ventricular, *EF* ejection fraction

ventilation after extubation, levosimendan) as an attempt to facilitate difficult cardiac-related weaning from positive-pressure ventilation (Fig. 29.5).

29.8 Mechanical Ventilation, RV Function, and Acute Cor Pulmonale

In ARDS, two factors combine to produce RV systolic overload:

1. The pathologic features of the syndrome per se, which can be associated with distal occlusion of the pulmonary arterial bed.
2. Mechanical ventilation, which increases RV outflow impedance.

In addition, PEEP may produce increased pulmonary vascular resistance. A high PEEP represents another potential factor for increased RV outflow impedance. However, when PEEP is able to reaerate part of the lung without overdistention, RV impedance may actually decrease.

Mechanical ventilation acts by direct mechanical augmentation of RV afterload in the inflation period. RV impairment may lead to RV dilatation, abnormal septal motion, and low cardiac output. When associated with high inflation pressures, acute cor pulmonale (ACP) can complicate ARDS. The ventilation respiratory strategy is fundamental for the tolerance of the right ventricle to plateau pressure and PEEP. In general, the ventilator should be set to the lowest level of positive pressure during both the inspiratory and the expiratory phase of the mechanical breathing which is still compatible with acceptable oxygenation and $PaCO_2$.

According to a recent study [3], ACP during the first day of mechanical ventilation depends mainly on the plateau pressure:

- A plateau pressure, below 26 cmH_2O, does not generally produce or almost never produces ACP and is associated with low mortality.
- A plateau pressure between 27 and 35 cmH_2O is associated with high mortality only if there is concomitant ACP.
- A plateau pressure above 35 cmH_2O is associated with a high incidence of ACP and mortality.

So, the increase of mortality related to mechanical ventilation (plateau pressure) depends on the presence or absence of ACP. The association of the following two echocardiographic findings are fundamental for the diagnosis of ACP in mechanically ventilated patients:

1. End-diastolic RV area to end-diastolic LV area ratio greater than 0.6, in the apical four-chamber view (TTE) or the mid-esophageal four-chamber view at 0° (transesophageal echocardiography).
2. Septal dyskinesia in the parasternal short-axis view (TTE), or the transgastric view at 0° (transesophageal echocardiography).

In ARDS, a major cause of ventilator-induced hypotension (and false fluid responsiveness) may not be venous return impairment (unless the patient is hypovolemic), but increased RV afterload. Thus, once the setting of the ventilator has been adjusted to the lowest level of positive pressure which guarantees acceptable gas exchange, a pulmonary vasodilator, such as nitric oxide, sildenafil, or prostacyclin, can be used to reduce pulmonary arterial pressure (Fig. 29.4).

Ventilator focus-oriented and RV goal-directed echocardiography has a irreplaceable role in assessment of the right side of the heart and patient monitoring to guide the setting of mechanical ventilation and any possible use of pulmonary vasodilator agents.

References

1. Bouhemad B et al (2011) Bedside ultrasound assessment of positive end-exipiratory pressure-induced lung recruitment. Am J Respir Crit Care Med 183:341–347
2. De Backer D, Cholley PB, Slama M, Viellard-Baron A, Vignon P (2011) Hemodynamic monitoring using echocardiography in the critically Ill. In: Viellard-Baron A (ed) Chapter 4 Heart-lung interactions in mechanical ventilation, Springer, Heidelberg
3. De Backer D, Cholley PB, Slama M, Viellard-Baron A, Vignon P (2011) Hemodynamic monitoring using echocardiography in the critically Ill In: Viellard-Baron A, Jardin F (eds) Chapter 17 Why and how to use echocardiography in acute respiratory distress syndrome, Springer, Heidelberg

Further Reading

Arbelot C, Ferrari F, Bouhemad B, Rouby JJ (2008) Lung ultrasound in acute respiratory distress syndrome acute respiratory distress syndrome and acute lung injury. Curr Opin Crit Care 14:70–74

Baron A et al (2002) Echo-Doppler demonstration of acute cor pulmonale at the bedside in the medical intensive care unit. Am J Respir Crit Care Med 166:1310–1319

Bouhemad B, Aberlot C et al (2010) Ultrasound assessment of antibiotic-induced pulmonary reaeration in ventilator-associated pneumonia. Crit Care Med 38(1):84–92

Caille V et al (2010) Echocardiography: a help in the weaning process. Critical Care 14:R120. doi:10.1186/cc9076

Feihl F, Broccard AF (2009) Interactions between respiration and systemic hemodymamics. Part II: practical implications in critical care. Intensive Care Med 35:198–205

Hypotension

30

Luigi Tritapepe, Cecilia Nencini, and Demetrio Tallarico

30.1 Introduction

Hypotension is always a symptom of hemodynamic instability, and when physicians talk about hemodynamic instability, they often speak of hypotension. Low systemic arterial pressure frequently develops in critically ill patients. Common causes of hypotension in ICU patients include left ventricular (LV) dysfunction due to myocardial infarction and heart failure due to different causes, such as hypovolemia, sepsis and septic shock, pulmonary embolism, and aggressive use of positive end-expiratory pressure. Hypotension is a symptom that physicians are often called to treat following the traditional algorithm of hemodynamic stability. This algorithm asks the physician to treat hypotension step by step by answering yes or no to the following question: Is the patient hypovolemic? If the answer is "yes," you should give fluid until the patient has a central venous pressure (CVP) of about 15 mmHg. If the patient does not respond, you must give inotropes, but if the patient does not have contractile dysfunction, you have to give vasopressors. If you have solved the instability, you are probably a good clinician or you have chosen the right type of monitoring in a patient without cardiac disease, but in the case of treatment failure, you have to reassess the clinical scenario. Where is the problem? The diagnosis of hemodynamic instability and hypotension is missing. Differently from both pressure and volume monitoring, echocardiography is the only diagnostic test that is easy to perform and useful in the early diagnosis of the previously described abnormalities which determine hypotension. The literature describes the use of echocardiography in patients with hypotension, but data are lacking or the results have limitations. One of the limitations is a selection bias that occurs because echocardiography is generally used for evaluation of hypotension only in patients with known or suspected cardiac abnormalities, so echocardiography may not be done on a noncardiac patient. It is certainly possible that other subgroups of patients may benefit from echocardiographic evaluation. In the guidelines endorsed by the various societies of physicians published in the *Journal of the American Society of Echocardiography* in 2007 [1], transthoracic echocardiography (TTE) and transesophageal echocardiography (TEE) have a maximal level of appropriateness (class A 9) in the diagnosis of hypotension. Echocardiography can make the difference in terms of time and accurateness. In fact, in skilled hands, it needs only a few minutes to resolve a diagnostic question and to guide the following therapy. Positive-pressure ventilation, high levels of positive end-expiratory pressure, intrathoracic surgery, and chest trauma all present challenges for adequate image acquisition using TTE. This means that TEE is frequently more useful in the ICU setting, and is the first-line echocardiographic examination whenever a patient has an endotracheal tube in situ.

L. Tritapepe (✉)
Department of Anesthesia and Intensive Care, Cardiac Surgery ICU, Policlinico Umberto I Hospital, Sapienza University of Rome, Rome, Italy
e-mail: luigi.tritapepe@uniroma1.it

A. Sarti and F. L. Lorini (eds.), *Echocardiography for Intensivists*,
DOI: 10.1007/978-88-470-2583-7_30, © Springer-Verlag Italia 2012

To return to the causes of hypotension, we can define the major factors that determine hypotension as problems of preload, contractility, afterload, and impairment of the relationship between the ventricles and between the heart and lungs. Assessment of all these variables may be accomplished with echocardiographic examination. Moreover, echocardiography can identify causes of hypotension that are not clinically suspected and that can alter clinical management, such as LV outflow tract obstruction (LVOTO). An early diagnosis of this condition is particularly important because it does not have other diagnostic possibilities and an incorrect treatment may result in a fatal outcome. The best approach is to perform a comprehensive evaluation of every patient. A comprehensive examination is less likely to miss an unexpected diagnosis. In this chapter, we to analyze the causes of hypotension and to describe the utility of echocardiography in detecting the causal abnormalities, especially in the ICU and the operating room.

30.2 Echocardiography in Hypotension

The use of echocardiography in the ICU is increasing. With use of an abbreviated focus-assessed protocol, TTE has been shown to contribute positively to patient care in 97 % of critically ill patients. Normally echocardiography allows the visualization of every cardiac structure and the recognition of the mechanical function of the heart. Ultrasonography can be used to detect the causes of hypotension and to understand why it is refractory to inotropic support or vasopressor infusions. Finally, echocardiography can help physicians in the diagnosis of a wide spectrum of syndromes that may or may not be related to the cardiovascular system.

Hypotension is a common problem in critically ill patients. Immediate treatment is mandatory to avoid prolonged hypotension that may lead to organ ischemia, dysfunction, and poor outcome. Rapid diagnosis and intervention may prevent this deterioration and eventually improve outcome. In the ICU, TTE is the first step in ultrasonography, but in certain cases it may not be able to provide good image quality because of structures which result in poor penetration of ultrasound, such as air or interposed equipment such as an extensive bandage. The failure rate of the transthoracic approach in the ICU setting has been reported to be between 30 and 40 %. TEE is particularly useful in every case of missed diagnosis due to technical impediment, and it is irreplaceable for the evaluation of suspected aortic dissection, malfunctioning of prosthetic heart valves, suspicion of embolization, endocarditis, possible intracardiac shunts, and unexplained hypotension. TEE allows better visualization of the heart in general and especially the posterior structures owing to the proximity of the esophagus without use of an unfavorable medium. The assessment of hypotension is commonly approached in terms of assessment of heart rate, rhythm, preload, contractility, and afterload. A complete view of all of these variables may be achieved by an echocardiographic study. The first differentiation in the case of hypotension must be made between acute patients with sepsis or trauma and long-term ICU patients. With a basic level of skill, a complete TTE examination may be performed in minutes. Preload, contractility, systolic function, diastolic dysfunction, and pericardial tamponade can be assessed quickly. Specific situations such as pericardial effusion or localized tamponade, pulmonary embolism, LVOTO, unexplained hypoxemia, and aortic dissection, among others, can all be assessed using TEE in a reliable fashion, and their assessment requires an intermediate level of skill.

30.3 Causes of Hypotension

30.3.1 Modification of Preload

Clinical assessment of intravascular volume can be extremely difficult or impossible to achieve in the ICU as well as during major surgery. This is a crucial problem because fluid loading is considered the first step during resuscitation of hemodynamically unstable patients. The literature indicates that

only about 50 % of hemodynamically unstable patients in the ICU and operating room respond to a fluid challenge. Cardiac filling pressures including the CVP and the pulmonary artery occlusion pressure (PAOP) have traditionally been used to guide fluid management. However, studies performed over the last 30 years have demonstrated that cardiac filling pressures are unable to predict fluid responsiveness. Over the last decade, a number of studies have been reported that have used heart–lung interactions during mechanical ventilation to assess fluid responsiveness. Specifically, the pulse pressure variation derived from analysis of the arterial waveform, the stroke volume variation derived from pulse contour analysis, and the variation of the amplitude of the pulse oximeter plethysmographic waveform have been shown to be highly predictive of fluid responsiveness when certain conditions are maintained (high tidal volume (TV), ventilator–patient synchrony, no spontaneous breathing, and absence of arrhythmias). Although the LV end-diastolic area as determined by TEE is a more accurate measure of preload than either the CVP or the PAOP, it does not predict fluid responsiveness as well as the dynamic indices. For many years in ICUs, physicians have argued over the best way to assess preload. On one side are those who rely on pressure monitoring, on the other side are those who chose volumetric monitoring. Nevertheless, the Swan-Ganz catheter has continued to be the most popular device, especially in ICUs. The literature describes the systematic failure of preload assessment through static measurement of the pressure, such as the CVP or capillary wedge pressure, but also for volumetric measurements, data are lacking. Dynamic monitoring, which uses the heart–lung interaction to better discover the preload deficit, does not reveal hypotension due to preload reduction. The complexity of every hemodynamic status and of the different abnormalities prevents the applicability of simple algorithms.

TTE and even better TEE provide a snapshot image of the patient and allow us to make a diagnosis either in the presence or in the absence of cardiac disease. First of all, the parasternal short-axis view at the mid-papillary level or the transgastric mid short-axis view are useful views to quantify the preload of the left ventricle. Short-axis images of the left ventricle provide real-time assessment of ventricular filling, which may not be accurately reflected by the pulmonary capillary wedge pressure. In the presence of a real hypovolemia, we can see a small LV area, in both systole and diastole, and it is possible to note the kissing of papillary muscles that represents the complete collapse of the left ventricle during systole. The diameters of the left ventricle can be measured in M-mode. The criteria for diagnosing hypovolemia include an end-diastolic diameter of less than 25 mm, systolic obliteration of the LV cavity, and a LV end-diastolic area of less than 5.5 cm^2/m^2. Moreover the measurement of LV areas, in both systole and diastole, can solve the question of true or false hypovolemia. In fact, in the case of true hypovolemia, both LV areas are small, whereas in the case of vasodilation with hypotension, only the systolic LV area is small. In general, a hypovolemic patient has a hyperdynamic status with a high ejection fraction. Patients with chronic cardiac failure have a dilated left ventricle and may be hypovolemic even with a higher LV end-diastolic area. In this case the study of cardiac function can be helpful for the diagnosis.

A new concept is fluid responsiveness instead of volume status or measurement of filling pressures. Fluid responsiveness means that a significant volume expansion, when performed, should induce a significant increase in cardiac output, reflecting the fact that the heart is on the steep portion of the Frank–Starling curve. Echocardiography has been widely demonstrated to predict fluid responsiveness accurately. This is now a complete and noninvasive tool able to determine hemodynamic status precisely in circulatory failure. We can draw the Frank–Starling curve of each patient through the TTE or TEE short-axis view of the left ventricle at different levels of loading, and we can identify a fluid-responder patient when his/her LV short-axis output is not on the flat portion of the curve. In mechanically ventilated patients, it is more useful to evaluate the dynamic indices of the cyclic modification of stroke volume to categorize a fluid-responder patient. A very useful index is the aortic volume–time integral

variation with the value of the aortic blood flow peak, measured by TTE in apical three-chamber and apical five-chamber views or by TEE in deep transgastric in transgastric long-axis views with pulsed wave Doppler imaging of the LV outflow tract at the level of the aortic valve. ΔV_{peak} is generally evaluated over each of five consecutive respiratory cycles. Beat-to-beat measurement of aortic blood V_{peak} allows the determination of $V_{peak\ max}$ and $V_{peak\ min}$ over a single respiratory cycle. ΔV_{peak} is calculated as the difference between $V_{peak\ max}$ and $V_{peak\ min}$ divided by the mean of the two values and is expressed as a percentage. A ΔV_{peak} of aortic blood flow greater than 12 % indicates a fluid-responder patient. In mechanically ventilated patients perfectly adapted to the respirator, respiratory variations in superior vena cava (SVC) and inferior vena cava (IVC) diameters have also been validated as parameters of fluid responsiveness. The SVC can be explored with TEE in the bicaval view, where it is represented on the right side of the screen. Simply, the eyeball or even better the M-mode show the collapse of the SVC in a hypovolemic patient during the respiratory cycle. Volume loading can stop the collapse of the SVC, which has a collapsibility variation of more than 36 % in a fluid-responder patient. The SVC collapsibility index is more reliable than the IVC distensibility index in predicting fluid responsiveness. However, the IVC is well recognized in almost all patients in the ICU and it is simple to visualize when it is not feasible to perform TEE. The IVC distensibility is often measured by a cardiologist to assess the value of the CVP, but the significance of its distensibility in the mechanically ventilated patient is more often used by intensivists. It can be easily visualized in mechanically ventilated patients by echocardiography, using a subxiphoid approach. When the distensibility variation of the IVC rises above 18 %, this means that the patient is a fluid responder. To better assess the ventricular loading, we need to know the LV end-diastolic pressure and the left atrial pressure (LAP). We can estimate this pressure by measuring the velocities of blood and tissue with tissue Doppler imaging of the mitral annulus and transmitral flow. Combining E′ from tissue Doppler imaging with the E wave of transmitral flow, we can obtain different values of the ratio E'/E: when this ratio less than 8, it is indicative of a low LAP and a compliant left ventricle, whereas for values greater than 15, LAP is high and the ventricle is not compliant. Other variables must be researched to precisely assess every intermediate value of LAP.

30.3.2 Myocardial Function

In the ICU many devices are used to measure cardiac output. Some are invasive others are non-invasive, but the Swan–Ganz catheter represents the gold standard. Nevertheless, despite the information derived from the pulmonary artery catheter, we need to know more about myocardial function to make a diagnosis. In fact, the measurement of flow does not provide information about the cause. The global systolic function of the left ventricle can be visualized with TTE or TEE by its contractility and by the increase in wall thickness in eyeball mode. It is very important to remember that each contracting myocardial segment moves toward a central point in the short-axis view during systole and simultaneously thickens. If you do not see the increase of wall thickness, the myocardial segment seems to thicken, but it is dragged from neighboring segments. The evaluation of wall motion is crucial in the ICU to verify if it is a new problem that causes hypotension or if it is a worsening of a known disease. This distinction, together with elevation of the level of biomarkers, can show an acute myocardial ischemia, which is treated differently from other forms of myocardial impairment such as stunning and global hypokinesia. Then it is crucial to study the global LV systolic function in terms of qualitative values. Qualitative methods used for assessing global LV systolic function using echocardiography are ejection fraction, fractional shortening, and fractional area change, as well as other methods that are not frequently used such as mitral annular motion, dP/dt using mitral regurgitant jet, and segmental wall motion abnormality assessment using strain-rate imaging. Evaluation of the right ventricle is

also essential, as tricuspid regurgitation, right ventricular (RV) overload (greatly increased size), limited tricuspid descent, and poor RV wall contraction may indicate right-sided heart failure. RV dilatation is often associated with LV underfilling and poor cardiac output. The explanation of these measures is given in other chapters in this book. However, it is important, especially in mechanically ventilated patients, to establish if the right ventricle is compromised or not because, despite all the modifications described for the dynamic parameters monitored, the patient will always be nonresponder to fluid challenge. The diastolic function is well described in another chapter in this book but it is important to underline its role in causing hemodynamic instability. Transmitral flow evaluation combined with measurement of the deceleration time represents the first step in diastolic evaluation. The examination is completed using tissue Doppler imaging of the mitral annulus, which represents an index of diastolic function not closely related to the load condition of the left ventricle. The Doppler imaging of the pulmonary veins helps to clarify the discrepancy from other measurements and to establish the degree of diastolic dysfunction. When patients with hypotension present with various degrees of diastolic dysfunction, they cannot be treated following the algorithms for hypotension with the use of catecholamines.

30.3.3 Modification of Afterload

Afterload is not often measured in the ICU. It is estimated from the clinical conditions such as peripheral vasoconstriction, oligoanuria, and cold extremities. It is measurable but we can only know the peripheral contribution to afterload because its value is determined more by aortic impedance, aortic elastance, and LV wall stress, which are difficult to obtain in clinical practice. TTE and TEE allow us to extrapolate the reduction of afterload whenever the mean arterial pressure is reduced but the LV diastolic area is normal and the left ventricle collapses during systole.

Table 30.1 The major clinical scenarios of hemodynamic instability

Pericardial tamponade
Pulmonary embolism
Left ventricular outflow tract obstruction
Unexplained hypoxemia
Blunt chest trauma
Aortic dissection

30.4 Different Scenarios of Hypotension

In the ICU, different clinical scenarios result from the physiopathologic causes of hypotension as previously described. These pathologic entities occur frequently, and echocardiography may represent a life-saving tool in many circumstances (Table 30.1).

Pulmonary embolism, unexplained hypoxia, and aortic dissection are described extensively in other chapters in this book (Chaps. 31, 35 and 32 respectively). Here we will describe pericardial tamponade, LVOTO, and blunt chest trauma.

30.4.1 Pericardial Tamponade

Cardiac tamponade is a true medical emergency, and the overall risk of mortality depends on early diagnosis, treatment, and the underlying cause. The most common cause of tamponade is pericardial effusion. Any condition that increases intrathoracic pressure such as a mediastinal mass or a large bilateral pleural effusion can also increase the pericardial pressure and cause hemodynamic compromise. In the case of pericardial effusion, there is an increase in intrapericardial pressure that rapidly causes a rise in intracardiac pressure, especially in the right side of the heart, where normally the intracavitary pressures are lower than in the left side. The rapid increase in intrapericardial pressure causes the diastolic collapse of the right ventricle in

the early phase of diastole, whereas during the late phase it can determine an invagination of the right atrium. Thus, the physiologic process of pericardial tamponade can result in hemodynamic instability with hypotension due to an increased intrapericardial pressure that precludes the cardiac filling. On TTE and TEE, in 2D views one sees the presence of pericardial effusion, the diastolic collapse of the right ventricle, the dilatation of the IVC with the loss of its respiratory variations reflecting the elevated right atrial pressure, and the respiratory increase of interventricular dependence. This increase of interventricular dependence can be revealed by pulsed wave and continuous wave Doppler imaging showing respiratory variations of more than 25 % in mitral, aortic, and/or tricuspid flow. This variation of right-sided and left-sided heart inflow is a sign of exaggerated interventricular dependence, which is also a hallmark of pericardial tamponade. The physiologic aspect of these changes during respiration is related to the constriction due to pericardial effusion that impedes the diastolic filling, so during inspiration the intrathoracic negative pressure causes suctioning of blood from the venae cavae with acceleration of transtricuspid flow and RV dilation. During expiration, the right ventricle is compressed and the transmitral and transaortic flow are accelerated. Flow respiratory variations can be assessed only in spontaneously breathing patients, in regular sinus rhythm. An important hemodynamic instability exists when the difference between the highest and the lowest velocity of transtricuspid or transaortic or transmitral flow is more than 25 %. The key element of the differential diagnosis is to identify that the patient has a moderate to large pericardial effusion. The amount of pericardial effusion can be estimated by measuring the diameter of the collection. A diameter greater than 1 cm is often considered significant. Also, the hypovolemia presents symptoms and echocardiographic findings similar to those of pericardial tamponade. However, all cardiac chambers are uniformly under filled without compression. In addition, and most importantly, a significant pericardial effusion is notably absent. Pericardial tamponade is well recognized in the subcostal view, but also in the apical four-chamber and parasternal long-axis views. TEE can be useful in the case of saccular compression such as after cardiac surgery when a frank cardiac tamponade can be difficult to diagnose, whereas the left atrial compression is better recognized.

30.4.2 Left Ventricular Outflow Tract Obstruction

In the emergency department and in the ICU, dynamic LVOTO occurs more often than is recognized. LVOTO has to be searched for whenever we encounter an unexplained hypotension. The patient who develops LVOTO has various degrees of aortic stenosis, not well-controlled hypertension, cardiac hypertrophy, and a hyperdynamic left ventricle. A particular predisposition is the eccentric hypertrophic interventricular septum associated with a long anterior leaflet of the mitral valve. In this case, the velocity of blood through the LV outflow tract, accelerated by the hypovolemia, tachycardia, or cathecolamines, determines a "Venturi effect" on the anterior mitral leaflet that obstructs the outflow tract and causes an aortic stenosis effect and mitral insufficiency. This situation quickly becomes serious and cannot be diagnosed with traditional monitoring. Indeed, if we monitor the patient with a Swan-Ganz catheter, we note a low cardiac output and a rise in PAOP. Immediately, with the diagnosis of low output syndrome, we administer inotropes, which leads to an irreversible hypotension. Many patients develop an LVOTO during hospitalization in the ICU because they have septic shock and the treatment with cathecolamines predisposes them to have a systolic anterior motion of the mitral valve and its chordal apparatus and the resulting consequences. This dynamic obstruction (systolic anterior motion) can result in cardiovascular collapse, and prompt diagnosis with echocardiography is essential to implement the correct management. Treatment includes the correction of hypovolemia with fluids, the use of vasopressors to raise the LV afterload, and β-blockade to relax the LV obstruction and reduce hypercontractility. Echocardiography, both TTE and TEE, is crucial in the

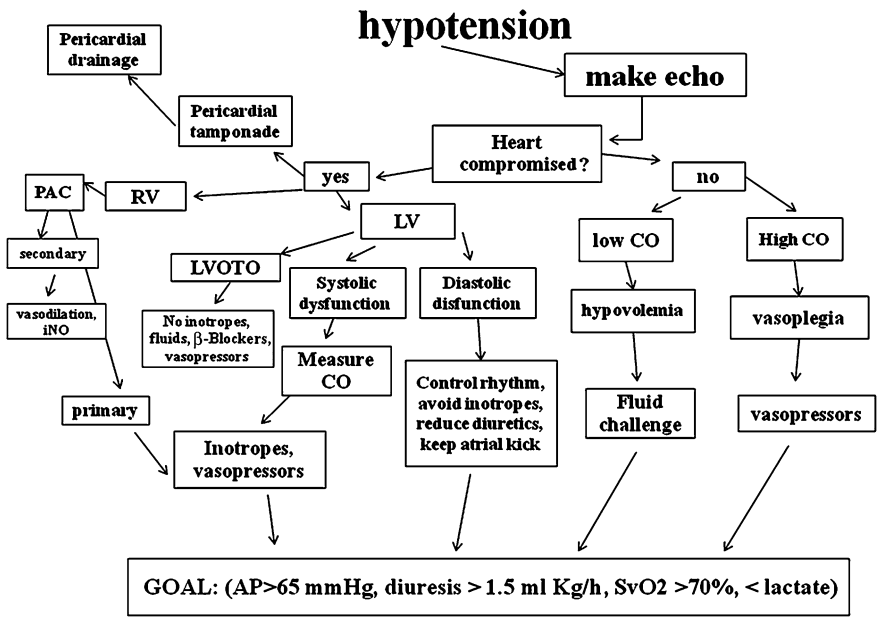

Fig. 30.1 Algorithm for diagnosis and treatment of unexplained hypotension. *AP* atrial pressure, *iNO* inhaled nitric oxide, *LV* left ventricle, *LVOTO* left ventricular outflow tract obstruction, *PAC* pulmonary artery catheter, *RV* right ventricle

diagnosis and management of therapy. TTE in the apical three-chamber view or the parasternal long-axis view and TEE in the deep transgastric view or mid-esophageal long-axis view at the level of the aortic valve provide the opportunity to immediately and simply make the diagnosis. The most important hallmarks are the presence of a septal bulge due to hypertrophy that is prominent toward the LV outflow tract. This bulge causes a subaortic stenosis, which revealed from the turbulence of the color flow Doppler imaging. The subaortic stenosis is associated with mitral insufficiency and color flow Doppler imaging shows a typical Y shape due to the contemporary turbulence in the aortic and mitral valves during systole. Continuous wave Doppler imaging across the LV outflow tract estimates a serious subaortic gradient that can exceed 100 mmHg and has a late-peaking "dagger shape."

30.4.3 Blunt Chest Trauma

Cardiac contusion is usually caused by blunt chest trauma arising from car accidents or falling injuries. The reported incidence of cardiac contusion in patients with blunt chest trauma ranges between 3 and 56 % depending on the diagnostic methods. This pathological condition leads to serious hypotension that has to be discriminated from other causes. Echocardiography, together with other examinations and blood samples, is now an important diagnostic tool also in thoracic trauma. The value of TTE in blunt chest trauma is limited because patients with severe chest wall injury often have suboptimal echocardiographic findings. TEE can provide high-quality images when the transthoracic image quality is poor. There are a few reports that blunt chest trauma may lead to acute myocardial infarction caused by coronary artery dissection, thrombosis, or fistula. Echocardiography can be used as a screening tool for ventricular dysfunction, which is one of the most serious complications of cardiac contusion. With respect to myocardial contusion, the right ventricle is nearest to the chest wall and on echocardiographic examination its apex can appear damaged, whereas the left ventricle is interested at level of septum and apex. This myocardial contusion is shown as an increase in wall thickness in diastole, alteration of segmental wall contractility, and increased brightness of the ventricular walls. Also, a rapid focused assessment with echocardiography can

detect pericardial collection, mediastinal hematomas, aortic intramural hematomas, aortic dissection or transection, and pleural collections (Fig. 30.1).

Reference

1. Douglas PS, Khandheria B, Stainback RF, Weissman NJ, Brindis RG, Patel MR et al (2007) ACCF/ASE/ACEP/ASNC/SCAI/SCCT/SCMR 2007 appropriateness criteria for transthoracic and transesophageal echocardiography. J Am Soc Echocardiogr 20:787–805

Further Reading

Beaulieu Y (2007) Bedside echocardiography in the assessment of the critically ill. Crit Care Med 35:S235–S249

Chockalingam A, Dorairajan S, Bhalla M, Dellsperger KC (2009) Unexplained hypotension: the spectrum of dynamic left ventricular outflow tract obstruction in critical care settings. Crit Care Med 37:729–734

Marcelino PA, Marum SM, Fernandes AP, Germano N, Lopes MG (2009) Routine transthoracic echocardiography in a general intensive care unit: an 18 month survey in 704 patients. Eur J Intern Med 20:e37–e42

Salem R, Vallee F, Rusca M, Mebazaa A (2008) Hemodynamic monitoring by echocardiography in the ICU: the role of the new echo techniques. Curr Opin Crit Care 14:561–568

Subramaniam B, Talmor D (2007) Echocardiography for management of hypotension in the intensive care unit. Crit Care Med 35:S401–S407

Vignon P (2005) Hemodynamic assessment of critically ill patients using echocardiography Doppler. Curr Opin Crit Care 11:227–234

Wasir H, Mehta Y, Mishra YK et al (2003) Transesophageal echocardiography in hypotensive post-coronary bypass patients. Asian Cardiovasc Thorac Ann 11:139–142

Suspicion of Pulmonary Embolism 31

Alessandro Locatelli, Carla Avallato, and Ilaria Nicoletti

31.1 Suspicion of Pulmonary Embolism

Acute pulmonary embolism (PE) consists in the acute obstruction of one or more branches of the pulmonary artery; the obstruction can be total or partial, and the material, usually of thrombotic origin, comes from deep vein thrombosis of lower limbs. Sometimes the material can be made up of fat, amniotic fluid, air, or CO_2. In cases of massive PE with cardiogenic shock, the symptoms are clinically obvious, but in most cases the symptoms are vague, so it is essential to assume clinical suspicion.

There are a few known factors predisposing the development of PE, including:

- Primary hypercoagulable conditions: the presence of Leiden factor V (resistance to activated protein C with a sharp increase in the risk of developing deep vein thrombosis and PE). Other predisposing factors include the prothrombin gene mutation, protein S deficiency, antithrombin III deficiency, hyperhomocysteinemia, antiphospholipid antibodies (anticardiolipin antibodies and lupus anticoagulant).
- Acquired hypercoagulable state: all the conditions that promote venous stasis predisposing to thrombosis. For example, prolonged immobilization from surgery, trauma, obesity, smoking, and use of CO.

The hemodynamic effects are the result of increased pulmonary vascular resistance caused by embolic obstruction and release of neurohumoral substances. The sudden increase in right ventricular (RV) afterload, with increased wall tension, is followed by dilation and dysfunction of the RV. The high wall stress leads to a reduction of right coronary blood flow with increased oxygen requirements and the risk of RV ischemia. The expansion of the right ventricle determines an interventricular septal shift to the left with reduced distensibility and filling of the left ventricle. The reduction in left ventricular (LV) filling causes a reduction in cardiac output resulting in hypotension, which in turn can lead to reduced coronary perfusion and myocardial ischemia.

The presence of dyspnea and tachypnea associated with a hemogas analysis in the presence of hypoxia, hypocapnia, and respiratory alkalosis in a patient with swelling of the jugular veins, deep vein thrombosis, and the presence of predisposing factors are strongly suggestive of acute PE. If these are associated with a complete or incomplete ECG right bundle branch block, S1Q3T3 complex, and negative T wave from V1 to V4, the probability is very high.

The diagnostic steps for acute PE with severe hemodynamic dysfunction have recently been described in the guidelines on the diagnosis and management of acute PE by the Task Force for the Diagnosis and Management of Acute Pulmonary Embolism of the European Society

A. Locatelli (✉)
Cardiovascular Anesthesia,
Santa Croce & Carle Hospital,
Cuneo, Italy
e-mail: locatelli.a@ospedale.cuneo.it

A. Sarti and F. L. Lorini (eds.), *Echocardiography for Intensivists*,
DOI: 10.1007/978-88-470-2583-7_31,

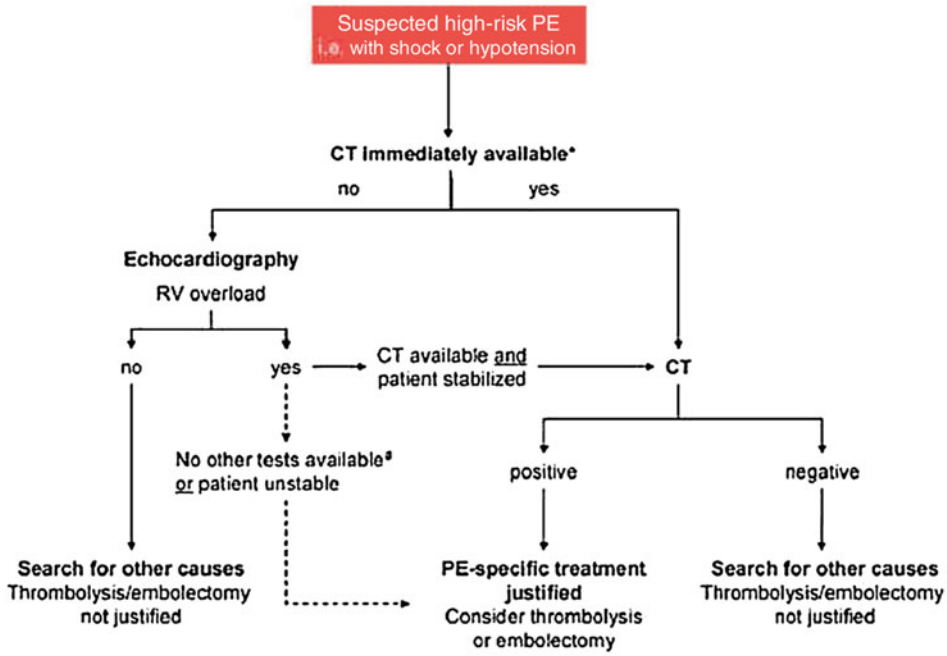

Fig. 31.1 Proposed diagnostic algorithm for patients with suspected high-risk pulmonary embolism (*PE*), i.e., presenting with shock or hypotension. * CT is considered not immediately available also if the critical condition of a patient allows only bedside diagnostic tests. # transesophageal echocardiography may detect thrombi in the pulmonary arteries in a significant proportion of patients with right ventricular (*RV*) overload and PE that is ultimately confirmed by spiral CT; confirmation of deep vein thrombosis with bedside compression ultrasonography might also help in decision-making (from Torbicki et al. 2008)

of Cardiology, to which we refer and which are shown in Fig. 31.1.

The algorithm shows the key role of echocardiography in the diagnosis of acute PE. Echocardiography should be performed whenever a CT examination is not readily available or if the patient, admitted to the ICU, is not in a state to be transported. The presence or absence of signs of RV overload determine the next diagnostic step.

31.2 Role of Echocardiography in PE

Echocardiography is used in the diagnosis, prognosis and evaluation of pulmonary hypertension. It has the advantage of being done easily at the bedside, of having a low cost, and of not being an invasive examination; it can therefore be done several times to monitor hemodynamic status and response to treatment. The echocardiographic signs suggestive of PE are direct and indirect. The direct signs are represented by direct visualization of the thrombus, whereas the indirect ones are mostly related to acute pressure overload in the right ventricle:

- RV dilatation and hypokinesis
- Abnormal interventricular septal motion
- Tricuspid valve regurgitation greater than 2.8 m/s
- Lack or decreased inspiratory collapse of the inferior vena cava (IVC)

Transthoracic echocardiography (TTE) can hardly visualize thrombi in the pulmonary artery; however, it is able to provide information on the hemodynamic status, on the RV and LV function, and on pulmonary pressure, and it also allows risk stratification. Transesophageal echocardiography (TEE) has a sensitivity ranging from 60 to 80 % and a specificity of 95–100 % in the diagnosis of acute PE. It highlights thrombi located in the trunk of the pulmonary artery and the two main branches as

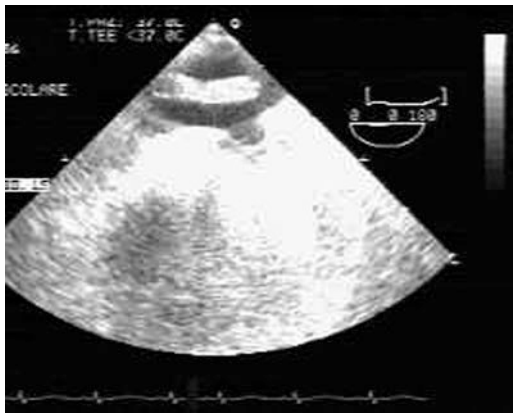

Fig. 31.2 Right branch of pulmonary artery. Upper esophageal long-axis view

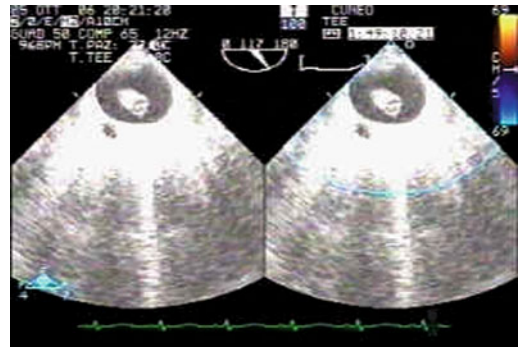

Fig. 31.3 Right branch of pulmonary artery. Upper esophageal short-axis view

well, although the left branch is only visible for a short distance (Figs. 31.2, 31.3).

TEE has a valuable role in the diagnosis of acute PE in patients who have had a sudden cardiac arrest or acute PE. The TEE shows floating thrombi in the right atrium very well. These are classified into three types: types A, B, and C. Type A thrombi have an elongated and serpiginous shape; they originate from peripheral veins and rapidly migrate to the pulmonary circulation. Thrombi of this type are associated with high mortality. Type B thrombi have a globular shape, a broad plant, and are motionless. They also migrate to the pulmonary circulation, but have a better prognosis than the other types. Type C is an intermediate form in its morphology, evolution, and prognosis.

Indirect signs of PE are due to overload pressure on the right ventricle, and this overload pressure is a consequence of obstruction of the pulmonary artery or its branches. For diagnosis of PE, 2D and Doppler echocardiographic parameters can be observed.

31.3 Two-Dimensional Echocardiography

The ultrasound views used to study the right ventricle are:

- TTE: parasternal views (long axis), and apical four-chamber and subcostal four-chamber views.
- TEE: upper esophageal views (trunk of the pulmonary artery and its division into right and left branches), and mid-esophageal views (four chamber, RV inflow-outflow, and bi-caval views)

The parasternal short-axis view for TTE and the transgastric short-axis view for TEE are useful to investigate the septum and the size of the right ventricle.

The findings in cases of acute RV overload are:

- Expansion of the right ventricle with LV deformity: the expansion can be measured both as the diastolic diameter of the right ventricle (DdRV) and as the relationship between the diastolic diameter of the right ventricle and diastolic diameter of the left ventricle (DdRV/DdLV). The finding of DdRV $>$ 30 mm and a DdRV/DdLV ratio of 0.7 or greater in parasternal long-axis and subcostal views and greater than 1 in the apical view is considered pathological. The area ratio of the two ventricles can be used if the images are of good quality. A right ventricle to left ventricle area ratio below 0.6 is normal; if it is greater than 1, a major expansion of the right ventricle is present.
- Right atrial dilation with interatrial septal shift to the left.
- Increased diameter and decreased collapse (less than 40–50%) of the IVC.
- Diastolic dyskinesia of the interventricular septum.

- Normal contraction of the RV apex with hypokinesis of the midportion of the RV free wall (McConnell sign). It has a high negative predictive value. This sign can be visualized from the apical four-chamber view.

31.4 Doppler Echocardiography

- *Estimation of pulmonary arterial systolic pressure*: The modified Bernoulli equation is applied on the tricuspid valve regurgitation jet to obtain the pressure gradient between the atrium and the right ventricle. Then the estimated right atrial pressure (RAP) is added to this gradient to obtain the pulmonary arterial systolic pressure. The RAP is estimated from the diameter and respiratory variation of the IVC. Usually, if the IVC collapse index is greater than 40–45 %, the RAP is estimated to be about 5 mmHg; if the index is between 35 and 40 %, the RAP is about 10 mmHg; an index less than 35 % means an RAP of about 15 mmHg.
  Pulmonary arterial diastolic pressure (PAPd) can be estimated from the end-diastolic pulmonary regurgitant jet, which depends on the diastolic pressure difference between the pulmonary artery and the right ventricle. The PAPd is obtained by applying the Bernoulli formula to the velocity of pulmonary regurgitation and then adding the diastolic pressure of the right ventricle. The RV diastolic pressure (RVPd) equals the RAP if there is no tricuspid valve stenosis ($PAPd = 4V^2_{PRd} + RVPd$).
- *Pulmonary acceleration time*: This represents the time necessary to reach peak pulmonary velocity and is calculated as the time interval between the beginning of the pulmonary valve flow and its peak velocity. In normal conditions this acceleration time is greater than 90 ms; if it is less than 60 ms, there is pulmonary hypertension. A pulmonary acceleration time of less than 60 ms associated with a tricuspid regurgitation pressure gradient below 60 mmHg (60/60 sign) is highly specific for PE. Another useful sign in the diagnosis of pulmonary hypertension is the shape of pulmonary blood flow; in the case of pulmonary hypertension, pulmonary blood flow has a triangular shape or shows a mesosystolic incision.

The detection of these parameters in a critical patient associated with a clinical suspicion of PE should point towards more specific tests if the condition of the patient allows this. If there is hemodynamic instability, an ultrasound examination compatible with PE can help the start of fibrinolytic therapy.

31.5 Echocardiography and Prognosis of Patients with PE

Echocardiography is able to show deterioration of the right side of the heart very well during PE. The gravity of RV dysfunction is a factor that can influence the outcome. Several studies have reported a decreased survival rate in patients with PE associated with RV dysfunction. Echocardiography is also able to predict the risk of developing chronic pulmonary hypertension: pulmonary arterial pressures greater than 50 mmHg at the time of diagnosis are associated with persistence pulmonary hypertension at 1 year from the acute event. In addition, ultrasonography performed 6 weeks after acute PE can highlight patients with persistent pulmonary hypertension and can be useful for a long-term treatment. In combination with ultrasonography there are some biomarkers that are useful in risk stratification, such as B-type natriuretic peptide (BNP), pro-BNP, and troponin. Several studies have shown an increased risk of mortality in patients with PE who had RV dysfunction associated with an increase in the levels of these markers.

31.6 Echocardiography and Therapy for Patients with PE

Early anticoagulation treatment can improve survival: therefore, in patients with a high clinical suspicion and a low bleeding risk, diagnostic investigations should not delay the start of anticoagulation therapy. In patients with clinical

suspicion of PE, echocardiography is a quick, accurate, and safe diagnostic tool; it can be used easily at the bedside and is able to show both direct (blood clots in the pulmonary artery or right atrium) and indirect (deterioration of the right side of the heart up to acute lung heart) signs of PE and to guide the therapeutic choice. Ultrasonography is also useful to monitor patients undergoing thrombolytic treatment for thrombosis of the right side of the heart. Thrombolysis is the treatment of choice for massive and submassive PE in patients with hemodynamic instability. It improves lung perfusion, reduces pulmonary hypertension, and improves function of the right side of the heart, but is burdened with increased bleeding complications. Echocardiography, however, has some limitations in the diagnosis of PE. It is a operator-dependent method, so the operator's experience and skill are fundamental. The display of thrombi, particularly in the left branch of the pulmonary artery, is obstructed by the interposition of the left bronchus. Furthermore, besides PE, some other diseases that can impair RV function (COPD exacerbations, right IMA, cardiomyopathies, and valvular disease) can be confusing, so it is important to make a differential diagnosis.

Further Reading

Goldhaber SZ (2002) Echocardiography in the management of pulmonary embolism. Ann Intern Med 136:691–700

Leibowitz D (2001) Role of echocardiography in the diagnosis and treatment of acute pulmonary thromboembolism. J Am Soc Echocardiogr 14:921–926

Mookadam F et al (2010) Critical appraisal on the echocardiography in the management of acute pulmonary embolism. Cardiol Rev 18(1):29–37

Torbicki A et al (2003) Right heart thrombi in pulmonary embolism: results from the international cooperative pulmonary embolism registry. J Am Coll Cardiol 41:2245–2251

Torbicki A, Perrier A, Konstantinides S, Agnelli G, Galiè N, Pruszczyk P et al (2008) Guidelines on the diagnosis and management of acute pulmonary embolism. The Task Force for the Diagnosis and Management of Acute Pulmonary Embolism of the European Society of Cardiology (ESC). Eur Heart J 29:2276–2315

Suspicion of Acute Aortic Diseases

32

Luigi Tritapepe, Francesca Pacini, and Maurizio Caruso

32.1 Introduction

In this chapter we will consider only the acute diseases of the aorta that quickly endanger the patient. This group of aortic diseases is now called "acute aortic syndrome" (AAS). AAS is a summary term for various acute life-threatening aortic conditions represented by aortic dissection, intramural hematoma, penetrating atherosclerotic ulcer, and thoracic aortic aneurysm rupture, excluding traumatic entities (Fig. 32.1). The incidence of AAS is 2.6–3.5 cases per 100,000 individuals per year. Two thirds of patients are male, and the average age of affected patients is 63 years. All of these diseases, namely, AAS, show a certain monotony in terms of symptoms. In fact, the patient complains of severe chest pain radiating to the neck and arms in the case of type A aortic dissection or intramural hematoma and into the abdomen and back in the case of type B aortic dissection. Also, very often, patients may have hypertension or hypertensive emergency with alteration of peripheral pulses which become asymmetric, and may have associated aortic valve regurgitation. Depending on the severity of the case, the patient may have hemodynamic instability with splanchnic hypoperfusion, metabolic acidosis, heart failure, and impaired cerebral perfusion. Also, patients may suffer from acute renal failure or respiratory insufficiency, and AAS can present itself as syncope related to cardiac tamponade or to occlusion of cerebral vessels. It may also occur as an acute coronary syndrome that sometimes is mistaken as the main pathologic entity instead of an accompanying syndrome. Therefore, differing AAS diagnoses may include myocardial ischemia/infarction, pulmonary embolism, pericarditis, acute aortic regurgitation without dissection, mediastinal tumors, perforating peptic ulcer, acute pancreatitis, cholecystitis, and musculoskeletal pain. Making a rapid diagnosis in these cases is essential to reduce mortality linked to AAS and especially to reduce morbidity. Normally, the most sensitive and specific imaging techniques are CT and MRI, whereas angiography has lost its diagnostic role. But nowadays echocardiography—transesophageal echocardiography (TEE) and transthoracic echocardiography (TTE)—plays an essential role because it is inexpensive, rapidly repeatable, and safe in experienced hands for the diagnosis of AAS. Furthermore, we also have to consider the time savings related to the examination with the ultrasound technique.

L. Tritapepe (✉)
Department of Anesthesia and Intensive Care, Cardiac Surgery ICU, Policlinico Umberto I Hospital, Sapienza University of Rome, Rome, Italy
e-mail: luigi.tritapepe@uniroma1.it

A. Sarti and F. L. Lorini (eds.), *Echocardiography for Intensivists*,
DOI: 10.1007/978-88-470-2583-7_32,

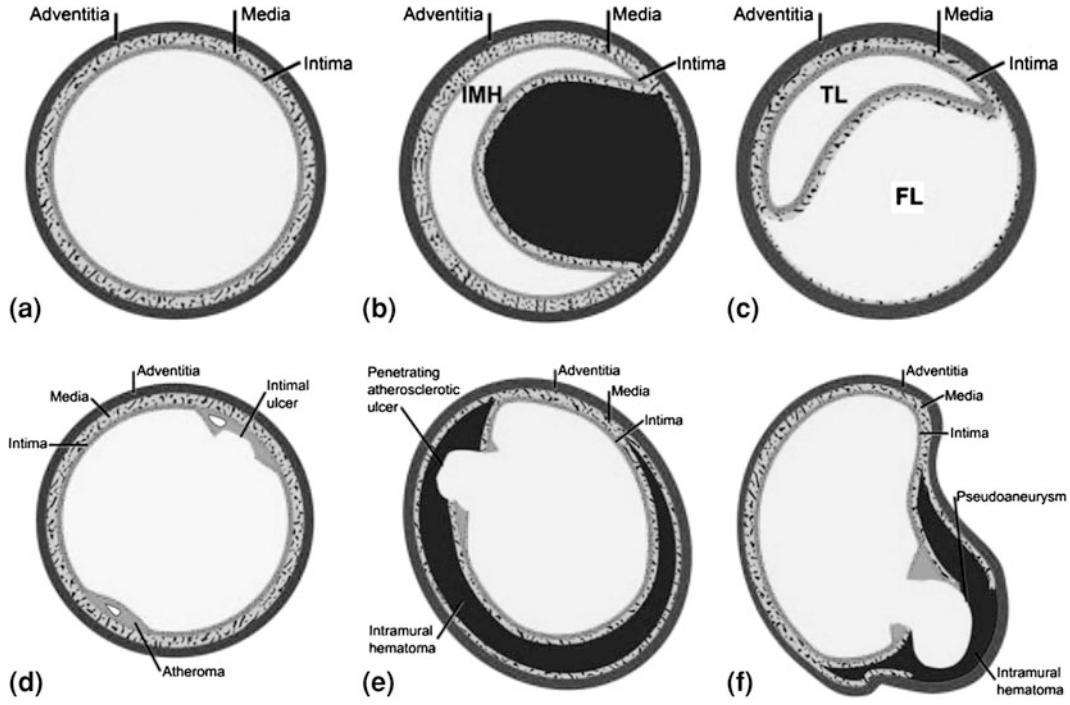

Fig. 32.1 The pathologic entities which determine acute aortic syndrome. **a** normal aorta, **b** intramural hematoma, **c** aortic dissection, **d** aortic atheroma and ulcer, and **e**, **f** penetrating ulcer with intramural hematoma and pseudoaneurysm. (Reproduced with permission from Shiau et al. [1])

32.2 TTE and TEE

The proximal ascending aorta is visualized in the parasternal long-axis view, and also in the modified right parasternal long-axis view and in the basal parasternal short-axis view, but to a lesser extent. The parasternal long-axis view allows us to correctly measure the aortic root diameters. In the parasternal long-axis view, directly in two dimensions or in M-mode, we can study the aortic root and the proximal ascending aorta at the end of diastole with the aortic leaflets closed. In all patients with suspected aortic disease, the right parasternal long-axis view, even if it is not routinely performed, is recommended for estimating the true size of the ascending aorta. The ascending aorta is also visualized in the apical three-chamber and modified apical five-chamber views; however, in these views, the aortic walls are seen with suboptimal lateral resolution and a false diagnosis could be made or the abnormality may remain unrecognized. The suprasternal view is a crucial tomographic view to visualize, above the right pulmonary artery, the aortic arch and the three supra-aortic trunks (innominate, left carotid, and left subclavian arteries), and again a variable tract of the descending and ascending aorta. Acute ascending aortic AAS (i.e., type A dissection flap) may be visible on TTE with a sensitivity of 60–80 % and specificity of 60–90 %. However, if there is inconclusive information or abnormalities are present, another imaging modality (e.g., TEE) is required to either complete or add diagnostic information. TEE has been shown to be a very sensitive diagnostic tool in the delineation and management of different aortic diseases. It is a fundamental examination to diagnose aortic

Table 32.1 Tomographic views for evaluation of the ascending thoracic aorta, the aortic arch, and the descending thoracic aorta

TTE	TEE
PSLAX, PSSAX (Asc + Desc Ao)	ME Asc Ao LAX, ME Asc Ao SAX (Asc Ao)
A4C, A2C, ALAX (Desc Ao)	UE aortic arch, UE aortic arch LAX (arch + Asc Ao)
Suprasternal (arch, Asc + Desc Ao)	Desc Ao LAX, Desc Ao SAX (Desc Ao)
Subcostal (abdominal + Asc Ao)	

TTE transthoracic echocardiography, *TEE* transesophageal echocardiography, *PSLAX* parasternal long axis, *PSSAX* parasternal short axis, *Asc* ascending, *Desc* descending, *Ao* aorta, *A4C* apical four chamber, *A2C* apical two chamber, *ALAX* apical long axis, *ME* mid-esophageal, *LAX* long axis, *SAX* short axis, *UE* upper esophageal

syndrome and differentiate other diseases in the case of chest pain. The anatomic proximity of the aorta to the esophagus allows us to have a good view of the aorta, almost entirely. The only invisible tract is the distal portion of the ascending aorta owing to the presence of air in the right main bronchus, whereas the proximal portion of the aortic arch is poorly visible because of the proximity of the trachea, which can cause a virtual blind spot in that area.

In routine practice, TEE evaluation of the aorta is possible through six views (Table 32.1): mid-esophageal ascending aorta short-axis view, mid-esophageal ascending aorta long-axis view, upper esophageal aortic arch short-axis view, upper esophageal aortic arch long-axis view, descending aorta short-axis view, and descending aorta long-axis view. In the mid-esophageal four-chamber view at 0°, the probe should be withdrawn 2 cm and the ascending aorta can then be shown in the short-axis view. This produces a circular image of the aortic root between the left atrium and the right atrium. Rotating the imaging plane to 90° will produce the long-axis view showing the ascending aorta. In this projection, however, the distal ascending aorta cannot be visualized because of the dispersion of echoes due to tracheal air. To view the descending thoracic aorta, we must return to the mid-esophageal four-chamber view and then rotate the probe through 180°, and then we see the aorta, which is positioned behind the esophagus. By slightly shifting the probe back, we can obtain the short-axis view of the thoracic aorta at various levels, making sure to rotate the probe slightly to center the image of the aorta because it runs laterally and then posteriorly to the esophagus at this level. Rotating the imaging plane to 90° will bring into view the long-axis image of the descending aorta. To view the arch, we return to the mid-esophageal four-chamber view at 0° and pull the probe back slowly until the aortic arch is seen. This is displayed in the upper esophageal long-axis view about 20 cm from the mouth rhymes. The proximal part of the aortic arch is not viewable because of air in the trachea; however we have a good view of the arch that shows the proximal portion to the left of the screen, and the distal part on the right with the posterior wall near the probe and at the top of the screen and the anterior wall further down. To obtain short-axis images of the aortic arch, we need to pull the probe back and rotate it 90° clockwise. The left subclavian artery and the left common carotid artery can also be viewed by pulling the probe further back. Study of the thoracic aorta should include wall thickness, tissue characteristics, dimensions, and blood flow patterns by Doppler assessment. The primary aim of TEE is to identify the intimal flap, false lumen, and entry tear, delineate the extent of aortic dissection , and identify intramural hematoma or penetrating atherosclerotic ulcer. TEE has a high sensitivity of 95–100 % and modest to high specificity of 75–100 % for identifying an intimal flap. More information about ultrasonography of the aorta can be found in Chap. 10.

Table 32.2 Acute life-threatening aortic conditions called acute aortic syndrome

Aortic dissection
Intramural hematoma
Penetrating atherosclerotic ulcer
Thoracic aortic aneurysm rupture

32.3 Acute Aortic Syndrome

Now we review the conditions that fall within the definition of AAS, as illustrated in Table 32.2.

TEE offers considerable advantages in the diagnosis of AAS. The technique has very high sensitivity and specificity, is rapid (5–10 min), readily available, and does not require the patient to be moved. Echocardiographic study should include transthoracic assessment of the upper third of the ascending aorta, aortic insufficiency quantification, pericardial effusion diagnosis, and assessment of segmental alterations of ventricular contractility. Only in the few cases in which TEE does not permit a definitive diagnosis or where intramural hematoma is suspected would it be advisable to perform MRI or CT. In patients with ascending aorta dissection, TEE offers sufficient information for surgery to be directly indicated. The delay of surgery while conducting other tests may increase the risk of death without any significant advantage.

32.4 Aortic Dissection

Acute aortic dissection occurs when there is a tear or separation of the aortic intima from the media. Flow of blood into the intima–media space allows the tear to propagate as a dissecting hematoma. Aortic dissection is usually classified on the basis of aortic tract involvement. DeBakey type I and Stanford type A include dissections that involve the proximal aorta, aortic arch, and descending thoracic aorta. DeBakey type II only involves the ascending aorta; this dissection is included in Stanford type A. DeBakey type III and Stanford type B include dissections that originate in the descending thoracic and thoracoabdominal aorta regardless of any retrograde involvement of the arch. Demonstration of the presence of an intimal flap that divides the aorta into two lumina, the true and the false (Fig. 32.2), forms the basis of echocardiographic diagnosis of the dissection.

Color Doppler imaging may help to evaluate the dissection when two different flow patterns, separated by the intimal flap, along the aorta, are identified. In the ascending aorta, particularly when it is dilated, linear artifacts are very common in the images and they may be confused with the intimal flap, which appears in the transverse or longitudinal plane. In most ascending aorta dissections, the movement of the intima is free and does not meet the reverberation criteria. Therefore, assessment of the location and mobility of intraluminal images by M-mode and their longitudinal extent permits correct identification of artifacts in the ascending aorta. Often, the false lumen is thrombosed. The differential diagnosis between total false thrombosis and aneurysm is not always easy by TEE. The high echogenicity on the internal surface, the semilunar form, and the smooth surface increase the probability of it being a thrombosed false lumen. Ascending aorta involvement has high mortality and urgent surgery is indicated; it is of importance to determine the proximal extent of the dissection. Treatment of type A is surgical and that of noncomplicated type B is medical. TEE permits correct assessment of the proximal extent of the dissection, except when it is located in the upper third of the ascending aorta and the proximal half of the aortic arch (Fig. 32.3).

It is very important to localize the intimal tear. With the use of color Doppler imaging, TEE permits small communications between true and false lumina, mainly in the descending aorta, to

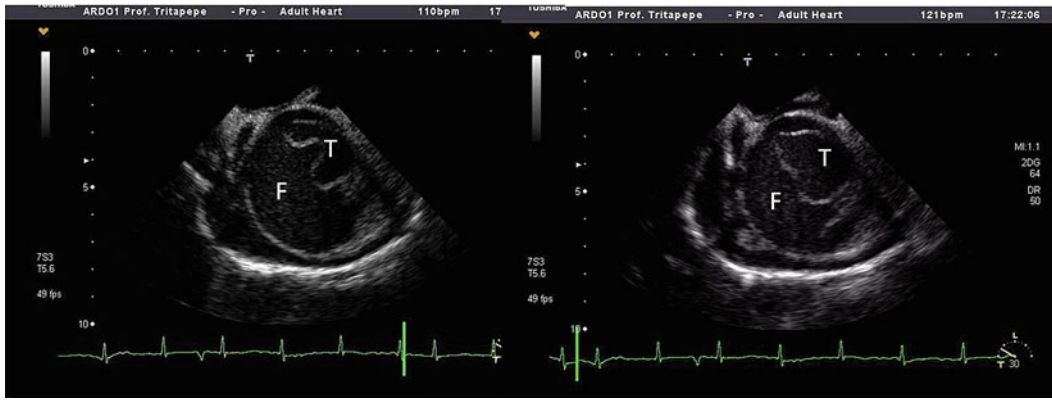

Fig. 32.2 TEE of the aortic dissection. False and true lumen during diastole and systole

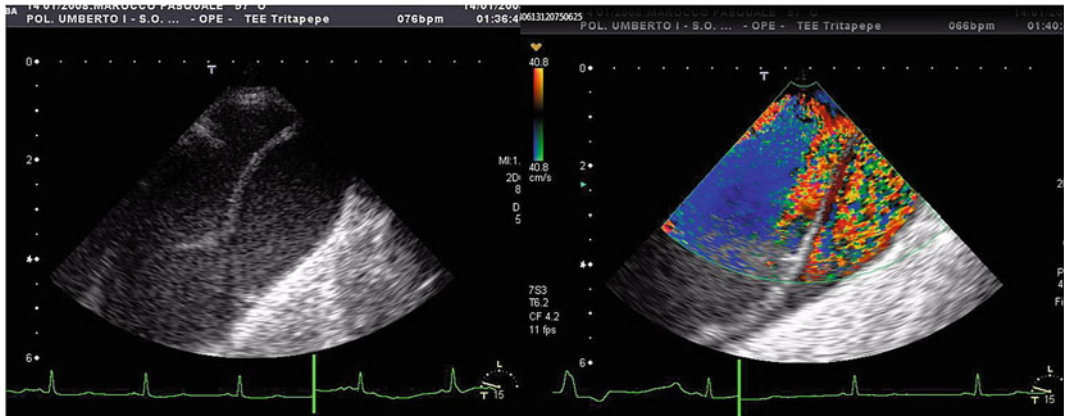

Fig. 32.3 TEE of the aortic arch dissection. False and true lumen without and with color Doppler imaging

be visualized. It is important to differentiate these secondary communications from the main intimal tear. The latter is usually identified by two-dimensional echocardiography and tends to measure more than 5 mm and be located in the proximal part of the ascending aorta in type A dissections and immediately after the origin of the left subclavian artery in type B dissections. With pulsed Doppler imaging, it can be verified that the flow velocity at the tear is usually below 1.5 m/s and the flow goes from the true to the false lumen in systole. In diastole, the velocity is lower and the flow usually goes from the false to the true lumen. In certain circumstances, identification of the false lumen is of special clinical interest. When the aortic arch is involved, the surgeon needs to know whether the supra-aortic vessels originate from the false lumen. Similarly, when the descending aorta dissection affects visceral arteries and ischemic complications arise, it may be important to identify the false lumen prior to surgery or endovascular treatment, such as intima fenestration or endoprosthesis implantation. Percutaneous fenestration of intima may be a therapeutic alternative when the main artery branches originate from the false lumen. On most occasions, the distinction between true and false lumina is easy. The false lumen is usually larger and has less flow than the true lumen. M-mode shows how the intima moves toward the false lumen at the start of systole by expansion of the true lumen. Partial thrombosis of the false lumen is frequently present and total thrombosis is occasionally present (Table 32.3).

Table 32.3 Complications and secondary findings detectable with transesophageal echocardiography

Complications	Secondary findings
Pericardial and pleural effusions	Secondary tears
Aortic rupture	False lumen thrombi
Aortic insufficiency	Intima movement
Arterial branch involvement	Predisposing factors

32.5 Aortic Intramural Hematoma

Aortic intramural hematoma forms part of AAS. Diagnosis by TEE is made when a circular or semilunar image, which may contain echolucent zones and which occasionally may be distributed in layers, is observed on the aorta wall. Wall thickness should be more than 7 mm and there should be no flow within. Diagnosis is straightforward in typical cases, but the hematoma may sometimes be mistaken for the presence of an intraluminal thrombus or a dissection with thrombosed false lumen. Other imaging techniques such as CT, which shows an attenuated signal zone, and MRI, with a hyperintense signal, confirm the diagnosis. On occasions, localized zones of the hematoma can be identified which break the intima, giving rise to saccular protrusions that may be confused with penetrating ulcers. In more than 10 % of cases, aorta zones with hematoma coexisting with others with classic intima dissection are detected; in these cases, the diagnosis is aortic dissection. In over 60 % of hematomas, the location is in descending aorta and is frequently accompanied by other signs of aortic arteriosclerosis. Evolution of the hematoma is highly dynamic, with complete reabsorption in more than half of cases or dissection in 40 % of cases being observed in the first 6 months.

32.6 Penetrating Aortic Ulcer

The diagnosis of penetrating ulcer is controversial. The presence of saccular protrusion outside the aorta profile is readily identifiable by contrast angiography and tomography. TEE is less useful in the diagnosis of these protrusions in the aorta profile, although recent studies have suggested its usefulness; nevertheless, it is highly useful for differentiating penetrating arteriosclerotic ulcers from ulcer-like projections secondary to thrombi with crater-like cavities in their surface and hematomas that evolve with disruption located in the intima. Absence of arteriosclerotic plaque in the intima of the aorta wall should lead us to suspect an ulcer-like projection and not a true penetrating ulcer. Aortic ulcers are also located more frequently in the descending aorta. Both color Doppler echocardiography and contrast echocardiography may be helpful to confirm the presence of flow within the external saccular protrusion to the aortic intima. Although TEE is highly accurate for the diagnosis of aortic dissection, its sensitivity and specificity in the diagnosis of intramural hematoma and penetrating ulcer have not been reported; thus, it is advisable to perform another imaging technique, particularly MRI, to confirm the diagnosis and provide information on bleeding persistence and the presence of periaortic hematoma.

Reference

1. Shiau MC, Godoy MC, de Groot PM, Ko JP (2010) Thoracic aorta: acute syndromes. Appl Radiol 1:6–16

Further Reading

Armstrong WF, Bach DS, Carey LM et al (1998) Clinical and echocardiographic findings in patients with suspected acute aortic dissection. Am Heart J 136:1051–1060

Evangelista A, Mukherjee D, Mehta RH et al (2005) Acute intramural hematoma of the aorta. A mystery in evolution. Circulation 111:1063–1070

Evangelista A, Flachskampf FA, Erbel R et al (2010) Echocardiography in aortic diseases: EAE recommendations for clinical practice. Eur J Echocardiogr 11:645–658

Golledge J, Eagle KA (2008) Acute aortic dissection. Lancet 372:55–66

Meredith EL, Masani ND (2009) Echocardiography in the emergency assessment of acute aortic syndromes. Eur J Echocard 10:i31–i39

Nienaber CA, Kische S, Skriabina V, Ince H (2009) Noninvasive imaging approaches to evaluate the patient with known or suspected aortic disease. Circ Cardiovasc Imaging 2:499–506

Shiga T, Wajima Z, Apfel CC, Inoue T, Ohe Y (2006) Diagnostic accuracy of transesophageal echocardiography, helical computed tomography, and magnetic resonance imaging for suspected thoracic aortic dissection. Arch Intern Med 166:1350–1356

Willoteaux S, Nedelcu C, Bouvier A et al (2011) Syndrome aortique: quelle imagerie réaliser? Presse Med 40:43–53

Chest Pain

33

Michele Oppizzi and Rachele Contri

33.1 Pulmonary Embolism

Chest pain in pulmonary embolism (PE) may be due to either peripheral embolism with pleural involvement or acute strain and ischemia of the right ventricle determined by a large, central embolism.

Echocardiography is an important diagnostic, monitoring, and prognostic tool in the treatment of patients with PE and also guides the choice of the most appropriate therapeutic strategy. Its applications are (a) diagnosis and differential diagnosis, (b) risk stratification, (c) decision making and echo-guided therapy, and (d) assessment of therapeutic efficacy in terms of thrombus size reduction, pulmonary pressure, and right ventricular (RV) function.

Taken together, clinical, echocardiographic, and biohumoral assessment allows a classification of patients with PE into high, intermediate, and low risk. Patients with hypotension (shock index greater than 1) or with shock are at high risk, with an in-hospital mortality rate between 15 and 30 %. Hemodynamically stable patients with at least one marker of RV dysfunction are classified as having intermediate risk, with an early mortality rate between 3 and 15 %. Stable patients with no RV dysfunction are at low risk, with an in-hospital mortality rate of less than 1 %.

33.1.1 Diagnosis and Differential Diagnosis

Echocardiographic findings suggestive of pressure overload induced by PE include RV dilatation and hypokinesia, abnormal leftward motion of the ventricular septum, functional tricuspid regurgitation, pulmonary hypertension, and a dilated inferior vena cava with lack of inspiratory collapse (Fig. 33.1). Moderate RV dilatation corresponds to a diastolic RV to left ventricular (LV) diameter or area ratio between 0.6 and 1, whereas a severe dilatation corresponds to a diastolic RV/LV ratio greater than 1. The RV/LV ratio is widely accepted as one of the most important and independent factors associated with elevated 30-day mortality.

Several patients with PE have a typical and distinct regional pattern of RV dysfunction, characterized by akinesia of the mid segment of the free lateral wall with a normal motion of the apex, known as the McConnel sign. This finding has a high specificity (94 %) for the diagnosis of PE and has an high positive predictive value (96 %). In patients with chest pain and suspected PE, echocardiographic signs of RV overload/dysfunction have a good positive predictive value for the indirect diagnosis of PE, whereas the sensitivity and specificity are reduced in the context of small PE. These findings are observed with a variety of other conditions associated with an increased RV

M. Oppizzi (✉)
Department of Cardiology, San Raffaele Hospital, Milan, Italy
e-mail: oppizzi.michele@hsr.it

A. Sarti and F. L. Lorini (eds.), *Echocardiography for Intensivists*,
DOI: 10.1007/978-88-470-2583-7_33, © Springer-Verlag Italia 2012

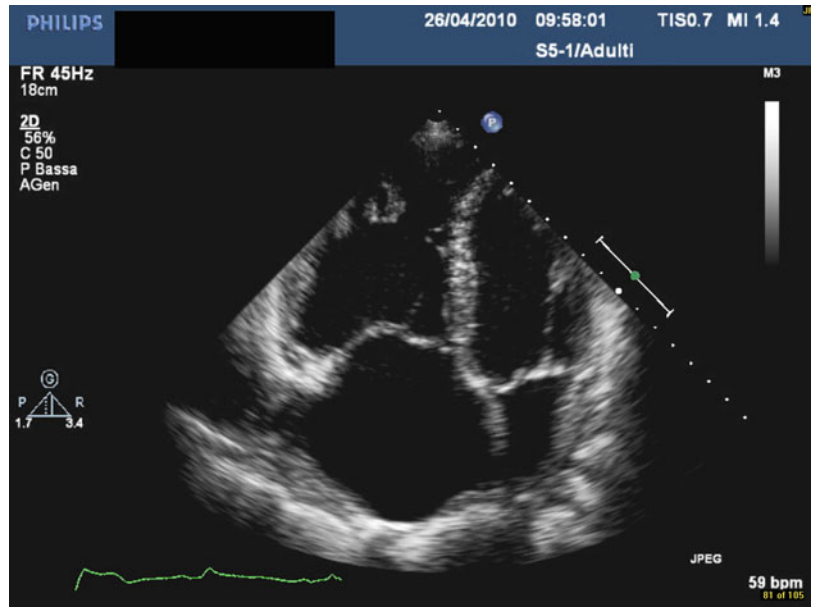

Fig. 33.1 Massive pulmonary embolism: right ventricular enlargement and paradoxical movement of septum

strain such as acute respiratory distress syndrome, asthma, chronic obstructive pulmonary disease, pneumothorax, and pneumonia.

RV dysfunction may be associated with inferior infarction, sepsis and myocardial contusion, and primitive RV myocardial diseases. In patients with a known cardiorespiratory disease, the specificity of the RV overload criterion decreases from around 80 to 20 %. On the other hand, the McConnell sign has a specificity and positive predictive value of around 100 %. Regional wall motion in the course of RV infarction may mimic the McConnell sign. Echocardiographic signs of pulmonary hypertension and pressure overload are required in order to avoid making a wrong diagnosis.

Adding RV dilatation/dysfunction to the clinical model substantially improves the risk stratification in terms of 1-month event-free survival, also in patients with clinically stable PE. Moreover, in patients who present with cardiac arrest, particularly in those with pulseless electrical activity, demonstration of RV enlargement by transthoracic echocardiography (TTE) or transesophageal echocardiography (TEE) has such a high positive predictive value for PE that the choice of fibrinolysis or of more aggressive treatments is justified.

Pulmonary artery (PA) systolic pressure is typically mild to moderate, around 40 mmHg. An acutely overloaded right ventricle cannot generate a higher pressure. A pulmonary pressure of more than 45 mm Hg suggests a chronic process or an acute PE superimposed on a chronic lung disease. Severe pulmonary hypertension (above 50 mm Hg) is associated with the persistence of pulmonary hypertension on follow-up.

If the patient is hemodynamically stable, the absence of echocardiographic signs of RV overload, which has a sensitivity of around 60–70 %, does not exclude PE, particularly when the clinical suspicion is moderate to high. Nonetheless, it is helpful to identify a low-risk group.

In patients presenting with critical conditions, echocardiography is particularly helpful because it allows a bedside and fast diagnosis, avoiding logistic problems associated with standard radiological diagnostic procedures, and is useful in the differential diagnosis of shock. The absence of signs of RV dysfunction/overload excludes PE as a cause of hypotension, whereas their presence is highly suggestive of PE and may justify an aggressive approach. Other causes of shock such as cardiac tamponade, acute valvular dysfunction, large myocardial

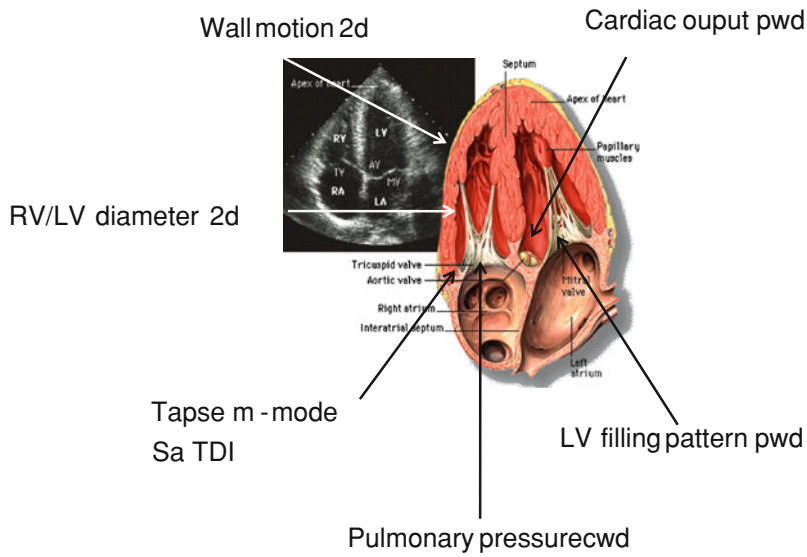

Fig. 33.2 Pulmonary embolism, apical four-chamber view. *AV* aortic valve, *cwd* continuous wave Doppler, *2d* two-dimensional, *LA* left atrium, *LV* left ventricle, *MV* mitral valve, *pwd* pulsed wave Doppler, *RA* right atrium, *RV* right ventricle, *Sa* systolic movement of annulus, *Tapse* tricuspid annular plane systolic excursion, *TDI* tissue Doppler imaging, *TV* tricuspid valve. (From Atlas of echocardiography, Yale University, with permission)

infarction, mechanical complications of acute myocardial infarction (AMI), and severe hypovolemia are rapidly detected.

We are not always able to visualize the thrombus in the inferior vena cava, right side of the heart, or main PA through TTE, whereas by using TEE we achieve a sensitivity of 92 % and a specificity of 100 % for central or right PA embolism. In the course medical treatment, echocardiography is useful in the evaluation of the efficacy of medications on RV function, PA pressure, LV filling, and thrombus dissolution.

33.1.2 How To Do It

Apical Four-Chamber View

By 2D echocardiography, an enlarged right ventricle is visualized and the free lateral wall seems severely hypokinetic on inspection. Typically the RV apex is spared. The atrial septum and the ventricular septum move toward the left ventricle during systole. A movement of the fossa ovalis greater than 1 cm is diagnostic of septal aneurysm, a condition not uncommonly associated with patent foramen ovale and with the risk of right-to-left shunt. After the image has been frozen, RV and LV end-diastolic diameters and areas are measured. The end-diastolic diameter is measured at the mid-portion of the cavity from the endocardium of the lateral wall to the endocardium of the septum. An RV/LV diameter or area ratio between 0.6:1 and 0.9:1 indicates a moderate dilatation, whereas a ratio greater than 0.9:1 indicates a severe enlargement that is associated with higher in-hospital mortality. RV end-diastolic and end-systolic areas are quantified and the fractional area change is calculated. After the image has been unfrozen, M-mode is applied on the tricuspid valve annulus, and the tricuspid annular plane systolic excursion (TAPSE) is recorded. An RV fractional area change below 30 % and TAPSE below 1.6 confirms RV dysfunction (Fig. 33.2).

PA systolic pressure is easily estimated by continuous wave Doppler (CWD) imaging from the velocity of the tricuspid regurgitant jet through the simplified Bernoulli equation. Color flow through the tricuspid valve is activated to visualize a regurgitant jet. Continuous wave Doppler imaging is aligned along the jet and the

velocity is recorded and frozen. The best envelope is chosen and encircled to measure the systolic right atrium–right ventricle gradient. Right atrial pressure, estimated from the inferior vena cava diameter, is added to the peak gradient to obtain the PA systolic pressure. If the spectral Doppler information is not well visualized, then 10 ml of agitated saline contrast agent can be used. Tricuspid regurgitation jet velocities are typically in the range of 2.5–3.5 m/s, corresponding to a PA systolic pressure of about 40 mmHg.

The leftward movement of the interventricular septum impairs LV filling and pulmonary hypertension reduces LV preload. The degree of LV impairment may be evaluated by examination of the diastolic function and cardiac output by positioning the pulsed wave Doppler beam first between mitral leaflets and afterward by moving it into the LV outflow tract (LVOT). E and A waves and the deceleration time are measured. A long deceleration time and an *E/A* ratio greater than 0.5 are common and indicate abnormal LV filling. Pulsed wave Doppler imaging is performed at the level of the LVOT, immediately under the aortic valve cusps. If the envelope of the LVOT is traced, the velocity–time integral (VTI) is automatically calculated. Stroke volume is obtained by multiplying the VTI by the aortic area calculated from the parasternal long-axis view.

Parasternal Long- and Short-Axis Views

The long-axis view is useful to measure the RV diameter and the aortic area to calculate the stroke volume. RV diameter is measured by M-mode at the end of diastole. A value greater than 33 mm is considered to represent RV dilatation. The aortic area is calculated from the systolic diameter of the LVOT according to the formula. The short-axis view at the level of the left ventricle is ideal for visualization of 2D paradoxical leftward ventricular septal motion and the degree of impairment of LV filling. At end diastole, the anteroinferior and the septal-lateral diameters can be measured; a ratio between them—the eccentricity index—less than 1 is a sign of severe pressure overload. In several cases, moving the probe cranially at the level of the aortic valve allows the visualization of the truncus and the bifurcation of the PA and the proximal tract of the right and left PA. In some cases, the thrombus can be identified in the main PA (Fig. 33.3).

Subcostal View

The subcostal view is well suited for the measurement of the inferior vena cava diameter. M-mode is applied perpendicular to the vena cava lumen so that its maximal and minimal diameter are measured, and the right atrial pressure can be calculated according to Table 33.1. In some cases, if the probe is turned clockwise, it is possible to visualize the truncus and the bifurcation of the PA.

TEE is usually needed to confirm the diagnosis of central PE, to assess whether the thrombus is sufficiently proximal to the PA to warrant surgical embolectomy, and to visualize any patency of the fossa ovalis. The main views to obtain the visualization of thrombus in the PA are the upper esophageal view for the PA and the mid-esophageal view for the RV inflow/outflow tract. In the upper esophageal view, the pulmonary truncus and the right PA can be visualized until branches to the right lung. The proximal tract of the left PA is obtained by rotation of the probe. The middle portion of the left PA is more difficult to investigate because of the presence of air in the left main bronchus. Nonetheless, the sensitivity of the TEE approach remains high (90–95 %), because the occurrence of an isolated left PA thrombus is uncommon. Thrombi can be classified by ultrasonography into two different morphological types: moving and hypoechoic or motionless and hyperechoic. Thrombolytic agents work better, in terms of a more effective lysis in vitro and a higher hemodynamic benefit in vivo, on the first, fresher, type of thrombus.

Finally, the TE probe is pushed some centimeters downward to achieve the mid-esophageal bicaval view in order to examine the fossa ovalis. Uncommonly, a thrombus straddling the

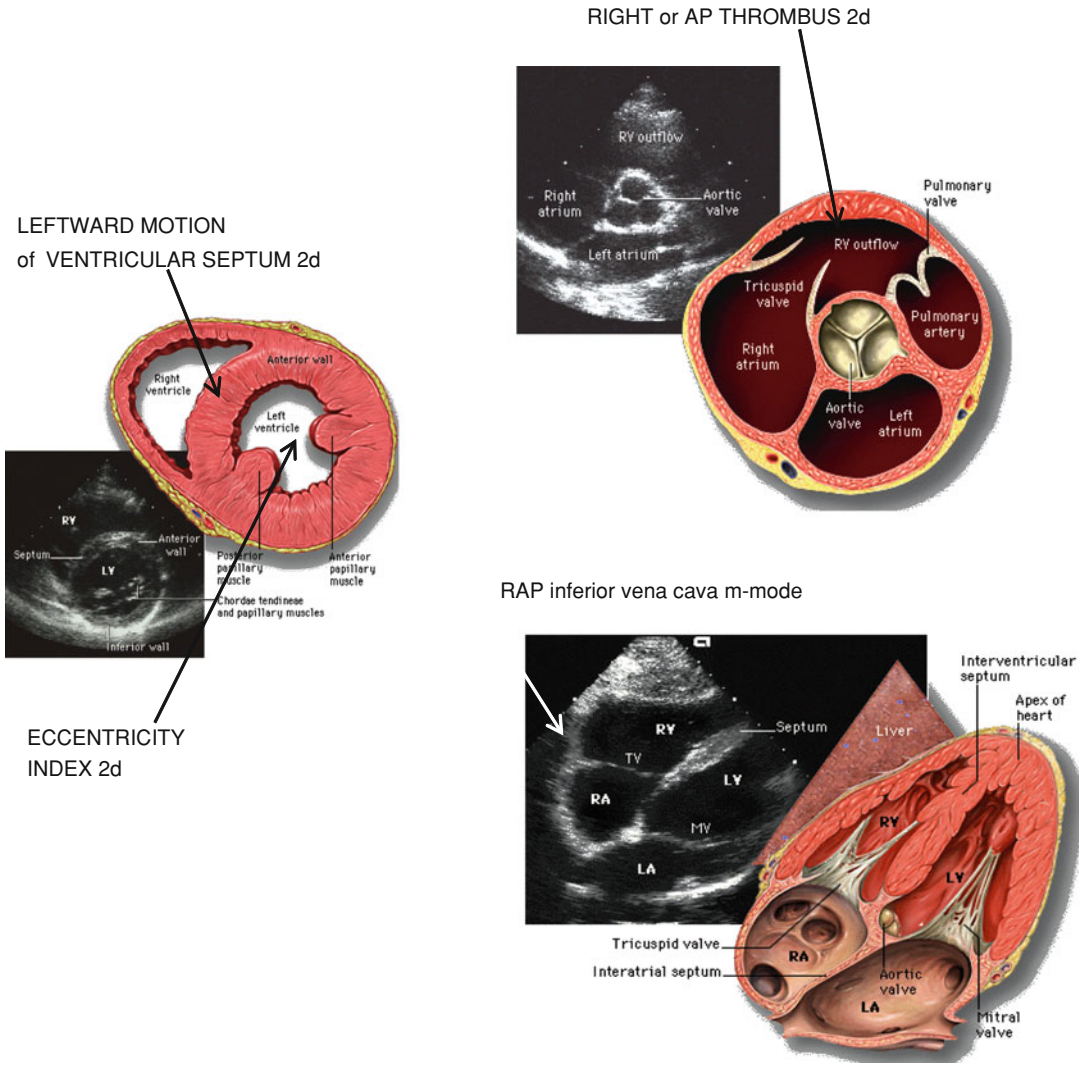

Fig. 33.3 Pulmonary embolism, parasternal and subcostal views. *PA* Pulmonary artery, *RAP* right atrial pressure. (From Atlas of echocardiography, Yale University, with permission)

Table 33.1 Data for calculation of right atrial pressure (*RAP*)

IVC diameter (cm)	SNIFF	RAP (mmHg)
<1.5	Collapse	0–5
1.5–2.5	>50 %	5–10
	<50 %	10–15
>2.5	>50 %	15–20
	<50 %	>20

IVC Inferior vena cava, *SNIFF*: inspiration

fossa ovalis with high risk of systemic embolism can be visualized.

33.1.3 Risk Stratification and Decision Making

Risk stratification achieved by echocardiography and additional to clinical findings has two goals: (1) the recognition of low-risk patients who can

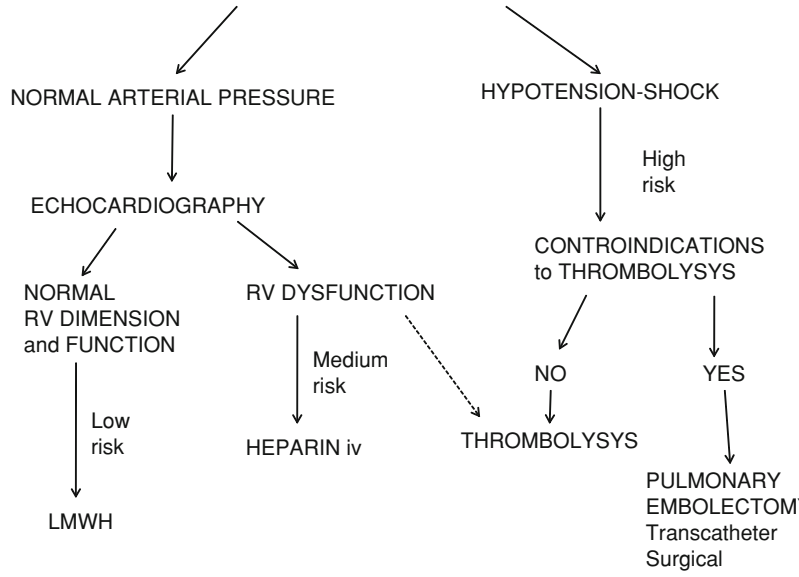

Fig. 33.4 Management of pulmonary embolism. *iv* intravenously, *LMWH* low molecular weight heparin, *RV* right ventricular

be treated as outpatients and (2) the identification, in hemodynamically stable subjects, of a subgroup at higher risk suitable for thrombolytic therapy (Fig. 33.4).

Hemodynamically stable patients with normal RV dimensions and function and normal PA pressure are a low-risk group with an in-hospital mortality of less than 1 %. They do not require admission to the ICU and could be eligible for early discharge and treatment at home with low molecular weight heparin.

The optimal treatment of stable patients with RV dilatation/dysfunction at intermediate risk is disputable. In-hospital mortality in these patients is undoubtedly higher than in the previous group, ranging between 5 and 10 %, but presently there is no compelling evidence of the benefits of fibrinolytic agents for survival. Intravenous administration of heparin is still generally considered the treatment of choice. Routine use of thrombolysis is not recommended because of the paucity of trials, the small number of patients involved, and disputed results, but it may be considered in selected patients, as long as the risk of bleeding is not elevated, particularly if RV enlargement is severe (RV/LV ratio greater than 0.9) and the cardiac troponin I level exceeds 0.1 ng/L, whereby the 30-day mortality reaches 38 % (Fig. 33.5).

Presently, we do not know if early inotropic treatment of normotensive patients with severe echocardiographic RV dysfunction could decrease the progression toward shock and their in-hospital mortality.

In high-risk patients with hypotension or shock, admission to the ICU is mandatory and thrombolytic therapy is the first-line treatment, unless there are absolute contraindications for its use. If thrombolysis is absolutely contraindicated or has failed to improve hemodynamics, surgical or percutaneous pulmonary embolectomy is a valuable therapeutic option. In emergency situations, TEE showing the presence of a thrombus in the main PAs is the only imaging modality to indicate this approach.

Echocardiography can also identify two other specific markers of high-risk PE and increased mortality: patent foramen ovale and right-sided heart thrombi. Patent foramen ovale is associated with right-to-left shunt with two consequences: (1) worsening of hypoxemia, pulmonary hypertension, and RV overload; (2) right thrombus crossing to the systemic circulation with the risk of cerebral or peripheral embolism. In the international registry, patients with free-floating right-sided heart thrombi have a mortality rate of 21 % compared with 11 % in those without RV thrombi.

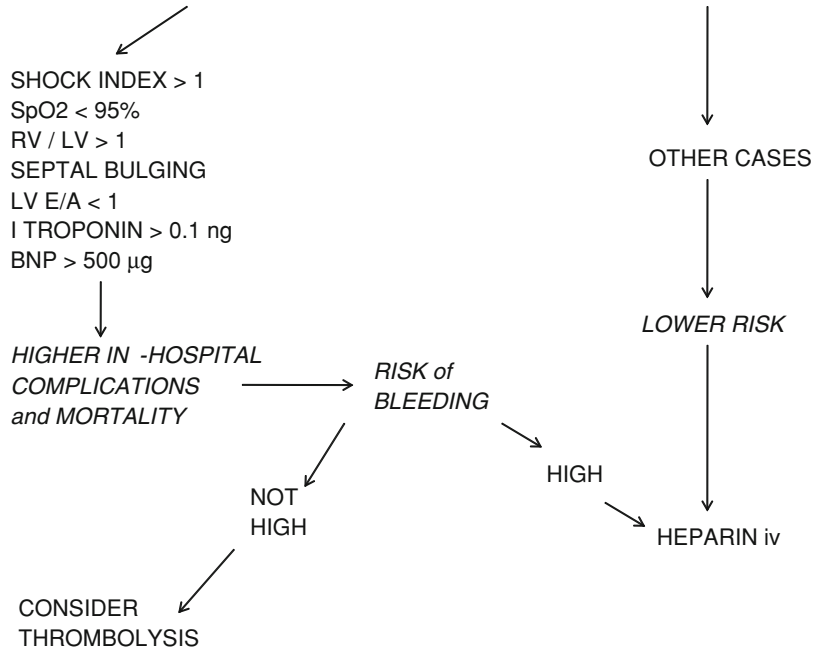

Fig. 33.5 Management of pulmonary embolism with right ventricular dysfunction. *RV* right ventricle, *LV* left ventricle, *E/A* transmitral Doppler E/A waves, *BNP* brain natriuretic peptide, *iv* intravenously

33.2 Acute Coronary Syndromes

33.2.1 Indications

There are two main indications for TTE in patients with ST elevation: (1) the differential diagnosis between AMI or myocarditis (regional wall motion abnormalities) and acute pericarditis (normal wall motion and in some cases pericardial effusion); (2) a rapid bedside examination to quantify the real extent of regional wall motion abnormalities. A mismatch between the number of leads with ST elevation and echocardiographic infarct extent is not uncommon. So echocardiographic examination is particularly useful in primary care hospitals to decide between in situ thrombolysis (small uncomplicated infarction) and transfer of the patient to tertiary centers for primary percutaneous pulmonary intervention (large infarction).

In patients with anterior ST depression, TTE allows the identification of the subgroup with posterior transmural AMI (regional wall motion abnormalities in the posterior wall) that must be treated with early reperfusion. When the baseline ECG is not diagnostic, segmental wall motion abnormalities are highly suggestive of AMI or acute myocarditis.

33.2.2 How To Do It

Diagnosis of Ischemia

Myocardial ischemia is characterized by regional wall motion abnormalities, described as hypokinesia, akinesia, and dyskinesia. Each segment is scored from 1 (normal) to 4 (dyskinesia). Hypokinesia is defined as a reduced endocardial motion and wall thickening in systole, akinesia as the absence of inward endocardial motion and systolic thickening, and dyskinesia as outward motion or bulging during systole, usually associated with a thin (thickness less than 5 mm), scarred (brighter) myocardium.

Site of Ischemia

From the base to the apex, the left ventricle is typically divided into three segments: basal, mid-ventricular, and apical. In the parasternal long-axis view, the basal and mid segments of the anterior interventricular septum and of the posterior LV wall are visualized (Fig. 33.6). In the short-axis views, all LV segments from the base to apex are visible. In clockwise order, the

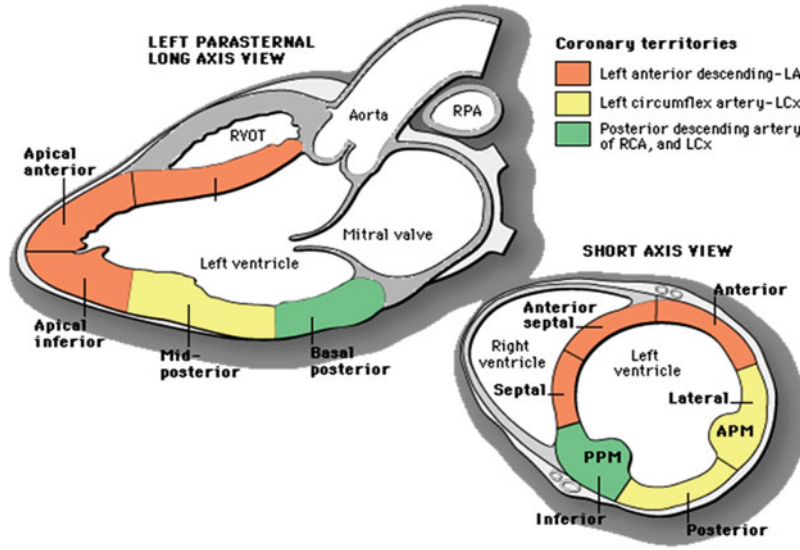

Fig. 33.6 Coronary vascularization, parasternal views. *APM* anterior papillary muscle, *PPM* posterior papillary muscle, *RCA* right coronary artery, *RPA* right pulmonary artery, *RVOT* right ventricular outflow tract. (From Atlas of echocardiography, Yale University, with permission)

anterior wall, lateral wall, posterior wall, inferior wall, inferior septum, and anterior septum can be seen. In the four-chamber view, the inferior septum, the anterior apex, and the lateral wall are visualized, in the two-chamber view the anterior and inferior walls and the inferior apex, and in the three-chamber view the anterior septum and the posterior wall. (Fig. 33.7) In the subcostal four-chamber view, the inferior septum and lateral wall are seen.

From the Site of Ischemia to the Identification of Coronary Artery Stenosis

The relationship between coronary artery anatomy and regional wall motion is usually as follows: The anterior septum (through the septal branches), anterior free wall, anterior apex, and lateral wall (through the diagonal branches) are supplied via the left anterior descending artery. If the left anterior descending artery extends around the apex, the apical segment of the inferior wall is usually affected in disease of the left anterior descending artery. Lateral and posterior walls are vascularized via the circumflex coronary artery. The right ventricle (RV branch), the inferior septum (posterior descending branch), and inferior and posterior walls receive blood from the right coronary artery. The pattern of wall motion is influenced by variations in coronary anatomy, the presence of collateral vessels, or previous bypass surgery.

33.3 Stress Cardiomyopathy, Apical Ballooning, Tako-tsubo Syndrome, Broken Heart Syndrome

Catecholamine-mediated myocardial stunning has been implicated in the pathogenesis of stress-induced cardiomyopathy. Apical ballooning is a unique and reversible acute cardiomyopathy frequently precipitated by a stressful event, whose pathogenesis seems to be related to catecholamine-mediated myocardial stunning. Despite a clinical presentation indistinguishable from that of AMI, stress cardiomyopathy is characterized by a normal coronary angiogram. Apical ballooning is diagnosed in about 1–2 % of all patients presenting with acute coronary syndrome.

Typical characteristics of apical ballooning are female prevalence, severe emotional stress as the precipitating factor, and wall motion abnormalities involving apical and mid segments, while the basal segments are typically spared.

Postmenopausal women account for 80 % of cases and it has been estimated that as many as 6 % of women presenting with acute coronary syndrome may have stress cardiomyopathy. A

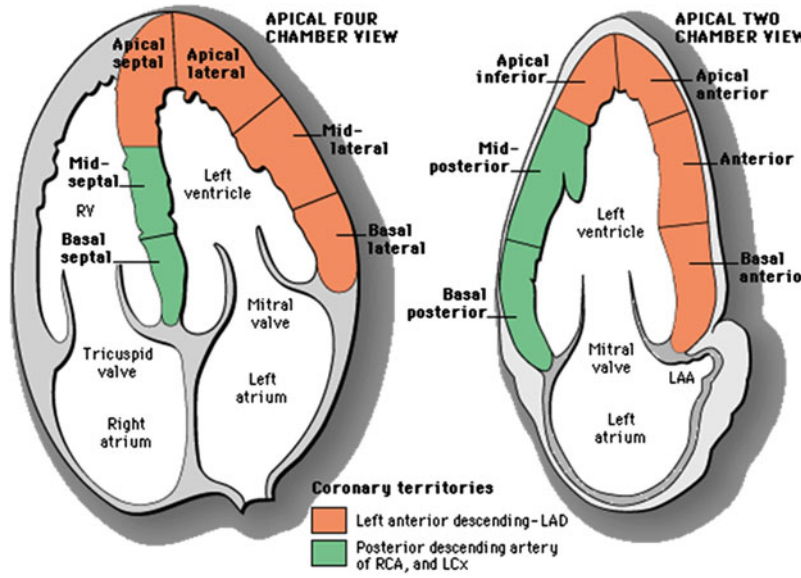

Fig. 33.7 Coronary vascularization, apical views. *LAA* left atrial area, *LCx*, left circumflex artery, *RCA* right coronary artery, *RV* right ventricle. (From Atlas of echocardiography, Yale University, with permission)

severe emotional stress, an acute illness, or a surgical procedure usually precedes the presentation of apical ballooning in approximately 40 % of cases. ST elevation usually occurs in the anterior precordial leads and the degree of ST elevation tends to be of a lesser magnitude when compared with AMI owing to coronary occlusion, but no ECG criteria are reliable in discriminating between apical ballooning and anterior ST-segment elevation myocardial infarction.

TTE is used to investigate apical ballooning and to identify the complications. In the classic form of apical ballooning, wall motion abnormalities (hypoakinesia or akinesia) involve the mid and apical segments of the left ventricle, sparing the basal segments, an alteration that outruns the distribution of any single coronary artery. The extent of areas of asynergy is typically disproportionate when compared with the degree of ST elevation and troponin release. It is necessary to pay attention to its variants, which are increasingly being recognized, where hypoakinesis/akinesis is limited to the mid or basal segments, sparing the apex (defined as inverted tako-tsubo). The final diagnosis relies on the absence of obstructive coronary artery disease on angiography.

The three main complications of the syndrome can be well visualized by TTE. They are:

1. RV involvement, present in up to 25–30 % of patients. The most affected segments are the apical, lateral (apical four-chamber view) ,and anterior (parasternal long- and short-axis views) segments. RV dysfunction is associated with a lower LV ejection fraction (between 35 and 45 %) and with a higher incidence of complications such as congestive heart failure, hemodynamic instability, intra-aortic balloon pump requirement, cardiopulmonary resuscitation, and prolonged hospitalization. Most patients with RV involvement have pleural effusions.
2. Dynamic LVOT obstruction (LVOTO) associated with mitral regurgitation due to systolic anterior movement, caused by hyperkinesia of the basal segments. This mechanism is especially observed in patients presenting with hypotension and acute heart failure. The patients at higher risk of LVOTO are elderly women with an abnormal basal–mid septal thickness—the so-called sigmoid septum—and with a small LV cavity owing to preexisting concentric LV hypertrophy, high levels of catecholamines, or acute hypovolemia.
3. LV mural thrombus formation in the akinetic apical segment. This is relatively rare, but it must be recognized since these patients require anticoagulation. Mechanical

complications, including ventricular septum and papillary muscle rupture, have been rarely reported, but they must be excluded by TTE, especially in patients with hemodynamic instability.

33.3.1 Echo-Guided Decision Making

Diagnosis requires a high index of suspicion, particularly in hospitals that do not have catheterization laboratories. Inappropriate administration of fibrinolytic drugs may be harmful without conferring any benefits.

No trial data are currently available. Therefore, optimal management has not been definitively established, but supportive therapy usually leads to a relatively prompt and spontaneous recovery. In-hospital mortality is around 1–2 %. In patients without congestive heart failure and/or severe reduction in LV/RV function, it is reasonable to start with beta-blockers empirically on the basis of the pathogenesis of the disease (i.e., cathecolamine-mediated myocardial stunning). Beta-blockers, possibly associated with cautious infusion of fluids or low dose of norepinephrine in hypotensive patients, are the first choice in the treatment of LVOTO. In subjects with congestive heart failure, diuretics are usually effective. Cardiogenic shock, after LVOTO has been excluded by echocardiography, is treated with inotropes and an intra-aortic balloon pump. Further echocardiographic examinations show a complete recovery from regional wall motion abnormalities and of ventricular function in virtually all patients 4–8 weeks after the acute event.

33.4 Aortic Dissection

In the evaluation of suspected aortic dissection, TTE should be performed as soon as possible, with all standard (i.e., left and right parasternal, apical, subcostal, suprasternal, and abdominal) and off-axis views, with the patient in the supine position and in both the left and the right lateral decubitus position in order to evaluate most of the thoracic aorta.

TTE may provide the diagnosis of aortic dissection and its complications, i.e., aortic valve regurgitation, signs of impending aortic rupture (pericardial or pleural effusion, cardiac tamponade), and coronary artery involvement. TTE is considered of limited value in the diagnosis of aortic dissection, with a sensitivity ranging from 35 to 80 % and a specificity from 39 to 86 %. These data are derived from studies performed at a time when the current imaging technology, such as harmonic imaging and multifrequency transducers, was not yet available. These recent advances in echocardiography have greatly improved image quality. The use echo contrast agents is safe and improves even further the sensitivity of the examination, yielding results similar to TEE. In addition, echo contrast agents eliminate the issue of artifacts, and easily identify the true lumen and improve the location of the entry tear.

33.4.1 Diagnosis of Aortic Dissection

The evaluation starts with the TTE approach (Fig. 33.8). Three echocardiographic signs are highly suggestive of type A aortic dissection: dilatation of the ascending aorta, new-onset aortic valve regurgitation, and pericardial effusion.

The visualization by 2D echocardiography of an intimal flap separating the true from the false lumen in the ascending aorta (type A) or the abdominal aorta (type B) or in both (type A) is diagnostic of aortic dissection. The specificity of TTE is high (about 95 %), but in some patients with a poor transthoracic window and in real-world experience the sensitivity is lower. Therefore, the TEE approach is usually needed to confirm the diagnosis, especially in the suspicion of type B aortic dissection when the abdominal aorta is not well visualized by TTE. TEE also provides further information which is useful for surgical planning. The sensitivity and specificity of TEE in the diagnosis of acute aortic syndrome in experienced hands approaches 100 %. The TEE blind zone, due to the interposition of the trachea between the esophagus and the upper ascending aorta, does not

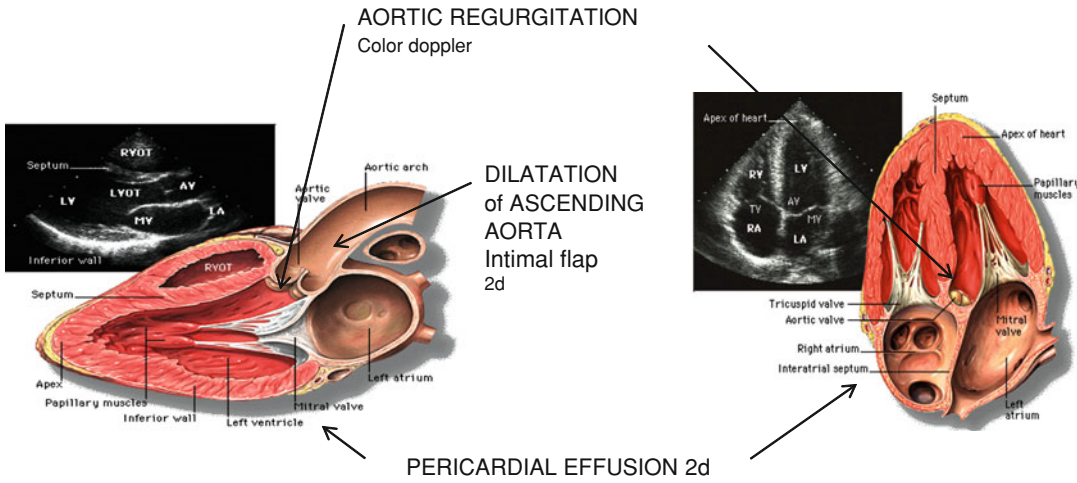

Fig. 33.8 Transthoracic echocardiography in suspected aortic dissection. *AV* aortic valve, *2d* two-dimensional, *LA* left atrium, *LV* left ventricle, *LVOT* left ventricular outflow tract, *MV* mitral valve, *RA* right atrium, *RV* right ventricle, *RVOT* right ventricular outflow tract, *TV* tricuspid valve. (From Atlas of echocardiography, Yale University, with permission)

represent a real problem because the probability of dissection confined to this location is extremely low.

33.4.2 Differential Diagnosis

TTE is also useful in establishing or excluding other diagnoses such as myocardial infarction (regional wall motion abnormalities), pericarditis (pericardial effusion), and PE (RV dilatation). ST elevation and regional wall motion abnormalities simulating AMI due to coronary thrombosis, particularly those involving the inferior wall, may be the consequence of the involvement of the ostium of the right coronary artery by type A aortic dissection. This complication is uncommon, but it must be well recognized in order to avoid the risk of aortic rupture as the consequence of the inappropriate choice of providing thrombolytic therapy or performing catheterization. Pericardial effusion is usually small in pericarditis, whereas it is large with signs of cardiac tamponade in aortic dissection.

33.4.3 Complications

Pericardial effusion occurs in up to 20–30 % of patients with ascending aorta dissection. It may be due to aortic rupture into the pericardium or to irritation of the visceral pericardial layer secondary to aortic intramural hematoma. Cardiac tamponade is a sign of poor prognosis with in-hospital mortality reaching 50 %. Among patients with type B dissection, a left pleural effusion identifies a group at higher risk of aortic rupture.

Both TTE and TEE are able to accurately quantify the diameter of the ascending aorta and the degree of aortic regurgitation, but TEE usually adds more information on the mechanisms of valve insufficiency, distinguishing valves with geometric distortion amenable to repair from those with organic disease that require replacement.

Coronary involvement in type A aortic dissection may be due to the propagation of the dissection to the coronary ostia, (usually the right) or, more frequently, may be due to preexisting coronary artery disease. Coronary involvement is suggested by regional wall motion abnormalities. TEE allows direct visualization of the coronary ostia and their spatial relationship with the dissection flap; TEE allows it to be established whether the coronary ostia originate from the true or the false lumen and if the dissection involves the coronary arteries. Wall motion abnormalities

in the absence of involvement of the coronary ostia by the dissection are typical of preexisting coronary artery disease. This information is of invaluable importance in guiding the decision making toward a surgical approach to perform myocardial revascularization, considering that coronary angiography is hazardous (in terms of aortic rupture, renal insufficiency) and not routinely used.

The aortic arch and the ostia of the neck vessels are better visualized by TEE than by TTE. In the evaluation of a surgical approach involving the aortic arch, it is important to assess the presence of an intimal tear in the arch, to distinguish between an entry or a reentry tear, and to establish whether flow in the innominate artery and in the left common carotid artery arises from the true or the false lumen.

Periaortic hematoma is well visualized only by TEE and appears as a collection of fluid around the aorta, near the site of the acute dissection. The hematoma is a harbinger of impending rupture.

33.4.4 How To Do It
Transthoracic Echocardiography

Parasternal Long-Axis View Two-dimensional echocardiographic inspection allows the diagnosis of type A aortic dissection by visualizing the intimal flap within the dilated aorta or indirect signs highly suggestive of aortic dissection: dilation of the ascending aorta, new onset aortic valve regurgitation, pericardial effusion.

Pericardial effusion is visualized as an anechoic (dark) space between the echogenic pericardium and the heart. A heart swinging into the pericardial fluid in a patient with pulsus paradoxus is suggestive of cardiac tamponade. The best view to visualize the hemodynamic effects of cardiac tamponade is the apical four-chamber view.

Two-dimensional echocardiographic inspection permits the immediate visualization of the ascending aorta dilatation. The aortic diameters ("annulus," Valsalva sinuses, sinotubular junction, and tubular tract) are obtained by M-mode or 2D echocardiography applied after freezing the image. The severity and the site of the dilatation are recorded. Aortic enlargement, due to intramural hematoma consequent to dissection, is usually located in the tubular tract of the ascending aorta. Dilatation involving the sinuses of Valsalva is a common occurrence in younger patients affected by connective tissue diseases. The right parasternal or high left parasternal views allow better visualization of the ascending aorta in some cases.

By positioning color flow into the LVOT, aortic regurgitation is visualized and quantified by the vena contracta method. Direction of the jet may be important to differentiate the various mechanisms of valve regurgitation (see TEE).

Parasternal Short-Axis View At the level of the aortic valve, the morphology of the cusps, the presence of a bicuspid aortic valve, and the diameter of the aorta can be assessed. Angulation of the transducer toward the LV apex allows the evaluation of the extent of the pericardial effusion and of LV regional wall motion and function. A swinging heart image caused by cardiac tamponade from aortic rupture may be easily appreciated.

Apical Views Apical views are useful to evaluate pericardial effusion, regional wall motion, LV and RV function, and the severity of aortic insufficiency. In the four-chamber view, the collapse of the right cavities by cardiac tamponade is immediately visualized. LV and RV function are quantified in terms of LV ejection fraction, RV TAPSE, and RV fractional area change. Usually RV and LV function are normal. A depressed ejection fraction may be due to acute severe aortic regurgitation (diffuse hypokinesia), the effect of intravenous beta-blockers (diffuse hypokinesia), regional wall motion abnormalities consequent to a previous AMI (akinesia or scar), or ongoing myocardial ischemia (asynergy without scar). RV dysfunction may be ascribed to acute dissection of the right coronary ostium if it is associated with inferior asynergy in the apical two-chamber view, or to a preexisting lung disease with RV hypertrophy and dilatation. Wall motion abnormalities are investigated in the four-, two-, and three-chamber views. Asynergy of the inferior wall is suggestive of right coronary dissection.

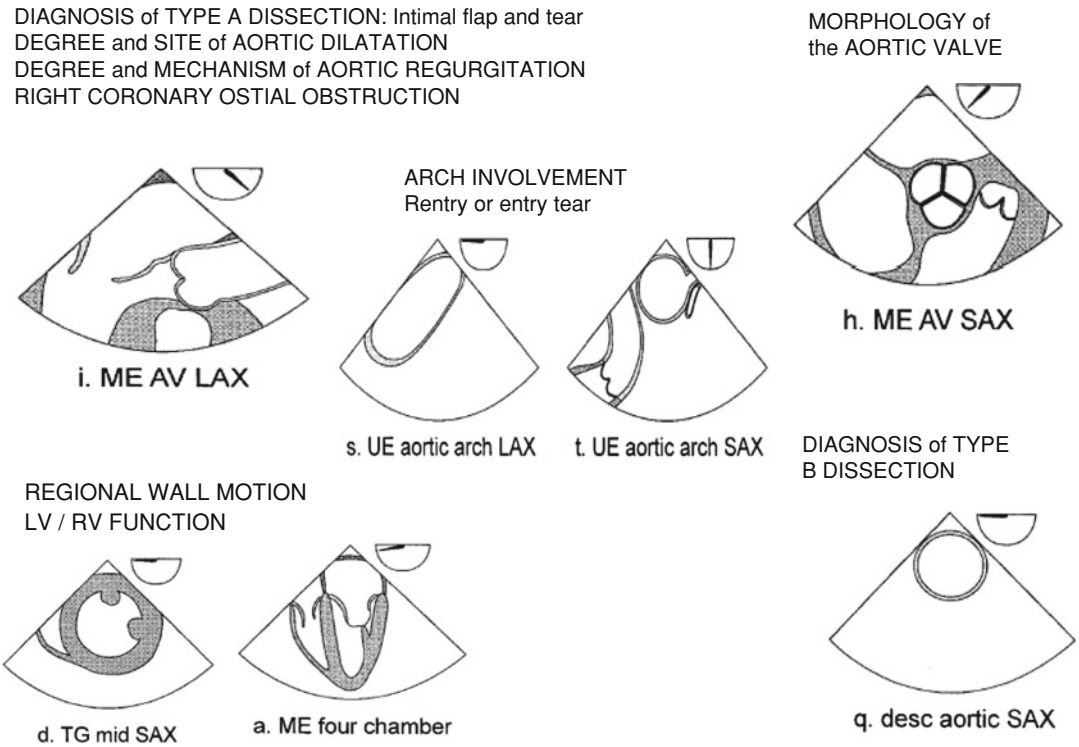

Fig. 33.9 Transesophageal echocardiography in aortic dissection. *AV* aortic valve, *LAX* long axis, *LV* left ventricular, *ME* mid-esophageal, *RV* right ventricular, *SAX* short axis, *TG* transgastric, *UE* upper esophageal. (From Shanewise et al. [4], with permission)

Abnormal motion of the other walls is usually associated with coronary artery disease. The presence and the degree of aortic regurgitation is assessed by color Doppler imaging in the four- and three-chamber views.

Subcostal and Abdominal Views These views easily allow the visualization of pericardial effusion (differential diagnosis with pleural effusion) and of the swinging heart phenomenon. By rotation of the probe to the vertical position, the abdominal aorta can be seen and the intimal flap dividing the true from the false lumen can be identified.

Suprasternal View In the suprasternal view the arch, the origin of the neck vessels, and the proximal descending aorta can be imaged and the intimal flap and tear may be visualized.

Pleura With the patient in the sitting position, and with the probe placed along the back of the thorax, pleural effusion is seen as an anechoic space between the probe and the lung. Its presence is suggestive of complicated type B dissection.

Transesophageal Echocardiography

TEE is the gold standard for the diagnosis of aortic dissection, with a sensitivity and specificity reaching 100 % (Fig. 33.9).

Mid-Esophageal Long-Axis View of the Ascending Aorta TEE examination starts with this view because it allows the diagnosis of type A dissection. In fact, the 2D examination shows the classic sign of aortic dissection, i.e., the presence of an intimal flap, which appears as a mobile linear echo separating the true from the false lumen. In most cases of type A dissection, a careful examination shows the intimal entry tear, which appears as an interruption in the flap crossed by turbulent color flow, located in the tubular tract of the ascending aorta usually a few

centimeters above the coronary ostia. The less common extension of the dissection to the sinuses of Valsalva and to the right coronary ostium is easily visualized. When the entry tear is not found in the ascending aorta or the aortic arch, it is usually located in the blind segment.

After the image has been frozen, all diameters of the ascending aorta should be measured: annulus, Valsalva sinuses, sinotubular junction, tubular tract. If the diameter of the Valsalva sinuses exceeds 45 mm, the more complex composite graft operation is required. A careful 2D echocardiographic inspection of the morphology and the movements of the valve cusps is helpful in distinguishing functional from organic regurgitation and to investigate the mechanisms of insufficiency. The presence of a bicuspid valve is suspected from systolic doming of the conjoint cusp. Cusp prolapse and the dissection flap are well visualized. Vena contracta imaged by Doppler color flow mapping predicts the severity of the regurgitation; moreover, information concerning jet direction (central versus eccentric) combined with morphological data are useful to characterize the mechanism of regurgitation.

Mid-Esophageal Short-Axis View of the Aortic Valve The short-axis view is complementary but superior to the long-axis view in distinguishing a normal from a diseased valve, especially in the evaluation of bicuspid aortic valve. The raphe is well visualized in diastole; in systole, the orifice has a characteristic elliptical shape and "fish-mouth" appearance.

Mid-Esophageal and Transgastric Short-Axis Views These views are useful to evaluate regional wall motion and pericardial effusion.

Descending Thoracic Aorta If the probe is turned toward the descending aorta, the extension of the dissection to the thoracic aorta and the abdominal aorta and the presence of reentry tears become visible.

Aortic Arch If the probe is withdrawn from the descending aorta, the aortic arch can be well visualized and it is possible to identify the origin of the neck vessels from the true or false lumen, the extension of the dissection into the ostia of the innominate and left carotid arteries, and the presence of a tear. In order to decide the most appropriate surgical approach, it is fundamental to distinguish the more common reentry rear (primary tear in the ascending aorta) from an entry tear (no tear in the ascending aorta).

True Lumen Versus False Lumen The true lumen is usually smaller, the flow is greater and anterograde during systole, and flap moves toward the false lumen. The presence of echo contrast or ongoing thrombosis is specific of the false lumen. When the entry tear is large, flow is similar in both lumens.

33.4.5 Timing of Sequence Examination

The primary objectives of the echocardiographer are to immediately identify an intimal flap and to delineate the extent of a thoracic dissection, categorizing it as type A, whose treatment is surgical, or type B, whose treatment is medical. The diagnosis of type A dissection and of type B dissection complicated by pleural effusion must be established as soon as possible, the cardiac surgeon must be alerted immediately, and all necessary procedures required before surgery must be done without delay. Meanwhile, secondary evaluations must be made in order to provide important information for the anesthesiologist and the surgical planning. The sequence of examinations must be tailored on the specific clinical situation.

In hypotensive patients (it is always necessary to check the arterial pressure in both arms to make sure there is not pseudohypotension) it is advisable to start with the subcostal view to visualize at the same time cardiac tamponade and an intimal flap in the abdominal aorta. If both complications are present, the diagnosis is type A aortic dissection with rupture in the pericardial space, a surgical emergency. More uncommonly, if the intimal flap is visualized but cardiac tamponade is not present, the apical five-chamber view must then be applied to search for other, more frequent causes of hypotension, such as a massive aortic regurgitation or a severe LV dysfunction.

In "stable" patients, TTE can be performed using the standard sequence of projections or starting from the subcostal and suprasternal

views to identify the aortic dissection in the shortest possible time.

After TTE examination has been completed, TEE is needed to confirm the diagnosis of aortic dissection or to identify other types of acute aortic syndromes (hematoma or aortic ulcer), which are usually poorly visible by TTE, and to provide further information useful for the decision making.

If the suspicion of type A aortic dissection is high, TEE examination should be performed in an environment where potentially life-saving cardiac surgery can be done without delay. To reduce the catastrophic risk of aortic rupture during esophageal intubation, continuous arterial pressure monitoring and deep sedation are mandatory.

33.4.6 Echo-Guided Decision Making

The goal of surgery in type A aortic dissection is to replace the tubular tract of the ascending aorta with a vascular prosthesis in order to prevent early death from aortic rupture, coronary dissection, and aortic valve insufficiency. It must be remembered that more complex repairs such as aortic valve replacement, coronary revascularization, composite graft procedure, and arch replacement do not influence in-hospital mortality but improve medium-term event-free survival. Their indications are based, in addition to age and concomitant diseases, on the extent of the dissection, the site of the entry tear, and surgical skill.

Type of Dissection

Acute type A aortic dissection is a highly lethal disease with an early mortality rate of 1–2 % per hour. In most patients with type A acute aortic dissection, emergent replacement of the ascending aorta is the only therapeutic option. Medical therapy is preferred as the initial treatment of type B dissection but, if there are echocardiographic signs of impending aortic rupture (pleural effusion, periaortic hematoma), interventional options (stenting or surgery) must be considered.

True Lumen Versus False Lumen

The distinction between the true and the false lumen has surgical relevance when the coronary arteries and/or neck vessels originate from the false lumen (see leter). It is also useful to guide safe cannulation in type A aortic dissection and endovascular graft positioning in type B aortic dissection.

Fluid Extravasation

Pericardial or pleural effusion and periaortic hematoma are signs of impending aortic rupture. All preoperative procedures must be expedited. Immediate surgery is mandatory. In type B aortic dissection, the presence of a pleural effusion results in a shift from medical to interventional therapy. Beta-blocking agents and coronary angiography must be avoided. Smooth induction is recommended. Sternotomy must be performed after femoral or axillary cannulation for extracorporeal circulation.

Aortic Regurgitation

If aortic insufficiency is acute (aortic valve of normal morphology) and the degree of regurgitation is severe, there is a high risk of pulmonary edema and tracheal intubation might be required. Obviously, in this situation beta-blockers must be avoided. In the elderly or in patients with a history of coronary artery disease, vasodilators must be used cautiously because of the risk of myocardial ischemia owing to further decreases in diastolic aortic pressure. Patients with severe aortic valve regurgitation, even when the cusps are normal, are best treated by aortic valve replacement (better 5-year event-free survival). More uncommonly (around 5 % of cases), valve replacement is necessary because of preexisting valve disease.

Aortic Root Involvement

If there is an aneurysm of the aortic root (larger than 45 mm), which is usually associated with Marfan syndrome, or a dissection involving the sinuses of Valsalva, a skilful surgeon performs a composite graft replacement (around 10 % of cases). The choice between the techniques of valve sparing (David operation) and valve replacement (Bentall operation) depends on the morphology of the aortic valve and the severity

of aortic regurgitation. The David procedure is preferred when the aortic cusps are normal and the degree of insufficiency is less than severe. In other cases, the Bentall operation is recommended.

Tear in the Aortic Arch

The surgical approach to the aortic arch may be different in reentry and entry tears.

Emiarch replacement, reimplantation of without neck vessels, is more easily performed and is indicated when the reentry tear is in the proximal tract of the arch. More complex total resection of the aortic arch with reimplantation of the neck vessels is preferable when there is a primary entry tear or a dilatation greater than 45 mm. Some skilful surgeons choose to perform extended arch repair also in young patients with Marfan syndrome in order to reduce the need for later arch resection.

Myocardial Ischemia

The treatment of patients with abnormal wall motion abnormalities on TTE has not been standardized. Coronary angiography may be applied but it is dangerous (false lumen cannulation) and time-consuming (high risk of aortic rupture in the first few hours from symptoms onset). Most surgeons perform coronary revascularization on the basis of the site of wall motion abnormalities and inspection of the coronary vessels.

Reference

1. Shanewise JS, Cheung AT, Aronson S et al (1999) ASE/SCA guidelines for performing a comprehensive intraoperative multiplane transesophageal echocardiography examination: recommendations of the American Society of Echocardiography Council for Intraoperative Echocardiography and the Society of Cardiovascular Anesthesiologists Task Force for Certification in Perioperative Transesophageal Echocardiography. Anesth Analg 89:870–884

Further Reading

Fremont B, Pacouret G, Jacobi D et al (2008) Prognostic value of echocardiographic right/left ventricular end-diastolic diameter ratio in patients with acute pulmonary embolism. Results from a monocenter registry of 1,416 patients. Chest 133:358–362

Meredith EL, Masani ND (2009) Echocardiography in the emergency assessment of acute aortic syndromes. Eur J Echocardiogr 10:131–139

Scridon T, Scridon C, Skali H, Alvarez A, Goldhaber SZ, Solomon SD (2005) Prognostic significance of troponin elevation and right ventricular enlargement in acute pulmonary embolism. Am J Cardiol 96:303–305

Torbicki A, Galie N, Covezzoli A et al (2003) Right heart thrombi in pulmonary embolism: results from the International Cooperative Pulmonary Embolism Registry. J Am Coll Cardiol 41:2245–2251

Tsai TT, Trimarchi S, Nienaber CA (2009) Acute aortic dissection: perspective from the International Registry of Acute Aortic Dissection. Eur J Vasc Endovasc Surg 37:149–159

Acute Dyspnea

34

Gino Soldati

Dyspnea, the subjective feeling of difficult, labored, or uncomfortable breathing, is a common complaint in intensive care medicine. It may result from many disorders involving the airways, pulmonary parenchyma, pleural space, chest wall, or pulmonary vessels (Table 34.1). Its differential diagnosis is not always immediate. Use of ecography for characterization of dyspnea and to aid in its diagnosis is interesting for different reasons:

1. Greater knowledge of the pleural acoustic plane in the normal subject and in the subject with pleural disease has allowed the creation of simple decisional algorithms with dichotomous (yes/no) answers relative to the causes of dyspnea.
2. Echography is a bedside, easily repeatable, noninvasive technique, so it may simply be considered as part of the clinical examination.
3. The echocardiographist may explore the heart, pleura, and lung in the same session, so defining through imaging the physiopathologic cross talk at the basis of the patient's symptoms (as in left ventricular failure and subpleural congestion).

G. Soldati (✉)
Emergency Medicine, Valle del Serchio General Hospital, Lucca, Italy
e-mail: g.soldati@usl2.toscana.it

34.1 Thoracic Sonography: Where and When

Lung echography is a focused method. The clinician will interpret a symptom (dyspnea) and then utilize "imaging" to potentiate the accuracy of an examination of a patient which may be poor when the symptoms are minor or initial. The answers obtained with echography are dichotomous—the sign is either present or absent—and the decisional algorithm leads to a "probable" diagnosis. Echography is thus an integrating part of clinical reasoning and as such is performed when the symptom is present and where the symptom is present.

Lung ultrasonography competes well with chest radiography when done in the ICU. In fact, in this setting, chest radiography is only performed in one projection and may be technically inefficient. The diagnostic accuracy for pleural disease is thus reduced (even to a reported sensitivity of 50 % or less). In the same way, an increase in extravascular lung water is only diagnosed through chest X ray when it is greater than 30 %. Analogous difficulties arise with the differential diagnoses of opacities hardly identified as of pleural, interstitial, alveolar, or at times even subdiaphragmatic origin.

Lung echography is a recent application of ultrasound on the thorax. The study of the pleura as in pneumothorax and effusions has been done for a long time, but its most innovative aspect is the study of artifacts. This unusual representation

A. Sarti and F. L. Lorini (eds.), *Echocardiography for Intensivists*,
DOI: 10.1007/978-88-470-2583-7_34, © Springer-Verlag Italia 2012

Table 34.1 Acute dyspnea and its differential diagnosis

Acute dyspnea	Differential diagnosis
Pleural diseases	Pneumothorax
	Hemothorax
	Pleural effusion
Parenchymal diseases	Cardiogenic edema
	Noncardiogenic edema
	Interstitial pneumonia
	Pulmonary consolidations (acute)
	Diffuse parenchymal lung diseases (acute)
	Trauma (contusion)
Obstructive diseases of the airways	Asthma
	Chronic bronchitis
Pulmonary vascular obstructive diseases	Pulmonary embolism

is typical of that type of lung disease which allows the lung to still have air in its subpleural periphery. In the next paragraphs artifactual aspects of lung echography characteristic of interstitial parenchymal disease will be described. These artifacts are present when the lung is edematous and thus characteristic of cardiogenic and noncardiogenic pulmonary edema, especially in the initial, nonconsolidating phases. Diagnostic characteristics of pleural effusion, pneumothorax, consolidations, and pulmonary embolism are described in Chap. 45.

Echographic interstitial syndrome is disease of lung parenchyma characterized by an increase in density, but not by consolidations. Parenchymal density is not enough to generate anatomic images, but is able to alter the subpleural lung geometry and density, generating artifacts. These artifacts, known as B lines (Fig. 34.1), may range in density up to coalescence and generation of a "white lung" (Fig. 34.2). A patient with acute dyspnea and diffuse echographic interstitial syndrome has a hyperdense, but not a consolidating, parenchymal lung disease. A patient with dyspnea and no interstitial syndrome is not affected by pulmonary, cardiogenic, or noncardiogenic edema or any other interstitial disease.

34.2 Instruments

Currently, to perform a thoracic sonography, a normal ultrasound machine equipped with convex and linear probes (with a frequency range between 3.5 and 10 MHz) is used. A low ultrasound frequency (using a convex probe) can penetrate deeply into lung consolidations and provides images of the vertical artifacts (B lines). A linear probe accurately explores the surface of the pleura, its irregularities, small subpleural consolidations, and pleural origin points of B lines. There is no evidence on the utility of advanced ultrasound features (e.g., harmonics).

The probe is placed in the intercostal spaces and, in the scan, normal chest wall planes look like real images, up to the pleural line. Visceral pleura appears as a regular echogenic line that moves through the act of breathing.

34.3 Pleural Line Artifacts

The lung in the normal subject has a cortical density of 0.15 g/ml, as it contains air for the most part. The pleural level is seen as a hyperechogenic line underneath the costae. The visceral pleura acts as a specular reflector which returns to the transducer around 90 % of the acoustic energy it receives. For this reason the subpleural space is echographically virtual and made of horizontal artifacts that reflect and repeat the pleural plane and the superficial planes crossed by the ultrasound beam (A lines) (Fig. 34.3). An increase in density of the lung (for an increase in interstitial edema, a reduction in air content, or both) increases the acoustic permeability of the pleural line. The ultrasound is able to penetrate the pleura through acoustic microdiscontinuities of the expanded interstitial space and thus interact with residual air in small reverberation "rooms" which are more or less concentrated and homogeneous. Multiple repetitive signals are thus sent the transducer and the machine interprets them as nonreal images. B lines are therefore a representation not of

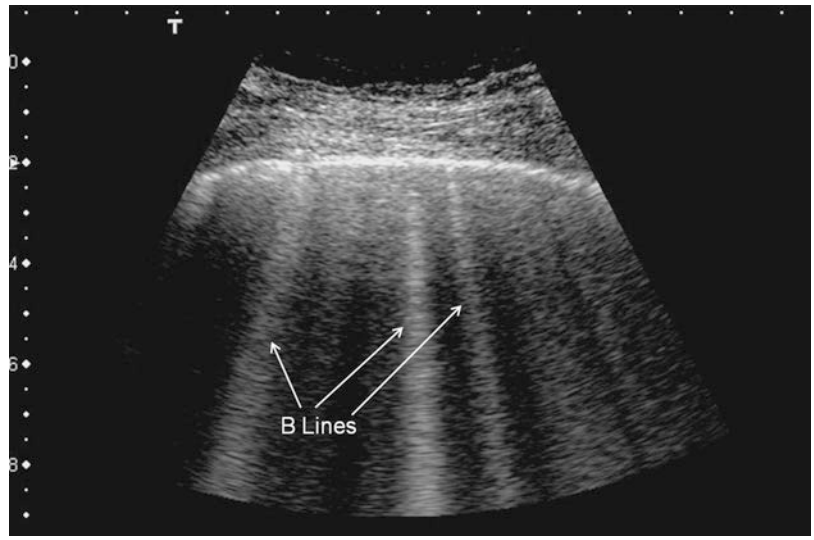

Fig. 34.1 B lines in a patient with cardiogenic pulmonary edema. They appear as vertical laser-like artifacts which extend to the inferior margin of the screen. A 5-MHz convex probe was used

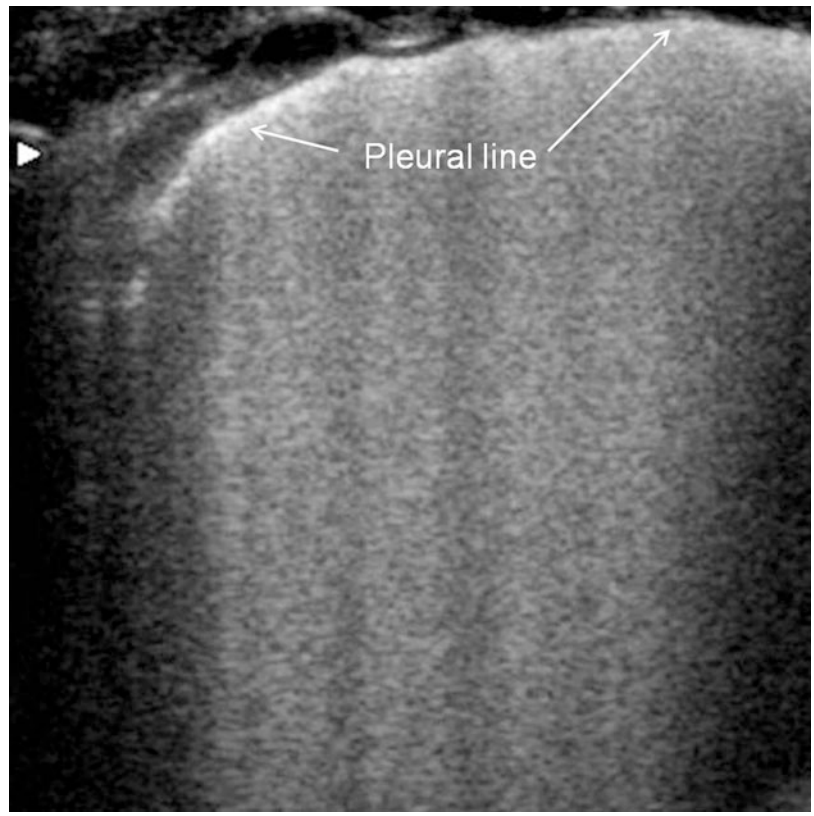

Fig. 34.2 Coalescent B lines generating the white lung effect in a patient with acute respiratory distress syndrome (ARDS). It is an echogenic subpleural field masking A lines. A 7.5-MHz linear probe was used

anatomic structures but of density-dependent small acoustic discontinuities of the pleural reflector. They define a hyperdense range of the lung up to the density of lung consolidation, which is 0.9–1 g/ml. The white lung pattern (Fig. 34.4) identifies elevated and homogeneous parenchymal densities seen on computerized tomography as "ground glass".

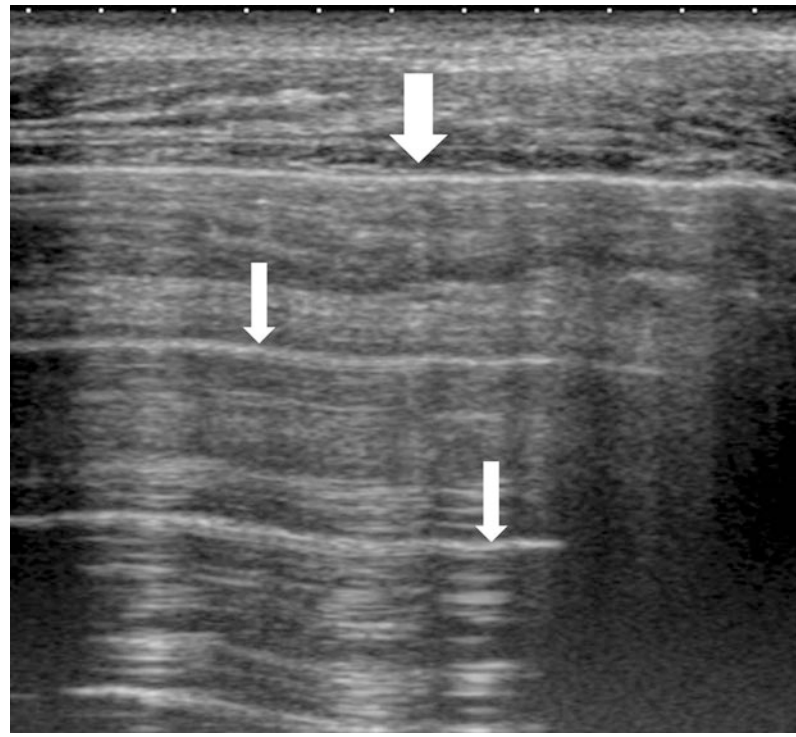

Fig. 34.3 Normally aerated lung. The pleural line is indicated by the *thick arrow*. *Thin arrows* indicate horizontal repetition lines, known as A lines. They represent reverberation artifacts which reflect the pleural line in depth. A 10-MHz linear probe was used

34.4 Clinical Use of Interstitial Syndrome

Instrumental evidence of B lines and of a white lung indicates interstitial lung disease and is useful when investigating the causes of acute dyspnea. Interstitial syndrome may be focal (with segmentary or random aspects) as in interstitial pneumonia or in lung contusions. It may be bilateral and diffuse as in hydrostatic pulmonary edema or in acute respiratory distress syndrome (ARDS). The presence of these signs places the patient in the category of parenchymal, nonconsolidating causes of dyspnea. B lines and white lung though are not specific signs as they appear in all interstitial diseases, including diffuse parenchymal disease as fibrogenic or granulomatous, both primary and secondary.

In terms of the decisional algorithm, what is extremely useful is finding the absence of B lines, which directs the clinical diagnostic process toward bronchial, pleural, or vascular lung disease.

34.5 Cardiogenic Pulmonary Edema

Cardiogenic pulmonary edema is a hydrostatic type of edema which generates B lines in variable concentration and up to their confluency. These B lines originate from the pleural line and extend like laser beams to the inferior margin of the screen. They move along with pleural sliding, which is preserved in this type of edema. The pleural line is usually regular, and the echographic signs are bilateral and contiguous with no spared areas. A small pleural effusion is usually present. A look at the heart aids in diagnosing a cardiac origin.

B-line concentration is correlated to the severity of pulmonary edema and with radiographic scores of pulmonary edema. There is a significant correlation between the numeric concentration of B lines and the B-type natriuretic peptide (BNP) and pro-BNP concentration. B lines are furthermore correlated with the New York Heart Association class, with the ejection fraction, with diastolic dysfunction, with wedge pressure, and with the degree of extravascular lung water.

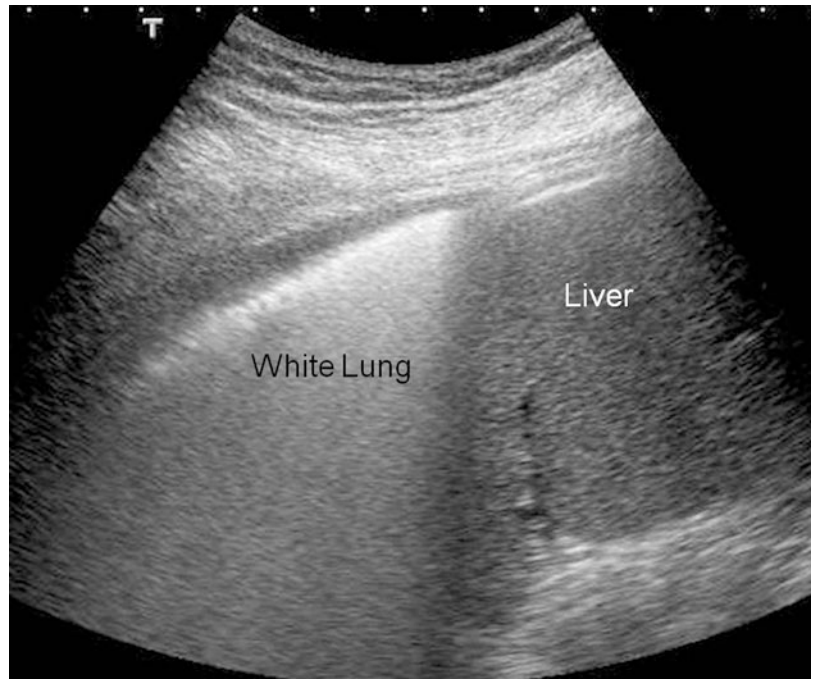

Fig. 34.4 White lung at the right pulmonary base in a patient with inflammatory edema. This variation of the subpleural pattern from A lines to an artifactual echogenic field represents a hyperdense nonconsolidating lung. A 3.5-MHz convex probe was used

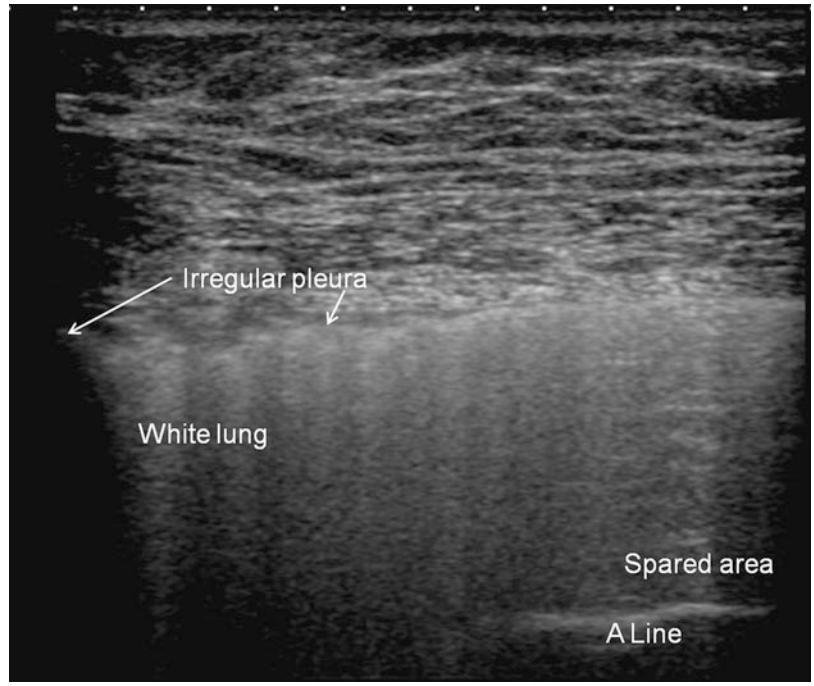

Fig. 34.5 Noncardiogenic pulmonary edema. The pleural line is irregular. On the *right* there is a normal horizontal reverberation artifact (*spared area*). On the *left*, the subpleural acoustic pattern is pathologic (white lung with many coalescent B Lines). A 7.5-MHz linear probe was used

A clinical and radiologic entity of pulmonary edema produces artifacts that are initially scattered (septal syndrome), with a greater concentration at the lung bases, and then extend through all the lung surface to become confluent.

B lines are often present in patients with pulmonary congestion and subclinical pulmonary edema. This could be due to venular perilobular congestion and subpleural septal edema. These artifacts tend to rapidly disappear after

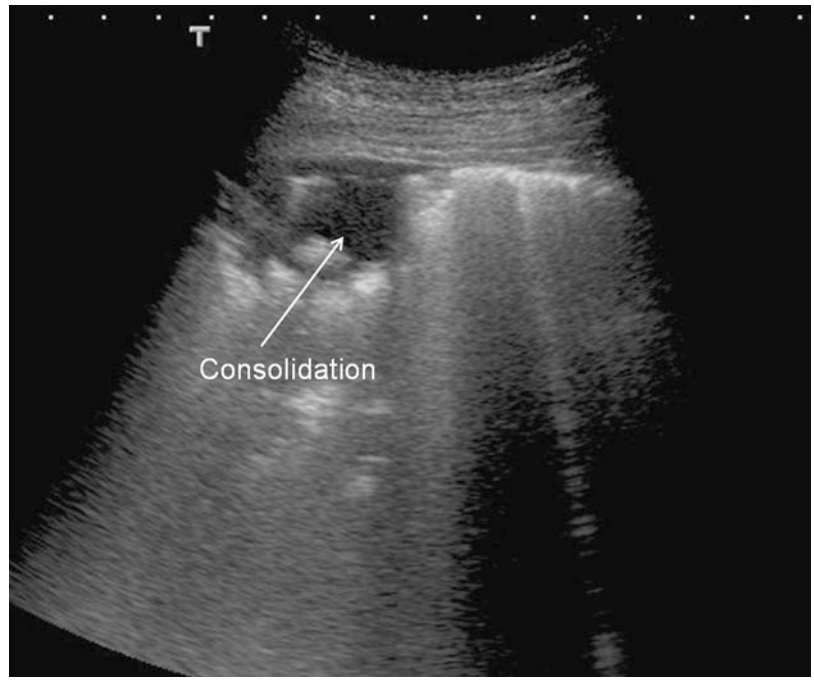

Fig. 34.6 Gravitational consolidation in ARDS. Organization (hepatization) of a pulmonary field with a solid appearance and posterior echogenic reinforcement. On the *right* there is interstitial disease. A 5-MHz convex probe was used

diuretic and vasodilator therapy. An increase in interstitial density explains the appearance of interstitial syndrome in patients with borderline congestive heart failure undergoing a cycle or echographic stress test, also correlated with an increase in wedge pressure after exercise.

34.6 Acute Lung Injury/ARDS Edema

Acute lung injury (ALI) and ARDS are inflammatory lung diseases characterized by edema due to alterations in the alveolocapillary membrane. They show interstitial and consolidating phases (alveolar), acute and chronic (fibrogenic), that follow a ventrodorsal gradient. Computerized tomography has clearly been able to demonstrate how this disease is inhomogeneous, with areas that are normally expanded, hypoexpanded, and consolidated. The echographic study of consolidations in ARDS shows dense regions with solid, tissue-like characteristics which may contain air in bronchograms or bronchiolograms, or as still ventilated alveoli. Interstitial syndrome is present wherever lung porosity is reduced to the hyperdense range and shows confluent B lines or white lung. Certain characteristics differentiate ALI/ARDS from hydrostatic edema. In noncardiogenic pulmonary edema, the pleural line loses its linearity (Fig. 34.5) and its physiologic motility (sliding), some "spared areas" are present (relatively normal looking areas in the context of diffuse interstitial disease), white lung pattern is well represented, and consolidations are present (Fig. 34.6).

34.7 Differential Diagnosis in Echographic Interstitial Syndrome

Differences between cardiogenic pulmonary edema and ALI/ARDS have been described. Isolated pleural regions with B lines and/or white lung are aspects of focal interstitial disease. They are present in interstitial pneumonia, around flogistic alveolar consolidations, or even in lung contusion without consolidation or parenchymal rupture. Bilateral interstitiopathy appears in subjects with diffuse interstitial lung disease, and in these cases a fibrous and/or micronodular pleural involvement is frequent. The pleura is not regular

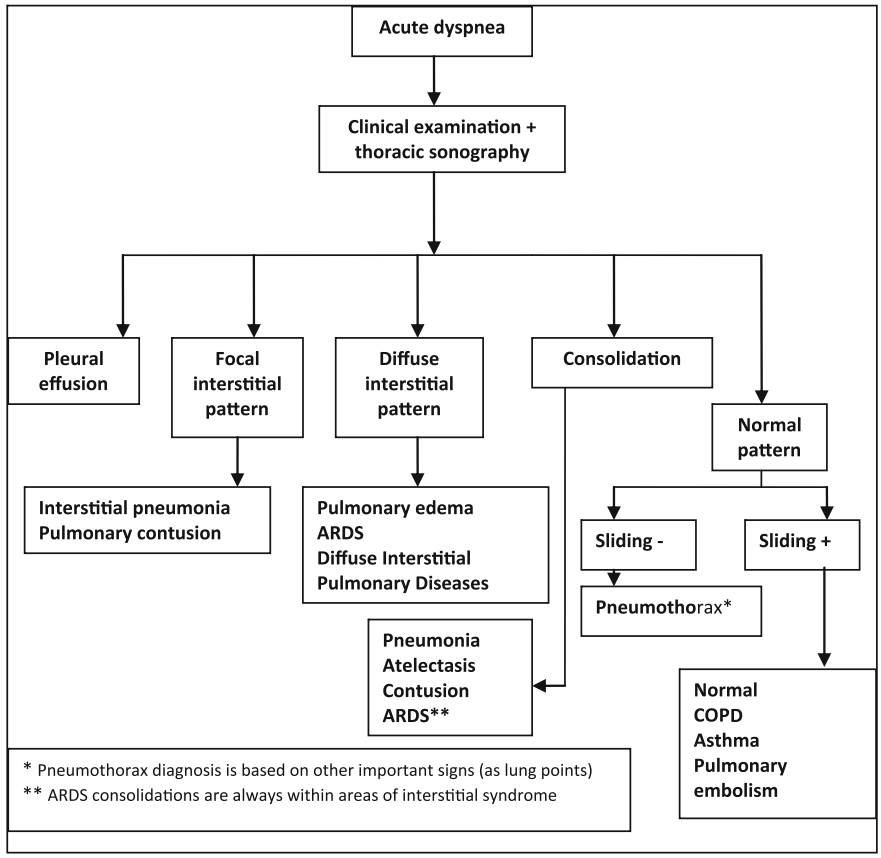

Fig. 34.7 Flowchart illustrating an algorithmic approach to acute dyspnea

as in cardiogenic edema but shows clear irregularities or micronodules on its surface. Areas of B lines and of white lung are present.

34.8 Acute Dyspnea: Sonographic Diagnosis

Diagnostic algorithms for dyspnea based on lung ultrasonography have been proposed recently. They all point to the evidence of echographic syndrome (or B-line pattern) in the initial differential diagnosis and the role of pleural disease in giving symptoms (Fig. 34.7). A sliding pleural line without B lines and with horizontal reverberations (A-line pattern) is typical of normal lung, asthma, pulmonary embolism, and uncomplicated chronic obstructive pulmonary disease. The absence of pleural sliding and of vertical artifacts is typical of pneumothorax (see Chap. 45). A focal pleural pattern of artifacts or an alveolar consolidation allows the diagnosis of pneumonia or pulmonary contusion. A bilateral interstitial syndrome defines pulmonary edema or diffuse interstitial lung disease. In these contexts, an echographic "cross talk" with cardiac function and sonographic hemodynamics results is extremely useful.

Further Reading

Copetti R, Soldati G, Copetti P (2008) Chest sonography: a useful tool to differentiate acute cardiogenic pulmonary edema from acute respiratory distress syndrome. Cardiovasc Ultrasound 6:16

Jambrik Z, Monti S, Coppola V et al (2004) Usefulness of ultrasound lung comets as a nonradiologic sign of extravascular lung water. Am J Cardiol 93:1265–1270

Lichtenstein D (2010) Whole body ultrasonography in the critically ill. Springer, Berlin
Lichtenstein D, Mezière G, Biderman P et al (1997) The comet-tail artifact: an ultrasound sign of alveolar-interstitial syndrome. Am J Respir Crit Care Med 156:1640–1646
Mathis G (2008) Chest sonography. Springer, Berlin
Soldati G (2006) Sonographic findings in pulmonary diseases. Radiol Med 111:507–515

Unexplained Hypoxemia

35

F. Luca Lorini, Bruno Rossetto, and Francesco Ferri

35.1 Introduction

Assessment of unexplained hypoxemia and the inability to wean a patient from ventilatory support are potential uses of echocardiography in the intensive care unit. Causes of hypoxemia that can be diagnosed by echocardiography include intracardiac right-to-left shunting, pulmonary embolus, and disorders of the left ventricle such as left ventricular systolic and/or diastolic dysfunction and mitral valvular abnormalities that can lead to pulmonary edema. If no cardiac abnormality is identified (ventricular or valvular dysfunction), right-to-left shunting must be considered, and the most common cause is patent foramen ovale (PFO).

35.2 Patent Foramen Ovale

The clinical relevance of PFO, a relatively frequent remnant of fetal circulation, has remained obscure for many decades. In fact, before the development of echocardiographic imaging techniques, detection of a PFO during life and clinical diagnosis of paradoxical embolism were rarely possible. In clinical practice, the diagnosis of paradoxical embolism is almost always presumptive and relies on indirect signs such as the presence of a PFO and the diagnosis of arterial embolism. During the past 20 years, initial studies reporting noninvasive detection of right-to-left shunt by contrast echocardiography were followed by extensive clinical research on the association between PFO and several pathological processes, including cryptogenic stroke, peripheral embolism, brain abscesses, decompression sickness, platypnea–orthodeoxia, and fat embolism syndrome. In these studies, PFO was confirmed as a source of paradoxical embolism caused by air, thromboemboli, and fat emboli [1].

Transient right-to-left shunt through a PFO can occur in the presence of normal right-sided hemodynamics. However, patients with submassive and massive pulmonary embolism and those with pulmonary hypertension and right ventricular dysfunction may be at particularly high risk of paradoxical embolism if they happen to have a PFO, with substantial impact on their in-hospital morbidity and mortality [2].

The prevalence of PFO in adults ranged from 25 to 35 % in autopsy series, and from 5 to 31 % in healthy volunteers. The size of the foramen ovale in normal hearts varied between 1 and 19 mm, with a mean of 4.9 mm.

F. L. Lorini (✉)
Department of Anesthesia and Intensive Care, Ospedali Riuniti di Bergamo, Bergamo, Italy
e-mail: llorini@ospedaliriuniti.bergamo.it

A. Sarti and F. L. Lorini (eds.), *Echocardiography for Intensivists*,
DOI: 10.1007/978-88-470-2583-7_35, © Springer-Verlag Italia 2012

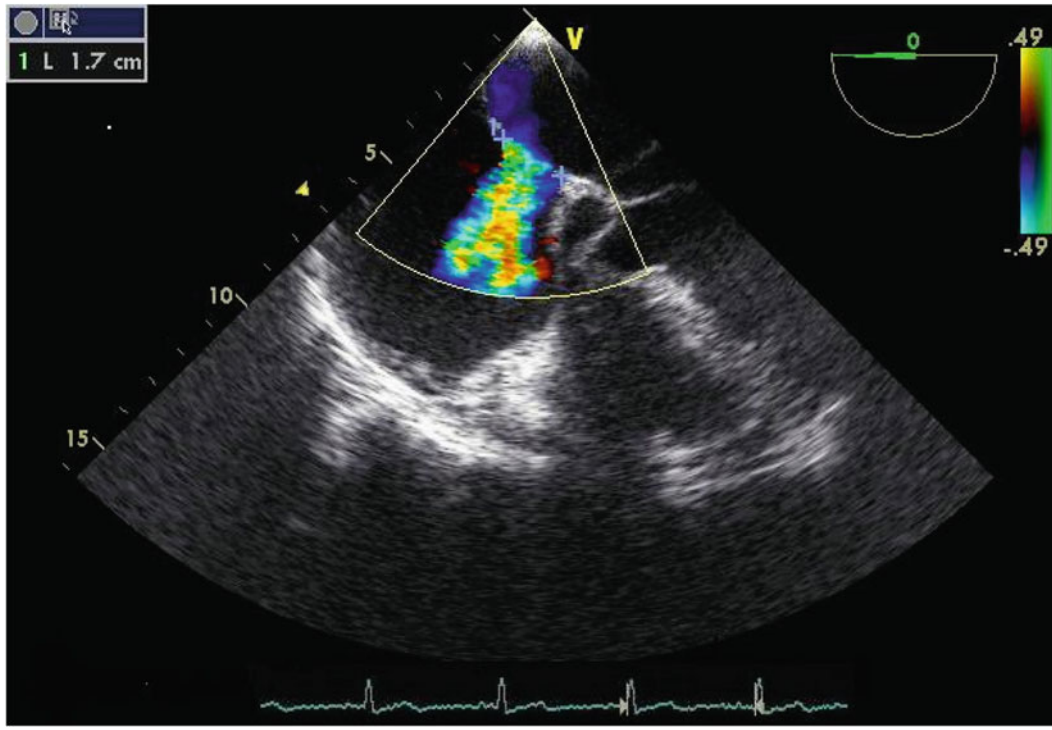

Fig. 35.1 Transesophageal view of the atrial septum. Color Doppler demonstration of left-to-right flow under mechanical ventilation

35.3 Diagnosis of PFO

The presence of a PFO generally does not affect the patient's history, clinical findings, ECG, or chest radiograph. Either invasive or noninvasive methods can be used for detection of an intracardiac shunt. Routine right-sided and left-sided cardiac catheterization is generally inadequate for definitive diagnosis of a PFO, and specialized techniques are required for shunt diagnosis [3].

Echocardiography is the primary imaging modality used to diagnosis PFO. Transthoracic echocardiography (TTE) and transesophageal echocardiography (TEE) can detect this structure by three different methods:

1. Color Doppler analysis
2. B-mode analysis
3. Contrast echocardiography—microbubbles

35.3.1 Color Flow Analysis

Color flow Doppler analysis with modern multiplane TEE and with variation of the Nyquist limit detects almost all adult PFO. There is no single view for color flow Doppler detection of PFO; the mid-esophageal bicaval and the mid-esophageal four-chamber views are both required for adequate examination.

By aligning the Doppler sample volume with the atrial septum, flow across the defect can be recorded. In the usual case, pulsed Doppler imaging will demonstrate low-velocity left-to-right flow extending from mid-systole to mid-diastole, with a second phase of flow coincident with atrial systole. Care must be taken to avoid confusing the low-velocity shunt flow with normal venous and atrioventricular valve flow (Figs. 35.1, 35.2).

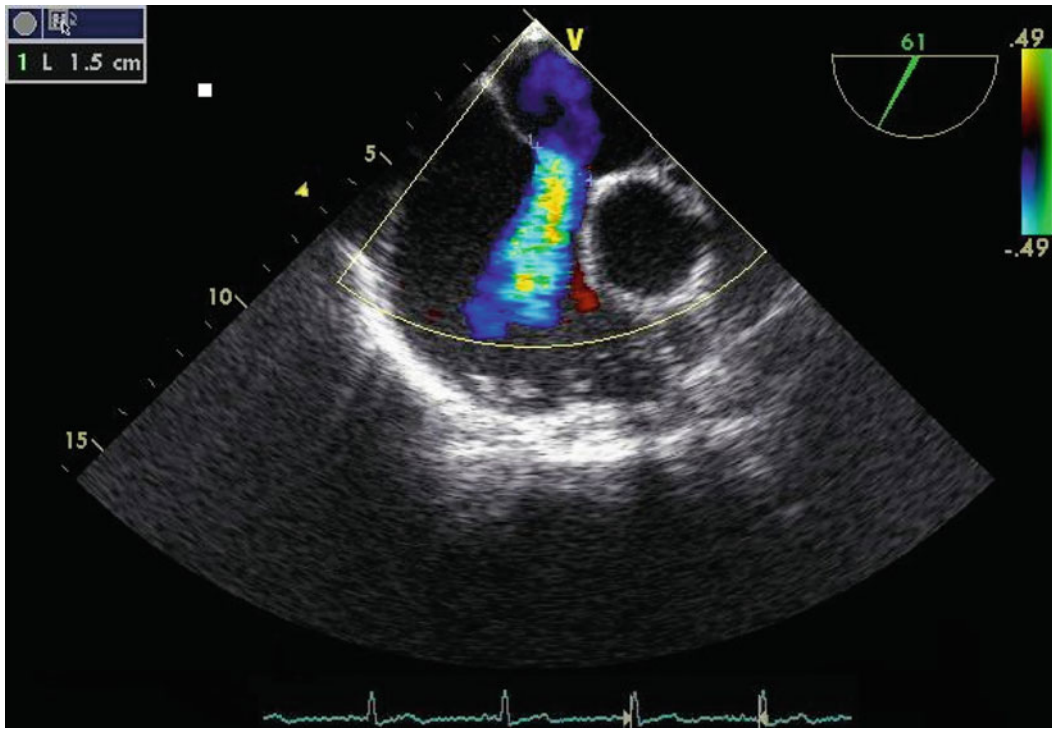

Fig. 35.2 Transesophageal aortic valve short-axis view. This may need to be rotated slightly to bring the atrial septum into the center of the image. Color Doppler visualization of left-to-right shunt in a young patient during the Valsalva maneuver

Color Doppler analysis will show flow across the interatrial septum. Since the pressure gradient between the atria is small, the velocity is low (usually below 1–1.5 m/s) and occurs in late ventricular systole and early in diastole. Calculation of the shunt ratio is usually not necessary. Right ventricular enlargement indicates a hemodynamically significant shunt, being present when the output of the right side of the heart exceeds that of the left side by 50 %. It is essential to obtain the right ventricular peak systolic pressure as part of the examination. The best tricuspid regurgitant Doppler signal should be sought from multiple views. By applying the modified Bernoulli equation to the peak velocity of the tricuspid regurgitation jet, one obtains the pressure gradient between the right ventricle and the right atrium.

35.3.2 B-Mode Analysis

It is important to recognize normal anatomic variants to avoid confusion. These include atrial septal aneurysm, Eustachian valve (associated with the entrance of the inferior vena cava into the right atrium), and the Chiari network (a strand-like structure that extends from the orifices of the superior vena cava and inferior vena cava).

Dropout of echo signal from the foramen ovale occurs when the echo beam is parallel to the interatrial septum in the apical four-chamber view. This give the false appearance of a septal defect. Whereas TTE can occasionally reveal a PFO, TEE demonstrates the interatrial septum in great detail. Various anatomic components (septum primum, septum secundum, fossa ovalis) can

easily be distinguished, and the actual size of the PFO can be defined [4, 5].

The standard TEE views for imaging the atrial septum are as follows:

1. Mid-esophageal four-chamber view (Fig. 35.2). This is useful for demonstrating ostium secundum and ostium primum defects.
2. Mid-esophageal bicaval view. This is useful for demonstrating a sinus venous defect and for identifying anomalous pulmonary veins.
3. Mid-esophageal aortic valve short-axis view (Fig. 35.2). This may need to be rotated slightly to bring the atrial septum into the center of the image.

TTE is also used. The sensitivity of TTE with agitated saline contrast medium for right-to-left shunts is inferior to that of TEE. However, in dimensional cardiac visualization, the development of contrast-based transmitral Doppler techniques and the use of second-harmonic imaging have improved the diagnostic accuracy of TTE.

35.3.3 Contrast Echocardiography

Contrast echocardiography including a provocative maneuver is the most sensitive modality for PFO detection. This happens by detection of microbubbles from intravenously injected agitated saline in left-sided chambers of the heart that would otherwise by filtered by lung capillaries.

The intravenous injection of 5–10 ml agitated saline (or any other sterile solution, including blood) creates a cloud of microcavitations that normally travel with the blood through the right-sided chambers into the pulmonary artery. The microcavitations are trapped in the pulmonary capillaries, and therefore no microcavitations appears in the left side of the heart. With the presence of a right-to-left shunt, the microcavitations bypass the pulmonary circulation and appear in the left side of the heart immediately (within one heart beat) after they appear in the right side of the heart. The appearance of three microcavitations in the left atrium after intravenous injection is considered diagnostic of PFO. The amount of right-to-left shunting (expressed by the number of microcavitations that appear in the left atrium) can be increased significantly by a "provocative" maneuver that augments venous return to the right atrium and increases right atrial pressure or decreases left atrial pressure. Such maneuvers include the release stage of the Valsalva maneuver, the Müller maneuver, cough, elevation of the lower limbs, and liver compression [6]. The risk of side effects of contrast TEE appear to be low. Nevertheless, several cases of neurological deficiency have already been described after contrast TEE using agitated saline with Valsalva maneuvers.

Total PFO detection is only obtained by combining multiple TEE modalities in various atrial views. Thus, a stepwise interrogation of the interatrial septum by multiplane TEE for detection of PFO should include the following:

- Step 1. Two-dimensional imaging of the interatrial septum should be performed in multiple views to rule out any major atrial septal defect.
- Step 2. If step 1 results in negative findings, then color flow Doppler interrogation of the interatrial septum is performed in at least two different views, preferably in the mid-esophageal four-chamber view and the mid-esophageal bicaval view. The Nyquist limit should be serially decreased to approximately 20–40 cm/s.
- Step 3. If step 2 results in negative findings, then contrast echocardiography should be performed with release of positive airway pressure as the provocative maneuver.
- Step 4. If step 3 results in negative findings, contrast echocardiography may be repeated without a provocative maneuver because this may still facilitate PFO detection.

35.3.4 Three-Dimensional Echocardiography

Real-time three-dimensional echocardiography (transthoracic or transesophageal) is more accurate than contrast TTE or TEE, and can avoid injection of saline contrast medium in a sizable number of patients, especially in those patients with larger PFO who are at higher risk of events

and procedure complications. Real-time three-dimensional echocardiography allows fast acquisition of dynamic pyramidal data sets that encompass most of the heart. Acquired data sets can be sliced in several planes and rotated, allowing the observer to visualize cardiac structures such as the interatrial septum "en face" from both the left and the right side with better understanding of its anatomy and its spatial relationship with adjacent structures. Addition of three-dimensional color flow Doppler flow mapping allows one to visualize shunt jets in relation to the anatomy of the interatrial septum and to locate exactly the origin of the jet and the size of the defect.

A limitation of real-time three-dimensional echocardiography is that current technology provides a suboptimal spatial and temporal resolution. When smaller defects that have dynamic shunts or shunts elicited only with the Valsalva maneuver/coughingare being imaged, the accuracy of real-time three-dimensional echocardiography may sometimes be hampered by the frame rate.

35.3.5 Closure of Atrial Septal Defects

TEE is also essential for closure of atrial septal defects with an Amplatzer septal occluder. TEE is vital in the recognition of morphologic variations of the atrial septal defects and patient selection. It allows clear visualization of the defect and the device during the procedure, precise measurement of stretch diameters, guidance of deployment, and stable positioning of the device. This is especially important in patients with large or multiple atrial septal defects and those with atrial septal aneurysm. With TEE, incorrect positioning of the device can be detected while is still screwed to the delivery cable, which allows its early redeployment, before any complications occur.

References

1. Kronzon I (2006) Patent foramen ovale: echocardiographic evaluation and clinical implications. Isr Med Assoc J 8(11):793–797
2. Alp N, Clarke N, Banning AP (2001) How should patients with patent foramen ovale be managed? Heart 85(3):242–244
3. Meier B, Lock JE (2003) Contemporary management of patent foramen ovale. Circulation 107(1):5–9
4. Di Tullio MR (2010) Patent foramen ovale: echocardiographic detection and clinical relevance in stroke. J Am Soc Echocardiogr 23(2):144–155
5. Kronzon I, Ruiz CE (2010) Diagnosing patent foramen ovale: too little or too much? JACC Cardiovasc Imaging 3(4):349–351
6. Sharma VK (2010) Diagnostic strategies for patent foramen ovale. Echocardiography 27(1):100–101

Further Reading

Seller C (2004) How should we assess patent foramen ovale? Heart 90(11):1945–1947

Sepsis and Septic Shock

36

Armando Sarti, Simone Cipani, and Germana Tuccinardi

36.1 Introduction and Background

Severe sepsis and septic shock are still a common cause for admission to the ICU, and are the leading cause of death, despite enormous scientific advances in understanding their complex pathophysiologic processes and biomolecular picture. The natural course of sepsis produces major and different hemodynamic changes depending on the type of immunological response of the patient and the evolution of the disease. All determinants of cardiovascular function, including both central and peripheral blood volume, preload, afterload, and both right and left pump function, may be involved simultaneously or at different times during the progression of the septic insult. Septic shock is often associated with vasoparalysis, microcirculatory dysfunction, and massive fluid leakage into the extravascular compartment. The pathophysiologic consequences of severe sepsis and septic shock include either absolute hypovolemia, due to third space losses, or relative hypovolemia, caused by abnormal distribution of blood volume between peripheral and central compartments. Regardless of whether hypovolemia is absolute or relative, the heart is not properly filled and both mean arterial pressure and cardiac output decrease. Vasodilation ensues owing to the failure of vasoconstrictor mechanisms. Nitric oxide activity seems to play a major role in the vasoconstriction disturbances. Most endothelial functions are disrupted in sepsis, resulting in a procoagulant, antifibrinolytic, and proadhesive state, altered red blood cell deformability, and sluggish or heterogeneous microvascular flow. Mitochondrial dysfunction occurs inside the cell.

Left ventricular (LV) systolic and/or diastolic dysfunction is common, and right ventricular (RV) dysfunction can also be frequently observed, either primary or secondary to increased pulmonary artery pressure, due to associated acute lung injury (ALI) or acute respiratory distress syndrome (ARDS) and concomitant positive-pressure mechanical ventilation. Myocardial contractility is depressed by circulating substances such as endothelin, endotoxin, and cytokines, in particular IL-1, IL-6, and TNF-α. Myocardial edema and cardiomyocyte apoptosis have even been invoked. LV systolic dysfunction may also reflect impaired adrenergic responsiveness. LV diastolic dysfunction may be isolated or observed in conjunction with decreased contractility and it is associated with myocardial edema and augmented cytokine activity, particularly IL-10, IL-8, and TNF-α. Controversy persists over whether LV systolic dysfunction with increased end-diastolic volume might be linked to improved survival, considering LV dilatation as

A. Sarti (✉)
Department of Anesthesia and Intensive Care, Santa Maria Nuova Hospital, Florence, Italy
e-mail: armando.sarti@asf.toscana.it

A. Sarti and F. L. Lorini (eds.), *Echocardiography for Intensivists*,
DOI: 10.1007/978-88-470-2583-7_36,

an adaptive mechanism leading to maintained cardiac output. LV diastolic dysfunction is clearly associated with increased mortality. The characteristic hyperdynamic high output and low peripheral resistance circulatory shock is only observed if the patient is readily resuscitated with copious fluid infusions as the heart maintains adequate, or at least acceptable, contractile function and filling properties on both right and left sides. Integrated into the specific bundles of treatment, early broad-spectrum antibiotics and prompt circulatory resuscitation are associated with improved survival.

36.2 Echocardiography in the Clinical Picture of Severe Sepsis and Septic Shock

Since hemodynamic derangement is a dominant feature of severe sepsis and septic shock, bedside echocardiography is paramount for the assessment, management, and reassessment of circulatory failure. In fact, cardiovascular ultrasonography has almost totally replaced right-sided heart catheterization in many ICUs, and a growing number of intensivists now advocate echocardiography as the first-line technique for hemodynamically unstable patients. However, this technique is still complementary to clinical judgment and to all other monitors of hemodynamics.

The initial echocardiography may show unexpected abnormalities of the heart, such as LV diastolic dysfunction, acute cor pulmonale, and pericardial effusion, which can certainly alter the management plan. Moreover, endocarditis as a cause of the sepsis and vegetations on vascular catheters, prosthetic valves, or electrical devices can be diagnosed by echocardiography. Other ultrasonographic techniques may help find the source of infection inside the chest, the abdomen, or the limbs without delay at the bedside.

Presently, our standard approach is using ultrasonography to evaluate and check again the unstable septic patient after any relevant change, while monitoring central venous oxygen saturation by means of a central venous catheter and cardiac output using a continuous semi-invasive method based on arterial trace pulse contour analysis.

36.2.1 Fluid Responsiveness

Volume expansion is a fundamental component of the initial resuscitation of the septic patient. Restoring blood flow to the organs is essential to prevent hemodynamic collapse. Each minute of tissue hypoperfusion at the onset of the septic insult will be paid for in terms of multiorgan dysfunction later on. On the other hand, considering the ongoing tendency for capillary leakage of severe sepsis and septic shock, once preload has been optimized, further fluid load does not increase delivery of oxygen to the tissues, but may only cause adverse consequences, such as pulmonary edema and edema of other tissues, thus enhancing organ dysfunction. Initial fluid loading is always started on a clinical basis. Fluid infusion should not be withheld while awaiting more sophisticated information, but it is not easy to establish the amount of fluid to infuse and for how long to maintain vascular filling. Echocardiography may definitely help to give sufficient fluid (which can be more than generally used) during the early phase of sepsis while restricting the volume load later on.

Traditional static measurements of vascular filling pressures, such as central venous pressure and pulmonary capillary wedge pressure (PCWP), have been found to be unreliable as a guide to volume resuscitation. The clinical picture may suggest severe hypovolemia, which can be clearly confirmed by echocardiography, which shows a small hyperdynamic fast-beating heart with decreased flows and end-diastolic areas or volumes of all cardiac chambers and the inferior (transthoracic echocardiography, TTE) or superior (transesophageal echocardiography, TEE) vena cava. If manifest hypovolemia is not clearly detected, the crucial question regarding whether a volume bolus might increase cardiac output must still be answered. Sonographic dynamic indices of fluid responsiveness based on heart and lung interaction, which are correlates of pulse pressure variation, have been proposed and validated as a guide to fluid management.

The most useful ultrasonographically derived parameters for assessment of fluid responsiveness are respiratory variation of vena cava diameter and of stroke volume (see Chap. 28). First, it is very important to fully understand the perequisite criteria and limitations for applying these measures. Sinus rhythm is required and patients must be fully ventilated (tidal volume of 8 ml/kg) without any spontaneous respiratory effort, even if a reduced tidal volume may still cause enough respiratory variations in patients with decreased lung compliance (ARDS). Abnormal intra-abdominal pressure may interfere with inferior vena cava diameter and respiratory variation. Most important, acute cor pulmonale and RV dysfunction may cause false dynamic signs of fluid responsiveness, owing to adverse effects of the mechanical ventilation on the dilated failing right side of the heart. If these limitations cannot be ruled out, the only way to predict a positive response to a fluid bolus is the measurement of cardiac output before and after passive leg raising. Passive leg raising, as a temporary test of volume expansion, can be used even in spontaneously breathing patients. The intensivist with competence limited to only basic TTE should rely on respiratory variation and the diameter of the inferior vena cava. Twelve percent as a threshold value for the respiratory variation index of the inferior vena cava can predict an increase of cardiac output of more than 15 % with good positive and negative predictive values. More competence in critical care echocardiography allows the skilful intensivist to measure even the diameter and variations (collapsibility index of 36 % or more) of the superior vena cava by TEE and to use Doppler interrogation of LV stroke volume variations by both TTE and TEE. A peak velocity variation index greater than 12 % and a velocity–time integral greater than 18 % can predict a sufficient increase in cardiac output.

36.2.2 Left Ventricular Systolic Dysfunction

"Ejection fraction" (EF) is not synonymous with "contractility," but simply refers to the proportion of blood pumped out of the left ventricle during a cardiac cycle. Thus, a normal or high EF is consistent with low cardiac output and a very low EF may be found together with a normal cardiac output, according to different end-systolic and end-diastolic volumes. Since traditional echocardiographic indices of systolic function, such as EF, are closely preload and afterload dependent, hypovolemia and decreased afterload due to vasodilatation must first be treated with fluids and/or vasopressors before LV pump dysfunction is established. For the septic patient, an initial normal or even increased EF in the emergency department may only show the unloading effect of reduced systemic vascular resistance on LV performance. Thus, after volume resuscitation and norepinephrine infusion, a further echocardiogram may only show depressed contractility, unmasking the "real" decreased EF, which is frequent after restoring afterload and alerts the clinician to consider inotropic support. In the case of a clinically shocked patient with systolic dysfunction, the PCWP should be assessed to distinguish genuine cardiogenic shock, characterized by high PCWP ($E/E' > 15$), from septic shock , characterized by normal, near normal, or decreased PCWP ($E/E' < 8$).

Visual estimation of EF is reliable only when performed by the expert echocardiographer intensivist. With competence in only basic TTE, it is preferable to measure EF using endocardial border excursion at the end of diastole and end of systole using both apical four-chamber and apical two-chamber views. Possible regional systolic dysfunction must also be detected, even if precise scoring and accurate localization of regional dysfunction requires an expert second opinion. If regional dysfunction is not observed, the easier-to-measure fractional area change or fractional shortening may be used, with the parasternal short-axis view or the parasternal long-axis view (TTE), respectively, for a quick assessment of systolic function.

The echocardiographer intensivist must also recognize two possible peculiar patterns of systolic dysfunction which lead to a major change of the management plan. Dynamic LV outflow

tract (LVOT) obstruction can occur as a consequence of ventricular septal thickening and systolic anterior motion of the anterior mitral leaflet. LV hypertrophy (most often caused by previous hypertension or aortic stenosis), hypercontractiliy, hypovolemia, and reduced systemic vascular resistance are all predisposing factors. When LVOT obstruction is diagnosed, inotropic support must be stopped immediately, a rapid fluid bolus must be provided, and just in case a pure vasopressor, such as phenylephrine, should be added to the management plan. Apical ballooning, also referred to as tako-tsubo myopathy, is the other systolic pattern to recognize. Tako-tsubo myopathy is characterized by concomitant hyperdynamic basal and reduced mid-chamber function with akinesis and aneurysmal dilatation of the apex. Intense physical or emotional stress may precede apical ballooning, which is associated with increased levels of endogenous or exogenous cathecolamines. β-blockers can be considered.

Cardiac output is the final parameter to consider along with the peripheral indices of tissue perfusion which guide the treatment, such as venous hemoglobin desaturation, venous to arterial carbon dioxide gradient, lactate levels, and organ dysfunction. Among those who survive, all aspects of systolic dysfunction seem to resolve in a few weeks, regardless of severity.

36.2.3 Left Ventricular Diastolic Dysfunction

It must be kept in mind that Doppler analysis of forward mitral flow (E and A waves) is load-dependent. Also, the inflow pattern of the LV filling depends significantly on the age of the patient. Most often, early diastolic relaxation, which is an active energy phenomenon, is involved in sepsis. Reduced LV compliance due to myocardial stiffness can coexist. An *E*/*A* ratio of more than 2 is generally associated with a pulmonary artery pressure greater than 18 mmHg. LV diastolic function may be better assessed by the tissue velocity (tissue Doppler imaging) of the longitudinal movement toward the base of the heart of the mitral valve annulus (E'), which is relatively load independent. The E/E' ratio is closely related to the PCWP. Whichever diastolic function is assessed during the initial phase of the sepsis, the measurement must be repeated after volume expansion to avoid excessive fluid load, which increases the risk of pulmonary edema, particularly in the presence of ALI or ARDS or if LV function is already depressed prior to the septic insult. New-onset septic diastolic dysfunction may completely reverse if the patient survives.

36.2.4 Right Ventricular Dysfunction

The right side of the heart may be compromised as well as the left side. The discovery of RV impairment, either primary or secondary, always leads to significant changes in drug therapy and in the mechanical ventilation setting. RV impairment may become manifest only after the institution of positive-pressure mechanical ventilation with or without positive end-expiratory pressure. Severe RV failure may alert the clinician to consider venous thromboembolism as a concomitant or alternative diagnosis. RV end-diastolic dilatation and the RV/LV area ratio in the apical four-chamber view allows the diagnosis of dysfunction, together with septal paradoxical motion (dyskinesia) or flattening, which is more related to pressure overload. The assessment of pulmonary artery systolic pressure by the Doppler velocity of tricuspid regurgitation is crucial to distinguish a RV primary involvement as a direct effect of all circulating factors of sepsis from a secondary involvement, due to increased afterload caused by chronic obstructive pulmonary disease, or factors such as acidosis, hypoxia, ALI/ARDS, and positive-pressure mechanical ventilation. Inotropic support is considered for primary systolic dysfunction, together with vasopressors, to sustain coronary perfusion pressure, whereas specific steps should be taken to reduce afterload, as in the presence of pulmonary hypertension. Pulmonary vasodilators, such as oxygen, nitric oxide, sildenafil, and prostacyclin, can be used to reduce pulmonary pressure. At the same time, mechanical ventilation is adjusted to reduce as

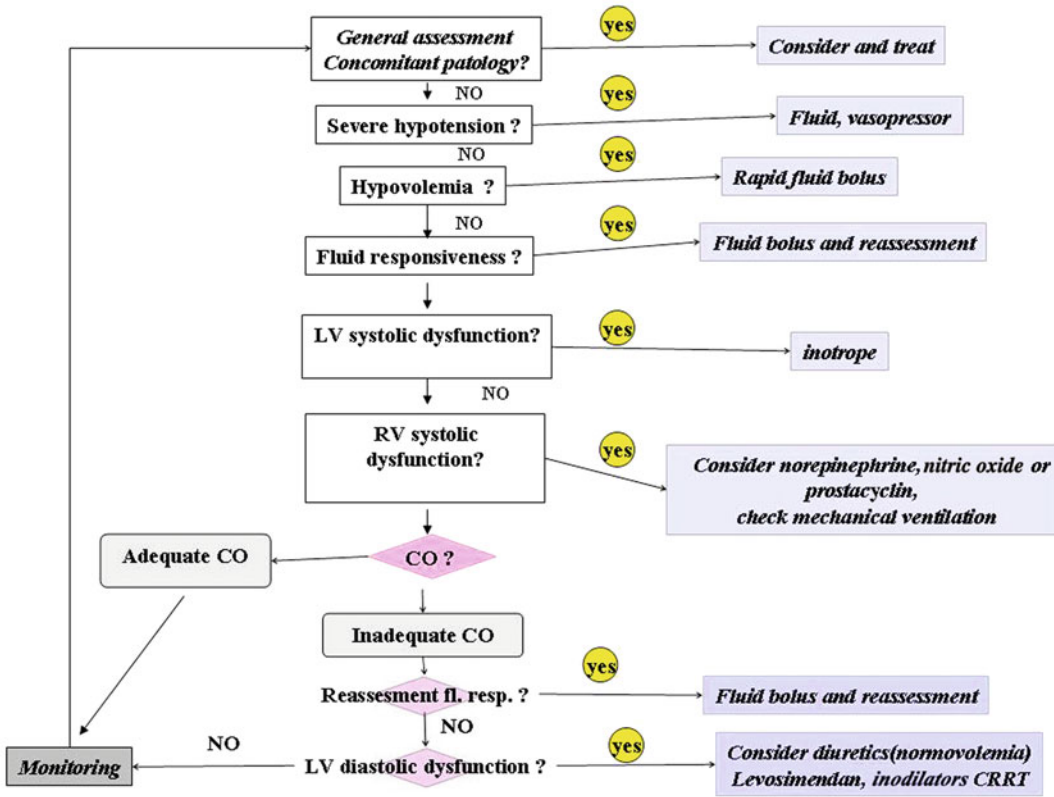

Fig. 36.1 Echo-guided assessment and management of the septic patient. See the text for details. *LV* left ventricular, *RV* right ventricular, *CO* cardiac output, *fl resp* fluid responsiveness, *CRRT* continuous renal replacement therapy

much as possible the inspiratory plateau pressure and the positive end-expiratory pressure, while maintaining arterial oxygen content and preventing excessive respiratory acidosis.

36.2.5 Vasopressors and Inotropes

Echocardiography, with all the information it provides on the entire cardiovascular function, may greatly help guide the rational use, if any, of vasopressors, inotropes, and vasodilators. Serial echocardiographic examinations are necessary to reassess the hemodynamic profile of the septic patient during the progression of the disease and after any relevant management change. The ideal vasopressor has not yet been found by researchers, the choice being guided by the clinical context and the type of patient. When the arrhythmic risk is high, it will be more appropriate to use norepinephrine than dopamine. Recent findings show that vasopressin may be considered to restore systemic arterial pressure if norepinephrine treatment fails or if high, potentially dangerous doses need to be used. Some authors now suggest vasopressin even before considering norepinephrine infusions. However, both vasopressin infusion to increase arterial pressure and dobutamine infusion to increase cardiac output imply adequate previous vascular filling. A good response to dobutamine infusion is a reduction of heart rate. Epinephrine is administered to sustain cardiovascular function if other drugs fail to restore pump function and arterial pressure. The calcium sensitizer levosimendan seems able to improve both systolic and diastolic ventricular function on both sides of the heart without increasing oxygen consumption. However, this

agent stimulates the endothelial release of nitric oxide and thus it might be speculated that this could exacerbate the sepsis-related fall of systemic vascular resistance and the tendency for hypotension. Both levosimendan and dobutamine seem to improve microvascular flow.

The LV ejection velocity–time integral is closely related to stroke volume since the LVOT area does not change acutely, and it can therefore be monitored to detect any inotropic change as long as both preload and afterload stay stable. Cardiac output is the final central determinant of tissues perfusion. It may be manipulated with fluids and drugs according to all the relevant clinical and hemodynamic data to reach peripheral therapeutic goals, such as:

- Adequate mixed venous oxygen saturation (above 70 %)
- Central venous–arterial carbon dioxide gradient below 6 mmHg
- Acceptable diuresis
- Decreasing lactate level
- Recovery of organ function

Figure 36.1 shows an algorithm for the assessment and the management plan of the septic unstable patient based on the echocardiographic findings.

Further Reading

Dellinger RP, Levy MM, Carlet JM et al (2008) Surviving Sepsis Campaign: International Guidelines for Management of Severe Sepsis and Septic Shock. Critical Care Med 36:296–327

Funk D, Sebat F, Kumar A (2009) A systems approach to the early recognition and rapid administration of best practice therapy in sepsis and septic shock. Curr Opin Crit Care 15:301–307

Gerstle J (2010) Echocardiographically derived parameters of fluid responsiveness. Int Anesthesiol Clin 48:37–44

Griffee MJ, Merkel MJ, Wei KS (2010) The role of echocardiography in hemodynamic assessment of septic shock. Crit Care Clin 26:365–382

Pinto B, Reheberg S, Ertmer C et al (2008) Role of levosimendan in sepsis and septic shock. Curr Opin Anaesthesiol 21:167–168

Chest Trauma

37

Fabio Sangalli, Lucia Galbiati, and Roberto Fumagalli

37.1 Introduction

Trauma is a major cause of morbidity and mortality worldwide and represents the leading cause of death for those between 1 and 41 years, and the fifth leading cause of death overall. Chest trauma, either blunt or penetrating, occurs in almost two thirds of multiple-trauma patients and contributes 15–35 % of the burden of trauma-related deaths. These injury mechanisms may result in pneumothorax, hemothorax, pulmonary contusion, or injuries to the mediastinal structures. Although pulmonary parenchymal injuries such as contusion and laceration represent the most common intrathoracic lesions—occurring in 30–70 % of blunt thoracic trauma victims—mortality from chest trauma is usually due to aortic or great vessel injury, and although only about 15 % of chest trauma patients require operative intervention, a considerable number of preventable deaths occur because of inadequate or delayed treatment of an otherwise remediable injury.

Echocardiography, particularly transesophageal echocardiography (TEE), is a key component of the diagnostic process. It has a higher sensitivity and specificity than transthoracic echocardiography, ranging in experienced hands between 91 and 100 % and between 98 and 100 %, respectively (Table 37.1). Besides providing accurate and real-time information on the morphological and functional aspects of the heart and intrathoracic great vessels, it allows point-of-care examination and can be performed without interrupting ongoing measures to stabilize the patient. The speed and portability of echocardiography make it an attractive alternative to other imaging technologies such as computed tomography (CT), arteriography and magnetic resonance imaging (Table 37.2). Although the sensitivity and specificity of TEE have been reported as comparable to those of CT in diagnosing traumatic aortic injury (TAI), TEE furthermore allows the identification of associated cardiac injuries, and is more sensitive than CT in the detection of intimal lesions. TEE now represents the primary diagnostic tool in unstable patients in most institutions where an experienced echocardiographer is available.

Ultrasonography also plays a role in the differential diagnosis of pulmonary lesions and may allow one to discriminate between them and to evaluate the effects of therapeutic interventions. Lung ultrasonographic techniques are described elsewhere in this book.

F. Sangalli (✉)
Cardiac Anesthesia and Intensive Care Unit, Department of Perioperative Medicine and Intensive Care, San Gerardo Hospital, University of Milano-Bicocca, Monza, Italy
e-mail: f.sangalli@hsgerardo.org

A. Sarti and F. L. Lorini (eds.), *Echocardiography for Intensivists*,
DOI: 10.1007/978-88-470-2583-7_37,

Table 37.1 Indications for echocardiography in the trauma patient

Problem	Class of evidence
Serious blunt or penetrating chest trauma	I
Mechanically ventilated patients with multiple trauma or chest trauma	I
Hemodynamically unstable polytrauma patients without obvious chest injury but with a mechanism of trauma suggesting potential cardiac or aortic injury (i.e., deceleration or crush injury)	I
Widening mediastinum or suspicion of postinjury aortic damage	I
Trauma patients with suspicion of preexisting valvular or myocardial disease	I
Evaluation of hemodynamics in multiple-trauma or chest trauma patients with PAC monitoring data that are disparate from the clinical scenario	IIa
As a follow-up study for victims of serious blunt or penetrating injury	IIa
Suspected myocardial contusion in hemodynamically stable patients with a normal ECG	III

PAC Pulmonary Artery Catheter

Table 37.2 Imaging techniques in chest trauma

	TEE	CT	MRI	Angiography
Pros				
- Portability (bedside)	X	–	–	–
- Rapidity	X	X	–	–
- No radiation	X	–	X	–
- Visualization of entire aorta and branches	–	X	X	X
- Specific advantages	Evaluation of cardiac function and cardiac valves, flow in the true/false lumen			
Cons				
- Invasive	–	–	–	X
- Requires experienced operator/ interpreter	X	–	X	–
- Expensive	–	–	X	X
- Requires contrast agent	–	X	–	X
-Specific risks	Aspiration in the nonintubated patient Damage to visceral structures (very rare)	Potential renal damage from contrast agent	Long acquisition time Not widely available 24h7 Contraindicated in patients with metal prostheses	Retrograde extension of dissection False negative if false lumen is completely thrombosed Potential renal damage from contrast agent

TEE transesophageal echocardiography, *CT* computed tomography, *MRI* magnetic resonance imaging

Table 37.3 Classification of chest trauma

	Mechanism of injury	Frequent causes	Structures involved	Clinical pictures
Blunt	Compression between spine and sternum Abrupt intrathoracic pressure shifts Shearing from rapid deceleration Upward displacement of intra-abdominal organs Blast injuries	Motor accidents Crush fractures Falls Kicks Sports injuries Explosions	Anterior structures (right chambers and aorta) more commonly involved	Cardiac contusion Rupture of myocardial free walls or interventricular septum Tamponade Aortic lesion (ranging from intramural hematoma to aortic rupture) Intrathoracic herniation of abdominal organs
Penetrating	Direct injury from penetrating object Damage to adjacent structures is directly related to the amount of energy exchanged (i.e., mainly to the missile velocity)	Stab wounds Impalement Low- and high-velocity missiles	Dependent on the site of penetration and the velocity and the intrathoracic path of the penetrating object	Penetrating injuries to the ventricles or the atria Tamponade

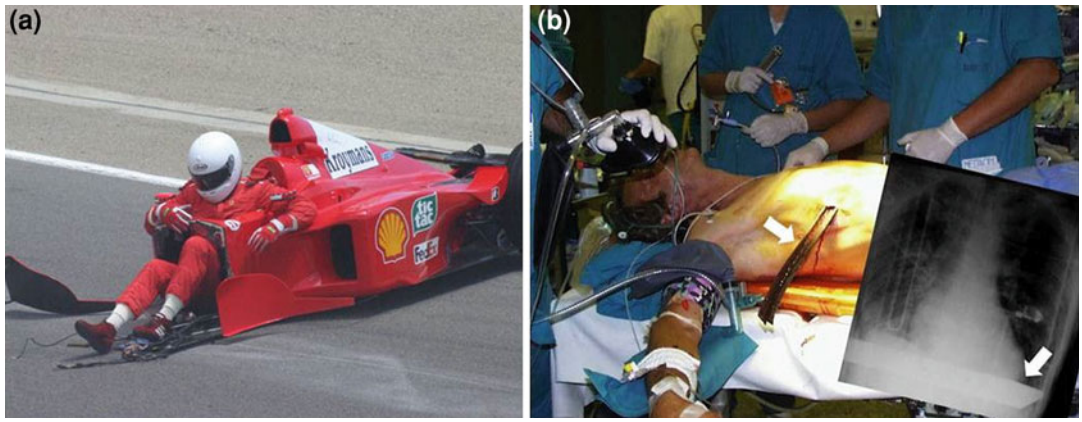

Fig. 37.1 Examples of blunt (**a**) and penetrating (**b**) chest trauma patients

37.2 Blunt and Penetrating Chest Trauma

Chest trauma is generally classified into blunt or penetrating, as different mechanisms of injury are involved (Table 37.3, Fig. 37.1).

Blunt chest trauma to the heart and intrathoracic great vessels—although relatively rare, accounting for less than 5 % of trauma-related vascular lesions—has an extremely high mortality, representing the leading cause of trauma-related death after head injury. The actual incidence is very likely underestimated, as up to

80 % of patients with TAI die before reaching the hospital, and traumatic aortic rupture accounts for nearly 18 % of all deaths related to motor vehicle accidents. A timely and accurate diagnosis and lifesaving interventions are essential to reduce the burden of preventable deaths due to inadequate or delayed management.

In penetrating trauma, injury occurs as a result of the extrinsic violation of the integrity of the thoracic cavity. Two different mechanisms contribute to the damage: direct injury from the intrusion, and damage to adjacent structures owing to the exchange of energy between the penetrating object and the surrounding tissue; this latter damage is directly proportional to the amount of energy exchanged, which is in turn directly related to the speed of the missile.

37.3 Cardiovascular Lesions in Chest Trauma

The most common trauma-related intrathoracic lesions are represented by TAI , myocardial contusion, cardiac rupture, and valve lesions, although nearly all possible cardiovascular lesions have been reported in trauma patients (Fig. 37.2). The most frequent and life-threatening clinical scenarios derived from these lesions are hemorrhagic shock, cardiac tamponade, and cardiac rhythm disturbances.

37.3.1 Traumatic Aortic Injury

Traumatic aortic injury is a rare, but very lethal condition and represents the most commonly diagnosed injury in unstable chest trauma patients. Deceleration injuries from high-speed motor vehicle collisions and falls from a height represent the most frequent causal mechanisms. As already mentioned, roughly 80 % of patients die at the scene, and up to 50 % of those who make it to the hospital die within 24 h if not promptly diagnosed and treated. The outcome of patients depends primarily on the extent of the lesion and on the rapidity of appropriate care (Table 37.4).

Most lesions are localized at the level of the aortic isthmus, between the left subclavian and the first intercostal arteries; this is due to the relative mobility of the ascending aorta with respect to this region, which is partially fixed by the ligamentum arteriosum, a postnatal remnant of the duct of Botallus (Fig. 37.3).

Three factors contribute to aortic rupture: shear stress, bending stress, and torsion stress. As deceleration occurs, the aortic isthmus is placed under tension by the gradient created between the mobile aortic arch and the relatively fixed descending aorta, with an ensuing shear stress that can lead to rupture or tear. Bending stress results from the hyperflexion of the aortic arch produced by the downward traction exerted by the heart, whereas anteroposterior compression of the chest with the heart displaced to the left leads to torsion stress. The combination of these three forces generates maximum stress to the inner aortic layer at the level of the ligamentum arteriosum (aortic isthmus), which represents the point of greatest fixation.

A traumatic lesion may be classified as (1) intimal hemorrhage, (2) intimal hemorrhage with laceration, (3) medial laceration, (4) complete laceration of the aorta, (5) false aneurysm formation, and (6) periaortic hemorrhage.

Most patients with free rupture die at the scene, whereas patients with a contained rupture who reach the hospital alive often exhibit inconsistent symptoms, owing to the variety of clinical presentations. For this reason it is of paramount importance to keep a high index of suspicion in all trauma patients with a potential TAI, even though they do not present evident signs of chest trauma.

Echocardiographic Findings

As mentioned already, TAI represents a wide spectrum of possible lesions, ranging from intimal lesion, to intramural hematoma, pseudoaneurysm, aortic dissection, and aortic rupture.

Whereas complete aortic transection leads to at-scene death in most patients, patients with an incomplete rupture may reach the hospital alive. When the tear does not extend to the adventitial layer of the aortic wall, a pseudoaneurysm will

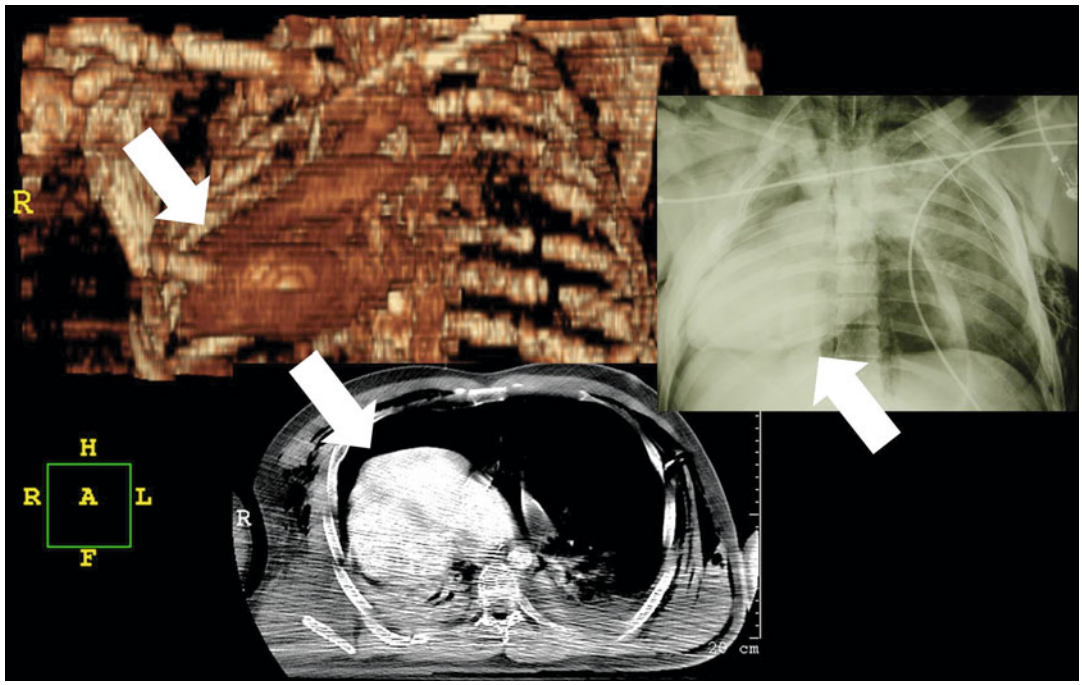

Fig. 37.2 Posttraumatic heart dislodgement, with a rotation of the cardiac chambers in the right side of the chest (*arrow*)

Table 37.4 Classification of traumatic aortic injury (*TAI*)

Grade 1	TAI consisting in superficial lesions; conservative management is safe and effective
Grade 2	Subadventitial injuries requiring repair (immediate or delayed depending on the clinical conditions)
Grade 3	Aortic transection with blood extravasation or aortic obstruction with ischemia; requires prompt repair

develop. Contained rupture is generally visualized by TEE as a discontinuity of the aortic arch from the descending aorta, with torn and mobile ends often visible (Fig. 37.4). Perivascular hematoma is generally present, but flow to and from the pseudoaneurysmal space is inconsistent (Fig. 37.5). Doppler imaging may detect a gradient across the lesion when the transection causes obstruction of flow.

Less severe trauma to the aorta may lead to intimal tearing, with the development of intramural hematoma; this scenario is generally characterized by stable hemodynamic conditions and has a more benign course. The echocardiographic signs are similar to those in spontaneous dissection, consisting in an aortic wall thickening (more than 7 mm is generally considered diagnostic) and/or an echolucent appearance within the aortic wall. Differential diagnosis with atherosclerotic lesions is not always straightforward, unless a tear is clearly visible. The site of the tear should be accurately inspected for perivascular hematoma—which represents a risk factor for a quickly progressing lesion—and for the patency of epiaortic vessels.

The information gained with TEE that is essential in the treatment of the patient does not differ from that in the setting of aortic dissection and is reported in Table 37.5.

The main limitation of TEE in the diagnosis of TAI is due to the "blind spot" caused by the trachea and the right main bronchus, which makes the distal ascending aorta and the proximal arch very difficult to scan. The incidence of TAI in this region has been reported as up to

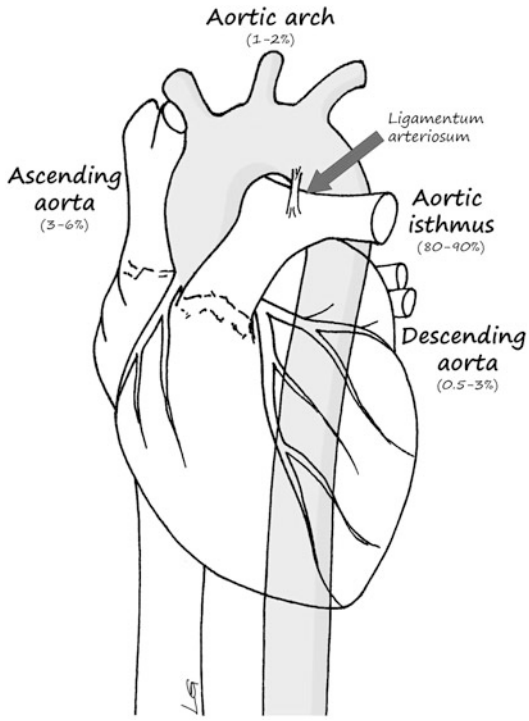

Fig. 37.3 The thoracic aorta, indicating the relative topographic distribution of traumatic aortic lesions

20 % of all TAIs, requiring careful observation and possibly a second imaging modality (i.e., CT scan) if the likelihood of aortic trauma is high.

Besides its fundamental role in the diagnostic stage of TAI, TEE also plays a key role during the operative period. Not only does it allow ongoing monitoring of cardiac function and hemodynamics, but it also represents a consistent aid in the evaluation of the intraoperative and early postoperative results of both surgical and endovascular interventions.

In the last decade, the endovascular treatment of traumatic aortic lesions gained an increasing role both in the acute and in the subacute settings. TEE, together with angiography, plays a pivotal role in the intraprocedural distinction of the true from the false lumen, guidewire positioning, graft positioning and deployment, and determining the patency of epiaortic branches and if there are periprosthetic leaks (Fig. 37.6, Table 37.6).

37.3.2 Blunt Cardiac Injury

Cardiac injury may occur as a result of direct blows, athletic trauma, industrial crush, blasts, rapid deceleration, or falls from a height. A direct blow to the precordium creates a force that compresses the myocardium against the spine. Because of the relatively free anterior–posterior movement of the heart, the momentum generated from a rapid deceleration accident maintains the heart in a uniform, straight-line motion, resulting in a direct strike against the internal sternum. Several forces may be involved in blunt cardiac injury, including compression of the heart between the spine and the sternum, abrupt pressure fluctuations in the chest and abdomen, shearing from rapid deceleration, and blast injury. In addition, fragments from rib fractures can directly traumatize the heart.

Blunt cardiac injury includes cardiac contusion and concussion (commotio cordis), cardiac chamber rupture (free wall, septa, papillary muscles, and chordae tendineae,) and valvular disruption. The right side of the heart is most commonly injured, probably because of its position closest to the anterior chest wall. In autopsy series, ventricular injuries predominate, whereas other findings such as valvular tear or rupture, septal tears, and coronary artery thrombosis are far less common.

37.3.3 Myocardial Contusion

The absence of a clear definition and accepted gold standard for testing makes the diagnosis of cardiac contusion difficult. This also leads to the wide variability of reported prevalence in the literature, ranging from 3 to 56 %. The right side of the heart is most commonly injured, probably because of its position closest to the anterior chest wall. Suggestive symptoms may be unrelated to blunt cardiac injury, whereas mild injuries may be clinically asymptomatic. Moreover, some of the other

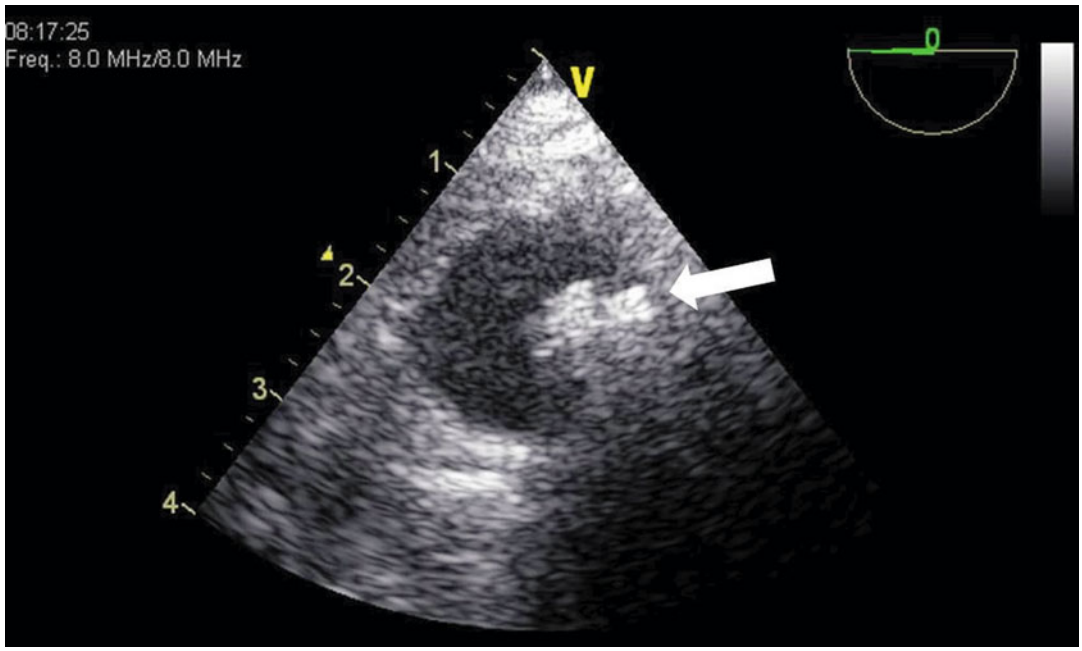

Fig. 37.4 Transesophageal echocardiography short-axis aortic view at the level of the aortic isthmus in a young man with incomplete posttraumatic aortic transection. The ruptured aortic wall is visible within the lumen of the vessel (*arrow*)

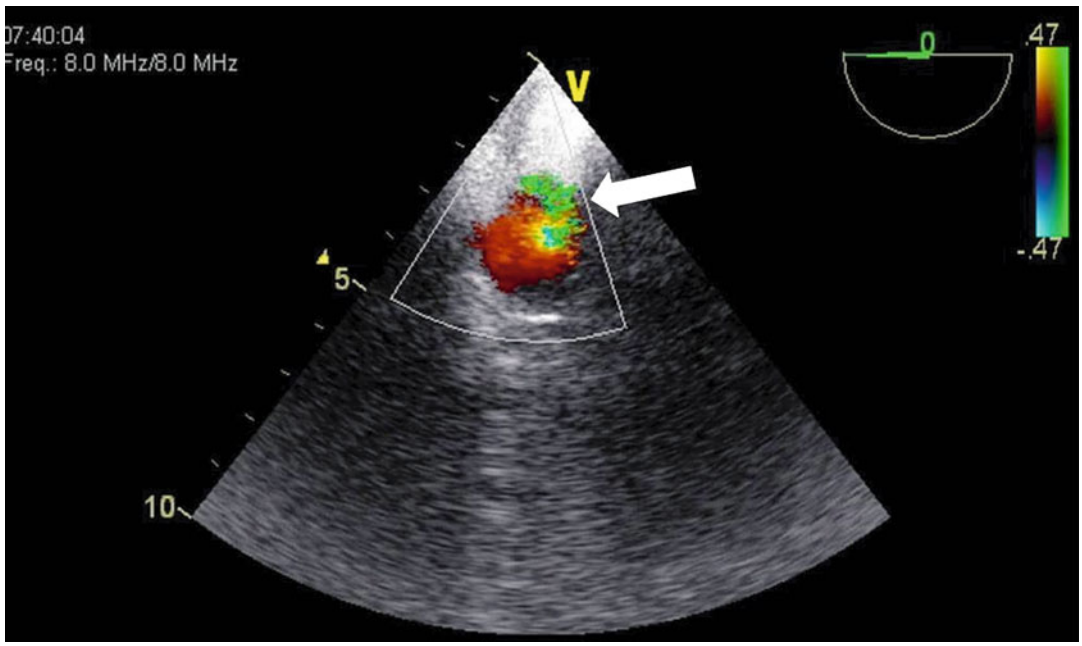

Fig. 37.5 In the same patient as in Fig. 37.3, color Doppler imaging demonstrates flow to and from the pseudoaneurysmal sac (*arrow*)

Table 37.5 Essential information gained by TEE in TAI patients

Proximal extent of dissection
Entry tear(s) location
Pericardial effusion and/or tamponade
Presence, mechanism, and severity of aortic regurgitation
Involvement of coronary ostia
Patency of epiaortic vessels
Systolic and diastolic ventricular function
Additional cardiac alterations

criteria used in the definition of myocardial contusion, such as dysrhythmias and troponin release, may be related to the patient's preexisting conditions, or to traumatic lesions remote from the chest.

Echocardiographic Findings

As significant cardiac contusion resembles myocardial ischemia and infarction, echocardiography is useful in detecting global and regional wall motion abnormalities, diastolic alterations, and associated lesions such as thrombi, pericardial effusions, and valvular lesions.

37.3.4 Cardiac Rupture

Cardiac rupture represents the most devastating form of blunt cardiac injury. As for complete aortic transection, most patients who sustain rupture of a heart chamber do not reach the hospital alive. Delayed rupture of the heart may also occur weeks after blunt trauma, probably as a result of necrosis of a contused or infarcted area of the myocardium.

The immediate ability of the patient to survive cardiac rupture depends mostly on the integrity of the pericardium. An intact pericardium or a very small pericardial tear may protect the patient from immediate exsanguination. These patients may survive for variable periods, but they eventually develop significant hemopericardium and pericardial tamponade.

Atrial rupture occurs far less often than ventricular rupture, most likely owing to anatomy and lower compliance, and presentation may be delayed and less acute. Right atrial rupture is seen in about 10 % of wall ruptures from blunt trauma, and left atrial rupture is seen less often.

Septal injury appears to be rare and its presentation is variable. Septal injury may involve insignificant tears or frank rupture and may be associated with valvular injury. There may be signs of acute heart failure.

Isolated valvular injury is likewise rare. The aortic valve is most often injured (Fig. 37.7), followed by the mitral and tricuspid valves. The lesion may consist of a tear of the leaflet or a partial or full-thickness tear of the papillary muscle or chordae tendineae. Presentation may differ depending upon the lesion, but falls somewhere on the spectrum of acute valvular insufficiency with right- or left-sided heart failure. Treatment of septal and valvular injury is generally surgical and the timing depends upon the stability of the patient and the associated lesions.

Echocardiographic Findings

Focused assessment with sonography for trauma (discussed elsewhere in this book) allows one to detect significant pericardial effusions in unstable trauma patients. Once pericardial tamponade has been ruled out, echocardiography (particularly TEE) permits one to identify wall motion abnormalities, to determine the need for fluid resuscitation or inotropic support, and to identify other lesions requiring intervention. Of particular interest is the recognition of pericardial effusion and its monitoring, in order to anticipate and avoid cardiac tamponade. The identification of free wall discontinuations may be challenging, since they are frequently subtle fistular fissures across the myocardial layers, rather than linear ducts. Doppler flow imaging and/or the intravenous injection of a small amount of echogenic contrast medium may be helpful when the diagnosis is particularly demanding. The same considerations apply to septal lesions; in this latter case, the presence, direction, and magnitude of intracardiac shunts should be clarified and signs of right-sided heart volume overload should be noted. For right chambers, a small volume of colloid solution shaken well with a small amount of air to form microbubbles

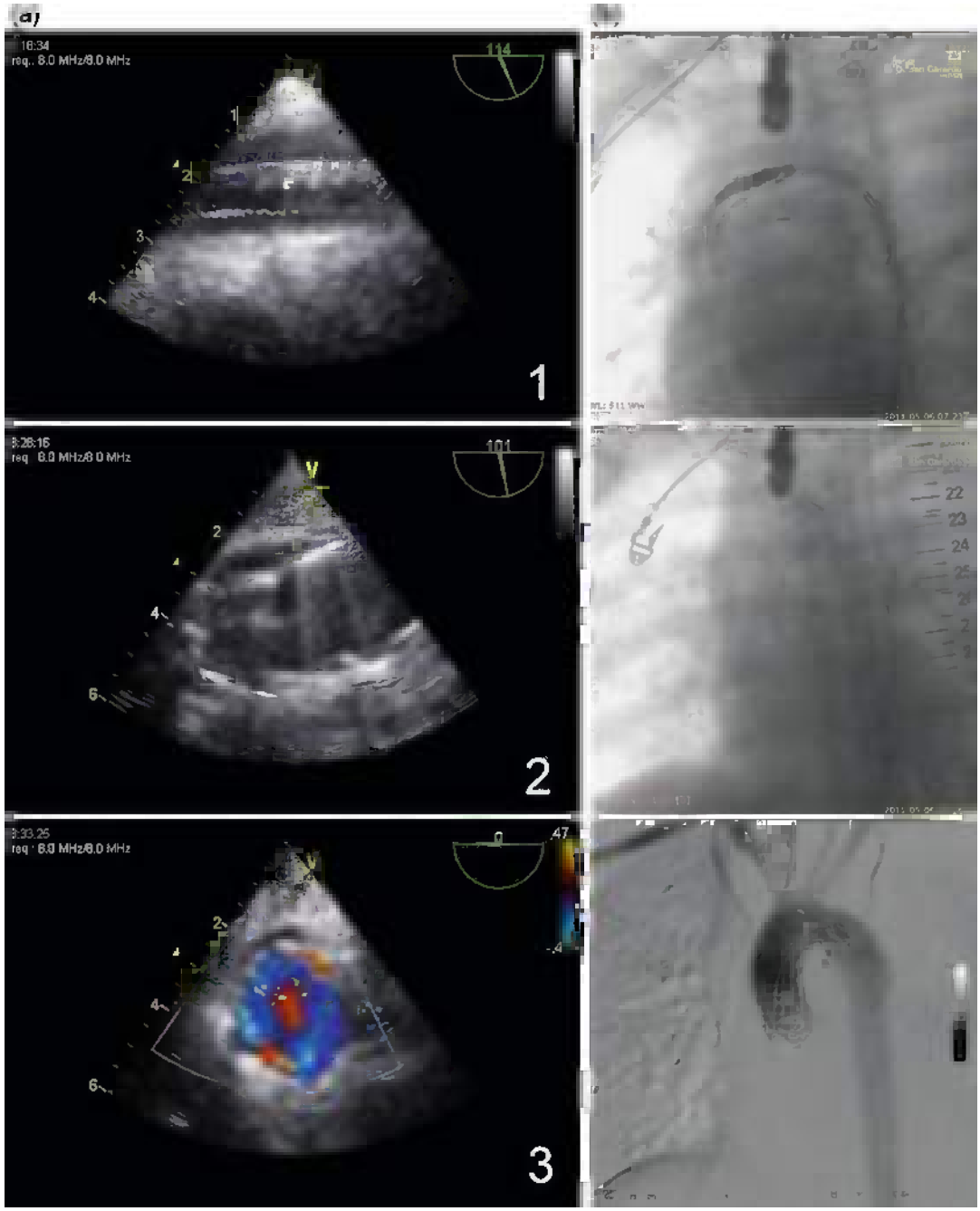

Fig. 37.6 Intraoperative echocardiographic (**a**) and angiographic (**b**) monitoring during endovascular repair of a traumatic lesion of the aortic isthmus. The graft is advanced in the descending aorta to cover the lesion, with the distal landing zone just distal from the emergence of the left subclavian artery (*1*); the graft is subsequently deployed in the correct position (*2*) and, finally, the procedure is verified for proper positioning, patency of the epiaortic vessels, and the absence of significant leaks (*3*)

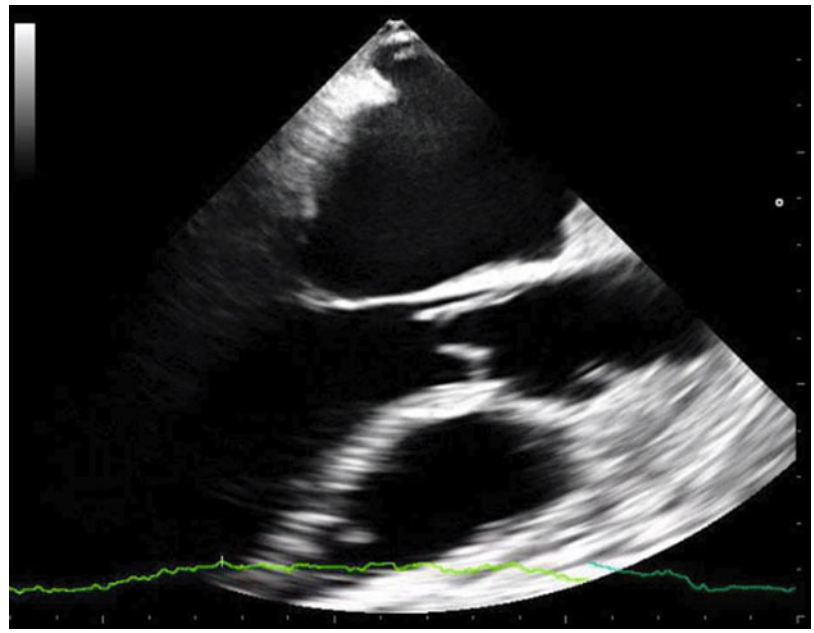

Fig. 37.7 Traumatic disruption of the aortic valve. The aortic cusps show a diastolic flail in the left outflow tract

Table 37.6 Classification of endoleaks

Type I	Endoleak originating from either the proximal (type Ia) or the distal (type Ib) end of the stent graft
Type II	Retrograde flow into the area of exclusion via side branches, i.e., intercostal arteries, inferior mesenteric artery, or lumbar arteries
Type III	Endoleak due to graft defect, or between stent graft components
Type IV	Endoleak due to graft porosity

may work as an intravenous contrast medium, whereas when the microbubbles need to persist across the pulmonary circulation and reach the left chambers, a contrast agent is indicated. These media contain small (1–8 μm) engineered microbubbles filled with a high molecular weight perfluorocarbon which have substantial persistence in the bloodstream (contrast effect lasting up to 10 min). It should be noted that this indication is off-label for all contrast agents registered by the Food and Drug Administration/ European Medicines Agency.

Traumatic valvular injuries encompass a wide spectrum of possible lesions from small fissures or perforations in the valve leaflets to complete disruption of the valve structure. The echocardiographic investigation of such lesions reflects the usual evaluation of cardiac valves done in the standard echocardiographic examination. Signs of volume or pressure overload associated with these lesions should be inspected as well.

37.4 Diagnostic Algorithm in the Chest Trauma Patient

To assess trauma patients in a consistent and reproducible way, the implementation of a diagnostic protocol is of paramount importance, as it allows one to minimize individual judgment and time loss in such a challenging situation. The diagnostic algorithm reported in Fig. 37.8 represents the guideline currently applied at our institution.

37.5 Summary

Although the involvement of the chest in trauma is quite common, serious injuries are relatively rare. Nevertheless, lesions of the heart and intrathoracic great vessels have an extremely high

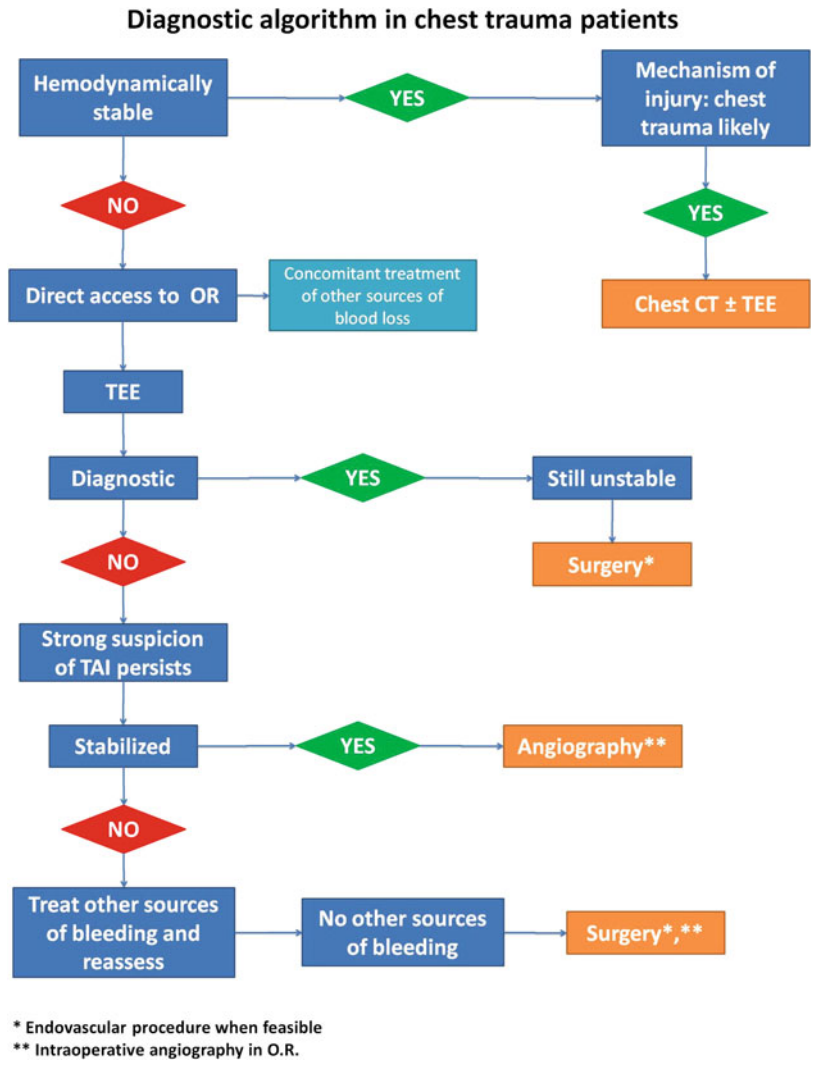

Fig. 37.8 The algorithm for the management of chest trauma patients in use at the authors' institution

mortality, which is attributable to delayed recognition and treatment in a number of patients.

Echocardiography—namely TEE—represents, in experienced hands, an invaluable tool in the acute treatment of chest trauma patients, as it allows continuation of ongoing resuscitative maneuvers, and provides point-of-care diagnostic and monitoring capabilities on the morphological and functional status of intrathoracic cardiovascular structures. TEE furthermore represents a fundamental aid during the operative moment to assess the adequacy of therapeutic interventions, particularly in the setting of endovascular aortic surgery, where its integration with intraoperative angiography allows optimal control of the procedure.

Although in stable patients CT still has some advantages in the morphological evaluation of the thoracic aorta, it nonetheless needs integrative information that only TEE can provide on the heart morphology and function and on the hemodynamic status.

We can state that TEE and CT represent complementary diagnostic techniques in the stable patient, whereas in the unstable critically injured patient, TEE proves superior in terms of portability and lifesaving information gained.

Further Reading

Evangelista A, Flachskampf FA, Erbel R et al (2010) Echocardiography in aortic diseases: EAE recommendations for clinical practice. Eur J Echocardiogr 11:645–658

Hiratzka LF, Bakris GL, Beckman JA et al (2010) 2010 ACCF/AHA/AATS/ACR/ASA/SCA/SCAI/SIR/STS/SVM guidelines for the diagnosis and management of patients with thoracic aortic disease: a report of the American College of Cardiology Foundation/American Heart Association Task Force on Practice Guidelines, American Association for Thoracic Surgery, American College of Radiology, American Stroke Association, Society of Cardiovascular Anesthesiologists, Society for Cardiovascular Angiography and Interventions, Society of Interventional Radiology, Society of Thoracic Surgeons, and Society for Vascular Medicine. Circulation 121:e266–e369

Meredith EL, Masani ND (2009) Echocardiography in the emergency assessment of acute aortic syndromes. Eur J Echocardiogr 10:i31–i39

Neschis DG, Scalea TM, Flinn WR, Griffith BP (2008) Blunt aortic injury. N Engl J Med 359:1708–1716

Ting JYS (2003) Blunt traumatic aortic injury traumatic aortic injury. A review of initial diagnostic modalities and a proposed diagnostic algorithm. Eur J Trauma 29:129–138

Acute Atrial Fibrillation and Other Arrhythmias

38

Vanni Orzalesi, Silvia Marchiani, and Armando Sarti

38.1 Background

Echocardiography can be used successfully in the diagnosis, monitoring, and treatment of patients with arrhythmias in the ICU. Echocardiography is important because the diagnostic and prognostic significance of any acute arrhythmia depends on its hemodynamic consequences, and on the existence of any associated cardiac structural disorder.

The presence of arrhythmia can alter systolic and diastolic functions, affecting the stroke volume and contributing to circulatory and respiratory failure. As any tachyarrhythmia persists long enough, it is possible to observe an acute dilation of the cardiac chambers which ultimately may result in a dilated cardiomyopathy. This dilation may be reversible after the interruption of the altered rhythm. Patients with a persistent arrhythmia always need hemodynamic assessment.

ECG is the most important tool in the investigation of arrhythmias, but the ultrasound technique may be of great assistance in making the right ECG diagnosis and the management plan as well.

V. Orzalesi (✉)
Department of Anesthesia and Intensive Care, Civil Hospital, Guastalla, Italy
e-mail: vorza@iol.it

38.2 Atrial Fibrillation

Atrial fibrillation (AF) is the most common supraventricular tachyarrhythmia seen in the intensive care setting and postoperative patients. It occurs in 1–2 % of the general population with a prevalence that increases with age. In a postoperative setting, AF affects around 30 % of post-cardiac-surgery patients. AF is associated with increased risk of death, thromboembolic events, stroke, heart failure, and left ventricular (LV) dysfunction. Echocardiography plays a particularly important role in the treatment of patients with AF. When facing a patient who has acute AF in the emergency or ICU setting, four issues must be considered (Fig. 38.1):

1. Assess hemodynamic stability and control ventricular rate
2. Look for and treat underlying causes
3 Rate and rhythm control
4. Consider the risk of thrombus formation and anticoagulation.

We will consider each of these in turn:

1. *Evaluation of systolic function*. In the four-chamber view [apical four-chamber transthoracic echocardiography (TTE) and mid-esophageal four-chamber transesophageal echocardiography (TEE) at 0–20°] it is possible to evaluate the systolic function either by ejection fraction calculation or by S wave from tissue Doppler imaging measurement. An S wave velocity below 8 cm/s or below 3 cm/s correlates with moderate and severe systolic dysfunction, respectively. Cardiac output is easily measured

A. Sarti and F. L. Lorini (eds.), *Echocardiography for Intensivists*,
DOI: 10.1007/978-88-470-2583-7_38, © Springer-Verlag Italia 2012

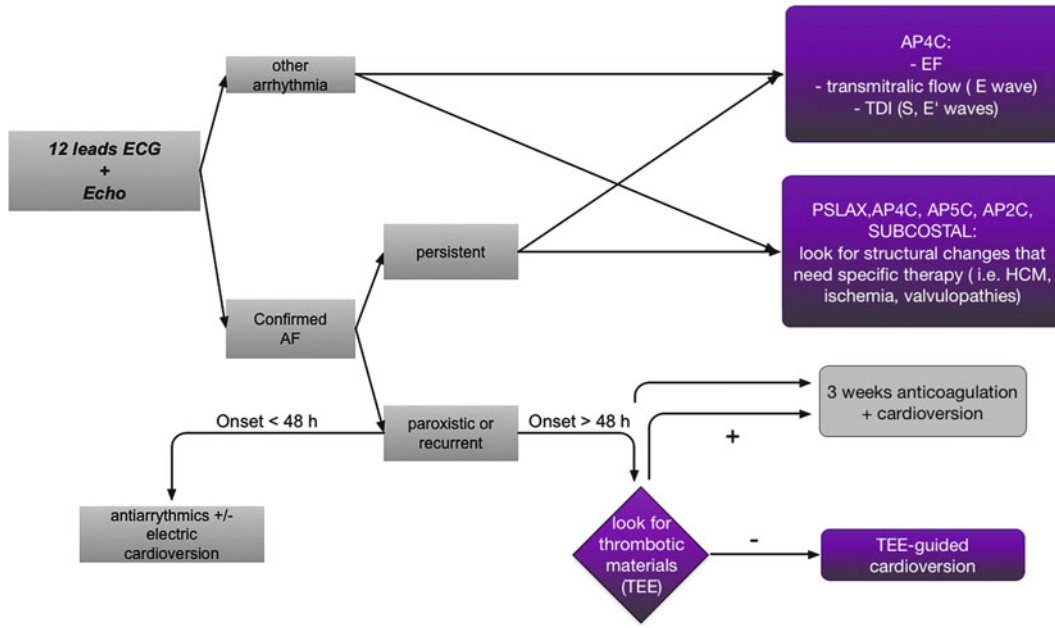

Fig. 38.1 Echocardiography-based approach to atrial fibrillation

by the product of the velocity–time integral of the ejected flow and the area of the LV outflow tract (apical five-chamber TTE or deep transgastric TEE). In the evaluation of diastole, the absence of Doppler A waves in the transmitral flow confirms the diagnosis of AF. Doppler E peak, E shape, and deceleration time can be considered to evaluate diastolic function, together with the tissue Doppler imaging E′ wave. The *E*/*E*′ ratio is used to evaluate LV filling pressure. An *E*/*E*′ ratio greater than 15 is related to a high left atrial pressure and high pulmonary capillary wedge pressure with excellent sensitivity and specificity.

2. *Search for structural causes of AF*. Left atrial dilation represents the most important risk factor for AF. The main structural alterations related to left atrial enlargement are LV hypertrophic cardiomyopathy, systodiastolic dysfunction, and mitral valve diseases.

3 *Rate and rhythm control*. The choice of the drug to be used depends on the clinical state. Beta-blockers and calcium channel blockers are effective in rate control but act as negative inotropes and are contraindicated in Wolff–Parkinson–White syndrome. Digitalis and amiodarone can be used if poor ventricular function is detected. Flecainide is another possible option to restore sinus rhythm in nonischemic patients, and propafenone may be used to prevent relapses. An electric shock is always considered for the hemodynamically unstable patient.

4. *Search for thrombotic material*. Left or right atrial appendages are the typical thrombus locations. In expert hands, TEE (mid-esophageal two-chamber view at 90° for the left appendage) is the most reliable noninvasive modality for localizing them. Its sensitivity approaches 100 %. TEE plays a role in early cardioversion of uncontrollable AF in a patient without proper anticoagulation. No detection of atrial thrombus permits one to safely cardiovert AF. TEE-guided cardioversion has the same thromboembolic risk as a cardioversion after an anticoaugulation period of 3 weeks.

A similar approach can be used to evaluate other supraventricular or ventricular tachyarrythmias. In particular, for ventricular arrythmias, echocardiography can help in diagnosing structural abnormalities such as:

- Regional wall motion abnormalities that can be found in ischemic diseases, in myocarditis, and in other cardiomyopathies
- Systodiastolic LV dysfunction
- Valvulopathies
- Cardiomyopathies
- LV dynamic outflow obstruction
- Right ventricular (RV) arrhythmogenic dysplasia.

38.3 Bradyarrhythmias and Atrioventricular Blocks

Echocardiography can also be helpful in identifying most of the causes of bradycardia or atrioventricular (AV) blocks, such as:

- Acute ischemia: regional wall motion abnormalities
- Hypovolemia—Bezold–Jarisch reflex: kissing ventricles, inspiratory collapse of the inferior vena cava (TTE) or superior vena cava (TEE), marked transaortic flow (velocity–time integral) variability
- Infiltrative processes such as amyloidosis: dilated atria with thickened interatrial septum and AV valves; LV concentric hypertrophy; granular-sparkling and hyperrefractile myocardium
- Valvulopathies: aortic stenosis.

Ischemia of the conduction system is an important cause of bradycardia. One third of patients with acute myocardial infarction develop bradycardia. The prognosis is less dependent on the presence of conduction system disease than on the extent of underlying ischemia and the severity of LV dysfunction.

The occurrence of a first- or second-degree AV block is suggestive of ischemia of the right coronary artery because it supplies blood to the AV node in 90 % of patients. Wall motion abnormalities (hypokinesia/akinesia) of the inferior wall can be easily identified in the apical two-chamber view (TTE) or mid-esophageal two-chamber view at 90° (TEE). RV involvement is observed by parasternal short-axis or apical four-chamber views (TTE) and the mid-esophageal four-chamber view at 0° or RV inflow–outflow view (TEE).

An ECG finding of third-degree AV block can be confirmed as a complete dyssynchrony between atria and ventricles (apical four-chamber view).

Ischemia of the left anterior descending artery can lead to left bundle branch block. Echocardiography can show hypokinesia/akinesia of the septum with septal asynchrony (B-mode and M-mode in parasternal long-axis TTE, or mid-esophageal long-axis TEE at the aortic valve level at 140°). In the presence of right bundle branch block, echocardiography can help in identifying important causes, such as pulmonary embolism or pulmonary hypertension (dilated right side of the heart and interventricular septal dyssynchrony), and arrhythmogenic RV cardiomyopathy (replacement of RV myocardium with fatty and fibrous tissue).

Further Reading

European Heart Rhythm Association, European Association for Cardio-Thoracic Surgery, Camm AJ, Kirchhof P, Lip GYH et al (2010) Guidelines for the management of atrial fibrillation. Eur Heart J 31:2369–2429

Morady F, Zipes DP (2011) Acute management of atrial fibrillation. In: Zipes DP, Libby P, Bonow R, Mann D (eds) Braunwald's heart disease: a textbook of cardiovascular medicine, 9th edn. Saunders, Philadelphia

Olgin J, Zipes DP (2011a) Tachyarrhythmias. In: Zipes DP, Libby P, Bonow R, Mann D (eds) Braunwald's heart disease: a textbook of cardiovascular medicine, 9th edn. Saunders, Philadelphia

Olgin J, Zipes DP (2011b) Bradyarrhythmias. In: Zipes DP, Libby P, Bonow R, Mann D (eds) Braunwald's heart disease: a textbook of cardiovascular medicine, 9th edn. Saunders, Philadelphia

Wann LS, Curtis AB, January CT et al (2011) 2011 ACCF/AHA/HRS focused update on the management of patients with atrial fibrillation (updating the 2006 guideline): a report of the American College of Cardiology Foundation/American Heart Association Task Force on Practice Guidelines. Circulation 123(1):104–123

Multiorgan Donor and Transplant Patients

39

F. Luca Lorini and Lorenzo F. Mantovani

39.1 Evaluation of the Donor Patient

Worldwide, physicians have made considerable effort to increase the number of transplants under the circumstances of an extremely severe organ donor shortage. There is a mandatory need to increase to the maximum graft availability. In this setting, the preharvesting evaluation of the candidate and the right management of the donor organ function and hemodynamics are of the utmost importance.

Usually a transthoracic examination is performed, but according to evidence that all those patients are mechanically ventilated (with worsening of the echo window) and owing to the extreme importance of exclusion of inadequate grafts, we think that in the absence of major contraindications a transesophageal examination should be always performed.

Ideally a consultant transplant physician or an expert transplant cardiologist should evaluate the patient before the procedure, but this is often impossible because of logistic difficulties in many countries, and sometimes even a nonexpert cardiologist is not immediately available. In this setting, the role of the intensivist is usually of pivotal importance. We can identify two aspects of the heart evaluation:

1. Function of the graft itself
2. Exclusion of direct heart damage

Moreover, it should be underlined that the possibility of comparing pretransplant images with postransplant ones provides a great chance of rapid identification of early postoperative dysfunction of the graft.

39.2 Function of the Graft

The assessment of a good cardiac function in a multiorgan donor is of utmost importance considering the role of the heart to perfuse and supply the whole body. The finding of an ineffective cardiac function should alert the clinician in order to better investigate the availability of other potential grafts.

The examination should certainly include the evaluation of standard echocardiographic parameters, the area and distribution of ventricular regional wall motion abnormalities. The presence of a possible atrial or ventricular defect should always be excluded, but remember that in the case of an atrial defect a surgical intraoperative closure is an option.

Obviously, we recommend the standard evaluation of all the heart valves with careful attention to the presence/absence of relevant valvular disease, including valvular calcification. Anyway, it should be remembered that the finding of a bicuspid aortic valve does not

F. L. Lorini (✉)
Department of Anesthesia and Intensive Care, Ospedali Riuniti di Bergamo, Bergamo Italy
e-mail: llorini@ospedaliriuniti.bergamo.it

A. Sarti and F. L. Lorini (eds.), *Echocardiography for Intensivists*,
DOI: 10.1007/978-88-470-2583-7_39, © Springer-Verlag Italia 2012

contraindicate the use of a donor heart. In the case of valvular disease associated with hemodynamic abnormalities, the donor heart may still be used for heart transplant. On some occasions bench repair or replacement of a donor aortic valve or repair of an incompetent mitral valve has been performed with favorable outcomes.

The myocardial function and the coronary tree of the patient should be evaluated as far as possible, especially in patients with relevant risk of such a disease defined as current or past existence of a history of hyperlipidemia, hypertension, diabetes, or smoking, and older than 50 years of age, but we recommend whenever possible this kind of evaluation for all patients. Discreet wall motion abnormalities on echocardiography or left ventricular (LV) ejection fraction less than 40 % despite optimization of hemodynamics with inotropic support should lead to exclusion of a graft.

Evaluation of left anterior descending coronary artery flow should be done whenever possible. The examination should include evaluation of end-systolic and end-diastolic LV diameters from M-mode or 2D imaging, ejection fraction evaluation, and measurements of the thickness of the ventricular septum and LV posterior wall, and as stated before an accurate observation of possible ventricular regional wall motion abnormalities. Another crucial evaluation is assessment of donor heart size expressed as LV diameter; it usually correlates very well with the LV mass index. This is very important especially in the case of a possible donor–recipient body mass index mismatch greater than 20 %. Anyway, we should always remember that there is a poor relationship between echocardiographic adult heart size and body weight. In such a case, the postoperative course of this kind of patient should be carefully monitored and inotropic support and hemodynamic monitoring should be prolonged.

The presence of LV hypertrophy in the donor heart suggests the need for early administration of cardioprotective agents (ACE inhibitors, angiotensin receptor blockers, and calcium antagonists) in the postoperative course. Some studies found that early mortality after transplant was increased only if the donor wall thickness was more than 14 mm and was associated with ECG abnormalities.

Finally, it should be remembered that a relative increase of LV wall thickness compared with previous measurements is a very clear sign of antibody-mediated rejection in the postoperative period.

Evaluation of mitral inflow obtained by pulsed wave Doppler echocardiography sampling the volume between the mitral leaflet tips during diastole, peak early (*E*) and late (*A*) transmitral filling velocities as their ratio (*E*/*A*), and the deceleration time of the E wave should be always done, but it should be remembered that very often discordances between the *E* and *E*/*A* parameters and the degree of valvular regurgitation between the donor and recipient are attributable to the difference in the volume status before and after transplant, so abnormalities in the donor heart should not exclude harvesting itself.

From the clinical decision perspective, the role of echocardiography prior to graft harvesting seems to be fundamental when there is LV dysfunction in the donor: LV dysfunction is a common finding in patients with intracranial disorders (about 20 %), with the singular feature of regional wall abnormalities covering multiple coronary territories without and with underlying coronary disease. In a peculiar way, the apical LV function is often preserved despite other regional abnormalities (probably due to a paucity of norepinephrine content leading to less sensitivity to the catecholamine storm especially during subarachnoid hemorrhage). So a further evaluation by means of coronary angiography is recommended when this kind of feature is found. Moreover in the case of a negative result after coronary angiography it should be remembered that this kind of ventricular dysfunction has proven to been reversible even many days after transplant (30 days). To distinguish donor cases likely to be transient, it seems useful to perform dobutamine stress echocardiography in association with assessment of troponin I plasma level. Some preliminary studies suggest that a reversible dysfunction after the stress test associated

with a low troponin level should lead to successful transplant of the organ. Another interesting issue is to perform prolonged donor management in order to obtain a series of echocardiographic examinations showing an improvement in LV function. All the above statements are very important especially in the evaluation of urgent transplant in sick pediatric patients because of the lack of donor hearts.

In conclusion, it has been demonstrated that an expert operator can obtain a good preoperative evaluation with a 5–10-min standard examination by means of recording the thickness of the ventricular septum and LV posterior wall and end-systolic and end-diastolic LV diameters from M-mode or 2D imaging. LV ejection fraction is measured with the two-chamber view and the four-chamber view by the biplane Simpson method.

39.3 Exclusion of Direct Heart Damage

Obviously this is perhaps the other important issue in evaluating a donor's heart. This kind of evaluation is made in order to exclude marked heart damage often caused by direct or indirect chest trauma. The examination should exclude a direct lesion of heart structures such as atrial or ventricular rupture and related acute cardiac tamponade or pericardial effusion, acute valve regurgitation due to a lesion of the valve apparatus (especially a mitral valve acute papillary muscle lesion but even an aortic lesion in the case of direct or indirect damage to the aorta), and a direct myocardial lesion leading to acute myocardial infarction. Even iatrogenic lesions (lesions of the great vessels or heart especially following resuscitation procedures or placement of intravascular monitoring–infusion lines or devices) should always be excluded. Always remember that heart lesions are not infrequent following deceleration trauma, a situation often leading to brain death and consequently to transplant.

39.4 Perioperative and Postoperative Monitoring During Heart and Lung Transplant

Intraoperative echocardiography has become a standard procedure during most cardiac procedures, including heart transplant. It can aid in identifying intracardiac thrombosis and a real-time assessment of the cardiac allograft during deairing, weaning from cardiopulmonary bypass, and after implantation of the donor heart as the chest is closed. Biventricular function, especially right ventricular (RV) function, valve function, and surgical anastomoses should always be assessed if possible. Particularly, attention should be given to exclude acute rejection, RV failure, or tamponade whenever acute hemodynamic instability arises.

Another specific issue is the presence of tricuspid regurgitation. The adverse impact of significant tricuspid regurgitation on mortality or need for retransplant has been stressed. In pediatric heart transplant, a prophylactic donor tricuspid annuloplasty (De Vega) was proposed in order to prevent postoperative valve regurgitation especially if a biatrial anastomosis technique is used.

Usually the newly transplanted heart allograft typically has a good LV systolic function, so observation of an early acute LV dysfunction following heart transplant in particularly worrisome and should always be investigated to exclude early rejection or poor graft quality or preservation. More frequently we can see the presence of a postoperative early RV dysfunction, often predictable in patients with high preoperative pulmonary vascular resistance, excessive perioperative bleeding with massive transfusion, pulmonary edema, poor RV protection during implantation, significant donor–recipient mismatch, or more infrequently acute right coronary air embolization.

Even a heart allograft with excellent early function typically shows a worsening of ventricular function over the first 12 postoperative hours, primarily due to ischemia time, reperfusion, and myocardial edema, This results in both systolic and diastolic dysfunction. In the intraoperative setting, it is not uncommon to see an increase in wall thickness and mass and a restrictive cardiac filling pattern (by means of a transmitral Doppler evaluation). In the early postoperative period, serial echocardiographic monitoring is very useful to lead the clinician decision to discriminate between a transient benign course associated with a good cardiac output status and impaired cardiac function with poor cardiac output with the need for prolonged inotropic support, an intra-aortic ballon pump, or a RV assist device/LV assist device. Anyway, it seems there is substantial evidence that an isovolumetric relaxation time less than 90 ms and a pulsed Doppler *E/A* ratio greater than 1.7 could be significant predictors of acute cardiac allograft rejection, even if each single echocardiographic feature is not able to confirm rejection alone. This kind of diagnosis should be confirmed by clinical, hematochemical clues and keeping in mind that endomyocardial biopsy of the right side of the heart is the gold standard.

Another important issue to consider is the surgical technique used during heart transplant. Orthotopic heart transplant has most commonly been performed with biatrial anastomoses according to the Lower and Shumway technique. More recently, bicaval and total techniques have been devised to improve cardiac anatomy and physiologic function. The bicaval technique leaves a large cuff of the recipient's atria and leads to a marked atrial enlargement and altered geometry with a predisposition to intracavitary thrombus formation.

Observation of an elevated transmitral *E/A* ratio could be explained as the result of an impaired overall atrial function after standard left atrial anastomosis rather than from a truly restrictive pattern. In this case, the observation of a "pseudorestrictive" pattern associated with elevated *E/A* ratios and paradoxically normal early diastolic mitral annular motion velocities avoids misdiagnosis of an advanced diastolic dysfunction status often associated with acute rejection, as stated above.

Key Points in Heart Transplant Echocardiography

1. Preoperative evaluation.
   - The finding of an ineffective cardiac function should alert the clinician in order to better investigate the availability of other potential grafts.
   - Discreet wall motion abnormalities on echocardiography or LV ejection fraction less than 40 % despite optimization of hemodynamics with inotropic support should lead to exclusion of a graft.
   - The presence of LV hypertrophy in the donor heart suggests the need for early administration of cardioprotective agents.
2. Intraoperative evaluation.
   - An early acute LV dysfunction following heart transplant is particularly worrisome and should always be investigated to exclude early rejection or poor graft quality or preservation.
   - More frequently we can see the presence of a postoperative early RV dysfunction, often predictable in patients with high preoperative pulmonary vascular resistance.
3. Postoperative evaluation.
   - In early postoperative period, serial echocardiographic monitoring is very useful to lead the clinician decision.
   - There is a substantial evidence that reduction of the pressure half time, an isovolumetric relaxation time less than 90 ms, and pulsed Doppler *E/A* ratio greater than 1.7 could be significant predictors of acute cardiac allograft rejection , but no single predictor or combination is powerful enough to eliminate surveillance by endomyocardial biopsies.

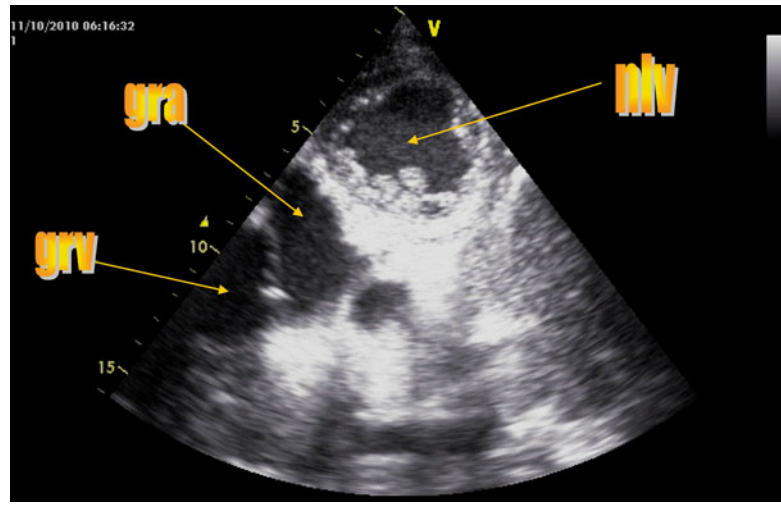

Fig. 39.1 Heterotropic heart transplant echo. *nlv* native left ventricle, *gra* graft right atrium, *grv* graft right ventricle

39.5 Heterotopic Heart Transplant

In this technique the donor heart is placed without recipient cardiectomy. The technique was initially developed in the precyclosporine era for patients whose myocardium was expected to recover. Now it is a technique adopted for patients with severe pulmonary hypertension because the preconditioned native right ventricle should cope better with the high transpulmonary pressure gradients. Moreover, it permits use of undersized allografts and it is sometimes used in size-mismatch patients, expanding the donor pool

The allograft is placed to the right to the native heart in the right side of the chest at an angle close to 90° to it. Both the left and the right donor atria are connected to the recipient's atria and both aortas are anastomosed. The donor pulmonary artery may be connected to the donor right atrium (LV assist configuration) or to the pulmonary artery by means of an interposed graft (biventricular configuration). Physiologically we have a situation in which the native and donor atria share the systemic and pulmonary venous return. The donor pulmonary artery and aorta are anastomosed to the respective native vessels, each receiving blood from both native and donor ventricles (Fig. 39.1).

Clinical experience demonstrates that owing to the huge space occupied by the two anastomosed hearts, it is often very difficult to obtain a single image covering of all the anatomical field. It is therefore very important to identify correctly the single structures, so in this case transesophageal echocardiography (TEE) is used to correctly identify the chambers in a step-by-step examination, considering the different orientation of the two hearts in the chest and their expected function and keeping in mind the 90° orientation between the native and donor chambers. Often it is possible to find a smoke-like effect in the native atria and dilatation and poor contractility obviously in the native left ventricle.

39.6 Lung Transplant

Owing to the close interrelation between the heart and lung, the TEE evaluation is considered an invaluable tool for intraoperative monitoring during anesthesia in this kind of surgical procedure. Induction and mechanical ventilation can exacerbate a preexisting pulmonary hypertension, leading to acute RV failure. Preoperative severe emphysema (always present in α_1-antitrypsin deficiency) can lead to acute pneumatic tamponade. Intraoperative hypoxemia due to ventilation

of one lung can exacerbate cardiac ischemia, so TEE is the right tool to inform the anesthesiologist about the necessity of extracorporeal intraoperative support. During the reperfusion of the lung, there is the possibility of coronary air embolism. Moreover, TEE is routinely used to assess possible thrombi, vascular strictures, and the permeability of pulmonary venous vascular sutures.

39.7 Conclusion

In conclusion, it can undoubtedly be stated that TEE is a fundamental tool for both standard monitoring and diagnosis in the transplant surgery environment. It could make a difference in saving or preserving grafts because of its early-warning capacity, enabling the decision-making process to be as fast as possible in virtue of its bedside utilization compared with more complex diagnostic procedures requiring the moving of the patient. A well-planned evaluation strategy in the preoperative, intraoperative, and postoperative settings plays a key role in success during anesthesia and in the intensive care unit.

Further Reading

Costanzo MR, Dipchand A, Sterling R et al (2010) The International Society of Heart and Lung Transplantation guidelines for care of heart transplant recipients. J Heart Lung Transplant 29(8):914–956

Hashimoto S, Kato TS, Komamura K, Hanatami A (2011) The utility of echocardiographic evaluation of donor hearts upon the organ procurement for heart transplantation. J Cardiol 57:215–222

Serra E, Feltracco P, Barbieri S (2007) Transoeshopageal echocardiographic during lung transplantation. Transplant Proc 39(6):1981–1982

Sun JP, Abdalla IA, Asher CR, Greenberg NL, Popovic ZB, Taylor DO, Starling RC, Thomas JD, Garcia MJ (2005) Non invasive evaluation of orthotopic heart transplant rejection by echocardiography. J Heart Lung Transpl 24(2):160–165

Venkateswaran RV, Bonser RS, Steeds RP (2005) The echocardiographic assessment of donor heart function prior to cardiac transplantation. Eur J Echocardiogr 6:260–263

New-Onset Cardiac Murmur in the Unstable Patient

40

Michele Oppizzi and Marco Ancona

There are several different clinical scenarios and causes of hemodynamic instability associated with cardiac murmur of new onset, including:

- Mechanical complications of acute myocardial infarction (AMI)
  - Free wall rupture
  - Ventricular septal defect (VSD)
  - Papillary muscle rupture
- Left ventricular outflow tract (LVOT) obstruction
  - Systolic anterior motion (SAM)
- Mitral regurgitation (MR) due to spontaneous rupture of chordae tendineae
- Endocarditis
  - MR
  - Aortic regurgitation (AR)
- Aortic dissection
- Prosthetic valve malfunction

40.1 Mechanical Complications of AMI

Patients at high risk of mechanical complications are elderly patients with the first ST-segment elevation myocardial infarction (STEMI) without a history of previous angina with late presentation to the emergency department and too late or no reperfusion.

40.1.1 Free Wall Rupture

40.1.1.1 Clinical Scenario

Free wall rupture typically appears within a few days from the onset of STEMI in the population previously mentioned: these patients suddenly develop a circulatory collapse, usually associated with bradycardia, within a few days after a small infarct. Free wall rupture represents an emergency because it leads to cardiac tamponade and death. On physical examination, cardiac tamponade manifests itself as distension of neck veins, pulsus paradoxus, and muffled heart sounds. Occasionally rupture of the septum or papillary muscle is associated.

40.1.1.2 Echo Diagnosis

Transthoracic echocardiography (TTE) is sufficient to diagnose a free wall rupture. Typically the presence of (a) pericardial effusion (2D; apical, parasternal ,or subcostal views), (b) an akinetic wall, usually inferior (two-chamber view) or lateral (four-chambers view), and (c) hyperkinesis of other segments, in patients with circulatory collapse, must raise the suspicion of free wall rupture. Increased contraction of remote walls produces a high intraventricular pressure; late thrombolysis converts ischemic necrosis into hemorrhagic necrosis, causing rupture of the infarcted wall. Free wall rupture occurs between viable and necrotic myocardium. A large anterior AMI in the

M. Oppizzi (✉)
Department of Cardiology,
San Raffaele Hospital, Milan, Italy
e-mail: oppizzi.michele@hsr.it

A. Sarti and F.L. Lorini (eds.), *Echocardiography for Intensivists*,
DOI: 10.1007/978-88-470-2583-7_40,

territories of the left anterior descending coronary artery is usually not associated with free wall rupture because it usually causes a severe left systolic dysfunction: the ventricle is not able to generate an intraventricular pressure high enough to cause wall rupture.

The diagnosis is confirmed by a turbulent systolic flow (color Doppler imaging) through the akinetic wall, usually in the mid-ventricular position of the anterior or lateral wall. In some patients the rupture is incomplete or closed by a cloth and is not well visualized by echocardiography. Blood pericardial effusions commonly cause cardiac tamponade: the right ventricle and both atria appear compressed and diastolic filling is impaired (swimming heart image).

40.1.1.3 Echo-Guided Therapy

Free wall rupture is a surgical emergency; in the absence of prompt treatment this condition is usually fatal. During surgery, the pericardial effusion is evacuated and the myocardial tear is closed by pledgeted sutures.

40.1.2 Ventricular Septal Defect

40.1.2.1 Clinical Scenario

The symptoms of VSD include a sudden relapse of chest pain, shortness of breath, and a rapid worsening of the patient's hemodynamic status with a low cardiac output and cardiogenic shock. In patients who have not been treated with reperfusion therapy, symptoms usually appear 3–7 days after the infarct, whereas rupture occurs earlier (median 24 h) if thrombolytic therapy has been used. Characteristically, a parasternal thrill is palpable in half of patients and a harsh, loud, and holosystolic new-onset murmur becomes audible along the sternal border and typically radiates to the right parasternal area. Signs of left-sided and right-sided heart failure are both present. In patients with cardiogenic shock, it can be difficult to identify a thrill or a murmur, and therefore shock may be erroneously attributed to extension of the AMI. The definitive treatment is the surgical closure of the VSD with a patch; in selected patients it is possible to close the VSD by placing a device percutaneously.

40.1.2.2 How To Do It and Echo-Guided Therapy

Echocardiography is useful in diagnosing septal rupture, to define the site, to estimate left-to-right shunt, to quantify right and left ventricular function, and to visualize, if any, MR.

VSD appears on color Doppler imaging as a turbulent systolic flow from the left to the right ventricle through the akinetic ventricular septum and is more commonly associated with hyperkinesis of other walls. Such findings are diagnostic of a VSD: the sensitivity and specificity of color Doppler imaging are about 100 %. The size of the defect ranges from a few millimeters to several centimeters. So a large VSD appears on 2D imaging as an echo dropout across the septum. In patients with an anterior AMI, the defect is simple (discrete with direct communication at the same level on both sides of the septum) and apically located, and it can be well visualized in the four-chamber view. In patients with an inferior AMI, the defect is more complex (irregular and serpiginous) and it involves the basal portion of the inferoposterior septum, close to the tricuspid and mitral valves; it may be seen in the basal septum in the four-chamber transthoracic or transesophageal views and in the parasternal short-axis views. Sometimes, multiple septal perforations are present. Given the high mortality rate for patients treated conservatively, the diagnosis of VSD is itself an indication for emergent surgery, even when the patient is stable. Previous controversies on the timing of surgical intervention are no longer an issue.

In most cases the right ventricle appears dilated in the four-chamber and long-axis views as a consequence of left-to-right shunt and/or right ventricular infarction. Right atrial pressure inferred from the inferior vena cava diameter and its degree of collapse in the subcostal view may be high. Right ventricular infarction is suspected in patients with an inferior AMI with ST elevation in the right precordial leads,

bradyarrhythmias, and reduced indexes of right ventricular function: diffuse hypokinesia, a tricuspid annular plane systolic excursion of less than 1.8 cm, and a systolic velocity on tissue Doppler imaging of less than 10 cm/s.

A posterior location of the VSD and right ventricular dysfunction, particularly if complicated by an increase in right atrial pressure, are echocardiographic predictors of poor outcome. Cardiogenic shock more commonly develops in patients with right ventricular dysfunction. Surgical closure of a complex posterior VSD is more technically demanding and carries a higher risk of recurrence. Percutaneous closure is not always feasible: the Amplatzer device may impinge the mitral and tricuspid valves, causing significant regurgitation. In-hospital mortality for anterior defects is 10–15 % and 30–35 % for anterior and for posterior VSD, respectively.

The estimation of the left-to-right shunt can be obtained by measuring the ratio between the right and the left cardiac output as recorded with pulsed wave Doppler imaging on the right ventricular outflow tract and the LVOT: its clinical relevance has recently declined because early surgery is now recommended in all patients, irrespective of the amount of the shunt. Nevertheless, it is valuable in patients who develop a recurrent defect after surgical closure: in these patients redo surgery is indicated when the shunt fraction is greater than 2.0.

Left ventricular function, quantified by ejection fraction in the four-chamber view, is usually mildly reduced. The preoperative hemodynamic status is a more powerful predictor of outcome than the left ventricular ejection fraction.

Simultaneous significant MR secondary to papillary muscle infarction or dysfunction may occur in up to 20 % of patients with VSD. It is well visualized and quantified in the apical four- and two-chamber views and in the parasternal long-axis view. If the regurgitation is severe, concomitant valve repair or replacement is indicated.

In the operating theater, transesophageal echocadiography (TEE) is used after the weaning from cardiopulmonary bypass in order to assess the completeness/efficacy of the repair of the septum and of the mitral valve, if performed, and the response of right and left ventricular function to inotropic and mechanical support. In the postoperative period, TTE is recommended to guide the weaning from drugs or devices and if a VSD recurrence (new-onset murmur, hemodynamic worsening) is suspected.

40.1.3 Papillary Muscle Rupture

40.1.3.1 Clinical Scenario

The population at risk of papillary muscle rupture is the same as that described for the other mechanical complications of AMI. Complete resection of papillary muscle is incompatible with life. Partial papillary muscle rupture is usually due to a small inferior infarction involving the posteromedial papillary muscle. Rupture of the posteromedial papillary muscle is three times more frequent than that of the anterolateral papillary muscle, because the former is vascularized only by the right coronary artery, whereas the latter usually has a double vascularization from the left anterior descending coronary artery and circumflex coronary artery. The clinical manifestations of papillary muscle rupture are similar to those of VSD—an abrupt onset of shortness of breath and hypotension—but the incidence of papillary muscle rupture is lower (about 1 %), the onset is early (median 1 day), pulmonary edema is more common and more severe, and signs of right-sided heart failure, such as distension of jugular veins, are missing. Physical examination reveals no thrill and the cardiac murmur is softer and radiated to the left axilla.

40.1.3.2 How To Do It

TTE (apical and parasternal views) with color Doppler imaging immediately identifies the MR, which is usually eccentric and severe, regional akinesia, usually of the inferior wall, and a hyperdynamic cardiac motion consequent to acute volume overload. The anterior or, more commonly, the posterior mitral valve leaflet, consequent to the rupture of the head of the medial or of the lateral papillary muscle, respectively, is flailed into the left atrium. TTE can often visualize the papillary muscle's head protruding in the left atrium, but in some

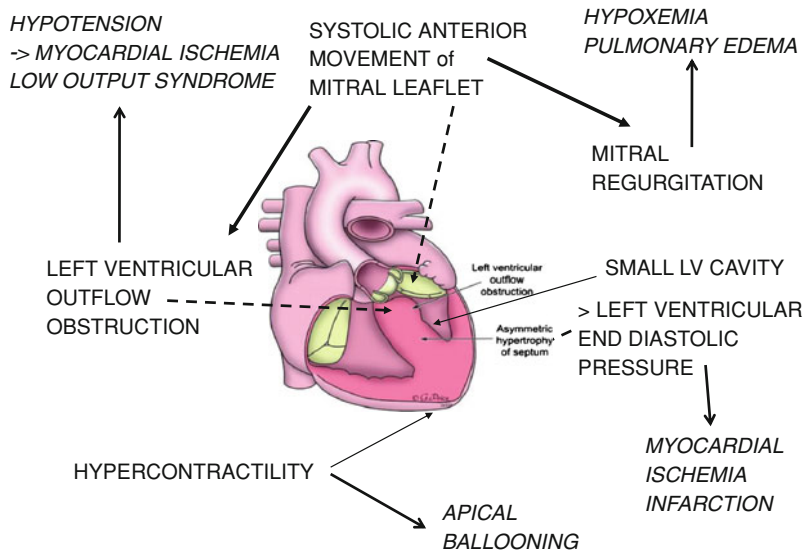

Fig. 40.1 Left ventricular outflow tract (LVOT) obstruction

patients TEE (mid-esophageal views for the mitral valve and transgastric long-axis views) is needed to confirm the diagnosis.

40.1.3.3 Echo-Guided Therapy

Partial papillary muscle rupture is a surgical emergency. The decision for repair or replacement is based on surgical preference and skill and not on echocardiographic data.

40.2 LVOT Obstruction and SAM of the Mitral Valve

40.2.1 Clinical Scenario

LVOT obstruction is a dynamic, functional obstruction due to systolic movement of the anterior mitral leaflet (SAM) into the outflow caused by suction (Venturi effect) or pushing (drag forces) of the anterior leaflet. These forces are generated by a combination of (a) *predisposing anatomic features of the left ventricle*, such as moderate to severe hypertrophy of the basal ventricular septum, in some cases associated with an anterior position of the papillary muscles, a small left ventricular cavity, and a hyperkinetic left ventricle, and (b) *predisposing conditions* such as a hyperdynamic state and a preload reduction (Fig. 40.1)

LVOT obstruction is typical of hypertrophic obstructive cardiomyopathy. However, it has also been described in patients with hypertensive heart disease, especially in elderly women, in pheochromocytoma, apical ballooning syndrome, after mitral valve repair or cerebral hemorrhages, and in those situations characterized by high catecholamine levels and/or low left ventricular preload (hypovolemia, use of nitrates, pericardial effusion, etc.)

High-risk populations are those with:

- Hypertrophic obstructive cardiomyopathy
- Asymmetric left ventricular hypertrophy associated with small left ventricular volumes and hyperkinetic let ventricle

High-risk conditions are all conditions causing underfilling of the left ventricle, tachycardia, and enhancing left ventricular contractility, such as:

- Hypovolemia
- Reduced preload
- Reduced afterload
- Hyperdynamic state
- Catecholamine infusion

SAM causes two different problems:

1. *LVOT obstruction*, which, if severe, may lead to a reduction in cardiac output, hypotension, myocardial ischemia, and cardiac arrest by ventricular fibrillation
2. *MR*, which increases the left atrial and pulmonary capillary pressure, leading to dyspnea, pulmonary edema, and hypoxemia

When a high-risk patient meets a high-risk condition, the prerequisites for the perfect storm are present. A typical scenario is a patient who becomes hypotensive with or without ST changes or pulmonary edema. If the hemodynamics do not respond to volume expansion, catecholamines are the first choice of therapy, but drugs are not effective and the arterial pressure remains low. So the anesthetist decides to position the Swan–Ganz catheter: but hemodynamic data from the pulmonary catheter are dangerously misleading, because low cardiac output (due to LVOT obstruction) and high left atrial pressure (due to MR) are interpreted as the consequences of a severe systolic left ventricular dysfunction. The levels of adrenergic agents are increased and administration of furosemide is started. LVOT obstruction is worsened with a positive feedback and if the loop is not interrupted by an echo-guided diagnosis, cardiac arrest eventually occurs.

40.2.2 How To Do It

The diagnosis of LVOT obstruction by SAM can only be performed by echocardiography, which can also quantify the gradient. SAM can be easily diagnosed with both TTE and TEE. First one has to identify, with 2D echocardiography, the anterior mitral leaflet being suctioned during systole into the LVOT. The more useful views are the parasternal long axis-view, the apical five-chamber view, and the mid-esophageal long-axis view for the aorta at 120°. In these views color Doppler imaging typically shows two contemporary turbulent systolic flows: one directed into the LVOT, i.e., the obstruction, and the other directed posteriorly in the left atrium, i.e., the MR, both caused by SAM. In the apical five-chamber and deep transgastric views, continuous wave Doppler imaging allows the quantification of the obstruction through the measurement of the gradient. The systolic gradient due to SAM has a typical *dagger-shaped* morphology, increasing during systole and reaching its peak in end-systole (Fig. 40.2). Its morphology is very different from that of aortic stenosis, whose peak is in mid-systole. A peak gradient value higher than 30 mmHg defines a critical gradient.

MR and turbulent flow of LVOT obstruction can be very close to each other and it can be difficult to understand which flow is being measured by continuous wave Doppler imaging. To discriminate between them, remember the dagger-shaped morphology of LVOT obstruction and the higher velocity of MR flow.

40.2.3 Echo-Guided Therapy

The diagnosis of LVOT obstruction in the setting of a hypotensive patient is critical: in this clinical condition every positive inotropic agent must be avoided, because these agents worsen the obstruction. Norepinephrine and low doses of beta blockers to cause volemic expansion and preload and afterload increases are the appropriate treatment of SAM (Fig. 40.3).

40.3 MR Due to Spontaneous Rupture of Chordae Tendineae

Spontaneous rupture of chordae tendineae (flail) in patients affected by myxomatous degeneration of the mitral valve gives rise to an acute MR which can quickly decompensate the patient.

40.3.1 Echocardiographic Findings

- On 2D echocardiography, the leaflet loses the normal concavity towards the left ventricle, becoming flat or with concavity directed at the left atrium, with a free movement during

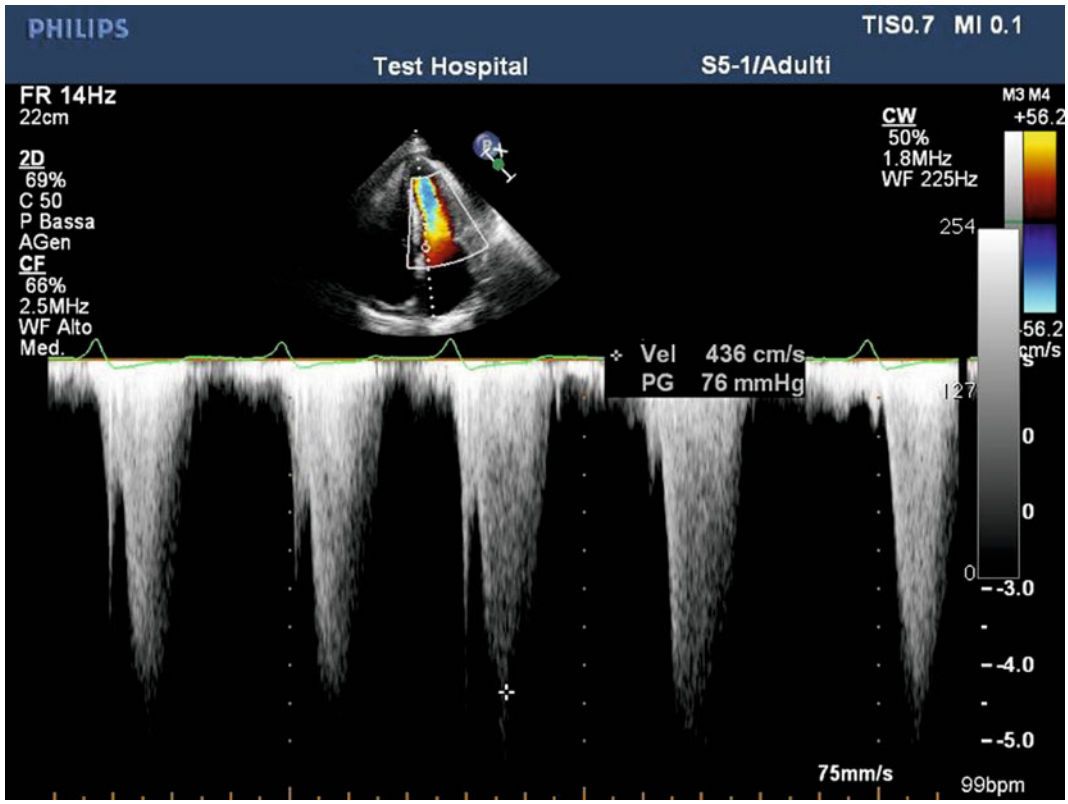

Fig. 40.2 LVOT gradient by continuous wave Doppler imaging

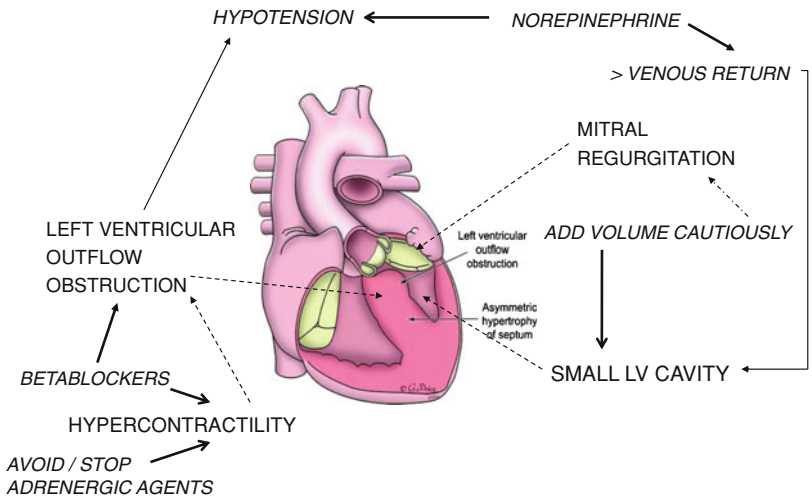

Fig. 40.3 Echo-guided treatment of LVOT obstruction

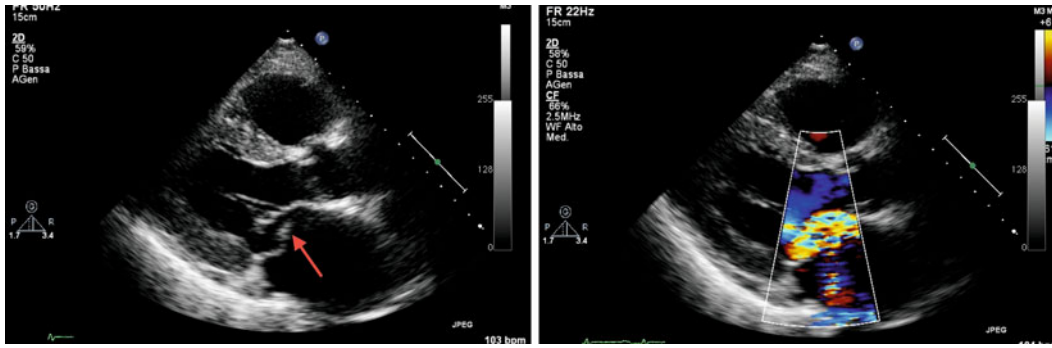

Fig. 40.4 Chordal rupture of posterior leaflet, parasternal long-axis view

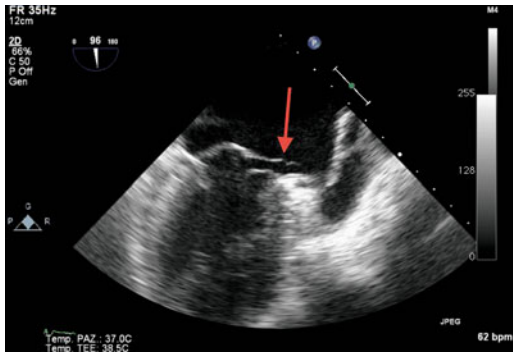

Fig. 40.5 Chordal rupture of posterior leaflet, transesophageal echocardiography two-chamber view

systole, giving the eversion of the leaflet (Fig. 40.4).

- Direct visualization of ruptured chordae tendineae protruding in the atrium during systole.
- Regurgitant jet is usually severe (color Doppler imaging) and holosystolic (color M-mode imaging). As in mitral valve prolapse, the jet is in a direction which is opposite to that of the leaflet whose chordae are ruptured (e.g., rupturing of the chordae of the posterior leaflet results in an anteriorly directed jet).

40.3.2 How To Do It

Usually TTE (parasternal long-axis and four-chamber views) allows the diagnosis. TEE is necessary to confirm the diagnosis through the direct visualization of the chordal rupture (Fig. 40.5).

40.3.3 Caveat

Rupture of chordae tendineae near the commissure gives rise to a markedly eccentric regurgitation jet which can be easily underestimated on TTE: it appears as a horizontal jet spreading over the opposite leaflet. TEE should be performed to confirm the diagnosis of rupture of chordae tendineae.

40.4 Endocarditis

Hypotension and acute congestive heart failure are not uncommon in infective endocarditis as a result of sepsis status and/or hemodynamic complications: severe MR or AR, prosthetic detachment or obstruction, cardiac shunts, or cardiac tamponade from fistula formation. The sensibility of TTE for infective endocarditis is suboptimal, especially in patients with prosthetic valves and/or periannular complications: TEE must be performed in high-risk populations. Infective endocarditis complicated by acute congestive heart failure is an indication for urgent surgical treatment.

40.4.1 Native Valve Endocarditis

Vegetation is the echocardiographic hallmark of infective endocarditis. It appears on 2D examination as an echogenic, irregularly shaped mass, usually oscillating with high-frequency movement, independent of that of the cardiac valve, typically attached to the ventricular layer of

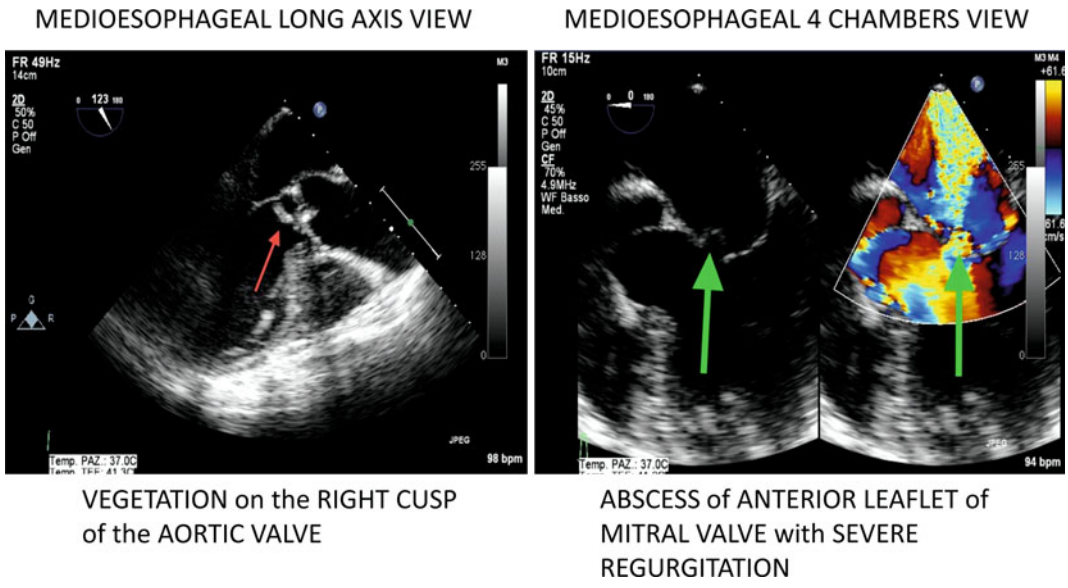

Fig. 40.6 Aortic and mitral valve endocarditis

aortic cusps or to the atrial layer of the mitral leaflet (Fig. 40.6). Sometimes, primary aortic vegetations can be responsible for the so-called kiss lesion on the anterior mitral leaflet. Other cardiac masses (Libman–Sacks lesions, marantic endocarditis, myxomatous valve, chordal rupture, Lambl excrescences) may mimic vegetations, but only spontaneous chordal rupture may cause acute severe regurgitation with hemodynamic instability.

Native valve endocarditis can cause acute regurgitation in three different ways: perforation, fistula formation (aortic valve), and chordal rupture (mitral valve).

Perforation is the most common lesion caused by endocarditis causing regurgitation: it appears early, usually in the first week after the onset of fever. On echocardiography it can be diagnosed/appears as a regurgitant flow originating from the body of the leaflet or cusp and not from the coaptation zone. *Fistula* is due to spread of infection to perivalvular tissue with the development of an aortocavitary communication creating intracardiac shunt: it can result in acute overload of the left or right ventricle. It is uncommon in aortic valve endocarditis; the incidence is a little bit higher in patients with an aortic prosthetic valve. Fistula is well visualized by color Doppler imaging in parasternal or mid-esophageal short-axis views of the aortic valve like a turbulent jet between periaortic tissue and a cardiac cavity. The left or right ventricle appears hyperkinetic because of acute overload. Patients with infective endocarditis complicated by fistula formation are, despite surgery, at increased risk of adverse outcome, including heart failure and death (up to 40 %). The fistula may break into the pericardial sac, causing cardiac tamponade.

40.4.2 Prosthetic Valve Endocarditis

Infective endocarditis of the prosthetic valve begins on the valvular cuff and usually extends to periannular tissue, resulting in prosthetic dehiscence and abscess and fistula formation. It can be difficult to visualize vegetations and extraannular complications with TTE owing to shadowing of the prosthetic valve, so TEE is usually needed.

There are three possible echocardiographic findings:

1. *Vegetations* are attached to the prosthetic anulus.
2. *Prosthetic detachment* appears as a paraprosthetic regurgitating jet. It is responsible for the development of severe regurgitation and

sometimes for the development of hemolysis. Extensive detachment can produce a "rocking" motion of the of the entire valve apparatus.

3. *Paraprosthetic abscesses* appear as an anechoic cavity surrounding the prosthesis. The echocardiographic appearance is usually nonhomogeneous. In many cases there is evidence on color Doppler imaging of a flow within the echo-free space, but this observation is not mandatory. Paraprosthetic abscesses are typical of prosthetic aortic valves and are usually localized posteriorly, i.e., in the left or the right fibrous trigone. They can fistulize in the surrounding cavity/cavities, such as the left atrium for posterior abscesses, the right atrium for lateral abscesses, and the pulmonary artery for anterior abscesses.

Vegetations and abscesses, when isolated, do not determine hemodynamic instability. In contrast, an acute prosthetic detachment causing severe AR or MR can lead to acute heart failure.

40.4.3 How To Do It

The native aortic valve can be well evaluated by TTE in the parasternal long-axis view, whereas the mitral valve can be also studied in the apical four-chamber view.

It is mandatory to perform TEE in the prosthetic valve setting when the clinical suspicion of endocarditis is high. Native and prosthetic aortic valves can be evaluated in the mid-esophageal short- and long-axis views: the short-axis view allows the evaluation of abscesses and detachments. Native and prosthetic mitral valves should be studied in every mid-esophageal view.

40.4.4 Differential Diagnosis

It can be difficult to distinguish a vegetation from a flail mitral valve on TTE. TEE allows a simple discrimination between the two. With a prosthetic mechanical valve it can be challenging to discriminate between vegetations and thrombi localized at the prosthetic annulus: thrombi are usually bigger and are associated with spontaneous echo contrast.

40.5 From Echo Images to Diagnosis: A Practical Approach

In the unstable patient in whom a new onset cardiac murmur is present, three different echocardiographic settings might be responsible for the instability: a new MR, a new AR, or a prosthetic malfunction. A practical overview of the differential diagnosis and the causes of these murmurs is described here.

40.5.1 New-Onset MR

MR appears on color Doppler imaging as a turbulent systolic flow directed from the left ventricle through the left atrium. All the causes of new-onset MR must be excluded: endocarditis, SAM, and papillary muscle rupture as a complication of AMI or flail mitral leaflet. One must proceed step-by-step in order to discriminate between them (Fig. 40.7).

Firstly, the LVOT must be inspected: normally there is a systolic nonturbulent flow. A turbulent flow in the LVOT associated with the MR is indicative of SAM: the anterior leaflet of the mitral valve, during systole, is suctioned by a Venturi effect through the LVOT, causing an obstruction; if the anterior leaflet is displaced in the LVOT, it cannot ensure an adequate coaptation, and therefore causes MR. This mechanism causes a reduction of the cardiac output, through the obstruction of the LVOT, and increases left atrial pressure through MR.

To confirm the diagnosis of SAM, one has to:

- *Evaluate the gradient on the LVOT*: SAM typically gives a dagger-shaped gradient whose peak value is greater than 30 mmHg.
- *Evaluate the direction of the MR jet*, which is typically directed posteriorly.

Once an LVOT obstruction caused by SAM has been excluded, the morphology of mitral valve leaflet should be evaluated, particularly at the concavity of the leaflet. When the valve is

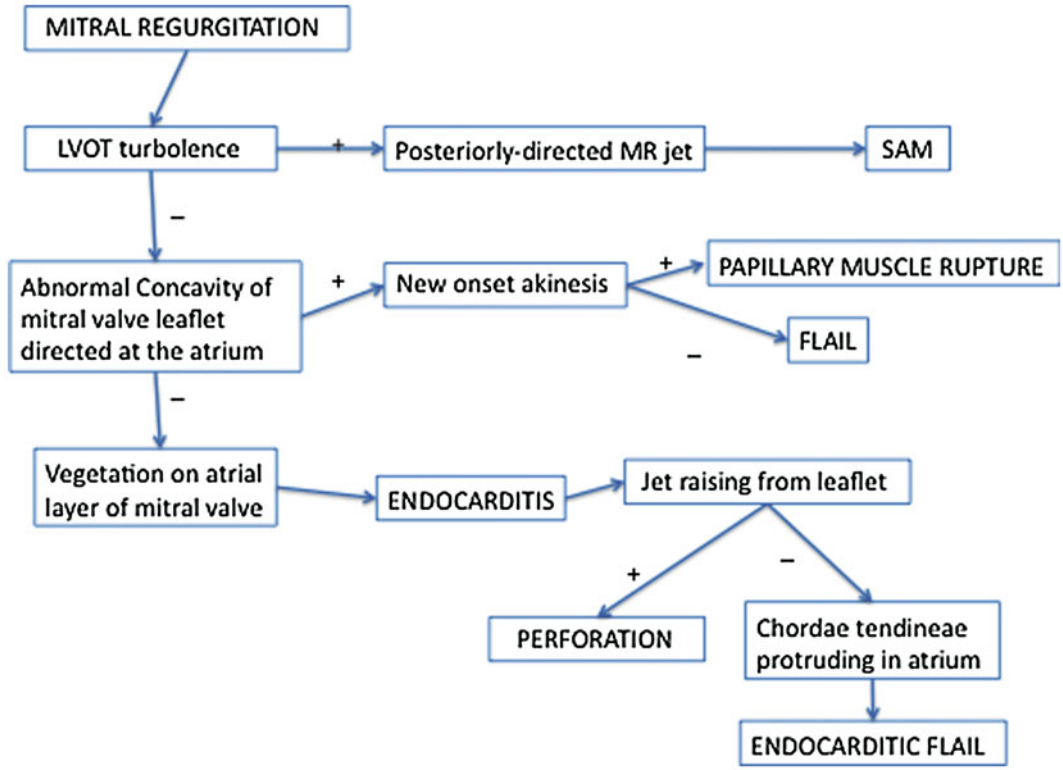

Fig. 40.7 Diagnostic algorithm for mitral regurgitation

closed, mitral leaflet concavity is normally directed to the ventricle and the chordae tendineae attached to the leaflet are visible. There are two pathological conditions in which the mitral leaflet concavity during systole is directed to the atrium, determining a leaflet eversion which causes MR: papillary muscle rupture as a complication of an AMI and a flail mitral leaflet. Therefore, in an unstable patient with MR and a mitral leaflet with an abnormal concavity directed to the atrium, a differential diagnosis must be performed. To do so, attention should be focused on *left ventricular wall kinesis*. An akinetic wall could be the consequence of an AMI which might have caused, a few hours from the beginning of the symptoms, the rupture of the papillary muscle. In this case the head of the papillary muscle attached to the mitral leaflet through the chordae tendineae is visible, moving during systole in the left atrium. If the left ventricular kinesis is normal, myocardial infarction can be excluded as the cause of the papillary muscle rupture. In the case of an MR with an abnormal concavity of the leaflet directed to the atrium, the likely diagnosis is flail mitral leaflet. Rupture of chordae tendineae can be difficult to visualize on TTE, and therefore TEE may be necessary to confirm the diagnosis.

Once LVOT obstruction, flail, and papillary muscle rupture have been excluded, another cause of new-onset MR causing hemodynamic instability should be considered, i.e., *infective endocarditis*. This is characterized by the presence of fluctuant vegetation attached to the atrial layer of the mitral valve; it can cause MR by two different mechanisms: perforation or chordal rupture. The origin of the regurgitant jet discriminates between them. In fact, when the jet originates from the leaflet, perforation is the

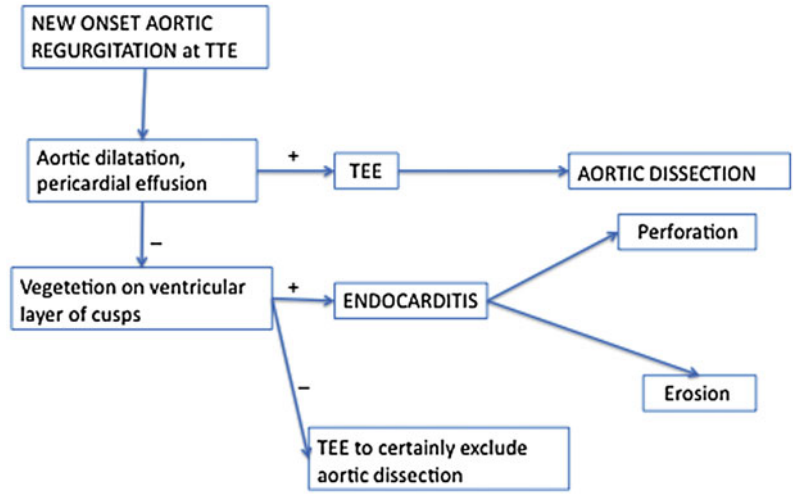

Fig. 40.8 Diagnostic algorithm for aortic regurgitation

culprit mechanism, whereas when the jet originates from the coaptation zone in presence of chordae tendineae protruding in the atrium during systole, it is obviously caused by chordal rupture. The sensitivity of TTE in the diagnosis of endocarditis is about 75 %: when clinical suspicion is high, TEE should be performed.

When an acute MR in an instable patient is diagnosed, the correct mechanism of insufficiency has to be known in order to institute the right treatment. The diagnostic process consists of three steps: (1) look at the LVOT, (2) look at the morphology of the valve, and (3) look for vegetations.

40.5.2 New-Onset AR

AR is characterized on color Doppler imaging by a turbulent diastolic flow from the ascending aorta to the left ventricle through the aortic valve. The cause of new-onset AR may be type A aortic dissection or infective endocarditis (Fig. 40.8).

In the unstable patient with acute AR, *type A aortic dissection must be excluded first* since it is a surgical emergency and, if not treated, it has 50 % mortality in the first 24 h. TTE shows direct signs of dissection of the ascending aorta, such as the visualization of the tear with the true and the false lumen, or signs that are indicative of dissection, such as a dilated ascending aorta or the presence of a pericardial effusion. The sensitivity of TTE in diagnosing ascending aorta dissection is only 70 %, whereas that of TEE reaches 100 %.

Firstly, *look for direct signs of dissection on TTE*, using also the suprajugular view, which allows better visualization of the aortic arch: if there are direct signs of dissection, the heart surgeon must be alerted as soon as possible.

When direct signs of dissection are not present, this is an *indicative sign*. If they are found, one should confirm the diagnosis of dissection by TEE as soon as possible. If neither direct nor suspected signs of dissection are found, one should look for other cause of acute AR, such as endocarditis: this is characterized by a fluctuant vegetation attached to the ventricular layer of aortic cusps. As in MR, endocarditis can cause AR by perforation or erosion.

Because of the high mortality of type A aortic dissection, one must be sure that this diagnosis is excluded in the setting of an acute AR: if it is not possible to understand the cause of an acute AR, it is mandatory to perform TEE in order to increase the sensibility of the examination. If there is high suspicion of a dissection, it is advisable to call the anesthetist and perform the TEE with the patient sedated, in order to avoid dangerous hypertensive peaks which can cause aortic rupture.

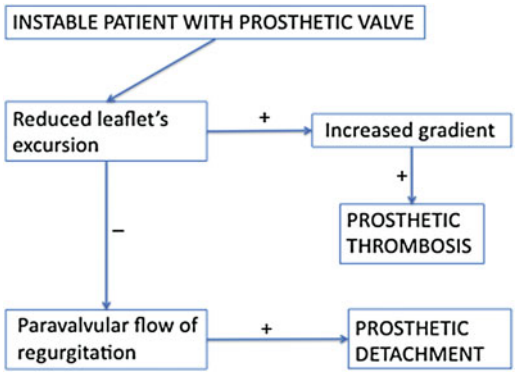

Fig. 40.9 Diagnostic algorithm for prosthetic valve dysfunction

40.5.3 Prosthetic Malfunction

In an unstable patient with a prosthetic *mechanical* valve, two pathologic processes must be excluded: firstly, a *prosthetic thrombosis* and, secondly, a *prosthetic detachment*. In patients with a prosthetic *biological* valve, thrombosis is unlikely; therefore, only *prosthetic detachment* must be excluded (Fig. 40.9).

40.5.3.1 How To Do It

Firstly, consider the mobility of the leaflet by M-mode imaging: if one or both leaflets show a reduced excursion, *prosthetic thrombosis* is likely.

If thrombosis is the causative agent of acute decompensation, an increased gradient on continuous wave Doppler imaging of the prosthetic valve is present. Continuous wave Doppler imaging of the mitral prosthetic valve also allows one to measure the pressure half-time, whose value is increased in prosthetic malfunction: a value higher than 250 ms is highly suggestive of thrombosis. Gradient measurements are more easily obtained by TTE, whereas the direct visualization of thrombosis is more likely visualized by TEE.

If a prosthetic mechanical valve has normal leaflet excursion with a gradient within the normal limits for that specific mechanical valve, or it is a prosthetic biological valve, thrombosis is excluded and one has to consider an *acute detachment*. Detachment can be diagnosed by using color Doppler imaging: it is visualized as a paravalvular turbulent flow of regurgitation. Mitral valve detachment can be missed on TTE because of the difficult visualization of the left atrium due to the presence of the prosthesis. If the suspicion of prosthesis detachment is high, TEE is needed to confirm the diagnosis and to accurately evaluate the extent of the detachment.

Further Reading

Beaulieu Y (2007) Bedside echocardiography in the assessment of the critically ill. Crit Care Med 35(Suppl):S235–250

Price S, Nicol E, Gibson DG, Evans TW (2006) Echocardiography in the critically ill: current and potential roles. Int Care Med 32:48–59

Lester SJ, Wilansky S (2007) Endocarditis and associated complications. Crit Care Med 35(Suppl):S384–391

41 ICU Echocardiography and Noninvasive Hemodynamic Monitoring: The Integrated Approach

Carlo Sorbara and Valeria Salandin

41.1 Left Ventricular–Arterial Coupling

The primary role of the cardiovascular system is to deliver energy sources and oxygen to the tissues. The periphery itself has the ability to autoregulate blood flow to the metabolic activity of any individual organ, but it needs an adequate perfusion pressure and a constant flow in the capillaries. Since the left ventricle functions as a volume phasic pump, the proximal arterial vascular system (the large arteries) acts as a large capacitor with a high output resistance (peripheral arterioles) to convert the pulsatile flow to a constant one, like a hydraulic filter (Fig. 41.1). Thus, optimal cardiovascular function requires appropriate coupling of the left ventricle and the arterial system and good interaction of its components. To fully appreciate the pathophysiology of cardiovascular function, we need a diagnostic and monitoring modality that explains the concept of a pump that generates flow (cardiac output), ejecting phasically in a pressurized compartment. In other words, we need an integrated monitoring modality that represents left ventricular–arterial coupling or the matching of ventricular elastance with arterial elastance. The clinical dilemma in a hypotensive patient with low cardiac output is whether the pump or the circuit is working out of the normal range or whether a combination of both exists.

Functional analysis of this interaction requires that the left ventricle and the arterial system be described in similar terms.

The left ventricle is evaluated best by plotting left ventricular pressure versus volume throughout the cardiac cycle (Fig. 41.2). With every heart beat a full loop is described. Starting at end-diastole, the first part of the loop is the isovolumic contraction. When the aortic valve opens, ejection begins and during the ejection period, the volume decreases and the pressure changes relatively little. After closure of the aortic valve, the isovolumic relaxation follows. When the mitral valve opens, filling starts and the volume increases with a very small increase in left ventricular pressure until the end-diastolic volume (EDV) is reached. The lower right-hand corner of the left ventricular pressure–volume loop is end-diastole, with EDV and end-diastolic pressure; the upper left-hand corner of the left ventricular pressure–volume loop is end-systole, with end-systolic pressure (ESP) and end-systolic volume (ESV). This is the point at which the left ventricle reaches maximal stiffness. The difference between EDV and ESV is the stroke volume (SV), and the ejection fraction (EF) is the relationship between SV and EDV. The area inside the loop is the ventricular effective stroke work (SW), which is the product of volume and pressure. Different loading conditions in different beats determine different SVs, so different ESVs come across different ESPs (Fig. 41.3).

C. Sorbara (✉)
Department of Anesthesia and Intensive Care, Regional Teaching Hospital, Treviso, Italy
e-mail: carlo.sorbara@gmail.com

A. Sarti and F. L. Lorini (eds.), *Echocardiography for Intensivists*,
DOI: 10.1007/978-88-470-2583-7_41, © Springer-Verlag Italia 2012

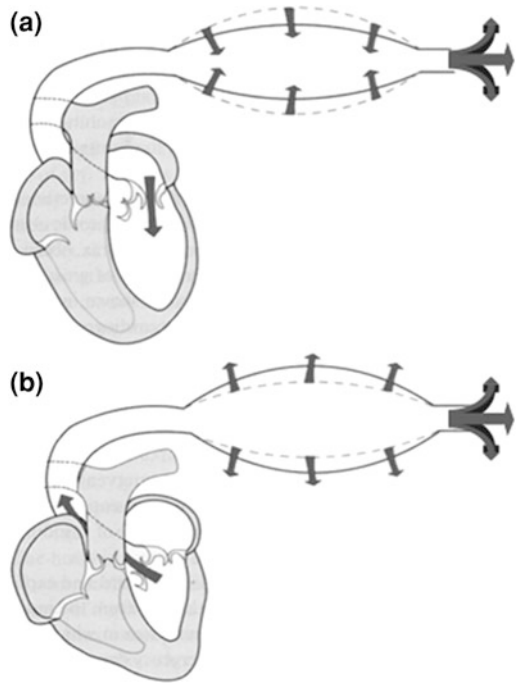

Fig. 41.1 Left ventricular–arterial coupling

Connecting the end-systolic points of variable loaded beats determines the left ventricular ESP–ESV relation (ESPVR) (Fig. 41.4). The points along this line indicate how much the left ventricular ESV will increase (and SV will decrease) in response to an increase of ESP. The slope of this relation expresses the left ventricular end-systolic elastance (E_{ES}). This is a property of the heart linked to the contractility itself, and is very little affected by the loading conditions. The original results suggest a linear ESPVR with an intercept with the volume axis (V_d). The linear relation implies that the slope of the ESPVR, the E_{ES}, with the dimension of pressure over volume (mmHg/ml), can be determined. An increase in contractility, as obtained with epinephrine, shifts the relation to the left and increases E_{ES}, but leaves the intercept volume (V_d) unchanged. ESPVR can be calculated as the ratio between ESP and (ESV − V_d).

On the other side of the aortic valve, the arterial system can be evaluated in an analogous manner [1]. Different SVs determine different expansions of the arterial system with different ESPs (Fig. 41.5): the higher the SV, the greater the arterial ESP, depending on compliance and resistance of the arterial tree (arterial mechanical properties). In this analysis, the arterial system is described by the relation between the SV and ESP. The slope of this relation expresses the effective arterial end-systolic elastance (E_A); then E_A can be calculated as the ratio of ESP to SV.

E_{ES} (ventricular function) indicates the variations of left ventricular ESV (and indirectly the variations of SV) in response to the variation of ESP (arterial pressure) [ESP/(ESV − V_d)], and E_A (arterial mechanical properties) indicates the variation of arterial pressure (ESP) in response to the variation of SV (ESP/SV).

The intersection of the E_{ES} slope (which represents ventricular function) and the E_A slope (which represents arterial mechanical properties) is the "coupling point" (Fig. 41.6) and expresses the concept of the left ventricular–arterial coupling (E_A/E_{ES} ratio): this coupling point is, from a hemodynamic point of view, the ESP (arterial pressure) when the aortic valve has just closed and the total amount of the corresponding SV at the end of ejection phase has been ejected in the arterial tree.

Thus, the SV, the SW, and the ESP (arterial pressure) are dependent beat-to-beat on the balance between E_{ES} (describing the left ventricle) and E_A (describing the arterial system) and their corresponding slopes: different E_A/E_{ES} and different slopes determine different ESP (arterial pressure), different SV, and different SW (Figs. 41.7, 41.8, 41.9).

It has been suggested that this E_A/E_{ES} ratio is the left ventricular–arterial coupling parameter and that when $E_A/E_{ES} = 1$, that is, when the E_A slope is equal to the E_{ES} slope, the external work (mechanical work) is optimized (Fig. 41.10), whereas for $E_A/E_{ES} = 0.5$, that is, the E_A slope is lower than the E_{ES} slope, cardiac efficiency is maximal (Fig. 41.11).

To determine these two parameters, several monitoring simplifications have been used in clinical practice.

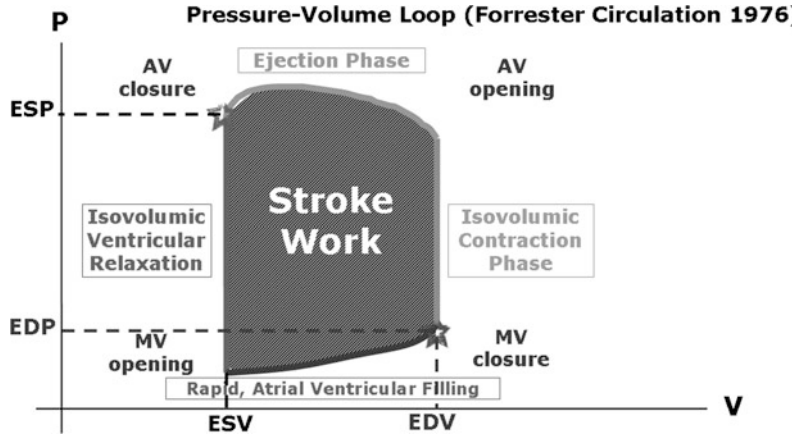

Fig. 41.2 Cardiovascular physiology: the pump. *AV* aortic valve, *EDP* end-diastolic pressure, *EDV* end-diastolic volume, *ESP* end-systolic pressure, *ESV* end-systolic volume, *MV* mitral valve

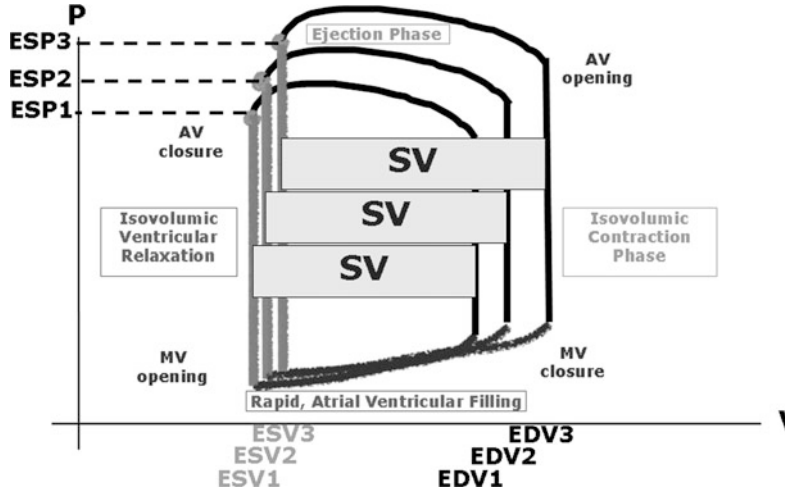

Fig. 41.3 Cardiovascular physiology: the pump. *SV* stroke volume

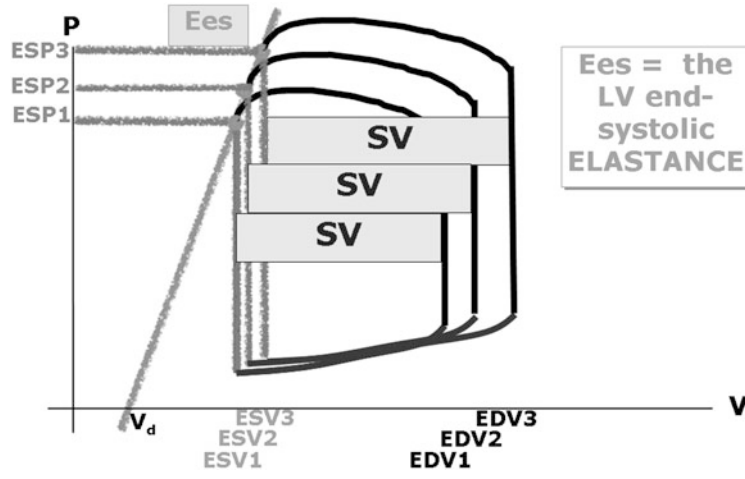

Fig. 41.4 Cardiovascular physiology: the pump. *LV* left ventricular

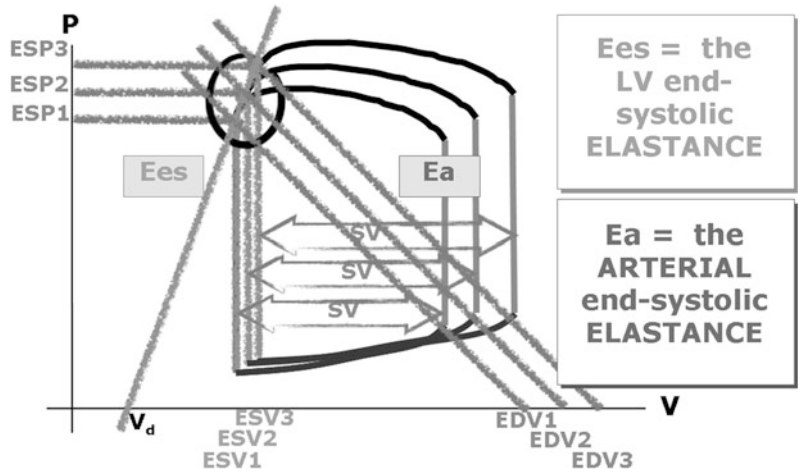

Fig. 41.5 Cardiovascular physiology: the pump

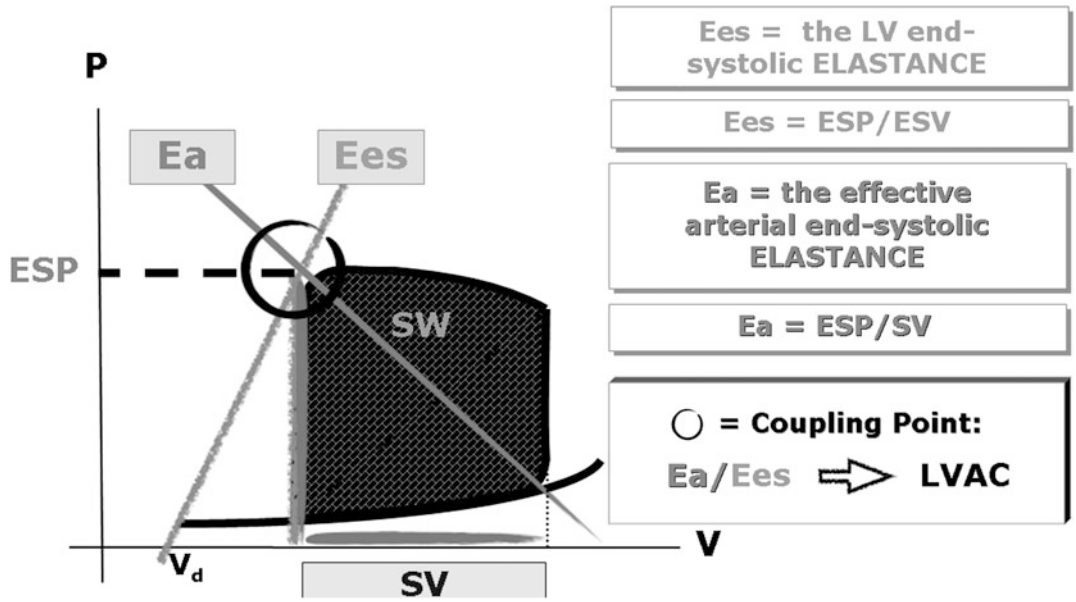

Fig. 41.6 Left ventricular–arterial coupling (*LVAC*). *SW* stroke work

The arterial elastance (E_A) can be approximated as follows. ESP is close to the mean arterial pressure (Fig. 41.12), and SV can be obtained through echocardiography (2D, 3D) or through continuous cardiac output with noninvasive hemodynamic monitoring systems (pulse contour methods). We can calculate E_A = ESP/SV ≈ (beat-to-beat) P_{mean}/cardiac output/heart rate.

The left ventricular end-systolic elastance (E_{ES}) is calculated from E_{ES} = ESP/(ESV − V_d). V_d (the intercept volume) is the volume of the heart at which the left ventricular ESPVR intercepts the *x*-axis (ideally the volume of the heart at zero ESP) (Fig. 41.13). ESV can normally be measured noninvasively by echocardiography (2D, 3D), but V_d is hard to estimate. To derive this intercept volume, at least one other point of the

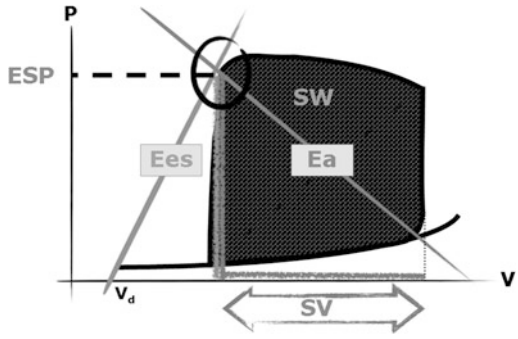

Fig. 41.7 Left ventricular–arterial coupling and stroke volume, stroke work, and arterial pressure

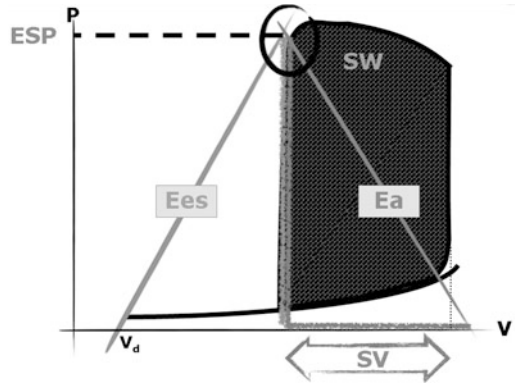

Fig. 41.8 Left ventricular–arterial coupling and stroke volume, stroke work, and arterial pressure

ESPVR should be obtained. This would require changes in diastolic filling that are often not feasible in very sick patients. In a number of studies, it has simply been assumed that $V_d = 0$.

This assumption leads to a very interesting simplification of the analysis (Fig. 41.14). With $V_d = 0$, $E_{ES} = ESP/ESV = ESP/(EDV - SV)$. The E_A/E_{ES} ratio then becomes $E_A/E_{ES} = (ESP/SV)/[ESP/(EDV - SV)] = (EDV - SV)/SV = ESV/SV = (1/EF) - 1$.

It is important to underline that the ESP disappears altogether, leaving only the determination of two volumes, the ESV "inside the heart" and the SV, or the EF. This implies that the mechanical work is maximal when $E_A/E_{ES} = 1$ and EF = 0.5, or when ESV and SV are equivalent. Similarly, the cardiac efficiency is maximal when $E_A/E_{ES} = 0.5$ and EF = 0.67, or when SV is greater than ESV. In contrast, when

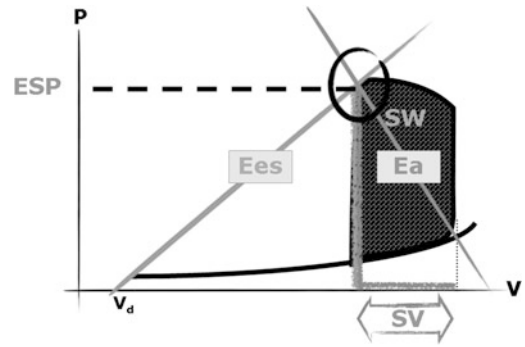

Fig. 41.9 Left ventricular–arterial coupling and stroke volume, stroke work, and arterial pressure

E_A exceeds E_{ES}, that is, when $E_A/E_{ES} > 1$, EF falls, and ESV is greater than SV.

In patients with systolic heart failure, E_{ES} is reduced and peripheral vascular resistance (and thus E_A) is increased. In this situation, the left ventricle and the arterial system are suboptimally coupled ($E_A/E_{ES} > 1$). Any increase in heart rate will further increase E_A, making the coupling worse. Vasodilator therapy, which lowers E_A, will bring the E_A/E_{ES} ratio back down toward 1.0, improving the coupling. Alternatively, or contemporarily, inotropic therapy, which increases E_{ES}, will also improve the E_A/E_{ES} ratio. Thus, in a patient with a failing heart, the left ventricle and the arterial system are inappropriately coupled, further reducing the heart's mechanical work and efficiency. The coupling and performance in systolic heart failure can be improved by vasodilator and/or inotropic therapy and can be monitored by the E_A/E_{ES} ratio by an integrated monitoring, echocardiography and noninvasive hemodynamic monitoring (pulse contour methods).

The assumption of a negligible V_d simplifies matters. However, negligible V_d values are difficult to verify, mostly not correct, and certainly lead to possible large errors in the very sick patient (dilated cardiomyopathy).

There are multiple potential sources of error in the noninvasive assessment of left ventricular–arterial coupling. However, this integrated monitoring approach (ESP, SV, ESV) gives appropriate attention to the concept of left ventricular–arterial coupling and it demonstrates the feasibility of monitoring the E_A/E_{ES} ratio throughout the

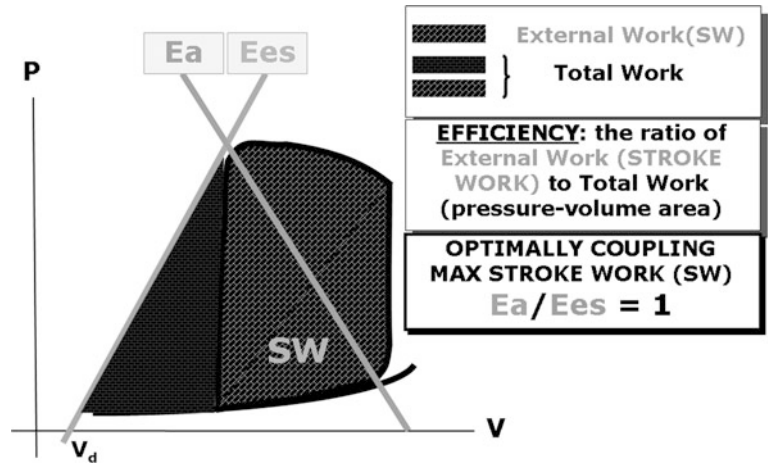

Fig. 41.10 Left ventricular–arterial coupling and maximum work and maximum efficiency

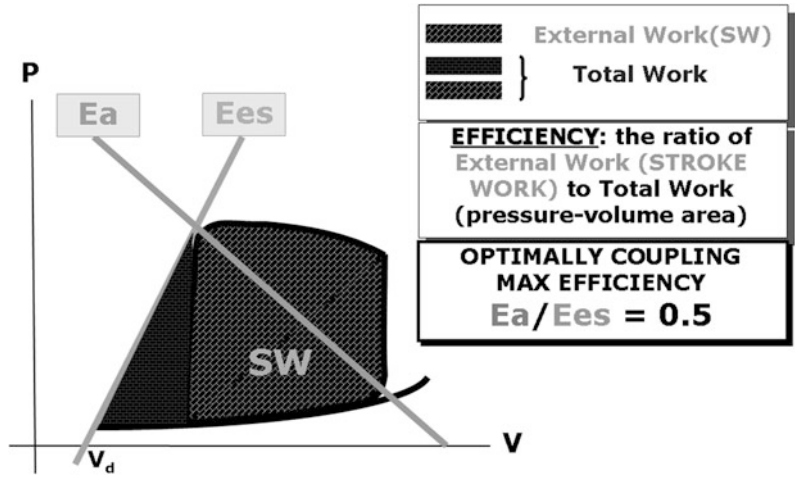

Fig. 41.11 Left ventricular–arterial coupling and maximum work and maximum efficiency

noninvasive echocardiographic assessment. Although not ready for routine use in the echocardiographic laboratory or in cardiac intensive care, this area certainly deserves further investigation and may ultimately improve our pathophysiologic understanding of cardiac disorders. Further studies may focus on assessing the effect of pharmacologic intervention on left ventricular–arterial coupling (improved E_{ES} and/or reduced E_A), on left ventricular function, on arterial compliance, and on left ventricular remodeling, thus leading to a correct prognostic evaluation.

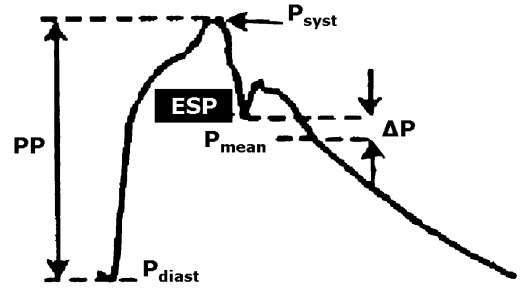

Fig. 41.12 End-systolic pressure

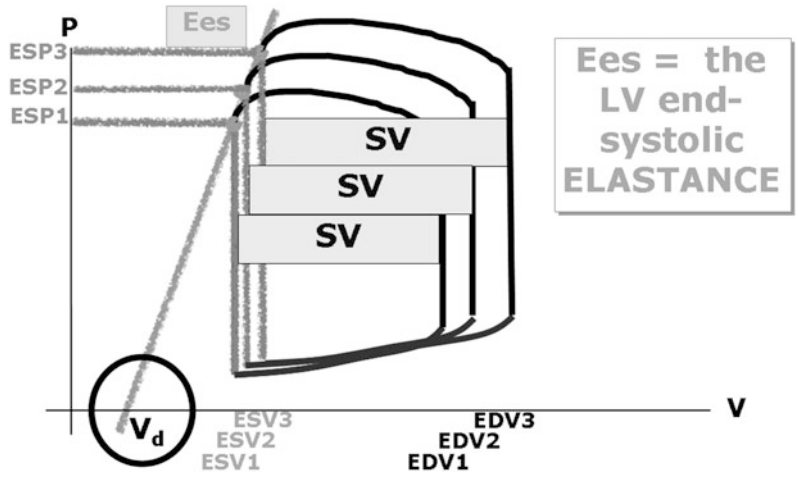

Fig. 41.13 Cardiovascular physiology: the pump

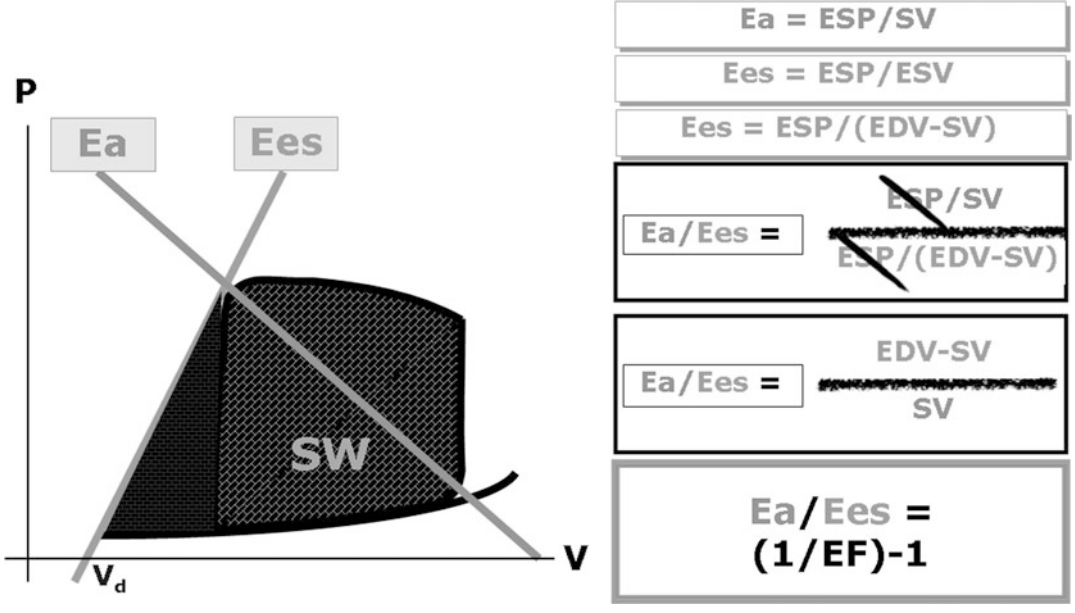

Fig. 41.14 Left ventricular–arterial coupling and ejection fraction

Reference

1. Sunagawa K, Maughan WL, Sagawa K (1985) Optimal arterial resistance for the maximal stroke work studied in isolated canine left ventricle. Circ Res 56:586–595

Further Reading

Antonini-Canterin F, Enache R, Popescu BA, Popescu AC, Ginghina C, Leiballi E et al (2009) Prognostic value of ventricular–arterial coupling and B-type natriuretic peptide in patients after myocardial infarction. A five-year follow-up study. J Am Soc Echocardiogr 22:1239–1245

Binkley PF, Van Fossen DB, Nunziata E, Unverferth DV, Leier CV (1990) Influence of positive inotropic therapy on pulsatile hydraulic load and ventricular–vascular coupling in congestive heart failure. J Am Coll Cardiol 15:1127–1135

Borlaug BA, Kass DA (2008) Ventriculo-vascular interaction in heart failure. Heart Fail Clin 4:23–26

Chen CH, Fetics B, Nevo E, Rochitte CE, Chiou KR, Ding PYA et al (2001) Non-invasive single-beat determination of left ventricular end-systolic elastance in humans. J Am Coll Cardiol 38: 2028–2034

Hettrick DA, Warltier DC (1995) Ventriculoarterial coupling. In: Warltier DC (ed) Ventricular function. Williams & Wilkins, Baltimore, pp 153–179

Little WC, Cheng CP (1991) Left ventricular–arterial coupling in conscious dogs. Am J Physiol 261:H70–H76

Ohte N, Cheng CP, Little WC (2003) Tachycardia exacerbates abnormal left ventricular–arterial coupling left ventricular–arterial coupling in heart failure. Heart Vessels 18:136–141

Saba PS, Roman MJ, Ganau A, Pini R, Jones EC, Pickering TG, Devereux RB (1995) Relationship of effective arterial elastance to demographic and arterial characteristics in normotensive and hypertensive adults. J Hypertension 13:971–977

Part V

Ultrasound in the ICU: Other Applications

Echocardiography and Advanced Life Support

42

Simone Cipani, Silvia Marchiani, and Armando Sarti

Focused ultrasonography has emerged as a useful diagnostic tool for a variety of life-threatening conditions in the emergency setting. As the intensivist is faced with periarrest conditions, rapid and safe interpretation of the clinical picture may improve patient outcome.

Physical examination has been shown to be unreliable in differentiating hypovolemic from cardiogenic causes of hypotension. Faced with a patient with hemodynamic instability and hypotension, what kind of information is obtainable with a quick ultrasonography scan?

- A quick scan with the apical four-chamber view may show significant reduction of systolic and diastolic volumes of the left ventricle (kissing ventricle) and a reduced size of all the other cavities with limited opening of valvular structures. With the subcostal window, a reduced diameter (less than 1 cm) of the inferior vena cava together with total inspiratory collapse allows us to confirm the diagnosis of *hypovolemia*, justifying an aggressive immediate fluid resuscitation.
- The diagnosis of *tamponade* is clinical (jugular turgor, hypotension to cardiac arrest, tachycardia, tachypnea, pulsus paradoxus), but the ultrasonographic assessment may greatly help to establish the right diagnosis and confirm this suspicion in the presence of hemodynamic instability. The echocardiographic findings are essentially pericardial effusion, interference with diastolic filling and compression of the right sections resulting in decreased cardiac output, and marked respiratory excursions in Doppler right-sided heart preload and ejection. Moreover, ultrasound-guided pericardial drainage is much safer than any blind technique.
- The quick ultrasonographic assessment may document significant dilatation of the right side of the heart. This imaging assumes a high probability of pulmonary embolism in the absence of significant valvular disease or previous ventricular or pulmonary diseases. *Acute cor pulmonale* ensues as more than two thirds of the pulmonary arterial bed is blocked because of an embolus. The diagnosis of thromboembolism has clear therapeutic implications (immediate thombolysis).
- *Coronary heart disease and myocardial infarction* are the major causes of cardiac arrest by malignant ventricular arrhythmia or severe acute ventricular dysfunction. In this circumstance, echocardiography can detect wall motion abnormalities that may be linked to previous or acute myocardial ischemia. Although these wall motion alterations do not have high specificity for coronary heart disease, they may ultimately lead to urgent cardiovascular support (aortic counterpulsation, rapid revascularization).
- The ultrasonographic assessment of the lung may be characterized by the absence of pleural

A. Sarti (✉)
Department of Anesthesia and Intensive Care,
Santa Maria Nuova Hospital, Florence, Italy
e-mail: armando.sarti@asf.toscana.it

A. Sarti and F. L. Lorini (eds.), *Echocardiography for Intensivists*,
DOI: 10.1007/978-88-470-2583-7_42, © Springer-Verlag Italia 2012

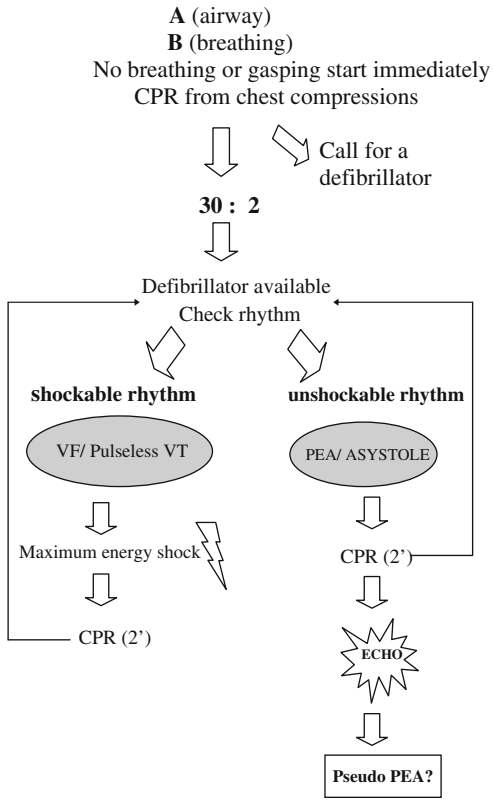

Fig. 42.1 Ultrasonographic assessment during advanced life support

"sliding" and B lines at the intercostal spaces on the mid-clavicular line. This diagnosis of *tension pneumothorax* is characterized by the presence of a"lung point" on the echocardiographic scan and severe hemodynamic instability due to intrathoracic high-pressure regimes. Immediate ultrasound-guided pleural drainage is mandatory to restore cardiopulmonary stability.

42.1 Pseudo Periarrest and True Periarrest

The complete absence of motion of the heart, visible only with echocardiography, allows us to identify *true periarrest* in a patient with no central arterial pulse (Fig. 42.1). This diagnosis implies immediate administration of vasoactive drugs (epinephrine) while maintaining basic life support and searching for the underlying causes.

Pseudo periarrest is defined as the presence of residual wall motion with no central pulse. This is often due to severe cardiogenic shock and pump failure. This echo pattern is more likely to be restored to that for spontaneous circulation compared with true periarrest. Thus, aggressive searching for and removal of the causes is paramount. It has been proposed to assess the Doppler flow velocity within the internal carotid artery by vascular ultrasound investigation during cardiopulmonary resuscitation. A telediastolic flow velocity of more than 20 cm/s seems to ensure adequate cerebral perfusion values during resuscitation.

Further Reading

Haas MM, Haas J, Allendorfer J, Allendorfer F, Walcher F et al (2010) Focused examination of cerebral blood flow in peri-resuscitation: a new advanced life support compliant concept-an extension of the focused echocardiography evaluation in life support examination. Crit Ultrasound J 2:1–12

Hayhurst CC, Lebus C, Atkinson PR et al (2011) An evaluation of echo on life support: Is it feasible? What does it add? Emerg Med J 28:119–121

Hernandez CC, Shuler K et al (2008) CAUSE: cardiac arrest ultrasound exam, a better approach to managing patients in primary non–arrhytmogenic cardiac arrest. Resuscitation 76:198–206

Nolan JP, Soar J, Zideman DA et al (2010) European Resuscitation Council Guidelines for Resuscitation 2010. Executive Summary. Resuscitation 81: 1219–1276

Price S, Uddin S, Uddin T et al (2010) Echocardiography in cardiac arrest Echocardiography in pacemakers arrest. Curr Opin Crit Care 16:211–215

Central and Peripheral Vein Cannulation

43

Antonio Franco, Cecilia Pelagatti, and Laura Pera

43.1 Introduction

The recommendations of the US Agency for Healthcare Research and Quality, the US Center for Disease Control and Prevention (CDC), and the UK's National Institute for Clinical Excellence have established ultrasound guidance as the current state of the art for the placement of central vascular access devices.

Unfortunately, even when performed by experienced operators, this procedure had always been burdened with a certain incidence of complications, primarily pneumothorax and arterial puncture: it was therefore necessary to seek a safer alternative to the "blind" method, and the application of ultrasonography came naturally.

The ultrasound-assisted" technique is not the same as the "ultrasound-guided" technique. In the former, a sonographic survey is performed in the region where the venipuncture will be made. In the latter, the advancement of the needle and its penetration into the vessel chosen are observed step by step. It is therefore clear that the ultrasound-guided technique is preferable in order to minimize complications and achieve the best results. However, it is also true that the mere fact of having a scanner in their hands can generate a false feeling of confidence in beginners; in fact, cautious climbing of the learning curve is essential to master the technique. On the other hand, no international scientific society has so far issued reference guidelines on ultrasonography for the placement of venous catheters, and only expert opinions and general advices are available on this ultrasound technique.

The choice of the central vessel is traditionally between the internal jugular vein (IJV) (Fig. 43.1) and the subclavian vein (SV) (Fig. 43.2) on both sides. The femoral vein is frequently used, but it is not really considered a central vessel because it does not allow central venous pressure monitoring or mixed venous blood sampling; moreover, it tends to suffer from unacceptable infection rates.

43.2 Procedure

Patients should receive clear and comprehensive oral and written information on the risks/benefits of catheters, and explanations for catheter care. Signed consent should be obtained prior to insertion of a catheter. It is generally accepted that the platelet count should be greater than 50×10^3/l prior to insertion of a catheter other than a peripherally inserted central catheter (PICC), and the international normalized ratio, INR, should be less than 1.5.

A. Franco (✉)
Department of Anesthesia and Intensive Care, Santa Maria Nuova Hospital, Florence, Italy
e-mail: antonio.franco@asf.toscana.it

A. Sarti and F. L. Lorini (eds.), *Echocardiography for Intensivists*,
DOI: 10.1007/978-88-470-2583-7_43,

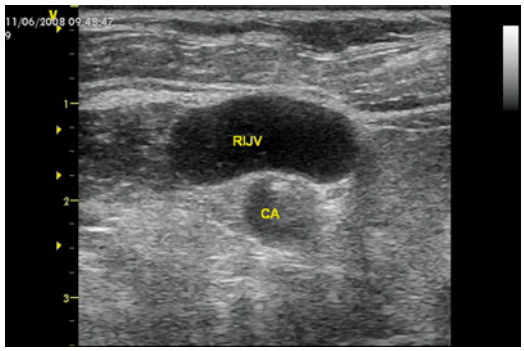

Fig. 43.1 Right internal jugular vein (*RIJV*) overlapping the carotid artery (*CA*). (From Sarti [1] with permission)

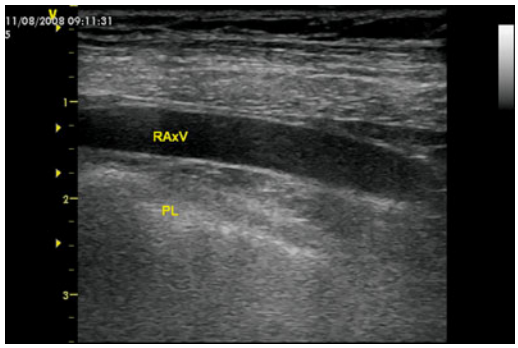

Fig. 43.2 Right axillary vein (*RAxV*) in the long axis and a little lower the pleural line (*PL*). (From Sarti [1] with permission)

A preliminary bilateral ultrasound study must be performed to compare the size of the vessels and detect thrombosis or anatomical variations. This is when ultrasonography best displays its value, as inappropriate access can be ruled out before starting the procedure. The soft tissue linear probe is the best for this technique; it should not be too long (2–5 cm), and should be used at a 7.5–13-MHz frequency, because the structures to be examined are at a depth ranging from 1–2 cm for the IJV up to 3–4 cm for the SV.

The ergonomic positioning of the operator, probe, and screen with regard to the patient (Table 43.1) is of the utmost importance. The screen must be positioned in front, and not to the side, of the operator. To facilitate the cannulation of the vessel, the probe must be held with the nondominant hand. It must be positioned with the benchmark (usually located on the left side of the screen) on the same side as the operator so that the needle can be seen moving on the screen normally, and the operator is spared complex mental reasoning.

Compression with the probe helps distinguish a vein from other structures: under pressure, a vein will disappear, whereas an artery's pulsation will be enhanced, and another structure will remain unchanged.

Another major issue is sterility: in compliance with CDC guidelines, the operator must perform surgical hand washing and use maximal sterile barriers (cap, mask, gown, and sterile gloves). After disinfection with 2 % chlorhexidine in isopropyl alcohol, the operative field is surrounded with sterile drapes. The ultrasound probe must be covered with a sterile sheath, which may just be a glove with jelly both inside and outside. Obviously, jelly applied outside should be sterile and may be replaced by sterile Vaseline normally used for urethral catheters. The air bubbles trapped between the probe and the jelly must absolutely be removed.

For central venous cannulation, the view to be achieved on screen is that of the needle advancing through the structures and penetrating into the chosen vein (Fig. 43.3). This is accomplished by aligning the needle with the probe along the long axis (usually this appears as a hyperechoic line), and the vessel may be visualized as a hypoechoic circle along the transverse axis (short axis). Vein puncture is also possible by using the transverse vein and needle axes (short axis–short axis): this is, however, not recommended where there are structures that must be avoided, such as the pleura and carotid artery, because the ultrasound beam covers a small area of tissue, and in the short axis it shows the needle as a dot, and the vessel as a small circle. This mode of vision (short axis–short axis) is recommended for peripheral venous cannulation (including PICC or midline) where viewing a larger area transversally is more useful.

A major problem for beginners is how to keep the needle within the ultrasound beam, which is only 1 mm at its origin and then spreads to become a cone. Therefore, even a small tilting or

Table 43.1 How to position the probe and the screen with regard to the patient

Vein	Operator position	Screen position	Probe position
Right IJV	Behind the patient's head on the right	On the patient's left side	The probe must always be aligned with its reference on the same side as the screen reference
Left IJV	Behind the patient's head on the left	On the patient's right side	
Right SV	On the patient's right side	Next to the patient's head to the left	
Left SV	On the patient's left side	Next to the patient's head to the right	

IJV internal jugular vein, *SV* subclavian vein

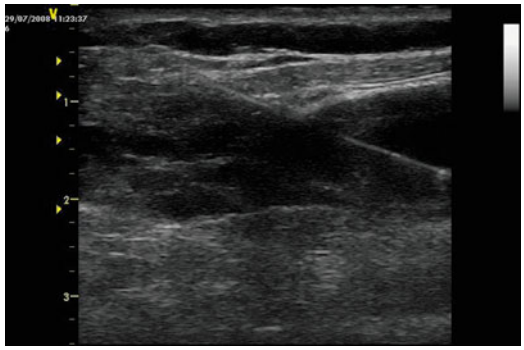

Fig. 43.3 Needle into the vein with a "curtain" sign. (From Sarti [1] with permission)

swinging of the probe is enough to lose the best view of the needle advancing.

In the opinion of most authors, the vein of choice for the placement of a central venous catheter is the right IJV, because of its superficial position (it is usually 1 cm deep), larger size, and direct continuity with the superior vena cava.

Using ultrasonography for venous cannulation requires a "Copernican revolution" in terms of approach: no more bony landmarks but muscular structures, very little imagination, and as much direct vision as possible. The best approach to the IJV to be used under ultrasound guidance is the technique described by Jernigan and modified by Pittiruti: a low approach, almost tangent to the clavicle, and made safe by direct vision. It allows excellent dressing for subsequent management, with patient comfort comparable to that with placement in the SV.

The patient lies supine, with the face turned in the direction opposite the side of the procedure. The puncture is performed behind the clavicular head of the sternocleidomastoid muscle with an angle of less than 90° to the vessel, with the needle sliding under this muscle to find the IJV in the space between the sternal and clavicular heads. On the ultrasound machine screen, the needle is visualized through the various planes until it reaches the target, where it pushes the vein's intimal wall inward toward the lumen ("curtain sign") and then punctures it (Fig. 43.3). Blood return should then be obtained in the syringe connected to the needle. After this, to facilitate the insertion of the guide wire, the needle is moved with great caution and under ultrasound vision toward the vein's major axis. The rest of the procedure is the same as the traditional technique, with the insertion of the guide wire, followed by the dilator and then the catheter. In our series, this technique has virtually eliminated the risk of pneumothorax, although there were a few cases of arterial puncture. These can be avoided by stricter control of the needle tip progression, achieved with more echogenic needles, or by letting some air in the needle during its progression, in order to increase the ultrasound contrast with surrounding tissues.

A collapsed vein in dehydrated patients, or variable vein lumen due to breathing, can make venipuncture very difficult even with ultrasonography. Such cases vividly show how risky these maneuvers are when performed blindly.

Even SV cannulation, which is still the first choice for many anesthesiologists, can be improved with ultrasonography. Although the clavicle prevents the transmission of ultrasound, the SV can be visualized in the infraclavicular area, where it is called axillary vein (AV), and is

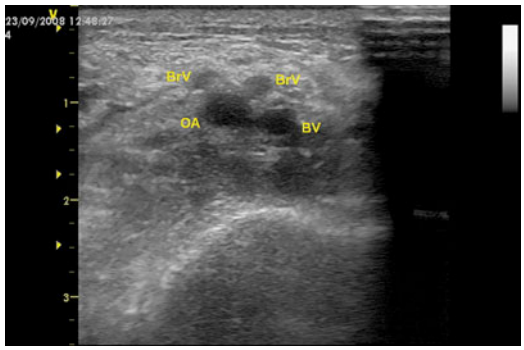

Fig. 43.4 Arm veins and brachial artery with a Mickey Mouse shape. *OA* brachial artery, *BV* basilic vein, *BrV* brachial vein. (From Sarti [1] with permission)

relatively shallow (about 2–2.5 cm) and can be easily cannulated with ultrasonography, preferably in the long axis–long axis modality. The AV remains a second choice versus the IJV because it is smaller, deeper, and closer to the pleural cupola.

At the end of the procedure, ultrasonography can also be used to confirm the absence of pneumothorax by positioning the beam longitudinally in the anterior region of the thorax and looking for the sliding sign. The pleural line is a fundamental sign in chest echography; it is located deeply under rib shadows and is visualized as an echogenic line. It glides with an apparently single movement that is related to lung excursion during breathing (gliding or sliding sign). The gliding sign disappears in the presence of pneumothorax.

43.2.1 Peripheral Cannulation

Ultrasound is also used to place a PICC. In classic sonographic anatomy of the arm veins above the elbow, the centrally located brachial artery, with its two satellite brachial veins, looks like a Mickey Mouse face (Fig. 43.4). The basilic Vein is located a few centimeters medially, whereas the cephalic vein (CV) is located laterally. Usually the best vein is the basilic vein, because it is larger, empties directly into the AV without valves, and has no structures at risk in its proximity. The brachial veins are the second choice, and the cephalic vein is the third choice because of its more complex anatomical configuration where it empties into the AV; it is often used in obese patients.

The most advanced venipuncture kits currently available on the market include a microintroducer, a 22G echogenic needle to minimize endothelial injury and reduce thrombotic complications, a guide wire and a peel-away dilator. The catheter is cut to the right size (matching the distance from the venipuncture site to the third intercostal space on the right hemiclavicular line) and is inserted into the dilator.

At the end of the procedure, ultrasonography is also useful to confirm that the catheter has not gone up in the ipsilateral IJV or in the contralateral SV.

43.2.2 Arterial Cannulation

More recently, ultrasound guidance has been proposed for arterial cannulation too. Undoubtedly ultrasonography helps to obtain the desired result in a higher percentage of cases and contributes to achieving cannulation with fewer attempts. Moreover, ultrasonography can be useful to achieve a better result when blind cannulation cannot be performed because of lack of pulsatility due to calcifications or plaques on the intimal wall of the vessel.

Reference

1. Sarti A (2009) Ecocardiografia per l'intensivista. Springer, Milan

Further Reading

Centers for Disease Control and Prevention (2002) Guidelines for the prevention of intravascular catheter related infections. MMWR Morb Mortal Wkly Rep 51:RR10

Chapman GA, Johnson D, Bodenham AR (2006) Visualisation of needle position using ultrasonography. Anaesthesia 61:148–158

Fry WR, Clagen GC, O'Rourke PT (1999) Ultrasound guided central venous access. Arch Surg 134:738–741

Karakitsos D, Labropoulos N, De Groot E et al (2006) Real-time ultrasound-guided catheterisation of the internal jugular vein. Crit Care 10:R162

Maecken T, Grau T (2007) Ultrasound imaging in vascular access. Crit Care Med 35:178–185

McGee DC, Gould MK (2003) Preventing complication of central venous catheterization. N Engl J Med 348:1123–1133

Modeliar SS, Severe MA, de Cagny B et al (2008) Ultrasound evaluation of central veins in the intensive care unit. Int Care Med 34:333–338

National Institute for Clinical Excellence (2002) Guidance on the ultrasound locating devices for central venous catheters. NICE technology appraisal, no. 49. National Institute for Clinical Excellence, London

Pittiruti M, Malerba M, Carriero C et al (2000) Which is the easiest and safest technique for central venous access? A retrospective survey of more than 5,400 cases. J Vasc Access 1(3):100–107

Sharma A, Bodenham AR, Mallick A (2004) Ultrasound-guided infraclavicular axillary vein cannulation for central venous access. Br J Anaesth 93:188–192

Shiloh AL, Savel RH, Paulin LM, Eisen LA (2011) Ultrasound-guided catheterization of the radial artery: a systematic review and meta-analysis of randomized controlled trials. Chest 139:524–529

Essential Ultrasonography for Venous Thrombosis

44

Federica Marini, Paola Pieraccioni, and Armando Sarti

44.1 Essential Ultrasonography for Venous Thrombosis

Point-of-care ultrasonography performed at the bedside by critical care physicians is easy and immediate. Mechanical ventilation, sedation, paralysis, surgical procedures, malignancies, central venous catheters, and prolonged hospital stay have all been shown to increase the risk of venous thrombosis in the ICU.

44.2 Lower Extremity Deep Venous Thrombosis

Lower extremity deep venous thrombosis (DVT) is a major national health problem, with an overall age- and gender-adjusted incidence of more than one case per 1,000 people annually. Because the incidence is so high and the progression from DVT to pulmonary embolism can lead to significant morbidity and mortality, the ability to rule in or rule out DVT in the emergency department and the ICU is paramount.

DVT is a common, serious, often underrecognized diagnosis in the critically ill patient. Factors that have been recorded to predict an increased risk of ICU-related venous thromboembolism include the following: increased age, previous venous thromboembolism, sepsis, heart failure, malignancy, major trauma, prolonged pre-ICU hospital stay, mechanical ventilation, use of paralytic drugs, high Acute Physiology, Age, and Chronic Health Evaluation (APACHE) score, need for emergency surgical procedures, insertion of a femoral venous catheter, and failure to use thromboprophylaxis. The importance of any of these clinical risk factors is not completely determined, nor is the role of inherited or acquired coagulation system abnormalities.

Focused ultrasonography is a sensitive and specific tool for the assessment of a patient at risk of DVT. The probe of choice to perform the examination is a 5–10-MHz linear probe. Two sonographic findings are diagnostic of a venous thrombosis:

- Noncompressibility of the venous segment.
- Echogenic intraluminal material.

44.3 Compression Strategy

Two methods are commonly used—compression and duplex:

- Compression ultrasonography works by the principle that normal veins collapse when extrinsic pressure is applied by the sonographer. Using B-mode 2-D imaging and a high-frequency linear transducer, the examiner locates the vessel of interest and performs a

F. Marini (✉)
Department of Anesthesia and Intensive Care, Santa Maria Nuova Hospital, Florence, Italy
e-mail: federica.marini@asf.toscana.it

A. Sarti and F. L. Lorini (eds.), *Echocardiography for Intensivists*,
DOI: 10.1007/978-88-470-2583-7_44, © Springer-Verlag Italia 2012

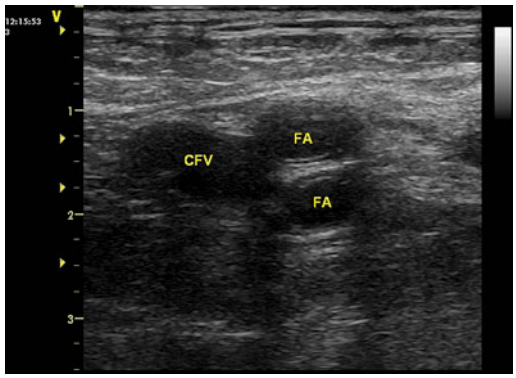

Fig. 44.1 The image shows the common femoral vein (CFV) and the superficial and deep femoral artery (FA) medially

compression maneuver using a transverse plane. Considering the adjacent artery as a reference point, full compression of the vein with minimal deformation of the artery indicates absence of thrombus. If a vein is compressible, the walls of the vessel will join together under direct probe pressure, resulting in the disappearance of the vessel lumen (Fig. 44.1).

- Duplex and triplex ultrasonography combine compression ultrasonography with pulsed wave Doppler imaging (duplex) and both pulsed wave and color Doppler imaging (triplex).

44.4 Intraluminal Material

Most acute thrombi are hypoechoic and not well visualized. If a thrombus is identified within the vessel lumen, a compression maneuver is not necessary and may even be harmful as excessive compression may dislodge the thrombus (Fig. 44.2).

The femoral and popliteal veins should be imaged to the fullest extent possible, and images should be recorded at each of the following levels:

- Common femoral vein.
- Junction of the common femoral vein with the great saphenous vein.
- Proximal deep and superficial femoral vein.
- Proximal, mid, and distal femoral vein.

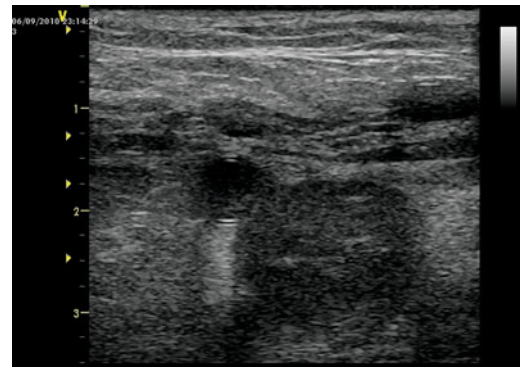

Fig. 44.2 Common femoral vein with a thrombus inside

- Popliteal vein: the patient's leg should be positioned at a 45° flexion angle at the knee and the transducer is placed in the popliteal fossa.

44.5 Venous Thrombosis of the Upper Extremities

Approximately 10 % of all cases of venous thrombosis involve the upper extremities, resulting in an annual incidence of 0.4 cases to one case per 10,000 people. The incidence is increased owing to the routine use of central venous catheters and possible cardiac pacemakers and defibrillators.

Axillary and subclavian veins are often involved. A secondary form, such as catheter-associated thrombosis, cancer-associated thrombosis, surgery or trauma of the arm or shoulder, pregnancy, use of oral contraceptives, and ovarian hyperstimulation syndrome, is more common than a primary form (e.g., venous thoracic outlet syndrome).

Symptoms of DVT of an upper extremity include discomfort, pain, paresthesias, and weakness of the arm.

Upper extremity evaluation consists of assessment of subclavian, innominate, jugular, and axillary veins. Duplex Doppler or color Doppler techniques are used to assess venous compressibility, wall thickening, spontaneous venous flow, cardiac and respiratory phasicity of flow, and venous filling defects.

Compression ultrasonography, which relies on the finding that a thrombosed vein cannot be compressed, is the preferred imaging test also for patients with suspected DVT of the upper extremities. However, the proximal subclavian and brachiocephalic veins are difficult to visualize because of overlying bony structures. When a proximal subclavian or brachiocephalic thrombosis is suspected, duplex ultrasonography of distal arm veins may reveal an abnormal Doppler pattern with reduced variability or no variability in flow velocity during a Valsalva maneuver.

Complications of DVT, which are less common in the upper extremities than in the lower extremities, include pulmonary embolism , recurrence at 12 months, and postthrombotic syndrome. Thrombosis of the axillary and subclavian veins and residual thrombosis at 6 months are associated with an increased risk of postthrombotic syndrome; the risk is lower for catheter-associated thrombosis as the catheter has been removed under appropriate anticoagulant treatment.

Vascular ultrasonography is rapid, repeatable, and easy to perform at the bedside. The learning curve for the intensivist is steep and rapid. Doppler ultrasonography is currently the gold standard for the diagnosis of venous thrombosis in the emergency department and ICU settings.

Further Reading

Di Bello C, Koenig S (2010) Diagnosis of deep venous thrombosis by critical care physicians using compression ultrasonography. Open Crit Care Med J 3:43–47

Fields M, Munish G (2008) Venothromboembolism. Emerg Med Clin N Am 26:649–683

Geerts W, Selby R (2003) Prevention of venous thromboembolism in the ICU. Chest 124:357S–363S

Kucher N (2011) Deep-vein thrombosis of the upper extremities. N Engl J Med 364:861–869

Lung and Pleural Ultrasonography in Emergency and Intensive Care

45

Gino Soldati

45.1 Introduction

Pleuropulmonary echography is a non-invasive diagnostic technique of great interest and value in the emergency department and in the intensive care unit. Its advantage is that of being able to show both anatomic and functional parameters and give categorical (yes/no) answers to diagnostic questions. This makes it an essential bedside, goal-directed instrument which should be present or accessible in every emergency department or ward.

Practically every patient with cardiorespiratory symptoms may be evaluated with echography. Acute dyspnea was discussed in Chap. 34 from its parenchymal (interstitial) cardiogenic and noncardiogenic aspects. In this chapter we will discuss diagnostic and monitoring pleuropulmonary uses with regard to dyspnea of pleural or vascular origin whether or not associated with chest pain and/or hemodynamic instability.

Topics of great interest are those related to residual lung air in alveolar syndromes and recruitment of pathologic areas in the critically ill. Great attention is also given to early diagnosis of the alveolar damage that accompanies the initial phases of acute lung injury (ALI) in many critically ill patients.

Chest radiography is used in the intensive care unit usually with portable X-ray machines at the bedside and often even with daily frequency. This efficacy of method though has never been clearly demonstrated. About 65 % of chest radiographs are able to show new alterations that may result in a variation in patient treatment. However, in emergency chest radiography, the diagnostic accuracy is quite low. The sensitivity and specificity for nosocomial pneumonia are 62 and 28 %, respectively. The sensitivity for pneumothorax (PNX) and pleural effusion may be very low (50 %) in the supine patient. Low values are also reported for the diagnosis of consolidations.

Computerized tomography is, by contrast, an efficient diagnostic tool for analysis of overimposed structures and for a volumetric and densitometric quantification of pathologic lungs. Its accuracy regarding pleural disease is practically absolute. Nevertheless, computerized tomography is costly, biologically invasive, may not be done at the bedside, and therefore exposes the patient to the risks of critical transport. The difficulties in performing this examination increase interest in every innovation existing in this context.

G. Soldati (✉)
Emergency Medicine, Valle del Serchio General Hospital, Lucca, Italy
e-mail: g.soldati@usl2.toscana.it

A. Sarti and F. L. Lorini (eds.), *Echocardiography for Intensivists*,
DOI: 10.1007/978-88-470-2583-7_45, © Springer-Verlag Italia 2012

Table 45.1 Definitions of echographic patterns

Echographic pattern	Definition
Lung sliding	Evidence of pleural line movement. This indicates pleural contact with the thoracic wall and excludes pneumothorax
Lung point	The point at which a partially collapsed lung is in contact with the chest wall. On the sonogram, the pleural sliding and vertical artifacts are only present in part of the visible "pleural line"
A lines	Horizontal repetition lines. Reverberation artifacts which reflect the pleural line in depth. Normal finding of aerated lung
B lines	Vertical laser-like artifacts which extend to the inferior margin of the screen. They define interstitial syndrome
White lung	Echogenic subpleural field masking A lines. Hyperdense preconsolidation state of the lung
Interstitial syndrome	Variation of the subpleural pattern from A lines to B lines. May be limited or diffuse to the whole surface of the lung
Consolidation (or alveolar syndrome)	Organization (hepatization) of a pulmonary field with a solid appearance. Posterior echogenic reinforcement
Air bronchograms	Sonographic evidence of aerated bronchi. This indicates a partially aerated consolidation

45.2 Use of Pleuropulmonary Echography in the Emergency Department and in the Intensive Care Unit

Echography has elevated sensitivity and specificity for acute pleural diseases such as pneumothorax, hemothorax, and effusions. In the critically ill patient, congestive heart failure and pulmonary edema are seen as typical interstitial–alveolar syndrome (B lines) (see Chap. 34) without "skip areas" (areas of normal lung in the context of abnormal lung). Acute respiratory distress syndrome (ARDS) has certain peculiar characteristics, such as anatomic (interstitial–alveolar syndrome) and topographic inhomogeneity. Lung consolidations, whatever their nature, appear as solid hypoechogenic areas containing residual air. The echographic sensitivity in this case is around 90 % and the specificity is 98 %.

Nosocomial pneumonia affects 12–29 % of intubated patients, with a mortality of 27–33 %. Diagnosis must discern pneumonia from acute pulmonary edema, ARDS, atelectasis, and aspiration syndrome. Echography is able to distinguish atelectasis from a phlogistic consolidation of nonobstructive origin and the latter from interstitial syndrome.

A cavitation inside a consolidation indicates an infective origin. Aspiration pneumonia is a chemical insult that may evolve to phlogistic pneumonia. It most often involves the right bronchial tree and the posterior regions. Echography is able to show consolidations and their evolution in time with antibiotic therapy and recruitment.

Aspiration of solid material induces distal hyperinflation or atelectasis, which may be seen and differentiated with the use of ultrasound. The Incidence of barotraumas in intubated patients ranges from 4 to 11 %, but may reach 60 % in patients with ARDS. Among the consequences of barotraumas, pneumothorax, which even if small could become hypertensive during mechanical ventilation, may be easily diagnosed with echography.

Table 45.1 describes the main signs in lung ultrasonography.

45.3 Pleural Effusion and Hemothorax

A pleural effusion is seen in echography as fluid (transonic, corpusculated, fibrinous, alveolar, or complex) in the bottom part of the pleural cavity. In the supine patient it will therefore lie in

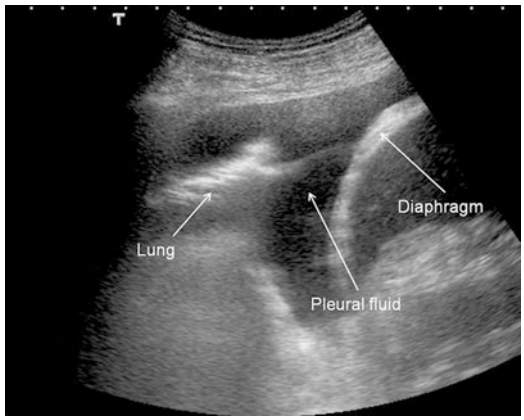

Fig. 45.1 An echofree small pleural effusion. Heart failure. The fluid offers an acoustic window for the diaphragm and for the lung. Lung appearance is artifactual (aerated lung). Seated patient, 7.5-MHz convex probe

the dorsal costovertebral region, whereas in the seated patient it will be above the diaphragm (retroparietal and subpulmonary), offering an acoustic window for the diaphragm and for the variably compressed lung (Fig. 45.1).

Generally, transudate is transonic, whereas exudate contains fibrin sheaths with an alveolar distribution or corpuscularity. A finely corpusculated aspect is typical of hemothoraxes. In the evaluation of the fluid characteristics of a pleural effusion, a semiquantitative estimate (Table 45.2) and the degree of parenchymal compression should be described in order to be also able to define the most appropriate way to drain the thorax.

Lastly, we recount how echography allows one to establish lung density. Normal lung density creates horizontal (specular) artifacts, called A Lines, a hyperdense range produces B lines, and white lung, whereas densities close to the density of water (tissue-like) create parenchymal consolidations with or without air bronchograms.

45.4 Pneumothorax

In pneumothorax air collects in the pleural space. Air is a total acoustic reflector that replaces the physiologic pleural image with pure air artifacts. The regions containing air (usually above) do not show normal pleural sliding. Absence of sliding is one of the signs of pneumothorax to be seen with a convex or linear probe by focalizing on the pleural line (Fig. 45.2). In those pleural regions containing air, all artifacts normally originating from the pleural plane will disappear, so the absence of B lines, white lung, or consolidations excludes a pneumothorax. A pathognomonic sign of pneumothorax is the presence of one or more "lung points" (Fig. 45.3). Evidence of a mobile pleural line, with or without artifacts, that is suddenly covered by pure air artifacts identifies with precision the peripheral extension of a nonmassive subpleural air collection.

With use of these described characteristics, diagnosis of pneumothorax may be made with sensitivity and specificity greater than 95 %. This fact is particularly interesting in the context of small (minuscule, anterior) pneumothoraxes that are usually occult on chest radiography done in the supine patient. These pneumothoraxes are usually collocated in the parasternal and paracardiac regions of the supine patient.

The echographic study of pneumothorax also plays a significant role in the evaluation of secondarily occult pneumothoraxes persisting after thoracostomic drainage. The reexpansion of a lung that was collapsed for pneumothorax may be followed in time by evaluating the medial progression of lung points up to their disappearance, confirming the reconstitution of pleural continuity in all explorable thoracic regions.

45.5 Consolidations and Their Ventilatory Dynamics

Lung consolidations are frequent in the intensive care unit. They are the expression of phlogistic consolidations, alveolar collapse in ARDS, obstructive atelectasis, and contusions. Necessary for their echographic visualization is a critical lung porosity creating a density close to that of solid tissues (0.8–0.9 g/ml), which may contain some residual air but only in

Table 45.2 Semiquantitative evaluation of pleural effusion

Volume	Definition
Minuscule	Only visible in the costophrenic angle
	About 10–30 ml
	Marginal lung compression in the costophrenic angle
Small	Over the costophrenic angle visible with a single echographic scan
	About 100–500 ml
	Compression of the supradiaphragmatic segments of the inferior lobes
Intermediate and large	Visible through two thoracic scans with a convex probe
	About 500–1,000 ml
	Collapse of the lower lobes
Massive	Occupies more than two thoracic scans with a convex probe
	Over 1,500 ml
	Submassive lung collapse

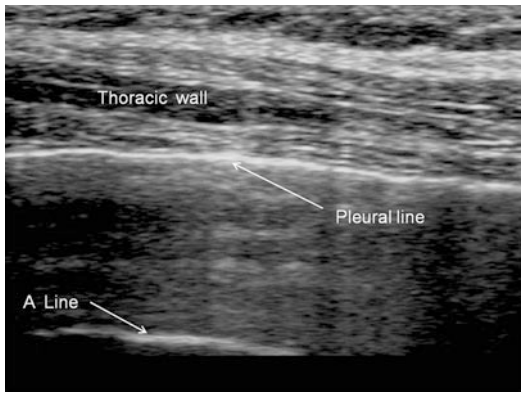

Fig. 45.2 The pleural line is a regular echogenic (specular) line underneath the costal plane. It moves through the acts of breathing, and this movement (lung sliding) is seen in a dynamic scan. Lung sliding indicates pleural contact with the thoracic wall and excludes pneumothorax. Normal subject, 10-MHz linear probe

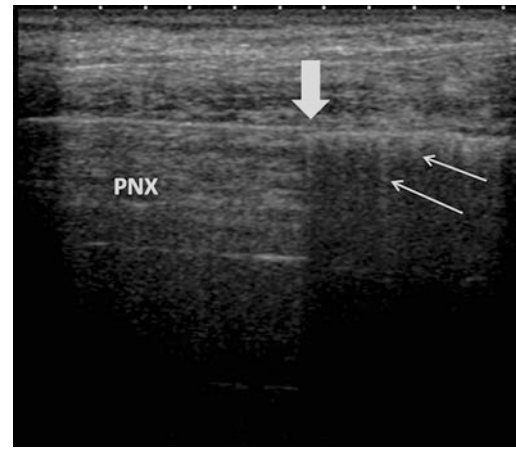

Fig. 45.3 The lung point (*large arrow*) represents the moving point in which a partially collapsed lung is in contact with the chest wall. The pleural sliding and vertical artifacts are only present in the explorable "pleural line," on the right of the picture (*small arrows*). *PNX* indicates the intrapleural air collection, masking the pleura. A 10-MHz linear probe was used

discontinuous and deep regions. The echographic appearance, if the consolidation is air-free, is that of a parenchymal organ (hepatization). A lobar, monosegmentary, or plurisegmentary image of this type is characteristic of atelectasis secondary to bronchial obstruction (Fig. 45.4). Within these images one may visualize blood vessels and fluid-containing bronchi (with echogenic walls) with a piled disposition owing to the lesion's volume loss. Residual air is present in phlogistic consolidations, in those of the critically ill patient, and in compressive atelectasis. It creates artifactual echogenic, linear, or arborescent images (air bronchograms) or punctual and peripheral (air bronchiolograms or air alveolograms) images (Fig. 45.5). The margins of the lesion are usually well defined and irregular with echogenic enhancement. The periphery shows interstitiopathic artifacts and

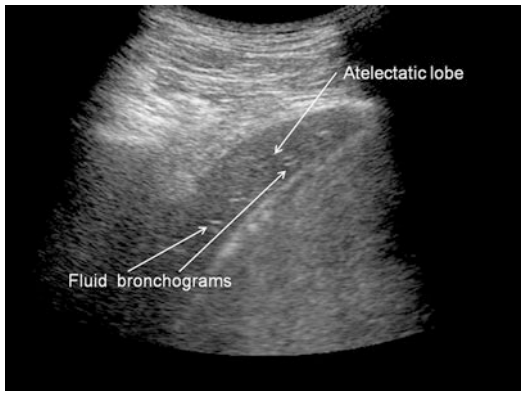

Fig. 45.4 Atelectatic right middle lobe (bronchial obstruction). The lobe is small and with a "parenchymal" appearance. Air artifact are absent. Small tubular images with echogenic walls represent fluid filled bronchi (fluid bronchograms). A 7.5-MHz convex probe was used

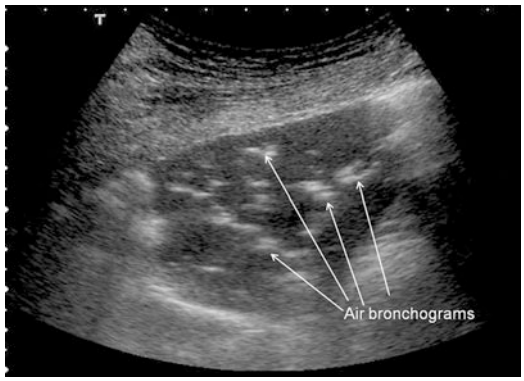

Fig. 45.5 Bacterial pneumonia. Organization of a pulmonary field with a solid appearance and posterior echogenic reinforcement. Many echogenic foci are seen inside the consolidations and they represent air brochograms. A 3.5-MHz convex probe was used

the pleura appears to be interrupted above the consolidation. To be seen, a consolidation or atelectasis must involve the pleura, but this condition is almost always present. Their position is usually lobar, monosegmentary, or plurisegmentary and is actually random in the case of contusions. Evidence of air bronchograms containing artifacts that move along with respiratory acts (dynamic bronchograms) excludes obstruction of the afferent bronchus.

Observing the air pattern inside a consolidation allows one to make a qualitative estimate of residual air and of the possibility of recruitment with ventilation. Table 45.3 reports dynamic ventilatory patterns and their clinical meaning.

Table 45.3 Sonographic ventilatory pattern in pulmonary consolidations

Sonographic pattern	Clinical significance
Consolidation without air	Obstructive atelectasis (subacute)
Consolidation with fluid bronchograms	Obstructive atelectasis (chronic)
Consolidation with dynamic bronchograms	Pneumonia without bronchial obstruction
Progressive disappearance of air bronchograms	Massive exudation, bronchial and bronchiolar obstruction
Gradual emergence of peripheral bronchiolograms	Healing of pneumonia
Sudden disappearance of a consolidation	Sliding +: presence Sliding −,absence +: presence
Rarefaction of B lines	Recruitment
Disappearance of white lung, appearance of A lines	Recruitment

45.6 Early Diagnosis of ALI/ARDS

Alveolar capillary membrane damage in this disease produces acute interstitial edema, hyaline membranes, and alveolar syndrome, whose manifestations are typically cortical. The interstitial syndrome of ALI/ARDS has a particular echographic appearance characterized by bilateral B–lines and white lung with an inhomogenous pattern. The presence of "spared areas" is characteristic (Fig. 45.6). Noncardiogenic pulmonary edema of ALI/ARDS is an early event in the context of systemic inflammatory response syndrome which is not evident or not specific on chest radiography. It has recently been demonstrated, in animal models of ALI/ARDS, how echography has a high sensitivity for the detection of the increase in extravascular lung water and that these modifications actually precede the alteration in the levels of blood gases.

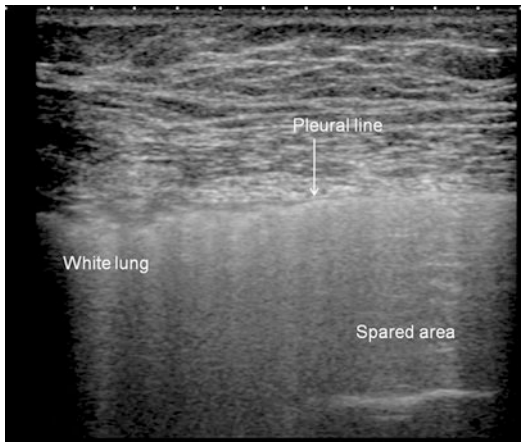

Fig. 45.6 Spared areas of uninvolved lung that abruptly interrupt a subpleural plane with dense interstitial syndrome (or white lung) are typical of noncardiogenic pulmonary edema. Patient with acute respiratory distress syndrome (ARDS), 7.5-MHz linear probe

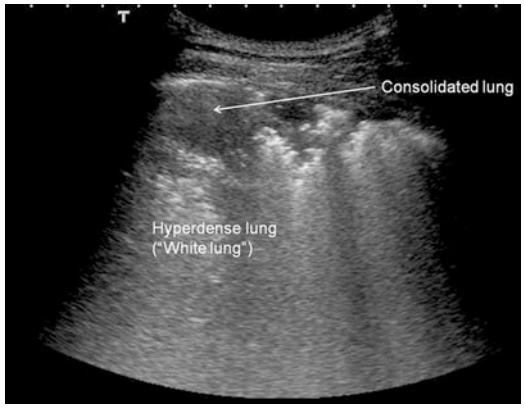

Fig. 45.7 Gravitational dorsal consolidation, containing a small air bronchogram, surrounded by fields of echographic interstitial pattern. Patient with ARDS, 7.5-MHz convex probe

Echographic monitoring of the subpleural fields in patients with pulmonary or extrapulmonary sepsis, lung contusion, trauma, pancreatitis, or other systemic diseases is important for the early detection of those alterations in lung density indicative of alveolar–capillary damage. The appearance and bilateral diffusion of a B-line pattern in previously normal, or only locally pathologic, lungs is strongly indicative of progressive lung damage.

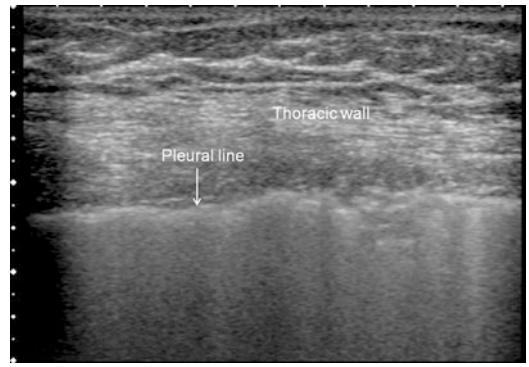

Fig. 45.8 An hyperdense nonconsolidated subpleural pattern expressed along the antigravitational pleura of a patient with ARDS. The pleural line is typically irregular.A 10-MHz linear probe was used

45.7 Lung Consolidations in the ARDS Patient

In ARDS patients, lung disease has an inhomogeneous expression through a wide range of parenchymal densities. A ventrodorsal aeration gradient shows a greater concentration of consolidations (Fig. 45.7) in the posterior gravitational regions. The echographic aspect of these lesions is not different from that of those described earlier with a more or less accentuated presence of air bronchograms. The lesser dense lung regions (usually ventral in the supine patient) show pleural artefacts in the preconsolidation phase such as white lung and compact B lines (Fig. 45.8). Normally expanded or hyperinflated lung areas show horizontal repetition artifacts known as A lines. An increase in artifactual air components or in dynamic bronchograms inside a consolidated lung region, or the variation of a subpleural pattern with dense B lines to one with rare B lines may be indexes of lung recruitability through ventilatory strategies.

45.8 Pulmonary Embolism

Pulmonary embolism may not determine the immediate formation of echographically visible lesions. They usually appear, in a couple of days, as small (1.5–3-cm), subpleural, multiple

consolidations with a segmentary distribution in the dorsal segments of the lower lobes. The nature of these lesions may be atelectatic from loss of surfactant, or infarctual. They are either triangular in shape with the pleura as the base or polygonal. In 50 % of cases, a small pleural effusion is also present. From the diagnostic point of view, these signs are important if they are associated with suggestive clinical symptoms and especially if they are associated with positive findings on venous compression ultrasonography. A perfectly normal lung parenchyma (A-line pattern) is also compatible with pulmonary embolism, and in fact a normal subpleural pattern in the context of dyspnea and positive findings on compression ultrasonography make the diagnosis of pulmonary embolism very likely.

45.9 Vascular Pattern of Pulmonary Consolidation

Use of last-generation contrast media (e.g., sulfur hexafluoride—contrast-enhanced ultrasonography) has allowed vascular characterization of visible lung consolidations. Endovenous administration of a contrast medium, using a low ultrasound mechanical index, results in typical real-time enhancement patterns. Arterial enhancement (5–7 s after injection) is characteristic of most pneumonias and atelectases in the acute phase. In these cases, abscesses do not absorb contrast medium. A systemic enhancement (bronchial), which appears in 18–20 s, is usually present in tumoral lesions that reach the pleura. A peripheral enhancement without signs of contrast medium inside the lesion is typical of pulmonary embolism.

Further Reading

Beckh S, Bolcskei PL, Lessnau KD (2002) Real time chest ultrasonography. A comprehensive review for the pulmonologist. Chest 122:1759–1773

Copetti R, Soldati G, Copetti P (2008) Chest sonography: a useful tool to differentiate acute cardiogenic pulmonary edema from acute respiratory distress syndrome. Cardiovasc Ultrasound 6:16

Lichtenstein D (2010) Whole body ultrasonography in the critically ill. Springer, Berlin

Soldati G, Sher S (2009) Bedside lung ultrasound in critical care practice. Minerva Anestesiol 75:509–517

Wilkerson RG, Stone MB (2010) Sensitivity of bedside ultrasound and supine anteroposterior chest radiographs for the identification of pneumothorax after blunt trauma. Acad Emerg Med 17:11–17

Focused Assessment with Sonography for Trauma

46

Alfonso Lagi and Federica Marini

46.1 Introduction

Focused assessment with sonography for trauma (FAST) is an echographic approach used for patients with abdominal trauma. It is a limited bedside ultrasound examination that seeks to quickly detect free intra-abdominal fluid, particularly blood. Extended FAST (E-FAST) expands the examination to assess whether there is pneumothorax or cardiac complications.

FAST answers one question only: Is there free fluid in the abdomen?

So, the indications for performing FAST are *blunt or penetrating trauma, trauma in pregnancy, or hypotension of unclear cause*.

FAST helps to select the patients requiring emergent laparotomy and who can be monitored or can await slower, more definitive studies. The FAST examination has many advantages over more traditional tests such as explorative laparatomy, peritoneal lavage, and abdominal CT scan, as listed below:

- It decreases the time needed for diagnosis because it can be executed at the bedside, it is noninvasive, and it does not require a contrast medium or radiation.
- It is safe in pregnant woman and in children.
- It can be performed serially.
- It has high specificity to detect free fluid (between 98 and 100%).
- It can be used to diagnose and assess the degree of hemoperitoneum.
- It needs a short training period, so its use can be extended to every emergency doctor.

On the other hand, FAST has many drawbacks:

- It has lower sensibility to detect peritoneal fluid (between 73 and 88%).
- It requires almost 200 ml of fluid for detection.
- It cannot detect retroperitoneal fluid.
- It has limited ability to detect organ lesions.
- It is operator-dependent.
- Difficult in obese subjects.

The conclusion is that negative findings from FAST do not exclude the presence of peritoneal fluid.

46.2 Indication for FAST or E-FAST and Examination Skill

1. Abdominal trauma
2. Trauma in pregnancy
3. Hypotension of unclear cause

The philosophy behind the FAST examination is that fluid pools in the lower areas of the abdomen and chest. Four views can be used for the abdomen:

A. Lagi (✉)
Department of Emergency, Santa Maria Nuova Hospital, Florence, Italy
e-mail: alfonso.lagi@asf.toscana.it

A. Sarti and F. L. Lorini (eds.), *Echocardiography for Intensivists*,
DOI: 10.1007/978-88-470-2583-7_46, © Springer-Verlag Italia 2012

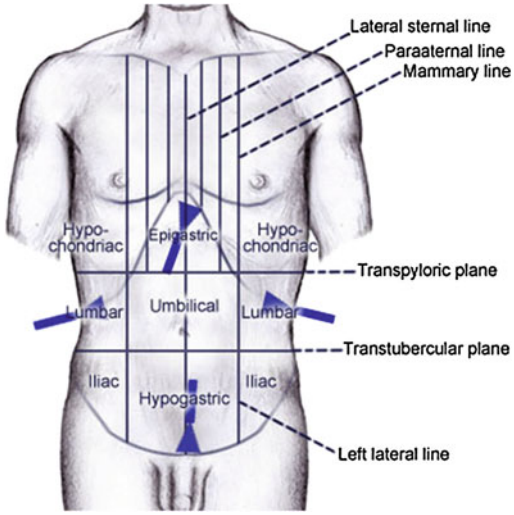

Fig. 46.1 Views and the position of the probe

- Right lumbar (hepatorenal recess)
- Left lumbar (perisplenic)
- Suprapubic window
- Subxiphoid pericardial window to evaluate the heart

A standard 3.5-MHz convex probe can be used.

Views and the position of the probe are shown in Fig. 46.1 .

46.3 Right Lumbar Side

With this view the hepatorenal space is explored. This is named the Morison pouch. The probe is placed on the right upper quadrant at the mid-axillary line between the ninth and 11th ribs. Both oblique and coronal views should be used. The examiner can see the liver and during deep inspiration the kidney appears and with it the Morrison pouch, which is the space between the liver and the right kidney. In a supine patient this space is chosen for drainage of ascites, the place where initially all peritoneal liquid, if enough, accumulates. Normally, it is free from fluid and appears hyperechoic. In cases of hemoperitoneum, the Morison pouch appears as an anechoic strip.

If there is copious fluid, over 200 ml, it may be detected in the perihepatic space (Fig. 46.2).

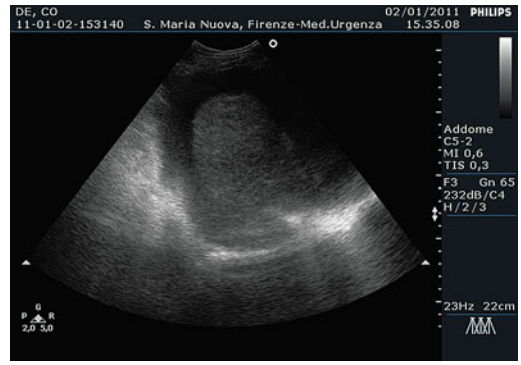

Fig. 46.2 Perihepatic fluid

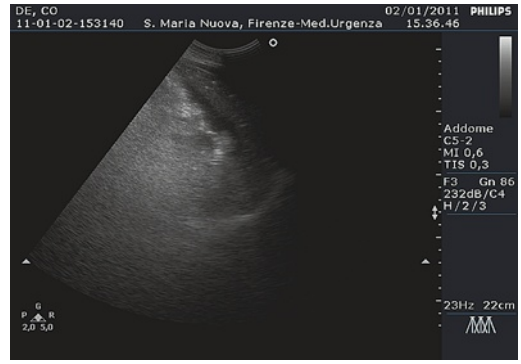

Fig. 46.3 Anechoic perisplenic space

46.4 Upper Left Lumbar Side

The probe is placed over the left flank, on the left upper quadrant at the posterior axillary line between the ninth and 11th ribs. Sliding the probe superiorly and inferiorly will help to detect free fluid above the spleen and along the spleen tip. Ascites can be seen at the upper splenic tip, in the subphrenic place over the spleen, or in the recess between the spleen and left kidney. It appears as an echogenic space which better defines the outline of the spleen (Fig. 46.3).

46.5 Suprapubic View

The probe should be placed just above the pubic symphysis and directed inferiorly (Fig. 46.1). The pelvis is the most dependent part of the

peritoneal cavity, so it is fluid collects there easily. Both sagittal and transverse views should be obtained. The bladder should be left full to provide a better window. So, fluid around and behind the bladder can be stressed and in women so can the Douglas pouch.

46.6 Subxiphoid View

The subxiphoid view is obtained by placing the probe in the subxiphoid space directed toward the left shoulder, at an orientation of 45°. This will allow the diaphragm and pericardium to be viewed and a four-chamber view of the heart. This view may be uncomfortable for many patients because it requires significant pressure on the upper abdomen to perform it.

Further Reading

ACEP Clinical Policies Committee and the Clinical Policies Subcommittee on Acute Blunt Abdominal Trauma (2004) Clinical policy: critical issues in the evaluation of adult patients presenting to the emergency department with acute blunt abdominal trauma. Ann Emerg Med 43(2):278–290

American College of Surgeons (2008) Advanced trauma Life support for doctors. Student course manual, 8th edn. American College of Surgeons, Chicago

Boulanger BR, Kearney PA, Brenneman FD et al (2000) Utilization of FAST (focused assessment with sonography for trauma) in 1999: results of a survey of North American trauma centers. Am Surg 66(11):1049–1055

Bode PJ, Edwards MJ, Kruit MC et al (1999) Sonography in a clinical algorithm for early evaluation of 1671 patients with blunt abdominal trauma. AJR Am J Roentgenol 172(4):905–911

Farahmand N, Sirlin CB, Brown MA et al (2005) Hypotensive patients with blunt abdominal trauma: performance of screening US. Radiology 235(2):436–443

Lee BC, Ormsby EL, McGahan JP et al (2007) The utility of sonography for the triage of blunt abdominal trauma patients to exploratory laparotomy. AJR Am J Roentgenol 188(2):415–421

Natarajan B, Gupta PK, Cemaj S, Sorensen M, Hatzoudis GI, Forse RA (2010) FAST scan: is it worth doing in hemodynamically stable blunt trauma patients? Surgery 148(4):695–700

Renal Ultrasound and Echo–Color Doppler Techniques in Kidney Failure

47

Andrea Masi, Filippo Nori Bufalini, and Federica Manescalchi

47.1 Introduction and Background

Today, ultrasonography represents the first phase in the morphologic and flowmeter study of the kidney and permits the use of more complex and invasive examinations to be reserved for more "targeted" situations.

The ultrasound examination of the kidney is usually done using convex probes, with a frequency of between 3 and 5 MHz, with longitudinal, coronal, and transverse scanning planes. In longitudinal scans, the kidney has an ellipsoid form; in the coronal scans, the external profile of the renal ellipsoid has a convex form; and in the transverse scans, the kidney has a rounded form. The adult kidney has a longitudinal diameter of between 9 and 12 cm; the renal parenchyma has medium-to-low echo density, that is, it is slightly inferior to that of the liver. The parenchymal thickness in the adult must be more than 15 mm.

In children and in adults, there may be differentiation between cortical echogenicity and medullary echogenicity, with greater cortical echogenicity (Fig. 47.1a) In the elderly person, there is a reduction of the parenchymal thickness along with an increase in echogenicity and the loss of visibility of the corticomedullary junction (Fig. 47.1b).

The renal sinus is characterized by the presence of very intense echoes due to the presence of fibrous–adipose tissue and the interfaces generated by multiple structural components such as the calyx; in the child, the adipose tissue is not well represented and the renal sinus is thin; in the elderly person, it generally has increased thickness owing to the presence of lipomatosis.

In the normally hydrated patient, the calyces are not identifiable; they become assessable in the case of hyperhydration, hyperdistension of the bladder, or because of a disease (congenital, inflammatory, obstructive, or due to reflux). The ureter, if not dilated, can only be recognized at a low pelvic level, using the bladder distension as the window; the ureteral meatus can be noted as a limited hump on the posterior bladder wall which extends up with its typical canalicular structure. The perviousness of the meatus with the assessability of the phenomenon of the ureteral jet has been thoroughly studied with color Doppler research.

Today, the great diffusion of color Doppler equipment and the experience acquired therewith have given rise not only to its very important role in the examination of the patient with hypertension and, more in general, in the evaluation of vascular nephropathy, but this diffusion has also resulted in color Doppler examination being considered as a complement to the basic ultrasound examination [1, 2].

A. Masi (✉)
Department of Radiology, Santa Maria Nuova Hospital, Florence, Italy
e-mail: antemasi@yahoo.it

A. Sarti and F. L. Lorini (eds.), *Echocardiography for Intensivists*,
DOI: 10.1007/978-88-470-2583-7_47,

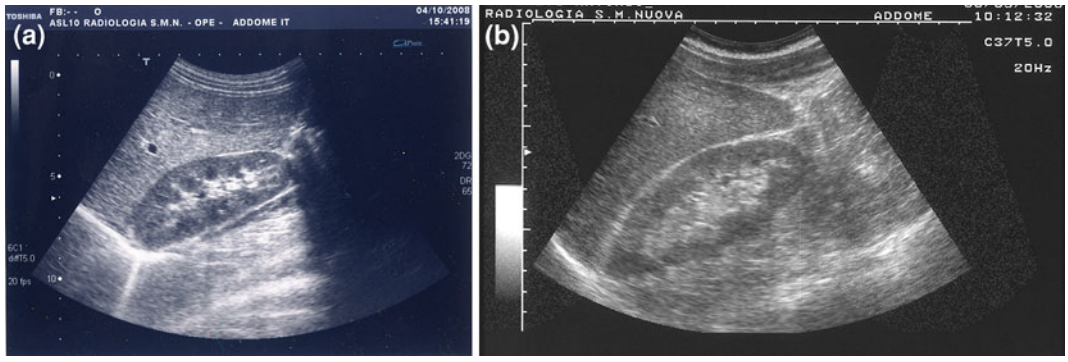

Fig. 47.1 Normal ultrasonographic appearance of the right kidney in an anterior longitudinal scan: **a** Young adult: it is possible to see the corticomedullary junction. **b** Old patient: moderately hyperechoic homogeneous appearance of renal parenchyma (From Sarti [3] with permission)

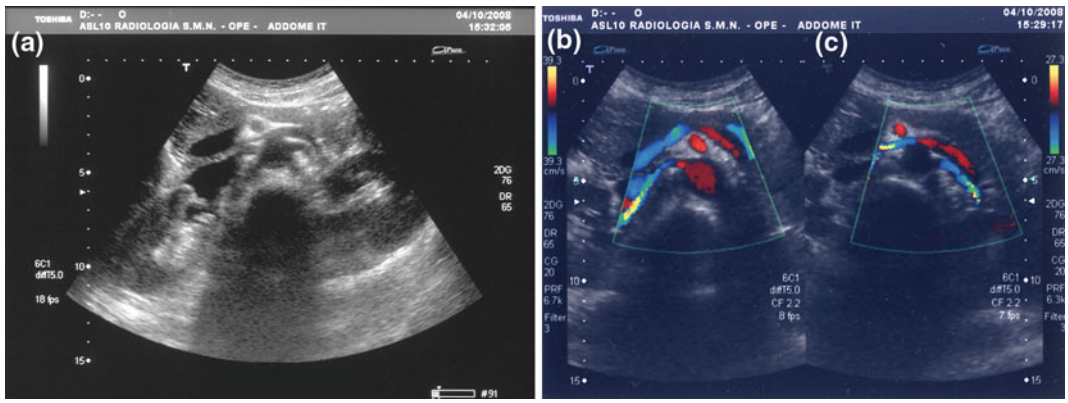

Fig. 47.2 Emergence of the renal arteries: **a** Transverse mesogastric scan: from anterior to lateral aortic walls the emergence of the right and left renal arteries can easily be seen. **b**, **c** Color Doppler image of the proximal origin of the right and left renal arteries (From Sarti [3] with permission)

The study of the principal renal arteries begins with transverse scans in the upper abdomen, through which the emergence of the renal arteries is identified. Both originate in the anterolateral aortic wall (Fig. 47.2); the right renal artery crosses behind the inferior vena cava (Fig. 47.3). Then a subcostal oblique scan must be performed (asking the patient to raise the side being scanned) in order to follow the intermediate section of the artery, which, on both sides, is located behind the ipsilateral renal vein (Fig. 47.4).

It may not always be possible to identify the emergence and the intermediate section of the renal arteries because of obesity or meteorism; on the right side the use of the liver window is an aid in the viewing the artery.

The study of the hilum vessels (anterior and posterior rami and segmented subdivisions) and the intraparenchymal renal arteries is performed using chiefly longitudinal–coronal scans of the patient in an oblique–prone position; at times transverse scans may also be used. Modern ultrasound equipment permits the interlobar, arcuated, and interlobular arterial vessels to be picked out (Fig. 47.5). The evaluation of the flow pattern is a consideration typical of parenchymatous organs with a systolic peak (which must not exceed 100–150 cm/s) and a diastolic component which is

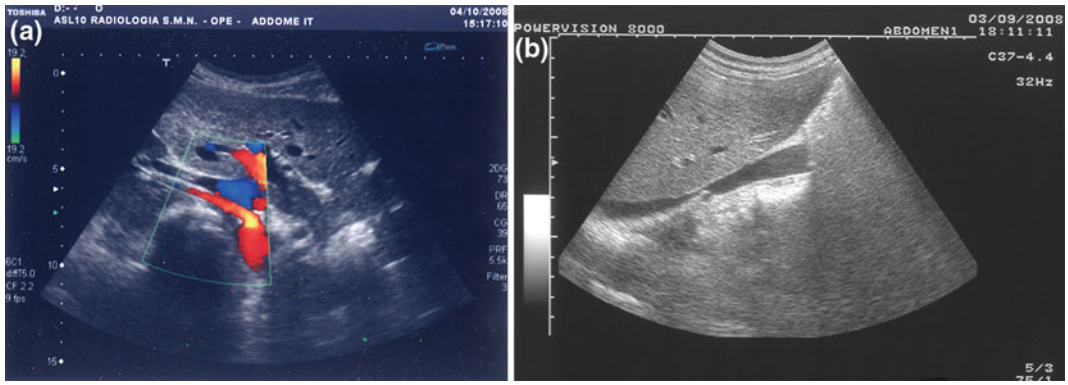

Fig. 47.3 Retrocaval position of the right renal artery: **a** Color Doppler oblique subcostal transverse scan. **b** Typical appearance in the longitudinal scan (From Sarti [3] with permission)

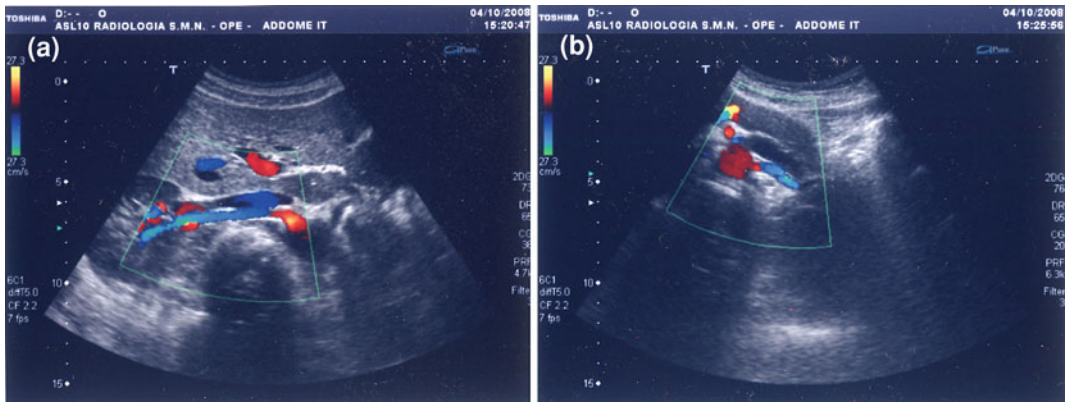

Fig. 47.4 Posterior and parallel localization of renal arteries against venous vessels (From Sarti [3] with permission)

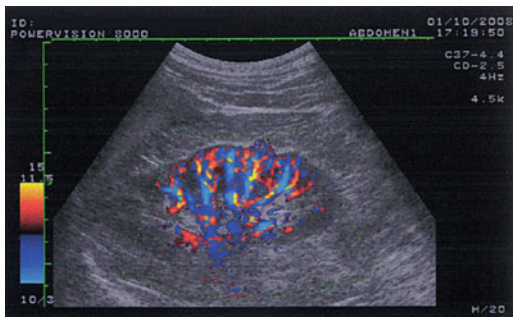

Fig. 47.5 Power color Doppler perfusion imaging (From Sarti [3] with permission)

well represented (Fig. 47.6). The presence of a stenosis which is not hemodynamically significant increases both the systolic and the diastolic velocity in the stenotic zone, whereas further along alterations in the morphology of the flow are not discernible.

On the other hand, a hemodynamically significant stenosis causes distally the presence of a flow with a tardus–parvus peak.

In the case of complete obstruction due to embolus or thrombosis of the renal artery, the color Doppler examination may show the absence of flow in the intraparenchymal renal arteries and the hilum vessels. Analogously, the obstruction of a hilum vessel or a segmental arterial vessel may be hypothesized in the case of a lack of flow in the interlobar vessels of certain segments. It must be kept in mind that the arterial system of the kidney is vulnerable since it is of the terminal type, without anastomosis.

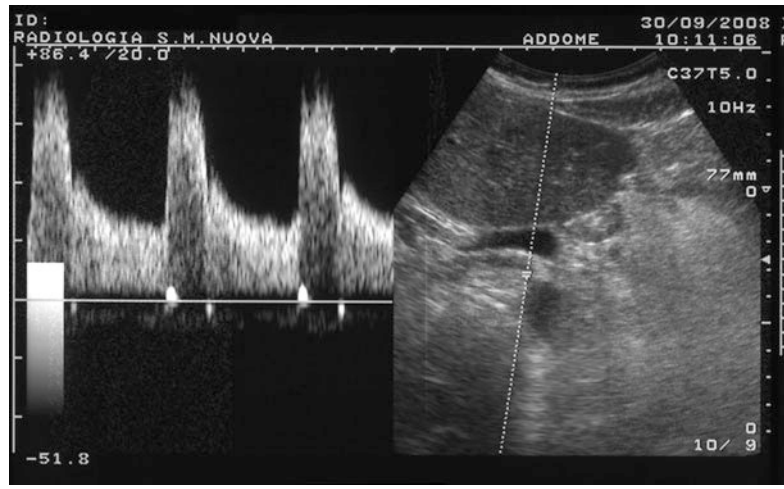

Fig. 47.6 Typical appearance of the flow pattern in the main renal artery with systolic acme following gradual flow decrease in diastole (From Sarti [3] with permission)

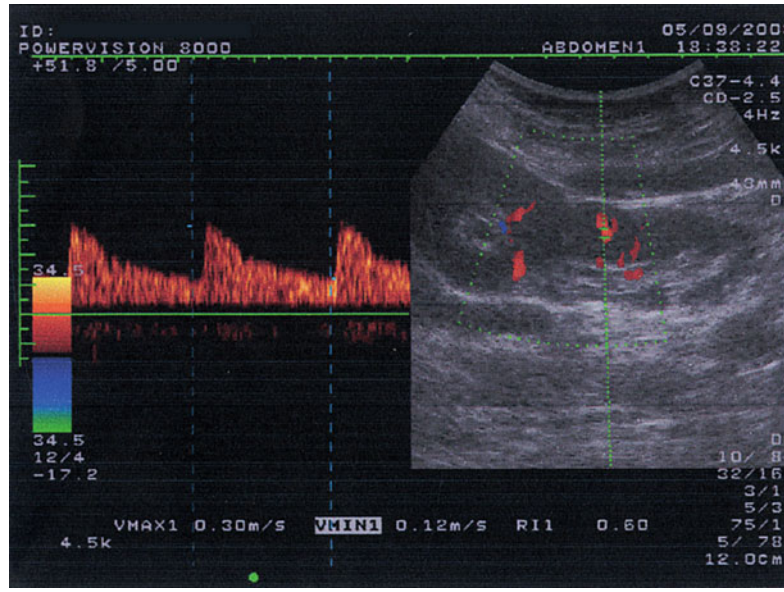

Fig. 47.7 Example of a normal flow pattern inside an interlobar artery (From Sarti [3] with permission)

In the intraparenchymal renal arteries, arterial resistance index (RI), an expression of the relation between the difference in the velocity of the systolic peak and the telediastolic velocity and the velocity of the systolic peak, must not be above 0.70 (Fig. 47.7); in elderly patients the presence of atherosclerotic alterations causes an increase in the resistance of the intraparenchymal vessels; for this reason the tolerance of the RI may be as high as 0.80. The evaluation of the RI is usually performed on the interlobar arteries.

The primary renal veins, tributaries of the inferior vena cava, are easily identifiable: they are found in front of the corresponding arterial vessels and they are characterized by a continuous flow with phasal oscillations from respiration or cardiac activity (Fig. 47.8).

The normal venous perviousness may be altered by the presence of a neoplastic thrombosis (partial or total), by a kidney tumor, or by a thrombosis which is a complication of acute or chronic nephropathies.

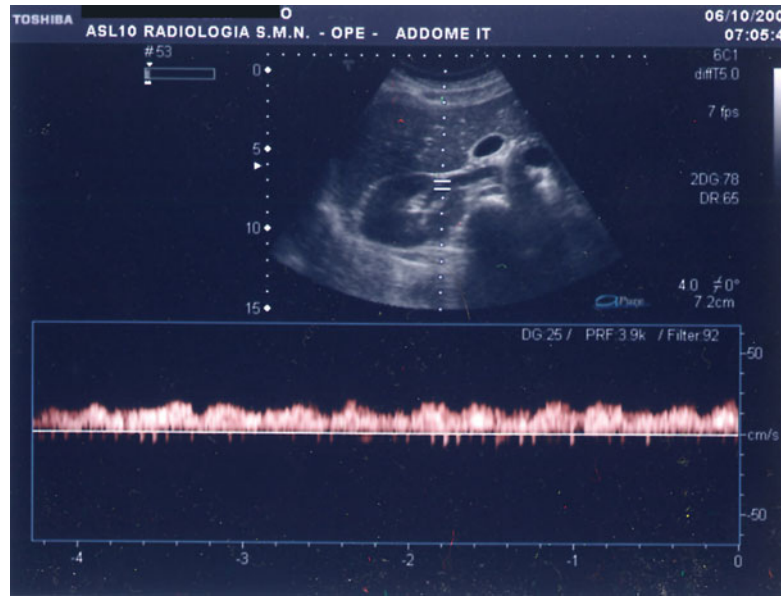

Fig. 47.8 Example of venous flow in the right renal vein; polyphasic appearance (From Sarti [3] with permission)

47.2 Renal Failure

47.2.1 Acute Renal Failure

Acute renal failure (ARF) is a complex clinical picture that includes the spectrum of renal physiopathological alterations. Its severity is currently studied according to RIFLE criteria that refer to the two main clinical components of the syndrome: diminished diuresis and the reduction of the glomerular filtration rate (GFR)/increase of creatininemia.

Traditionally, ARF can be classified as prerenal, renal, and postrenal .

Prerenal ARF accounts for over half the cases and is a potentially reversible functional condition, secondary to real intravascular hypovolemia or to a drop in effective volemia as in heart failure, contrast-medium-induced intrarenal vasoconstriction, drug treatment (cyclosporine), endotoxins, and borderline hypovolemia associated with the intake of drugs that alter the self-regulation of the renal blood flow (ACE inhibitors).

Renal intrinsic or parenchymal ARF represents about 25 % of cases and, in addition to the acute tubular necrosis, there may be vascular (vasculitis, uremic–hemolytic syndromes), glomerular (acute glomerular nephritis and rapidly progressive), and interstitial causes (acute pyelonephritis).

Postrenal ARF is caused by urinary outflow obstruction at either the intrarenal level (e.g., tubular obstruction by paraproteins) or, above all, at the level of the excretory ducts, caused by lithiasis, tumors, and retroperitoneal fibrosis.

The differential diagnosis among the different causes of ARF is mainly based on the anamnesis (patient history) and clinical and laboratory data. We should remember that today, with increasing patient age and comorbidities, acute renal damage is frequently a consequence of preexisting chronic damage which is often not recognized.

The use of renal ultrasound and echo–color Doppler techniques to diagnose the different forms of acute renal damage must take into account the influence of preexisting damage regarding the size of the kidney, but, above all, the thickness and echogenicity of the parenchyma, as well RIs.

Ultrasound techniques supplemented with color Doppler examination are generally the only diagnostic imaging examination requested for these patients, who are often hospitalized in intensive care units because they need rapid and noninvasive surveys to obtain anatomical, morphological, and functional information useful for the specialists to identify a correct diagnostic course and help define an adequate therapeutic medical and/or surgical

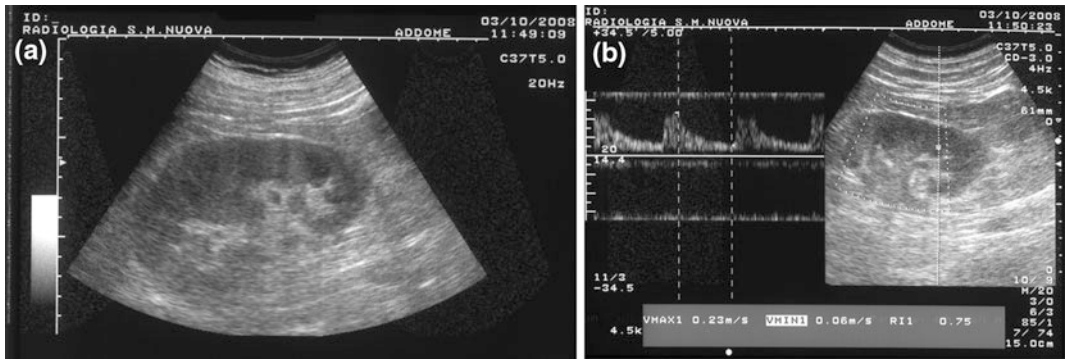

Fig. 47.9 Acute interstitial nephritis. **a** Normal ultrasound appearance. **b** The Doppler examination shows a reduced diastolic flow component with a resistance index of 0.75 (From Sarti [3] with permission)

strategy. In particular, this method is highly sensitive in detecting the dilation of the excretory ducts.

The morphological alterations that occur in the kidneys of patients with ARF are nonspecific. In most cases, the echogenicity and parenchymal thickness are regular in renal ARF. The kidneys may sometimes be larger and show an increased cortical echogenicity, and low medullary echogenicity size, with a visible corticomedullary junction even in elderly patients.

In acute tubular necrosis, the color Doppler survey also highlights a parenchymal hypoperfusion: vessels are difficult to see and the RI is increased by the reduction, even up to the possible absence or inversion, of the diastolic component. Such a situation is determined by the high vascular resistances consequent to the vasoconstriction of small intraparenchymal arteries.

The flow, and consequently the RI, tends to fall back within the limits simultaneously with the recovery of the renal function. The RI is generally increased in the pathological processes that involve the tubulointerstitial compartment (Fig. 47.9), whereas it is normal in the diseases with a prevalent glomerular localization.

In clinical practice, the performance and interpretation of the color Doppler survey in elderly or noncompliant patients are often difficult, with flow patterns being recorded in technically unsatisfactory conditions.

In prerenal ARF cases, the ultrasonographic aspect of the kidneys is normal and there are no intrinsic flow variations in the renal vessels. In these cases, it is usually rather difficult to identify significant changes in the RI, except for cases of severe hypovolemic shock, where the diastolic component is lowered until it is almost completely flat (RI increase). The correction of the hypovolemia or cardiac output deficit can almost always resolve the kidney failure condition and normalize the RI, if it was altered.

Postrenal ARF is caused by bilateral obstructive calculi or neoplastic alterations infiltrating the ureters or retroperitoneal fibrosis.

Ultrasonography is a highly sensitive technique for the diagnosis of dilation of the urinary excretory system, which can frequently identify the level and cause of the obstruction. Finally, the thickness of the renal parenchyma and the level of dilation of the excretory ducts must always be evaluated (Fig. 47.10). The presence of an obstructive process produces an increase in the RI because of the reduction of the diastolic component.

A summary of RI behavior in the different nephropathies is provided in Table 47.1.

Some patients (up to 30 %) with acute obstruction do not show an evident calicopyelic dilation in the first few hours, particularly elderly patients and dehydrated patients.

The echo–color Doppler study of the ureteral output may be useful in the diagnosis of an obstruction: if there is output, a complete obstruction can be excluded, whereas in the case of incomplete obstruction, we can observe a continuous low-intensity output and a marked asymmetry between the two sides.

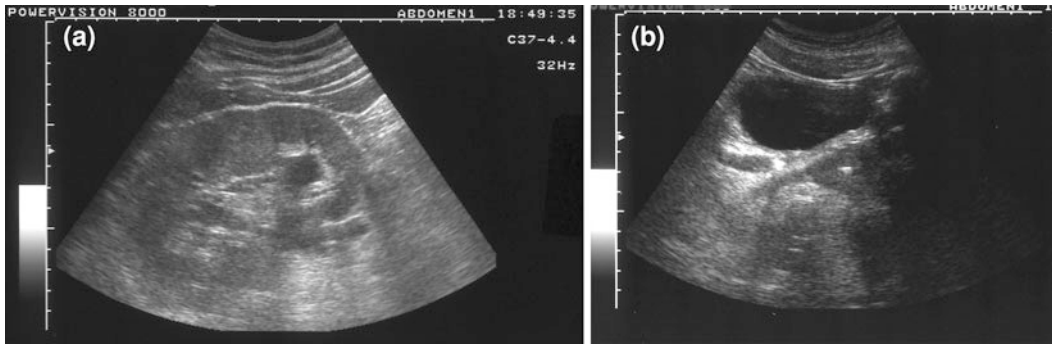

Fig. 47.10 Dilatation of the urinary tract caused by a stone placed in the distal ureter (From Sarti [3] with permission)

Table 47.1 Renal resistance index in several acture renal failure conditions (from http://www.medinterna.net/85323.php)

Cause of renal failure	RI	Notes
Acute tubular necrosis	I	Reflex vasoconstriction
Prerenal	U–R	Reduced systolic flow
Chronic renal failure	I	Reduced diastolic flow
Glomerular nephropathies	U	Glomerular influence on resistances
Vascular or tubulointerstitial nephropathies	I	Alteration of sensitive and early RI
Acute obstructive nephropathy	I	Obstructed side, even without hydronephrosis
Uremic–hemolytic syndrome	I	Reduced diastolic flow
Renal artery stenosis	R	If upstream stenosis >75%
Nephroangiosclerosis	I	In the advanced forms
Diabetic nephropathy	I	Early, related to progression of diabetic nephropath
Hepatorenal syndrome	I	Precedes the syndrome onset by a long time
Vasculitis	I	Reduced vascularization

RI resistance index, *R* reduced, *I* increased, *U* unchanged

47.2.2 Chronic Renal Failure

Chronic renal failure (CRF) is the persistence for at least 3 months of abnormal kidney structures and/or functions. These structural abnormalities may be microalbuminuria/proteinuria, pathological urinary sediment, and anomalies detected by instrumental examinations.

The GFR can be determined on the basis of creatininemia levels by using several validated formulas (Modification of Diet in Renal Disease Study/Chronic Kidney Disease Epidemiology Collaboration) to classify the condition in five stages (Table 47.2).

Kidney failure starts from stage 3 (GFR < 60 ml/min/1.73 m^2).

Chronic renal failure is usually caused by renal diseases with a chronic course that can last for a long time in the latent form and, as they become progressively more severe, may determine the onset of a clear organ failure. Clear chronic kidney failure is characterized by asthenia, anorexia, polyuria, arterial hypertension, hypernatremia, hypercreatinemia, hyperuricemia, hyperkalemia, and metabolic acidosis. Virtually all acquired or congenital chronic renal conditions can lead to chronic renal failure, but the main causes are diabetes and atherosclerosis.

Ultrasound signs of nephropathy are often not sufficient to distinguish individual diseases, except for some particular cases. In polycystic

Table 47.2 Classification of chronic renal failure based on the value of the glomerular filtration rate (*GFR*) in Kidney Disease Outcomes Quality Initiative (KDOQI) guidelines

Stage	Description
I	GFR normal or increased; evidence of kidney damage is proven by microalbuminuria/ proteinuria, hematuria
II	Small reduction of GFR (89–60 ml/min/ 1.73 m^2)
III	Moderate reduction of GFR (59–30 ml/min/ 1.73 m^2)
IV	Severe reduction of GFR (29–15 ml/min/ 1.73 m^2)
V	GFR < 15 ml/min/1.73 m^2)

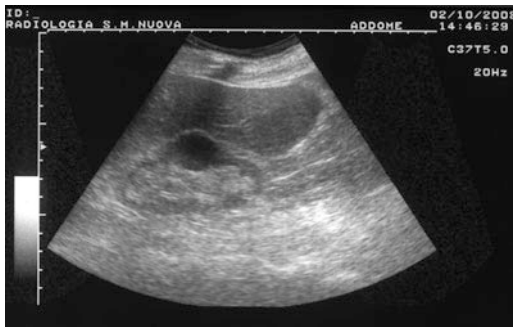

Fig. 47.11 Chronic nephropathy: the kidney is smaller, and the parenchymal thickness is considerably less. In this situation it is practically impossible to identify an intraparenchymal flow pattern also present a cortical cisty (From Sarti [3] with permission)

kidney diseases in young and adult individuals, for example, the kidney size is progressively increased until the kidneys appear as masses that occupy most of the abdominal cavity, with the presence of many cystic formations, some of which may show a corpuscle content due to hemorrhagic or infective phenomena. Sometimes, there may be cysts in the liver, pancreas, and spleen. Nephrocalcinosis (the deposition of calcium salts generally in the renal medulla, but also in the interstitial, vascular, and tubular walls) is characterized by a hyperechogenic appearance of the pyramids, which can be accompanied by a cone of shade at the back.

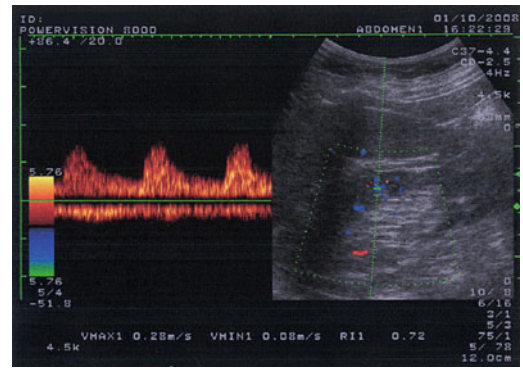

Fig. 47.12 Glomerular chronic nephropathy with a decrease of the diastolic component and an increase of the resistance index (From Sarti [3] with permission)

The size of the kidneys is mostly reduced (Fig. 47.11), even though they can be normal in a high number of cases. Their morphology can be preserved. An irregular morphology with areas of greater parenchymal retraction is typical of chronic pyelonephritis. Parenchymal echogenicity is increased in most cases, with a greater intensity than that of hepatic parenchyma. The corticomedullary junction is frequently not visible.

On color Doppler imaging, the intraparenchymal vessels are often rarefied, thin, and difficult to localize; therefore, it is easy to understand the complexity of the task of sampling the Doppler signal. The RI is increased in vascular–interstitial conditions (RI > 0.70); it exceeds 0.70 in glomerular nephropathies only at advanced stages (Fig. 47.12).

References

1. Barozzi L, Valentino M, Santoro A et al (2007) Renal ultrasonography in critically ill patients. Critical Care Med 35(Suppl):198–205
2. Gerhard-Herman M, Gardin JM, Jaff M, Mohler E, Roman M, Naqvi TZ (2006) Guidelines for noninvasive vascular laboratory testing: a report from the American Society of Echocardiography and the Society of Vascular Medicine and Biology. J Am Soc Echocardiogr 19(8):955–972
3. Sarti A (2009) Ecocardiografia per l′intensivista. Springer, Milan

Ultrasound for Percutaneous Tracheostomy

48

Massimo Barattini, Carla Farnesi, and Silvia Marchiani

Many ICU patients needing prolonged tracheal intubation for respiratory distress or neurological problems receive a tracheostomy. In recent years, intensivists have preferred a bedside percutaneous technique instead of a surgical one. In 1985, Ciaglia introduced dilatational tracheostomy, which is, with all the new variations, still widely performed. Except for Fantoni's translaryngeal tracheostomy, all percutaneous tracheostomies utilize the Seldinger technique with a frontal approach guided by anatomical landmarks such as the cricoid cartilage and the jugular notch.

It is a simple technique. With local anesthesia, a needle is inserted through the membrane between the second and third tracheal rings. A guidewire enters the trachea, passing inside the needle, which is then removed, giving the possibility to introduce various kinds of dilators to create a passage for the tracheostomy tube. Absolute and relative contraindications are anatomical features such as a short neck, obesity, difficult anatomical identification, thyroid enlargement, and previous neck surgery. The most common complications are breaks of tracheal rings, puncture of the posterior wall of the trachea and esophagus, and bleeding. In 20 % of cases venous bleeding can occur, rarely necessitating wound revision or blood transfusion even if there are descriptions of dramatic hemorrhages by fortuitous punctures of anomalous arterial vessels.

Bronchoscopy is suggested to locate the correct site for insertion of the needle on the sagittal midline of the trachea far from vascular structures, and to control all the dilatational procedures but a long-lasting reduction of oro-tracheal tube lumen can cause dangerous ventilation mismatch in hypoxic patients' lumen. For many years ultrasound has been commonly utilized in neck imaging. Also, an echographic study of the airways is currently widely used by intensivists.

We routinely use an ultrasound study of the neck and trachea before a blind tracheostomy to accurately evaluate the operating site and the underlying tissues, thus reducing the risk of vessel puncture and complication (Figs. 48.1, 48.2).

Then, with the vascular probe on the upper neck, we gently withdraw the endotracheal tube just above the needle insertion point (Figs. 48.3, 48.4, 48.5).

During the procedure we follow the needle insertion by continuous ultrasound imaging and control the correct tracheostomy cannulation within the tracheal lumen with the bronchoscope.

M. Barattini (✉)
Department of Anesthesia and Intensive Care,
Santa Maria Nuova Hospital, Florence, Italy
e-mail: massimo.barattini@asf.toscana.it

A. Sarti and F. L. Lorini (eds.), *Echocardiography for Intensivists*,
DOI: 10.1007/978-88-470-2583-7_48, © Springer-Verlag Italia 2012

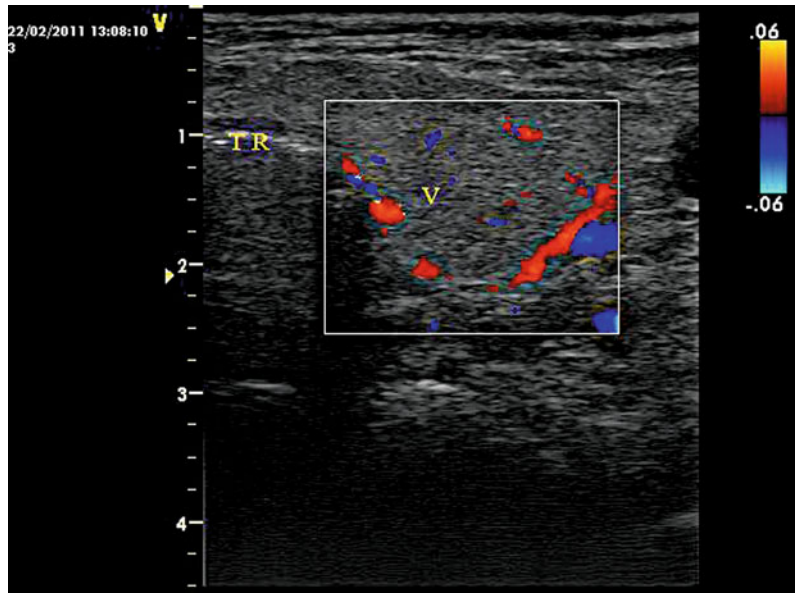

Fig. 48.1 Blood vessels near the tracheal ring. *TR* tracheal ring, *V* vessels

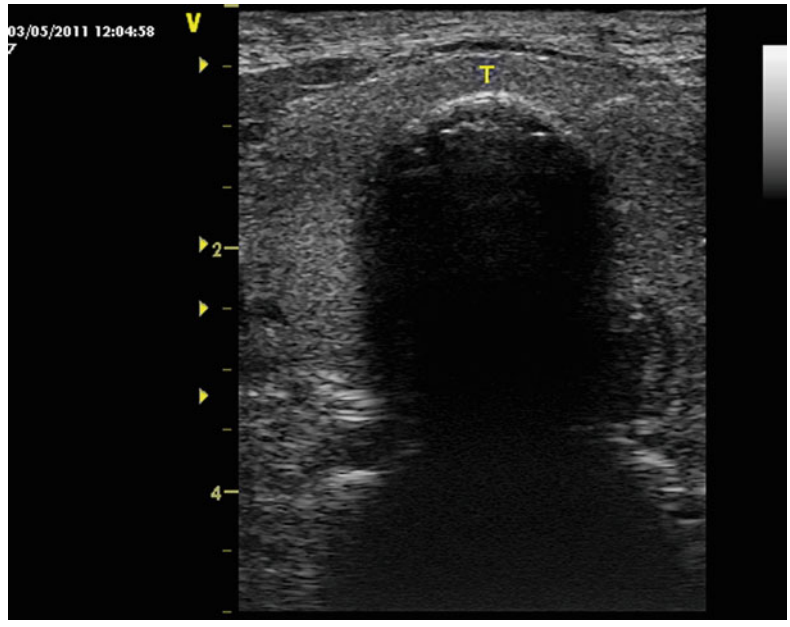

Fig. 48.2 Thyroid over the tracheal ring. Whenever possible the gland should not be punctured. *T* thyroid

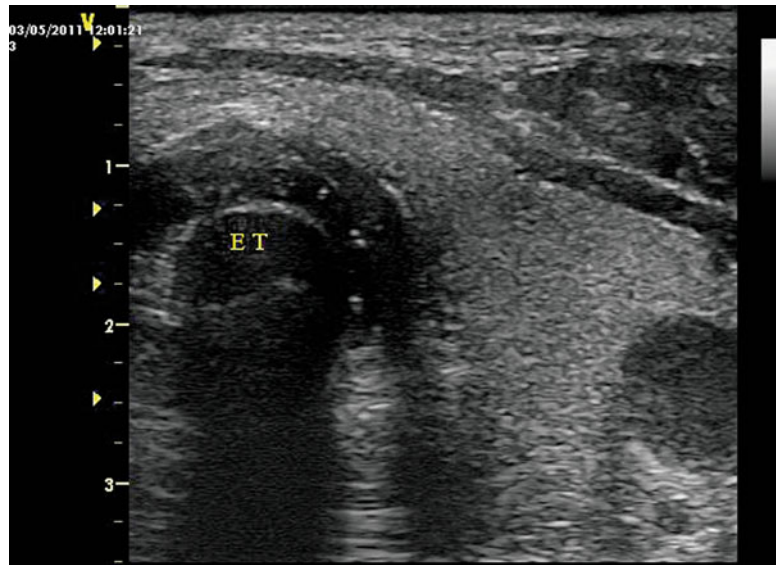

Fig. 48.3 Note the tracheal tube inside the tracheal lumen. *ET* endotracheal tube

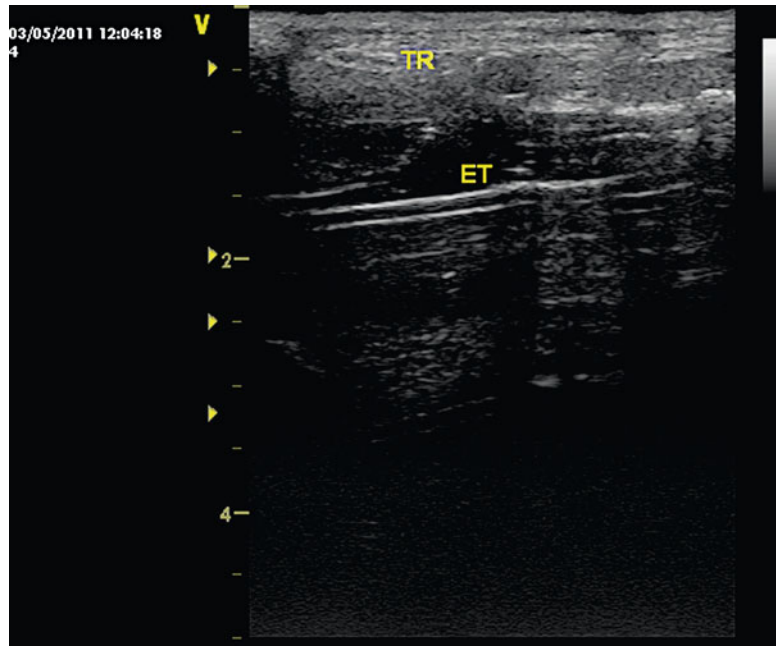

Fig. 48.4 Longitudinal scan of the neck. Note the tracheal tube. *TR* tracheal ring, *ET* endotracheal tube

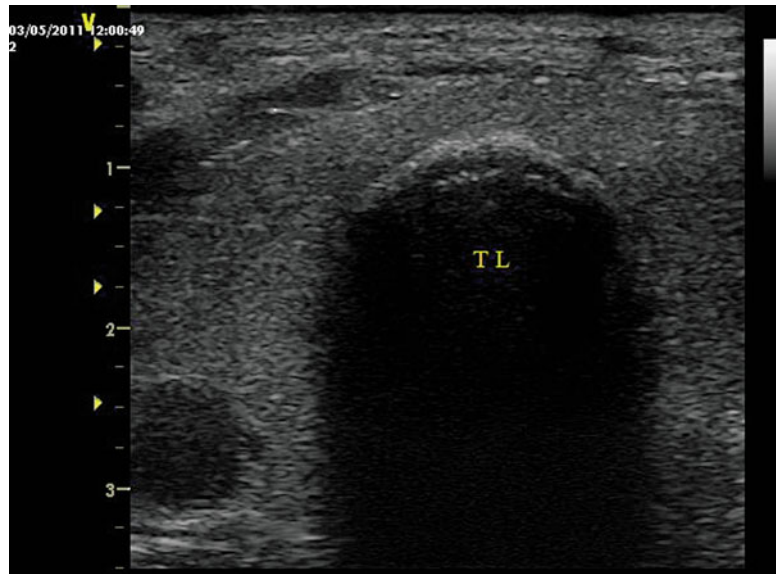

Fig. 48.5 The tracheal lumen appears empty as the tube has been withdrawn. *TL* tracheal lumen

Further Reading

Hatfield A, Bodenham A (1999) Portable ultrasonic scanning of the anterior neck before percutaneous dilatational tracheostomy. Anaesthesia 54:660–663

Hsieh KS, Lee CL, Lin CC et al (2004) Secondary confirmation of endotracheal tube position by ultrasound image. Crit Care Med 32(Suppl):374–377

Shlugman D, Satya-Krishna R, Loh L (2003) Acute fatal haemorrhage during percutaneous dilatational tracheostomy. Br J Anaesth 90:517–520

Sustic A (2007) Role of ultrasound in the airway management of critically ill patients. Crit Care Med 35(Suppl):173–177

Winkler WB, Karnik R, Seelmann O et al (1994) Bedsided percutaneous dilatational tracheostomy with endoscopic guidance: experience with 71 ICU patients. Intensive Care Med 20:476–479

Transcranial Doppler Ultrasonography in Intensive Care

49

Simone Cencetti and Daniele Cultrera

49.1 Introduction

Transcranial Doppler (TCD) ultrasonography is a validated noninvasive, reproducible, economical, and easily executable method that can be used at the bedside for the study of indirect markers of brain hemodynamics, although it is burdened by the limitation of not being the "gold standard" for any application. The method is applied with ultrasound scanning, using devices with a 2-MHz pulsed Doppler probe with special focus and dedicated software. The TCD study allows one to explore the main arteries of the circle of Willis, the ophthalmic artery, many portions of the carotid siphon (except the intrapetrosal tract and, in many cases, the intracavernosal tract), the intracranial vertebral arteries (V4 segment) ,and the basilar artery by ultrasonic scanning through special topographical extracranial areas, called windows (ophthalmic, temporal, and suboccipital). Special conditions and anatomical variability exclude the use of appropriate windows in 8–13 % of cases; the failure rate increases to 5–10 % when color-coded TCD ultrasonography is used, and that is the reason for fewer indications for its use in the ICU. The approach through the temporal window (zygomatic arch located above the protrusion in a route between the tragus and the orbital process, which differs depending on the subject) allows the study of the middle cerebral artery (MCA) (at scanning depths between 40 and 60 mm), the anterior cerebral artery (ACA) (depth 55–70 mm), the posterior cerebral artery (PCA) (depth 60–75 mm), and the termination of the internal carotid artery (ICA) (depth 58–68 mm), and only if activation of collateral circulation, interconnecting the front and rear. The polarity of the Doppler signal (positive, which is represented above the zero line, for the MCA, ICA, and PCA precommunicating segment, and negative for the ACA and the distal segment of the PCA) is indicative of the direction of flow with respect to the transducer. The investigation through the suboccipital window allows the study of the infratentorial major intracranial major arteries, namely, the vertebral arteries (depth 50–80 mm) and the basilar artery (depth 75–120 mm), which are all slack from the probe signal (negative polarity), i.e., the TCD ophthalmic window is used extensively for the analysis of signals from the carotid siphon and the ophthalmic artery. Standard reference values for the average speed for the intracranial arteries investigated by TCD ultrasonography are widely available in the literature, although it is good practice for each laboratory to set its own standards. The TCD study at the bedside in the ICU for elective indications is used for (1) monitoring severe head injury, (2) monitoring vasospasm after subarachnoid hemorrhage, and (3) determination of brain death.

S. Cencetti (✉)
UO Emergency Medicine, Santa Maria Nuova Hospital, Florence, Italy
e-mail: simone.cencetti@asf.toscana.it

A. Sarti and F. L. Lorini (eds.), *Echocardiography for Intensivists*,
DOI: 10.1007/978-88-470-2583-7_49,

49.2 Severe Head Injury

One should always remember that TCD ultrasonography does not provide measurements of cerebral blood flow, but provides dynamic assessments of cerebral hemodynamics. In many centers the findings of the investigation are used to instigate more significant investigations (e.g., scintigraphy, angiography, pressure measurements bloody intracranial) and also to drive some choices for the primary purpose of avoiding brain damage secondary to reduced perfusion, increased intracranial pressure, and vasospasm. Except for cases of reduced reactivity (CO_2 and barbiturates, which require the implementation of targeted testing), the TCD findings are mainly represented by decreases in average speed and increase in cerebral resistance (this is mainly expressed by a decrease or reset of flow velocity in the diastolic phase), obviously representing findings very specific to the individual concerned, but rather indicative of evolution if they are interpreted on the basis of repeated checking.

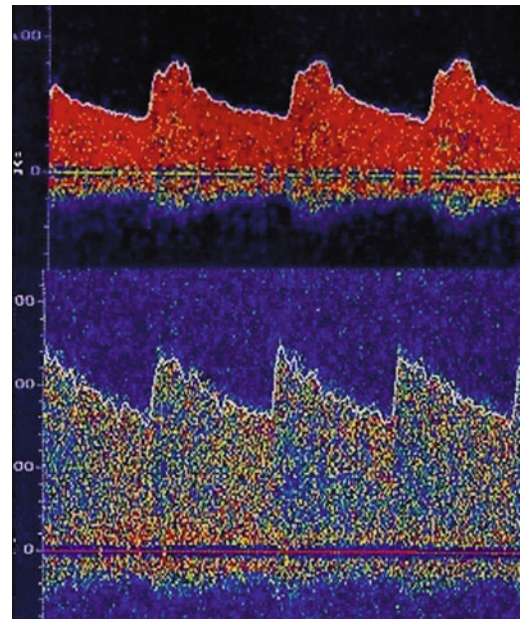

Fig. 49.1 Transcranial Doppler waveforms from a normal middle cerebral artery (*upper trace*) and cerebral vasospasm (*lower trace*). (Modified from Sarti [1] with permission)

49.3 Cerebral Vasospasm

Intracranial arterial vasospasm is a complication associated with subarachnoid hemorrhage and spontaneous posttraumatic hemorrhage, causing severe secondary neurological damage, with a trend of occurrence and intensity between the third and the 12th day after bleeding first occurred (with a peak between the sixth and the eighth day). TCD ultrasonography is not the gold standard for diagnosis and localization: the gold standard is cerebral angiography. TCD ultrasonography, however, can be performed serially at the bedside, and allows early recognition of the onset of vasospasm with a sensitivity of 42–67 % and a specificity of 76–99 % depending on the location. The hemodynamic effects of vasospasm of the proximal arteries of the circle of Willis are similar to those of a hemodynamic stenosis (Fig. 49.1) (significant increase of mean velocity, turbulence, decreased pulsatility index), whereas the distal vasospasm is expressed as a hemodynamically velocimetric decrease and an increase in pulsatility due to reduction of the diastolic component. It is therefore obvious that a single finding cannot be considered significant, and only monitoring by repeated tests may allow early recognition of hemodynamic alteration. Purely for guidelines, a classification has been proposed on the basis of the findings of TCD ultrasonography of the MCA during subarachnoid hemorrhage:

- Mean velocity lower than 120 cm/s: nonspecific increase in velocimetric
- Mean velocity greater than 120 cm/s: proximal vasospasm (if confirmed by a velocimetric MCA/ICA between 3 and 6)
- Mean velocity greater than 200 cm/s: severe spasm of the proximal (if MCA/ICA > 6)

These criteria, however, have value only if they are interpreted in an evolutionary context, emerging from repeated examinations.

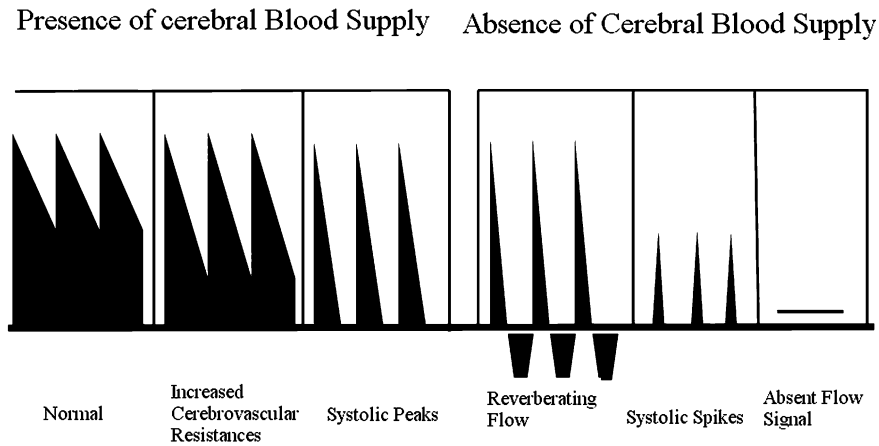

Fig. 49.2 Progression of transcranial Doppler waveforms toward brain death. (Modified from Sarti [1] with permission)

49.4 Assessment of Brain Death

The imbalance in the ratio between cerebral perfusion pressure and intracranial pressure, when a trend toward an increase in the intracranial pressure causes a progressive reduction until the arrest of cerebral blood flow. In Italy, the law provides for recourse to the determination of the arrest of cerebral blood flow in the following circumstances, which reasonably represent valid indications for common practice everywhere:

1. Children younger than 1 year
2. Presence of concomitant factors (e.g., neurodepressant drugs, hypothermia) that may interfere with the general clinical picture
3. Situations that prevent certain etiopathogenetic diagnoses, and can prevent or interfere with the EEG and brain stem reflexes.

Among the available methods that are allowed and recommended (i.e., cerebral angiography, brain scintigraphy, and TCD ultrasonography), the use of TCD ultrasonography according to the protocols defined an endorsement by type A class II evidence. It is obvious that TCD ultrasonography is a velocimetry and flowmetry technique, so it can be expected that the criterion for arrest of cerebral blood flow is represented by zero speed (no Doppler signal). The TCD findings, as summarized in Fig. 49.2, cover a spectrum of evolutionary change which sees the waveform in the sense of an increase in distal resistance (reduction up to disappearance of the diastolic component) and then evolves into a stream signal suggestive of reverberation (negative diastolic component, i.e., reverberation), the simple transmission of progression-free rate of the intracranial blood column (very small systolic spikes) until the final disappearance of the signal. These findings were validated in several studies by comparing them with the blood flowmetry methods and measurement of intracranial pressure, leading to confirmation that the patterns of reverberating flow, systolic spikes, and no Doppler signal correlate with the arrest of cerebral blood flow. When interpreting these findings, TCD ultrasonography forms part of the agreed protocols defined in the consensus. The sensitivity of the method reaches 91 % with a specificity of 100 %. The criteria for use in determining brain death are:

1. The test can be correctly interpreted only for systolic blood pressure greater than 70 mmHg
2. The investigation must necessarily be conducted through both the temporal windows and the occipital window
3. There must be evidence of cerebral circulatory arrest patterns: reverberating flow, systolic spike, and no signal. Necessary conditions for the appropriate interpretation of the absence of a signal are that through each of the three investigation windows at least one signal must be obtained with the flow characteristics of

reverberating or systolic spikes (exclusion of a false positive depends on the inadequacy of the window) or that a previous examination has shown the presence of a Doppler signal through the windows used.

Given the dynamic characteristic of the TCD findings and the evolutionary framework, the findings must emerge from two consecutive investigations at least 30 min apart.

Reference

1. Sarti A (2009) Ecocardiografia per l'intensivista. Springer, Milan

Further Reading

Bacalli S, Cencetti S, Cipriani M, Lagi A (1992) Débit sanguin cérébral et âge. Etude par Doppler transcrânien tridimensionnel. JEMU 13:260–263

Lysakowsky C, Walder B, Costanza MC, Tramer MR, Lysakowsky C, Walder B, Costanza MC, Tramer MR (2001) Transcranial Doppler versus angiography in patients with vasospasm due to ruptured cerebral aneurysm. Stroke 32:2292–2298

Newell DW, Aaslid R (1992) Transcranial Doppler. In: Aaslid R, Newell DW (eds) Transcranial Doppler. Raven, New York, pp 9–33

Steiner LA, Andrews PJD, Steiner LA, Andrews PJD (2006) Monitoring the injured brain: ICP and CBF. Br J Anaesth 97:26–38

Wijdicks EFM (2001) The diagnosis of brain death. New Engl J Med 2001(344):1215–1221

Ultrasonography of the Optic Nerve 50

Vanni Orzalesi and Daniele Cultrera

Despite the fact that the utility of intracranial pressure monitoring is still debated, evidence exists that intracranial hypertension is usually an acute event that can reduce cerebral perfusion and oxygen delivery, leading to cerebral ischemia and brain herniation. Invasive measurement of intracranial pressure remains the gold standard; however, it cannot always be performed because of the lack of neurosurgeons or because of the presence of contraindications such as coagulopathies and thrombocytopenia. The clinical diagnosis in comatose patients is often difficult and delayed, whereas neuroimaging, in addition to exposing the patient to ionizing radiation, cannot always be performed because of lack of equipment or hemodynamic instability and difficulty in transporting the patient. Transcranial Doppler ultrasonography is a viable alternative but it requires trained personnel and the presence of an acoustic window that is lacking in 10 % of the population.

Recently, optic nerve ultrasonography has been proposed as a noninvasive method for assessing intracranial hypertension. It is an easy to learn and feasible method with high intra- and interobsever reliability and a good correlation with MRI measurements. The optic nerve has an average diameter of 3 mm and is covered with a sheath made of leptomeninges, whose thickness is about 0.4 mm. Between the sheath and the nerve there is a subarachnoid compartment which continues with the intracranial compartment and that contains cerebrospinal fluid and a complex structure of trabeculae and septa.

When intracranial pressure increases, the shift of cerebrospinal fluid within the perineural subarachnoid space determines an increase in the optic nerve sheath diameter, which can be easily visualized by ultrasonography. The expansion tends to affect the anterior segment of the sheath, 3 mm posterior to the eyeball. Posterior regions tend to be affected to a lesser extent, probably due to the different distribution of trabeculae within the perineural subarachnoid space or to the decreased thickness of the sheath in the retrobulbar area.

Basically, the procedure consists in placing a linear probe (more than 7.5 MHz) on the closed eyelid either in the longitudinal or in the sagittal plane. The optic nerve appears as an anechoic/hypoechoic structure surrounded by echogenic material consisting of retrobulbar fat. The nerve sheath, rarely seen in healthy patients, appears as a hypoechoic structure that runs parallel to the nerve, enclosing a hyperechoic area (Figs. 50.1, 50.2).

Recent studies indicate a cutoff value of 5.7–6.0 mm to suspect intracranial hypertension with sensitivity between 87 and 95 % and specificity

V. Orzalesi (✉)
Department of Anesthesia and Intensive Care, Civil Hospital, Guastalla, Italy
e-mail: vorza@iol.it

A. Sarti and F. L. Lorini (eds.), *Echocardiography for Intensivists*,
DOI: 10.1007/978-88-470-2583-7_50, © Springer-Verlag Italia 2012

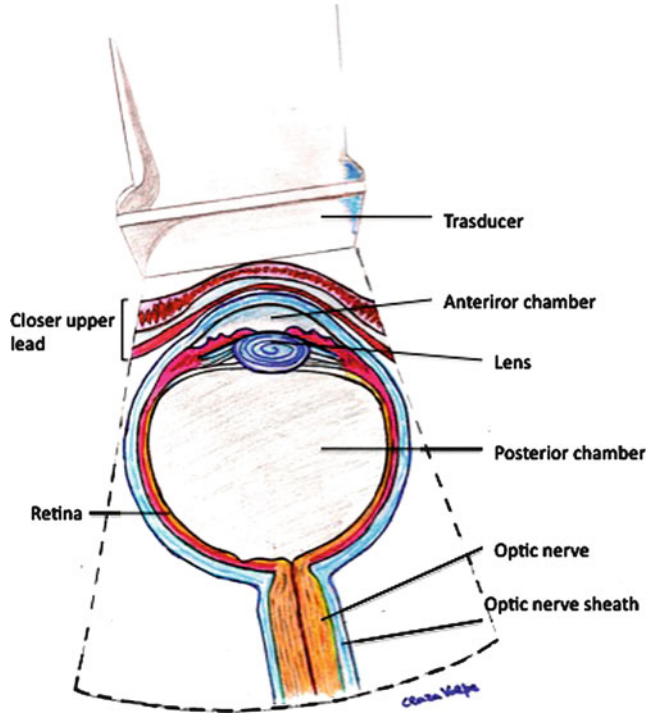

Fig. 50.1 Ocular ultrasound anatomy

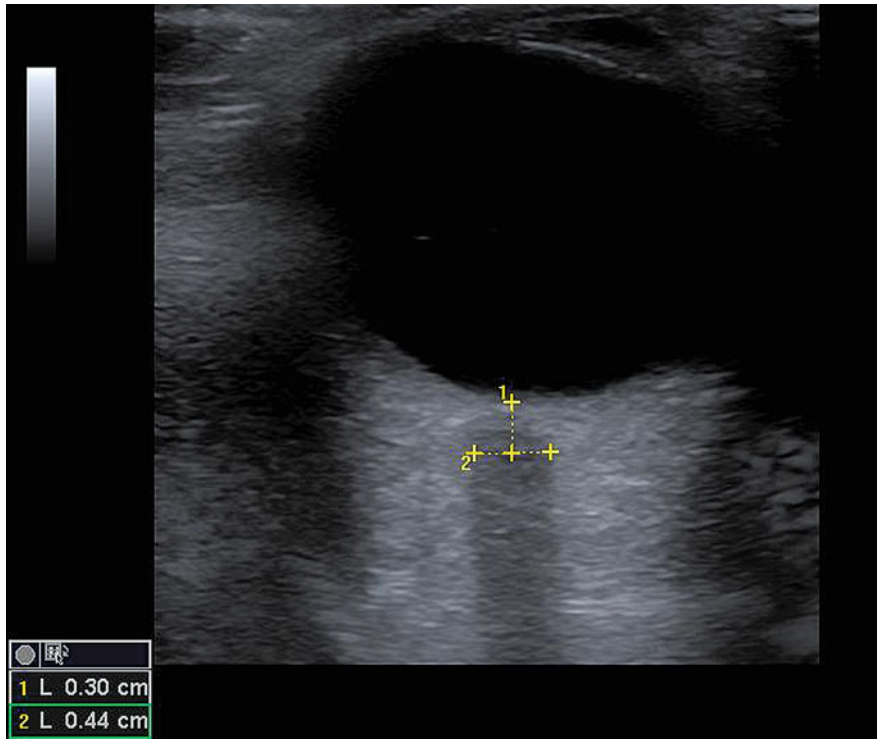

Fig. 50.2 Ultrasonography of the optic nerve: the ONSD is measured 3mm posterior to the eyball

between 79 and 100 %. However further research is needed to assess the optimal ONSD cut-off.

Further Reading

Geeraerts T, Duranteau J, Benhamou D (2008) Ocular sonography in patients with raised intracranial pressure: the papilloedema revisited. Crit Care 12(3):150

Major R, Girling S, Boyle A (2011) Ultrasound measurement of optic nerve sheath diameter in patients with a clinical suspicion of raised intracranial pressure. Emerg Med J 28(8):679–681

Skoloudík D, Herzig R, Fadrná T, Bar M, Hradílek P, Roubec M, Jelínková M, Sanák D, Král M, Chmelová J, Herman M, Langová K, Kanovsky P (2011) Distal enlargement of the optic nerve sheath in the hyperacute stage of intracerebral haemorrhage. Br J Ophthalmol 95(2):217–221

Soldatos T, Chatzimichail K, Papathanasiou M, Gouliamos A (2009) Optic nerve sonography: a new window for the non-invasive evaluation of intracranial pressure in brain injury. Emerg Med J 26(9):630–634

Steinborn M, Fiegler J, Kraus V, Denne C, Hapfelmeier A, Wurzinger L, Hahn H (2011) High resolution ultrasound and magnetic resonance imaging of the optic nerve and the optic nerve sheath: Anatomic correlation and clinical importance. Ultraschall Med 32(6):608–613

Appendix
Formulae and Normal Value

BSA	Body surface area	Jacobson Formula = (Ht in cm + Wt in Kg–60)/100		
MAP	Mean arterial pressure	N. = 65–100 mmHg	Low: <65 mmHg;	High: >100 mmHg
CVP	Central venous pressure	N. = 2–6 mmHg		
MPAP	Mean pulmonary arterial pressure	N. = 15–20 mmHg		
LAP (PAWP)	Left atrial pressure (PA wedge pressure)	N. = 6–12 mmHg		
MPAP-PAWP	Transpulmonary gradient	N. = <15 mmHg		
SVRI	80 x (MAP–CVP)/CI	N. = 1970–2390 dynes x sec/cm^5/m^2 (25–30 units)		
PVRI	80 x (MPAP–PAWP)/CI	N. = 255–285 dynes x sec/cm^5/m^2 (3.0–3.5 units)		
AVA	AVA1 = S^2 x 0.433 (with CWD)	N. = 2.5–4.5 cm^2		
	AVA2 = LVOT diameter^2 x 0.785 (with PWD)			
AV VTI (CWD)	AV velocity time integral	N. = 18–22 cm		
LVOT VTI (PWD)	LVOT velocity time integral	N. = 18–22 cm		
LVOT ET	LVOT ejection time	N. = 265–325 msec		
SI	AVA x AV/LVOT VTI (CWD/PWD)	N. = 33–47 ml/m^2/beat		
	BSA			
CI	AVA x AV/LVOT VTI x HR	N. = 2.4–4.2 l/min/m^2		
	BSA			
RVEDA (4-ch)	RV end diastolic area (4-ch)	N. = 20 ± 4 cm^2 or <65 % LV size;	Trivial and mild: 65 % LV size	Moderate and severe: >LV size
RVESA (4-ch)	RV end systolic area (4-ch)	N. = 11 ± 3 cm^2		

A. Sarti and F. L. Lorini (eds.), *Echocardiography for Intensivists*,
DOI: 10.1007/978-88-470-2583-7, © Springer-Verlag Italia 2012

LVEDA (4-ch)	LV end diastolic area (4-ch)	N. = 33 ± 8 cm^2 (17.7–47.3) & Apex = LV		
RVFAC (4-ch)	RV fractional area change	N. = 46 ± 6 %		
RVDd (4-ch)	RV end diastolic diameter	N. = 3.0 ± 0.3 cm		
RVFWd	RV free wall diastolic thickness	N. = 0.5–0.7 cm	Hypertrophy: >0.7 cm	
TAPSE	Tricuspid annular plane systolic excursion	N. = >20 mm		
LVEDV (MOD)	LV end diastolic volume (4-ch/2-ch)	N. = Male: 111 ± 22 ml (62–170); Female: 80 ± 12 ml (55–101)		
LVEDVi (MOD)	LV EDV (MOD)	N. = 67 ± 17 ml/m^2		
	BSA			
LVESV (MOD)	LV end systolic volume (4-ch/2-ch)	N. = Male: 34 ± 12 ml (14–76); Female: 29 ± 10 ml (13–60)		
LVESVi (MOD)	LV ESV (MOD)	N. = 28 ± 8 ml/m^2		
	BSA			
LVEF (MOD) %	LVEDVi–LVESVi (MOD)	N. = 70 ± 7 %(M), 65 ± 10 %(F)		
	LVEDVi			
LVEDA (SAX)	LV end-diastolic area	N. = 15 ± 5 cm^2		
LVEDAi (SAX)	LV end-diastolic area/BSA	N. = 5.5–12 cm^2/m^2		
LVESA (SAX)	LV end-systolic area	N. = 6 ± 2 cm^2		
LVESAi (SAX)	LV end-systolic area/BSA	N. = 2.4–6.4 cm^2/m^2		
LVFAC %	LVEDA–LVESA	N. = 65 ± 15 %;	Moderate dysfunction: 30–50 %	Severe dysfunction: <30 %
	LVEDA			
LVIDd (SAX) M-mode	LV end diastolic diameter	N. = 4.7+/− 0.8 cm (<5.5 cm)	Trivial/mild: 5.5–6.0 cm	Moderate/ severe: >6.0 cm
LVIDs (SAX) M-mode	LV end systolic diameter	N. = 3.1 ± 0.8 cm		

Mean Vcf	LVIDd–LVIDs	N. = 1.2 circ/sec (1.0–1.9)		
	LVIDd x (LVOT ET)			
LVPWd (SAX) M-mode	LV posterior wall end-diastolic thickness	N. = 0.6–1.1 cm	Hypertrophy: >1.1 cm	
EDLV mass [C]	End-diastolic LV mass (cubic):	N. = 90–100 ± 15 g/m^2		
	0.8 x (1.04) x [(LVIVSd + LVIDd + LVPWd)3−LVIDd3] + 0.6			
ESWS (merid.)	End-systolic meridional wall stress (Grossman):	N. = 65 ± 20 x 10^3 dynes/cm^2 or 44 ± 12 gr/cm^2 (LVPWs ≤ 1.2 cm)		
	1.35 x ESAP x LVIDs/4 x LVPWs x (1 + PWLVs/LVIDs)			
IVRT (MV–AV PWD)	Iso-volumic relaxation time	N. = 70–90 msec		
	'R'-MV/TVopen–'R'-AV/PV close			
IVCT (MV–AV PWD)	Iso-volumic contraction time			
	MV/TV close-MV/TV open–(LVET + IVRT)			
MPI	Myocardial performance index	Mild dysfunction: 0.40–0.60	Moderate dysfunction: 0.60–1.00	Severe dysfunction: >1.00
	(MV/TV close-MV/TV open–LVET)/LVET N. = < 0.40			
PA PWRmax	Preload adjusted maximal power	[ABF (max vel) x SAP x AVA]/EDV2		
MV E/A ratio	MV 'E' wave peak velocity	N. = 1.0–2.2	E vel N. = 70–120 cm/s	
	MV 'A' wave peak velocity		A vel N. = 42–70 cm/s	
MV DT - E	MV deceleration time 'E' wave	N. = 160–240 msec (lower in young people)		
MV A dur	MV 'A' wave duration	N. = >120 msec (A dur ≥ a dur)		
MV Vp (CMM)	MV flow propagation velocity	N. = >45 cm/sec (A); >55 cm/sec (Y)		
MV Ea vel (TDI)	MV annulus 'E' (early) wave peak velocity	N. = >8 cm/sec		

dp/dt (with Mit. Reg.)	Change in pressure over time (32.000/time 1–3 m/sec [CWD])	N. = >1,200 mmHg/s	Borderline: 1,000–1,200 mmHg/s;	Abnormal: <1,000 mmHg/s
PV VTIs/VTId	PV velocity–time integral syst/diast	N. = VTIs ≥ VTId (0.6−1.2) (smaller in young people)		
PV a vel	PV 'a' wave peak velocity	N. = <20 cm/sec		
PV a dur	PV 'a' wave duration	N. = > 110 msec (a dur ≤ A dur)		
LA(RA) L (A/P) Des	LA(RA) end-syst. Longitudinal diameter	N. = 3.8 ± 0.6 cm	Trivial and mild: 4.4–5.0 cm	Moderate and severe: >5.0 cm
LA(RA) T (L/L) Des	LA(RA) end-syst. Transverse diameter	N. = 3.8 ± 0.6 cm	Trivial & Mild: 4.4–5.0 cm	Moderate and severe: >5.0 cm
LA index	LALDes x LATDes	N. = <16 cm^2	Moderate dilatation: 16–24 cm^2	Severe dilatation: >24 cm^2
LAP (with Mit. Reg.)	Bernoulli equation SAP−[4 x (MAX vel for MR)2]	N. = 6–12 mmHg		
LAP (LVEF ≤35%) (MV DT-E)	Deceleration time of MV early diastolic filling	N. = 6–12 mmHg	DT-E ≥150 msec: LAP ≤10 mmHg	
	(DT-E)–1.12 x 2380		DT-E ≤120 msec: LAP ≥20 mmHg	
LAP (LVEF ≥35%) (MV Vp with CMM)	[(E vel/Vp) x 5.9] + 2.5	N. = 6–12 mmHg; N. = E vel/Vp: <2.5		
LAP (LVEF ≥35%) (MV Ea vel with TDI)	[(E vel/Ea) x 1.3] + 2.0	N. = 6–12 mmHg; N. = E vel/Ea: 8 ± 2		
LAP (LVEF ≥35% (MV IVRT)	1,000/[(2 x IVRT) + Vp]	N. = 6–12 mmHg		
LAP (LVEF ≥35%) (PV SF = VTIs/VTId)	Systolic fraction: VTIs/(VTIs + VTId) x 100	N. = >55%		
LAP (LVEF ≥35%) (PV a dur–MV A dur)	[(PV a dur–MV A dur) x 0.164] + 17.1	N. = 6–12 mmHg		

Diastolic function	Normal	Impaired filling	Pseudonormal filling	Restrictive filling
MV IVRT	70–90 msec	>90 msec	<90 msec	<70 msec
MV E/A ratio	1.0–2.2	<1.0	1.0–1.5	>1.5
MV DT-E	160–240 msec	>240 msec	160–200 msec	<160 msec
PV VTIs/ VTId	VTIs > VTId	VTIs >>> VTId	VTIs < VTId	VTIs < << VTId
PV a dur/ MV A dur	MV A dur ≥ PV a dur	MV A dur ≥ PV a dur	MV A dur < PV a dur	MV A dur <<< PV a dur
PV a vel	PV a vel <35 cm/sec	PVa vel >35 cm/ sec	PVa vel >35 cm/ sec	PVa vel >35 cm/ sec
MV Vp (CMM)	Vp >45 (A) cm/sec, >55 (Y) cm/sec	Vp <45 (A) 55 (Y) cm/sec	Vp <45 (A) 55 (Y) cm/sec	Vp <45 (A) 55 (Y) cm/sec
MV Ea vel(TDI)	Ea >8 cm/sec	Ea <8 cm/sec	Ea <8 cm/sec	Ea <8 cm/sec
LA Index	<16 cm^2	<16 cm^2	>16 cm^2	>>>16 cm^2

Hemodynamics calculations

Pressure estimated	Required measurement	Formula	Normal values (mmHg)
CVP	Respiratory IVC collapse (spontaneously breathing)	≥40% <10 mmHg	
RVSP	Peak velocity$_{TR}$, CVP estimated or measured	$RVSP = 4(V_{TR})^2 + CVP$ (No PS)	16–30 mmHg
RVSP + VSD	SBP, Peak $V_{LV–RV}$	$RVSP = SBP\text{-}4(V_{LV\text{-}RV})^2$ (No AS or LVOT obstruction)	Usually >50 mmHg
SPAP	Peak velocity$_{TR}$, CVP estimated or measured	$SPAP = 4(V_{TR})^2 + CVP$ (No PS)	16–30 mmHg
DPAP	End diastolic velocity$_{PR}$, CVP estimated or measured	$PAEDP = 4(V_{PR\ ED})^2 + CVP$	0–8 mmHg
MPAP	AT to peak V_{PA} (m/s)	$MPAP = (-0.45)\ AT + 79$	10–16 mmHg
RV dP/dt	TR spectral envelope, $T_{TR\ (2\ m/s)}$-$T_{TR\ (1\ m/s)}$	$RVdP = 4\ V^2{}_{TR(2\ m/s)} - 4V^2{}_{TR(1m/s)}$ $RVdP/dt = dP/T_{TR(2m/s)} - T_{TR(1m/s)}$	>150 mmHg
LASP	Peak V_{MR}, SBP	$LASP = SBP\text{-}4(V_{MR})^2$ (No AS or LVOT obstruction)	3–15 mmHg
LA + PFO	Velocity PFO, CVP estimated or measured	$LAP = 4(V_{PFO})^2 + CVP$	3–15 mmHg
LVEDP	End diastolic velocity$_{AR}$, DBP	$LVEDP = DBP - 4(V_{AR})^2$	3–12 mmHg
LV dP/dt	MR spectral envelope $T_{MR\ (3\ m/s)} - T_{MR\ (1\ m/s)}$	$LVdP = 4\ V^2{}_{MR(3m/s)} - 4V^2{}_{MR(1m/s)}$ $LVdP/dt = dP/T_{MR(3m/s)} - T_{MR(1m/s)}$	>1,000 mmHg

AR aortic regurgitation, *AS* atrial stenosis, *AT* acceleration time, *CVP* central venous pressure, *DBP* diastolic blood pressure, *ED* end diastolic, *IVC* inferior vena cava, *LA* left atrium, *LV* left ventricle, *LASP* left atrium systolic pressure, *LVOT* left ventricle outflow tract, *MR* mitral regurgitation, *PA* pulmonary artery, *PAEDP* pulmonary artery end-diastolic pressure, *SPAP* systolic pulmonary arterial pressure, *DPAP* diastolic pulmonary arterial pressure, *MPAP* mean pulmonary arterial pressure, *PFO* patent foramen ovale, *PR* pulmonary regurgitation, *PS* pulmonary stenosis, *RV* right ventricle, *RVSP* right ventricle systolic pressure, *SBP* systolic blood pressure, *TR* tricuspid regurgitation, *VSD* ventricular septal defect

Index

A. Sarti and F. L. Lorini (eds.), *Echocardiography for Intensivists*,
DOI: 10.1007/978-88-470-2583-7, © Springer-Verlag Italia 2012